The Selective Trimerisation of alpha-Olefins with Chromium Triazacyclohexane Catalysts

Coxon, Alex

Award date:
2015

Awarding institution:
University of Bath

The Selective Trimerisation of α-Olefins with Chromium Triazacyclohexane Catalysts

Alexander Gregory Nicholas Coxon

A thesis submitted for the degree of Doctor of Philosophy

Department of Chemistry
University of Bath

November 2015

Signed _____

Contents

Abbreviations

1-C_n	A linear α-olefin containing n carbon atoms
1D / 2D	One Dimensional / Two Dimensional
^2H	Deuterium
BP	Beyond Petroleum (formerly British Petroleum)
C_n	A hydrocarbon containing n carbon atoms
COSY	Correlation Spectroscopy (Two dimensional NMR spectroscopy)
Cr^{IV}	A chromium cation with the oxidation state given in superscript
Cy	Cyclohexyl
DABCO	1,4-Diazabicyclo[2.2.2]octane
DCM	Dichloromethane
DFT	Density Functional Theory
DMAB	Dimethylanilinium tetrakis(pentafluorophenyl)borate
Eq.	Molar equivalents
FID	Flame Ionisation Detector
GCMS	Gas Chromatography – Mass Spectrometry
HDPE	High Density Polyethylene
^{i}Bu	*iso*-Butyl
IR	Infrared
L	Undefined neutral ligand
LAO	Linear α-Olefin
LLDPE	Linear Low Density Polyethylene
M	An undefined metal atom or ion.
(m/z)	Mass spectrometry peak representing mass over charge, in all cases the charge is equal to one and therefore the peak value equals the relative atomic mass.
M Peak	Peak corresponding to the monoisotopic mass of a molecule in a mass spectrometry fragmentation spectrum
MAO/DMAO	Methylaluminoxane / Dry (Depleted) Methylaluminoxane
MMAO	Modified Methylaluminoxane
Na/K	Sodium/Potassium liquid alloy
NMR	Nuclear Magnetic Resonance
PET	Petroleum Ether
o-$C_6H_4F_2$	*ortho*-difluorobenzene
PNP	Bis(diarylphosphino)amine based compounds
PNPNH	(Diarylphosphino)(aminoarylphosphino)amine based compounds
RT	Room Temperature
R_3TAC	1,3,5-Trisalkyl-1,3,5-triazacyclohexane
(R_3TAC)$CrCl_3$	A generic chromium chloride triazacyclohexane complex
TAC	1,3,5-Triazacyclohexane
TACN	1,4,7-Triazacyclononane
THF	Tetrahydrofuran
TM	Transition Metal
TOF	Turnover Frequency
TON	Turnover Number
TOF-MS	Time Of Flight – Mass Spectrometry
UV/Vis	Ultraviolet/Visible light (spectroscopy)
^nC	The isotope of carbon with a relative atomic mass of n amu

Catalyst Notation

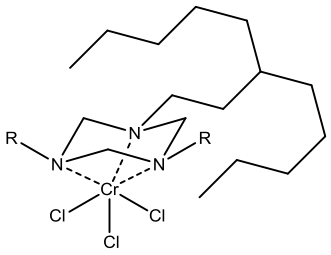

γ-Pe_2H

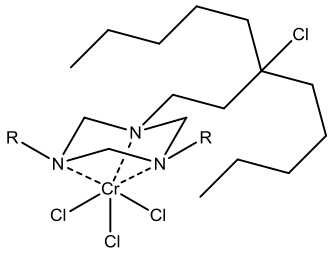

γ-Pe_2Cl

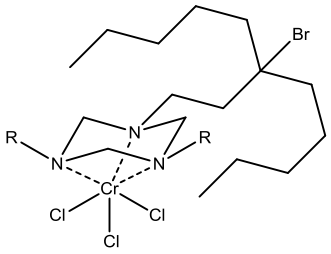

γ-Pe_2Br

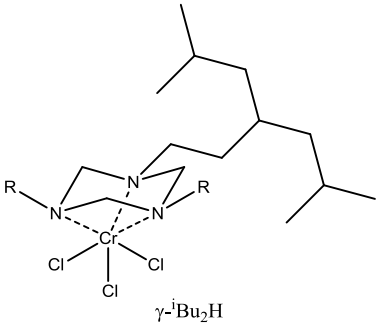

γ-$^{i}Bu_2H$

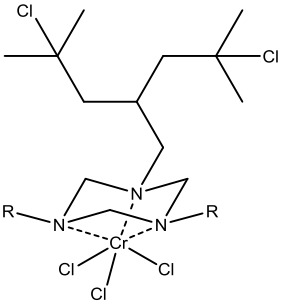

β-$^{i}Bu_2(Cl_2)$

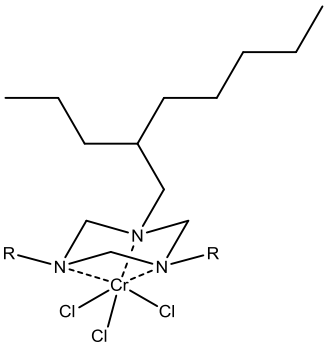

β-PrPe

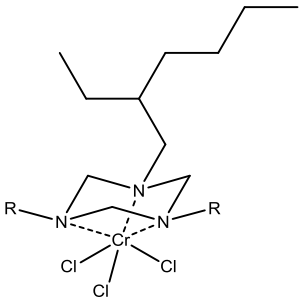

β-EtBu

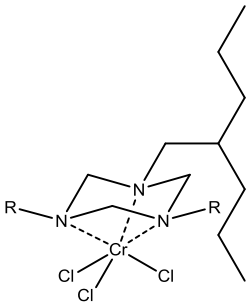

β-Pr_2

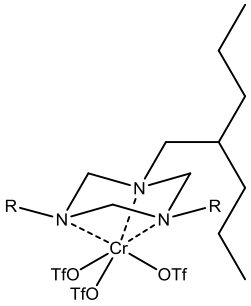

β-$Pr_2(OTf)$

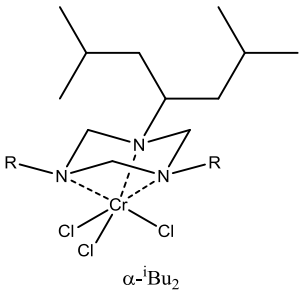

α-$^{i}Bu_2$

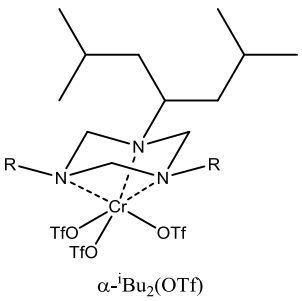

α-$^{i}Bu_2(OTf)$

Abstract

Described herein is research into the production of hydrocarbons suitable for various industrial applications *via* α-olefin trimerisation.[1] This work has been split into three principal chapters that each describe a different aspect of the research carried out. In addition, a comprehensive review is presented into the development of selective oligomerisation, with an emphasis on the role of metallacyclic intermediates.

α-Olefin Trimerisation: Catalyst Synthesis and Optimisation

The synthesis and characterisation of eight novel chromium triazacyclohexane catalysts is described, including a series of catalysts containing alternative abstractable anions. All were shown to be active towards trimerisation, with optimisation resulting in exceptional selectivities of over 95 w%, with the remainder consisting of isomerised LAO and dimer. Investigation of the 'halogen' effect indicated the inducement of catalyst decomposition *via* oxidation.

Mechanistic Insights into α-Olefin Trimerisation

The proposed metallacyclic mechanism was investigated using a variety of techniques.[2] The regioisomers of the trimer were identified down to an abundance of 0.1% with the use of ^{13}C labelling. All matched those expected, allowing the relative abundance of differently substituted intermediates to be determined. ^{2}H labelling identified competition between elimination pathways, which can only occur for metallacyclic intermediates. Characterisation of the catalyst activation products supported the mechanism, while chain transfer reactions were also identified. Air sensitive mass spectrometry led to observation of peaks matching those expected for proposed intermediates.

Ethylene Trimerisation: Process Optimisation and Product Identification

Optimisation of experimental procedures and increasing the catalyst bulk, led to selectivities of 93 w% and activities beyond 250,000 mol(C_2H_4) mol(Cr)$^{-1}$ h^{-1}. Kink kinetics resulted in three distinct periods of differing ethylene consumption for which a mechanism has been proposed. Tetramerisation was detected for these systems for the first time alongside several co-trimerisation products.[3] The C_{10} species were most abundant and have been fully characterised, supporting the proposed co-trimerisation mechanism.[4]

1. Olefin Oligomerisation

Oligomerisation has been of interest for decades as a means of producing useful hydrocarbons from simple and readily available α-olefins, principally ethylene. The ability to convert short chain length alkenes, collected during natural gas and oil extraction, into more useful $C_6 - C_{30}$ alkenes is of great commercial interest. This is due to the cost of the highly energy intensive alternatives for production and separation, such as cracking of paraffins, metathesis of olefins or electrolysis of carboxylic acids.[1] The oligomer products are in high demand for a variety of applications, principally as polymerisation co-monomers,[5] surfactants,[5] lubricants[3] and precursors for oxo-alcohols[6].

This field of research has expanded rapidly since the discovery of selective oligomerisation systems. An overview of these advances is presented here and covers both academic and industrial research. By following a broadly chronological approach, this section aims to demonstrate the progress made towards highly efficient selective oligomerisation catalysts and better understanding of the corresponding mechanisms.

Across the published literature a wide variety of units have been used to describe both the conditions and the performance of the catalyst systems developed. In order to enable meaningful comparison, it has been necessary to convert the reported activities and conditions into standardised units. The unit chosen for the presentation of activity data is mol(olefin consumed) per mol(catalyst) per hour, using the notation mol(C_nH_{2n}) mol(TM)$^{-1}$ h^{-1}, where TM represents the elemental symbol of the transition metal used in catalysis. In this manner the catalyst activity is comparable between non-selective oligomerisation, dimerisation, trimerisation and tetramerisation without distortion of the values. The key units used for the data reported are shown in Table 1.1.

Table 1.1 - The standard units used for comparison of catalyst systems.

Value	Unit
Activity	mol(C_nH_{2n}) mol(TM)$^{-1}$ h^{-1}
Turnover Number	mol(product) mol(TM)$^{-1}$
Equivalents	mol(compound) mol(TM)$^{-1}$
Time	h
Pressure	bar
Temperature	°C

1.1 Non-Selective Oligomerisation

The non-selective oligomerisation of olefins has been known since 1949 and quickly received considerable industrial attention, particularly for ethylene. In that year, Karl Ziegler discovered that exposure of $LiAlH_4$ to an ethylene atmosphere resulted in a rapid drop in pressure.[7, 8] Originally linked to the presence of lithium in the solution, it was quickly realised that the aluminium accounted for the activity. GCMS analysis indicated a range of α-olefins had been produced, the first example of oligomerisation as an efficient route to these valuable compounds. Importantly, it was also discovered that the system was easily tuneable to produce a desired product range by variation of the temperature. At high temperatures (200 °C or more) short chain olefins were produced, while at lower temperatures (80-100 °C) waxy oligomers of up to C_{200} were formed.

The activity of the aluminium species was found to result from the formation of triethylaluminium, a novel species at the time, which soon became a widely adopted catalyst for the 'Aufbau' reaction. The later serendipitous discovery that certain transition metals demonstrate far greater activities for these chain growth reactions led to the development of one of the largest research areas in chemistry.[7] A vast array of catalysts have since been discovered which are capable of oligo- and polymerisation; based principally on three transition metals: titanium, zirconium and nickel.[1]

The most established Ziegler-Natta type catalyst consists of solid-state titanium chloride with an alkyl aluminium co-catalyst.[9] This heterogeneous system involves the deposition of a mixture of α-$TiCl_3$ and $TiCl_4$ onto $MgCl_2$ followed by subsequent addition of Et_3Al. The Cossee-Arlman mechanism has now been generally accepted as the best representation of Ziegler-Natta type oligomerisation, Scheme 1.1.[10] However, the heterogeneous nature of the catalyst means very little is understood about the catalyst cycle and its intermediates. Since its discovery, considerable research has gone into analogous homogeneous systems in an attempt to improve the understanding and activity of the original catalyst, which was around 340 mol(C_2H_4) mol(Ti)$^{-1}$ h^{-1}.[1] More recently, research continues into multidentate ligands, which have recorded activities of around 3500 mol(C_2H_4) mol(Ti)$^{-1}$ h^{-1}, though with reduced selectivity.[11]

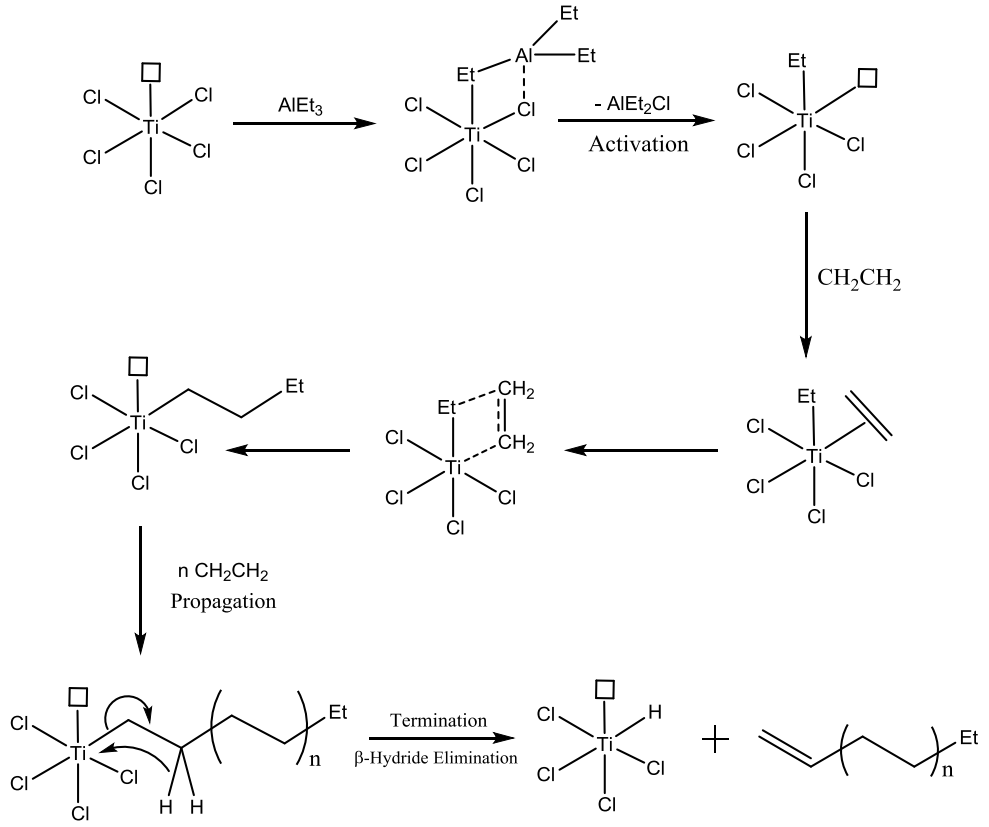

Scheme 1.1 - The Cossee-Arlman mechanism for Ziegler-Natta Ti-catalysed oligomerisation.

In the 1970s work into effective homogeneous analogues by Keim *et al.* led to the discovery of highly active nickel hydride species.[12-14] What became known as the Shell Higher Olefins Process (SHOP) represented a simple and cheap route to light α-olefins in the C_4-C_{30} range. These catalysts present the best activities out of the oligomerisation catalysts applied in industry, with activities at least a factor of ten higher than for titanium chloride based systems.[15] The mechanism is thought to be analogous to the Ziegler-Natta catalysts, with matching propagation and termination routes.[16]

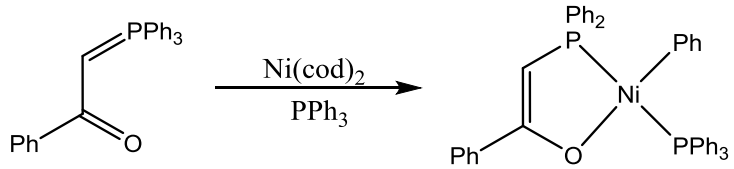

Scheme 1.2 - Synthesis of a typical SHOP precatalyst.

As well as the improved activities, these systems demonstrate a considerable advantage over the Ziegler-Natta catalysts in relation to their activation. The conventional synthesis of the precatalyst from a ketone stabilised phosphorus ylide and $Ni(cod)_2$ results in the formation of a metal-aryl bond, Scheme 1.2. On exposure to ethylene the labile phosphine is substituted and the coordinated ethylene subsequently inserts into the Ni-C bond. This produces a species capable of β-hydride elimination, leading to formation of the nickel hydride catalyst and vinylbenzene as a side product, Scheme 1.3. As a result, SHOP catalysts can be considered self-activating in the presence of ethylene, avoiding the considerable cost associated with aluminium alkyl activators.

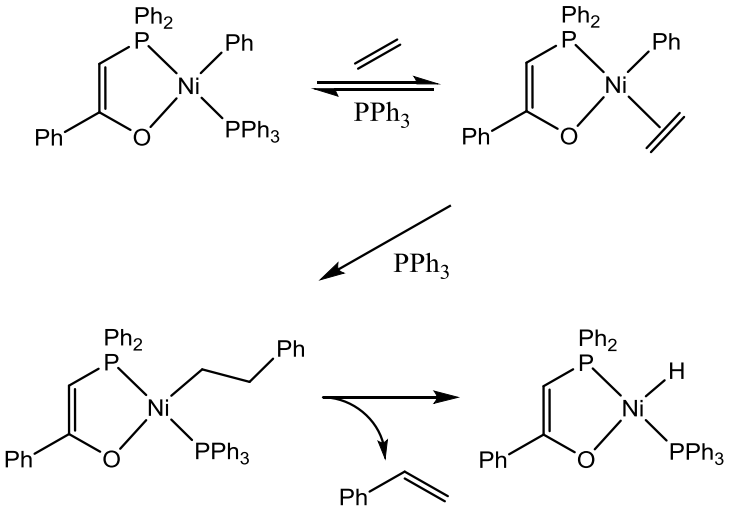

Scheme 1.3 - Activation of a SHOP catalyst with ethylene.

There has been considerable work into variation of the aryl groups and the labile phosphine donor since the original discovery.[14] This has led to improvements in the activity of the system but the core features of the catalyst have changed little since its conception. Both the titanium and nickel systems have been applied extensively in industry, yet they have significant drawbacks due to the broad range of LAOs produced.

Both catalysts produce a Shulz-Flory distribution of α-olefins containing an even number of carbon atoms, predominantly in the C_4-C_{40} range. This is dictated by the relative probabilities of propagation and termination. The isolation of the desired products either requires fractional distillation or more complex refining, which adds considerable cost to the process. Furthermore, demand for the properties demonstrated by the different chain lengths is not consistent. To avoid wasting the excess larger olefins, separation and chain length reduction via isomerisation and metathesis is required, further adding to the cost.[1]

Oligomerisation of larger α-olefins is also possible using variations of these catalysts, though with low activities. The increased bulk of the olefin leads to less favourable insertion and as such these species favour short (branched) chain oligomerisation, though they still produce a variety of products. The oligomerisation of larger olefins for application as lubricants has, therefore, not been actively pursued using these catalysts. Instead, the low abundance higher molecular weight products from propylene or ethylene oligomerisation are used. As such, the field of LAO oligomerisation has been investigated to a much lower degree.[1]

In all cases the process is inefficient due to the additional costs associated with isolating the desired product. This has led the industry to look at more selective processes, which demonstrate far more efficient routes to specific molecular weight products. The first breakthrough came in the form of selective dimerisation.

1.2 Selective Dimerisation

1.2.1 Ethylene Dimerisation and the Discovery of Metallacycles

The selective dimerization of ethylene was discovered by Ziegler at around the same time as the oligomerisation catalysts that bear his name.[8] Both titanium and zirconium alkoxide catalysts, when used in conjunction with alkyl aluminium co-catalysts, were shown to produce 1-butene at very high selectivities. The titanium analogue was later adopted by industry as the foundation of the Alphabutol process, accounting for approximately 25% of worldwide production as of 2009.[17]

The active form of the catalyst and the mechanism that the dimerisation proceeds by is still poorly understood. The most recent experimental evidence points towards a Cossee-Arlman mechanism similar to that of the non-selective processes.[18] However, in this case the β-hydride shift that terminates the oligomerisation is significantly more favourable than further propagation after the first ethylene insertion. Following the original discovery, it was found that a considerable number of catalyst systems were capable of the dimerisation of ethylene, though with a range of selectivities.[19, 20] The vast majority of these are proposed to proceed *via* the same mechanism with only very minor variations.

However, about a decade after the discovery of the Ziegler catalysts, a new range of selective dimerisation catalysts was beginning to emerge that followed a different mechanism. In 1970 M. L. H. Green reported the first metallacyclopentane complex, produced by reaction of a coordinatively unsaturated Fe species with fluorinated ethylene, Scheme 1.4.[21]

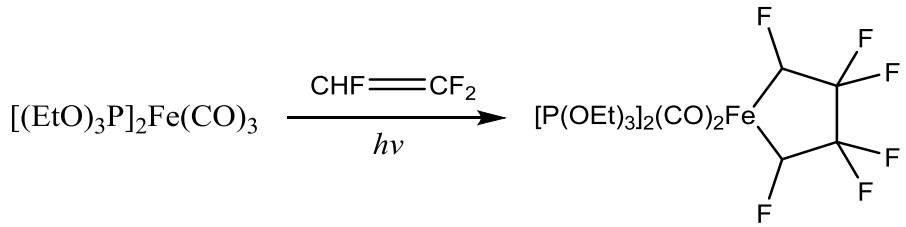

Scheme 1.4 - Synthesis of the first known metallacyclopentane.

Subsequently, it was found that strained olefins, typically norbornadienes and methylenecyclopropanes, were capable of forming metallacyclopentanes with Ir and Ni.[22-24] Importantly, the decomposition of these species led to cyclodimerisation and the first catalyst, based on Ni, was discovered in 1972 by P. Binger, Scheme 1.5.[25, 26] The addition of strongly binding bipyridyl ligands allowed the isolation and characterisation of the nickelacyclopentane species as an intermediate. This confirmed the existence of a second mechanism capable of dimerisation; one which gave considerably different products compared to the Cossee-Arlman pathway.

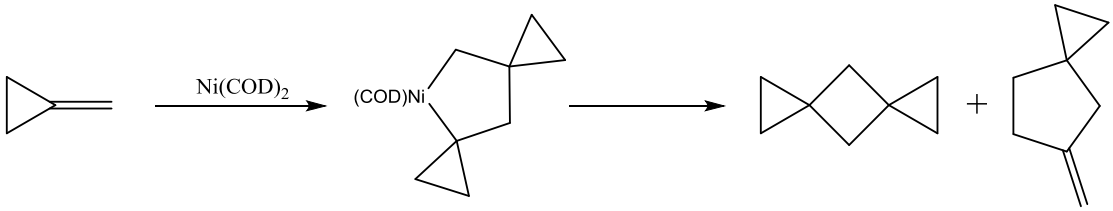

Scheme 1.5 - The cyclodimerisation of methylenecyclopropanes *via* a nickelacyclopentane intermediate.

The next significant step for this growing area of research was the successful synthesis of non-functionalised metallacyclopentanes. This was possible by reaction of transition metal dihalides with either 1,4-dilithiobutane or 1,4-di-Grignards of butane. Complexes of Pt,[27, 28] Ni,[23] Ti,[29] Co,[30] Ir,[30] Rh,[31] Zr,[32] Hf,[33] and Pd[34] have been successfully synthesised in this manner. Of these, single crystals of Pt, Co, Rh and Ir species have been isolated and the structures resolved by single crystal X-ray diffraction.[27, 30] It was found that the metallacycle was strained with C-M-C angles significantly more acute than would be expected for the square planar systems (80.9° for the Pt system and 80.2° for Co). The ring adopted the 'folded envelope' conformation in each case and regardless of ligand variation, with the two alpha-carbons on either side of the L-M-L plane.

Whitesides *et al.* took metallacycle synthesis one step further, however, by demonstrating for the first time that these species could be synthesised directly from ethylene with a titanium (IV) complex.[35] Once formed he also demonstrated that carbon monoxide reacts with the resulting metallacycle to form cyclic ketones *via* a proposed metallacyclohexane, the first time a ring containing a carbonyl group had been suggested, Scheme 1.6.

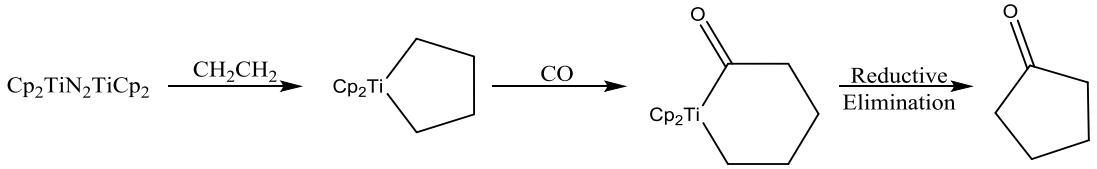

Scheme 1.6 - Formation of the first titanacyclopentane and the formation of cyclic ketones.

The formation of ketones, either cyclic or acyclic, cannot be replicated with the use of Cp_2TiBu_2, indicating a significant difference in the reactivity of the two potential intermediates of dimerisation. It was also demonstrated that the titanacycle could be reacted with bromine to form 1,4-dibromobutane and Cp_2TiBr_2, further confirming the existence of a metallacyclic species.[32]

Prior to this breakthrough, Whitesides *et al.* had conducted significant research into the stabilities of analogous complexes of Pt as well as those of additional, previously unknown metallacycles.[28] Using a variety of di-Grignard reagents with $Pt(COD)Cl_2$ and PPh_3, platinacyclohexanes and heptanes were synthesised for the first time as well as alkyl substituted platinacyclopentanes, Figure 1.1. Each of these species was fully characterised with elemental analysis, mass spectrometry and NMR spectroscopy.

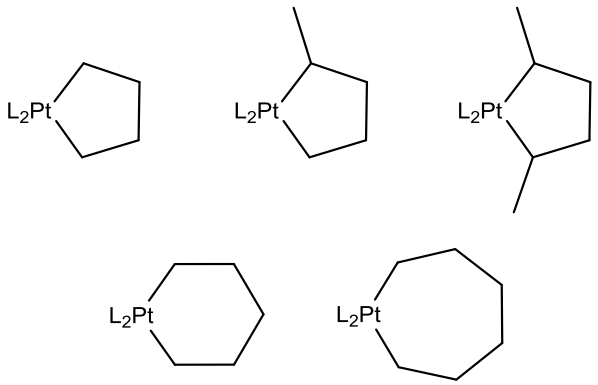

Figure 1.1 - The novel platinacycloalkanes, where L = PPh_3.

It was found that the platinacyclopentane species demonstrated considerably greater stability in relation to β-hydride elimination when compared with the analogous dibutyl complex. The rate of decomposition was approximately 20,000 times slower than the dialkyl, which eliminates butane and 1-butene rapidly at -50 °C. Interestingly, the platinacycle does not decompose to give solely 1-butene but also gives off ethylene, suggesting the ring formation is in fact in equilibrium. For this to occur the elimination must proceed *via* C-C bond cleavage, which is postulated to be feasible as the ring can distort such that the Pt-C-C-C dihedral angle is approximately 0°, as would be required.

The dihedral angle was also found to be extremely important in regards to the stability of the different organometallic species to β-hydride elimination. Where ring strain was found to effectively prevent the occurrence of a 0° Pt-C-C-H dihedral angle, the complex was far more stable. For example, the platinacycloheptane, which exhibits considerably less ring strain than the smaller analogues, was found to undergo β-hydride elimination at about 10,000 times the rate. This work demonstrated clearly that a considerable reduction in metallacycle stability is induced by increasing the ring size beyond six members.

The synthesis of both mono- and di-alkyl substituted metallacyclopentanes for the first time hinted at the potential for LAO dimerisation. In both cases the branching was at one or both of the alpha positions, such that an additional site from which β-hydride elimination could occur was presented in each case. It is notable therefore that no significant variation in decomposition rate was observed between these species and the non-substituted platinacyclopentane. This suggests that *exo*-cyclic elimination is less favourable and therefore, presumably, the methyl cannot be orientated such that a Pt-C-C-H dihedral angle of 0° occurs.

In relation to the work described herein, the most important metallacycle synthesis described previously is that involving chromium. The formation of chromacycles proved considerably more difficult than for the species described above and wasn't achieved until 1997 by Jolly *et al.*[36] Using tertiary amine pendent stabilised Cp complexes of $CrCl_2$, both chromacyclopentanes and chromacycloheptanes were synthesised, in the presence of activated magnesium, from dilithio and digrignard species respectively, Figure 1.2. It was also shown that in the presence of a large excess of trimethylphosphine these products could be isolated without the need for pendent stabilisation.

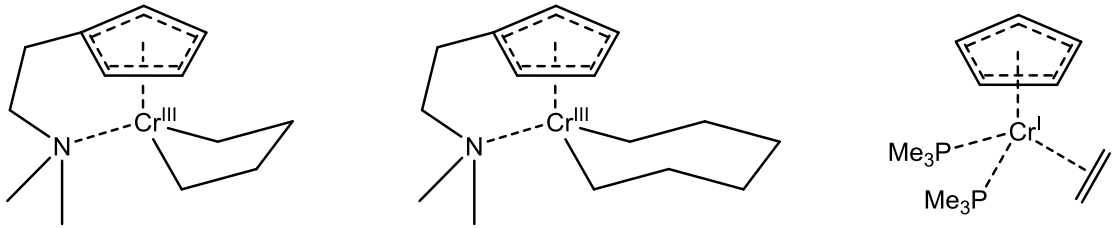

Figure 1.2 - The novel chromium complexes isolated and characterised by single crystal X-ray diffraction.

The relative thermal stability of the two ring sizes was measured in the same manner as for the platinacycles, with the metallacyclopentane again demonstrating considerably greater stability. It was also shown that 1-hexene was the principal decomposition product for the chromacycloheptane, as observed for other metals. Synthesis directly from ethylene was also repeated, with high yields recorded for the formation of Cp ligated chromacyclopentanes with either a pendent amine or phosphine secondary donor. Remarkably, the authors were also able to isolate and characterise the first example of a Cr^{I} ethylene adduct by single crystal X-ray diffraction. The three species isolated in this work, Figure 1.2, provide considerable support for the viability of the metallacyclic trimerisation mechanism discussed in Chapter 4.

Whitesides *et al.* also discovered a further novel method for the synthesis of platinacyclopentanes by which at high temperatures cyclometalation of a dialkyl species is possible.[37] However, the method is highly restricted by the fact that the original alkyl groups cannot contain hydrogens at the β-position, due to more favourable β-hydride elimination. Using this method a large selection of differently substituted platinacyclopentanes and hexanes were synthesised *via* aliphatic C-H bond activation. The mechanism, oxidative addition of the C-H bond to the metal centre to form the metallacyclopentane, followed by reductive elimination of the hydride and the remaining alkyl chain, was confirmed by deuterium labelling experiments, Scheme 1.7.

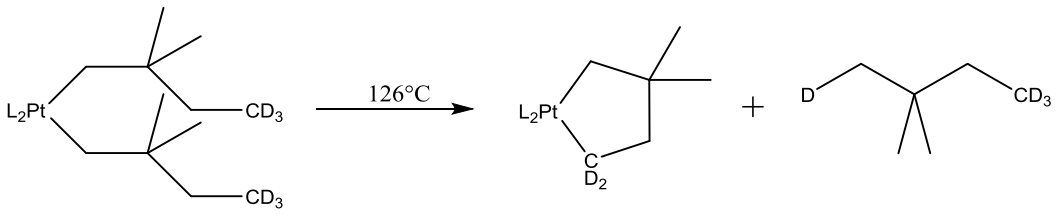

Scheme 1.7 - Cyclometalation of a deuterium labelled dialkyl titanium complex.

Later work by the group focused on other thermal decomposition pathways that can be observed, principally by increasing the temperature and using alkyl rather than aryl phosphines.[29, 38] This led to cyclobutane as the majority decomposition product, suggesting favourable carbon-carbon bond formation. It also led to 5% butadiene, indicating that in a minority of cases two β-hydride eliminations are possible from a single metallacycle.

This selectivity can be explained by assuming two distinct elimination steps, β-hydride elimination followed by reductive elimination of the alkyl and hydride or a second β-hydride shift. The location of the hydride would be expected to have a considerable effect on the favourability of the reductive elimination. A *cis* arrangement would facilitate elimination while a *trans* arrangement would prevent it, requiring a second β-hydride shift before complete decomposition, Scheme 1.8. Based on the selectivity, it can be assumed that *cis* is the favoured arrangement of the intermediate.

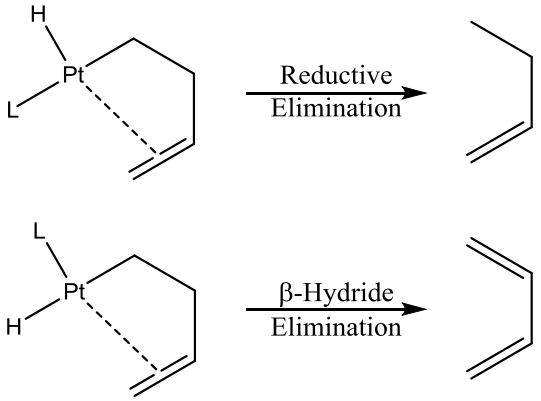

Scheme 1.8 - The proposed effect of the hydride position on the elimination product, L = Bu_3P.

A more in-depth look into the decomposition pathways of metallacycles was conducted at around the same time by Grubbs *et al.* using Ni based systems.[39] Using the same di-Grignard based synthesis it was found that nickelacyclopentanes of varying coordination number could be made by using different phosphines. Three, four and five coordinate species were isolated and characterised with the use of Cy_3P, $Ph_2PCH_2CH_2PPh_2$ and PPh_3 respectively. The gaseous thermal decomposition products of these species were identified, with each showing a marked difference in their selectivity, Scheme 1.9.

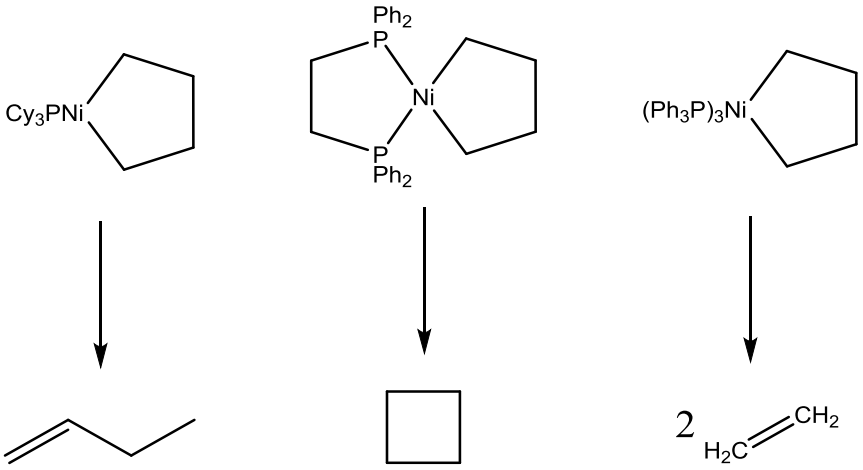

100% 90% 100%

Scheme 1.9 - The major thermal decomposition products of nickelacyclopentanes of various coordination numbers.

The coordinatively unsaturated Cy_3P species produced 1-butene as the sole gaseous decomposition product. This is unsurprising as the β-hydride elimination pathway that results in 1-butene is the only route requiring an additional coordination site. The 100% selectivity suggests that, if a vacant site is readily available, this pathway is by far the most favourable. Therefore, the catalytic dimerisation of ethylene to 1-butene can only be possible *via* a metallacyclic pathway when a vacant site is present in the active catalyst.

The selectivity of the four and five coordinate species is less easily explained. Repetition of the experiments in the presence of oxidising agents led to a considerable increase in the proportion of cyclobutane produced for all three complexes. This suggests that the electron density on the metal centre is of key importance. When the electron density is high, such as for the five coordinate species, C-C bond cleavage as a means of reductive elimination is preferred over C-C bond formation. This can be demonstrated by use of acetonitrile or pyridine as solvents for the Cy_3P complex, resulting in a 50:50 ratio of 1-butene to ethylene. Using electron withdrawing olefins led to increased production of cyclobutane containing products, further supporting this hypothesis.

Grubbs *et al.* conducted further research into the reactivity of the five coordinate species because of the apparent equilibrium between labile coordinated olefins and metallacyclopentanes.[40] This proved to be the case and could be demonstrated by the addition of different olefins to the preformed metallacyclopentane complex (in this case an analogous Ti species) to give 1:1 dimers of the two after protonolysis.[41] This was the first time that co-dimerisation of α-olefins had been demonstrated and marked another considerable advance in the field.

The equilibrium presented the possibility of catalytic cyclodimerisation and was explored extensively with the $(Ph_3P)_3Ni(CH_2)_4$ complex.[42, 43] Although turnover numbers never exceeded 10 for the production of cyclobutane this was the first example of catalytic dimerisation of ethylene *via* a metallacyclic mechanism. On top of this, with the addition of chlorobenzene as a solvent, it was found that the nickelacyclopentane was a pre-catalyst for Cossee-Arlman dimerisation, reaching turnovers numbers of around 60. While this is especially poor compared to the established Ziegler catalysts,[8] this represented the first catalytic system which did not require activation by aluminium alkyls.

A few years later Erker *et al.* demonstrated a system based on the Group 4 metallocenes which was capable of the linear dimerisation of ethylene.[44, 45] The facile reaction of butadiene with zirconocene and hafnocene leads to a precursor which, under an ethylene atmosphere, is substituted by two ethylene units before oxidative cyclisation to form a metallacyclopentane. Importantly, the complex formed then enters a catalytic cycle that leads to the dimerisation of ethylene, Scheme 1.10.

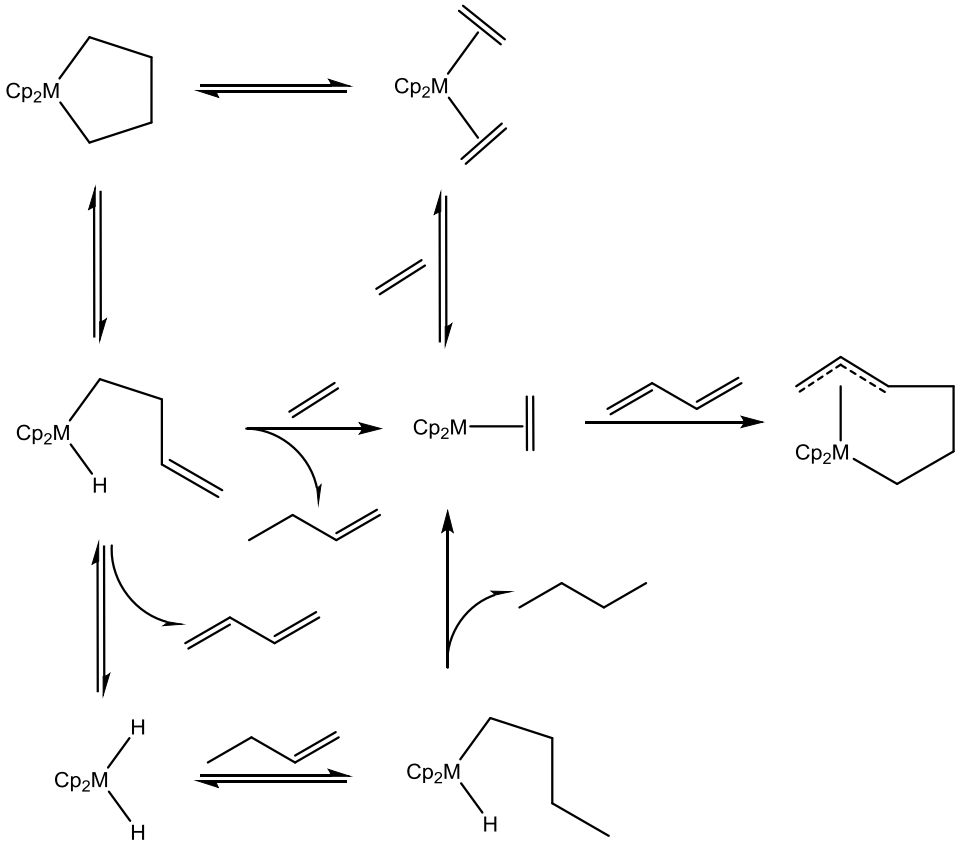

Scheme 1.10 - The catalytic cycles and decomposition of the metallocene dimerisation catalysts, where M = Zr or Hf.

This system only produces 0.66 equivalents of C_4 olefin per complex and therefore barely constitutes a catalytic cycle. However, this is the first proposed mechanism for the metallacyclic dimerisation of ethylene to 1-butene. In all, 0.66 equivalents of 1-butene are produced, alongside 0.94 equivalents of butane and 0.06 equivalents of ethane. The butane and ethane result from the bottom cycle which, due to the formation of butadiene, leads to the decomposition of the catalyst to form the tethered allyl species. The decomposition product was isolated at stoichiometric yield and its identity confirmed by X-ray diffraction. It was also demonstrated that a similar product distribution was observed when using Cp_2MH_2 as the initiator, confirming the interlinked nature of the two mechanisms.

These Zr and Hf systems, of which the Hf catalyst is very poor, demonstrated a considerable step towards the catalytic dimerisation of ethylene *via* a metallacyclic mechanism. Firstly, the facile synthesis of a metallacyclopentane without the need for lithium or Grignard reagents was demonstrated. It has since also been shown that substitution of phosphine ligands provides a facile route to the same zirconacyclopentanes.[46] Secondly, the well characterised cycle showed clearly that metallacycles can exist as catalytic intermediates in the formation of LAOs from ethylene.

Ironically, the first highly active and definitively metallacyclic ethylene dimerisation catalyst was discovered while Girolami *et al.* were attempting to synthesise the intermediates of the Cossee-Arlman mechanism.[47] Hf and Ti complexes containing both alkene and alkyl ligands were synthesised and isolated, with the Hf species characterised by X-ray diffraction. The Ti complex, which proved to be an active dimerisation catalyst (880 mol(C_2H_4) mol(Ti)$^{-1}$ h^{-1}), was formed by exposure of *trans*-$TiMe_2(dmpe)_2$ to ethylene at -40 °C.

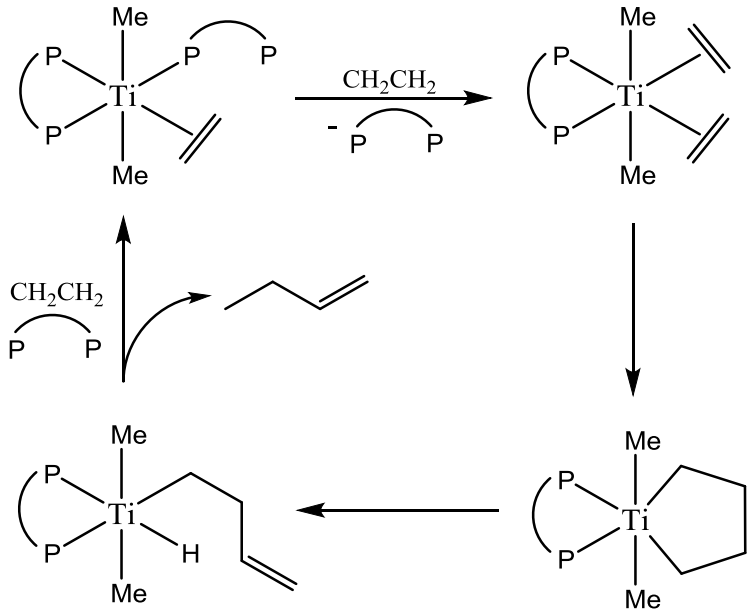

Scheme 1.11 - The proposed mechanism for the selective production of 1-butene.

The presence of the alkene and alkyl groups adjacent to one another would be expected to lead to a Cossee-Arlman type di- or polymerisation. However, this is not observed and the methyl groups remain present and unchanged throughout the catalyst cycle, Scheme 1.11. It is proposed that this is because of strong π-back-bonding, which makes the loss of the π-interaction *via* migratory insertion thermodynamically unfavourable. In contrast, the strong metal-alkene bond encourages the substitution of the monodentate phosphine donor by an additional alkene. Once bound, the back-bonding interaction orientates the alkenes into a co-planar orientation, encouraging the formation of the titanacyclopentane.

This catalyst also demonstrates limited activity towards dimerising propylene, though at very low turnover frequency. The regioselectivity of the propylene dimer goes against that observed for other systems, see below, as it is principally made up of head-to-head or head-to-tail dimers instead of the typical tail-to-tail. This further supports the coplanar orientation hypothesis, as this would induce significant steric repulsion on the tail-to-tail conformation.

This catalyst demonstrates that a metallacyclic mechanism can account for an active dimerisation system and that under certain conditions it is actually preferred over a Cossee-Arlman mechanism. Girolami *et al.* later improved on this system to give catalysts with a TOF of over 2000 mol(C_2H_4) mol(Ti)$^{-1}$ h^{-1}.[48] Amazingly, the most effective catalyst included a metal hydride that was not affected by the catalysis, Figure 1.3. This increased activity comes at the expense of selectivity, however, due to the ability of the catalyst to co-dimerise ethylene with the 1-butene product. To the best of my knowledge, this catalyst remains the most active example of a dimerisation system which is definitively metallacyclic in nature.

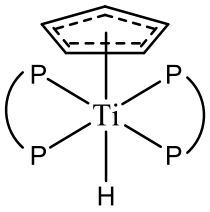

Figure 1.3 - The improved ethylene dimerisation catalyst, where the bidentate ligand is bis(dimethylphosphino)ethane.

There is still disagreement over whether the Alphabutol and other more active catalysts proceed *via* Cossee-Arlman or metallacyclic mechanisms. However, the systems have demonstrated deuterium scrambling and are therefore unlikely to be metallacyclic.[49] Overall, the catalysts thought to proceed through Cossee-Arlman intermediates are far superior for the dimerisation of ethylene, but it is not so clear cut for LAOs.

1.2.2 Linear α-Olefin Dimerisation

The dimerisation of propylene is renowned as one of the most active homogeneously catalysed reactions. It was discovered in 1968 by Wilke *et al.* during an investigation into the properties of nickel allyl complexes.[50-52] When activated with aluminium alkyls, these species were capable of converting propylene into a mixture of 1-hexene and 4-methyl-1-pentene at activities of up to 1,250,000 mol(C_3H_6) mol(Ni)$^{-1}$ h^{-1}. These catalysts operate *via* a mechanism similar to Cossee-Arlman but with considerable differences. The accepted mechanism, originally proposed by J. K. Hambling,[53] has been dubbed the 'Anionic Mechanism' because of the key role played by the negatively charged allyl ligand, Scheme 1.12.

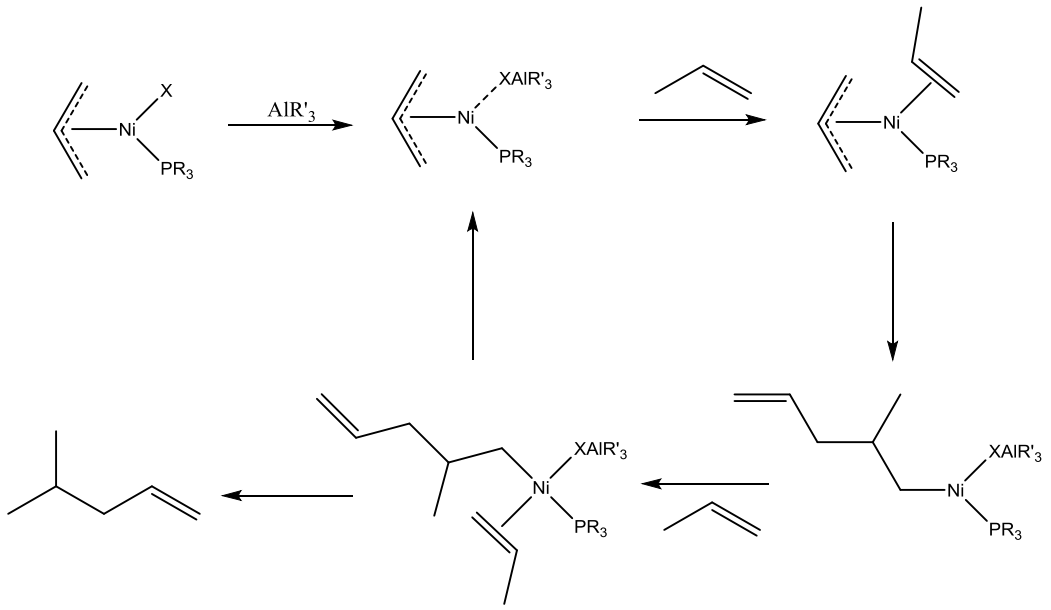

Scheme 1.12 - The generalised mechanism for propylene dimerisation with nickel allyl catalysts. Where the XAlR'$_3$ counter-ion is not shown in the catalyst cycle the nickel complex is mono-cationic.

Halide abstraction with a trialkylaluminium activator gives the active species, which coordinates a propylene unit. This then inserts into the Ni-C bond to form a nickel alkyl complex; it is at this stage that the selectivity between 4-methyl-1-pentene and 1-hexene is determined. [2,1]-Insertion of propylene is electronically favoured, leading to 4-methyl-1-propene as the majority product according to the pathway shown in Scheme 1.12. The product is released *via* a concerted β-hydride shift from the aliphatic carbon of a third propylene unit to the coordinated carbon of the dimer, reforming the nickel allyl catalyst in the process.

This highly active system makes up the Dimersol process, which has been broadly commercialised due to the demand for isopentene as a monomer in the production of thermoplastic resins. The production of 1-hexene as a minor side-product is inconvenient due to separation requirements but is also valuable as a monomer for LLDPE production. Unfortunately, the reliance of this process on the allyl ligand results in little scope for application to larger LAOs.

The selective dimerisation of longer chain α-olefins to produce an olefinic dimer was discovered in 1980 by Schrock *et al.* with the use of tantalum based catalysts.[54] The Ta(η^5-C_5Me_5)(cyclooctene)Cl_2 catalysts react with two equivalents of α-olefin to predominantly form a highly stable 2,3-substituted tantalacyclopentane, Scheme 1.13. This could be determined by identification of the products, which were 98% 2-methyl-3-methylenebutane for propylene dimerisation. Decomposition of the metallacyclic species was found to occur *via* β-hydride elimination, resulting in a vinylidene dimer. In the presence of excess LAO the species proved to be an active dimerisation catalyst (For example, 2400 mol(C_3H_6) mol(Ta)$^{-1}$ h^{-1}), being >85% selective for the tail-to-tail dimer for any linear α-olefin.

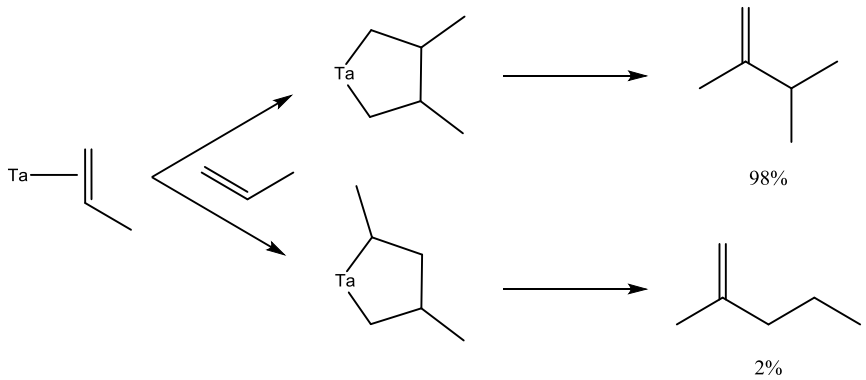

Scheme 1.13 - The catalytic pathways of propylene dimerisation.

Variation of the α-olefin resulted in considerable changes to the reaction rate and product distribution. Increasing the chain length of the LAO caused the catalyst to become less selective towards tail-to-tail dimers, ie. 98% selective for propylene compared to 86% for 1-octene. Introduction of branching into the olefin led to a considerable shift towards head-to-tail selectivity, with 4,4-dimethyl-1-pentene giving 100% head-to-tail. It is evident therefore that steric factors have a considerable influence over the selectivity of the tantalacyclopentane ring formation.

Kinetic analysis of the system indicated that the rate determining step is the elimination, rather than insertion, because no link between olefin concentration and rate could be observed. This was further confirmed by dimerisation of 2-deutero-1-pentene and NMR analysis of the products formed, as shown in Scheme 1.14. A slower rate of dimerisation was observed for this study in comparison to non-deuterated reactions. There was also a considerable difference in the effect on tail-to-tail ($k(H)/k(D) = 3.3$) and head-to-tail ($k(H)/k(D) = 1.2$) dimerisation. A relative ratio of 3.3 indicates a strong kinetic isotope effect and suggests that a hydride/deuteride migration accounts for the rate determining step. A ratio of 1.2 is indicative of secondary kinetic isotope effects and suggests that the deuterated position is not directly involved in the elimination.

The location of deuterium atoms in the product indicated that the mechanism does not occur *via* the simple β-hydride elimination pathway expected. The labelling studies showed that in fact the initial β-hydride elimination is followed by re-cyclisation to form a tantalacyclobutane in a ring contraction process. A second β-hydride elimination then occurs before the reductive elimination that gives the product.

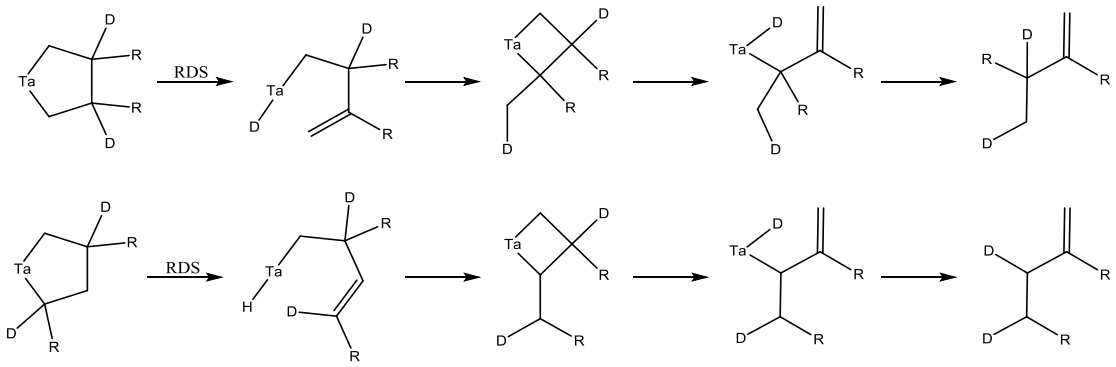

Scheme 1.14 - The mechanism proposed to explain the location of the deuterium atoms in the products. RDS = Rate Determining Step.

The presence of only secondary kinetic isotope effects for the head-to-tail dimer formation proves that it is β-hydride elimination from the metallacyclopentane that is the rate determining step. The kinetic isotope effect would have been the same for both products had elimination from the metallacyclobutane been rate determining, suggesting that the greater strain of the smaller ring does not hinder the migration. The marked difference between the two pathways also demonstrates that elimination from a secondary carbon is considerably more favourable than a tertiary position.

Schrock *et al.*[54] also investigated niobium analogues of their tantalum catalysts but with limited success. It was ten years later that Bercaw *et al.* discovered a system that could replicate the dimerisation of LAOs with similarly high selectivities of over 95%.[55] Using bulky scandium hydride complexes it was found that LAOs could be dimerised catalytically, though at low turnover numbers of around 40, Figure 1.4. The products also demonstrated high regioselectivity by favouring [1,2]-insertion of the olefin due to electronic and steric influences.

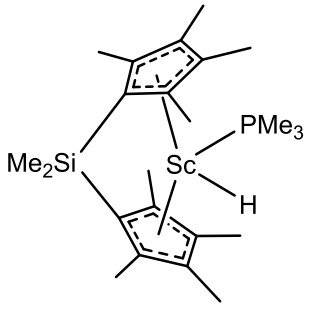

Figure 1.4 - The structure of the most effective scandium based LAO dimerisation catalyst.

The mechanism of this species, as would be expected for metal hydride catalysts, was found to follow a Cossee-Arlman mechanism. Similar dicyclopentadiene scandium species have been shown to be effective ethylene polymerisation catalysts and are also proposed to follow this mechanism. It appears that the high steric bulk of this ligand system results in the selectivity towards dimerisation due to hindrance of further insertion. It was found that in the presence of a vast excess of LAO a small quantity of trimer was also detected, supporting this hypothesis.

Numerous other LAO dimerisation catalysts have since been designed with the use of cyclopentadienyl ligands.[56-60] Each of these systems is thought to proceed *via* the Cossee-Arlman mechanism, supported by Bergman *et al.* with the use of Cp_2ZrCl_2 catalysts.[61] By using a 1:1 ratio of catalyst to MAO activator (equivalents of aluminium) they found that the selectivity of this well-known polymerisation catalyst could be switched to almost exclusive dimerisation.

This selectivity was attributed to the catalyst retaining a chloride at 1 equivalent of MAO, as compared to complete methylation at the high equivalents used for polymerisation. It is proposed that the presence of this chloride within the coordination sphere promotes β-hydride elimination, avoiding further oligomerisation. Turnover numbers of up to 500 were recorded, an improvement over the related scandium systems but still falling short of those demonstrated by the tantalum system.

In order to establish the Cossee-Arlman mechanism for these species it was necessary to demonstrate that a metal hydride was formed. The synthesis and application of $Cp_2Zr(H)Cl$ to this system demonstrated a five-fold increase in turnover frequency and, importantly, a substantial reduction in activation time was observed. Detailed analysis of the products of low-equivalent tests with the original catalyst showed that 2-methyl-1-hexene was detected during 1-hexene dimerisation, Scheme 1.15. This demonstrates the formation of the zirconium hydride during activation and strongly supports the proposed mechanism.

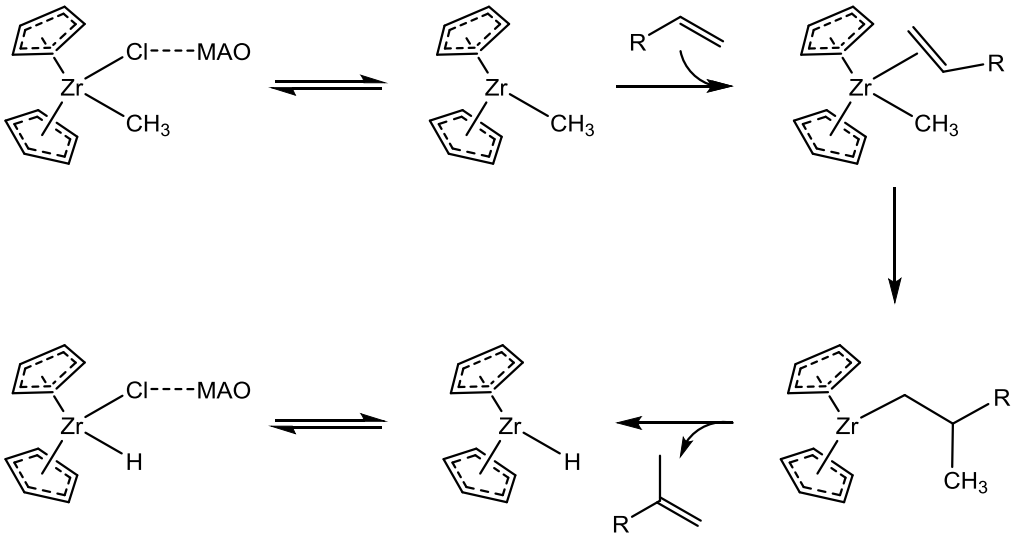

Scheme 1.15 - Activation of the Cp_2ZrCl_2 catalyst after the initial methylation.

Deuterium labelling studies were carried out on this system to further support the mechanism in much the same way as those performed by Schrock *et al.*[54] Dimerisation of 2-deutero-1-hexene led to the predicted products being formed with both deuterium atoms on the same carbon, in stark contrast to the results for the metallacyclic mechanism, Scheme 1.16. This confirmed the existence of two different mechanisms for the selective dimerisation of LAOs.

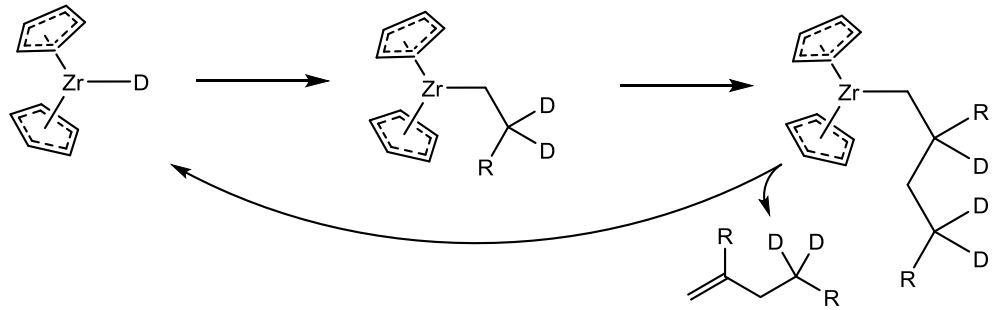

Scheme 1.16 - The proposed mechanism accounting for the location of the deuterium atoms in the product.

The dimerisation of ethylene, strained rings and LAOs have been covered here but there are also numerous examples of functionalised olefin dimerisation and co-dimerisation. Functionalised olefin dimerisation has focused on conjugated olefins such as methyl acrylate, acrylonitrile and styrene.[62-64] The various conjugations lead to increased selectivity towards tail-to-tail dimers due to the stabilisation of negative charge on the substituted carbon of the olefin. The reactions proceed through a rapid insertion and elimination mechanism similar to the Cossee-Arlman systems.

Co-dimerisation of conjugated olefins with ethylene is a significant field of research, a comprehensive review of which has been compiled by T. V. RajanBabu.[65] Its importance is due to the ability to selectively form simple chiral olefins of the form PhC*H(Me)CH=CH_2. The olefin can be converted to numerous functional groups to form extremely important compounds, especially carboxylic acids for biochemical applications.

A wide range of transition metal catalysts have been shown to be active. Nickel halide based systems are by far the most common but others based on Pd, Rh, Ru and Co have also been demonstrated. Activation can be achieved by the near stoichiometric addition of a Lewis acid in the presence of a phosphine donor. The mechanism is analogous to that of styrene dimerisation with the [2,1]-insertion of the conjugated olefin into the metal hydride preceding ethylene insertion, Scheme 1.17.

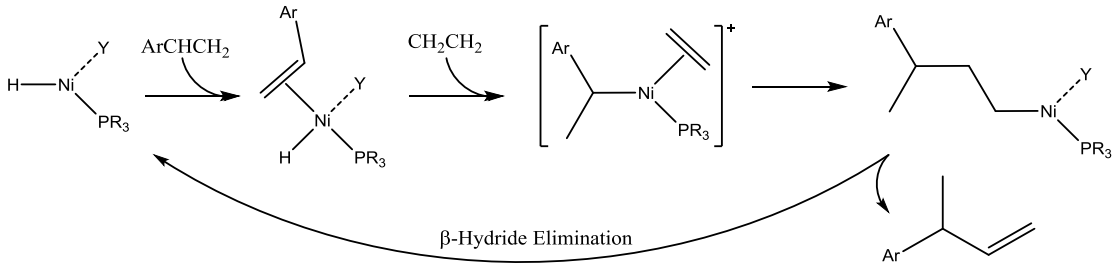

Scheme 1.17 - Co-dimerisation of a styrene derivative and ethylene *via* a selective Cossee-Arlman mechanism.

A significant advance was made in 2010 with the discovery of an (NHC)NiH system capable of co-dimerising styrenes with LAOs.[63] Steric control promotes tail-to-tail dimer formation despite the absence of any favourable electronic properties in the LAO. Yields are good for this system at over 80% for most substrates, with the loss attributed to homo-dimerisation of the styrene. The mechanism proposed is analogous to that of the ethylene work.

1.3 Ethylene Trimerisation and Tetramerisation

Selective trimerisation and tetramerisation were discovered later and signalled a move away from the titanium, zirconium and nickel catalysts that previously dominated the field of olefin oligomerisation. The major breakthrough was achieved with the development of the Chevron-Phillips trimerisation catalyst, based on chromium.

The first indication that chromium was able to selectively trimerise ethylene was observed during the development of the Phillips polymerisation catalyst. The catalyst is based on CrO_3 supported on silica in the presence of strontium oxide and other agents to protect the catalyst from decomposition.[66] A significant advantage of this catalyst is its self-activation by ethylene, which drastically reduces the cost and complexity of industrial application, Scheme 1.18.[67] It accounts for a significant proportion of HDPE production worldwide, at over 7 megatons per year as of 1998.[68]

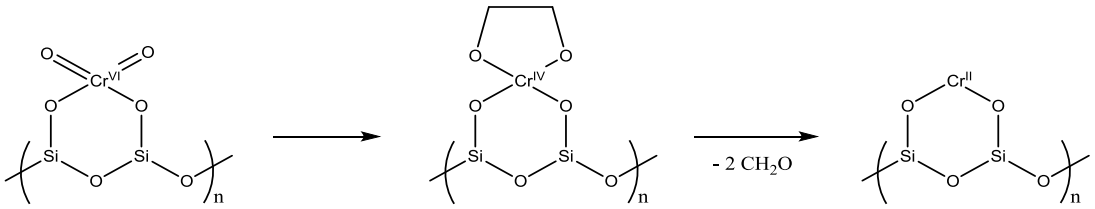

Scheme 1.18 - The proposed self-activation of the Phillips polymerisation catalyst.[67]

The polymer produced according to this method demonstrated different physical properties compared to HDPE made using other catalysts. The Phillips polymer is unusual, it features a considerable number of butyl side-chains, has a broad PDI and can be a terminal alkene, internal alkene or vinylidene.[69] Such side chains could only logically occur due to incorporation of 1-hexene into the polymer, suggesting the ethylene was being simultaneously trimerised.

Investigation of new potential catalysts for selective trimerisation began with exploration of the use of pyrrolide ligands due to their similarity to Cp ligands, which had proved so effective for polymerisation.[70] Reaction of $CrCl_3$ with sodium pyrrolide was found to produce a polymeric $Cr(C_4H_4N)_2Cl$ species. Addition of a triethylaluminium activator produced a catalyst capable of trimerising 1-hexene with very high selectivities of up to 99% but with low activities of just over 1800 $mol(C_2H_4)\ mol(Cr)^{-1}\ h^{-1}$. Following on from this discovery, it was found that production of the defined pre-catalyst was not necessary and that reacting chromium(III) 2-ethylhexanoate with pyrrole and triethylaluminium *in situ* gave similar activities.

The original reaction demonstrated poor activity but replacement of the pyrrole with 2,5-dimethylpyrrole and the alkyl aluminium with diethylaluminium chloride greatly improved its efficiency. The proposed active species is shown in Figure 1.5. The improved performance was attributed to greater catalyst stability and the 'halide effect', achieving impressive activities of over 275,000 $mol(C_2H_4)\ mol(Cr)^{-1}\ h^{-1}$ at selectivities of over 93%.[71] This performance led to the commercial realisation of the process in 2003 and this remains the only ethylene trimerisation system currently operating in industry.[19]

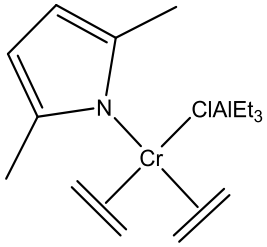

Figure 1.5 - The proposed active species of the Chevron-Phillips trimerisation catalyst.[72]

The exact nature of the active catalyst is still disputed but it is proposed that the mechanism proceeds *via* a Cr^{II}/Cr^{IV} redox cycle.[72] It should also be stated that there have been proposals that the mechanism proceeds through an alternative Cr^{I}/Cr^{III} pathway.[73, 74] The Cr^{I}/Cr^{III} redox cycle gained some experimental credibility in 2002 when an extensive X-ray photoelectron spectroscopy study was carried out by Hu *et al.*[75] It was found that as much as 95% of the chromium present in the activated solution occupied the Cr^{III} oxidation state. Therefore, the suggestion is that the resting state of catalysis is Cr^{III}, indicating a Cr^{I}/Cr^{III} redox cycle in contrast to the Cr^{II}/Cr^{IV} cycle predicted by computational experiments.

Whilst the identity of the active catalyst and the oxidation states of the chromium species are disputed, considerable experimental evidence suggests that the trimerisation occurs via a metallacyclic mechanism. This mechanism was first proposed in 1989 by J. R. Briggs while working with a slightly different catalyst system.[19, 76] This system relied on activating the chromium(III) 2-ethylhexanoate with partially hydrolysed tri-*iso*-butylaluminium in the presence of dimethoxyethane as an additive. Selectivities of up to 74% were achieved, of which 99.9% 1-hexene, with the remainder being accounted for principally by polyethylene. Such high 1-hexene selectivity could not be accounted for by Cossee-Arlman type mechanisms, leading to the proposal of the metallacyclic mechanism shown in Scheme 1.19.

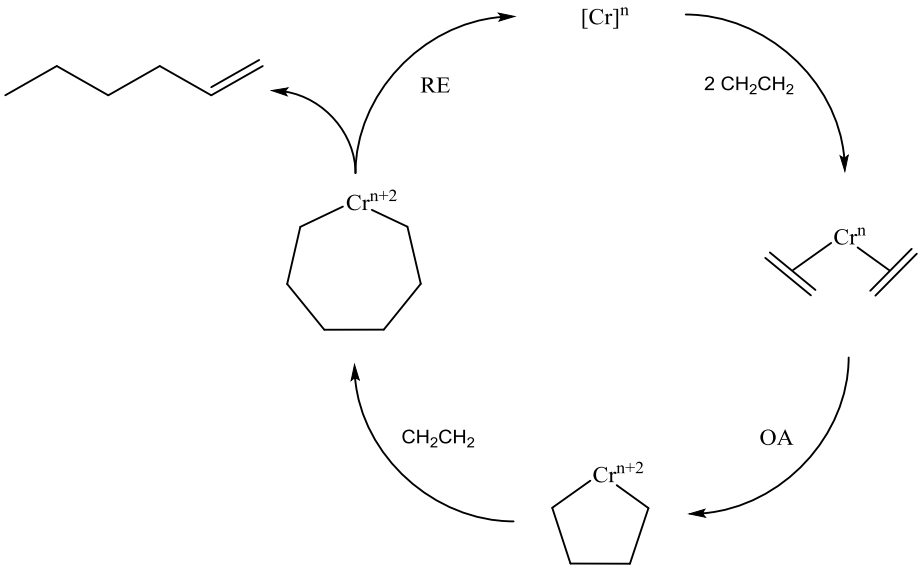

Scheme 1.19 - The proposed metallacyclic mechanism.
OA = Oxidative Addition, RE = Reductive Elimination.

Oxidative cyclisation of two ethylene molecules bound to the reduced state of the chromium forms a metallacyclopentane intermediate. Co-ordination of a further ethylene molecule is followed by migratory insertion into the ring to form a metallacycloheptane intermediate. β-Hydride shift occurs after formation of the more flexible seven-membered ring, followed by reductive elimination to give 1-hexene and an ill-defined reduced chromium species. Further coordination of two additional ethylene molecules then completes the catalyst cycle.

The rate of β-hydride shift for the metallacycloheptanes has been demonstrated by Whitesides *et al.* and Jolly *et al*. to be very fast and therefore the formation of higher α-olefins would be kinetically discouraged.[36, 38] When combined with the unfavourable hydride shift for the constrained metallacyclopentane observed in the same study, this accounts for the high selectivity for trimerisation. However, insertion of an olefin into a metallacycle had never been proven to be possible.

The only experimental evidence put forward for this mechanism was the observation of a second order rate dependence on ethylene pressure.[77] This observation suggests that the rate determining step is therefore the original complexation of the olefins to the reduced chromium species. Interestingly, the rate dependence of polymerisation was markedly different, indicating that the two products are produced *via* independent mechanisms. In effect, the observation suggested that polymerisation did not result from continued insertion into ever-growing metallacycles.

Since the discovery of this process there has been considerable interest in the chromium catalysed trimerisation of olefins. The activities of Phillips-type catalysts have been considerably improved since the first patenting of this reaction, with some optimisations recording incredible activities of over 6,300,000 mol(C_2H_4) mol(Cr)$^{-1}$ h^{-1}.[71] This was achieved principally by further exploitation of the so-called halide effect by incorporation of hexachloroethane as an additive as well as more general optimisation of temperatures and pressures etc.

More recently, the focus of research into selective trimerisation has shifted towards producing better defined, pre-formed catalysts which facilitate greater understanding of the mechanism and the inherent oxidation states. This has been broadly confined to ethylene, however, due to industrial interest in 1-hexene as a co-monomer for LLDPE among other applications.

This broad based research into homogeneous trimerisation catalysts resulted in the surprise discovery of selective tetramerisation in 2004.[78] However, such selectivity appears to conflict with the reasoning ascribed to the high selectivities observed for trimerisation systems. The need to explain this new found selectivity from a mechanistic point of view triggered further research, with two mechanisms proposed since the original discovery.

Firstly, the simplest explanation is that a fourth ethylene unit is inserted as part of an extended metallacyclic mechanism. The difficulty results from the similarity in ring strain between metallacycloheptanes and metallacyclononanes, as well as larger metallacycles. The selectivity must, therefore, not be reliant on the favourability of β-hydride elimination for the different ring sizes. A combination of kinetic and computational analysis performed by McGuiness *et al*. resulted in the proposal of a new metallacyclic mechanism, which offers an explanation for the selectivity towards 1-octene formation.

A system which produced both 1-hexene and 1-octene at high selectivities relative to other α-olefins was studied for kinetic analysis. It was found that the formation of 1-C_6 was first order relative to ethylene concentration whilst 1-C_8 formation was near second order. Such a difference suggested that a simple ring growth mechanism was unlikely as ethylene co-ordination and insertion would be first order regardless of ring size. This led to computational analysis of the effects of having more than one ethylene unit coordinated to the metal centre in each intermediate.

The calculations indicated that the metallacyclopentane intermediate, widely assumed to be the resting state for trimerisation systems that display first order kinetics, is stabilised by coordination of ethylene. In the case of tridentate ligands, only one ethylene unit is capable of binding to the metal. However, bidentate ligand systems are stabilised to a greater degree when two ethylene units are bound. A detailed DFT computational study was then undertaken to determine whether the number of ethylene units coordinating to the metal affected the selectivity.

This was found to be the case. When one ethylene unit is present within the coordination sphere of the metallacyclopentane, insertion is immediately followed by β-hydride elimination. On the other hand, when two ethylene units are present, insertion leads to a metallacycloheptane with the unaffected ethylene unit still available. This greatly increases the favourability of a second insertion relative to β-hydride elimination. On insertion there are no longer any ethylene units within the coordination sphere, resulting in β-hydride elimination again becoming the most favourable pathway, as shown in Scheme 1.20.

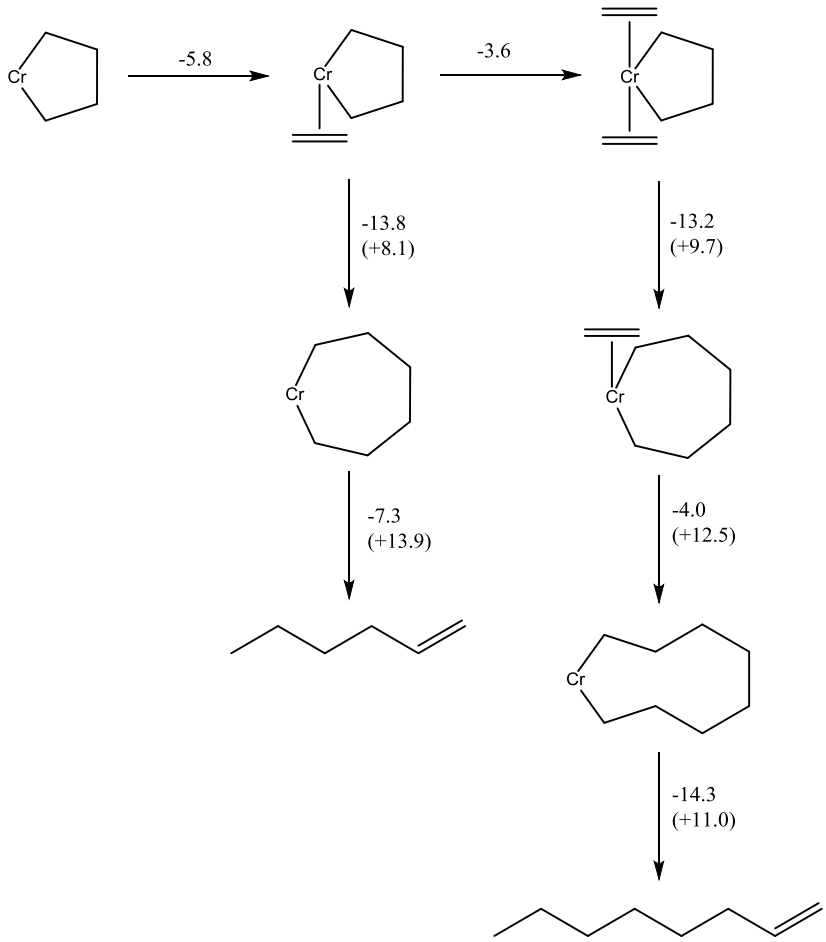

Scheme 1.20 – The proposed ring-expansion mechanism for selective tetramerisation. ΔΔG is quoted for each transformation and for the transition state in parenthesis.

A second mechanism, based strongly on that proposed and subsequently disproved by Theopold *et al.*,[79] has been proposed by Rosenthal *et al.*[80] It also incorporates metallacycle formation as a key driver of tetramerisation selectivity. Referred to as the dinuclear mechanism, it is hypothesised that dimeric species stabilised by bridging ligands may feature alternative reactivity. Principally, it is proposed that formation of metallacylopentanes on both of the adjacent metal centres could be followed by coupling between them to form a C_8 chain linking the two metals. β-Hydride elimination would then occur at one end of the chain, followed by reductive elimination between the metals, as shown in Scheme 1.21.

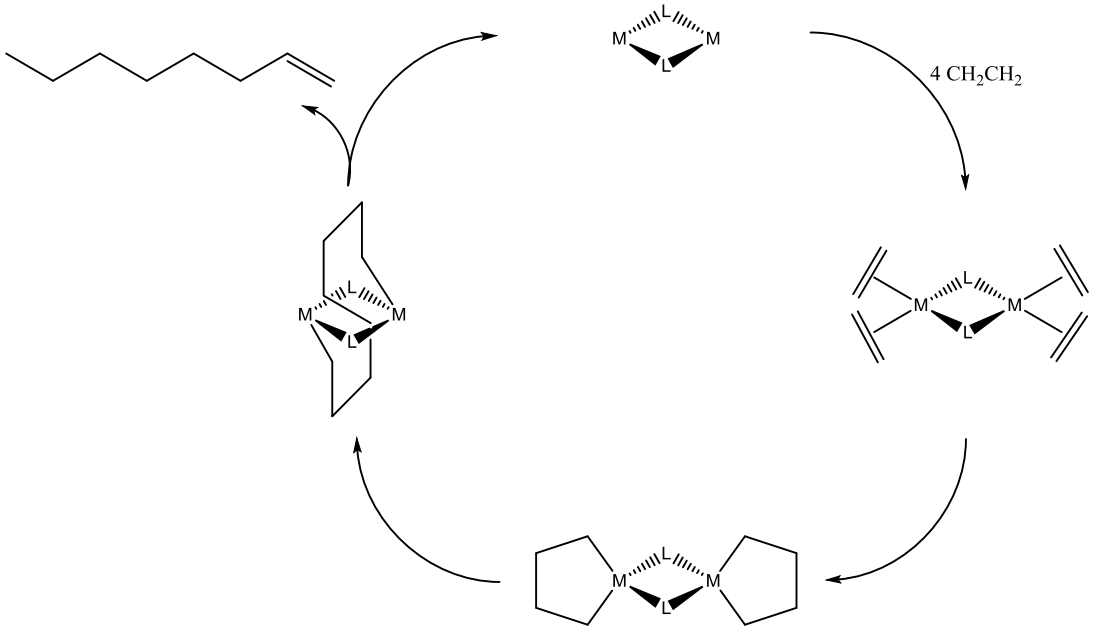

Scheme 1.21 – The proposed dinuclear mechanism for ethylene tetramerisation.

The dinuclear mechanism provides a good explanation for the selectivity towards tetramerisation due to the stability of the metallacyclopentanes. However, coupling of metallacycles in the manner described has not been demonstrated experimentally. In addition, no ethylene tetramerisation systems to date have been reported to exhibit greater than first order kinetics in relation to the chromium concentration. This would be expected for systems in which the dinuclear catalyst is formed *in situ* in equilibrium with a mono-nuclear species.

To date, neither of the mechanisms have been conclusively proven, though a considerable amount of research is being devoted towards this goal. The following sections will cover, on a catalyst by catalyst basis, the advances made towards well-defined homogeneous systems capable of selective tri- and tetramerisation. Particular attention will be paid to the mechanistic studies carried out using each catalyst and whether they support or contradict the mechanisms described previously.

1.3.1 Non-Chromium Catalysed Systems

The search for a well-defined trimerisation system led to the development of complexes consisting primarily of transition metals from group 4, 5 or 6 bound by a multidentate ligand. A common feature of these systems is also that one of the donors will be labile in nature while the other/s are more strongly bound. Of these metals, chromium has remained by far the most prominent but other systems based on nickel, vanadium, tantalum, zirconium, hafnium and especially titanium have shown considerable promise.

1.3.1.1 Group 4 Catalysts

The first effective alternative to chromium based trimerisation was again discovered during research into polymerisation systems. Pellecchia *et al.* discovered in 1999 that co-polymerisation of styrene and ethylene with $Cp^*TiMe_3/B(C_6F_5)_3$ resulted in a product containing a considerable proportion of butyl and 4-phenylbutyl side chains.[81] This was the first time evidence for titanium catalysed trimerisation had been observed and led to further study of Cp^*TiMe_2 cations. It was already known that group 4 cations could be stabilised by coordination of arenes and this approach proved the most common for investigation of this new found activity.[82, 83]

Hessen *et al.*, at the same time as Sassmannshausen *et al.*, synthesised methylated titanium and other group 4 species that contained a Cp ligand with a tethered arene group.[84-87] Each of these systems could be activated by the addition of stoichiometric amounts of $B(C_6F_5)_3$ to abstract a methyl group. This then led to the co-ordination of the arene to the metal centre as proven by ^1H and ^{13}C NMR spectroscopy of the arene group, Scheme 1.22.

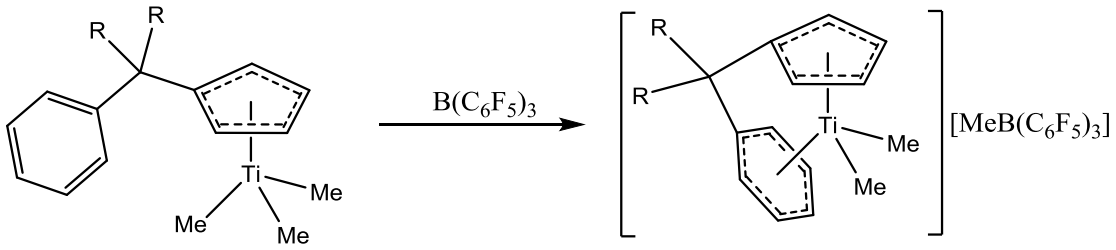

Scheme 1.22 - The general structure of the titanium complexes featuring Cp ligands with arene tethers both before and after activation. In some cases additional alkyl groups were present on the conjugated rings.

This class of compound proved to be highly active (TOFs of up to 220,000 $mol(C_2H_4)\ mol(Ti)^{-1}\ h^{-1}$ were achieved) and 86 w% selective towards the production of 1-hexene, with very little polyethylene produced (<3%). The selectivity has been attributed directly to the role played by the pendent arene, based primarily on comparison to non-aromatic analogues which showed much greater polymerisation. It was also observed that extending the tether to two carbons resulted in reduced activity. This was put down to stronger arene coordination resulting from removal of the ring strain in the cycle formed after coordination.

The magnitude of the ring strain plays a key role in determining the activity of the catalyst. Where R represents hydrogen atoms, the strain is reduced and this results in reduced catalytic performance due to overly strong arene binding. Where the two R groups are linked by a cyclohexyl ring then the ring strain increases and the arene is thought to bind less strongly, resulting in increased activity. If the arene donation became too weak, however, due to fluorine substitution of the aryl group for example, then selectivity dropped off sharply.

Kinetic analysis of the system indicated that it is first order in ethylene concentration, suggesting that insertion of the third ethylene group is the rate-determining step. It was also found that introduction of methyl groups onto the aryl ring, thereby increasing its propensity for π-donation, led to a marked reduction in the rate of trimerisation. This strongly suggests that the titanacyclopentane intermediate with the arene bound accounts for the resting state of the catalyst cycle.

Analogues of these systems that incorporated zirconium and hafnium metal centres have also been synthesised and applied to ethylene trimerisation. Unfortunately, each of the systems demonstrated poor selectivity for 1-hexene at less than 10% and favoured the production of polyethylene. Mechanistic studies indicate that the 1-hexene is formed as a result of a metallacyclic mechanism, while the polymer is more likely to be Cossee-Arlman derived. Therefore it appears that activation of these heavier metal complexes results in the majority formation of an undesired species which favours chain growth polymerisation over metallacyclic trimerisation.

Cp ligands with more conventional labile pendent donors such as thioethers, thienyls and ethers have also been explored but without much success, Figure 1.6.[88, 89] Catalysts featuring a donor atom well orientated for coordination to the titanium demonstrate good selectivities for 1-hexene at over 90% in some cases. However, in all cases these systems demonstrate far worse TOFs of less than 10,000 mol(C_2H_4) mol(Ti)$^{-1}$ h^{-1}. Thienyl donors gave the best activities but with reduced selectivity, while ether donors gave the best selectivity but with TOFs of under 2000 mol(C_2H_4) mol(Ti)$^{-1}$ h^{-1}. Thioethers proved to be ineffective and only produced polyethylene.

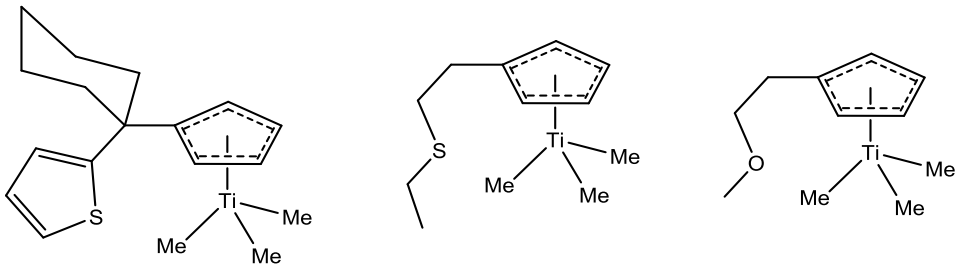

Figure 1.6 - Alternative non-aryl pendent donors.[19]

This work was followed by further investigations by Huang *et al.* which focused on variation of the Cp ring itself by addition of a fused phenyl group to give an indenyl species.[90] This resulted in a considerable improvement in overall activity over the cyclopentadienyl catalysts whilst improving the selectivity to around 95%. For example, for the cyclohexyl-bridged catalyst with a phenyl group as the pendent donor, the indenyl species demonstrated a 40% increase in activity at comparable ethylene pressure. Optimal activities were reported as 70,000 mol(C_2H_4) mol(Ti)$^{-1}$ h^{-1} at 8 bar ethylene pressure, though investigation of these catalysts at higher pressures has not been carried out. Variation of the bridging bulk, arene substituents and pendent donor all demonstrated the same relationship to activity as observed with the Cp systems.

More recently, a new titanium catalyst has been discovered by Suzuki *et al.* that demonstrates extremely impressive activities while retaining the high selectivity.[91] Phenoxyimine ligands with a pendent ether donor (abbreviated to FI) form titanium (IV) chloride complexes, Figure 1.7, which are readily activated with MAO. These catalysts demonstrate TOFs of over 11,200,000 mol(C_2H_4) mol(Ti)$^{-1}$ h^{-1} under ethylene pressures of 50 bar with 1-hexene selectivities of up to 93%. This remarkable activity is not only greater than that of the established Cp-arene titanium based systems but also outperforms the commercial Phillips trimerisation catalyst at comparable pressures. As such, this system represents the most active yet discovered.

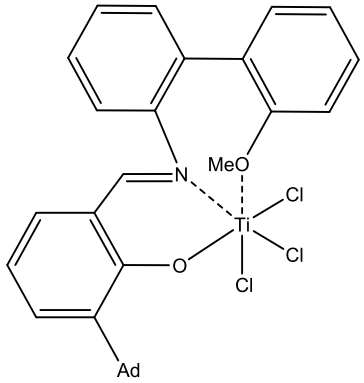

Figure 1.7 - An example of a highly active (FI)$TiCl_3$ pre-catalyst. Ad = adamantyl.

As observed with many of the trimerisation systems, it is the nature of the labile donor that affects the catalyst performance most. In this case, for example, it was found that replacing the methoxy group with a phenoxy group produced a catalyst selective for polymerisation with only limited trimerisation observed. The bulk of the catalyst was also found to have an impact around the phenoxy donor, whereby the larger adamantyl substituent produced a better catalyst than having a cumyl group in the same position.

The initiation process for this catalyst is proposed to occur *via* olefin insertion into the dimethyl species formed after methyl abstraction by the activating agent. Cossee-Arlman chain growth then proceeds for both until β-hydride elimination occurs, followed by reductive elimination of the remaining chain, Scheme 1.23. This then results in the 'naked' titanium cation, which is the entry point for the catalyst cycle.

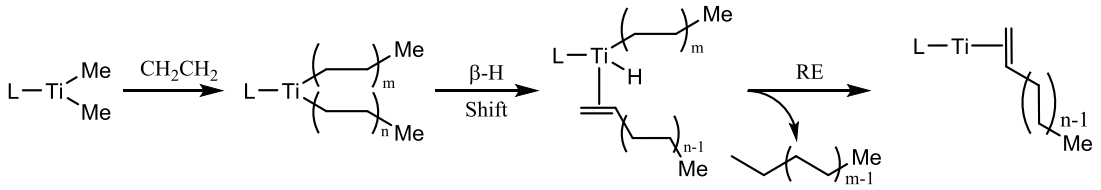

Scheme 1.23 - The proposed activation mechanism for the (FI)$TiCl_3$ catalyst. Each species is cationic in nature after abstraction of a methyl group by MAO.

An NMR and EPR spectroscopic investigation into the initiation pathway has been carried out by Soshnikov *et al.*[92] Using these techniques it was possible to look at the intermediates of activation even when using the usually restrictive MAO. Two key ionic intermediates were identified as playing an active role in the catalysis. Within the first few minutes of reaction between the pre-catalyst and MAO, the vast majority of the titanium species adopts the expected outer-sphere ion-pair $[(FI)TiMe_2]^+[MeMAO]^-$. Exposure to ethylene then leads to observation of peaks attributed to $[(FI)Ti]^+[MeMAO]^-$ formation. These results confirm the expected role of the MAO as an alkylating and abstracting agent, while also showing that ethylene is required to complete the initiation. As part of the work it was also established that MAO was the only effective activator, ruling out standard aluminium alkyls.

1.3.1.2 Tantalum Catalysts

It has been known since the discovery of α-olefin dimerisation catalysts by Schrock *et al.* that tantalum readily forms metallacycles. It is surprising therefore that Ta based ethylene trimerisation has only been explored to a very limited degree with the use of $TaCl_5$ as a catalyst.[93] After activation with $ZnMe_2$ the system produced 1-hexene at TOFs of around 500 mol(C_2H_4) mol(Ta)$^{-1}$ h^{-1} and very high selectivities exceeding 96%. The system was later modified by using bis(TMS)cyclohexadienes as activating agents and this resulted in an increase in TOF to 2500 mol(C_2H_4) mol(Ta)$^{-1}$ h^{-1}.[94]

The low turnover frequencies and diamagnetic nature of the tantalum chloride catalyst makes it an ideal candidate for mechanistic investigations. ^1H and ^2H NMR spectroscopy were used to examine the intermediates and side-products of the catalyst cycle. It was discovered that an active catalyst was formed only when $TaCl_3Me_2$ was present after activation. In addition, it was found that at -20 °C it was possible to observe the ^1H NMR peaks of the tantalacyclopentane present at 2% abundance. On heating these peaks were no longer observed, suggesting that this intermediate is very short lived.

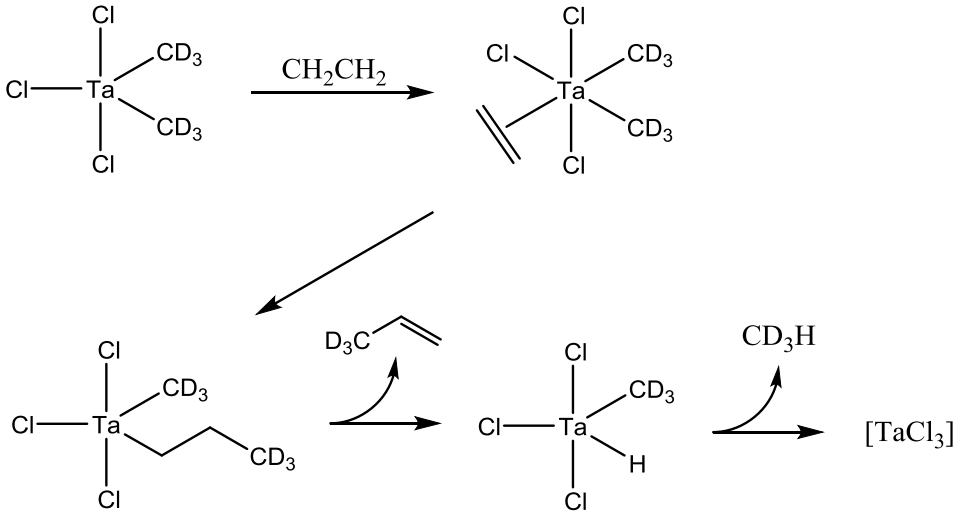

Scheme 1.24 - The observed deuterated side-products when $Zn(CD_3)_2$ is used as an activating agent.

When deuterated dimethyl zinc was used as the activating agent it was possible to identify the side-products of initiation and confirm the existence of the dimethyl tantalum species, Scheme 1.24. The discovery of propene deuterated at the methyl position alongside trideuteromethane confirms the predicted initiation sequence and establishes the dimethyl tantalum species as the active precatalyst. These catalysts show considerable potential because they are yet to be investigated with ligand systems that are known to be effective for other metals. In particular, the chloride anions are unlikely to exhibit much lability, a quality that features in the ligands of all of the most active catalysts.

1.3.1.3 Vanadium Catalysts

In 2001 a patent was filed by Enichem on the trimerisation of ethylene, as well as limited application to higher olefins, using vanadium sandwich compounds.[95] The $(arene)_2VX$ catalysts, Figure 1.8, in which X corresponds to a halide or weakly coordinating anion demonstrate modest activities, with maximum TONs of 600 at 7 bar ethylene pressure. While only moderately active, these catalysts demonstrate extremely good cost efficiency relative to other trimerisation systems because they require no activator. This self-activation simplifies their application to industry whilst also avoiding the large costs associated with the use of aluminium alkyls

In addition, the selectivity recorded at high pressures was remarkable at >99%, with no other olefinic species observed by GCMS and no polymer collected. At ambient pressure, considerable polymerisation is observed with 1-hexene selectivities of just 40-60%, suggesting a higher order rate dependence on ethylene for the trimerisation as compared to polymerisation.

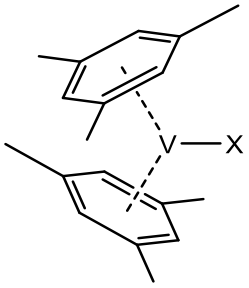

Figure 1.8 - The most active vanadium based trimerisation catalyst recorded to date. Where X = BF_4.

The different substituents have considerable impact on the catalysis as would be expected. Improved overall activity was observed when arene ligands of greater π-basicity, principally mesitylene, were used, suggesting an improvement in the stability of the catalyst. In contrast, the more weakly binding the anionic moiety the greater the activity. A marked improvement was observed when moving from halides to anions with a more widely distributed charge such as BF_4. This indicates that a more labile or even solvent separated interaction with the anion is required for the catalysis to proceed.

1.3.1.4 Nickel Catalysts

Nickel was evaluated for its potential to trimerise ethylene by Phillips Petroleum soon after the original discovery of the chromium system.[71] Reasonable selectivities were observed of up to 69% 1-C_6 enrichment of a Shultz-Flory distribution. Unfortunately, the observed activities of these systems, formed *in situ* from $Ni(acac)_2$, pyrrole and $AlMe_3$, were extremely poor at just 550 mol(C_2H_4) mol(Ni)$^{-1}$ h^{-1}. For this reason nickel has not attracted much attention until very recently.

A well-defined nickel based trimerisation system was discovered in 2015 by Ogoshi *et al*.[96] The process cannot truly be considered ethylene trimerisation because of the need to use a 2:1 ratio of ethylene to tetrafluoroethylene. However, it is notable as the only highly selective four-coordinate trimerisation system yet reported and for the fact that Ni is so well established as a non-selective oligomerisation catalyst. The catalyst is synthesised easily from $Ni(cod)_2$ and two equivalents of PPh_3 to give the active species. The activity of the system is extremely low at a maximum turnover number of just 13 but the selectivity towards '1-hexene' is very high. The location of the fluorine atoms in the product is fixed by the consistent inclusion of the fluorinated species in the nickelacyclopentane and the absence of β-fluoride shift in the nickelacycloheptane.

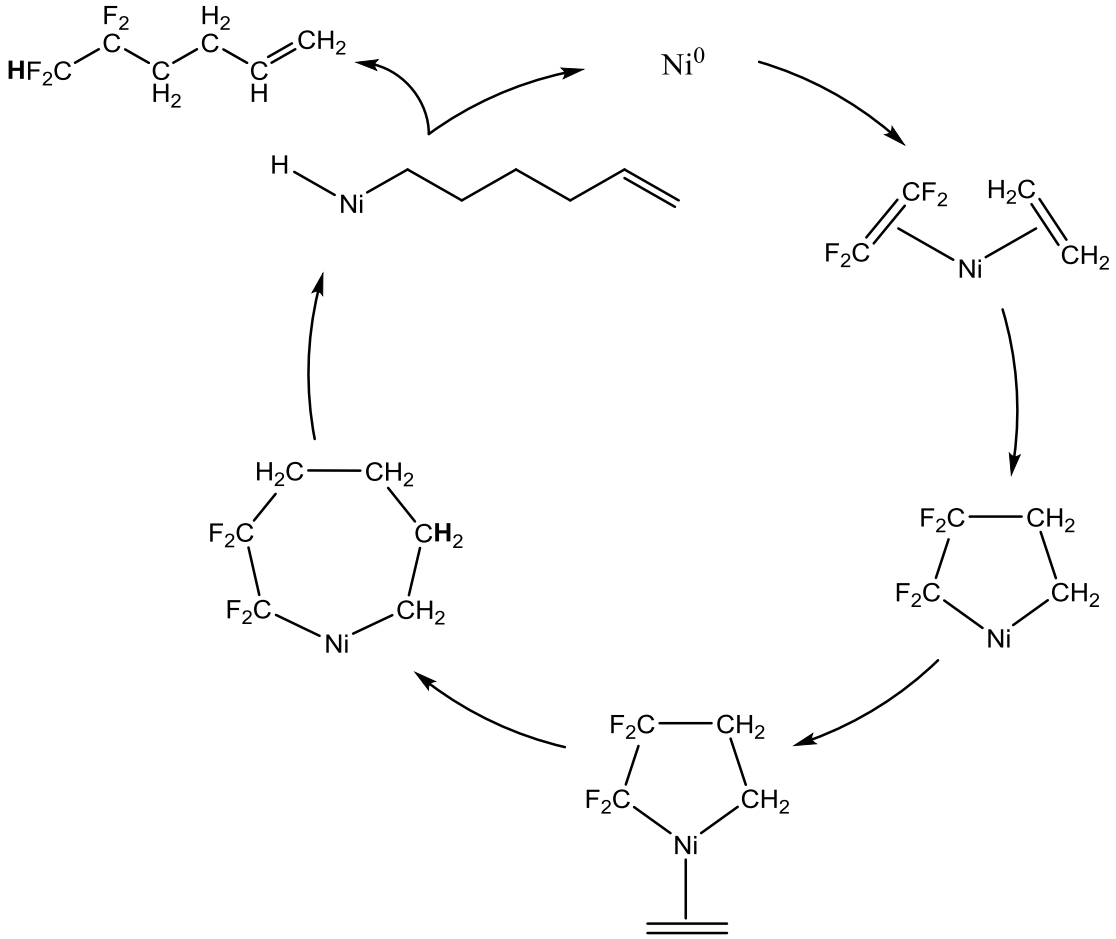

Scheme 1.25 - Co-trimerisation of ethylene with tetrafluoroethylene. PPh_3 ligands have been omitted for clarity.

The catalytic cycle is highly selective for a co-trimerisation system. This is driven by the electron withdrawing effect of the fluorine atoms and the strong C-F bond, Scheme 1.25. These features ensure that insertion into the nickelacyclopentane occurs into the Cr-CH_2 bond as this is more easily broken and that β-hydride shift can only occur from one position (shown in bold). The difficulty of insertion into the Cr-CF_2 bond is the primary cause of the low turnover numbers as the Ni(C_4F_8) metallacycle is stable to insertion and thus removes Ni from the catalyst cycle if formed. Although this system shows little scope as an effective ethylene trimerisation system, it does demonstrate that more metals may be capable of catalysing the reaction than currently thought.

Since 2000 there has been a considerable increase in the amount of research into non-chromium based ethylene trimerisation. Despite this, most have failed reach the standard set by the original Phillips catalyst, with the exception of the latest (FI)$TiCl_3$ system. Despite the considerable advances made, however, chromium based catalysts continue to demonstrate the most favourable properties and attract the most attention.

1.3.2 **Chromium Catalysed Ethylene Tri- and Tetramerisation**

Since the original discovery of the Phillips trimerisation system there has been a concerted effort to better understand the mechanism and hence intelligently design more effective catalysts. This has focused on the use of well-defined pre-catalysts which feature multidentate ligands in order to improve stability and direct the olefin coordination.

Pyrrolyl based donors were the first ligands found to be beneficial for chromium catalysed olefin trimerisation. Since then, research has focused primarily on incorporating group 15 elements as the principal donors, in addition to various pendent donors. This has led to the production of numerous ligand systems that demonstrate impressive activities and selectivities for ethylene tri- and tetramerisation.

1.3.2.1 The PNP Catalyst

Bis(diarylphosphino)amine (PNP) chromium complexes have been the most successful at emulating the activities of the Phillips trimerisation catalyst with a defined system. They were first discovered in 2002 by researchers at BP, with the catalyst formed *in situ* and activated by MAO.[97] While activities do not quite reach those of the optimised 2,5-dimethylpyrrole based system, high pressure runs have been shown to achieve over 1,700,000 mol(C_2H_4) mol(Cr)$^{-1}$ h^{-1}. This system is also 90% selective towards 1-hexene and produces less than 0.1 w% polymer, a key factor for any industrial application. The impurities are principally regioisomers of C_{10}, C_{14} and C_{18} olefins that are likely to result from reinsertion of 1-hexene after formation.

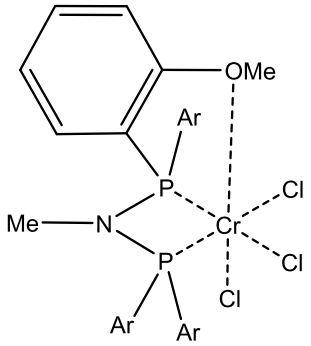

Figure 1.9 - The structure of one of the most active PNP catalysts prior to activation with MAO. Ar = *o*-methoxyphenyl.[98]

The interaction of the PNP ligand with the chromium centre in the pre-catalyst occurs as shown in Figure 1.9 and has been identified by X-ray crystallography.[98] The Cr-O bond was found to be weak, with a bond distance of greater than 2.3 Å. Deuterium labelling experiments have also shown that coordination of the methoxy group is highly labile, leading to fast exchange between the four pendent groups. Despite their highly labile nature, interaction between the ether groups and the metal centre was found to be essential to the trimerisation activity.

Situating the methoxy groups in the *para*-position of the phenyl group, for example, rendered the catalyst inactive, indicating it is the coordination rather than electronic effects which induce trimerisation. In addition, replacing the methoxy group with a sterically equivalent ethyl group resulted in no conversion to 1-hexene. This indicated the presence of this weak bond, and thus a pseudo-vacant site, is essential for trimerisation activity in this system. Under the conditions used no evidence for tetramerisation was observed in each case.

Analogous ligands were also synthesised in which the amine was replaced by a methylene or ethylene spacer. Both again demonstrated no activity, meaning the electronic effect of the amine linker plays a key role in the activity despite no evidence to suggest any interaction with the metal. Another impressive feature of the catalyst was that very little catalyst deactivation was observed over the course of an hour long run. It was also demonstrated that the active catalyst demonstrates good thermal stability, with little or no increase in deactivation up to 110 °C.

The extremely high activities and selectivities of the PNP catalyst made it a strong candidate for analysis of the mechanism. Many basic features of the metallacyclic trimerisation mechanism originally proposed by Briggs had no experimental basis or evidence to support them beyond kinetic observations. This led Bercaw *et al.* to conduct a series of experiments using the optimised PNP catalyst to test the key assumptions.[98, 99]

The first challenge was to produce clear evidence that the high selectivities observed could not be accounted for by the Cossee-Arlman mechanism. An established feature of chain growth oligomerisation is the formation of a metal hydride after elimination of the α-olefin, which is then incorporated into the next α-olefin formed.[100] Importantly, the proposed metallacyclic mechanism does not leave a hydride behind after elimination of the α-olefin and instead retains it in an intramolecular fashion, Scheme 1.26. This led to a crossover study in which a 1:1 mixture of CD_2CD_2 and CH_2CH_2 was trimerised. Should the metallacyclic mechanism account for the selectivity then only 1-hexene containing 4n deuterium atoms would be expected. This is due to complete retention of the deuterium atoms present in the constituent ethylene units in the product.

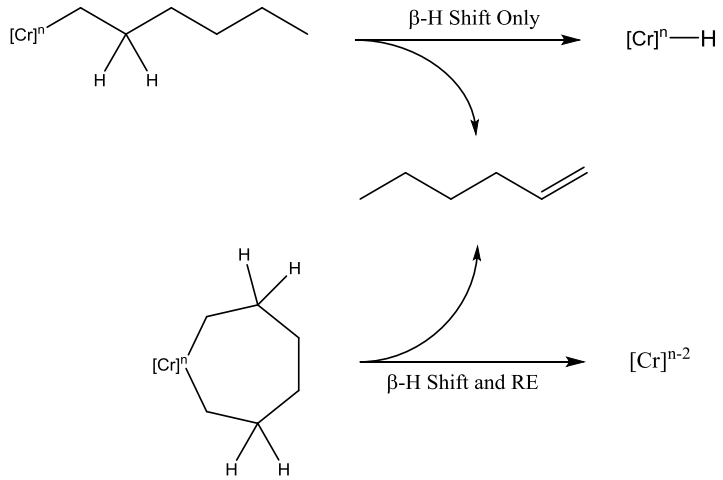

Scheme 1.26 - Comparison of the elimination pathways of the Cossee-Arlman (top) and metallacyclic (bottom) mechanisms.

Analysis of the partially deuterated product using GCMS allowed the number of deuterium atoms in the different isotopomers to be observed. The mass spectrum displayed four (m/z) peaks at a ratio of 1:3:3:1 at 84, 88, 92 and 96 respectively, corresponding to 0, 4, 8 and 12 deuterium atoms being present. The observation that all products contained 4n deuterium atoms gave conclusive evidence for an intramolecular hydride shift. As this selectivity can only occur for the metallacyclic and not the Cossee-Arlman mechanism, this provided convincing evidence of its existence.

In order to confirm the results, the same investigation was conducted with the SHOP catalyst and it was indeed observed that deuterium scrambling occurred. Numerous (m/z) peaks corresponding to partially deuterated 1-hexene were observed compared to the four seen for the PNP system. There was also only a minor peak at 96 compared to a much larger peak at 95, while each of the other 4n peaks had a significant peak at 4n-1. The low abundance of the entirely deuterated product reflects the kinetic isotope effect's influence on selectivity, such that the likelihood of a hydride undergoing β-hydride shift is considerably higher than that of a deuteride. This results in the ratio of metal hydride to metal deuteride being skewed significantly towards the hydride, causing the '4n-1' peak of the products to dominate over '4n+1' peaks.

Key questions remained, however, into the initiation mechanism and the nature of the catalyst itself. To investigate this further a defined precatalyst was synthesised that featured two alkylated sites on the chromium as well as a readily abstractable bromide ligand. The system was then run under different conditions to determine whether the catalyst was cationic in nature. Two experiments were performed, one in the presence of an abstracting agent and one without an activator. If bromide abstraction was necessary for catalysis then a cationic complex must account for the active species. This was found to be the case, while near-stoichiometric reaction with ethylene also allowed observation of the side-products of initiation, Scheme 1.27.

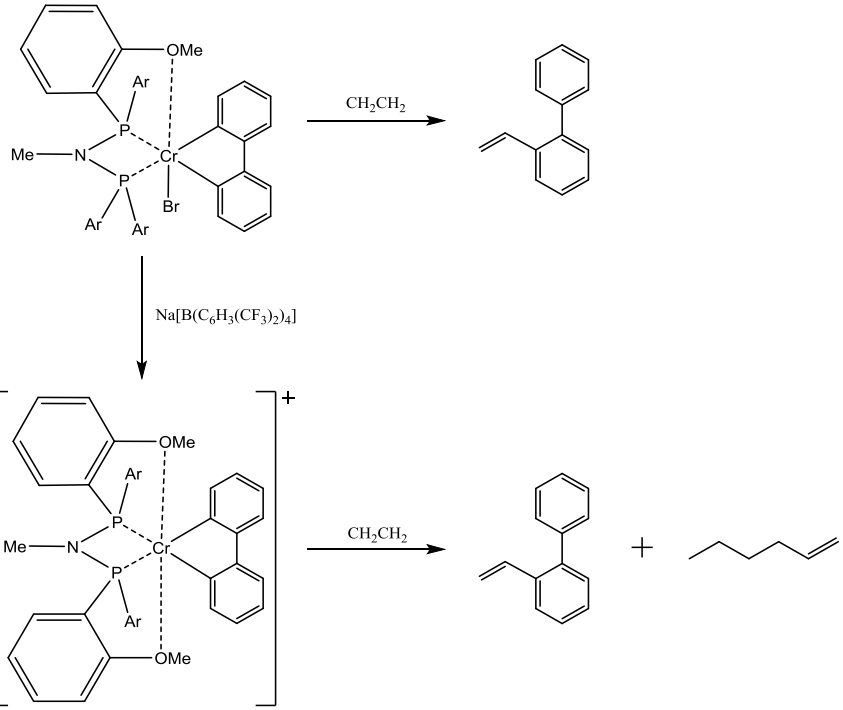

Scheme 1.27 - The alkylated precatalyst and the products of initiation under the different conditions.

The neutral complex gave no ethylene trimerisation, indicating that the cationic nature of the catalyst is essential for activity. In contrast, the initiation process appears to be the same for both complexes, with vinylbiphenyl produced in each case. This fits the proposed activation, by which ethylene inserts into the Cr-C bond prior to β-hydride shift and reductive elimination to give the active catalyst. Both the neutral and cationic species are therefore able to coordinate ethylene, demonstrating that the methoxy group is indeed labile enough to present a vacant site. The inability of the neutral species to trimerise must therefore derive from an inability to form chromacyclopentanes as ethylene insertion, β-hydride elimination and reductive elimination all occur during the formation of vinylbiphenyl. The greater electrophilicity of the cationic metal centre is therefore presumably a key factor in the oxidative cyclisation of two ethylene molecules with the chromium.

A different analytical approach was then employed in an attempt to observe the active species *in situ*. Low temperature UV-Vis and EPR spectroscopy were applied in order to search for the activation intermediates as well as the intermediates of the catalyst cycle.[101] UV-Vis analysis at -40 °C indicated rapid formation of a single product on addition of the MAO activator, followed by the gradual formation of a second activated species. On addition of ethylene several different species were formed. EPR analysis performed at -196 °C, with the solution frozen at the different stages identified by UV-Vis spectroscopy, also indicated a single species on addition of MAO. This initial product is proposed to be (PNP)$CrMe_3$ based on shift similarity to similar species. Comparison of the second activation product in the same manner suggested the abstraction of a methyl by the remaining MAO to give $[(PNP)CrMe_2]^+$.

In the presence of ethylene the situation becomes more complex, principally as a result of the majority of the chromium occupying an EPR-silent state, proposed to be Cr^{II}. The trimerisation reaction was run with ethylene added both before and after the activator and this gave different results. Prior addition of ethylene resulted in $[(PNP)CrMe_2]^+$ as the major species with ~2% of an unknown Cr^I species. In contrast, post addition of ethylene resulted in ~94% of suspected Cr^{II}, ~6% $Cr^I(arene)_2$ and traces of both $[(PNP)CrMe_2]^+$ and the unknown Cr^I, as shown in Scheme 1.28. However, both experiments produced highly active trimerisation systems, ruling out the Cr^{II} species as well as $Cr^I(arene)_2$ and $[(PNP)CrMe_2]^+$ as the active species. The unknown Cr^I species is therefore the most likely candidate for the active species although it is only present at very low concentrations in each case. This suggests that the activity of the true catalyst is up to 100-fold greater than previously thought.

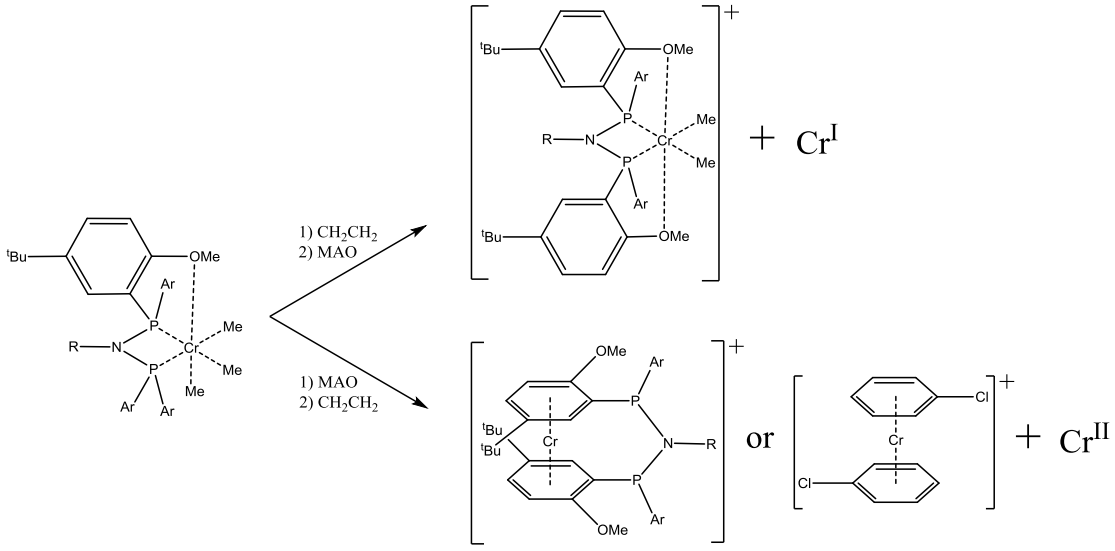

Scheme 1.28 - The activation and catalytic intermediates suggested by EPR spectroscopy.

This research provides important evidence that complete alkylation of the chromium by the activator occurs followed by a slower abstraction of one of the alkyl groups. In addition, the observation of a Cr^I species within the active catalyst solution strongly supports a Cr^I/Cr^{III} redox cycle while also contradicting previous suggestions that a Cr^{III} species acts as the resting state.

The success of the original PNP catalyst led to intensive industrial research into its modification. Further experimentation by Sasol Technology led to the surprise discovery of selective tetramerisation.[78] This was achieved by the complete removal of pendent donors to give a strictly bidentate PNP ligand. A considerable amount of research was then conducted into the effects of altering the bulk and functionality of the P- and N-alkyl or aryl groups. The optimum N-substituent for tetramerisation selectivity as well as overall activity was found to be either an *iso*-propyl or cyclohexyl group, with α-branching seeming to be a key feature. Increasing the bulk even further, by incorporating *ortho* substituents into the cyclohexyl ring for example, led to the selectivity shifting back towards trimerisation.[102]

The shift in selectivity observed on variation of the N-substituent's steric influence has been extensively explored by Cloete *et al.*[103] In combining crystallographic data with DFT calculations a linear arrangement was observed between the Tollman cone-angle of the N-substituent and the 1-C_6:1-C_8 ratio, Figure 1.10. The greater the steric bulk of the ligand, the higher the proportion of 1-hexene produced relative to 1-octene. Observation of this relationship allows the selectivity of a catalyst to be accurately predicted and was shown to hold true even when extremely bulky moieties were used.

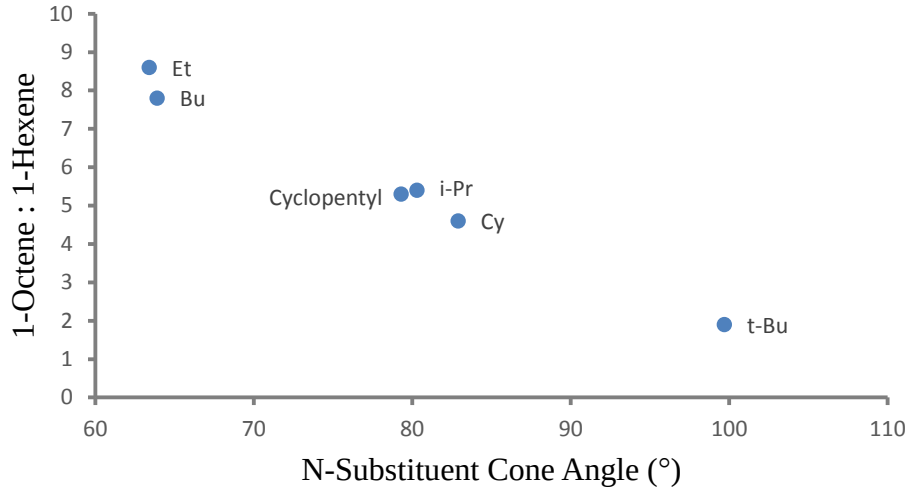

Figure 1.10 - A sample of the data showing a linear relationship between the ratio of 1-octene to 1-hexene and the N-substituent cone angle.[103]

It was also found that formation of the cyclic side-products does not follow the same trend and instead the abundance increases markedly at a cone angle of 80° and continues to rise as the angle decreases further. The hypothesis of the authors is therefore that the three pathways that yield 1-hexene, 1-octene and the two cyclopentanes are of similar energy and easily influenced by increased strain within the ligand environment. The linear relationship between N-substituent cone angle and the tri-/tetramerisation ratio is proposed to result from increasing encroachment of the ligand into the remaining coordination sites of the chromium. As the steric bulk of the ligand is augmented it increasingly replicates the effect of a labile donor and therefore the selectivity shifts towards trimerisation.

Increasing the bulk of the P-substituent did not lead to any improvements in selectivity or activity.[19] Similarly, investigations into PNNP and ethylene bridged diphosphine ligands also gave no improvement in catalyst performance, suggesting an increased bite-angle is not advantageous.[78] The absence of a third donor leads to dimer formation on coordination of $CrCl_3(THF)_3$ as opposed to the mononuclear species observed for the traditional PNP catalyst, Figure 1.11.

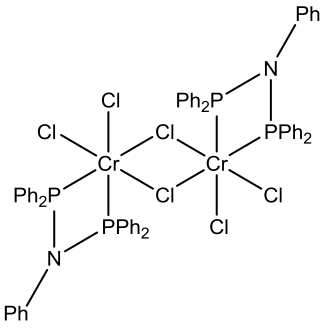

Figure 1.11 - The structure of the species formed on complexation of the bidentate ligand with $CrCl_3(THF)_3$ as proven single crystal X-ray spectroscopy.

Bollmann *et al.*, who first observed tetramerisation, propose that the tetramerisation system proceeds through a ring-expansion mechanism adapted from that originally put forward by Briggs, Scheme 1.29.[76, 78] This hypothesis is based principally on the observation that subtle alterations to the ligand environment can shift the selectivity, suggesting that both 1-hexene and 1-octene result from the same intermediate, the chromacycloheptane. It must be noted that this work was published prior to the proposed ring expansion mechanism and therefore variations in ethylene coordination were not considered. This could be considered as the original ring expansion mechanism proposal, though no supporting evidence was provided.

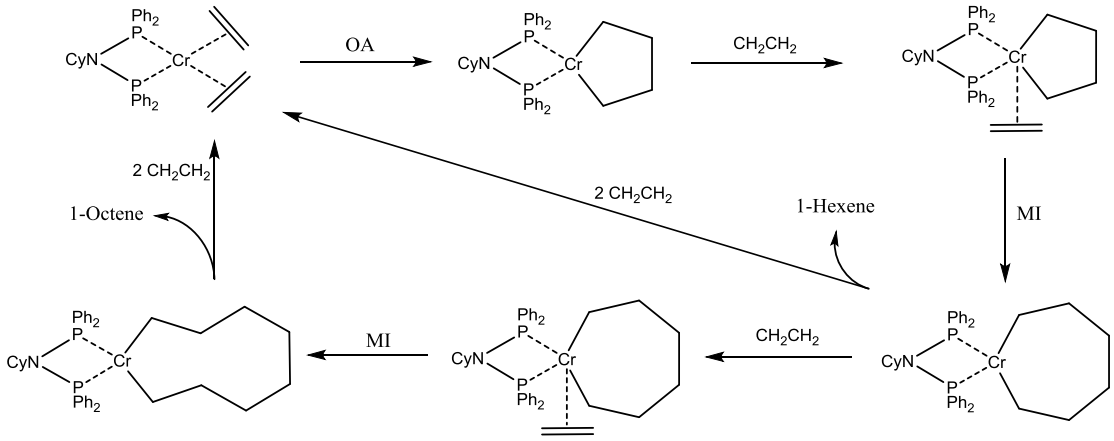

Scheme 1.29 - The proposed mechanism for the tri- and tetramerisation of ethylene by PNP ligands. OA = Oxidative Addition, MI = Migratory Insertion. All chromium complexes have a +1 charge, counter-ions have been excluded for clarity.

Mechanistic studies into the PNP tetramerisation catalyst have focused principally on the cyclic side-products observed as a considerable proportion of the C_6 fraction.[104] These consist of both methylcyclopentane and methylenecyclopentane in a 1:1 ratio. The fact that these products are formed in equal quantities suggests that they result from the same pathway. The authors therefore propose an intermolecular disproportionation reaction occurs after insertion of the intermediate hexenyl species into itself, Scheme 1.30.

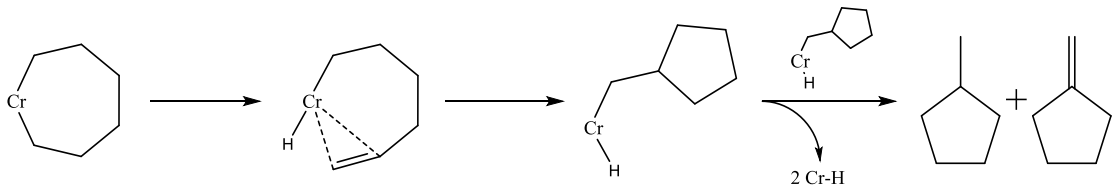

Scheme 1.30 – The proposed pathway for the formation of the cyclic side-products.

Further mechanistic studies were carried out using the deuterium labelling techniques first described by Bercaw *et al.* in order to eliminate the possibility of the Cossee-Arlman mechanism playing a role. It was once again found that on using a 1:1 mixture of CH_2CH_2 and CD_2CD_2 no deuterium scrambling was observed in the 1-octene product. As such, the formation of 1-octene *via* a metallacyclic mechanism was strongly supported.

This technique was also applied to the cyclic side-products for the first time, with deuterium scrambling found to occur in both products. This strongly suggests that methylcyclopentane is not formed through an intramolecular mechanism, in which the chromium hydride is formed from and then reincorporated into the same C_6 unit. In addition, the intramolecular formation of methylenecyclopentane would result in the loss of two hydrides/deuterides from the same C_2 segment, therefore retaining an even number of deuterium atoms in the product. Observation of scrambling therefore lends further support to the proposed intermolecular mechanism.

The disproportionation reaction proposed to account for the cyclic side-products is only feasible with radical intermediates. For this reason a catalyst run was doped with triphenylmethane as a ready source of hydride radicals. If the two products resulted from a radical pathway then a significant increase in the abundance of methylcyclopentane relative to methylenecyclopentane would be expected. However, this was not observed and the ratio remained 1:1, effectively ruling out any role for radical species. With this in mind a new dinuclear mechanism was postulated for their formation, Scheme 1.31.

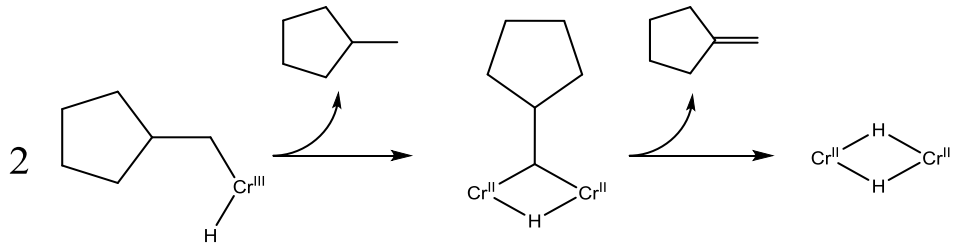

Scheme 1.31 – The proposed route for the production of a 1:1 ratio of cyclic products.

While this mechanism appears to result in Cr^{II}, which is known to result in non-selective oligomerisation, the authors propose disproportionation of this species to re-enter the Cr^{I}/Cr^{III} redox cycle. In addition to the products already mentioned, a range of longer chain α-olefins are also observed for each run. Unlike most systems, however, the relative abundance of these larger products does not fit to a Shulz-Flory distribution. This effectively rules out their formation resulting from a linear chain growth mechanism. Instead, the authors hypothesise that the distribution occurs from a ring-growth pathway in which the abundance is determined by the rate of ethylene insertion into the ring verses elimination.

Modification of the standard PNP tetramerisation system has been carried out by Sa *et al. via* the incorporation of tertiary amines into the N-substituent, Figure 1.12.[105] Surprisingly, despite the presence of a third donor typically being associated with selectivity towards trimerisation, these systems demonstrated good activities for tetramerisation. Variation of the spacer length between the amines was found to be key to catalyst reactivity, with a propylene bridge proving most effective at 60% 1-octene selectivity. Catalysts containing an ethylene spacer showed the best activities, the optimal dibutylamine system produced 1,100,000 mol(C_2H_4) mol(Cr)$^{-1}$ h^{-1}.

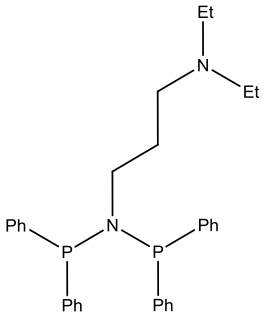

Figure 1.12 - The most selective PNP catalyst featuring a tertiary amine donor on complexation with $CrCl_3(THF)_3$.

The catalyst systems featuring ethylene spacers replicated the loss in tetramerisation activity with increasing temperature seen for the standard PNP system. For these species there was a considerable drop-off in performance on increasing the reaction temperature from 30 °C to 60 °C. The selectivity of the system was not effected suggesting that these systems demonstrate poor thermal stability while the tri- and tetramerisation pathways are of similar energy. In contrast, the propylene bridged species demonstrated similar or even improved activities at higher temperatures. This represents a considerable improvement over the systems not containing a pendent donor.

A similar investigation into modifying the PNP tetramerisation catalyst with pendent donors has also been carried out by Suttil *et al.*[106] This broader investigation found that pendent amine donors of the type described by Sa *et al.* are indeed the most effective modifications. Hydrazine type modifications in which a secondary amine is located adjacent to the tertiary amine of the PNP moiety produced polymer as the majority product. The use of aryloxy, siloxy and hydroxy pendent groups was also investigated with only limited success due to poor activities and selectivities. The most active catalyst was found to be a tertiary amine pendent donor with an ethylene spacer, matching the results observed by Sa *et al*.

Wass *et al.* took a different approach and investigated variation of the phosphine donors in these catalysts by incorporating them into phospholes.[107] Both tetraethylphosphole and dibenzophosphole substituents were investigated and were found to be selective for either tri- or tetramerisation, Figure 1.13. The tetraethylphosphole systems were found to be the more active, while the extended conjugation of the dibenzophosphole moiety led primarily to polymer formation. The best trimerisation system contained an *iso*-propyl N-substituent and achieved 37,000 mol(C_2H_4) mol(Cr)$^{-1}$ h^{-1} at 90% selectivity.

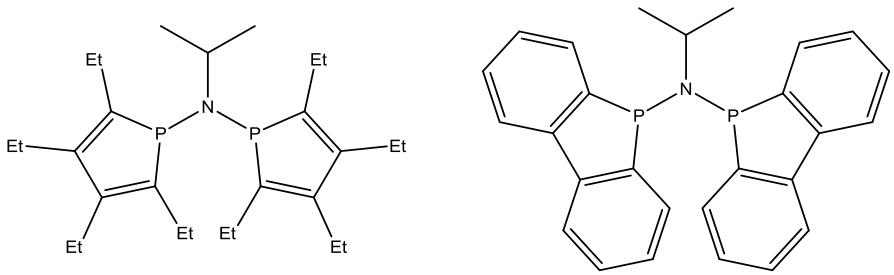

Figure 1.13 - The most effective symmetrical *N,N*-bis(phopholyl)amine ligands for each of the phosphorus donors.

Interestingly, the catalyst which demonstrated the best activity for 1-hexene and 1-octene formation combined represents the only successful application of an unsymmetrical PNP ligand. The use of one tetraethylphosphole donor alongside a diphenylphosphine donor led to activities approaching 55,000 mol(C_2H_4) mol(Cr)$^{-1}$ h^{-1} at a ratio of 65:35 in favour of trimerisation. Overall, the incorporation of the phosphine donors into a conjugated ring system resulted in retention of the selectivity of oligomerisation in some cases but with considerable loss in activity. The additional synthetic complexity associated with these catalysts therefore renders this family of ligands unable to compete with the original ligand design.

1.3.2.2 Adaptations of the PNP Catalyst

One modification of the PNP ligand which has attracted considerable attention is the PNPNH ligand, which was first published in 2009.[108] Addition of a secondary amine can be achieved according to Scheme 1.32 to give a highly stable ligand. However, the four step ligand synthesis is complex and poor yields are typically recorded. Complexation to chromium(0) carbonyl species demonstrated the same bidentate coordination behaviour as the established PNP ligand, with only the two phosphorus donors interacting with the metal.[109] This complex was found to demonstrate some ethylene trimerisation activity despite the Cr^0 oxidation state. Analogous reactivity was also observed with $CrCl_3(THF)_3$ to form a catalyst which demonstrated considerably better trimerisation activity, as expected.[110]

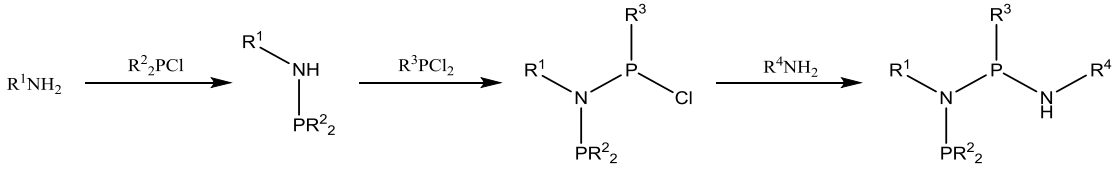

Scheme 1.32 - Synthetic route to the PNPNH ligand.

The catalysts derived from $CrCl_3(THF)_3$ reach peak activity when activated with just 15 equivalents of triethylaluminium, making them a highly cost efficient catalyst system. Optimised activities of up to 130,000 mol(C_2H_4) mol(Cr)$^{-1}$ h^{-1} fall a long way short of those seen for the original PNP system though, limiting any potential application. Extensive kinetic studies have been performed on this system and have revealed that the rate shows first order dependence on ethylene. This further confirms that the rate determining step is dependent on the ligand environment as well as the metal involved, as this differs from the kinetics of other chromium systems.[111]

Due to its extremely cheap activation procedure this catalyst system has been investigated heavily in regards to its potential application in industry. With this in mind, this is one of the few catalysts for which immobilisation on a scaffold to produce a heterogeneous system has been properly investigated.[112] Rosenthal *et al.* have shown that the ligand can be covalently bound to polystyrene resins containing primary amine moieties, Scheme 1.33. The ligand system retains its coordination chemistry on complexation of $CrCl_3(THF)_3$ to give an active trimerisation catalyst when activated with $AlEt_3$.

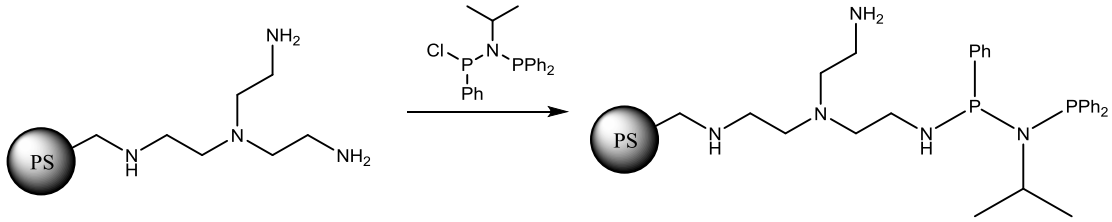

Scheme 1.33 - Covalent binding of a PNPNH ligand to tris(2-aminoethyl) polystyrene resin.

Unfortunately, preparation of the catalyst in this way results in a drop in activity to approximately 550 $mol(C_2H_4)\ mol(Cr)^{-1}\ h^{-1}$ and the selectivity falls to around 80 w% 1-hexene compared to 87 w% for the homogeneous system. These observations are attributed to incomplete reaction of the amines on the resin which could also bind chromium to form non-selective catalysts or hinder the reaction pathways.

Immobilisation does have a significant advantage in that it results in extremely stable and consistent catalyst systems, with no deactivation observed after 40 hours under ethylene. This is an important property if any of these trimerisation systems are to be commercialised and goes some way towards offsetting the disappointing loss in selectivity and activity. Interestingly, one of the biggest drawbacks of the PNP system is its rapid deactivation at higher temperatures, indicating that introduction of the additional amine moiety significantly affects the stability of the active catalyst.

While investigation of the precatalysts showed analogous coordination chemistry to the PNP catalyst, later experiments have shown that under catalytic conditions the ligand behaves very differently.[113] The use of two tertiary amines resulted in no catalytic activity at all, indicating a strong link between the presence of an acidic proton and activity. Reaction of a PNPNH ligand with an aluminium alkyl was found to result in deprotonation of the secondary amine to produce a neutral $(PNPN)AlR_2$ complex, which was confirmed by single crystal X-ray diffraction. Binding occurs *via* phosphorus and amide donation in this case and analogous binding to a model chromium compound $Li[CpCrCl_3]$ has also been observed. The use of the aluminium complex as a precatalyst under standard conditions resulted in similar trimerisation activity to the use of the unreacted ligand, strongly suggesting it exists as an intermediate.

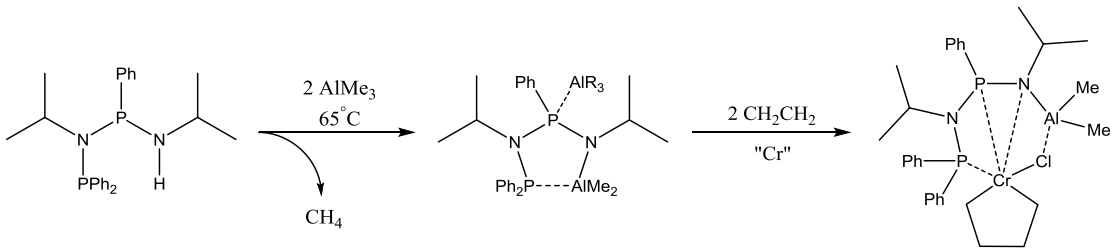

Scheme 1.34 - Reaction of a PNPNH ligand with trimethylaluminium and the proposed resting state of the catalyst cycle.

Rosenthal *et al.* propose therefore that the aluminium 'counter-ion' is bound in an intramolecular fashion to the active species. While this would result in reduced availability of the vacant site, and therefore reduced activity, it may also explain the high stability of these systems. An intermediate of this type would also prevent the strong coordination of the amide, which would likely have a negative impact on the catalyst. Instead, the additional coordination sites are proposed to be occupied by the second phosphorus and the now tertiary amine, preserving the neutral nature of the ligand.

This ligand also shows switchable selectivity for tri- and tetramerisation by variation of the substituent on the internal phosphine. The ligand shown is highly selective for trimerisation, while if the phenyl group on the phosphorus is replaced by a methyl group the reduced steric bulk leads to predominantly tetramerisation.[113]

Following a similar methodology, Zhang *et al.* explored the effects of incorporating an ether donor into the PNP catalyst in much the same way as the additional amine.[114] These PNPO ligands can be synthesised readily with the use of sodium aryloxides instead of a primary amine in the last step of Scheme 1.32. *In situ* catalyst formation with the use of $Cr(acac)_3$, the ligand and MMAO led to catalysts selective towards formation of a mixture of 1-hexene and 1-octene, Figure 1.14.

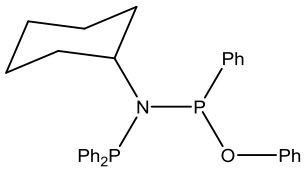

Figure 1.14 - The best performing PNPO ligand for ethylene tri-/tetramerisation to date.

The optimised system, featuring a cyclohexyl N-substituent, phenyl O-substituent, chlorobenzene solvent and 800 equivalents of MMAO, recorded high combined tri- and tetramerisation activities of over 550,000 $mol(C_2H_4)\ mol(Cr)^{-1}\ h^{-1}$ and were up to 85 w% selective for $1\text{-}C_{6/8}$. The solvent and temperature both had a considerable effect on the catalyst activity and selectivity. Toluene favoured polymerisation while methylcyclohexane led to improved oligomerisation selectivity. The use of chlorobenzene led to a significant improvement in activity and better selectivity compared to the use of toluene. The catalyst was found to have extremely poor thermal stability and performed best at 40 °C. However, reducing the temperature to 20 °C led to significant levels of polymerisation, suggesting the catalyst is only effective within a fairly narrow operating window.

Another later modification of the PNP catalyst took the opposite approach and instead investigated the effect of removing one of the phosphine groups to give amidophosphine ligands. These so-called PN catalysts were first explored by Gambarotta *et al.* in order to test the performance of an anionic ligand similar to PNPNH but with different coordination behaviour.[115] Both Cr^{II} and Cr^{III} complexes were synthesised and found to demonstrate considerably different geometries, with Cr^{II} forming dinuclear complexes containing a very weak Cr-Cr single bond, Scheme 1.35.

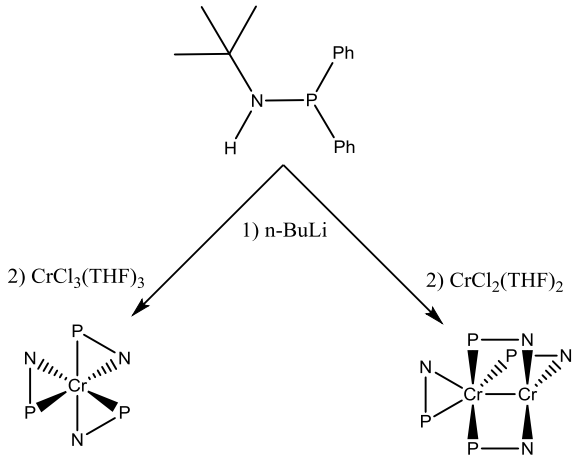

Scheme 1.35 - Synthesis of Cr^{II} and Cr^{III} complexes with amidophosphine ligands. The R-substituents have been removed for clarity.

Overall, these catalysts failed to replicate the successes observed with the PNPNH system due to poor activities (optimised TOFs of around 3000 mol(C_2H_4) mol(Cr)$^{-1}$ h^{-1}) and selectivities on activation with 1000 equivalents of MAO. Production of a Shultz-Flory distribution of olefins was observed for the Cr^{II} species in toluene. Meanwhile, considerable polymer formation and only slight enrichment of the C_6 fraction of a Shultz-Flory distribution was observed for the Cr^{III} species. However, changing the solvent to methylcyclohexane led to almost 100% selectivity within the liquid fraction, though polymer production was still high. The poor performance of this ligand system was attributed to the stability of the complexes formed preventing facile access to Cr^{I}, thought to be a key intermediate of the metallacyclic mechanism.

An important result within this research was the isolation and structural elucidation of the complex formed on addition of diethylaluminium chloride to the Cr^{III} species. It was observed that the prediction by Rosenthal *et al.* of complexation of the aluminium activator was true for this pre-catalyst. The chromium species undergoes a complex rearrangement to form a distorted square-planar geometry in which the chromium and aluminium ions are bridged by chlorine, Figure 1.15. This species acted as a reasonably active non-selective oligomerisation catalyst without the need for an activator.

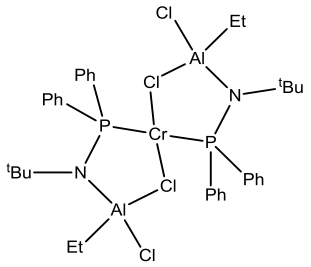

Figure 1.15 - The complex formed on reaction of $Cr(PN)_3$ with $AlEt_2Cl$, as confirmed by single crystal X-ray diffraction.

Gambarotta *et al.* went on to adapt the PN ligand into neutral $PN(CH_2)_nNP$ ligands with the aim of producing a tetramerisation catalyst, Figure 1.16.[116] Based on the idea of the dinuclear mechanism, first proposed by Rosenthal *et al.*, it was hoped that separation of the donating units would induce the formation of suitable bimetallic species. In the presence of $CrCl_3(THF)_3$ and DMAO the best resulting catalyst was found to be capable of tetramerising ethylene with a selectivity of over 91%, with the remainder 1-hexene. While the combined tri- and tetramerisation activity of this system was low at under 4000 $mol(C_2H_4)\ mol(Cr)^{-1}\ h^{-1}$, this was the first example of a truly selective (>90%) catalyst for the tetramerisation of ethylene .

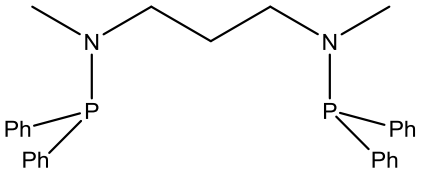

Figure 1.16 - The most effective $PN(CH_2)_nNP$ ligand at inducing tetramerisation. Ligands with an ethylenic spacer and ethyl or *iso*-propyl N-substituents were also tested.

Both ethylenic and propylenic spacers were explored, with the chain length found to have a marked effect on the selectivity of the catalyst. The ethylenic spacer demonstrated far greater preference for 1-hexene formation, with selectivities in the order of 60 w%, in contrast to the longer chain, which favoured tetramerisation. In addition, replacing the methyl N-substituent with a bulkier *iso*-propyl group leads to a switching of the selectivity towards trimerisation. The authors propose that this contrast results from the binding mode of the ligand switching based on the spacer length and substituent bulk. Bidentate coordination to one chromium for the ethylenic spacer and monodentate bridging coordination to two chromium centres for the propylenic spacer are hypothesised based on steric considerations, Figure 1.17.

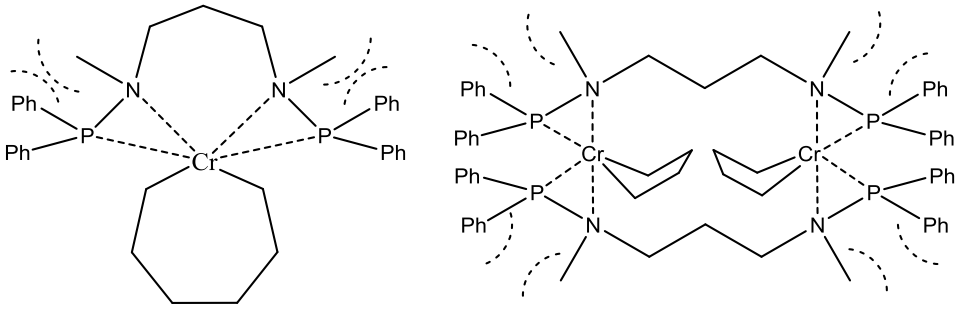

Figure 1.17 - The proposed reduction in steric hindrance between the P and N-substituents for the dinuclear propylene-bridged structure proposed to result in tetramerisation compared to the mononuclear alternative proposed to result in trimerisation. Shown are the proposed metallacyclic intermediates formed prior to olefin elimination.

The manner in which selective tetramerisation was achieved in this study, ie. by increasing separation between donor groups, lends considerable support to the proposed dinuclear mechanism. The steric observations associated with the bulk of the N-substituent also match nicely to those observed for the PNP ligand system, with increased bulk favouring trimerisation. Both factors observed to induce tetramerisation would also be expected to promote a bridging ligation, which correlates well to the proposed mechanism.

Later work by Gambarotta *et al.* continued to explore the effects of pendent donors by incorporating amine, pyridyl and phosphorus donors into neutral PN ligands, Figure 1.18.[117] In this case ethylenic spacers were used on each occasion in order to assess the impact of donor variation. The use of a phosphorus pendent donor proved ineffective and resulted in a Shultz-Flory distribution of olefins with only slight enrichment of C_6 and C_8. The pyridyl donor showed strong selectivity for 1-octene at 75 w% but with considerable polymer production and poor activities. The amine pendent containing ligand performed best with 89 w% selectivity for tetramerisation in the liquid products. Activities were also high, with combined tri- and tetramerisation activities recorded at over 22,000 mol(C_2H_4) mol(Cr)$^{-1}$ h^{-1}. However, polymer was still produced at over 25 w%, meaning none of these catalysts demonstrated selectivities close to that of the original PN(CH_2)$_n$NP system.

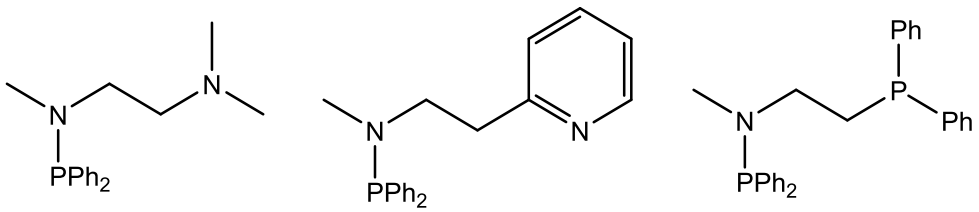

Figure 1.18 - The three ligands investigated.

The pyridyl containing ligand system has been used to investigate the effect of altering the spacer length more closely with the use of a methylenic spacer as well as no spacer at all.[118] Overall, these new systems presented poor combined activities of around 2000 mol(C_2H_4) mol(Cr)$^{-1}$ h^{-1} alongside high levels of polymer production. In addition, while selectivity for tri-/tetramerisation was very high, variation of the ligand structure was not able to induce selectivity for either beyond 80%.

Duchateau *et al.* also explored neutral PN ligands by incorporation of the nitrogen donor into a conjugated N-heterocyclic ring to give an analogue with just one PN moiety in the ligand, Figure 1.19.[119] On complexation with $Cr(acac)_3$ these ligands proved to completely alter the selectivity compared to the anionic PN ligand. The systems investigated produced a mixture of 1-hexene and 1-octene at a combined selectivity of over 99 w%, with specific optimisation resulting in up to 74 w% selectivity for 1-octene in some cases. This suggests that the stabilisation that results from amide donation is not necessarily beneficial and neutral ligand systems are more effective. Observation of impressive 1-octene selectivities without the presence of pendent or separated donors suggests this is not the only factor capable of inducing tetramerisation.

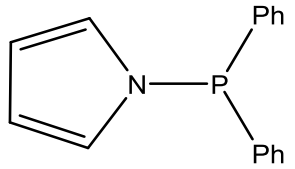

Figure 1.19 - The most effective heterocyclic PN ligand for the tri-/tetramerisation of ethylene.

It was also found that toluene significantly affected the catalysis, as in the work by Gambarotta *et al.*, with >10 w% within the solvent rendering the catalyst completely non-selective. The best activities were achieved with a *N*-pyrrolyldiphenylphosphine ligand and were very similar to the amidophosphine system at around 6000 $mol(C_2H_4)\ mol(Cr)^{-1}\ h^{-1}$ for $1\text{-}C_{6/8}$.

The principle of combining the PN motif with pendent nitrogen donation was recently explored by Carney *et al.* with the use of imine donors.[120] The catalysts differ considerably from prior PNP adaptations, however, because the amine is not alkylated and is instead retained as a secondary amine, Figure 1.20. These proved to be far more effective than previous attempts at modification, with trimerisation activities reaching 1,800,000 $mol(C_2H_4)\ mol(Cr)^{-1}\ h^{-1}$ and selectivities of 94 w%. As such, these catalysts demonstrate similar efficiencies to the original PNP catalyst, indicating that use of the PN moiety within different ligand arrangements can yield impressive results. The precatalyst was activated with up to 800 equivalents of MMAO and, unusually, the reactions were run in the presence of hydrogen. These extremely bulky ligand systems also produce 1-octene when the bulk of the imine or carbon substituent is reduced compared to the optimal trimerisation system. So far a selective tetramerisation system has not been demonstrated but considerable scope remains to reduce the bulk further.

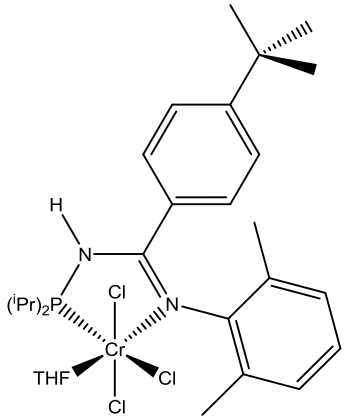

Figure 1.20 - The most effective PNN pre-catalyst described for ethylene trimerisation.

This appears to be the first highly selective ethylene trimerisation system based on a bidentate ligand system, suggesting the active complex may differ from that expected. For example, deprotonation of the amine may result in a tridentate donor or the THF present in the precatalyst could be retained. An additional pendent tertiary amine donor was incorporated to produce a defined tridentate complex. This resulted in a catalyst that was completely inactive towards oligomerisation and suggests that additional donation from the backbone may indeed occur in the activated catalyst.

One final catalyst system presented by Albahily *et al*. can also be considered to be an adaptation of the PNP catalyst due to the presence of a covalent P-N bond in the catalyst backbone.[121] However, the NPN catalysts presented are in truth very different because no phosphine donors are present. Despite this, catalysts synthesised by reaction of ^{t}BuNHP=N(2,6-diisopropylphenyl) with BuLi prior to complexation with $CrCl_2(THF)_2$ were found to be highly selective towards ethylene trimerisation, Figure 1.21.

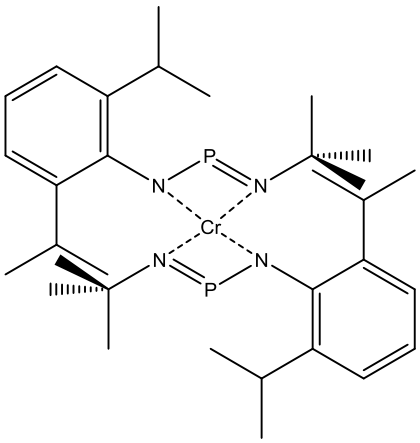

Figure 1.21 - The Cr^{II} precatalyst identified by single crystal X-ray diffraction.

Crystallographic investigation of the activation products indicated that the phosphorus of the backbone is alkylated and the ligands open up to bridge between two aluminium units and the chromium centre. The Cr^{II} product observed is unlikely to act as the active catalyst, however, and instead likely represents an activation intermediate. Overall the catalyst activities were very poor at an optimised 0.02 mol(C_2H_4) mol(Cr)$^{-1}$ h^{-1} but with high selectivities exceeding 90 w%.

Further work was conducted into alkylation of the phosphorus with the use of MeLi in an attempt to probe the active ligand system.[122] It was observed that a Cr^{III} species was formed with a partially solvated lithium ion rendering the complex electronically neutral. It is proposed that the presence of the reducing MeLi induces the disproportionation of the Cr^{II} as well as alkylating the ligand to give the product, though the corresponding Cr^{I} complex could not be identified. Unfortunately, when activated with MAO or Et_3Al these products produced a Shultz-Flory distribution of α-olefins on exposure to ethylene. A considerable shift was observed on activation with $RAlCl_2$ (R = Me, Et), whereby selective trimerisation was observed, though at even lower activities of less than 0.01 $mol(C_2H_4)\ mol(Cr)^{-1}\ h^{-1}$.

1.3.2.3 Bis(phosphino)amine and Bis(sulfanyl)amine Catalysts

At around the same time as progress was being made into the bidentate PNP ligand, several catalysts were being developed at Sasol based on tridentate bis(phosphino)amine ligands.[123] It was found that these ligands, in combination with $CrCl_3(THF)_3$ and MAO, were highly selective catalysts for the trimerisation of ethylene. The structures of various pre-catalysts have been analysed by single crystal X-ray diffraction and were found to feature the bis(phosphino)amines as meridional tridentate ligands, Figure 1.22. This differs from the highly active PNP and FI catalysts, which each feature facial coordination.

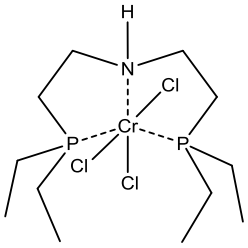

Figure 1.22 - The optimised bis(phosphino)amine trimerisation catalyst.

This catalyst was shown to be capable of producing 1-hexene at selectivities over 93 w% but at relatively low activities of 70,000 $mol(C_2H_4)\ mol(Cr)^{-1}\ h^{-1}$. Limited bulk on the phosphine substituents, ideally ethyl groups, demonstrated the best activity whilst phenyl or larger groups led to considerable deterioration. In analogy to the PNPNH ligand system it was found that replacing the N-H moiety with a tertiary amine led to almost complete loss of trimerisation activity.

The ligand structure was later altered in further work carried out by Alzamly *et al*. in which the secondary amine was replaced by a pyridyl group and the ethyl groups replaced by phenyl moieties.[124] This modification almost completely eliminated the selectivity of the prior system and instead resulted in a Shultz-Flory distribution of α-olefins with slight enrichment of the 1-hexene fraction. These systems are notable, however, for the lack of polymer produced, a common problem for non-selective systems.

Single crystal X-ray diffraction studies on the intermediates of both Cr^{II} and Cr^{III} ligated species demonstrated alkylation and cationisation by aluminium alkyls. A single crystal of a mononuclear Cr^{I} intermediate was also isolated, strongly suggesting the presence of monovalent chromium in the active catalyst solution. The authors propose that this may result from the parallel trimerisation mechanism. This observation would suggest the trimerisation reaction pathway for the pyridyl system differs from the more established secondary amine system in which a Cr^{II}/Cr^{IV} redox cycle is proposed. Such a non-selective system cannot be reliably studied for crystallographic intermediates of a trimerisation system, however, and as such the redox cycle of these systems remains unclear.

Based on the idea that the phosphines act as relatively weak donors and are likely to be quite labile, research was conducted into other weak donors, principally thioethers, Figure 1.23. Analogous catalysts were synthesised which demonstrated considerably better attributes for this process, with greater activities, lower equivalents of MAO required and more facile synthesis.

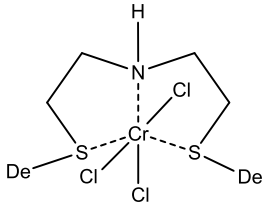

Figure 1.23 - The optimised bis(sulfanyl)amine trimerisation catalyst. De = Decyl.

The high solubility of the complex containing the decyl S-substituent resulted in improved activity over the ethyl analogue that, based on the bis(phosphino)amino results, would have been expected to perform best. Activation of this species with 30-100 equivalents of MAO led to activities in the region of 300,000 $mol(C_2H_4)\ mol(Cr)^{-1}\ h^{-1}$. Also, the selectivities observed for this catalyst are amongst the highest ever observed at over 98% 1-hexene. This represents a considerable improvement over the phosphine ligand system and remains one of the only examples of a highly active trimerisation catalyst which features sulphur donors.[125]

Further investigation of both systems showed that they could also be activated with $AlR_3/B(C_6F_5)_3$ to give catalysts with slightly reduced efficiency.[126] This method, in accordance with the observation that AlR_3 alone did not produce an active catalyst, demonstrated that a cationic species was responsible for catalysis. It was found that the effectiveness of the activator was related directly to the bulk of the ligand, with reduced bulk preferring MAO activation. This suggests that the interaction between the active species and the counter-ion is of key importance for these systems. Activation of some bulky SNS systems, such as $^{t}BuS(C_2H_4)NH(C_2H_4)S^{t}Bu$, with $AlR_3/B(C_6F_5)_3$ led to selectivities exceeding 99 w%.

This alternative activation route allowed for mechanistic studies to be carried out on this system and more specifically the oxidation state of the chromium centre.[126] Cr^{II} congeners were synthesised of the different pre-catalysts and tested for trimerisation under the same conditions. The activities and turnovers observed for these species were very similar to those of the Cr^{III} catalysts, indicating that a reduced species, either Cr^{I} or Cr^{II}, occurs during the catalyst cycle. It is hypothesised that the aluminium reagent may be capable of one electron reduction of the chromium species in order to access these oxidation states.

It was also found that synthesis of both Cr^{II} and Cr^{III} complexes with the deprotonated ligand resulted in pre-catalysts that demonstrated similar activities on activation. This suggests that deprotonation of the secondary amine is induced by the aluminium alkyl, as observed by Rosenthal *et al.*, to produce an anionic ligand. The complex must then, by implication, contain a Cr^{II} metal centre in order to maintain the cationic nature of the catalyst throughout the cycle. The evidence therefore points towards a Cr^{II}/Cr^{IV} redox cycle, contradicting the observations of other groups working on chromium based systems. The suggestion is therefore that the redox cycle may be dependent on the ligand environment, especially in the presence of an easily deprotonated ligand. However, it should be noted that this has been disputed by others based on similar species and non-catalytic conditions.[127]

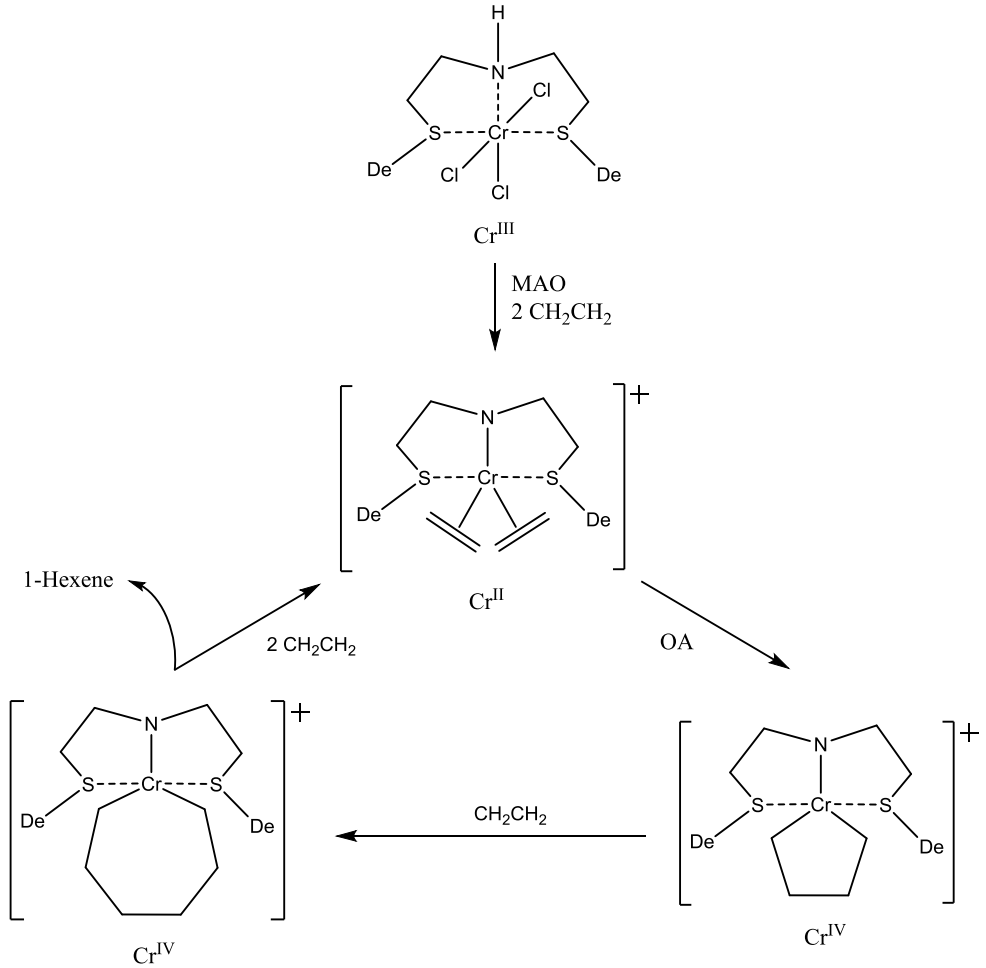

Scheme 1.36 - The proposed oxidation states for the optimised SNS catalyst. Counter-ions have been excluded for clarity. OA = Oxidative Addition. De = Decyl.

As with the original PNP catalyst the good activities and extremely high selectivities of these systems led to further research into their modification.[19] This was broadly focused on alteration of the donating atoms to test the effects. The majority of variations had a negative effect. Combinations of phosphorus and sulphur donors, or three of a kind, led to unstable complexes prone to ligand abstraction. This resulted in production of a Shultz-Flory distribution of oligomers similar to that of unligated chromium. Variation of the spacer length between the donors has also been explored but showed similar losses to selectivity.

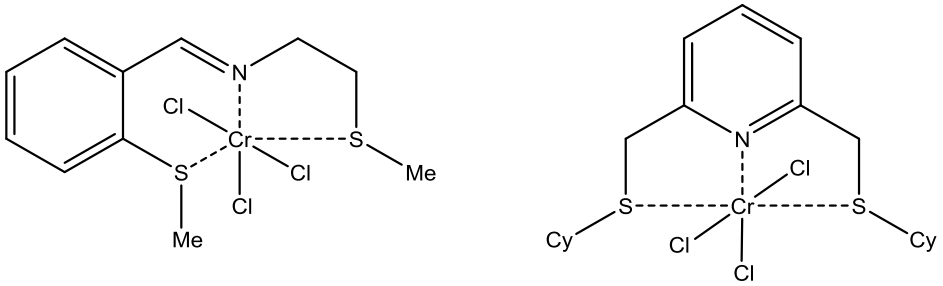

Figure 1.24 - Two of the more successful adaptations of the Bis(sulfanyl)amine ligand.

Some examples of alteration of the ligand, in which the nitrogen was retained, have displayed some limited success. For example, Gambarotta *et al.* explored the use of pyridyl donors to replace the secondary amine in much the same way as for the bisphosphino analogue, producing catalysts that demonstrate a TOF of approximately 30,000 mol(C_2H_4) mol(Cr)$^{-1}$ h^{-1}, Figure 1.24.[128] This is surprisingly high given the absence of the acidic proton that was thought to be essential for the activity. Bluhm *et al.* also explored the use of more strongly donating nitrogen donors with the application of imines as the central donor, Figure 1.24.[129] These catalysts performed less well, with TOFs of below 18,000 mol(C_2H_4) mol(Cr)$^{-1}$ h^{-1} and poor selectivity. Overall, adaptation of the bis(sulfanyl)amine and bis(phosphino)amine ligands has failed to produce catalysts of greater activity or utility.

1.3.2.4 Diphosphine Catalysts

The success of the PNP ligand resulted in considerable industrial research into alternative diphosphine ligands. This was led by Overett *et al.* at Sasol Technology who investigated a broad range of catalysts to determine the best bite angle, P-P alkyl bridging length and phosphine substituent bulk.[130] Methylene bridges were found to perform poorly but ethylene spacers gave some very active catalysts for selective oligomerisation. The effect of bite angle and substituent bulk was principally to switch the selectivity between tri- or tetramerisation.

Large bite angles and bulky substituents gave high selectivities for trimerisation, most likely due to prevention of the more sterically demanding intermediates of tetramerisation. Incorporation of labile donors such as methoxy groups into the phosphine substituents also favours trimerisation, as was the case for the PNP ligand.

Alteration of the electronic environment of the phosphine donors was also shown to have a considerable effect and resulted in by far the most active catalyst, Figure 1.25. A phenyl backbone, which conjugates the phosphines, gave extremely high 1-hexene and 1-octene activities (1-Hexene TOF = 3,300,000 mol(C_2H_4) mol(Cr)$^{-1}$ h^{-1} and 1-octene TOF = 7,300,000 mol(C_2H_4) mol(Cr)$^{-1}$ h^{-1}) but unfortunately demonstrated poor selectivity between them. This cheap, easily made and flexible range of ligands is therefore of intense commercial interest, though mainly for tetramerisation. This research also demonstrated that these readily available ligands can display comparable catalytic performance to the relatively expensive to synthesise PNP and FI based systems.

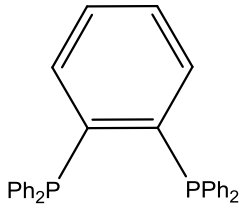

Figure 1.25 - The most active diphosphine ligand reported by Sasol.

This family of ligands was later taken forward by Zhang *et al.*, who looked at incorporating additional steric bulk into the preferred ethylene bridges.[131] Both saturated and unsaturated spacers were investigated that contained an alkyl substituent on one of the carbon atoms of the backbone, Figure 1.26. The unsaturated spacer proved to form a far more active catalyst system (1-$C_{6/8}$ TOFs of up to 4,800,000 mol(C_2H_4) mol(Cr)$^{-1}$ h^{-1}), in agreement with the observations of Overett *et al.*[130]

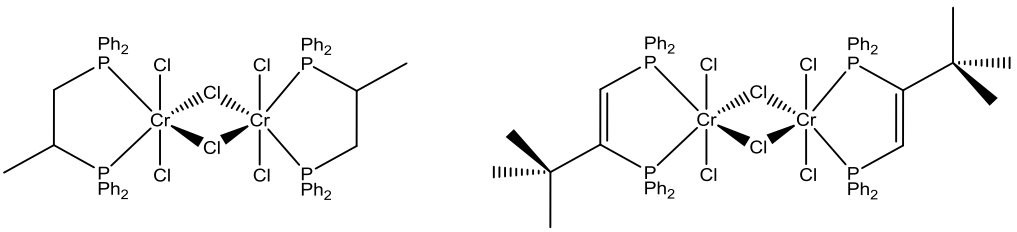

Figure 1.26 - The highly selective saturated tetramerisation pre-catalyst and the highly active unsaturated tri-/tetramerisation catalyst.

Polymer formation was limited for these systems and was typically less than 0.5 w%. However, the selectivity between 1-hexene and 1-octene was poor for the more active unsaturated ligands. The saturated ligand that contained only a methyl substituent demonstrated the highest overall tetramerisation selectivities at 65 w%.

The steric bulk within both ligand types played a significant role in their selectivity for either tri- or tetramerisation. The larger the alkyl moiety present in the spacer the more 1-hexene formation was favoured over 1-octene and usually the better the overall activity. The authors propose that, contrary to previous assumptions, it is the C^{Ph}-P-Cr bond angle rather than the bite angle which influences the selectivity. Crystallographic comparison with PNP and PCP catalysts demonstrates a considerably lower C^{Ph}-P-Cr angle for the highly active unsaturated systems. Based on other comparative studies, this property would appear more likely to induce the shifts in selectivity observed. The improved activity on incorporation of greater steric bulk is attributed to greater catalyst stability.

1.3.2.5 NNC Catalysts

Alternative chromium catalysts have moved away from the sulphur and phosphorus donors which dominate the field of olefin trimerisation. Recently, Enders *et al.*, following up on original work by Ackerman *et al.*,[132] published a ligand containing a carbon donor as part of a tridentate system, Figure 1.27.[133] This also allowed synthesis of bidentate analogues to investigate whether the denticity of the ligand plays a significant role in catalysis.

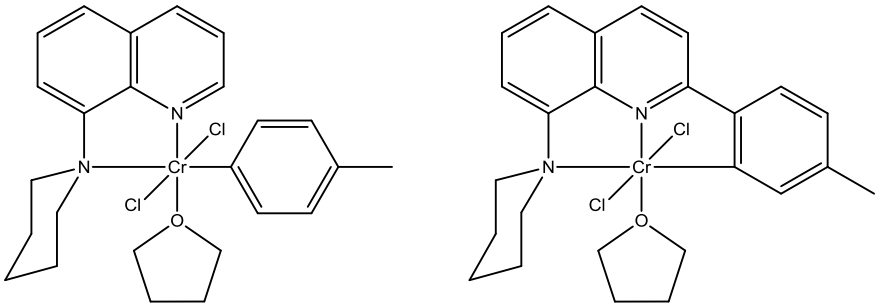

Figure 1.27 - Example catalysts from each of the two classes explored by Enders *et al.*

Both classes of catalyst produced 1-hexene at peak activities of around 50,000 mol(C_2H_4) mol(Cr)$^{-1}$ h^{-1} for optimised systems and at selectivities of up to 85 w%. The denticity of the ligand was therefore shown to have minimal effect on catalysis in this case, though this may be due to the unusual nature of the aryl donor. For this system it was discovered that a considerable improvement in activity was observed when $MeCrCl_2(THF)_3$ or (*o*-tolyl)$CrCl_2(THF)_3$ was used as the chromium source. The improvement was attributed to facilitation of the activation procedure and did not affect the overall selectivity.

The products of activation were also analysed for this catalyst type with the use of the bidentate ligand and with all three chlorides replaced by tolyl groups. This was achieved through reaction with Grignard reagents to give a rare square-pyramidal geometry. This species thermally decomposed to form 4,4'-dimethylbiphenyl as the sole organic product, excluding the ligand, indicating that C-C bond forming reductive elimination is possible for certain chromium systems. A similar experiment in the presence of ethylene produced 4,4'-dimethylbiphenyl as well as 4-methylstyrene, demonstrating the ability of ethylene to coordinate and insert into the Cr-tolyl bond.

In the presence of MAO, trimerisation was observed as expected, indicating the active species was successfully formed. In this case no 4,4'-dimethylbiphenyl or 4-methylstyrene were observed and instead a range of products representing further insertion of ethylene were observed, as shown in Figure 1.28. The authors hypothesise that the C_{11} compounds result from Cossee-Arlman chain growth after insertion of the original ethylene molecule. The C_{13} products are attributed to insertion of 1-hexene into a Cr-tolyl bond for the internal alkene and three ethylene insertions for the terminal alkene. However, it appears that these products would be better explained by metallacyclic co-trimerisation of two ethylene molecules with one 4-methylstyrene unit.

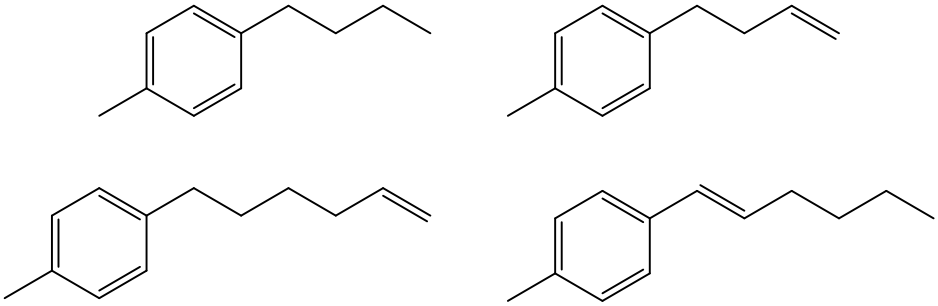

Figure 1.28 - The four tolyl-containing products identified after $Cr(tolyl)_3$ catalyst activation.

1.3.2.6 Solely Nitrogen-Based Catalysts

In an attempt to selectively tetramerise ethylene, Gambarotta *et al.* developed a dipyridyl ligand in which the two heterocyclic rings are bridged by a tertiary amine. It was found by single crystal X-ray diffraction that the tertiary amine is not involved in the coordination, such that the ligand binds in a bidentate manner with one THF group retained after synthesis from $CrCl_3(THF)_3$, Figure 1.29. Overall, these catalysts proved to be ineffective due to the production of a considerable quantity of low molecular weight polyethylene alongside 1-octene.

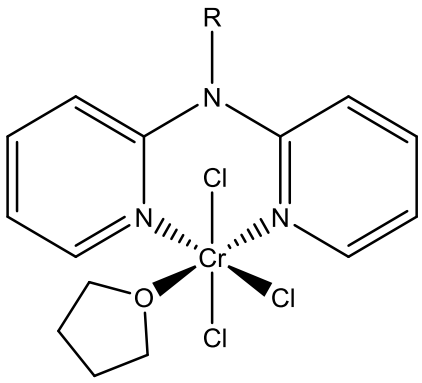

Figure 1.29 - The coordination mode of the dipyridyl ligand in the pre-catalyst.

From a mechanistic perspective, it was found that accessing the active species *via* a divalent chromium source led to no activity at all, indicating that Cr^{II} plays no role as an intermediary in this system. The authors also explored the effect of steric influence on the system by introducing a methyl group at the *ortho*- and *para*-position of the pyridyl donors. Catalysts with *ortho*-substitution produced 1-hexene at high selectivities, indicating that sterics play a key role in selectivity. Meanwhile, *para*-substitution led to 1-octene and polymer being produced in much the same way as the un-substituted catalyst. It is clear therefore that it is a steric rather than electronic effect.

Research has also been performed into NNN tridentate donors which bind in a facial manner rather than the meridional orientation observed for the bis(phosphino)amine and bis(sulfanyl)amine ligands. The best among them are heteroscorpionate or 'tripod' type systems based on pyrazolyl donating groups that are each bound to a central carbon atom. A series of symmetrical systems containing a variety of dialkylated pyrazolyl groups was first investigated by the Tosoh Corporation.[134] Of these, the least bulky ligand, tris(2,5-dimethyl-1-pyrazolyl)methane, led to the most effective catalyst on complexation of $CrCl_3(THF)_3$ and activation with MAO. The trimerisation activity for this system was moderate at approximately 75,000 mol(C_2H_4) mol(Cr)$^{-1}$ h^{-1} but this was compensated by the >99 w% 1-hexene selectivities observed, the best achieved to date.

More recently, Hor *et al.* have investigated these systems further by replacing one of the pyrazolyl groups with alternative donors.[135, 136] The focus of this research was the use of ethers, thioethers and various forms of nitrogen donor in the third position. Ethers proved to be more effective than thioethers and produced a catalyst that demonstrated activities of up to 39,000 mol(C_2H_4) mol(Cr)$^{-1}$ h^{-1}.[136] However, the alternative heterocyclic nitrogen donors were considerably more effective and use of an imidazolyl donor produced the most active catalyst at 98,000 mol(C_2H_4) mol(Cr)$^{-1}$ h^{-1}, Figure 1.30.[135] Importantly, substitution of one of the pyrazolyl groups did not lead to any considerable reduction in selectivity, with >97 w% achieved in each case. These tri-nitrogen catalysts marked a shift away from the more established systems in which a labile donor is present.

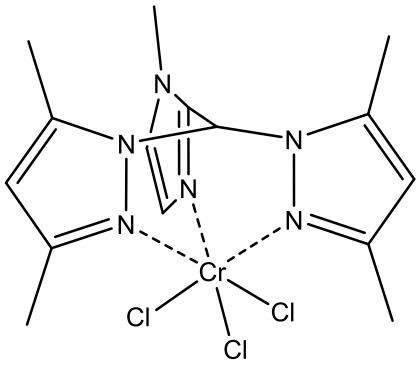

Figure 1.30 - The Bis(pyrozolyl)imidizolylmethane based chromium pre-catalyst.

A related system based on triazacyclononanes was patented by Wu *et al.* that demonstrated some limited enrichment of the C_6 fraction of a Shultz-Flory distribution of α-olefins.[137] The catalyst could either be formed *in situ* or prior to reaction and activation was achieved, unusually, with n-hexylaluminoxane. Increasing the bulk of the ligand and removing the ligand acidity by alkylation of the secondary amines was found to reduce polymerisation to very low levels. This bulky ligand system constitutes the only other example, outside of triazacyclohexane ligands, of a tri-nitrogen facially coordinated chromium chloride pre-catalyst.

The strong performance obtained for the heteroscorpionate species demonstrates the potential for facially bound tridentate nitrogen ligands for ethylene trimerisation. It is also notable that, despite the similarity to triazacyclononane ligands, its performance is vastly superior. An amine donor was trialled in the third position of the heteroscorpionate system resulting in a massive reduction in activity.[135] This suggests that relatively weakly bound facially coordinating ligands with a low steric bulk around the metal centre offer considerable potential for selective trimerisation. Further investigation into this type of ligand was undertaken by Köhn *et al*. with the use of triazacyclohexanes.

1.3.2.7 Other Chromium Trimerisation Catalysts

The catalysts discussed throughout this chapter constitute the most active and selective homogeneous systems as well as those that have been used for mechanistic studies. In addition to these, there have been numerous less active and ill-defined catalysts, in which the pre-catalyst is formed *in situ*, described in the literature that have been found to trimerise ethylene.

An adaptation of the Phillips catalyst in which the 2,5-dimethylpyrrole ligand was replaced by a maleimide ligand proved to be a moderately effective replacement and achieved activities of nearly 550,000 mol(C_2H_4) mol(Cr)$^{-1}$ h^{-1}, Figure 1.31. Selectivities were less impressive however at just under 80 w% 1-hexene. During testing of this system it was found that alternative inorganic chlorides, such as $GaCl_4$, also produced the 'halide effect'.[138]

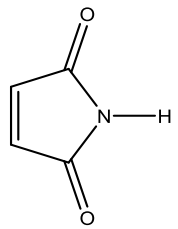

Figure 1.31 - The maleimide ligand.

Another simple adaptation of the Phillips trimerisation catalyst carried out by Licciulli *et al.* involved increasing the bulk of the pyrrole by replacing the methyl groups with *tert*-butyl moieties at the same position.[139] Deprotonation of the ligand followed by addition of $CrCl_3(THF)_3$ and activation with $AlEt_3$ gave a 91 w% selective system with an activity of nearly 110,000 mol(C_2H_4) mol(Cr)$^{-1}$ h^{-1}. There is therefore a considerable detrimental effect associated with increasing the bulk around the nitrogen atom.

The use of this ligand did allow for several structures to be elucidated by single crystal X-ray diffraction however. The key observation as a result of extensive crystallographic analysis of catalytic intermediates was that the pyrrolide binds facially through the π-system rather than through the nitrogen. This has considerable consequences for the proposed mechanism of the Phillips system, which has traditionally been thought to feature nitrogen bonding. Interestingly, only one species in which the chromium occupied the Cr^{II} oxidation state featured nitrogen bonding. This suggests that such binding could lead to catalyst decomposition as regards trimerisation or even form an active polymerisation catalyst.

Duchateau *et al.* went further in adapting the original 2,4-dimethylpyrryl ligand by incorporating fused phenyl and cyclohexyl rings, Figure 1.32.[140] *In situ* catalyst formation from a $Cr(octanoate)_3$ chromium source and Et_2AlCl activation produced a 93 w% selective system capable of trimerising ethylene at an activity of around 7500 $mol(C_2H_4)\ mol(Cr)^{-1}\ h^{-1}$. Single crystal X-ray analysis of the pre-catalysts formed indicated that several coordination modes are possible with this ligand. Nitrogen, η^6 phenyl and η^5 pyrryl donation were all observed under different conditions.

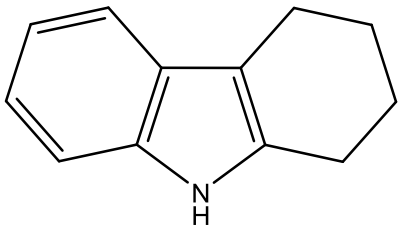

Figure 1.32 - The fused ring ligand structure capable of various coordination modes.

The authors hypothesise that these different binding modes lead to stabilisation of a variety of oxidation states, which in turn determine the catalytic process. It is proposed that Cr^{I} systems lead to trimerisation, Cr^{II} systems lead to polymerisation and Cr^{III} systems lead to non-selective oligomerisation. This was supported by observation of considerably higher levels of polymerisation for systems in which it was known that nitrogen donation led to stabilisation of divalent chromium.

Cyclopentadienyl ligands were of natural interest to oligomerisation due to their wide application to polymerisation systems. It was discovered at Sasol Technology that these usually entirely non-selective catalysts could be tuned towards trimerisation by incorporation of bulky substituents onto the ligand.[141] The use of a $CpPh_4(4\text{-}^tBuPh)$ ligand alongside $Cr(2\text{-}Ethylhexanoate)_3$, $AlMe_3$ and hexachloroethane was found to give a 77 w% selective trimerisation catalyst at activities up to 110,000 $mol(C_2H_4)\ mol(Cr)^{-1}\ h^{-1}$.

Another ligand type that has been adapted to trimerise rather than polymerise ethylene is diimine-containing ligands.[142] In much the same way as for the cyclopentadienyl catalysts the introduction of significant bulk into the N-substituents resulted in the switch in reactivity, Figure 1.33. $Cr(2\text{-Ethylhexanoate})_3$ and $AlMe_3$ were again used as chromium source and activator, with bromoalkanes employed as selectivity enhancing additives. These 58 w% selective systems proved less suitable for adaptation to trimerisation, with activities not exceeding 40,000 $mol(C_2H_4)$ $mol(Cr)^{-1}$ h^{-1}.

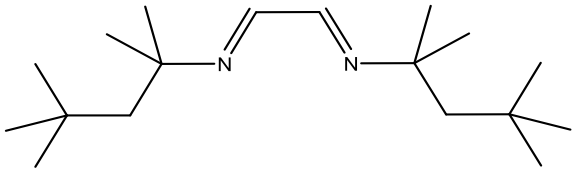

Figure 1.33 - An example of a diimine ligand capable of trimerisation.

So-called aryloxide systems are more unusual in that the 'ligand' constitutes a phenol derivative which has been shown to be deprotonated by the trialkylaluminium activator and bound as an aryloxide.[143] Nevertheless, the up to 83 w% selective systems demonstrated activities in the order of 50,000 $mol(C_2H_4)$ $mol(Cr)^{-1}$ h^{-1}. By far the best efficiencies were demonstrated when anisole was used as a solvent, however, indicating that this may in fact act as the ligating species.

The vast majority of trimerisation systems developed to date have been homogeneous in nature. A number of the catalysts already described have been deposited onto silica and retained their activity towards trimerisation, though in each case this has led to reduced selectivity and more prevalent polymer formation. The Phillips,[70] PNP[144] and maleimidyl[138] catalysts have all been explored as heterogeneous systems in this manner.

To the best of my knowledge, only one heterogeneous system has been described which does not lose activity and/or selectivity when deposited onto a silica support. $Cr[N(SiMe_3)_2]_3$ catalysts, activated by *iso*-butylaluminoxane, have been investigated in homogeneous systems but, while 75 w% selective, displayed low activities of around 2000 $mol(C_2H_4)$ $mol(Cr)^{-1}$ h^{-1}.[145] Despite this poor performance, these catalysts were applied to a heterogeneous system by supporting the catalyst onto silica and then calcining the product at 600 °C.[146] This procedure led to a considerable improvement in activity, reaching 110,000 $mol(C_2H_4)$ $mol(Cr)^{-1}$ h^{-1} without any loss in selectivity and no polymer production. It was also discovered that selectivities could be increased to just over 86 w% with the use of diether additives in much the same way as for the system discovered by Briggs.[76]

1.4 Triazacyclohexanes as Ligands

Following on from the highly selective NNN heteroscorpionate systems reported by Hor *et al.* research into tri-nitrogen facially binding tridentate ligands was pursued by Köhn *et al.*[2, 135, 147] This work was based on the use of 1,3,5-trisalkyl-1,3,5-triazacyclohexane (R_3TAC) ligands, which are well-established and readily synthesised.

The formation of R_3TACs from the condensation of primary amines with formaldehyde has been known since 1895.[148] Since then it has been found that numerous alkyl and aryl amines can form these structures, which are arranged in the chair conformation. Typically, the most stable arrangement of the alkyl substituents is such that two occupy equatorial positions and one axial (eea), Figure 1.34, although there are some exceptions, such as Bz_3TAC (eaa) for example.[149, 150]

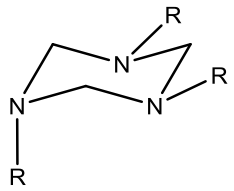

Figure 1.34 - The most stable conformation of the free 1,3,5-trisalkyl-1,3,5-triazacyclohexane ligand. R = linear alkyl.

In solution, however, it is observed by ^{1}H NMR spectroscopy that the protons of the heterocycles are all equivalent. This indicates that ring-flip and nitrogen inversion occur on the NMR time-scale such that a broad peak is observed, rather than the four environments that would be expected otherwise, Scheme 1.37.[151]

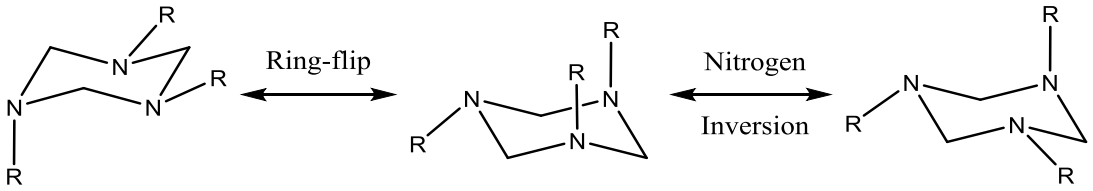

Scheme 1.37 - The rapid conformational changes of TAC compounds in solution. R = alkyl.

Species of this type have been of considerable interest since the second world war when 1,3,5-trisnitro-1,3,5-triazacyclohexane (RDX or Hexogen) was exploited as a powerful explosive. Its stability in air and resistance to shock, in combination with its explosive velocity greatly exceeding that of TNT and other established explosives, led to its widespread adoption.[152] This particular species and adaptations of it are still the focus of a considerable amount of research to this day.[153, 154]

TACs were first applied as ligands in 1959, with several molybdenum and chromium carbonyl compounds characterised by IR spectroscopy.[155] Limited detailed experimentation was carried out, however, until the 1990s when Fuchs *et al*. (Cu),[156] Schumann (Mo),[157] and Baker *et al.* (Mo, W, Cr)[158-164] began research into its complexation to a variety of metal carbonyl species. The results of these groups show that R_3TACs bind facially to group 6 metals to form stable κ^3 complexes. In contrast, Fuchs *et al.* showed that Cu is bound on a κ^1 basis and that the R_3TAC can act as a bridging ligand. A range of other metals have since been complexed with R_3TAC ligands to give a variety of coordination modes. Ti,[165, 166] Y,[167] La,[167] Sm,[167] Pr,[168] Re,[169] Ge,[170] Sn,[170] Sc[171] and Ca[172] have each been shown to adopt the κ^3 coordination mode, while lithium is capable of either κ^3 or μ^3-κ^1.[173]

The unusual co-ordination behaviour, namely the ability to switch between acting as a mono-, bi- or tridentate ligand via ring-slip, is due to the fixed orientation of the nitrogen lone pairs, Figure 1.3. Unpublished computational studies have shown that the predicted activation energy for ring-slippage is relatively low. This is explained by the increased orbital overlap achieved by ring-slip from κ^3 to either κ^2 or κ^1. The binding mode adopted appears to be almost entirely dependent on the metal centre rather than the ligand itself.

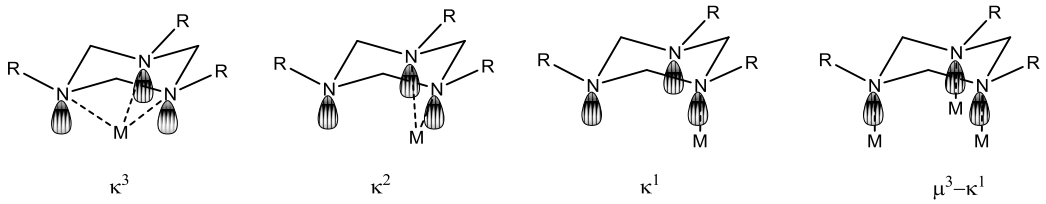

Figure 1.35 - The possible co-ordination modes of triazacyclohexanes ligands. R = alkyl, M = metal. The co-ordinations possible are dependent on the metal.

The majority of research was based on the use of Me_3TAC ligands until Baker *et al*. demonstrated that facile variation of the pendent arms could add further functionality and alter the ligand bulk.[158, 174] During this research it was also demonstrated that exposure of an $(R_3TAC)MCl_3$ complex to an excess of uncoordinated R'_3TAC led to a ligand exchange equilibrium, clearly demonstrating the lability of TAC ligands. Meanwhile, Fuchs *et al*. demonstrated the synthesis of unsymmetrical Me_2HTAC ligands, leading to different coordination characteristics and reactivity. It was also found during this synthetic work that modification of the ligand was possible '*a postieri*' (post-complexation) without any loss of or effect on the bound Cu.

At around the same time Köhn *et al*. synthesised and characterised TAC complexes of both $CrCl_3$ and $FeCl_3$ for the first time.[175] Using Me_3TAC and $^iPr_3$TAC ligands, κ^3 complexes were synthesised from $CrCl_3(THF)_3$ and directly from $FeCl_3$. The structure of $(Me_3TAC)FeCl_3$ was observed by single crystal X-ray diffraction to be highly symmetrical, with all alkyl substituents equatorial (eee), and Fe-N 'bend-bonding' interactions all measured at 2.25Å.

The ‘bend-bonding’ coordination is proposed to occur because the orbitals are constrained to a parallel orientation, relative to one another, by the ring strain of the ligand. The orbital interaction between metal and ligand is therefore analogous to that of cyclopentadienyl complexes, though ligation is far weaker for TAC compounds due to the absence of ionic attraction. The weak binding is also ascribed to the rigidity of the complexed TAC ring preventing orbital alignment, this is supported by comparison with triazacyclononanes (TACNs).

In TACNs the ethylene bridges between each nitrogen donor introduce considerable flexibility into the ring and allow full alignment of the nitrogen lone pairs with the metal, Figure 1.36.[176] This leads to chromium complexes in which it is significantly more difficult to substitute or remove the ligand. Despite the difference in binding energies, the average Fe-N bond lengths are almost identical for $(Me_3TAC)FeCl_3$ (2.25Å) and $(Me_3TACN)FeCl_3$ (2.25Å).[177] Though it should be noted that the TACN species is not completely symmetrical like the TAC system, with variation of approximately 0.03Å between Fe-N bonds. The key structural difference is instead the N-M-N bond angle which increases markedly from 65.9° for $(Octyl_3TAC)CrCl_3$ to 82.4° for $(Bu_3TACN)CrCl_3$ for example.[2, 178]

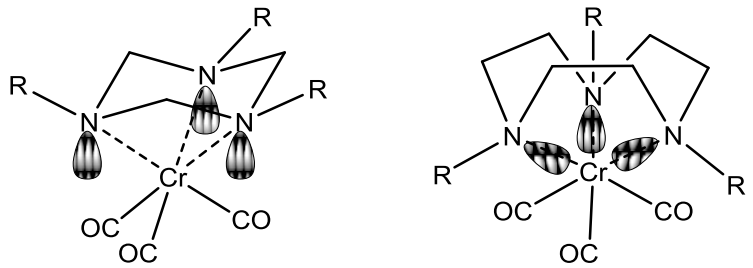

Figure 1.36 - Comparison of the nitrogen lone-pair orientations of κ^3 TAC and TACN ligands. R = alkyl.

Further research by Köhn *et al.* led to modification of the N-substituents to produce more strongly binding higher denticity ligands or incorporate greater functionality. The use of methylpyridene N-substituents, for example, was found to completely alter the coordination chemistry towards copper(II) chloride because of the stronger pyridyl donors.[179] The ligand remained tridentate but single crystal X-ray diffraction showed a meridional coordination with two pyridyl donors and one TAC donor.

In this work, the facile synthesis of unsymmetrical $R'R''_2TACs$ was demonstrated by the reaction of paraformaldehyde with a mixture of two amines, of which $R''NH_2$ is in significant excess. The statistical mixture produced could be separated by column chromatography to give $(PyCH_2)Et_2TAC$ in this case. Remarkably, reaction of this ligand with copper dichloride resulted in bidentate coordination and the formation of chloride bridged dimers. This clearly demonstrates the unfavourable nature of κ^3 TAC binding in the presence of stronger donors.

By contrast, reaction of donor functionalised TACs with copper(I) chloride results in highly stable halide bridged tricopper clusters. Such clusters are present in important enzymes such as copper oxidases and were first reproduced synthetically, with the use of triazacyclohexanes, in 2002 by Kickelbick *et al.*[180] Ester and tertiary amine pendent donors stabilised the κ^1 coordination of Cu^I with bromide bridges in an equidistant triangular arrangement, as observed in nature. The insolubility of these compounds hindered full spectroscopic analysis, leading Köhn *et al.* to investigate the use of a variety of thioester pendents and alternative halides.[181]

Highly soluble tricopper complexes were successfully synthesised with the use of branched alkyl or aryl substituted thioesters that allowed improved analysis of the compounds, Figure 1.37. It was also shown that halide substitution was facile to produce chloride and iodide bridged species without any effect on the ligand.

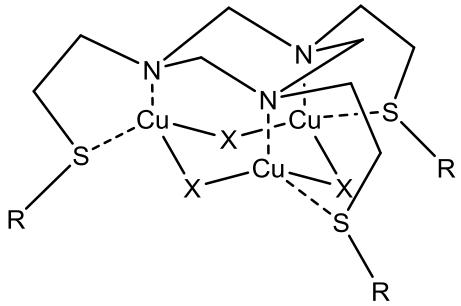

Figure 1.37 - The general structure of the tricopper clusters formed by TAC ligands with thioester pendent donors. X = Halide, R = branched alkyl or aryl.

Later work with copper by Köhn *et al.* demonstrated the first example of bidentate coordination of a non-functionalised TAC ligand.[182] A dinuclear Cu^I sandwich compound was formed on reaction of Bz_3TAC with $[Cu(MeCN)_4][BF_4]$ to give a μ^2-κ^2 coordination mode. Exposure of this species to air resulted in oxidation of the metal centre and formation of a Cu^{II} sandwich compound, $[(Bz_3TAC)_2Cu][BF_4]_2$, the first such complex of a transition metal. Analogous chemistry was also demonstrated with zinc, with the sandwich compound again formed on oxidation to Zn^{II}. Coordination of the TAC ring is unsymmetrical due to Jahn-Teller distortion and demonstrates the potential for ring slip towards lower denticities, Figure 1.38.

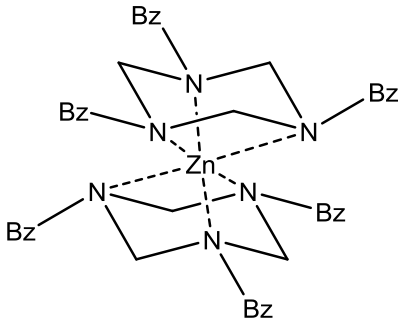

Figure 1.38 - The isolated Zn^{II} sandwich complex.

The constrained nature of the nitrogen donors within the triazacyclohexane presents an interesting ligand system. The acute N-M-N bond angle results in low steric bulk and a very open environment around the metal centre. Meanwhile, the poor orbital overlap results in a highly labile ligand stabilised principally by the chelate effect rather than coordination strength. The ability of the ring to slip and adopt a new denticity also suggests considerable promise for catalytic application due to the potential availability of a vacant site. Such behaviour could lead to unstable systems but it has been shown that larger alkyl substituents increase the stability of TAC complexes, most likely due to kinetic hindrance to substitution, potentially offsetting the risks of decomposition.[183]

Importantly, it was also discovered that the ($^{i}Pr_3TAC$)$CrCl_3$ complex could be dialkylated with Me_3SiCH_2Li without any adverse effect on the ligand.[175] Complete alkylation has also been demonstrated on reaction of benzyl sodium with (Cy_3TAC)$CrCl_3$ to give a species of comparable structure to alkylated chromium Cp complexes.[184] This opened up the possibility for these species to be used as catalysts, particularly for oligomerisation and polymerisation, as this is often one of the activating steps.[19]

1.5 Chromium Triazacyclohexane Complexes in Catalysis

To the best of my knowledge only Köhn *et al.* have applied triazacyclohexane ligands to catalysis with the exception of Nenu *et al.*, who demonstrated a near stoichiometric ethylene trimerisation catalyst with a TON of less than 10. The system was also moderately active towards ethylene polymerisation.[185-187] This single site heterogeneous chromium catalyst presents very poor trimerisation activities and selectivities, potentially indicating that heterogenising TAC based catalysts has a devastating effect on trimerisation activities. Further conclusions are difficult based on the poor performance of the system and the fact that their system is derived from the highly active Phillips catalyst. The low activity observed could therefore be a result of residual active catalyst.

During early investigations into the coordination chemistry of Me_3TAC it was discovered that sandwich complexes of praseodymium(III) triflate could be synthesised in high yield, Figure 1.39.[188] Due to the high lewis acidity expected, this highly sensitive compound was tested as a lactide polymerisation catalyst.[189] It was discovered that the complex was indeed active, recording total lactide conversions of >95%, and producing polylactide of high molecular weight (18,000 amu). Unfortunately the catalyst demonstrated a relatively poor polydispersity index (PDI) at over 2.2. However, it was shown that the presence of the TAC ligands was essential to the activity, as $Pr(OTf)_3$ alone performed poorly.

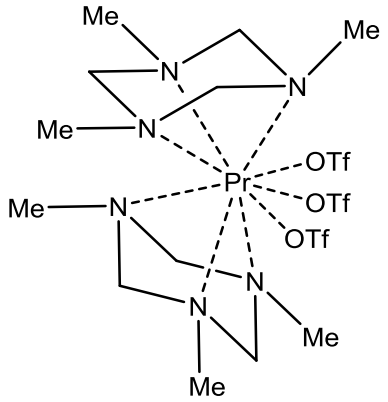

Figure 1.39 - $(Me_3TAC)_2Pr(OTf)_3$, an active lactide polymerisation catalyst.

Aside from the work on lactide, Köhn *et al.* focused on chromium complexes based on 1,3,5-trisalkyl-1,3,5-triazacyclohexanes as models for the heterogeneous Phillips polymerisation catalyst described earlier.[147] The mechanism and the intermediates of the catalyst cycle are poorly understood and as such there has been considerable research into defined homogeneous models. The unusual selectivity of the catalyst had previously proven difficult to replicate due to the proposed presence of both the Cossee-Arlman and metallacyclic mechanisms.

$(R_3TAC)CrCl_3$ catalysts featuring linear alkyl N-substituents were shown by Köhn *et al.* to be active ethylene polymerisation systems that accurately reproduce the selectivity of the heterogeneous system.[147] While the molecular masses of the products differ, suggesting a greater rate of chain transfer or catalyst decomposition, other properties are very similar to the commercial product. Principally, the various olefinic terminal groups observed for the Phillips polymer were observed at a similar abundance. In addition, butyl side chains were found to be present in the TAC produced polymer, indicating that both trimerisation and polymerisation mechanisms occur in tandem. As such, it was discovered that TAC based complexes also demonstrate the ability to trimerise ethylene to 1-hexene. The especially broad PDI of the commercial system was also successfully replicated, such that the $(R_3TAC)CrCl_3$ system proved to be an impressive homogeneous model.

The best of the TAC catalysts, incorporating n-dodecyl N-substituents, demonstrated polymerisation activities of over 25,000 $mol(C_2H_4)\ mol(Cr)^{-1}\ h^{-1}$. The activity was found to rise with increasing N-substituent chain length and as such was likely linked to solubility. Catalyst activation was best achieved with 300 equivalents of MAO but was also shown to be possible with DMAB and 20 equivalents of $^{i}Bu_3Al$. The activity of this system far outstripped the performance of any other non-cyclopentadienyl alternative. In fact, only one model was known to exhibit greater activity at the time of publishing and featured less accurate replication of termination groups. The strong performance of this novel catalyst led to its protection in patents by BASF.[190]

In much the same way as for the original discovery, the observation of trimerisation led to future investigations being focused on this new field of research. An overview of the work by Köhn *et al.* towards the selective trimerisation of ethylene is provided in Chapter 5.

1.6 Summary

This comprehensive review into selective oligomerisation provides a detailed account of the progress made towards the specific synthesis of linear α-olefins from ethylene. Particular attention has been paid to the catalysts that induce these transformations and the mechanisms by which they occur. A wide range of catalysts have been exploited within this field that incorporate a range of transition metals and ligand designs.

Dimerisation of both ethylene and LAOs is now well established and has been commercialised as the Alphabutol process with the use of titanium alkoxide catalysts. The mechanism by which this selective oligomerisation occurs remains poorly understood, with systems described that demonstrate both metallacyclic and chain-growth mechanisms. Selective trimerisation and later tetramerisation of ethylene have become increasingly intensively researched as demand for 1-hexene and 1-octene continues to increase. As a result, a broad range of ligand designs have been applied to chromium and titanium to give highly active systems.

In relation to the work described herein the trimerisation of ethylene is most relevant. Therefore, the results reported for 1-hexene trimerisation systems have been collated in Table 1.2 in order to allow facile comparison of the most impressive systems.

Table 1.2 - A selection of the optimised activities and selectivities of each major catalyst type discussed. The ligand abbreviations are those used by the original author.

Ligand Abbreviation	Transition Metal	Activity (TOF)	Selectivity (w%)
FI	Ti	11,250,000	92
Phillips	Cr	6,300,000	95
PP	Cr	3,300,000	25
PNN	Cr	1,800,000	94
PNP	Cr	1,700,000	90
PNPO	Cr	550,000	85
SNS	Cr	300,000	98
CpAr	Ti	225,000	86
PNPNH	Cr	130,000	87
NNN	Cr	100,000	97
NNC	Cr	50,000	83
Cl_5	Ta	2,500	96

It can be seen that the commercialised Phillips catalyst has only been surpassed to date by the (FI)$TiCl_3$ system, which demonstrates extremely high activities and goes against the established view that chromium catalysts are most effective. Diphosphine donors then make up the remaining catalysts that demonstrate TOFs of over 500,000. The remaining systems are more varied and have struggled to achieve such a high performance despite considerable optimisation in some cases. The work described herein is based on the use of (R_3TAC)$CrCl_3$ catalysts, which are similar in structure to the NNN heteroscorpionate systems. It is hoped, therefore, that these systems can improve on the current record of nitrogen based ligands and compete with the phosphine based catalysts.

A critical overview was also presented into the proposed mechanisms that account for each of the selective tri- and tetramerisation reactions. The vast majority of ethylene trimerisation catalysts are proposed to proceed *via* a metallacyclic mechanism for which considerable evidence has been obtained. Meanwhile, the mechanism that accounts for ethylene tetramerisation is poorly understood and continues to be intensively researched, though the consensus is for a metallacyclic mechanism of some sort. However, significant questions remain around the oxidation states, resting state and intermediates of selective oligomerisation catalysis. This has prompted further mechanistic investigations into this rapidly expanding field.

2. Chromium Catalysed Linear α-Olefin Trimerisation

During research into ethylene trimerisation Köhn *et al.* also discovered that the same TAC catalysts are capable of trimerising the 1-hexene produced, the first time this had ever been observed.[2] Several patents have since been claimed into this novel process.[191, 192] This is due to potential applications in the production of oxo-alcohols for surfactant production,[6] as well as automotive lubricants or fuels.[3] A collaborative project with Wasserscheid *et al*. into lubricants followed, which showed that the viscosity indexes (an important factor for the efficiency of lubricants relating to viscosity change with increasing temperature) of the trimers were better than the commercial alternatives.[3]

The first α-olefin trimerisation system was based on (Dodecyl$_3$TAC)$CrCl_3$ activated with 100 equivalents of MAO. Turnover numbers of around 700 were achieved and it was shown that the catalyst could be applied to propene, 1-hexene and even styrene without any polymerisation being observed. The system was also highly selective, no trimerisation or alternative reactivity was observed in the presence of internal olefins or conjugated dienes. Application of the system to donor-functionalised α-olefins led to rapid decomposition of the catalyst.

Investigation of analogous complexes confirmed the specific reactivity of (R_3TAC)$CrCl_3$ complexes. (R_3TAC)VCl_3 complexes were synthesised as part of this work because of the similar reactivity of vanadium and chromium species, with the exception of redox processes. It was found that no activity was observed for the vanadium complex, indicating that the catalysis does indeed proceed through a redox cycle. (R_3TACN)$CrCl_3$ complexes were also synthesised and applied to catalysis under the same conditions but again the adaptation showed no activity towards trimerisation. This was attributed to the larger steric bulk of this ligand hindering the reaction and reaffirms the importance of the small N-Cr-N bond angle of TAC compounds.

This work was taken forward with a more detailed analysis of the effect of ligand bulk and N-substituent branching. It was found that branching greatly improved the solubility and in turn the activity of the catalyst. ((2-Ethylhexyl)$_3$TAC)$CrCl_3$, featuring β-branching, proved to be the most effective catalyst and recorded turnover numbers in excess of 1000. On the other hand, methyl branching at the α-position resulted in a considerable drop in turnover number, with almost no activity observed when two methyl groups were present at this position.

Decomposition of the catalyst was shown to be highly dependent on temperature, with all studies carried out at 0 °C in order to minimise this. Kinetic studies indicated a considerable activation period of up to 30 minutes occurred, with the reaction complete after approximately 5 hours. The rate of reaction did not appear to be affected by ligand bulk except for those doubly branched at the α-position, suggesting steric hindrance. The similarity in the rate of trimerisation for the other catalysts indicated that lower turnover numbers likely resulted from issues with decomposition or solubility over time.

Since the original discovery only one other system has been found to demonstrate highly selective α-olefin trimerisation.[193] Interestingly, the catalyst used by Bercaw *et al.* is based on titanium rather than chromium and is much bulkier than the R_3TAC catalysts.

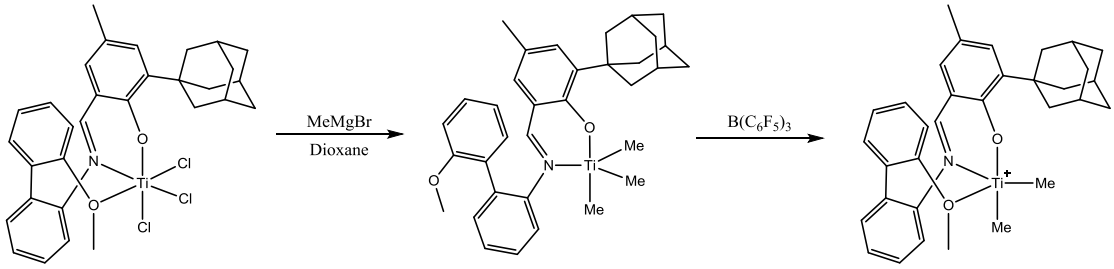

Scheme 2.1 - The two-step activation procedure of $[(FI)TiMe_2][MeB(C_6F_5)_3]$. The borate counter-ion has been removed for clarity.

The pre-catalyst, $(FI)TiCl_3$, was first discovered by Fujita *et al*. and applied to the trimerisation of ethylene, as described in Chapter 1.[91] The system had a significant restriction however in that it required up to 10,000 equivalents of MAO to get the best performance. This work explored potential methods of avoiding such an expensive activation procedure and discovered a more cost-effective stoichiometric pathway.

Using a two-step process it was found that alkylation is possible with three equivalents of methylmagnesium bromide to form a stable complex, the structure of which was determined as 5-coordinate by X-ray crystallography. One of the methyl groups can then be abstracted by the addition of $B(C_6F_5)_3$ to give the active cationic catalyst. The structure of this species was determined by NMR spectroscopy, which showed that the methoxy group takes up the position vacated by the abstracted methyl.

The catalyst was tested for ethylene trimerisation and it was found to give turnover frequencies of around 8100 $mol(C_2H_4)\ mol(Ti)^{-1}\ h^{-1}$, though considerable quantities of higher olefins were produced. Although this system was only tested at ambient pressure it can be extrapolated that this broadly agrees with the activities observed by Fujita *et al.* This activation route therefore demonstrates a considerable improvement over the previously described procedure and suggests that this catalyst has considerable potential for commercialisation.

The deuterium scrambling experiments carried out previously with the PNP system were repeated for this catalyst.[98] The absence of scrambling was again observed which rules out a Cossee-Arlman mechanism and lends considerable weight to a metallacyclic pathway. The metallacyclic mechanism would therefore proceed *via* Ti^{2+} and the reductive elimination of methane, which was observed by ^1H NMR spectroscopy as CH_3D when deuterated ethylene was used.

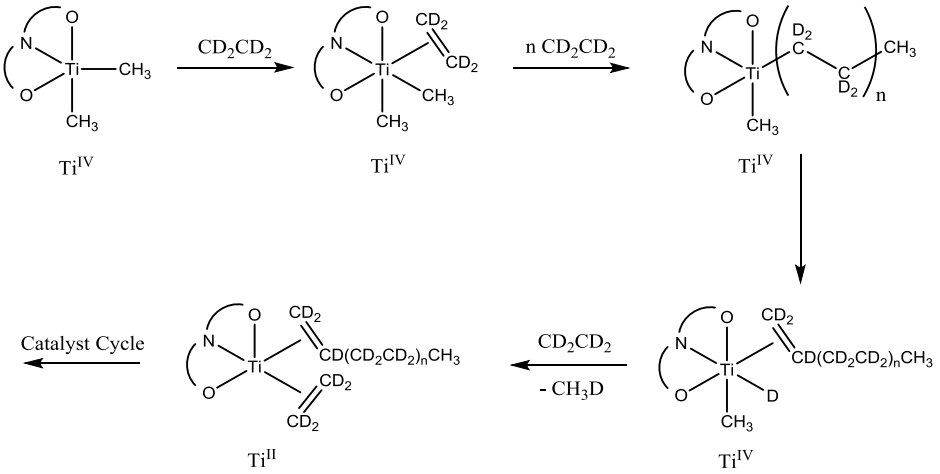

Scheme 2.2 - The activation steps leading into the catalyst cycle. All species are mono-cationic with the borate counter-ion removed for clarity.

As part of this research it was discovered that the system is also active for the trimerisation of LAOs, in this case 1-pentene, 1-hexene and 1-decene. Having established that ethylene trimerisation proceeds *via* a metallacyclic mechanism it follows that trimerisation of LAOs using the same catalyst results from an analogous pathway. 1-Pentene and 1-hexene both recorded relatively high turnover numbers of around 350 while the use of 1-decene restricted the reaction to around 100 turnovers. These activities are significantly lower than those observed for R_3TAC chromium catalysts, which may be due to the greater steric bulk of the ligand.

This chapter describes the synthesis of a range of (R_3TAC)$CrCl_3$ catalysts with varying halogen incorporation and steric bulk to fully test the effects on turnover and activity. The trimerisation procedure was then optimised using these species to give a highly reproducible system capable of reliably comparing the different features of the catalysts. Alternative pre-catalysts are then explored in which the abstractable anion has been altered to test the effects on activation and the counter-ion.

2.1 Catalyst Synthesis

In designing improved 1,3,5-trisalkyl-1,3,5-triazacyclohexane ligands for LAO trimerisation there were several properties that the catalyst needed to feature, based on the results published by Wasserscheid *et al.*[3]

Firstly, the low activity demonstrated by the previous catalysts was attributed to poor solubility in non-donor solvents. These solvents are used due to the sensitivity of the activated catalyst towards substitution of the TAC ligand by donating species. Catalysts which incorporated alkyl branching into the N-substituent demonstrated by far the best solubilities and produced the most active systems as a result. Therefore, it was essential that branching was incorporated in an attempt to emulate the high activities observed for ((2-Ethylhexyl)$_3$TAC)$CrCl_3$.

However, it was also observed that branching at the α-carbon of the alkyl substituent dramatically reduced the catalyst activity. The branching point must therefore be located further from the TAC ring in order to ensure that the steric bulk of the catalyst remains low. With this in mind, it was decided that branching should be situated at the γ-position, as this was unlikely to induce steric hindrance around the metal centre.

The 'halogen effect' has played an important role in improving the efficiencies of a range of selective trimerisation systems, most notably the Phillips trimerisation catalyst.[194] While poorly understood, it has been shown that the presence of a halogen atom within an additive or the activator greatly improves catalyst activity. However, incorporation of alkyl halides such as hexachloroethane or 1-bromobutane in this manner adds a layer of complexity to commercial application, which could be avoided if the halogens were incorporated directly into the ligand. In order to test whether this was possible, a set of ligands were designed in which halogens were present in positions capable of interaction with the metal centre.

Based on these requirements the synthesis of two ligand types was attempted in which symmetrical alkyl branching, in order to avoid the formation of chiral centres, was present at the γ-carbon. Halogenation was also targeted at the γ-carbon, as this location should facilitate any potential interaction with the chromium centre after complexation. Both pentyl and *iso*-butyl branches were investigated to compare their effects on solubility and steric bulk, Figure 2.1.

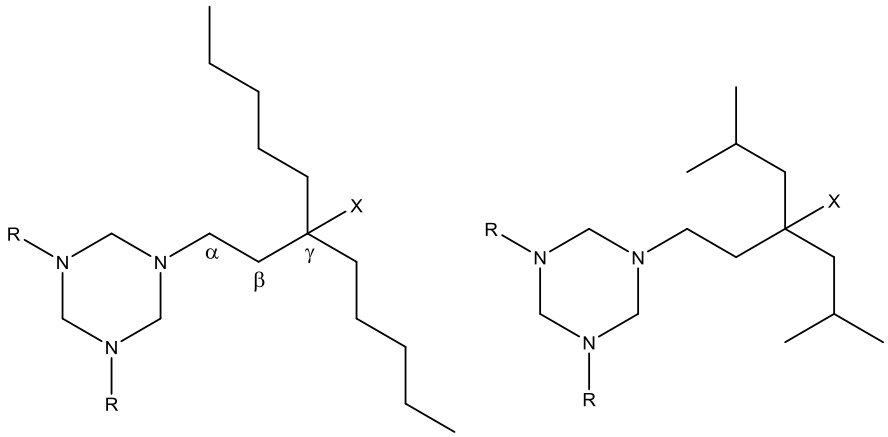

Figure 2.1 - The target triazacyclohexane ligands, where R = repetition of the shown alkyl chain and X = H, Cl or Br.

The method by which the synthesis was undertaken will be described briefly within this chapter. More detailed information on experimental procedures is available in Chapter 5. The synthesis of the hydrochlorinated pentyl branched ligand has been achieved previously within the group as a potential ethylene polymerisation catalyst.[151] The syntheses shown here are an adaptation of this work, with improvements made at several stages.

2.1.1 The Wittig Reaction

One of the most well established and reliable methods of halogen incorporation is addition across a double bond. Therefore, the Wittig reaction was identified as a good starting point for the synthesis of an unsaturated ligand. The ketone corresponding to the required branching was reacted with a Wittig-Horner reagent containing a nitrile, to allow subsequent access to the amine, Scheme 2.3.[195]

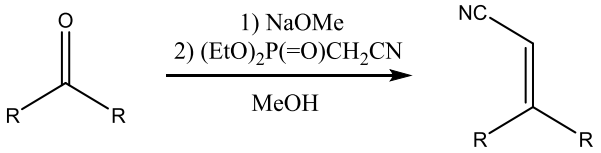

Scheme 2.3 - The Horner-Wadsworth-Emmons reaction. R = Pe or ^{i}Bu.

The phosphonate reagent was first deprotonated with a solution of sodium methoxide in methanol to produce an ylide. The ketone was added after 30 minutes and the solution refluxed overnight at 70 ˚C. The undecan-6-one reaction was attempted first and produced a poor yield of just 45%.

Investigating the reaction using ^{13}C pendent and ^{31}P NMR spectroscopy indicated that the phosphonate was not fully deprotonated by the sodium methoxide. It also indicated nucleophilic attack on the phosphorus centre by the methoxide base was occurring, leading to the formation of $P(=O)(OEt)_2(OMe)$ and acetonitrile. An intense singlet, attributed to acetonitrile, was observed at 2ppm in the ^{1}H NMR spectrum taken of the phosphonate in the basic solution. This peak increased over time and corroborated with ^{31}P NMR spectra which showed increasingly intense peaks in the region associated with $P(=O)(OR)_3$ compounds.[196, 197]

In order to prevent nucleophilic attack and ensure deprotonation, potassium *tert*-butoxide in THF was used as the basic solution. This proved to be much more effective, with NMR spectroscopy indicating 100% deprotonation of the phosphonate. 87% conversion had been achieved three hours after addition of the ketone, rising to 97% after three days without any heating required, as measured by ^{1}H NMR spectroscopy. This alteration to the initial synthetic step greatly reduced wastage of the expensive Wittig-Horner reagent and, as such, reduced the overall cost of catalyst synthesis significantly.

The potassium *tert*-butoxide process was taken forward to the 2,6-dimethylheptan-4-one reaction. Unfortunately, only a 38% spectroscopic conversion was achieved. Isolated yields when using sodium methoxide as the base were worse, at just 26%. The reduced yield was attributed to the greater steric bulk of the ketone, which would likely restrict the nucleophilic attack of the bulky ylide on the carbonyl. As the associated bulk is a key feature of the desired ligand the reaction was repeated until a satisfactory yield was isolated.

2.1.2 Selective Nitrile Reduction

Reduction of the nitrile to gain access to the amine required for R_3TAC formation proved more complicated than expected. Use of lithium aluminium hydride as the reducing agent, as is typical for nitrile reduction, resulted in partial hydrogenation of the alkene up to a maximum of 22%. Such reactivity has been observed previously for conjugated or functionalised double bonds.[198] The procedure was altered according to literature techniques by using a $LiAlH_4/AlCl_3$ 3:1 mixture to produce 'AlH_2Cl' as a reducing agent, Scheme 2.4, giving greatly improved results.[199]

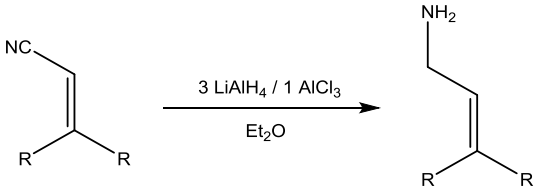

Scheme 2.4 - Reduction of the conjugated nitrile. R = Pe or ^{i}Bu

The pentyl branched amine was produced at a yield of 82% after 1 hour at room temperature. Importantly, there was no evidence of alkene hydrogenation, which would complicate isolation of the product due to the difficulty in separating the saturated and unsaturated amines. The *iso*-butyl branched amine was also produced with an isolated yield of 82%, suggesting the greater steric bulk no longer affected the functional group. There was again no evidence of alkene reduction, indicating that this technique is effective at selectively reducing conjugated nitriles.

2.1.3 Triazacyclohexane Formation

The condensation reaction between amines and formaldehyde is well established and produces 1,3,5-trisalkyl-1,3,5-triazacyclohexanes over the course of several hours, Scheme 2.5.[148]

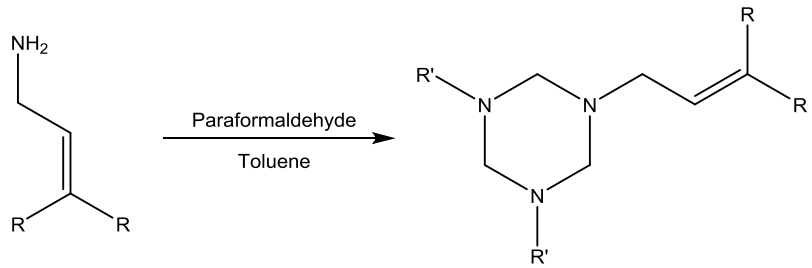

Scheme 2.5 - The condensation of the synthesised amines with formaldehyde.
R = repetition of the shown substituent.

The polymer form of formaldehyde, paraformaldehyde, was used rather than an aqueous solution due to ease of handling and this does not affect the reactivity. A 93% yield was obtained for the pentyl branched TAC while the isolated yield was 92% for the *iso*-butyl branched TAC. The high efficiency of this reaction is dependent on ensuring the 1:1 stoichiometry of reagents, as excess formaldehyde results in the incorporation of oxygen into the ring. This can easily be removed during the subsequent purification of the complex however.

2.1.4 Complexation

The ligand and $CrCl_3(THF)_3$ were combined before dissolution into a dry DCM solution to form the strongly coloured purple complex, Scheme 2.6.

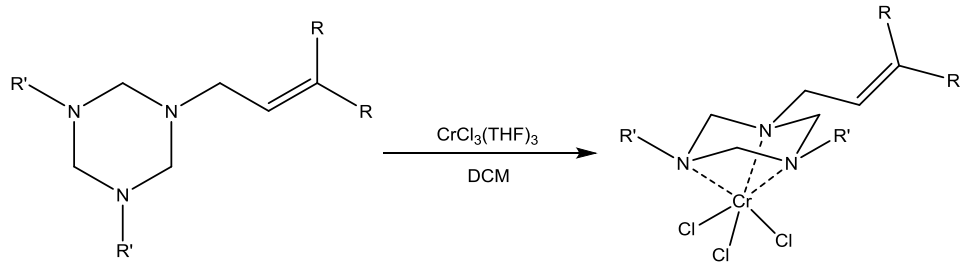

Scheme 2.6 - Complexation of the ligand. R = Pe or ^{i}Bu, R' = repetition of shown substituent.

After four days the purple solutions were eluted through silica columns with DCM. A small quantity of green hydrolysed chromium was retained on the column in each circumstance, along with a yellow compound likely to be excess ligand or a different organic contaminant. Removal of the DCM from the purple eluent gave a 90% yield of the pentyl branched complex and a 77% yield of the *iso*-butyl branched catalyst. Both were characterised using mass spectrometry and elemental analysis.

2.1.5 Hydrohalogenation

Hydrohalogenation was attempted after complexation because TAC compounds are unstable in acidic conditions and so would likely decompose in the presence of HCl or HBr. The nitrogen atoms are protected once coordinated to the chromium centre, however, leaving the alkene to react without any detrimental effect to the ligand. The kinetic inertness of the chromium centre prevents ligand substitution, such that addition across the double bond proceeded as hoped, Scheme 2.7.

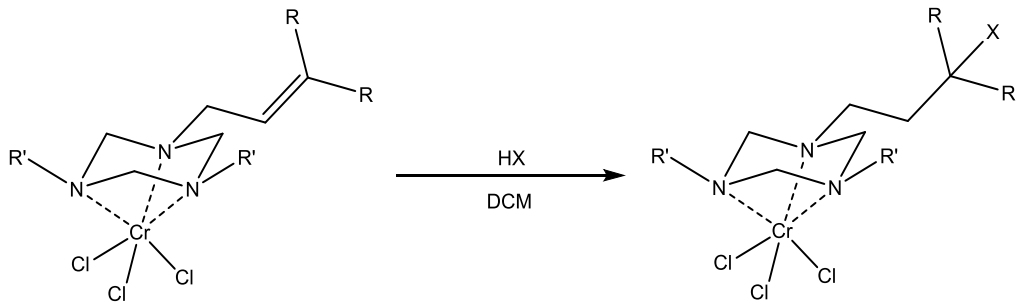

Scheme 2.7 - Hydrohalogenation of the alkene. R = Pe, R' = repetition of shown alkyl group, X = Cl or Br.

The HCl/HBr was formed *in situ* by reaction of acetyl chloride/bromide with methanol in the same vessel as the complex. The rate of reaction of acetyl halides with methanol greatly exceeds that of the complex, ensuring the chromium complex is only exposed to a minimal quantity of alcohol. The pressure was controlled using an addition funnel for the methanol which did not incorporate a side arm. Therefore, as the methanol was added and the reaction evolved acidic vapour this produced excess pressure, preventing further addition. As the vapour dissolved in the solvent or was taken up by addition across the double bond, further addition of methanol was then possible. As such, the rate of addition was self-regulating.

The reaction was cooled to 0 ˚C throughout in order to increase the solubility of the acids and moderate the temperature increase associated with this highly exothermic reaction. After four hours nitrogen was blown through the system to disperse the vapour and the reaction halted. An isolated yield after column chromatography of 77% was recorded for the chloride reaction and 69% for the bromide. Both complexes were characterised using TOF-MS, ^{13}C NMR spectroscopy and elemental analysis. The *iso*-butyl branched complex did not react with either HBr or HCl, suggesting that the greater steric bulk of the *iso*-butyl groups again hindered the reaction and prevented addition.

It was possible to crystallise the hydrobrominated catalyst using anti-solvent techniques to give a well-defined structure, Figure 2.2.

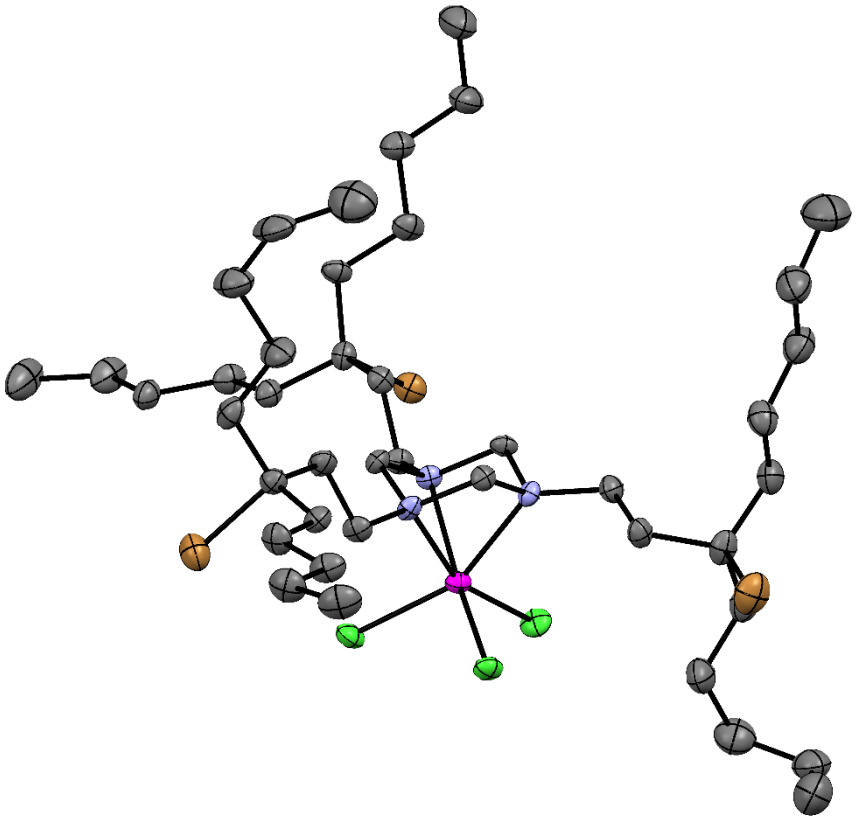

Figure 2.2 - The crystal structure of the hydrobrominated catalyst.
Grey = C, Mauve = N, Pink = Cr, Green = Cl, Brown = Br.

This complex adopted a monoclinic unit cell and had the pentyl groups orientated almost perpendicular to the plane of the TAC ring. Cr-N bond distances were quite short for Cr^{III} TAC species (2.123(3), 2.128(3) and 2.133(3)Å), indicating that the branching and halogen bulk does not influence the ligand binding to any great degree.[164, 175] The acute N–Cr–N bond angles of 65.70(13)˚, 65.86(13)˚ and 65.62(13)˚ demonstrate the low steric bulk of the ligand around the chromium centre.

Several attempts were also made at addition of hydrogen iodide across the double bond but all proved futile. The successful method used for bromide and chloride addition was not attempted for iodine due to the violent reaction that occurs between methanol and acetyl iodide. The focus of our efforts was the extraction of HI from the commercially available aqueous solution using DCM and phosphorus pentoxide. This was achieved and added to the unsaturated complex. After an extended work-up a purple solid was extracted which, according to mass spectrometry, contained complexes with varying levels of addition across the double bond. Repetition of the experiment resulted in the iodide containing complexes being lost and iodine being given off, suggesting the species formed were highly unstable.

2.1.6 Hydrogenation

Palladium catalysed hydrogenation of the unsaturated complex was unsuccessful and led to decomposition of the ligand as observed by ^{1}H NMR. This was attributed to the fact that the TAC ring is analogous to three N-methylidenealkylamines and as such may be vulnerable to hydrogenation itself despite protection of the nitrogen atoms by chromium complexation, Scheme 2.8.[200]

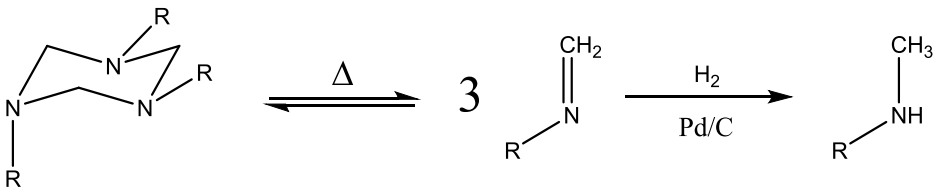

Scheme 2.8 - Predicted decomposition of the ligand. R = alkyl.

The failure of this reaction meant hydrogenation had to be performed at the amine stage, Scheme 2.9. This allowed the partially hydrolysed amines from the non-selective nitrile reduction to be recovered and further reacted. The double bond was reduced by stirring the amine in a methanol solution containing a Pd/C suspension under a hydrogen atmosphere. The hydrogen atmosphere was produced via the reaction of calcium hydride with water in an attached flask and maintained at one atmosphere with the use of an oil bubbler. The isolated yield of the saturated amine was 80%.

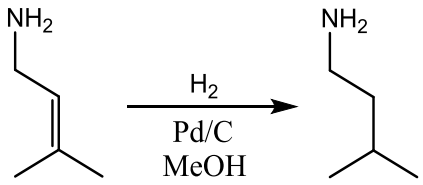

Scheme 2.9 - Amine hydrogenation.

The *iso*-butyl branched amine was synthesised anew before being reacted in the same way to give a 91% yield. Such a high yield further indicates that the alkene's low activity with respect to halogenation must be due to the steric bulk of the *iso*-butyl groups. Hydrogen appears to be small enough to add across the double bond but the increased bulk when one proton is replaced with a halogen appears to be sufficient to completely prevent reaction.

No significant difference in reactivity was observed during the TAC formation and complexation reactions compared to the unsaturated analogues. These catalysts should provide a control with which the effects, if any, of the incorporation of halides can be compared. A crystal structure of the pentyl branched catalyst was obtained over the course of several days using anti-solvent techniques, though the crystal was of a poor quality and low R_{int} values were recorded.

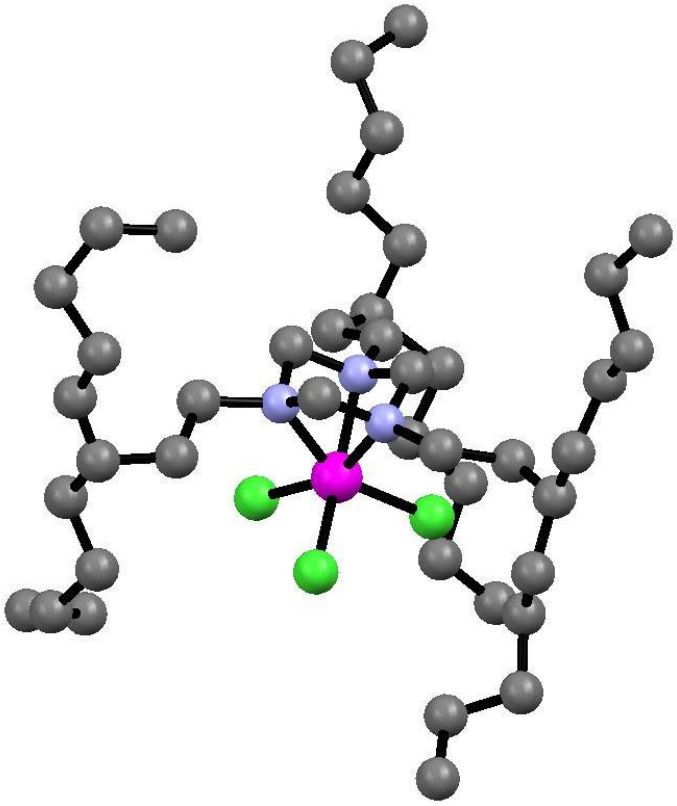

Figure 2.3 - The crystal structure of the hydrogenated pentyl branched catalyst.
Grey = C, Blue = N, Pink = Cr, Green = Cl.

The crystal structure of $((Pe_2CHCH_2CH_2)_3TAC)CrCl_3$ occupied a monoclinic unit cell much like the hydrobrominated analogue. The Cr-N bond lengths contrasted considerably, however, with shorter lengths of 2.006(17)Å, 2.06(2)Å and 2.069(19)Å. This indicates the chromium is shifted slightly towards one nitrogen donor and this is reflected in the N-Cr-N bond angles (63.0(9)˚, 61.6(9)˚ and 65.2(7)˚). The bond lengths are contracted compared to the hydrobrominated complex which suggests the bulk of the bromine atoms may destabilise the ligand – metal interaction to a limited degree. The Cr-N distances seen here are very low for this type of compound and hopefully indicate a highly stable complex.

2.2 Catalyst Optimisation

The catalytic procedure initially applied broadly matches that described by Wasserscheid *et al*. in collaborative work.[3] Catalyst optimisation was undertaken using 1-hexene as the LAO reagent due to its ready availability and low cost. 1-Hexene is also of interest as the product of ethylene trimerisation, Chapter 4.

The catalyst requires activation by an alkylaluminium co-catalyst in the form of methylaluminoxane (MAO), which acts as an alkylating and chloride abstraction agent.[3] In this work, 'dry' or 'depleted' methylaluminoxane (DMAO) was used instead of the commercially available toluene solution of MAO. This was desirable because it allowed both toluene and trimethyl aluminium to be avoided, which have been proposed to play key roles in catalyst decomposition.[201]

DMAO takes the form of a flaky white solid which is easier to work with than the solution, for which the concentration is hard to accurately define. It was produced by reducing down the commercial toluene solution under high vacuum to give a sticky white solid, which was then suspended in hexane. Filtering the suspension through sintered glass separated out the solid DMAO and repeated washes with hexane removed any remaining $AlMe_3$ and toluene.

The non-donor solvent used for all catalyst runs was 1,2-difluorobenzene, which was chosen because its relatively high polarity means both the catalyst and the DMAO are readily soluble, whilst 1-hexene is still miscible. Using *o*-$C_6H_4F_2$ instead of aliphatic hydrocarbon solvents should ensure that the solubility of the catalyst does not influence the catalyst performance, improving the reproducibility and accuracy of results. While there is evidence of aromatic solvents leading to catalyst decomposition, it is hoped that the weak π-basicity of *o*-$C_6H_4F_2$ will render this negligible. The complexes tested as trimerisation catalysts will be identified by abbreviations throughout the rest of this chapter, Figure 2.4.

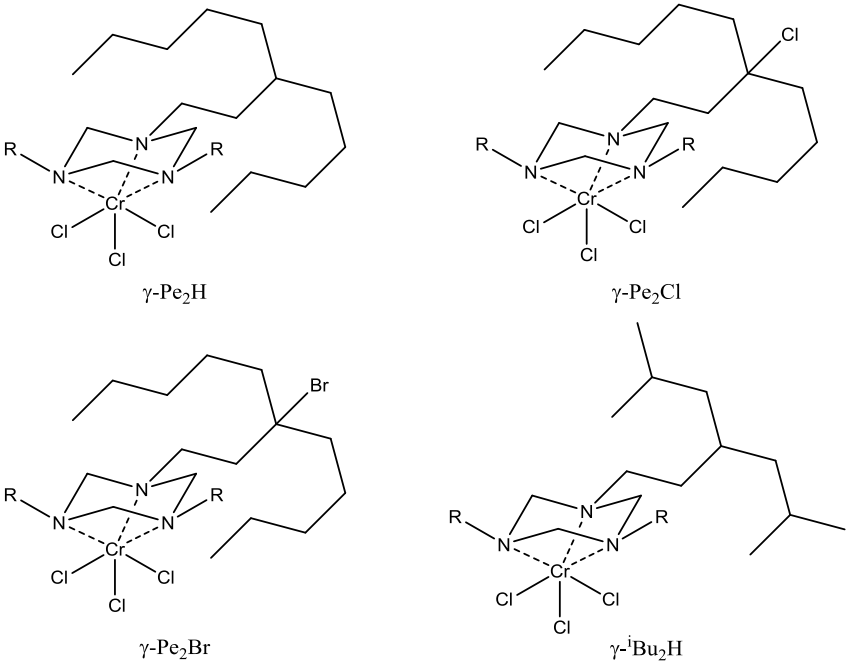

Figure 2.4 - Catalyst abbreviations.

MAO is a very ill defined material and as such its molecular weight is not consistent, it is typically described as either $(MeAlO)_n$ or $(Me_{1.5}AlO_{0.75})_n$. Throughout this report the molecular weight has been given the arbitrary value of 60 amu per aluminium as a compromise between these two possibilities. Conversions, activities, selectivities and turnover numbers have all be calculated on the basis of ^{1}H NMR integration. The distinctive peak corresponding to the internal olefinic hydrogen of 1-hexene was used as a reference, with integrations of the other regions taken relative to this signal, Figure 2.5.

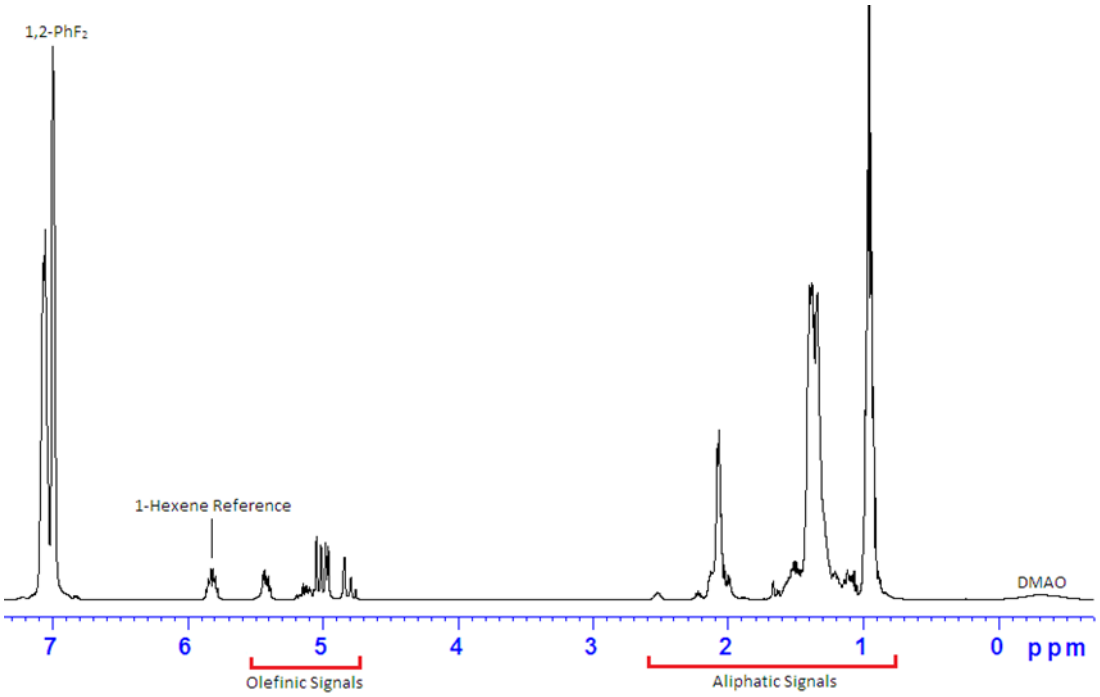

Figure 2.5 - A typical ^{1}H NMR spectrum for a catalyst solution.

The percentage conversion, C_{Total}, was calculated based on comparison of the reference signal integration, set as 1, to integration of the olefinic signals, $I_{olefinic}$.

$$C_{Total} = 100 \times \frac{x}{1+x}$$

$$Where\ x = \frac{I_{olefinic} - 2}{2}$$

The selectivity (mol%), S_{Trimer}, was calculated based on the ratio of the olefinic signals to the aliphatic signals, $I_{aliphatic}$, after taking account of the remaining 1-hexene.

$$S_{Trimer} = 100 \times \frac{\left(\frac{I_{aliphatic} - 9}{I_{olefinic} - 2}\right) - 5}{12}$$

The activity (mol(C_6H_{12}) mol(Cr)$^{-1}$ h^{-1}), A_{Trimer}, was calculated based on the conversion to trimer, C_{Trimer}, achieved after a given time, T. This was measured at the beginning of the reaction after either 1 or 1.5 hours.

$$A_{Trimer} = \frac{C_{Trimer} \times \left(\frac{Mol(C_6H_{12})}{Mol(Cr)}\right)}{T}$$

$$Where\ C_{Trimer} = \frac{C_{Total}}{100} \times \frac{S_{Trimer}}{100}$$

Finally, the turnover number (mol(C_6H_{12}) mol(Cr)$^{-1}$), *TON*, was calculated based on the conversion to trimer after complete reaction.

$$TON = C_{Trimer} \times \left(\frac{Mol(C_6H_{12})}{Mol(Cr)}\right)$$

Using these equations for calculation of catalyst performance allowed accurate comparison of the catalysts synthesised. The initial results, in which a relatively low ratio of catalyst to 1-hexene was used, are shown in Table 2.1 alongside the quantities and equivalents of the reagents used.

Table 2.1 - Initial Trimerisation Results for each N-substituent.

Catalyst	γ-Pe_2H	γ-Pe_2Cl	γ-Pe_2Br	γ-$^{i}Bu_2H$
Mass (mg)	5.2	4.7	5.0	3.7
Moles (μmol)	6.7	5.6	4.8	5.2
DMAO				
Mass (mg)	57	50	45	48
Moles (mmol Al)	0.94	0.84	0.75	0.80
Equivalents (Al)	140	150	156	154
1-Hexene				
Mass (mg)	634	646	674	499
Moles (mmol)	7.5	7.7	8.0	5.9
Equivalents	1124	1373	1669	1139
***o*-$C_6H_4F_2$**				
Mass (mg)	592	559	510	609
Moles (mmol)	5.2	4.9	4.5	5.3
Equivalents	775	875	931	1026
Conversion after 1.5 hrs (%)	67	76	15	4
Conversion after 3 days (%)	88	91	49	22
Trimerisation (mol%)	94	78	65	85
Isomerisation (mol%)	6	22	35	15
Activity (TOF)	500	697	167	30
Turnover Number	932	975	535	212

Both the hydrogenated and the hydrochlorinated catalyst gave high overall conversions and activities. For these two catalysts the turnover numbers are of a comparable magnitude to the best catalyst observed by Wasserscheid *et al*., which was recorded as 1026.[3]

The result for the hydrobrominated catalyst was disappointing and suggests much lower catalyst stability compared to γ-Pe_2H and γ-Pe_2Cl. This may result from thermal decomposition due to a severe exotherm observed for this catalyst which did not occur for the others. Exotherms are expected for catalytic reactions involving carbon-carbon bond formation but it is surprising that it only occurs for γ-Pe_2Br. The increase in temperature likely indicates a rapid reaction, indicating that the catalyst is potentially highly active but instability prevents a high turnover number.

The result for γ-$^{i}Bu_2H$ is very poor and can be attributed to limited solubility despite the use of *o*-$C_6H_4F_2$. While the light green solution attributed to the activated catalyst formed in the same manner as for the other catalysts a dark green film-like substance also formed on the glass. This is attributed to the catalyst dropping out of solution on addition of the 1-hexene, at which point the polarity of the solution is reduced. These observations match those made by Wassersheid *et al.* for poorly soluble catalysts.[3] Based on this result it was clear that γ-$^{i}Bu_2H$ was not suitable for application under these conditions and as such has not been investigated further.

The principal waste product observed for these catalytic runs was isomerisation of the 1-hexene to form 2-hexene. Isomerisation was observed for γ-Pe_2H at a similar level as for ((2-Ethylhexyl)$_3$TAC)$CrCl_3$.[3] However, the quantity of 2-hexene produced increased dramatically for the halogenated catalysts and accounted for a considerable proportion of the products. The route by which isomerisation occurs is unclear but there are three potential sources. Firstly, the aluminium activators, as lewis acids, could act as isomerisation agents. Secondly, a species produced from decomposition of the active catalyst could induce isomerisation. Thirdly, a side reaction occurring between 1-hexene and the active catalyst could account for the observed production of 2-hexene.

The aluminium alkyls were ruled out as the source by running a series of control reactions that tested the ability of the three variations of aluminium alkyl present to isomerise 1-hexene. Solutions of DMAO, MAO and $AlMe_3$ were made up in *o*-$C_6H_4F_2$ before addition of 1-hexene in a quantity equivalent to a catalytic run. The proportion of internal hexenes present in the 1-hexene sample was calculated at just 0.003% and this has been deducted from the isomerisation data in Table 2.2. The conversion was calculated by peak integration of the olefinic region of ^{1}H NMR spectra.

Table 2.2 – The proportion of 1-hexene trimerised on exposure to aluminium alkyl activators. Further experimental data available in Section 5.4.1.

	Isomerisation (%)	
Activator	1 hour	5 days
DMAO	0.01	0.51
MAO	0.00	0.07
$AlMe_3$	0.01	0.02

Minimal isomerisation was observed for the activators which could potentially be present within the catalytic system. Although DMAO in particular did gradually isomerise 1-hexene over the course of five days, almost no conversion had been observed after an hour suggesting a very slow rate of reaction. The activators are therefore unable to account for the high levels of isomerisation that occur within the time scale of catalysis. Based on this data the first possibility for the source of internal hexenes can be ruled out. This also agrees with the observation that different catalysts produced varying levels of isomer despite being run under the same conditions.

The lower turnover numbers seen here in comparison to the work conducted by Wasserscheid *et al.* may be due to the absence of reaction cooling.[3] The observed exotherm for the hydrobrominated complex caused a dramatic colour change to give a red solution while the other reactions gradually went from green to yellow. The colour change likely indicates the formation of a new chromium species, presumably through catalyst decomposition. The considerably higher level of isomerisation observed for γ-Pe_2Br could well be linked and supports the possibility that isomerisation is induced by a decomposition product.

It is unclear whether decomposition was induced thermally or through an innate instability in the catalyst. However, thermal decomposition would be prevented by cooling and may therefore have prevented the decay of the catalyst previously.[3] With the equipment available cooling was impractical and would have introduced further variables. Instead, in future experiments the level of dilution was increased to more rapidly dissipate the heat produced and hopefully prevent decomposition.

2.2.1 Variation of Dilution

γ-Pe_2Cl gave the best initial results and was therefore used to test the effects of increased dilution. Three experiments were performed with dilutions matching, doubling and tripling those of the initial tests. The relative quantity of 1-hexene was also increased to approximately 2000 equivalents in each case to explore the limit of the turnover number.

The key information relating to this investigation is shown in Table 2.3. All of the data not shown (reagent quantities, conditions and conversions) are provided in Section 5.4.2. This method for the presentation of data from LAO trimerisation reactions will be maintained throughout the remainder of this chapter, with all additional information provided on a section by section basis in Chapter 5.

Table 2.3 - Results of increased dilution on γ-Pe_2Cl catalysed 1-hexene trimerisation.

Run	*o*-$C_6H_4F_2$ (Eq.)	1-Hexene (Eq.)	Activity (TOF)*	Selectivity (%)	TON
1	853	2135	1269	79	1500
2	1584	2004	2085	83	1451
3	2504	2033	2052	91	1499

*TOF = mol(C_6H_{12}) mol(Cr)$^{-1}$ h^{-1}.

The turnover numbers recorded on increasing the 1-hexene equivalents are 50% higher than the best performing catalyst yet described and demonstrate considerable potential for γ-branched catalysts.[3] It can be seen that increasing the dilution has no significant effect on the turnover number, suggesting that decomposition is not influenced by decreasing concentration within this range. The high turnover numbers represent a significant improvement over the initial results and are most likely due solely to the availability of more 1-hexene.

The most notable effect is that increased dilution results in a considerable reduction in the proportion of 1-hexene that undergoes isomerisation. This is an important advance, as while internal hexene side-products are easily separated from the trimer product, wastage needs to be minimal for the process to be industrially viable. This data appears to support the hypothesis that a thermal decomposition product accounts for the isomerising species, as greater dilution should reduce any temperature increase. However, it could also be the case that the rate of isomerisation has a greater barrier to activation and is therefore only favoured at higher temperatures such that the active species could induce isomerisation.

The second notable change on increased dilution is the increase in catalytic activity from Run 1 to Runs 2 and 3. A decrease in catalyst concentration would be expected to result in a loss in activity and yet the opposite is observed. The most likely explanation, based on the mechanistic investigations of Bercaw *et al.*,[98] is that the greater polarity of the system favours the cationic active catalyst. By increasing the relative concentration of *o*-$C_6H_4F_2$ over 1-hexene the polarity of the solution will increase. As a result, dissociation of the active catalyst and its counter-ion will become more favourable, providing greater access to a vacant site for incoming 1-hexene molecules. The absence of an increase from Run 2 to 3 indicates the reduced increase in polarity is offset by decreasing catalyst concentration.

2.2.2 Variation of 1-Hexene Concentration

To test the maximum activity of the system, γ-Pe_2Cl was tested with increasing relative quantities of 1-hexene taken from the same sample.

Table 2.4 - The effects of increasing 1-hexene concentration. Further experimental data available in Section 5.4.3.

Run	1-Hexene (Eq.)	*o*-$C_6H_4F_2$ (Eq.)	Activity (TOF)*	Selectivity (%)	TON
1	1013	2504	1497	87	827
2	2049	2529	2055	91	1499
3	2989	2554	1488	87	1627
4	4107	2515	510	38	311

*TOF = $mol(C_6H_{12})\ mol(Cr)^{-1}\ h^{-1}$.

The results shown in Table 2.4 demonstrate that the turnover number can be increased by the addition of further 1-hexene, up to 3000 equivalents, but the activity drops off sharply beyond 2000 equivalents. The poor activity observed for Run 4 could result, in part, from the reduced polarity of the solution but it is highly unlikely this would have such a notable effect.

The reduction in conversion as the concentration of 1-hexene is increased suggests that a contaminant may be present within it. It is known that the catalysts are highly moisture sensitive once activated and so water was the most likely impurity. Before use, the 1-hexene was vacuum transferred off a calcium hydride suspension without heating and under high vacuum, allowing only half of the volume to pass across each time a new batch was required. In order to ensure the system was completely free of moisture an improved drying procedure was put in place.

2.2.3 The Effect of 1-Hexene Purification

Molecular sieves are a convenient drying agent and have been shown to be very effective at reducing moisture levels to very low concentrations.[202] Fifty grams of 3 A (8-12 mesh) molecular sieves were dried under vacuum at 300 °C for four hours, before a 100 mL sample of 1-hexene was added after cooling. The 1-hexene was tested by ^1H NMR spectroscopy to ensure that the molecular sieves did not induce isomerisation and it was found not be the case. The 1-hexene was left over the molecular sieves for three days before half the total volume was transferred under high vacuum and without heating.

Under an argon atmosphere one drop of sodium potassium alloy (Na/K) was added, which was prepared by melting together a 3:1 ratio by mass of K:Na.[203] A small amount of effervescence was observed suggesting some moisture still remained, thus the sample was left for a further two days over several drops of Na/K. Now that a 1-hexene sample was available that had been thoroughly dried the activity of γ-Pe_2Cl was again tested. A higher level of dilution was also used which should prevent any impact on the values derived from solubility.

Table 2.5 – Activity testing with the use of Na/K as 1-hexene drying agent. Further experimental data available in Section 5.4.4.

Run	1-Hexene (Eq.)	*o*-$C_6H_4F_2$ (Eq.)	Activity (TOF)*	Selectivity (%)	TON
1	1037	9278	1536	82	767
2	2130	9908	3462	83	1661
3	3081	9213	4992	92	2644
4	4375	9829	7140	93	3778

*TOF = mol(C_6H_{12}) mol(Cr)$^{-1}$ h^{-1}.

The improvement in catalyst performance after drying 1-hexene with molecular sieves and Na/K is considerable and increases the turnover numbers to almost quadruple the best previously published results.[3] The consistent improvement also indicates that these catalysts have considerable potential and that the results for Run 4 are far from the optimum activity of this catalyst. This catalyst has the potential to reach performance levels suitable for commercial development, considered to be a turnover number of over 10,000.[204]

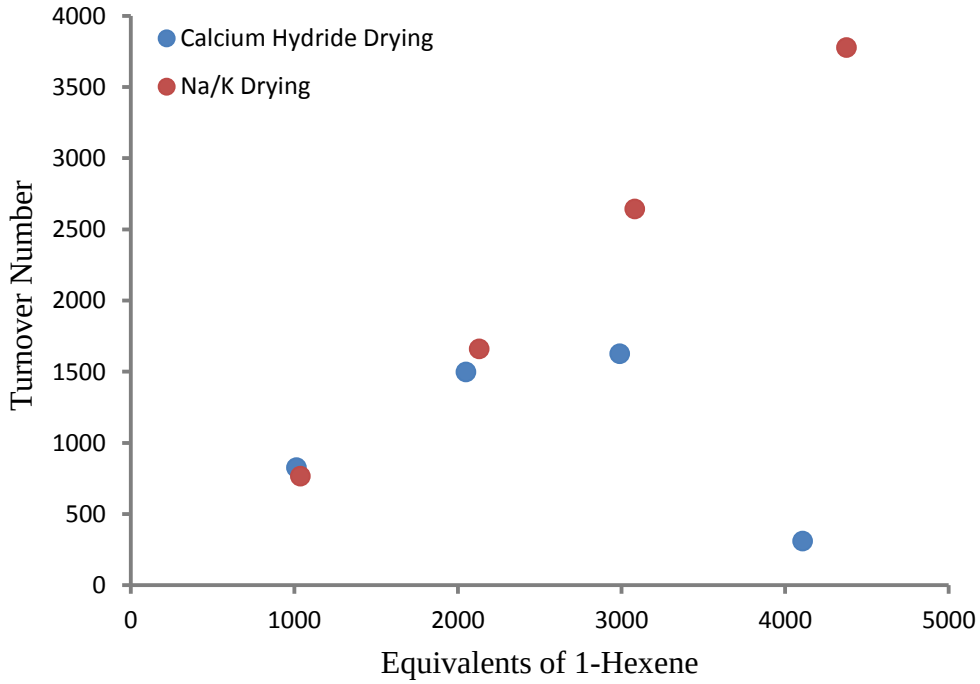

Figure 2.6 - The marked improvement in turnover numbers when Na/K is used as the drying agent rather than calcium hydride. The results shown are for γ-Pe_2Cl.

Comparison of the turnover number, as shown in Figure 2.6, demonstrates that a catalyst poison must indeed have been present within the 1-hexene. Na/K appears to be effective at removing the contaminant, presumed to be water, with a linear relationship between 1-hexene and turnover number observed, as would be expected for a system with low catalyst decomposition.

The proportion of isomerisation decreases with increasing 1-hexene concentration, suggesting a lower rate dependence than that of trimerisation. Selectivities of 93%, considering the internal hexenes are easily removed after complete reaction, suggest the system is highly suitable for application to industrial processes.

The most important conclusion to be drawn from the data is the observation of first order rate kinetics relative to 1-hexene concentration, Figure 2.7. Of the numerous ethylene trimerisation systems known, some have displayed first order rate dependence while others have recorded second order kinetics.[19] This is proposed to result from the influence of the ligand determining whether oxidative cyclisation or insertion into the metallacyclopentane is the rate determining step. The data presented here strongly suggest that for $(R_3TAC)CrCl_3$ α-olefin trimerisation systems the insertion step is rate determining. By implication, the resting state of the catalyst cycle is proposed to be the metallacyclopentane species, as has been proposed for other systems displaying first order kinetics.

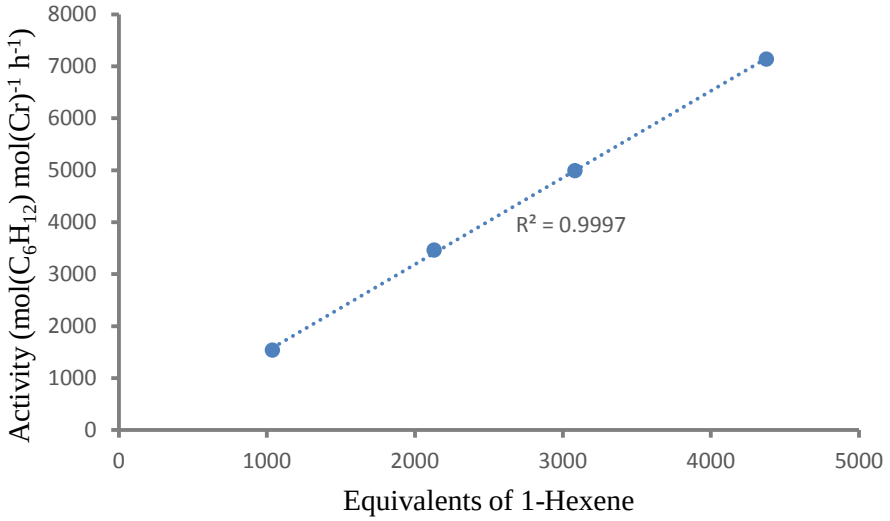

Figure 2.7 - The linear increase in the activity of γ-Pe_2Cl with increasing 1-hexene concentration.

In order to confirm that moisture was responsible for the loss in activity, a series of Karl-Fisher titrations were set up to test the water content of the *o*-$C_6H_4F_2$ and 1-hexene directly. Each value quoted in Table 2.6 is the average of three titrations taken across a range of sample weights. The ppm value represents the mass of water relative to the total mass. *o*-$C_6H_4F_2$ could not be dried with Na/K due to the risk of fluoride abstraction.

Table 2.6 – The water content of *o*-$C_6H_4F_2$ and 1-hexene after drying with different agents.

Reagent	Drying Agent	Water Content (ppm)
o-$C_6H_4F_2$	None	238.9
o-$C_6H_4F_2$	Molecular Sieves	1.1
1-Hexene	None	2336.1
1-Hexene	Calcium Hydride	33.0
1-Hexene	Molecular Sieves	15.5
1-Hexene	Na/K	6.9

The *o*-$C_6H_4F_2$ solvent demonstrated the low hydrophilicity typical of hydrofluorocarbons and was extensively dried with the use of molecular sieves. In contrast, the commercial 1-hexene contained ten times more water by weight and proved to be very hydrophilic. This hindered the efficiency of drying agents, with molecular sieves observed to be far less effective when used with 1-hexene compared to *o*-$C_6H_4F_2$. Overall, a considerable improvement was observed on moving from CaH_2 to Na/K drying, indicating the water content could well cause the drop in activity observed on increased 1-hexene concentration.

The data shown in Table 2.6 for molecular sieve dried *o*-$C_6H_4F_2$ and Na/K dried 1-hexene indicate that under optimised catalytic conditions 0.1 µmol of water would be introduced by the *o*-$C_6H_4F_2$ and 0.4 µmol from the 1-hexene. The maximum catalyst decomposition that could result is therefore 22 mol%, assuming stoichiometric reaction. In practice, it is likely to be negligible due to the greater reactivity of the aluminium alkyl activator towards water. As a result, with the use of Na/K drying, only very limited catalyst decomposition can be attributed to the presence of water.

2.2.4 Optimisation of DMAO Concentration

The final component of the catalyst system, which plays a key role in the overall activity, is the aluminium activator. The high costs associated with the use of these species means that optimisation of the equivalents required for complete catalyst activation is essential. However, it has also been shown for some systems that further increases in activator concentration continue to increase the catalytic activity.[19] This is attributed to an equilibrium existing for abstraction of the methyl/chloride to produce the active cationic catalyst, which is shifted towards cationisation by increased activator concentration. The performance of γ-Pe_2Cl across a range of DMAO concentrations was tested at higher equivalents of 1-hexene than previously to investigate whether the turnover number could be further improved.

Table 2.7 – The effect of activator concentration on catalyst performance. Further experimental data available in Section 5.4.5.

Run	DMAO (Al Eq.)	1-Hexene (Eq.)	Activity (TOF)*	Selectivity (%)	TON
1	45	7611	741	76	687
2	89	7238	1962	90	2820
3	218	7451	3315	93	5441
4	439	7345	3516	92	5302

*TOF = mol(C_6H_{12}) mol(Cr)$^{-1}$ h^{-1}.

The data shown in Table 2.7 demonstrate clearly the significant influence that activator concentration has on the overall activity. Increasing the equivalents up to around 200 results in vastly improved performance in terms of activity, selectivity and turnover number. Interestingly, a further increase in the concentration of DMAO does not lead to an overall improvement, suggesting complete activation of the catalyst has already been achieved. The absence of further improvement indicates that the abstraction equilibrium can be shifted towards the ion pair to its maximum extent with relatively few equivalents of MAO relative to other systems.[91]

A disappointing result obtained during this experiment is that even with optimised DMAO and dilution conditions the catalyst activity failed to reach the expected levels for the higher concentrations of 1-hexene. This suggests that, while the contaminant has been considerably reduced in concentration, a residual quantity remains and at high 1-hexene concentrations still detrimentally affects the catalyst. The poor selectivity observed when relatively few equivalents of DMAO were used strongly supports the hypothesis that the activator does not account for the isomerisation. In combination with the results of the control reactions it can be concluded that a chromium species accounts for this reactivity.

The optimal cost efficiency of the catalyst system was analysed more closely by looking at the costs associated with using the various quantities of activator. The overall cost of a catalyst run is attributed principally to the amount of DMAO used and as such, the quantity of activator required per gram of trimer produced provides a good estimate the overall production cost. The price of DMAO was based on the typical extracted yield from a commercial sample of 10% MAO in toluene. Based on this assumption the cost was calculated to be approximately £1,000 mol^{-1}.

Table 2.8 – The trimer production costs associated with each run.

Run	DMAO (Al Eq.)	Cost (£)	C_{18} Trimer (g)	Production Cost (£ g^{-1})
1	45	0.1	0.4	0.29
2	89	0.2	1.6	0.14
3	218	0.5	3.1	0.17
4	439	1.1	3.0	0.35

Remarkably, the high costs associated with the use of DMAO result in the relatively poorly performing Run 2 producing trimer the most cheaply, Table 2.8. However, Run 3 represents the most feasible operating conditions despite the slightly higher production costs due to the higher activity, selectivity and turnover number recorded. These conditions therefore represent a far more efficient system for commercialisation when everything is taken into account.

On the basis of the results discussed herein an optimised procedure was established for testing future catalysts. This was comprised of 250 equivalents of DMAO, 5000 equivalents of Na/K dried 1-hexene and 7500 equivalents of molecular sieve dried *o*-$C_6H_4F_2$. This technique proved to be reliable and to give highly reproducible results in later testing.

2.3 Investigation of the Halogen Effect

The revised drying technique provided a system which gave vastly improved results and consistently high yields. This allowed reliable investigation of the effects of halogen incorporation at the γ-position of the ligand. It has been proposed that the major decomposition pathway for these catalysts is the transfer of the TAC ligand to the aluminium co-catalyst.[205] Therefore, additional interaction between the ligand and the chromium centre should stabilise the active complex. The halide has been specifically located to facilitate any potential interaction with the chromium centre as a weak pendent donor. It is hoped that such an interaction could strengthen ligand binding and stabilise the catalyst. The intramolecular interaction would most likely consist of dipole attraction between the chromium cation and the electronegative halogen atom, Figure 2.8.

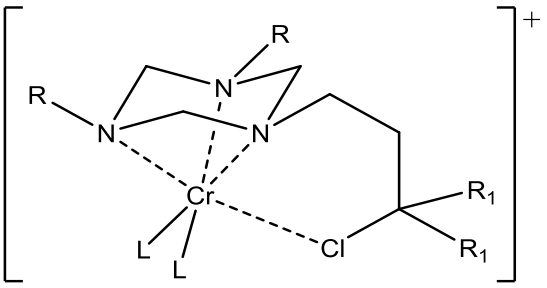

Figure 2.8 - The proposed stabilisation via weak intramolecular interaction. Where R = repetition of the shown substituent and R_1 = pentyl.

2.3.1 Activity Testing

The halide effect was first investigated by repetition of the activity testing performed on γ-Pe_2Cl. Both γ-Pe_2H and γ-Pe_2Br were investigated at increasing 1-hexene concentrations and high dilution as before. If the theory of catalyst stabilisation *via* pendent donor interaction is accurate, it would be expected that the hydrogenated catalyst would perform worse at higher equivalents of 1-hexene.

Table 2.9 – The effect of 1-hexene concentration on activity for the three γ-branched catalysts. Further experimental data available in Section 5.4.6.

Run	1-Hexene (Eq.)	*o*-$C_6H_4F_2$ (Eq.)	Activity (TOF)*	Selectivity (%)	TON
γ-Pe_2H					
1	1002	8480	528	91	274
2	2260	8637	3513	87	1918
3	3194	8467	3954	90	2558
4	4520	8938	7041	92	4042
γ-Pe_2Cl					
5	1037	9278	1536	82	767
6	2130	9908	3462	83	1661
7	3081	9213	4992	92	2644
8	4375	9829	7140	93	3778
γ-Pe_2Br					
9	1019	11118	1197	98	675
10	1926	10918	2496	94	1401
11	2915	10194	4260	86	2009
12	4113	10827	5673	66	2119

*TOF = $mol(C_6H_{12})\ mol(Cr)^{-1}\ h^{-1}$.

The results for γ-Pe_2H, shown in Table 2.9, are broadly similar to those of the hydrochlorinated catalyst for both selectivity and turnover number. The observed reaction rates appear to contain some anomalies, however, with Run 2 recording a considerably better activity than would be expected for linear rate dependence. Overall, the activity of γ-Pe_2H was lower than for γ-Pe_2Cl, suggesting halogenation has a beneficial effect on reaction rate.

In contrast, the hydrobrominated catalyst demonstrated far poorer turnover numbers and selectivities at higher 1-hexene concentrations. At 98%, Run 9 demonstrated the best selectivity observed so far. However, the selectivity declines rapidly with increasing 1-hexene, which results in far lower turnover numbers compared to the other catalysts. The activity of the catalyst increases linearly in an analogous manner to the other catalysts, Figure 2.9, such that in the case of Run 12 the trimerisation is almost complete after one hour. This strongly suggests rapid decomposition of the catalyst, which must presumably be linked to the corresponding increase in isomerisation.

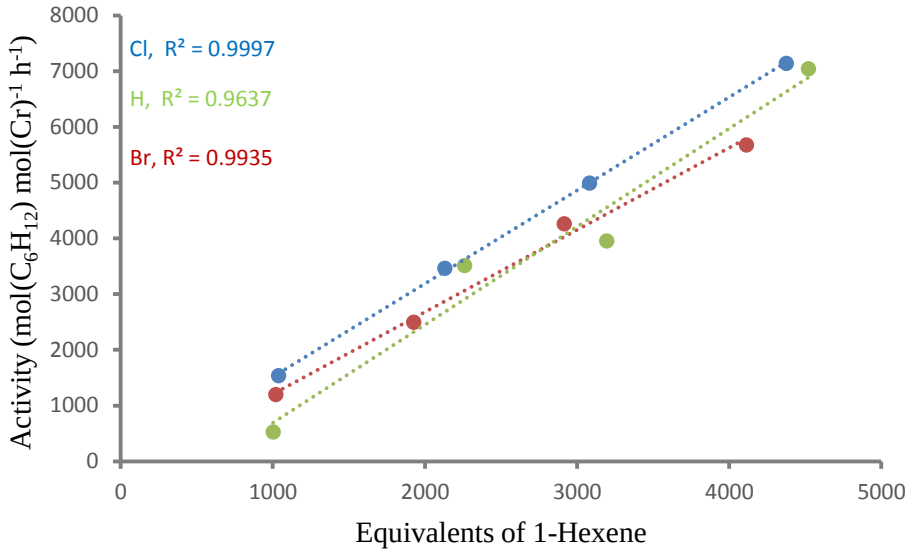

Figure 2.9 - The linear rate dependence of activity with increasing 1-hexene concentration.

Overall, the effect of incorporating a halogen into the ligand appears to be reliant on the halogen itself. The presence of bromine in the N-substituent appears to have a considerable and detrimental effect on the stability of the catalyst. However, the activities recorded remained high despite this and the chlorinated catalyst demonstrated the best trimerisation rate of the three. To test the effect of the halogens on catalyst stability more directly, a series of decomposition experiments were conducted.

2.3.2 Stability Testing

In order to test the stability of the activated catalysts, methylation and cationisation with DMAO in *o*-$C_6H_4F_2$ was performed according to the standard procedure. On this occasion, however, the addition of 1-hexene was delayed by varying degrees. The activity of the systems was then tested as usual after trimerisation was initiated. As demonstrated by Bercaw *et al.* and Arteaga-Muller *et al.*, the catalyst should adopt the form of $[(R_3TAC)CrMe_2]^+$.[94, 206] While this species would be present in the initial stages of reaction, it is also likely to demonstrate stability similar to the metallacyclopentane resting state predicted by the kinetic studies. This method should therefore give a good indication of the stability of the active catalyst to ligand migration, predicted by Köhn *et al.* to be the principal decomposition pathway.[201]

These reactions were carried out on an NMR tube scale to aid analysis and to ensure a closed system throughout the reaction. In order to achieve this, the dilution was reduced to the level of the initial testing and 1000 equivalents of 1-hexene were used. For this reason it was expected that selectivities would be poor compared to the optimised system but entirely comparable between experiments.

Table 2.10 – The effect of delaying1-hexene addition on catalysis. Further experimental data available in Section 5.4.7.

Run	Delay (h)	1-Hexene (Eq.)	Activity (TOF)*	Selectivity (%)	TON
γ-Pe_2H					
1	0	943	1263	72	651
2	1	1136	1362	69	739
3	2	1016	1341	69	650
4	3	1011	1374	67	637
5	24	1015	1218	71	659
γ-Pe_2Cl					
6	0	995	1353	82	776
7	1	1051	1491	91	914
8	2	1113	1491	79	846
9	3	1060	1398	98	954
10	24	1031	1341	93	907
γ-Pe_2Br					
11	0	1161	627	97	859
12	1	1077	516	95	754
13	2	1036	768	99	818
14	3	1208	411	86	689
15	24	1120	66	85	683

*TOF = $mol(C_6H_{12})\ mol(Cr)^{-1}\ h^{-1}$.

Due to the reduced dilution used for this experiment the 1-hexene was added dropwise over the course of approximately 3 minutes in each case. This proved effective in avoiding the occurrence of exotherms in all but two cases. Runs 8 and 12 both underwent a noticeable rise in temperature after addition of the 1-hexene. As a result the catalyst performance appears to have been degraded, particularly regarding selectivity. The time period for which the activity data was collected was taken from addition of the first drop and therefore the data likely include a minor underestimate.

The γ-Pe_2Br catalyst again performed poorly by comparison and showed considerable loss in activity on increased delay which was matched by diminished selectivity and turnover number. This provides further evidence that the catalyst is intrinsically unstable, presumably due to the presence of the alkyl halide in the N-substituent. While this suggests a negative influence by the halogen, γ-Pe_2Cl performed the best of the three and demonstrated only limited catalyst decay.

Both γ-Pe_2Cl and γ-Pe_2H performed well under these conditions with fairly consistent results across the various addition delays. γ-Pe_2H in particular demonstrated almost no loss in performance even when addition was delayed by 24 hours, suggesting the dialkylated cation is highly stable under reaction conditions. A greater effect was observed for γ-Pe_2Cl but not in the manner expected. Excluding the anomalous Run 8, turnover number and selectivity increase in line with delay up to a peak at three hours. This suggests that either alkylation or abstraction are slow and complete activation is not achieved before 1-hexene addition under normal circumstances.

Overall, both of the effective catalysts seem to be highly stable towards ligand abstraction by the aluminium species in the activation stages. This suggests an alternative pathway may account for the majority of decomposition. In order to test the presence of a 'halogen effect' it was also necessary to test the reaction in the presence of alkyl halide additives similar to those used in industry.

2.3.3 External Halogen Effects

While in industry relatively light 1-halogenoalkanes such as 1-bromobutane are used, this was not possible with the equipment available. It was necessary to use non-volatile compounds and therefore long chain 1-halogenoalkanes were used that should accurately replicate the reactivity.

The non-halogenated catalyst, γ-Pe_2H, was run under optimised conditions in the presence of either 1-chlorohexadecane or 1-bromododecane at a range of concentrations. The non-volatility of the additives aided their purification, with each dried under high vacuum before being transferred under vacuum at ~300 °C without cooling of the collecting flask. Each of the additives was then stored over molecular sieves for five days before use to ensure the samples were as dry as possible. A bulk catalyst solution was made up before samples were added to vessels containing the halogenoalkane additive. Using this method the relative quantities of catalyst, DMAO, *o*-$C_6H_4F_2$ and 1-hexene remained constant for each reaction.

Table 2.11 – The effect of halogenoalkane additives. Further experimental data is available in Section 5.4.8.

Run	Additive (Eq.)	Activity (TOF)*	Selectivity (%)	TON
Control	0	479	93	4214
1-$ClC_{16}H_{33}$				
1	33	335	94	1429
2	55	94	81	473
3	335	38	76	210
4	535	7	~	~
1-$BrC_{12}H_{25}$				
5	33	39	34	77
6	55	34	32	63
7	334	44	38	104
8	542	1	18	31

*TOF = mol(C_6H_{12}) mol(Cr)$^{-1}$ h^{-1}.

Surprisingly, the results shown in Table 2.11, rather than demonstrating the increases in activity observed for the Phillips catalyst and others, displayed completely the opposite relationship. Addition of 1-bromododecane led to rapid and complete decomposition of the catalyst. This could explain the decomposition observed for γ-Pe_2Br in which the alkyl bromide of the N-substituent interacts with the chromium centre, leading to decomposition.

The 1-chlorohexadecane displays the same relationship, though the effect is much less severe and the catalyst retains satisfactory activity at 30 equivalents of additive. This could explain why no loss in activity is observed for γ-Pe_2Cl, as in effect only 3 equivalents are present per chromium. The chlorine atom is also more constrained when incorporated into the ligand relative to an intermolecular interaction, which would also be expected to lessen the detrimental influence. The decomposition may well occur *via* the same pathway for both additives, with chloroalkanes less reactive.

Another halogenated compound commonly associated with trimerisation systems, chlorobenzene, has been applied much more broadly and has become the standard solvent for many systems, including the best performing PNP system.[97] On this occasion, the effect of *ortho*-dichlorobenzene was explored instead of chlorobenzene so as to better replicate the polarity of the original system. Two experiments were run to test the effects, one in which *o*-$C_6H_4Cl_2$ was used as the solvent and one in which *o*-$C_6H_4Cl_2$ was used as an additive. The *o*-$C_6H_4Cl_2$ was prepared according to the procedure previously described for *o*-$C_6H_4F_2$.

Table 2.12 – Catalyst performance on introduction of *o*-$C_6H_4Cl_2$. Further experimental data available in Section 5.4.9.

Run	*o*-$C_6H_4F_2$ (Eq.)	*o*-$C_6H_4Cl_2$ (Eq.)	1-Hexene (Eq.)	Activity (TOF)*	Selectivity (%)	TON
1	7891	0	4923	1361	95	2199
2	8414	470	4433	879	86	1476
3	0	6460	4928	104	82	349

*TOF = $mol(C_6H_{12})\ mol(Cr)^{-1}\ h^{-1}$.

The data shown in Table 2.12 show that aryl chlorides also have a significant detrimental effect on catalyst performance. It is notable, however, that the effects are far less marked than for alkyl halides, with a far greater relative concentration still producing an active system. It appears, therefore, that there is considerable variation in the magnitude of the negative effects of halogen containing additives.

The process most strongly associated with halogenoalkanes applicable to the observed decomposition is that of reduction.[207] There are numerous examples of primary halogenoalkane reduction with low valent metals in both protic and aprotic environments. The best example is the use of SmI_2 to reduce halogenoalkanes in an aprotic medium.[208] As observed here, it was found that primary brominated species were far more reactive than their chlorine analogues, though they could also be reduced in certain conditions with $SmBr_2$.[209] It is even more unfavourable to reduce aryl halides, especially chlorides, which again supports the trend observed here. It is therefore conceivable, based on the known chemistry of metals in relatively unstable low valent oxidation states, much like Cr^I, that direct oxidation of the chromium in its reduced state breaks the Cr^I/Cr^{III} redox cycle of catalysis.

In further support of the oxidation hypothesis is the unusual reactivity of the ligand. R_3TAC ligands readily form a cationic species *via* the loss of a hydride according to Scheme 2.10.

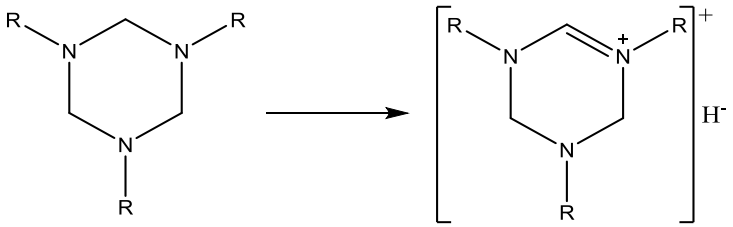

Scheme 2.10 - The 1,3,5-trialkyl-2,3,4,5-tetrahydro-1,3,5-triazin-1-ium hydride ionic compound formed by loss of a hydride. R = Alkyl.

The formation of these ionic compounds can be observed at high intensities by positive TOF-MS from samples of the free ligand. Importantly, the same signals can be observed on occasion from samples of chromium chloride complexes after extensive purification. For example, the corresponding peak was observed as the second most abundant signal for $((Pe_2CCHCH_2)_3TAC)CrCl_3$:

ESI-MS (m/z) $[C_{42}H_{80}N_3]^+$: Calculated exact mass: 626.6352; found: 626.6334.

The ability of the ligand to act as a hydride source further supports the hypothesis that reduction accounts for decomposition. The increasing propensity for reduction as you move from chlorine to bromine containing additives also agrees with established experimental precedent for hydride induced reduction.[207] The formation of the cationic TAC species would almost certainly result in catalyst decomposition due to the loss of a donor site and resulting cation-cation repulsion.

This hypothesis could also explain the strong performance of γ-Pe_2Cl in the decomposition experiment. Prior to addition of the α-olefin the chromium is proposed to remain in the Cr^{III} oxidation state and as such is not prone to oxidation. Any interaction between the metal centre and the chlorine may therefore be beneficial in preventing decomposition *via* alternative pathways such as ligand migration. The absence of the 'halogen effect' for this system as compared to others may be due to different redox cycles in the catalysis. The Phillips trimerisation system, which has benefitted most from exploration of halogenated additives, is proposed to operate *via* a Cr^{II}/Cr^{IV} redox cycle for example.[72] This mechanism may well benefit from an oxidative environment to stabilise the relatively unfavourable Cr^{IV} oxidation state.

Overall, a distinctly negative 'halogen effect' has been observed for this catalyst system. The effect is not observed for γ-Pe_2Cl due to the reduced potency of chloroalkanes as catalyst poisons relative to bromoalkanes, which have a considerable detrimental effect on the system. It is proposed that the decomposition is prompted by oxidation of the Cr^{I} centre by the alkyl halide either through direct interaction or due to hydride inducement. All sources of oxidation should therefore be avoided for $(R_3TAC)CrCl_3$ trimerisation systems.

2.4 Kinetic Analysis

Another observation made during the 1-hexene delay experiment, Table 2.10, was that activities peaked for each catalyst when a delay was introduced. This indicates that activation may be slower than originally thought, resulting in an extended induction period before complete catalyst activation. Kinetic analysis allowed observation of the reaction throughout and identification of the point at which peak activity and complete reaction were achieved. The catalytic performance of γ-Pe_2Cl was twice analysed by integration of ^1H NMR spectra obtained over the course of the reaction. The investigation was repeated in order to compare the effects of the purification process on the catalyst's behaviour. The first kinetic run, using 1-hexene dried with calcium hydride, was successful and gave a total conversion similar to those observed previously, Figure 2.10.

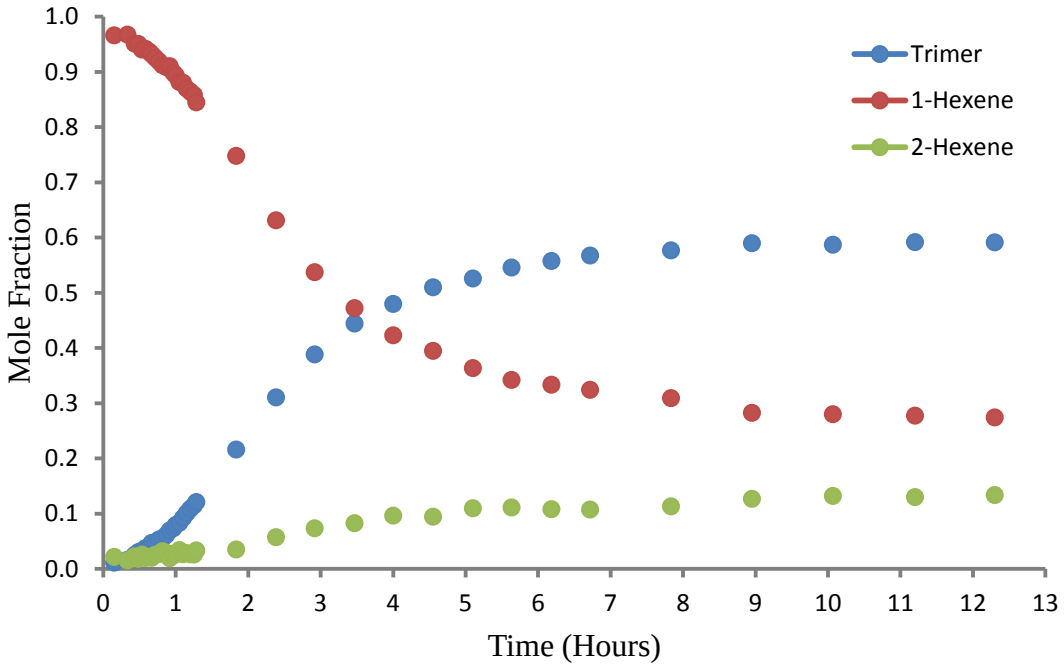

Figure 2.10 - The molar fraction of calcium hydride dried 1-hexene and products over time. Amounts used: 155 Al Eq. MAO, 16720 Eq. *o*-$C_6H_4F_2$, 2280 Eq. 1-Hexene.

As expected, the overall trimerisation was relatively poor and achieved just 60% conversion after 12.5 hours. The most notable feature is that there is indeed a period of initiation, with the reaction only reaching its peak rate after approximately two hours. Based on the decomposition results and the rapid colour change observed on addition of DMAO to the pre-catalyst, it can be hypothesised that slow methyl abstraction causes this initiation period. This process has been described as the rate determining step of activation by others in explanation for the requirement for large quantities of MAO.[19] The absence of 1-hexene in the decomposition tests, combined with the observance of the beneficial effects of delaying addition, suggests that the proposed 2-methylhex-1-ene/methane elimination step does not account for the induction period and is fast.

Regarding isomerisation, the formation of 2-hexene appears to follow the same trend as trimer production, though at considerably lower abundance. This strongly suggests that the active catalyst itself isomerises the 1-hexene, or that a short-lived decomposition product is formed from the active catalyst which is active towards formation of 2-hexene.

The Na/K dried 1-hexene kinetic experiment was run with 6000 equivalents of olefin in an attempt to investigate the catalytic behaviour over an extended period of time, Figure 2.11. Otherwise, the equivalents of DMAO and *o*-$C_6H_4F_2$ were maintained at the same level as for the previous kinetic study.

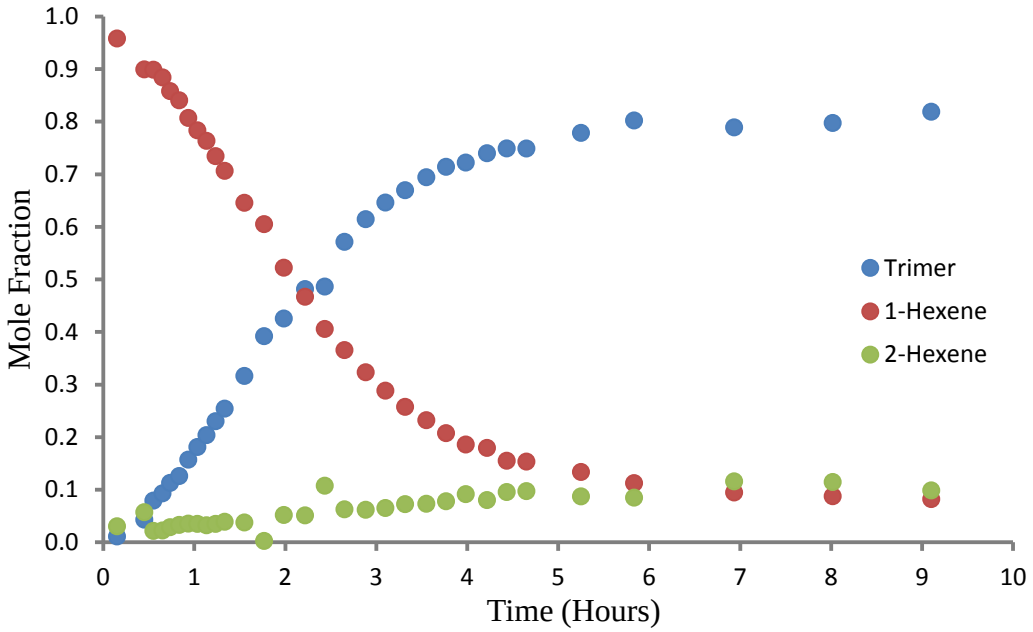

Figure 2.11 - The molar fraction of Na/K dried 1-hexene and the products over time. Amounts used: 165 Al Eq. MAO, 16956 Eq. *o*-$C_6H_4F_2$, 5950 Eq. 1-Hexene.

Despite the higher equivalents of 1-hexene the formation of products plateaued at a similar time as for the contaminated run at around 5 hours. The conversion to trimer, at around 80%, was slightly lower than for previous tests due to greater isomerisation. The purification appears to shorten the initiation period, observed at around one hour in this case, indicating a potential rate dependence on 1-hexene concentration. This would correlate with the observation that the peak rate for this kinetic test was five times greater than for the contaminated test, and therefore the curve would be less pronounced.

The mole fraction of 2-hexene again demonstrated that formation occurs over the same time frame as trimerisation. It appears that this is due to the same apparent dependence on the concentration of active catalyst. It seems clear therefore, with this system known to display considerably less decomposition, that isomerisation results from a side reaction of the active chromium complex. Should 2-hexene be produced by a relatively short-lived decomposition product then the rate of formation would be expected to peak towards the end of trimerisation activity and this is not observed.

The mechanism by which the isomerisation would occur is unclear. Of the two accepted metal catalysed alkene isomerisation mechanisms, ie. the metal hydride addition-elimination mechanism and the π-allyl complex mechanism, the allyl complex mechanism is considered the more likely. The absence of a pre-existing metal-hydride complex or hydrogen source suggests the metal hydride system could not be accessed. While it was shown previously that the ligand can provide access to a hydride which could well be taken up by the chromium centre, this is highly likely to lead to catalyst decomposition. The occurrence of isomerisation at up to 10% of conversion for highly active systems suggests that the production of 2-hexene does not induce catalyst decomposition.

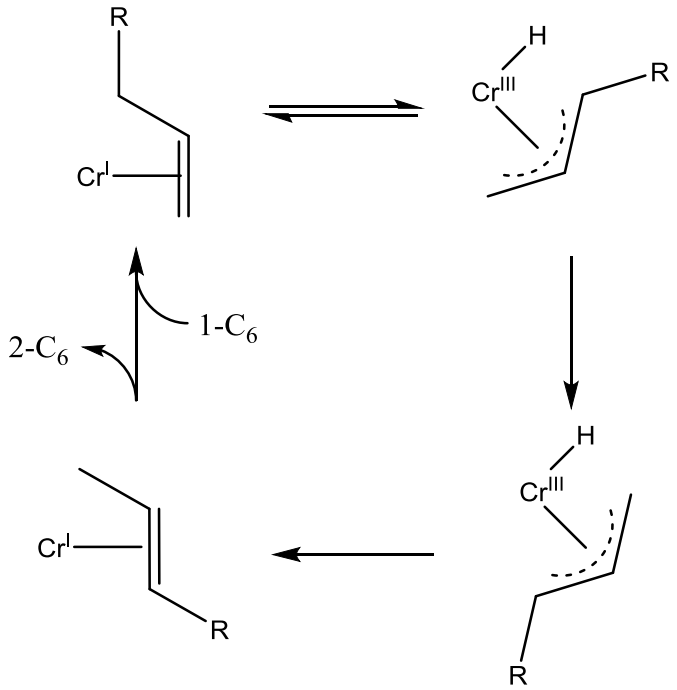

Scheme 2.11 – The proposed isomerisation mechanism.

Several other factors support the proposed allyl complex mechanism shown in Scheme 2.11. The proposed mechanism is reliant on a Cr^{I}/Cr^{III} redox cycle analogous to that of the trimerisation mechanism. Therefore there would be no decomposition induced by oxidation/reduction of the active species. The entry point of the catalytic cycle, the Cr^{I}-LAO adduct, is proposed to exist as an intermediate for both mechanisms. The proposal is therefore in agreement with the observation of tandem reactivity.

The selectivity between the allyl complex isomerisation mechanism and the metallacyclic trimerisation mechanism would be expected to be significantly affected by LAO concentration. If two LAO molecules are bound to the Cr^{I} species then trimerisation would likely be preferred, while if only one molecule is present then isomerisation is the only mechanism able to proceed. Such a relationship was indeed observed for both γ-Pe_2Cl and γ-Pe_2H, with optimal selectivities observed at the highest 1-hexene concentrations investigated, Table 2.9.

Similar conclusions can also be drawn from the results of increasing the solvent and activator concentration. In both cases the increases are predicted to lead to greater dissociation of the active catalyst and the counter-ion. This increased dissociation improves the availability of vacant sites and would therefore be expected to favour coordination of two 1-hexene molecules. In turn, based on this proposal a corresponding increase in trimerisation selectivity would be expected. Variation of the concentration of each reagent led to changes in selectivity that agree with the proposed kinetic control induced by coordination of a second 1-hexene molecule.

The selectivity of isomerisation towards 2-hexene also agrees with the proposed mechanism due to the reduced stability of di-substituted allyl moieties. This combines with the reduced favourability of adduct formation for more highly substituted alkenes such that almost no 3-hexene is observed. However, the relationship would likely be the same for an alternative metal hydride system based on the adduct formation step, as demonstrated by Rajanbabu *et al*.[210]

Synthetically this approach is supported by the high stability of Cr^{III} allyl complexes.[211] $(\eta^3\text{-}C_3H_5)_3Cr$ has been known for decades and has even been applied to oligo- and polymerisation reactions. Two other Cr^{III} allyl complexes that have been isolated and characterised include $Cp(\eta^3\text{-}C_3H_5)_2Cr$ and $Cp(\eta^3\text{-}C_3H_4R)_2Cr$. These species are interesting because of the similarity in bonding between Cp and TAC ligands. Most significant is the second complex, which clearly demonstrates the ability of Cr^{III} to bind mono-substituted allyl ligands.

To the best of my knowledge, no examples of Cr^{III} hydrides have been isolated. This again favours the π-allyl mechanism, as the chromium hydride in this mechanism is proposed to be a short-lived intermediate, as opposed to the stable resting state required by the metal hydride mechanism.

Overall, the evidence collected during the course of this study strongly suggests the existence of a second chromium triazacyclohexane based catalytic pathway that leads to the production of 2-hexene. This activity occurs in tandem with the established trimerisation reaction and the two reaction pathways appear to be interlinked, with the relative activities remaining near-constant throughout reaction. A Cr^{I}/Cr^{III} redox cycle is proposed based on the established π-allyl complex mechanism. The proposal is supported by both synthetic procedures relating to the intermediates and observation of expected trends based on limited kinetic control.[211]

2.4.1 Methane Observation

During these kinetic studies a ^{1}H NMR signal was observed at 0.2 ppm, which appeared to grow during the early stages of the reaction, Figure 2.12. The sharp singlet could be characterised as methane by comparison to a known *o*-$C_6H_4F_2$ solution. 2D ^{1}H NMR analysis indicated that no through bond coupling was observed, supporting the assignment. Minor broad peaks associated with DMAO overlapped with the methane peak, leading to small inaccuracies in peak integration.

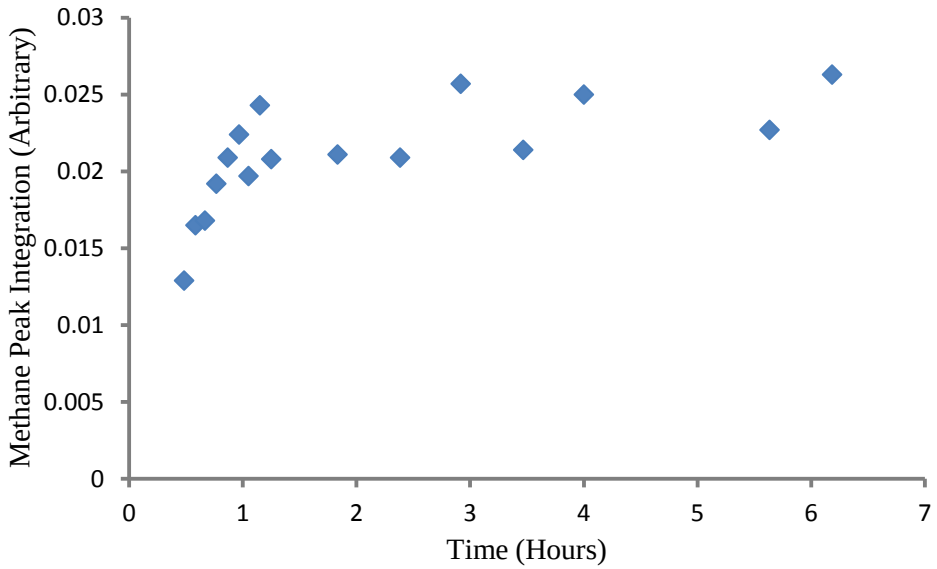

Figure 2.12 - Plot of methane peak integration over the course of the reaction. The integration value was calculated relative to the DMAO peak.

In further support of this characterisation the T_1 relaxation times were calculated for the different ^{1}H signals observed. It was discovered that the T_1 nuclear spin decay for the peak at 0.2 ppm was approximately 40 seconds, as compared to below four seconds for all other peaks. Such extended T_1 relaxation times are only found for proton environments in very small and highly symmetrical molecules. This is due to the loss of intramolecular relaxation pathways that results in stabilisation of the excited spin-state. The magnitude of the T_1 for methane meant that to obtain reliable signal integrations scans should only be taken every 200 seconds ($5.T_1$). As this was not feasible the integration values are only comparable between themselves and could not be analysed quantitively.

The data do, however, suggest a rapid increase in methane concentration during the first hour of the reaction, after which the abundance appears to plateau. The Youngs tube was sealed throughout and as such this is not considered to be a solubility limit but rather the point at which complete catalyst activation had been achieved. The peak concentration is reached at approximately the same reaction duration as the peak activity of the system. This strongly suggests that the methane proposed to result from the final stage of catalyst activation can be directly observed to monitor the production of the active catalyst. The methane could also result from hydrolysis of the DMAO, though the Karl-Fisher titrations indicate such a reaction would only account for a minor proportion.

2.5 Counter-Ion Variation Using Chromium Triflates

MAO and DMAO are very effective alkylating and abstraction agents but, as has been described in this report, they have serious drawbacks. The most significant of these is the high costs associated with their use. From a commercial perspective these costs are often prohibitive to the application of catalysts reliant on activation by these species. In addition, MAO is poorly defined and prevents crystallisation of ionic intermediates or decomposition products. Also, due to the synthetic procedure used to manufacture MAO, and thus DMAO, there is often considerable variation in performance between samples, another significant problem for commercialisation. As such, there has been considerable research towards developing catalysts that can be activated by cheaper and more readily available compounds.

The most established method for avoiding the use of MAO, which has been applied in numerous catalytic studies, involves the use of a fluorinated borane as an abstracting agent in concert with an aluminium alkyl as an alkylating agent.[126, 201] While this method leads to a better defined system and aids analysis of intermediates, the costs associated with the borane are still high. Aside from the Phillips trimerisation catalyst and adaptations thereof, only the PNPNH and NPN catalysts have shown the potential to be cheaply activated, by $AlMe_3$ and $AlCl_2Et$ respectively.[113, 212] In both cases relatively few equivalents of activator were required, presenting a far cheaper activation route. Unfortunately, the performance of the resulting catalysts fell well short of the MAO activated analogues and again rendered the catalyst unsuitable for industrial application.

An alternative activation route for the benchmark PNP trimerisation and tetramerisation catalysts has also been published, which avoids the use of expensive borane and MAO derivatives. McGuinness *et al.* carried out an extensive review into the use of perfluorinated aluminium oxides as counter-ions.[213] Aluminate counter-ions of this type were first described by Krossing *et al.* and were shown to act as extremely weakly coordinating ions.[214-216] By using trityl salts it was possible to abstract an alkyl group to form a neutral compound, such that the counter-ion of the active species could be specifically designed.

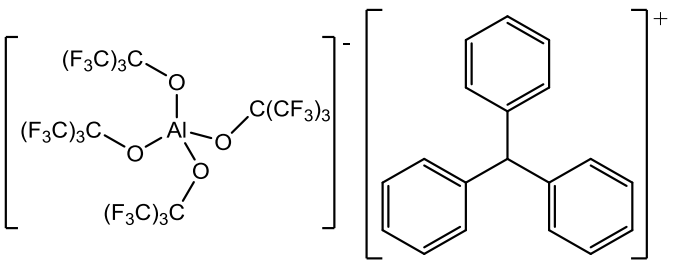

Figure 2.13 - The most effective co-catalyst, in combination with $AlEt_3$.

It was discovered that the $[Al(OC(CF_3)_3)_4]^-$ salt, Figure 2.13, performed well as the counter-ion and effectively mimicked the selectivity and performance of the MAO activated analogue. Optimisation of the $AlEt_3$ alkylating agent demonstrated peak activities at 100 equivalents, considerably lower than most MAO systems. The binding strength could be accurately judged based on the relative selectivity for tri- or tetramerisation. Stronger binding hindered a coordination site and favoured trimerisation in agreement with the proposed ring-expansion mechanism.[217]

It was judged therefore that aluminates of this type were sufficiently weakly binding to imitate the behaviour of aluminoxanes while remaining a defined structure. For the first time, a highly active system was described in which activation without the use of MAO or boranes led to a highly active system. It is reasonable to assume therefore that there is considerable further scope to explore the use of alternative activators and counter-ions.

In an adaptation of this work Wass *et al*. discovered that a cationic precatalyst could be synthesised directly to eliminate the need for an abstracting agent on activation.[218] Formation of the cationic chromium complex was achieved according to Scheme 2.12 using a ferrocenium salt to oxidise $CrCl_2(THF)_2$. Subsequent addition of the PNP ligand led to substitution of the THF to produce the precatalyst.

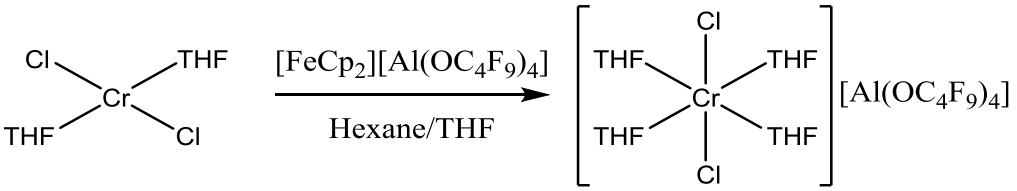

Scheme 2.12 – Synthesis of a cationic chromium complex with a weakly coordinating anion.

Activation of this system was achieved with just 10 equivalents of $AlMe_3$, representing a very cheap activation procedure overall. Unfortunately, this system suffered from the same problem as the borate systems. The peak activity of this system was reported as around 75,000 $g(C_2H_4)\ mol(Cr)^{-1}\ h^{-1}$ at 40 bar ethylene pressure. This represents a 50% reduction in performance relative to the MAO activated system under the same conditions. The additional synthetic step required for formation of the precatalyst in combination with the loss in activity suggests this method would not be employed over the original MAO based method.

Based on the results of McGuiness *et al.*, the $(R_3TAC)CrCl_3$ LAO trimerisation system was tested with $KAl(OC(CF_3)_3)_4$ as an additive. The salt was synthesised according to Scheme 2.13 in adaptation of the original synthesis described by Krossing *et al*.[215] The reaction was performed at low temperature to avoid the formation of aluminium fluoride species such as $KAl(OC(CF_3)_3)_3F$. A small quantity of these species were still produced but proved considerably more prone to sublimation, allowing purification.

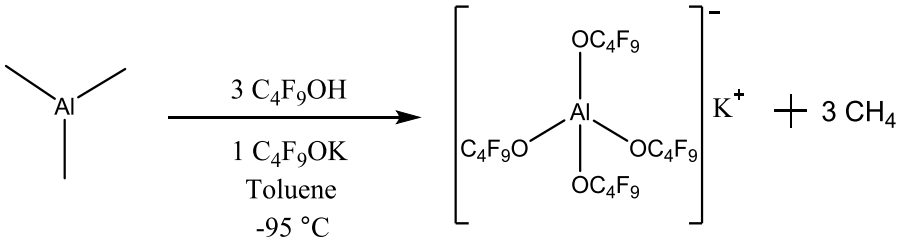

Scheme 2.13 - Synthesis of the defined aluminate counter-ion.

Should the aluminate act as a more weakly coordinating anion than MAO then it would be expected that catalyst performance would remain unchanged. However, should the additive bind more strongly, it would be expected that the activity of the system would fall as 1-hexene insertion is restricted. An excess of the aluminate relative to the catalyst was added to a 1-hexene trimerisation run in order to investigate its effects. A parallel control reaction was run to allow direct comparison.

The activity of the control and doped reactions were found to be almost identical at 1002 and 1065 mol(1-C_6) mol(Cr)$^{-1}$ h^{-1} respectively. Both systems demonstrated good selectivities of over 90% and high turnover numbers, suggesting that the aluminate has no detrimental effect under these circumstances. Further experimental data are available in Section 5.5. This result suggests that considerable scope exists for modification of the counter-ion to give similarly active R_3TAC catalyst systems, as observed by McGuinness *et al*.[213]

While considerable research has focused on the use of various activating agents and counter-ions, little attention has been paid towards variation of the abstractable anion of the catalyst. The favourability of alkylation/abstraction must be directly related to the binding strength of the anionic ligand to be removed. The strength of the abstracting agent required is then likely to be directly related to this feature of the pre-catalyst. The use of more weakly bound anions in the pre-catalyst may, therefore, result in a broader range of activators displaying suitable reactivity. In addition, in cases where a single activating agent is applied, the abstractable anion is incorporated into the counter-ion and likely plays a key role in its behaviour. Thus, this under-investigated aspect of catalyst systems could have a considerable effect on overall activities.

Bercaw *et al.* have undertaken some theoretical investigations into catalyst modifications of this type by exploring synthetic routes to alternatively halogenated pre-catalysts.[219] It was found that oxidation of (PNP)Cr(CO)$_4$ by exposure to Br_2 or I_2 led to the production of (PNP)CrX_3. Though the resulting compounds were never investigated as trimerisation catalysts.

Due to the apparent absence of research into this aspect of the catalyst activation, investigations were conducted into the synthesis of novel chromium catalysts containing alternative anionic ligands. The synthesis of (Me_3TAC)CrBr_3 has been demonstrated previously by Baker *et al.*[164] The synthesis was carried out using an analogous procedure to that of Bercaw *et al.*, in which (Me_3TAC)Cr(CO)$_3$ was oxidised with N-bromosuccinimide in the presence of tetrabutylammonium bromide. To the best of my knowledge, this is the only example of ligand substitution with a chromium triazacyclohexane complex reported to date.

TACN systems have been investigated more thoroughly in this regard. Ryu *et al.* have reported that (H_3TACN)CrCl_3 reacts directly with trifluoromethanesulphonic acid to give (H_3TACN)Cr(OTf)$_3$ complexes in high yields.[220] The triflate ligands of this species proved to be highly labile and numerous substitution reactions were demonstrated. Addition of simple sodium salts to the chromium triflate resulted in the facile synthesis of chromium chlorides, bromides, cyanides and thiocyanates. Analogous chemistry was also reported by Brorson *et al.* with the use of triammines, in this case achieving substitution of the triflate ions with lithium salts.[221]

Based on the success of these more stable tri-nitrogen donor systems, similar chemistry was explored with the use of triazacyclohexane ligands. It had previously been shown by R. D. Köhn that $(R_3TAC)CrCl_3$ complexes react with trifluoromethanesulphonic acid to form $(R_3TAC)Cr(OTf)_3$ complexes in an analogous manner to that described for TACN chromium complexes. A novel set of chromium triflates were therefore synthesised according to the same procedure in order to investigate their substitution chemistry.

2.5.1 Synthesis of Chromium Triflate Triazacyclohexane Complexes

The synthesis of $(R_3TAC)Cr(OTf)_3$ complexes from $(R_3TAC)CrCl_3$ requires direct solvent free addition of trifluoromethanesulphonic acid, which is then removed under high vacuum. In order to completely remove the acid the resulting solids must be washed repeatedly with diethyl ether.[220] For this reason, the highly soluble γ-branched catalysts proved unsuitable for application to triflate chemistry as the majority of the yield was lost during purification.

It was therefore necessary to synthesise new, less soluble, ligands for use in these reactions. In order to obtain a set of ligands with a range of branching points, two new ligands were synthesised. $((Pr_2CHCH_2)_3TAC)CrCl_3$ is unpublished but has previously been used during investigation of chromium carbonyl chemistry within the group and was shown to readily crystallise. It was therefore synthesised anew as a sparingly soluble β-branched complex, the procedure is described in Chapter 5. The synthesis of α-branched ligands has not been described previously, with the exception of those with commercially available α-branched amines as the precursor.

The novel synthesis of $(^iBu_2CH)_3TAC$ described herein has been carried out according to a technique adapted from work by Manning *et al.*[222] The one-pot technique described for the synthesis of α-branched primary amines allowed the introduction of *iso*-butyl moieties to produce a low solubility and high steric bulk ligand. The procedure was carried out according to Scheme 2.14 and recorded a yield of 67%.

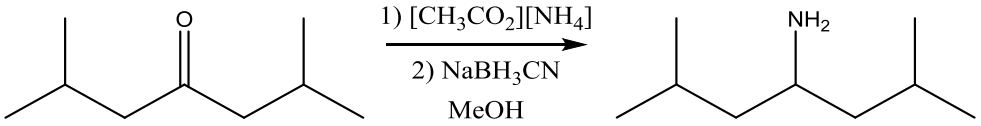

Scheme 2.14 – α-Branched amine formation from the corresponding ketone.

The synthesis was carried out in two steps. Firstly, imine formation was carried out with ammonium acetate over the course of 1.5 hours. Secondly, imine reduction was carried out with sodium cyanoborohydride over the course of 30 minutes. The use of this reducing agent, reported to be the most effective for this reaction, led to considerable safety concerns. The necessary hydrolysis of the cyanoborohydride on work-up results in the formation of hydrogen cyanide. The risks associated with the evolution of this potent poison were mediated by bubbling through a cooled trap containing an aqueous solution of NaOH and $FeSO_4$. Exposure of HCN to this solution results in deprotonation and complexation of the cyanide anion to form a far less dangerous iron cyanide complex, which can then be safely disposed of.

The colourless non-viscous oil extracted after purification was then reacted with paraformaldehyde according to the same procedure described previously. After stirring for 2 days and removal of the water formed during the condensation reaction, the product was analysed by NMR spectroscopy. Rather than the expected TAC formation, a 2:3 equilibrium mixture of $(^{i}Bu_2CH)_3TAC$ and $^{i}Bu_2CHN{=}CH_2$ had formed, Scheme 2.15. This clearly demonstrates that incorporation of α-branching increases the bulk around the TAC ring to such an extent that formation is significantly hindered. Such behaviour was not observed for the β-branched N-substituent, suggesting a far lower steric effect.

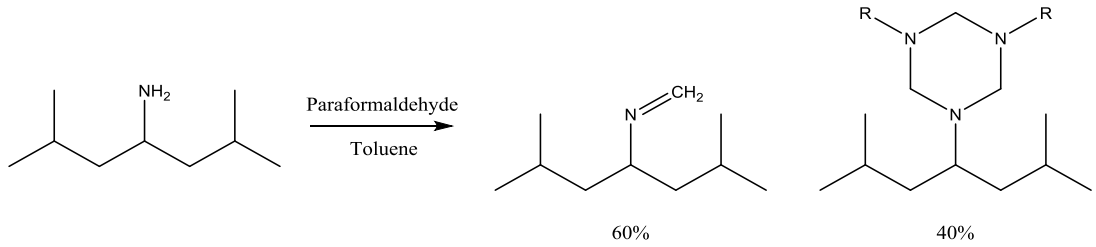

Scheme 2.15 – Formation of the 3:2 mixture of imine and TAC.

Formation of the imine complicated purification due to its far greater volatility relative to most TAC ligands, leading to a low yield for this reaction at 75%. The mixture was taken forward without any attempt to separate the two products. Complexation to $CrCl_3(THF)_3$ was carried out according to the method previously described, Scheme 2.16, and the resulting purple solution eluted through silica with DCM. After solvent removal a yield of 71% was isolated, with losses attributable to the diminished purification of the ligand.

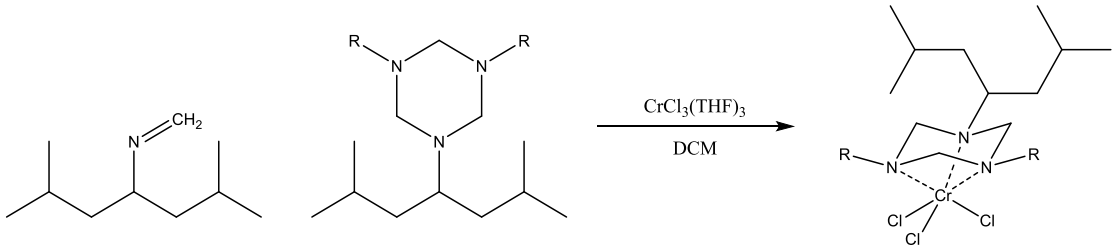

Scheme 2.16 – Complexation of chromium chloride using the mixture of TAC and imine ligands.

The presence of the imine in the mixture does not seem to affect the complexation, with a high yield recorded. This could result from two possible processes. Either the complexation of the TAC ligand shifts the equilibrium and results in further TAC formation, or three imine ligands bind to the chromium and ring formation occurs *a postieri*. The second process appears more likely based on the observation made previously by R. D. Köhn that adamantylamine reacts with formaldehyde to form 100% imine. No equilibrium exists in this case but complexation still proceeds to give the $(Ad_3TAC)CrCl_3$ complex, supporting the idea of ring formation post complexation.

The resulting $(({}^{i}Bu_2CH)_3TAC)CrCl_3$ was separated into two equal samples, one was kept for chromium chloride catalysis while the second was taken forward to investigate the behaviour of chromium triflates. In adaptation of the original procedure described by Ryu *et al.* for TACN chromium chlorides, excess pure CF_3SO_3H was condensed with liquid nitrogen under high vacuum onto the chromium chloride complex. On melting, this resulted in a rapid and violent reaction in which severe effervescence was observed due to the evolution of HCl gas, which was collected in a secondary trap. A prussian blue solution was formed almost immediately, with the reaction considered complete after no further bubbling was observed. The excess trifluoromethanesulphonic acid was then distilled off by heating the solution to 40 °C under high vacuum over the course of 6 hours. The remaining blue solids were washed repeatedly with diethyl ether until the washings were colourless.

After further drying under vacuum the solids were collected at a yield of 87% and stored under argon. Characterisation of the resulting complex proved difficult. Mass spectrometry, which proved to be a highly reliable method for the characterisation of $(R_3TAC)CrCl_3$ complexes, was not suitable for identification of these compounds. With or without the addition of ammonium salts, only low intensity signals were observed for which the identities could not be determined. Only the triflate ion could be reliably observed and identified during negative runs, suggesting catalyst decomposition may have occurred in the aqueous environment of the TOF-MS. This was not unexpected due to the high lability of triflate ions.

The paramagnetic nature of the chromium species prevented accurate ^{1}H NMR spectroscopy. Meanwhile, ^{13}C NMR analysis gave a very similar spectra to that of $(({}^{i}Bu_2CH)_3TAC)CrCl_3$, indicating the ligand remained bound to the chromium but giving little information on the presence of triflate groups. ^{19}F NMR analysis was then performed in an attempt to look at the triflate groups directly.

An extremely broad peak was observed at -44.4 ppm, set relative to the known shift of *o*-$C_6H_4F_2$. The line width of this peak, at 3400 Hz, demonstrated the close proximity of fluorine atoms to the paramagnetic centre. Larger Cr^{III}-F distances attributed to outer sphere interaction have been shown to exhibit line widths in the order of 100-300 Hz.[201] As such, such a large line width can be attributed to inner sphere coordination of the triflate group to the chromium metal, indicating the successful synthesis of $(({}^{i}Bu_2CH)_3TAC)Cr(OTf)_3$. The bulk chromium triflate was also characterised with air sensitive elemental analysis.

The synthesis of $((Pr_2CHCH_2)_3TAC)Cr(OTf)_3$ from $((Pr_2CHCH_2)_3TAC)CrCl_3$ was carried out according to the same method, with an isolated yield of 88%, and characterised in the same manner. A broad ^{19}F peak at almost identical shift (-45.6 ppm) and line width (3300 Hz) was again observed by NMR analysis and the elemental analysis was satisfactory. All four complexes will be referred to by the abbreviations shown in Figure 2.14 throughout the remainder of this thesis.

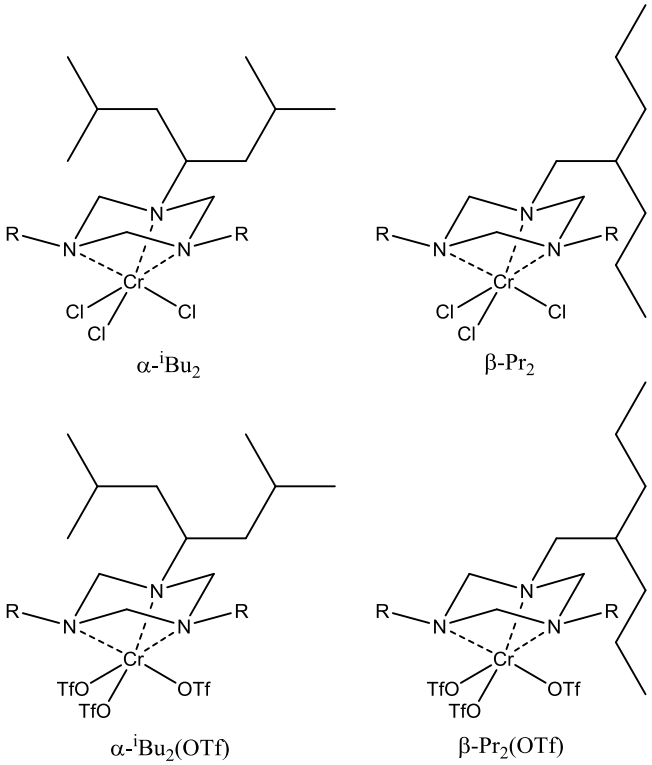

Figure 2.14 - The abbreviations used for the newly synthesised catalysts.

This method for the synthesis of chromium triflates has obvious drawbacks due to the additional synthetic step required compared to chromium chloride catalysts. Alternative routes were therefore explored in which chromium triflates could be directly accessed. It has been known since 1971 that trifluoromethanesulphonates are able to form Cr^{III} complexes in aqueous media.[223] The weakly coordinating nature of the anion means that in the presence of dilute CF_3SO_3H and oxygen $[Cr(H_2O)_6][OTf]_3$ is formed from chromium metal.

This procedure was repeated at 90 °C and over the course of 12 hours the expected blue/violet solution was formed. Removal of the water under reduced pressure produced a sticky blue solid, which was then dried further under high vacuum at ~200 °C to give a green solid at a yield of 89%, Scheme 2.17. The green solid proved to be extremely hydrophilic, as would be expected from the synthetic route, with the sticky blue solid reformed within seconds on exposure to air.

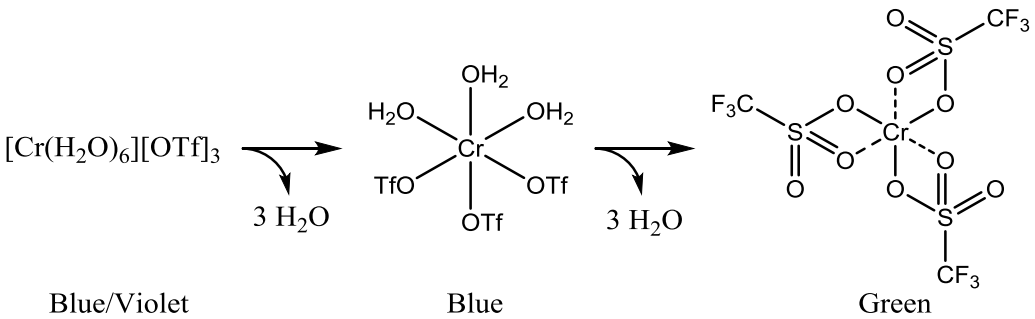

Scheme 2.17 – Synthesis of $Cr(OTf)_3$.

Purification and analysis of this material was complicated by its high hydrophilicity. Air sensitive elemental analysis only gave limited information because of the absence of hydrogen and nitrogen from the structure. The carbon content matched that expected but just over 1% hydrogen was detected, suggesting the sample was not completely dry. ^{19}F NMR spectroscopy displayed a broad peak with a line width indicative of direct binding of the triflate. The peak shift differed to that of the TAC complexes, as would be expected, and was observed at -53 ppm, again set relative to *o*-$C_6H_4F_2$. In agreement with the elemental analysis results, a smaller peak was observed at -76 ppm with a line width of 178 Hz. This suggests that outer sphere triflates give signals at around -76 ppm, much like the acid itself, and that the material is not completely dry.

Unfortunately, use of this species in the synthesis of $(R_3TAC)Cr(OTf)_3$ catalysts proved difficult. Insolubility in *o*-$C_6H_4F_2$ and less polar solvents severely hindered its use within the glovebox. Meanwhile, reactions undertaken in more polar dry solvents using Schlenk techniques did not produce any isolatable product. The reason for the failure of this synthetic pathway is unclear but no further investigations were undertaken due to the ready availability of the catalysts using the original method.

Exploration and optimisation of LAO trimerisation with chromium triflates was carried out first by R. D. Köhn and later by C. Heron under my supervision in a parallel project to my Ph.D. It was found that these catalysts could be activated by aluminium alkyls without the need for an additional abstraction agent. This resulted in a more defined system and removed the need for expensive MAO derived activators. However, as has been observed by other groups, the avoidance of MAO led to considerably reduced activities and selectivities.[19]

$AlEt_3$ was found to be the most effective activating agent in regards to the catalyst activity but these systems suffered from rapid deactivation. $AlMe_3$ proved to produce a more stable system with lower activities. It was also found that activation was best achieved with just 20 equivalents of $AlMe_3$, reducing the cost of the system further. The greater reliability of this activation route led to its adoption for later work described herein.

2.6 Synthesis of Alternative Chromium Halides and Pseudo-Halides

Due to the reduced steric bulk of β-Pr_2(OTf) relative to α-$^{i}Bu_2$(OTf), based on the results of the original TAC formation, it was decided to investigate the substitution chemistry of chromium triflate with this complex first. Initially, the procedures described by Ryu *et al.* and Brorson *et al.* were adapted with the use of simple potassium salts, rather than lithium or sodium. The greater instability of TAC complexes relative to those of the strong TACN and ammine donors meant that the procedure had to be altered considerably. All experiments were run under argon and *o*-$C_6H_4F_2$ was used as the most polar solvent available. This meant that the solubility of the salts was much lower than for the systems previously described.

Initial tests were performed with potassium chloride, bromide and iodide. A solution of 50 mg of β-Pr_2(OTf) was made-up in *o*-$C_6H_4F_2$ before addition of a large excess of the potassium halide. The salt was insoluble and formed a suspension which was stirred vigourously. No immediate colour change was observed in each case and the reactions were left to stir for 15 hours overnight. During this time the potassium bromide reaction had become a vivid purple in colour. The solution was eluted through a silica column with *o*-$C_6H_4F_2$ to remove the remaining salts and any unreacted chromium triflate. After removal of the solvent a 73% yield of purple solids was collected. The chromium tribromide complex was confirmed by TOF-MS and elemental analysis.

The remaining reactions were left for a further 24 hours but became cloudy blue/green solutions. The solutions were worked up in the same manner as for the bromide reaction to give purple solids in the case of the chloride and an orange/brown material in the case of the iodide. Based on the poor yield for these reactions and the observation that the salt was highly insoluble, an alternative halide source was used.

To test the effect of salt solubility the chloride reaction was repeated with Bu_3BzNCl. The colour change indicative of the reaction occurred within minutes and TOF-MS analysis indicated complete reaction. The good solubility of this ammonium salt presented complications to the purification however as, surprisingly, it could not be separated from the product with the use of column chromatography. This is likely due to adduct formation in an analogous manner to that observed for the TOF-MS analysis.

To simplify the purification a compromise was made with the use of Me_4NX as a cheap halide source expected to be more soluble than potassium salts but not to fully enter solution. The use of tetraalkylammonium salts should also aid the reaction due to the greater favourability of interaction between the soft cation and the soft anionic triflate, as compared to the hard halides. The reaction and subsequent purification steps were repeated according to the same method, using a large excess of Me_4X. The results are presented in Table 2.13 alongside a comparison with the KX reactions.

Table 2.13 – The results of triflate substitution with the two halide sources.

	KX		Me_4NX	
Target Compound	Isolated Yield (%)	Reaction Time (h)	Isolated Yield (%)	Reaction Time (h)
$((Pr_2CHCH_2)_3TAC)CrCl_3$	14	39	74	< 1
$((Pr_2CHCH_2)_3TAC)CrBr_3$	73	15	75	2
$((Pr_2CHCH_2)_3TAC)CrI_3$	15	39	42	39
$((^iBu_2CH)_3TAC)CrBr_3$	~	~	12	48
$((^iBu_2CH)_3TAC)CrI_3$	~	~	0	48

A significant improvement can be seen with the use of Me_4NX over KX both in terms of yield and reaction time. The general trend for the improved reaction method appears to be increasing reaction time as the Cr-X bond strength decreases, as would be expected on thermodynamic considerations. The low yield recorded for formation of $((Pr_2CHCH_2)_3TAC)CrI_3$ is as a result of losses incurred during purification by column chromatography. The chromium triiodide demonstrates far lower stability than the trichloride and tribromide, which gave no indication of decomposition on the column. TOF-MS analysis indicated an equally pure product prior to chromatography, indicating that, decomposition aside, roughly the same yield would be expected. All complexes were confirmed by TOF-MS and elemental analysis.

This synthetic method represents, to the best of my knowledge, the first example of chromium triiodide synthesis by substitution of triflate groups. This procedure was attempted by both Ryu *et al.* and Brorson *et al.* without success, with the steric bulk of the iodide ion attributed to the lack of reactivity.[220, 221] This further demonstrates how the open environment around the chromium centre, induced by the acute N-Cr-N bond angles of TAC ligands, can beneficially influence the coordination chemistry of the complexes.

The success of these experiments led to the attempted synthesis of $((^iBu_2CH)_3TAC)CrBr_3$ and $((^iBu_2CH)_3TAC)CrI_3$. However, these complexes did not form so easily and it was not possible to synthesise the chromium iodide, as shown in Table 2.13. The chromium bromide was formed after two days of vigourous stirring but was shown by TOF-MS to be impure. Three main peaks were observed that corresponded to $[((^iBu_2CH)_3TAC)CrBr_3.Me_3NH]^+$, $[((^iBu_2CH)_3TAC)CrBr_2]^+$ and $[((^iBu_2CH)_3TAC)CrBr_2(OTf).Me_3NH]^+$ respectively:

$[C_{30}H_{63}Br_3CrN_3.C_3H_{10}N]^+$: Calculated exact mass: 816.2770; found: 816.2744.

$[C_{30}H_{63}Br_2CrN_3]^+$: Calculated exact mass: 677.2773; found: 677.2749.

$[C_{30}H_{63}Br_2CrF_3N_3O_3S.C_3H_{10}N]^+$: Calculated exact mass: 886.3107; found: 886.3089.

The chromium dibromide and the chromium dibromide monotriflate signals are both likely to derive from the monotriflate species due to the known favourability of triflate dissociation. The monotriflate peak was observed at considerably lower intensity than the chromium dibromide and represents the first mass spectrometry derived evidence for complexation of triflate anions. It is remarkable that the $CrBr_2(OTf)$ complex could be observed in aqueous media and survived adduct formation. This suggests that substitution of the third triflate group is considerably less favourable than for the previous two, resulting in the incomplete reaction. This can most likely be ascribed to the large steric bulk of the triflate ion, once only one remains the strain is considerably reduced and the kinetic inertness of the chromium leads to greater retention.

Surprisingly, the $CrBr_2(OTf)$ complex was even stable on contact with silica and the two products could be separated. In this manner, $(({}^{i}Bu_2CH)_3TAC)CrBr_3$ was isolated and confirmed by TOF-MS and elemental analysis. The increased steric bulk of the α-branched ligand has a considerable effect on the chemistry of the complex. The stabilising effect towards substitution indicates that this complex may demonstrate much improved resistance to decomposition. In an attempt to push the reaction towards completion the reaction was repeated in dry acetone, with an aim to reduce any solubility restrictions and therefore increase the concentration of the halide source.

With the use of acetone as the solvent the reaction proceeded quicker, a purple solution was formed within 15 hours, but the product consisted entirely of the $CrBr_2(OTf)$ complex. The reaction was then repeated with β-$Pr_2(OTf)$ and the analogous product was observed, which had not been seen previously for this ligand. It appears that the acetone plays an active role in the reaction and prevents substitution of the final triflate group. While this prevented an improved synthetic route to the bulky chromium bromide, it does present a method for the synthesis of unsymmetrically ligated chromium triazacyclohexane complexes, Scheme 2.18.

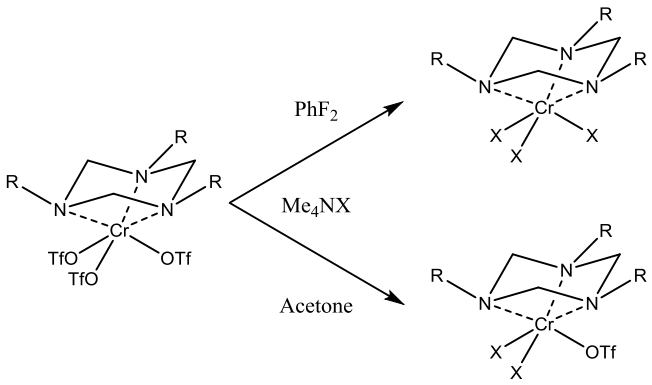

Scheme 2.18 - The effect of the solvent on triflate substitution.

The success of these reactions naturally led to investigation of chromium trifluoride synthesis. These species, though expected to be highly stable, could not be synthesised in our hands by the method described above. In each case a pale green suspension was formed, which was shown by TOF-MS not to contain the desired product. Similar colour changes are typically associated with hydrolysis of the chromium. The renowned difficulty in drying fluoride salts was therefore considered to prevent this reaction, despite numerous attempts at drying the fluoride source.

An alternative route was adapted from that originally described by Andersen *et al.* that relies on aqueous chemistry and is therefore not vulnerable to the hydrophilicity of fluoride salts.[224] NH_4F was added to $Cr(NO_3)_3$ under aqueous conditions to produce $[Cr(H_2O)_6]F_3$ in a similar reaction to that of the chromium triflate synthesis. Reaction with an excess of pyridine followed by drying then resulted in the isolation of $Cr(py)_3F_3$ as a purple solid, as described. In the original work a triammine complex was then formed by exposure to ammonia. Adaptation to form an R_3TAC complex was attempted by exposure to the ligand at 150 °C and refluxing under high vacuum in an attempt to remove any pyridine produced. Unfortunately, despite the highly forcing conditions the substitution of the pyridine donors could not be achieved.

The weak donating ability of the TAC ligand relative to the pyridine donors is the likely cause of the barrier to substitution, with the chelate effect unable to compensate for the loss in binding strength. L_3CrF_3 formation directly from a chloride has also been demonstrated *via* exposure of the complex to hydrogen fluoride in the presence of an Hg^{II} catalyst.[224] However, the equipment required for this hazardous procedure was not available and this route could not be explored further. The chromium chloride, bromide and iodide were taken forward for further investigation without further attempts to synthesise the fluoride analogue.

In addition to the introduction of alternative halides, the substitution of the triflate groups with thiocyanate moieties was also investigated. An excess of NaSCN was added to a solution of β-Pr_2(OTf) in *o*-$C_6H_4F_2$ and stirred for two days. No colour change was observed in this time, suggesting no reaction, but isolation of any trace product was attempted by eluting through a silica column with *o*-$C_6H_4F_2$. A turquoise solution was collected before the solvent was removed to give a sticky blue solid, at a yield of 14%, which could not be dried under vacuum. TOF-MS confirmed the product to be $((Pr_2CHCH_2)_3TAC)Cr(SCN)_3$ by formation of the typical Me_3NH adduct but also by observation of a $((Pr_2CHCH_2)_3TAC)Cr(SCN)_4$ anion:

$[C_{30}H_{57}CrN_6S_3.C_3H_{10}N]^+$: Calculated exact mass: 709.4025; found: 709.4060.

$[C_{31}H_{57}CrN_7S_4]^-$: Calculated exact mass: 707.2963; found: 707.3060.

The formation of an anion in this way suggests adduct formation through an alternative pathway to the established hydrogen bond formation with halide groups.[201] Instead, the hydrogen bonding must result from the protons of the TAC ring in a similar manner to that observed for the extended crystal structures of low steric bulk $(R_3TAC)CrCl_3$ systems, described in the same publication. As a result, thiocyanate anions appear to present a method of ionisation which is independent of the abstractable anion, Figure 2.15. This discovery could aid the identification of future chromium triazacyclohexane species in which the abstractable ion does not act as a hydrogen bond acceptor.

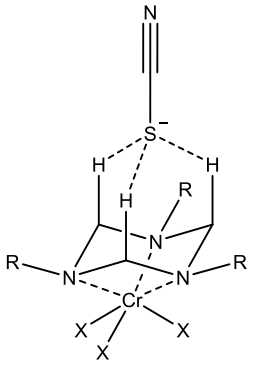

Figure 2.15 - The proposed $(R_3TAC)CrX_3$.SCN adduct observed by TOF-MS.

2.6.1 The Catalytic Potential of Alternative Chromium Halides

In a novel approach to olefin trimerisation catalyst modification, the selective oligomerisation of 1-hexene was attempted with a chromium tribromide and a chromium triiodide catalyst. The optimised procedure was used and the experiments run alongside the analogous chromium chloride catalyst as a control.

Table 2.14 – The trimerisation performance of the different chromium trihalide catalysts. Further experimental data available in Section 5.4.10.

Run	Catalyst	1-Hexene (Eq.)	Activity (TOF)*	Selectivity (%)	TON
1	β-Pr_2	5347	1191	84	759
2	β-Pr_2(Br)	5532	237	90	196
3	β-Pr_2(I)	5420	192	68	97

*TOF = mol(C_6H_{12}) mol(Cr)$^{-1}$ h^{-1}.

As shown in Table 2.14, alteration of the halide ligand from the chloride has a marked detrimental effect on the catalyst performance. However, the alternative halides, especially the bromide, still represent highly selective α-olefin trimerisation catalysts and demonstrate moderate activities. The overall activities of all three runs is disappointing, demonstrating that the $(Pr_2CHCH_2)_3$TAC ligand is considerably less effective than the γ-branched systems. This is most likely attributed to the reduced solubility of these systems, which has been shown in the past to drastically reduce catalyst activities.[2]

The marked loss in catalytic performance is surprising as the active species should not retain the halide and as such, once formed, should demonstrate the same activity. The observed trend of decreasing turnover number and activity from Run 1 to 3 can best be explained by comparison to the work of Bergman *et al.*[61] As described in Chapter 1, it was shown that the efficiency of halide abstraction can have a remarkable influence on the activity and selectivity of a catalyst. Based on these observations, and those of McGuinness *et al.* regarding the effect of the counter-ion,[213] it is proposed that the weaker Al-X bonding reduces the favourability of abstraction.

It follows that the detrimental effect results from the favourability of formation of the counter-ion. Al^{III}, as a harder cation than Cr^{III}, would be expected to form weaker bonds with the softer halides and this seems the most likely explanation for the loss in performance. The existence of an equilibrium between the chromium halide and the aluminium halide would effectively determine the concentration of the active species. When the equilibrium is shifted towards the chromium halide the effective concentration of the active catalyst would be reduced, resulting in the corresponding loss in activity.

2.7 Single Crystal X-Ray Diffraction Analysis

The (($^{i}Bu_2CH)_3TAC)CrBr_2(OTf)$ complex synthesised selectively by the reaction carried out in acetone was isolated and successfully crystallised under air by the gradual concentration of a DCM solution, Figure 2.16.

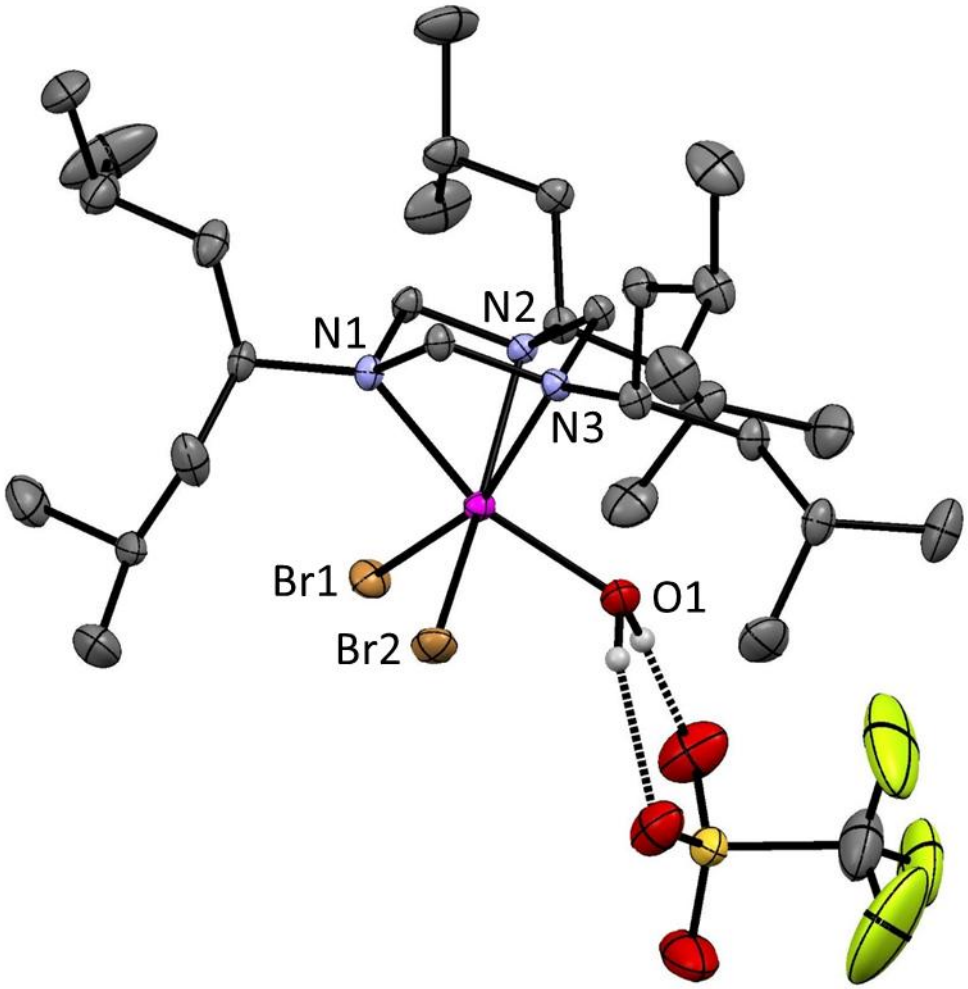

Figure 2.16 - The structure of $[(($^{i}Bu_2CH)_3TAC)CrBr_2(H_2O)][OTf]$ as calculated by single crystal X-ray diffraction. Grey = C, Mauve = N, Pink = Cr, Red = O, Brown = Br, Green/Yellow = F and Straw Yellow = S. All hydrogens have been removed for clarity except those of the water molecule in order to demonstrate the hydrogen bonding. Ellipsoids are set to 50% probability.

Despite the complex demonstrating considerable stability towards silica and aqueous environments it appears that the triflate group is susceptible to substitution by water over longer time periods. That is demonstrated nicely by the X-ray diffraction structure, in which the triflate has been substituted from the coordination sphere by a water molecule. Referring back to previous TOF-MS experiments in which the dihalides were formed, it was found that minor peaks corresponded to this same product, for example $[((Pr_2CHCH_2)_3TAC)CrCl_2(H_2O)]^+$:

$[C_{27}H_{59}OCl_2CrN_3]^+$: Calculated exact mass: 563.3440; found: 563.3434.

Upon substitution the triflate group is then bound to the water molecule by strong hydrogen bonding (1.86 and 2.03 Å). This may make the substitution reaction more thermodynamically favourable despite the displacement of the negative charge away from the cationic chromium centre.

Table 2.15 – Structural information on the coordination environment of the chromium centre.

Coordination Bonds	Bond Length (Å)
Cr – O	2.019(2)
Cr – Br1	2.4138(5)
Cr – Br2	2.4197(6)
Cr – N1	2.096(2)
Cr – N2	2.121(3)
Cr – N3	2.123(3)
Donor Bond Angles	**Bond Angle (°)**
N1 – Cr – N2	66.90(9)
N1 – Cr – N3	66.9(1)
N2 – Cr – N3	65.6(1)
Br1 – Cr – Br2	101.07(2)
Br1 – Cr – O1	94.32(7)
Br2 – Cr – O1	88.74(7)

The hydrogen bonding distorts the symmetry of the molecule, in addition to the trans effect of the oxygen donor, Table 2.15. The bond angles between each of the bromide ions and the oxygen donor of the water molecule would be expected to be similar. The steric influence of the unsymmetrically bound triflate appears to cause greater repulsion between the counter-ion and Br1, distorting the octahedral geometry. In addition, the electronegative neutral oxygen donor results in stronger binding of the *trans* nitrogen donor (N1) due to the trans effect. This leads to slightly off-centre binding of the TAC ligand towards N1, as demonstrated by the bond angles.

Single crystal X-ray diffraction was also possible with other target products, which enabled accurate comparison of the structural effects of halide variation. The chromium chloride, bromide and iodide of the $(Pr_2CHCH_2)_3TAC$ complex were all characterised in this manner and their structures are shown below in Figure 2.17, Figure 2.18 and Figure 2.19.

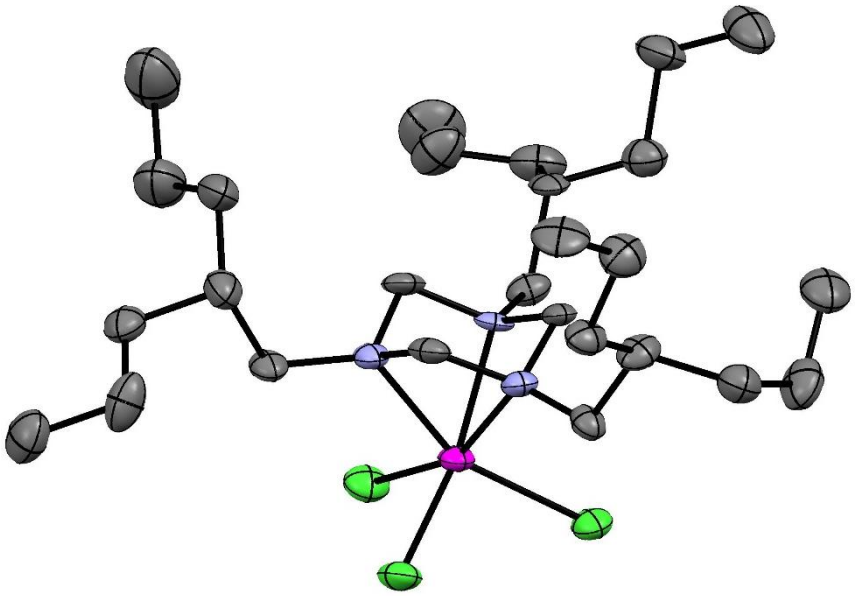

Figure 2.17 - The structure of $((Pr_2CHCH_2)_3TAC)CrCl_3$ as calculated by single crystal X-ray diffraction. Grey = C, Mauve = N, Pink = Cr, Green = Cl. Hydrogens have been removed for clarity. Ellipsoids are set to 50% probability.

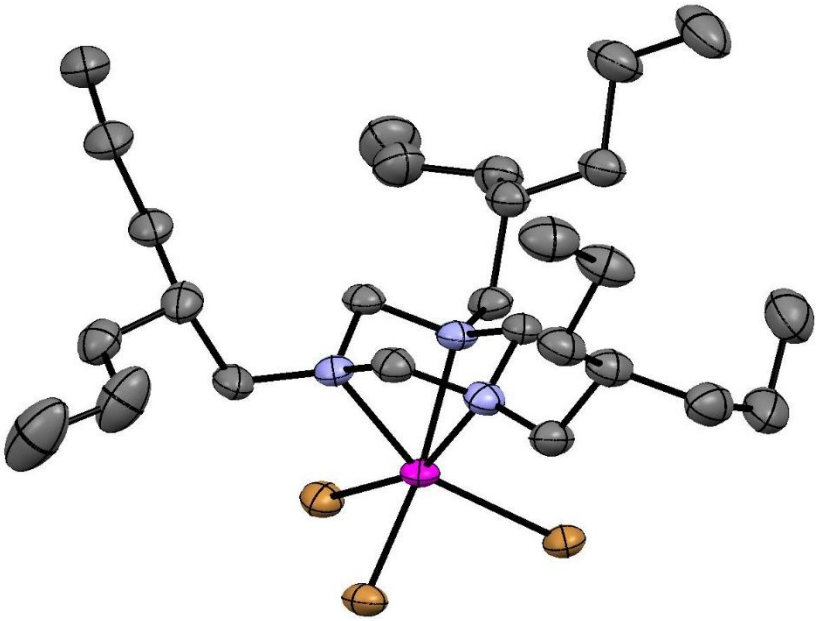

Figure 2.18 - The structure of $((Pr_2CHCH_2)_3TAC)CrBr_3$ as calculated by single crystal X-ray diffraction. Grey = C, Mauve = N, Pink = Cr, Brown = Br. Hydrogens have been removed for clarity. Ellipsoids are set to 50% probability.

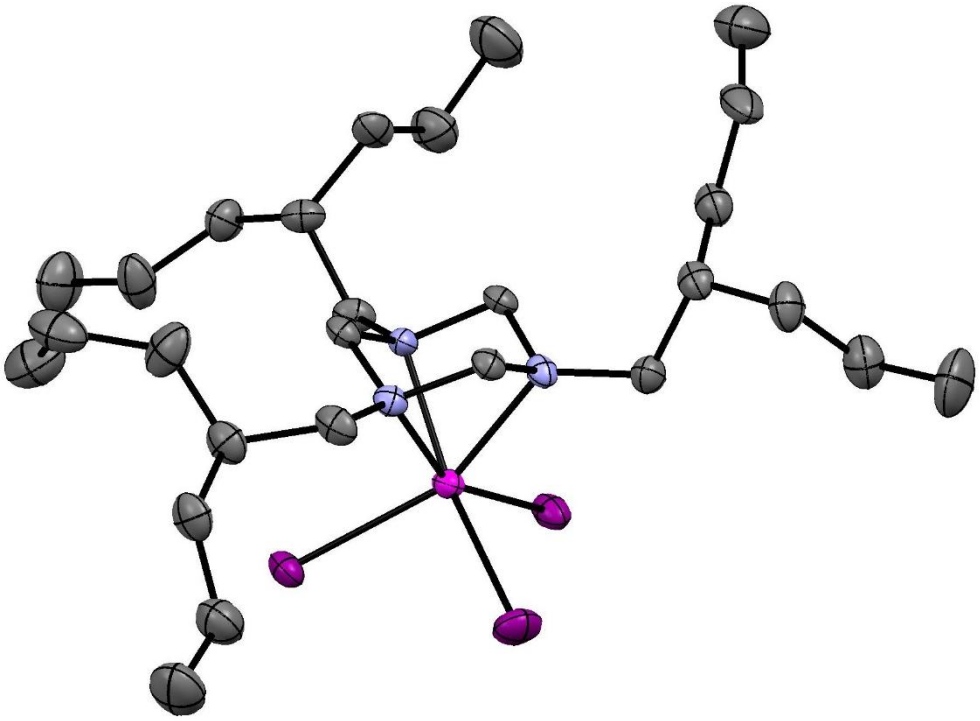

Figure 2.19 - The structure of $((Pr_2CHCH_2)_3TAC)CrI_3$ as calculated by single crystal X-ray diffraction. Grey = C, Mauve = N, Pink = Cr, Purple = I. Hydrogens have been removed for clarity. Ellipsoids are set to 50% probability.

Each of these complexes were crystallised by the gradual concentration of DCM solutions. The chromium tribromide was found to adopt an orthorhombic unit cell while the trichloride and triiodide adopted a monoclinic unit cell. The structural information of the coordination sphere is shown in Table 2.16 and demonstrates the effects of varying the size and binding strength of the halides.

Table 2.16 – Structural data for the $((Pr_2CHCH_2)_3TAC)CrX_3$ complexes, where X = Cl, Br or I.

	Bond Lengths (Å)		
Coordination Bonds	$CrCl_3$	$CrBr_3$	CrI_3
Cr – X1	2.285(3)	2.4417(8)	2.677(1)
Cr – X2	2.288(3)	2.4312(8)	2.631(1)
Cr – X3	2.280(3)	2.4407(8)	2.644(1)
Average Cr-X	2.285	2.438	2.651
Cr – N1	2.097(7)	2.109(4)	2.129(6)
Cr – N2	2.118(8)	2.112(3)	2.140(7)
Cr – N3	2.080(8)	2.111(3)	2.115(5)
Average Cr-N	2.098	2.111	2.128
	Bond Angles (°)		
Donor Bond Angles	$CrCl_3$	$CrBr_3$	CrI_3
N1 – Cr – N2	66.3(3)	66.1(1)	66.1(2)
N1 – Cr – N3	66.1(3)	66.2(1)	65.4(2)
N2 – Cr – N3	66.0(3)	66.0(1)	65.3(2)
Average N-Cr-N	66.1	66.1	65.6
Cr – N1 – C1	124.1(6)	126.2(3)	127.4(5)
Cr – N2 – C2	122.9(6)	124.3(3)	134.6(5)
Cr – N3 – C3	125.9(5)	124.7(3)	125.0(5)
Average Cr-N-C	124.3	125.1	129.0
X1 – Cr – X2	101.0(1)	99.25(3)	99.33(4)
X1 – Cr – X3	99.1(1)	100.07(3)	98.12(4)
X2 – Cr – X3	99.6(1)	98.84(3)	97.59(4)
Average X-Cr-X	99.9	99.39	98.35

As expected the Cr-X bond length increases from the chloride to the iodide with the increasing ionic radius of the halide. The average Cr-N bond length follows the same trend, suggesting that the increasing steric bulk interacts with the ligand. This is best reflected in the average Cr-N-C bond angle, where the carbon atom referred to is the α-carbon of the N-substituent. This structural feature is a good indicator of any steric strain on the ligand as it represents how well the ligand can distort to align the nitrogen lone pair with the chromium centre. Large angles indicate that steric strain prevents this distortion, leading to less effective orbital overlap. The average Cr-N-C angles increase significantly from the chloride to the iodide indicating increasing steric clash, which in turn results in weaker TAC ligation.

The steric strain can also be observed in the loss in symmetry for the iodide which is not observed for the chloride or bromide. Variation in the Cr-N bond length and N-Cr-N bond angle is considerably greater due to misalignment of the TAC ring. In contrast, identical N-Cr-N angles, within error, are observed for the other complexes. It is unclear if the distortion of the geometry or the weakening of TAC ligation results in the loss of stability, with the binding strength of the iodide itself also likely to be a significant factor. The monomeric facial chromium triiodide described here is only the second crystal structure of its type to be reported and as such represents a highly unusual species.[219]

The structures of α-$^{i}Bu_2$ and α-$^{i}Bu_2$(Br) were also determined by single crystal X-ray diffraction, allowing structural analysis of these catalysts which demonstrated considerably different chemistry. This difference has been attributed to increased steric bulk around the metal centre, induced by branching at the α- rather than β-position. It would be expected therefore that considerable differences would be observable in the structures of the complexes, Figure 2.20 and Figure 2.21.

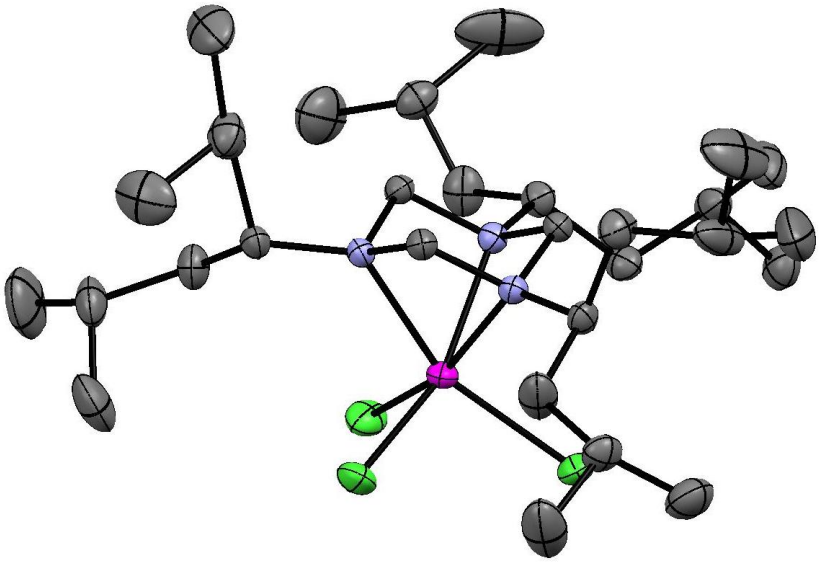

Figure 2.20 - The structure of (($^{i}Bu_2CH)_3$TAC)$CrCl_3$ as calculated by single crystal X-ray diffraction. Grey = C, Mauve = N, Pink = Cr, Green = Cl. Hydrogens have been removed for clarity. Ellipsoids are set to 50% probability.

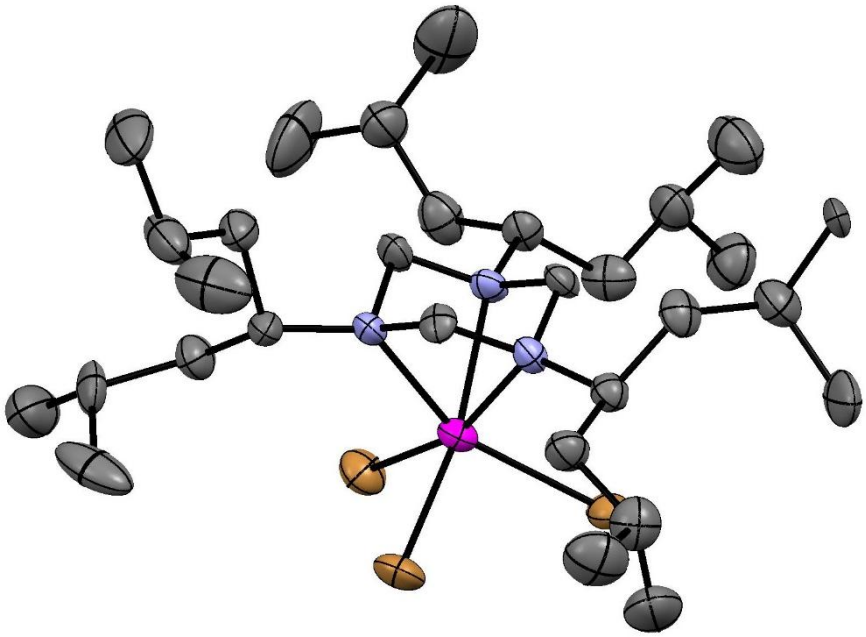

Figure 2.21 - The structure of (($^{i}Bu_2CH)_3$TAC)$CrBr_3$ as calculated by single crystal X-ray diffraction. Grey = C, Mauve = N, Pink = Cr, Brown = Br. Hydrogens have been removed for clarity. Ellipsoids are set to 50% probability.

Table 2.17 - Structural data for the (($^{i}Bu_2CH)_3TAC)CrX_3$ complexes, where X = Cl or Br.

	Bond Lengths (Å)	
Coordination Bonds	$CrCl_3$	$CrBr_3$
Cr – X1	2.2783(6)	2.431(2)
Cr – X2	2.2940(6)	2.451(2)
Cr – X3	2.2788(6)	2.435(2)
Average Cr-X	2.284	2.439
Cr – N1	2.143(2)	2.151(9)
Cr – N2	2.148(2)	2.15(1)
Cr – N3	2.129(1)	2.155(8)
Average Cr-N	2.140	2.152
	Bond Angles (°)	
Donor Bond Angles	$CrCl_3$	$CrBr_3$
N1 – Cr – N2	65.35(6)	65.7(3)
N1 – Cr – N3	65.96(6)	64.9(3)
N2 – Cr – N3	65.13(6)	64.5(3)
Average N-Cr-N	65.48	65.03
Cr – N1 – C1	136.6(1)	136.4(7)
Cr – N2 – C2	130.8(1)	126.6(7)
Cr – N3 – C3	130.9(1)	133.0(7)
Average Cr-N-C	132.8	132.0
X1 – Cr – X2	96.21(2)	96.33(7)
X1 – Cr – X3	98.23(2)	95.73(7)
X2 – Cr – X3	95.14(2)	96.68(7)
Average X-Cr-X	96.53	96.25

The weaker ligation of the TAC ring due to increased steric strain is immediately apparent from the Cr-N bond lengths and resulting N-Cr-N bond angles. Between the chloride and bromide there is a significant increase in the Cr-N bond length, whereas this was not seen for the $(Pr_2CHCH_2)_3TAC$ systems. This leads to the most acute N-Cr-N bond angles for a R_3TAC chromium complex observed to date.[164, 201] The increased steric clash observed between the TAC ligand and the bromide ions could indeed explain the difference in chemistry observed. This suggests that, once formed, α-branched complexes are considerably more stable towards substitution.

Structures were obtained for chromium chloride species with branching points at the α-, β- and γ- position and allowed a true comparison of the steric effects. γ-Pe_2Br, β-Pr_2 and α-$^{i}Bu_2$ are compared in Table 2.18. While these species are not perfectly comparable because of variation in the branching moieties, the key steric aspect of the ligand appears to be the branching point.

Table 2.18 – Key structural information on the $(R_3TAC)CrCl_3$ complexes with varying branching points.

	Bond Lengths (Å)		
Coordination Bonds	γ-Branched	β-Branched	α-Branched
Cr – X1	2.289(1)	2.285(3)	2.2783(6)
Cr – X2	2.286(1)	2.288(3)	2.2940(6)
Cr – X3	2.280(1)	2.280(3)	2.2788(6)
Average Cr-X	2.285	2.284	2.284
Cr – N1	2.128(3)	2.097(7)	2.143(2)
Cr – N2	2.124(3)	2.118(8)	2.148(2)
Cr – N3	2.134(3)	2.080(8)	2.129(1)
Average Cr-N	2.129	2.098	2.140
	Bond Angles (°)		
Donor Bond Angles	γ-Branched	β-Branched	α-Branched
N1 – Cr – N2	65.7(1)	66.3(3)	65.35(6)
N1 – Cr – N3	65.6(1)	66.1(3)	65.96(6)
N2 – Cr – N3	65.8(1)	66.0(3)	65.13(6)
Average N-Cr-N	65.7	66.1	65.5
Cr – N1 – C1	127.9(2)	124.1(6)	136.6(1)
Cr – N2 – C2	125.3(2)	122.9(6)	130.8(1)
Cr – N3 – C3	131.8(2)	125.9(5)	130.9(1)
Average Cr-N-C	128.3	124.3	132.8
X1 – Cr – X2	99.12(5)	101.0(1)	96.21(2)
X1 – Cr – X3	98.06(5)	99.1(1)	98.23(2)
X2 – Cr – X3	97.57(5)	99.6(1)	95.14(2)
Average X-Cr-X	98.25	99.9	96.53

The expected trend, of greater strain as the branching point approaches the triazacyclohexane ring, did not materialise on comparison of the Cr-N-C bond angles. Branching at the α-position resulted in a considerable increase in the steric bulk of the ligand, as indicated by each of the structural components shown. Meanwhile, the β-branched complex displayed the least steric hindrance, considerably less than the γ-branched species. This indicates that the branching groups may well have a greater effect on the structure than previously thought, with the two pentyl and a bromine groups being larger than the two propyl groups. This could result from interaction between the branching groups 'above' the TAC ring, which prevents further orientation away from the chromium metal.

The average Cr-N bond length for the α-branched bromide species is 0.04 Å greater than for the β-branched bromide, a considerable loss in binding strength due to the change in branching point. This also results in considerably greater distortion of the octahedral geometry as compared to the species with branching points at greater separation from the TAC ring. It seems reasonable, therefore, to conclude that the markedly different chemistry towards ligand substitution is a direct result of the increased steric bulk of the N-substituent.

2.8 Summary

Four novel chromium chloride triazacyclohexane catalysts have been synthesised and shown to be highly active LAO trimerisation catalysts. γ-Pe_2Cl and γ-Pe_2H outperformed the best $(R_3TAC)CrCl_3$ catalysts reported to date in terms of activity, selectivity and turnover number. The turnover numbers recorded here demonstrate a five-fold improvement over $((2\text{-Ethylhexyl})_3TAC)CrCl_3$, the previous record holder, and a twenty-fold increase compared to the only other known LAO trimerisation system.[193]

The system has been extensively optimised by variation of the relative concentrations of the different components. High dilution is essential for highly active catalyst systems, which show a considerable reliance on the polarity of the reaction medium. 200 equivalents of DMAO was shown to be most efficient, both in terms of cost and activity, a considerably lower abundance than most ethylene trimerisation systems, which operate in the 300 - 10,000 equivalent range.[218] Addition of Na/K proved to be by far the most effective 1-hexene drying technique and led to the production of a highly reproducible procedure.

The rate of LAO trimerisation was shown to demonstrate a first order dependence on 1-hexene concentration. In accordance with the kinetic studies of alternative ethylene trimerisation systems, this indicates that olefin insertion into the metallacyclopentane is the rate determining step of catalysis.[19] By implication, the resting state of the catalyst cycle is the chromacyclopentane.

The effect of incorporating halogenoalkanes into the system was studied extensively and found to be detrimental to catalysis. External halogen sources led to rapid catalyst decomposition, especially in the case of 1-bromoalkanes. Halogen sources incorporated into the N-substituent of the ligand displayed less potency, though the presence of bromine again led to reduced performance. The γ-Pe_2Cl catalyst demonstrated a strong performance and greater catalyst stability in the Cr^{III} oxidation state. This reactivity is attributed to the ability of the alkyl halides to oxidise the Cr^{I} intermediates of the catalyst cycle. This hypothesis is supported by reactivity trends between the halogenated additives and comparable reactivity in other systems.[208]

Kinetic studies on the catalysis indicated that isomerisation of the 1-hexene, the principal side reaction of the system, is induced by the active catalyst. This waste product is proposed to result from the π-allyl complex mechanism. This proposal is based on the chemistry of similar complexes and the observation that isomerisation occurred in tandem with trimerisation. The kinetic analysis also suggested that catalyst activation could be monitored by observation of methane evolution.

The synthesis of novel chromium triflates has also been achieved, with high yields recorded in each case. Investigation of the substitution chemistry of the resulting complexes led to the formation of seven novel chromium species, six of which were analysed by single crystal X-ray diffraction. Amongst these, the first example of a symmetrically α-branched $(R_3TAC)CrX_3$ (excluding R = ^{i}Pr and ^{t}Bu) is described. Chromium(III) bromides and iodides were also applied to selective trimerisation for the first time and were shown to be active under standard conditions.

3. Mechanistic Insights into α-Olefin Trimerisation

Since the original discovery of LAO trimerisation by Köhn *et al*. in 2000 it has been assumed to proceed *via* an analogous mechanism to ethylene trimerisation.[2] However, detailed analysis of the system has proven problematic due to the sensitivity and paramagnetism of the active complexes. Despite this, limited analysis of the catalytic intermediates has been achieved with the use of UV/Vis and ^{2}H NMR spectroscopy. As a result of this analysis, a metallacyclic mechanism was proposed based on that identified for the ethylene systems, Scheme 3.1.

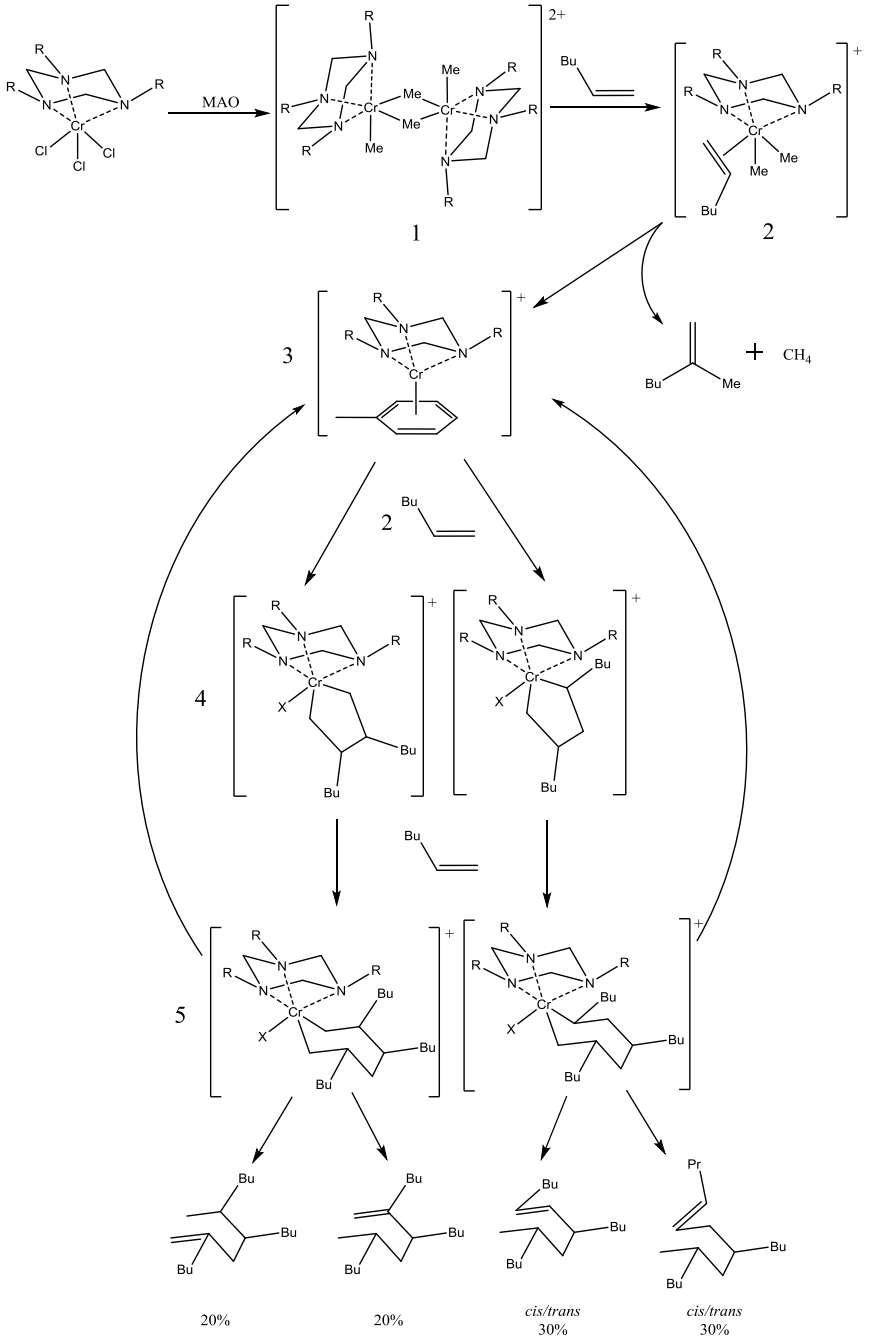

Scheme 3.1 - The detailed α-olefin trimerisation mechanism and product distribution proposed by Köhn *et al*. for the trimerisation of 1-hexene. X = counter-ion or solvent interaction. Counter-ions have been removed for clarity. The toluene is taken from the solvent.

The proposed mechanism follows the basic mechanistic pathways of the original metallacyclic catalyst cycle.[76] Alkylation and cationisation by MAO is followed by the binding of one olefin unit, insertion of the olefin into a Cr-C bond and β-hydride elimination to give 2-methyl-1-hexene in the 1-hexene based example shown. The resulting chromium hydride species then undergoes reductive elimination to give a Cr^{I} complex and methane. The Cr^{I} complex is proposed in this case to be a toluene adduct, where the toluene is taken from the solvent. Two olefin units then bind and undergo cyclic oxidation before a third olefin unit coordinates and inserts to give a chromacycloheptane. This complex is then unstable towards β-hydride elimination, which gives the desired trimer and reforms the Cr^{I} toluene adduct. The proposed distribution of trimer products is an estimate based on kinetic and steric considerations.

Using UV/Vis and ^{2}H NMR spectroscopy none of the intermediates could be characterised but the transitions could be observed. UV/Vis spectroscopy demonstrated that the chromium remained in the Cr^{III} oxidation state after addition of the MAO while ^{2}H NMR spectroscopy indicated a distinct transition in the ligand environment. Addition of 1-hexene led to another transition being observed, which resulted in a Cr^{III} species. This species was observed to exist throughout the period in which the catalyst was active towards trimerisation and was therefore assigned as the resting state of the catalyst cycle. This suggested that Cr^{III}, with the R_3TAC still bound, remains present throughout the catalyst cycle and accounts for the resting state.

The analysis also indicated a gradual transition over the course of several hours to give two inactive decomposition products, one of which was observed to be diamagnetic by ^{2}H NMR spectroscopy. In order to investigate the system and its decomposition products more closely a more defined system was required. This led to the discovery some years later that the system could be activated with DMAB/$Al^{i}Bu_3$ (dimethylaniliniumborate/tri-*iso*-butylaluminium), which resulted in a more favourable counter-ion for spectroscopy.

A detailed investigation into this system was then undertaken with the extensive use of NMR analysis.[205] Addition of DMAB prior to the aluminium activator led to vastly increased catalyst solubility. This was found to be a result of hydrogen bonding of the acidic anilinium proton to two of the chloride ligands, as proven by X-ray crystallography. The strong intermolecular interaction then restricted the weak hydrogen bonding observed between the catalyst species, improving the solubility. This allowed the facile creation of catalyst solutions and improved reproducibility.

The complex was then alkylated with $Al^{i}Bu_3$, which formed a stable species in solution in which the borate anion ($[B(C_6F_5)_4]^-$) was coordinated to the chromium. This was ascertained using ^{19}F NMR spectroscopy. The ^{19}F signals were found to be severely broadened, indicating interaction with the paramagnetic chromium, with the signal for the *meta*-position completely unobservable. The observance of just two peaks and the absence of the *meta*-F indicates that the interaction is fluxional between all C_6F_5 groups, indicating weak interaction. This gives strong support to the idea that interaction between the catalyst and the counter-ion plays a key role in catalyst activity.[213]

The Cr-F interaction between the metal centre and the *meta*-F of the borate anion is proposed to prevent the formation of the dimer predicted on MAO activation. However, *iso*-butyl groups are also known to be considerably weaker bridging ligands, which would also lead to the dimer being disfavoured. The presence of the inner sphere ionic interaction indicates the formation of a mono-cationic alkylated chromium complex in the activation stage, Figure 3.1.

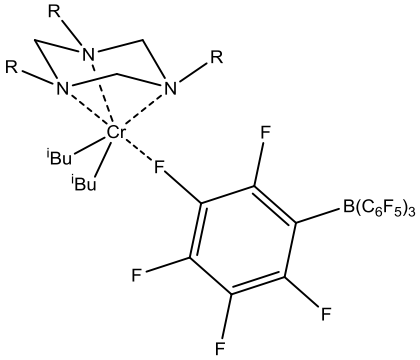

Figure 3.1 - The proposed complex formed on activation of an $(R_3TAC)CrCl_3$ precatalyst with DMAB/$^{i}Bu_3Al$. R = Alkyl.

After addition of 1-hexene, the catalysis was monitored for 48 hours using ^{19}F NMR spectroscopy. It was observed that the line width of all peaks gradually decreased over time, with the *meta*-signal observable after one day. The reduction in line width broadly agreed with the decrease in activity attributed to decomposition of the catalyst. The strong suggestion is therefore that X in the proposed mechanism, Scheme 3.1, is the borate counter-ion. The broadened ^{19}F NMR signals indicate interaction between the counter-ion and the resting state of the active catalyst is maintained throughout catalysis. In contrast, no direct interaction with a paramagnetic species is observed for the decomposition products.

Even after extended time periods, the line-widths of the ^{19}F signals do not return to those expected in the absence of a paramagnetic species. This strongly suggests outer sphere interaction with a paramagnetic species, likely due to formation of a conventional ionic pair. This was confirmed by single crystal X-ray diffraction analysis of a yellow precipitate that formed during catalysis. This was found to be $[(toluene)_2Cr][B(C_6F_5)_4]$ and represented confirmation of a major decomposition product, Figure 3.2. Importantly, the formation of this chromium species confirms that Cr^{I} can be formed under catalytic conditions. As such, this lends considerable support to the existence of a Cr^{I}/Cr^{III} redox cycle in addition to the UV/Vis spectrometry, with both oxidation states being directly observed.

^{1}H NMR analysis of the catalyst solution after complete reaction resulted in observation of sharp peaks at shifts associated with the coordinated TAC ligand. This indicated that the ligand was no longer coordinated to a paramagnetic chromium centre. Therefore, the TAC ligand must have formed a complex with a diamagnetic Al^{III} centre, as this was the only diamagnetic metal present. This was confirmed by reaction of R_3TAC, $Al^{i}Bu_3$ and DMAB to form $[(R_3TAC)Al^{i}Bu_2][B(C_6F_5)_4]$. The NMR spectra of this ionic compound was found to match the signals observed for the suspected decomposition product and as such confirmed its identity, Figure 3.2.

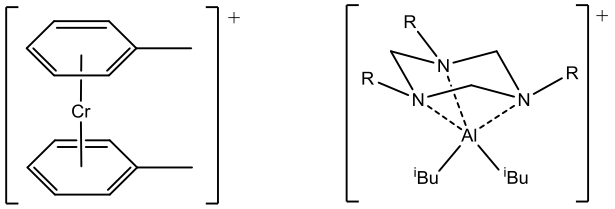

Figure 3.2 - The characterised decomposition products. R = alkyl. The $[B(C_6F_5)_4]$ counter-ion has been removed for clarity.

This work provided significant new insights into the decomposition mechanism of the catalyst for the first time. Identification of the decomposition products also confirmed the accessibility of Cr^{I} under catalytic conditions, which strongly supports the proposed redox cycle. However, further insights were hindered by poor catalyst activities and the fact that the trimer product was poorly understood.

This chapter describes further mechanistic investigation into LAO trimerisation. The principal aims of this research were to characterise the full range of trimers and side products, identify the catalytic intermediates and their substitution patterns and determine the factors that influence selectivity. In achieving these goals, it was hoped that a chain growth mechanism could be conclusively ruled out and the proposed mechanism confirmed. A variety of spectroscopic techniques have been deployed in order to improve upon the results already discussed and to support the existence of metallacyclic mechanisms in selective trimerisation.

3.1 Characterisation of the Trimer Products *via* ^{13}C Labelling

Characterisation of the full range of LAO trimerisation products has, to the best of my knowledge, not yet been achieved experimentally. There are only two examples in which an LAO trimer or trimer mix has been produced and characterised. Firstly, the system recently described by Bercaw *et al*. using the (FI)$TiMe_3$ catalyst was described in detail in Chapter 2.[193]

The major 1-pentene trimer regioisomer produced by this system was identified using ^{13}C NMR spectroscopy and agreed with the proposed mechanism. It is notable that this catalyst, with its hindered environment around the metal, leads to the formation of one regioisomer at a selectivity of 85%. It is proposed that this is due to highly favoured formation of the 2,3-substituted metallacyclopentane, Scheme 3.2.

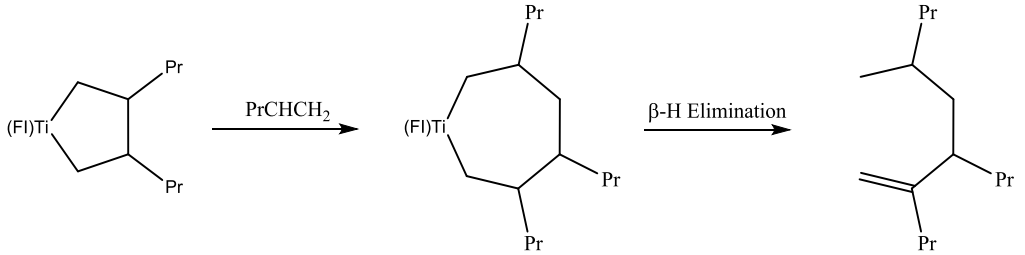

Scheme 3.2 - The proposed pathway to the majority 1-pentene trimer *via* a 2,3-substituted metallacyclopentane and 2,3,5-substituted metallacycloheptane.

This research lent considerable support to the proposed mechanism for LAO trimerisation by confirmation of metallacyclic trimerisation of ethylene with the same catalyst. However, regarding the use of LAOs, limited direct information was obtained. Only one product was successfully identified, which could potentially be formed by either a metallacyclic or chain growth mechanism. In order to better understand the catalytic pathways, characterisation of all the predicted products is required.

Secondly, a partially selective oligomerisation system based on Cp_2ZrCl_2 was described by Harvey *et al*. in 2013 using the methodology first demonstrated by Bergman *et al*. for analogous ethylene dimerisation.[61, 225] Activation with MAO using a low Al:Zr ratio of 50 successfully led to the formation of only low molecular weight 1-hexene oligomers. The system was found to be 25 w% selective towards trimerisation and produced only one isomer of each oligomer. This is ascribed to the Cossee-Arlman mechanism by which they are formed. The far greater favourability of [1,2]-migratory insertion leads to an organometallic chain in which β-hydride elimination is only possible from one position to produce a vinylidene product. As such, the sole trimer was easily separated by distillation and fully characterised by ^{13}C NMR spectroscopy, Figure 3.3. This product can be produced by either mechanism and, as such, its characterisation lent considerable support to later identification of trimer products.

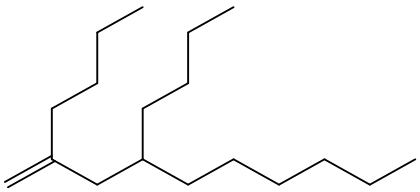

Figure 3.3 - The fully characterised product of 1-hexene trimerisation using Cp_2ZrCl_2 pre-catalysts.

Elucidation of the full range of products possible, while useful in itself, should also give considerable information about the mechanism by which trimerisation occurs. The location and orientation of the butyl chains, in the case of 1-hexene trimerisation, present an opportunity to further explore the mechanistic intermediates of the catalyst cycle. It has been shown previously within the group that $(R_3TAC)CrCl_3$ catalysts produce a diverse range of trimer products. As such, these catalysts are ideal candidates for attempting to identify all of the C_{18} regioisomers possible from selective trimerisation of 1-hexene.

Based on the adapted metallacyclic mechanism proposed by Köhn *et al*. there are a significant number of regioisomers possible.[2] Assuming only [1,2]-migratory insertion and *endo*-cyclic β-hydride elimination occurs, then the eight regioisomers shown in Scheme 3.3 can be formed. Furthermore, six of these regioisomers also feature diastereomers, such that 14 different isomers (excluding enantiomers) are possible. All of the isomers predicted are proposed on the assumption that isomerisation of the trimer product does not occur.

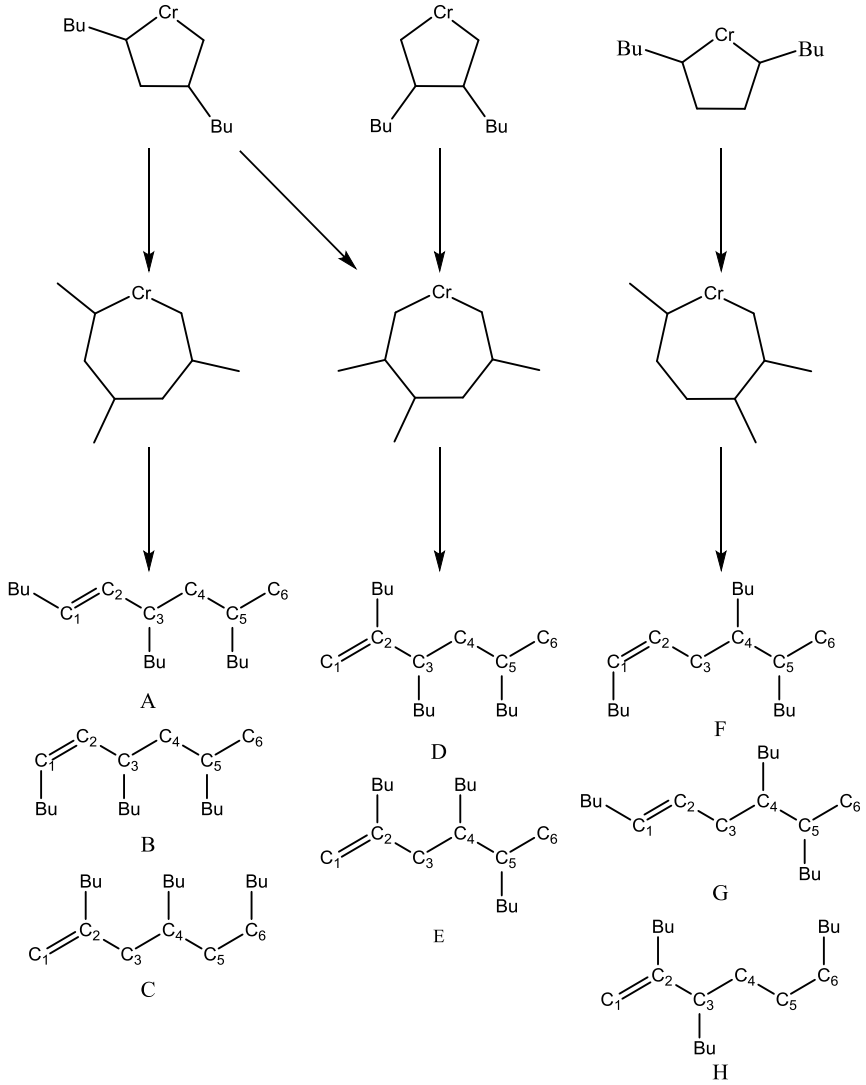

Scheme 3.3 - The range of possible isomers and the pathways to their formation assuming only [1,2] migratory insertion occurs.

However, should these assumptions be incorrect then a considerably higher number of isomers are possible. [2,1] migratory insertion would lead to a new set of isomers based on the same pathways, although some of these are identical to those produced by [1,2] insertion, as shown in Scheme 3.4.

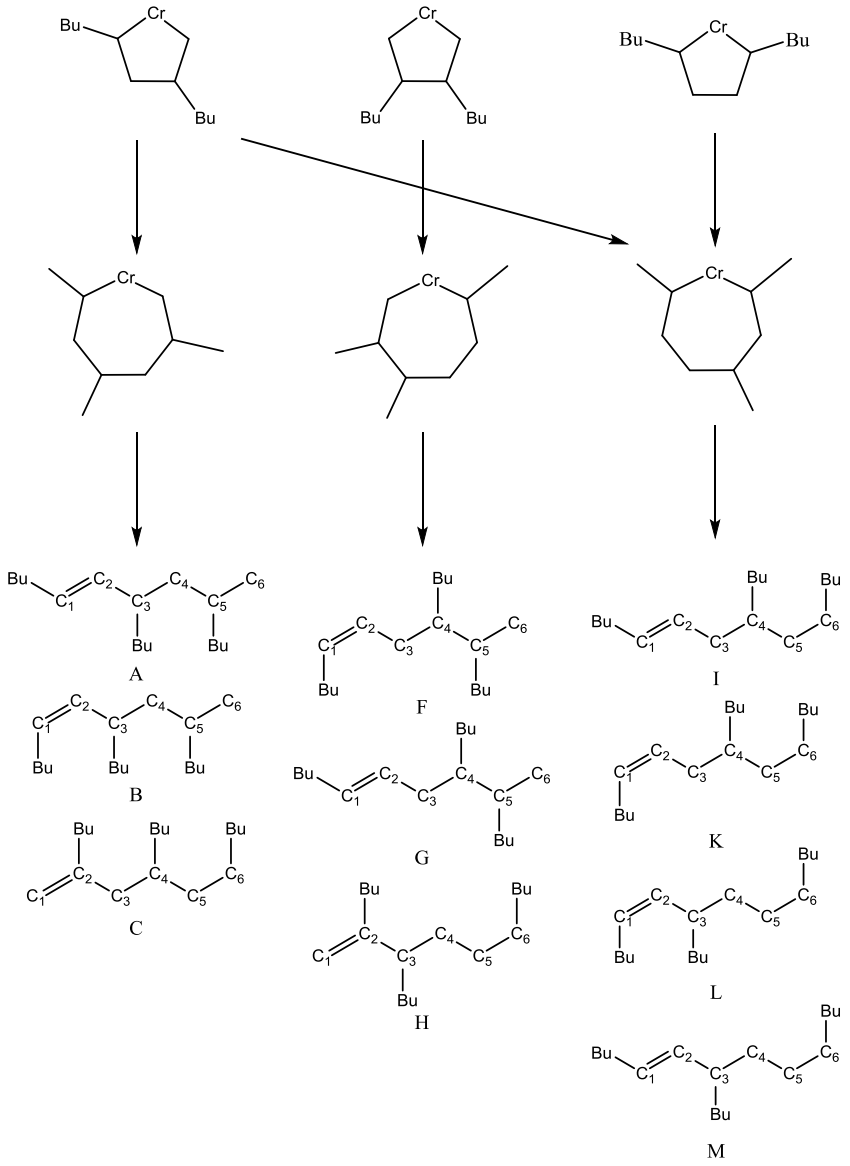

Scheme 3.4 - The range of regioisomers and their formation pathways possible when the third 1-hexene unit inserts with a [2,1] orientation.

It can be seen that an additional four regioisomers can be formed if [2,1] migratory insertion plays a role in the catalysis. These isomers do not contain any diastereomers and therefore the total number of possible isomers, excluding enantiomers, is brought to 18. The second assumption, that *exo*-cyclic elimination does not occur, could also be incorrect despite the observations of Whitesides *et al*.[38] Should this be the case then for each isomer formed as an internal olefin another would also be possible. The pathways would be identical to those already described except that β-hydride elimination would occur from the butyl chain to give the isomers shown in Figure 3.4.

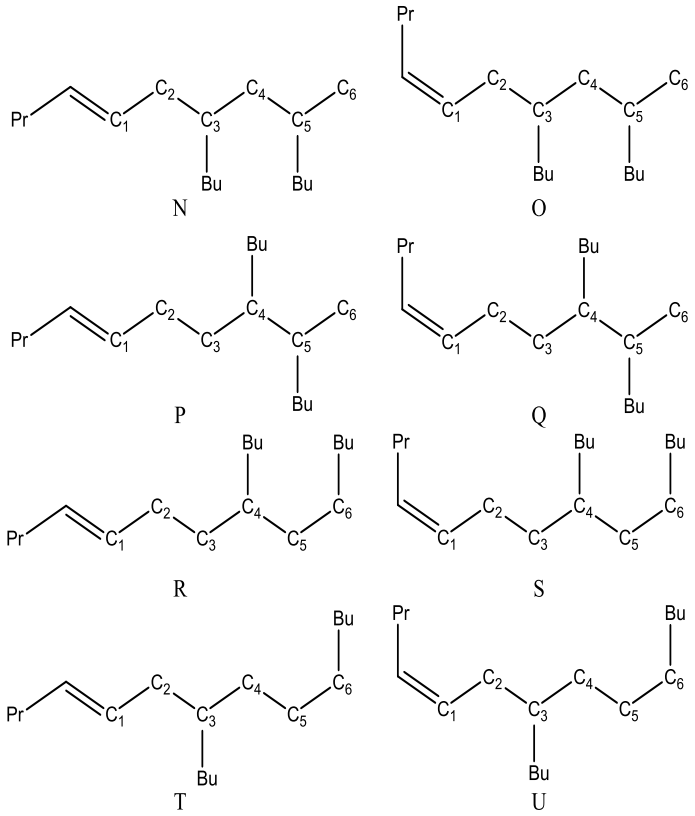

Figure 3.4 - The isomers that could be formed if *exo*-cyclic elimination occurs.

It can be seen that a further eight regioisomers can be formed, of which four contain diastereomers. Removing this assumption adds a further 12 possible isomers and brings the total number, excluding enantiomers, to 30. The work described in this section attempts to identify which of these isomers are formed in order to gain insight into, and prove the existence of, the metallacyclic mechanism for LAO trimerisation.

The extremely similar structures of the different products meant that a highly sensitive method was required in order to characterise each isomer. This led to the use of ^{13}C NMR, which had been shown in initial investigations to present numerous separate peaks corresponding to the olefinic region of the products, although they could not be adequately assigned. It was necessary, therefore, to identify the signals which corresponded to each of the products and subsequently to assign them as a complete set.

In order to directly link the carbon atoms present in the same isomer, it was necessary to carry out 2D NMR spectroscopy and observe the through-bond coupling. With the ^{1}H NMR spectrum difficult to interpret due to numerous overlapping peaks, ^{13}C-^{13}C COSY NMR spectroscopy was used to identify the signals corresponding to each stereoisomer. COSY NMR spectroscopy between carbon atoms is difficult due to the low natural abundance of ^{13}C, leading to just 0.01% of C-C interactions being observed. In order to use this technique effectively, it was necessary to synthesise ^{13}C enriched trimers to enable observation of the ^{13}C-^{13}C couplings. The trimers are perfect candidates for this type of analysis, as trimerisation of enriched 1-hexene results in three enriched carbon atoms per molecule. This then allows the facile observation of coupling between them.

With the intention of maximising the coupling between enriched carbon atoms, the terminal carbon of 1-hexene was labelled. This then ensured that all of the enriched carbons would be present within the metallacycloheptane intermediate and in close proximity to the key differentiating elements of the structure. Synthesis of terminally ^{13}C labelled 1-hexene from $^{13}CH_3I$ was performed according to literature techniques, Scheme 3.5.[226]

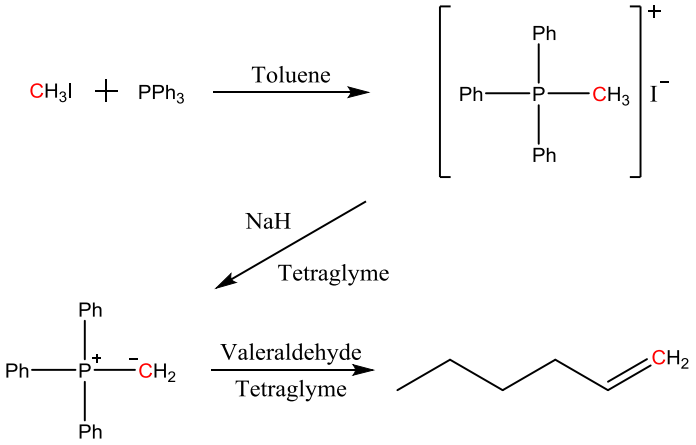

Scheme 3.5 - Synthesis of terminally labelled 1-hexene. The carbon indicated by red colouration represents the position enriched in ^{13}C.

The ^{13}C labelled iodomethane was stirred with triphenylphosphine over the course of three days to ensure complete reaction. The product was formed as a precipitate and filtered before being re-dissolved into tetraglyme. The ylide was formed with the use of sodium hydride, with the resulting sodium iodide precipitating out of solution. Pentanal was then added directly to this solution to form terminally enriched 1-hexene *via* a Wittig reaction. $^{i}Bu_3Al$ in *p*-cymene was then added in order to induce non-volatile adduct formation with the tetraglyme. Removal of the remaining volatile components gave the product as a *p*-cymene solution at an overall yield of 74%.

The trimerisation was carried out according to the standard procedure, though a reasonable quantity of *p*-cymene was present, using γ-Pe_2Cl as the catalyst. The trimerisation proceeded as hoped and acceptable yields of around 70% C_{18} trimer were recorded. The trimer was extracted from the catalyst solution and purified by vacuum transfer to give a pure sample for NMR spectroscopic analysis.

Conventional inverse-gated 1D ^{13}C NMR spectroscopy was run at 125 MHz with a 15 second delay between acquisitions and a 3 second acquisition time to ensure complete relaxation of all nuclei. The T_1 relaxation times for the trimer signals were measured prior to analysis and it was found that all carbon atoms had relaxation times below three seconds. Therefore, as is typical good practice, the delay was set at $5.T_1$ to ensure comparable integration and allow the relative abundance to be calculated.

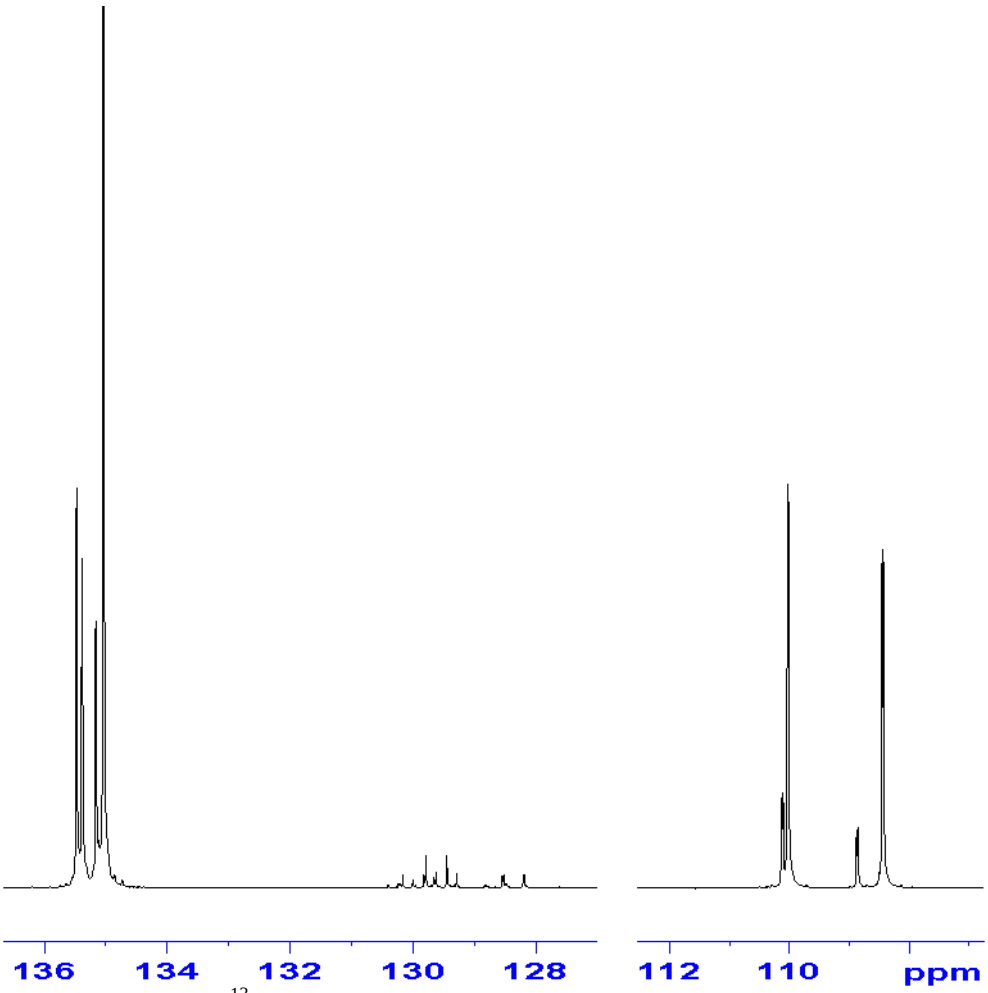

Figure 3.5 - The ^{13}C peaks present in the olefinic region of the enriched trimer.

The ^{13}C NMR spectrum indicated that there are eight major isomers present within the trimer mix, Figure 3.5. Four were observed in the 134-136 ppm region associated with internal alkenes with alkyl branching at the α-position, while four others were observed in the vinylidene region between 108 and 111 ppm. Several minor isomers were also observed in the 128-131 ppm region associated with internal alkenes without branching at the α-position. Each peak was observed as a doublet, indicating spin-spin coupling between the enriched carbon atoms. ^{13}C-^{13}C coupling constants are highly dependent on orbital hybridisation and bond separation between nuclei. This allows considerable information about the structure to be determined based on the magnitude of spin-spin coupling. The typical ranges for ^{13}C-^{13}C coupling constants expected for these species are shown in Table 3.1.[227] The ranges are induced by additional environmental factors that affect the coupling constant.

Table 3.1 – The effect of orbital hybridisation and bond separation on ^{13}C-^{13}C coupling constants.

$^{13}C_1$ Hybridisation	$^{13}C_2$ Hybridisation	Bond Separation	Coupling Constant (Hz)
sp^2	sp^2	1	70 - 75
sp^2	sp^3	1	40 - 45
sp^3	sp^3	1	30 - 40
sp^2	sp^3	2	1 - 3
sp^3	sp^3	2	0.1 - 1
sp^2	sp^3	3	1 - 3
sp^3	sp^3	3	1 - 3
sp^2	sp^3	4/5	< 0.1
sp^3	sp^3	4/5	< 0.1

The distinctive coupling constants between ^{13}C nuclei separated by one bond enabled considerable structural information to be determined from the 1D NMR. A closer look at the olefinic carbons immediately gave an indication of their environment and position relative to the other enriched ^{13}C atoms. In the 108-111 ppm and 134-136 ppm regions the signals were observed as doublets, with coupling of 1-3 Hz, Figure 3.6. This indicates that the enriched olefinic position is not adjacent to another enriched position and that the third enriched position is four or five bonds away.

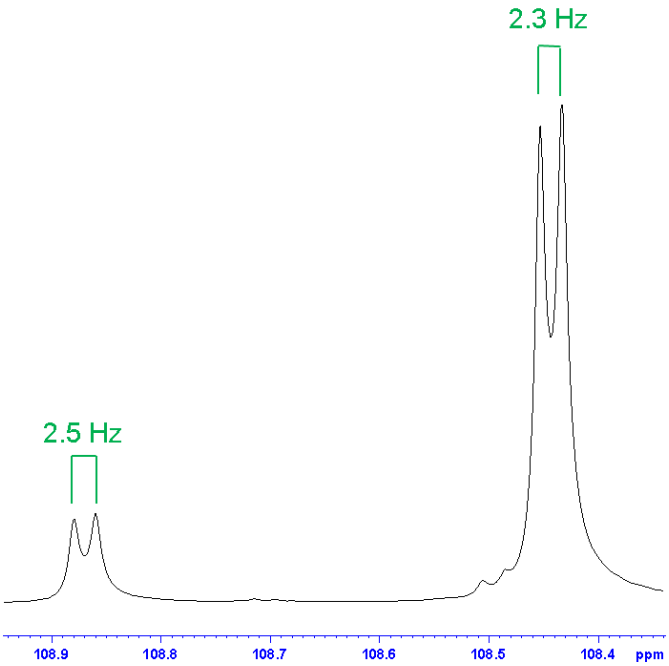

Figure 3.6 - An example of the coupling observed for two signals between 108 and 111 ppm in the 1D ^{13}C NMR spectrum of the enriched trimer.

In contrast, ^{13}C-^{13}C coupling in the 128-131 ppm region was more complex due to observation of doublets of doublets. The coupling constants were calculated at 40-45 Hz and 1-3 Hz, indicating sp^2-sp^3 one bond coupling as well as two or three bond coupling with another enriched position, Figure 3.7.

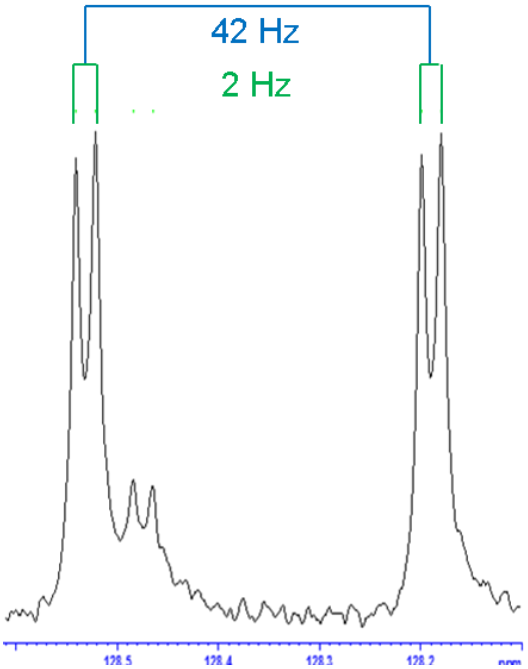

Figure 3.7 - An example of the coupling observed for one signal between 128 and 111 ppm in the 1D ^{13}C NMR spectrum of the enriched trimer.

Looking at the non-enriched carbon signals was difficult due to the far lower peak intensities. However, in some rare cases when the signal appeared at a distinctive chemical shift the peak splitting could be identified. These signals demonstrated even more complex splitting patterns, providing more detailed information about their location within the structure relative to the enriched positions. An example is shown in Figure 3.8, in which the data has been fitted to facilitate observation of the low intensity peaks.

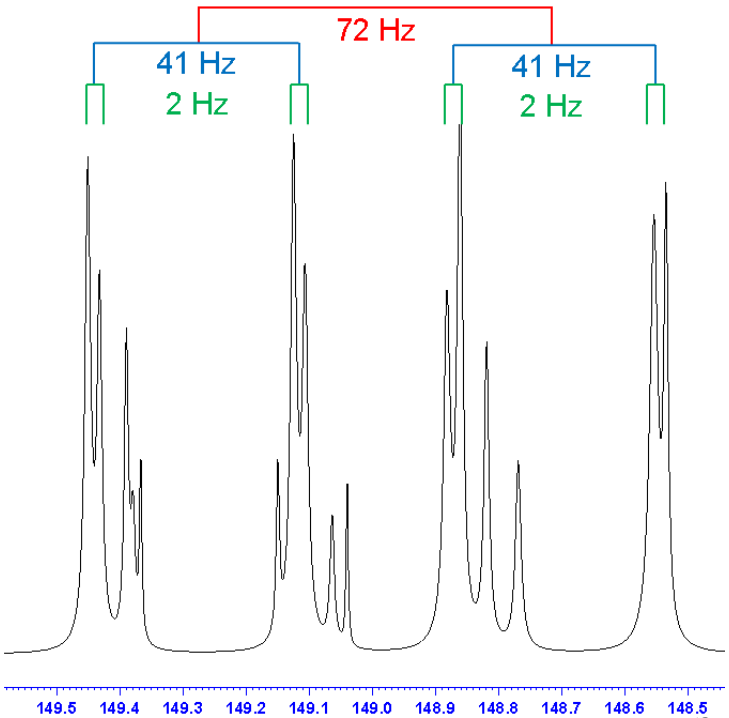

Figure 3.8 - An example of the coupling observed for a natural abundance ^{13}C atom in the 1D ^{13}C NMR spectrum of the enriched trimer.

For the signal shown, the coupling constants reveal that the natural abundance ^{13}C couples with all three of the enriched positions in the trimer. The magnitude of the coupling indicates one bond coupling with two enriched positions and two or three bond coupling with the third. A considerable amount of information on the structure is therefore made available by observing the coupling constants for the non-enriched positions. Unfortunately, where numerous carbon atoms were found to exist in similar environments this information could not be obtained due to the severe overlap of peaks. As a result, the $J_{13C\text{-}12C}$ coupling constants could not be calculated in the vast majority of cases.

The enriched positions of each of the observed isomers could be identified and linked to coupled nuclei based on the observation of cross peaks in the 2D ^{13}C-^{13}C COSY spectrum. Large one bond couplings were readily observed as sets of four peaks in a square formation. Smaller couplings were more difficult to quantify and were typically observed either as a singlet or as overlapping doublets. While this prevented accurate calculation of the coupling constant it indicated the existence of coupling between the two environments. Calculation of the coupling constants was undertaken with the use of the 1D spectrum for this reason. An example of the cross peaks observed for one bond sp^2-sp^2 coupling with this technique is shown in Figure 3.9.

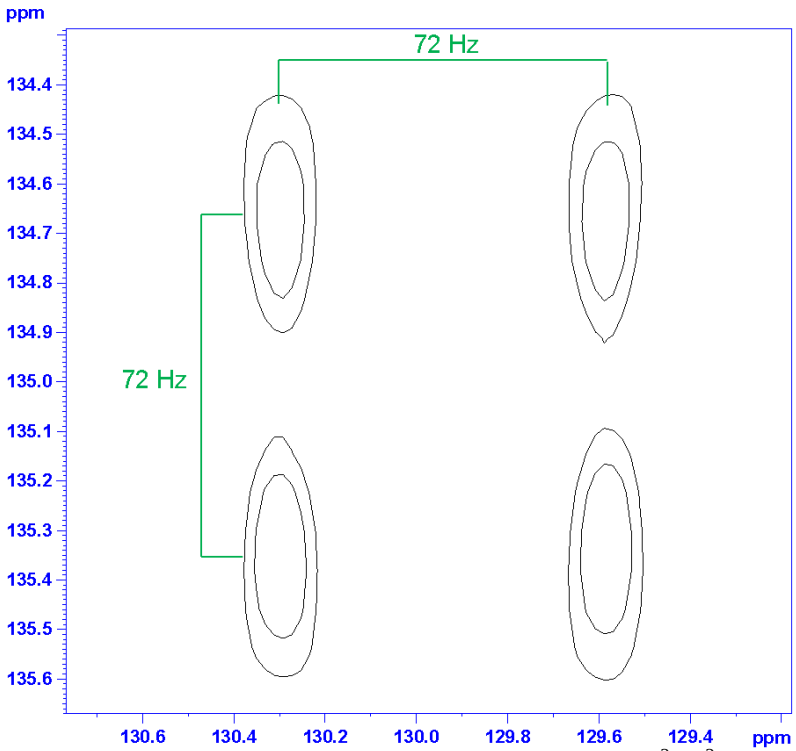

Figure 3.9 - An example of the cross peaks observed for one bond sp^2-sp^2 spin-spin coupling.

The high intensity of the signals corresponding to enriched positions allowed the facile observation of coupling between them. Starting from the olefinic region it was therefore possible to find the chemical shifts of the two other enriched positions in the same molecule. The coupling between the nuclei could then also be assigned to give the first information on the structure. The identification and correlation of all of the enriched signals allowed the number of isomers to be calculated, as listed in Table 3.2 in order of decreasing chemical shift of the enriched olefinic carbon.

Table 3.2 - The coupling constants and chemical shift data corresponding to enriched positions in the trimer products. The carbons are labelled sequentially according to their position in the isomer backbone relative to the olefinic carbon, based on the coupling constants observed.

C_1 (ppm)	J_{12} (Hz)	C_2 (ppm)	J_{23} (Hz)	C_3 (ppm)	J_{13} (Hz)
135.50	1.3	44.00	0.1	20.48	< 0.1
135.39	1.5	43.51	< 0.1	20.43	< 0.1
135.18	1.3	43.62	0.4	19.60	< 0.1
135.09	1.7	27.28	35.5	35.64	1.0
135.04	1.5	43.20	0.5	19.25	< 0.1
135.02	1.6	27.40	35.1	36.00	< 0.1
130.01	43.5	33.28	2.8	15.64	< 0.1
129.85	43.6	34.57	1.3	15.46	< 0.1
129.65	43.1	27.69	2.8	15.65	< 0.1
129.49	43.1	28.99	1.4	15.56	< 0.1
128.67	43.6	33.47	2.4	36.60	< 0.1
128.32	43.1	33.62	2.5	31.26	< 0.1
110.11	2.1	38.27	1.1	15.17	< 0.1
110.09	2.3	36.90	2.8	15.44	< 0.1
110.00	2.2	41.32	< 0.1	33.47	< 0.1
108.84	2.5	41.50	0.4	19.52	< 0.1
108.50	2.5	34.17	35.1	27.54	< 0.1
108.41	2.6	42.27	< 0.1	20.31	< 0.1

In total, 18 isomers were observed at an abundance greater than 0.1%, all of which contained an enriched olefinic carbon atom. Analysis of the aliphatic region did not lead to the discovery of any further peaks that corresponded to additional enriched signals. This led to the conclusion that the signals observed represented all of the isomers formed. This gave a strong indication that isomers N to U are not formed by this catalyst system, as they would not feature an enriched olefinic signal. The fact that 18 isomers are observed is also significant, as this would suggest that all of the other isomers predicted are indeed formed. This suggests that it cannot be assumed that [2,1] migratory insertion is so disfavoured as to yield negligible quantities of product. These conclusions are again made on the assumption that isomerisation of the trimer product does not occur.

With the three enriched positions identified for each of the isomers, the ^{13}C-^{13}C COSY spectrum could be used to determine the chemical shifts of the adjacent non-enriched positions. In this manner, the six positions for which the chemical shift was required to characterise the structure could be determined. Based on this data, each of the isomers proposed by the metallacyclic mechanism could be identified. The chemical shifts of the carbon positions present in the butyl side chains were determined by correlation of long-delay ^{13}C NMR integration values. The ^{13}C NMR peak assignments of any additional positions are provided in Appendix 2.

The characterisation of each of the regioisomers was achieved using the chemical shifts and $J_{13C\text{-}13C}$ coupling constants of the six structurally significant positions, which are provided here for each isomer. The identification was also supported by observation of $^{1}J_{CC}$ coupling between enriched and non-enriched positions in the COSY NMR spectrum. As a result, the connectivity of the compound could be identified. However, the majority of the low intensity cross peaks were obscured or distorted such that the coupling constant could not be accurately measured. In all cases the data was only of a suitable quality to ascertain a coupling constant of greater than 10 Hz, indicative of one bond coupling.

Diastereomers of a given regioisomer have been denoted as X and X', whereby X' is the stereoisomer of lower abundance. The diastereomers were determined by comparison to the results of Enders *et al*., who demonstrated that when chiral centres are separated by a methylene bridge the two diastereomers can be distinguished by ^{13}C NMR spectroscopy.[228] With the use of compounds with very similar branching arrangements to the C_{18} trimers investigated here, it was shown that the chemical shift of the carbon atoms adjacent to a chiral position are influenced by the stereoisomerism of the other chiral centre. Observation of the shifts induced on these positions allowed the assignment of the diastereomers. Characterisation of the diastereomers of A and B using this technique are shown in Scheme 3.6 as an example.

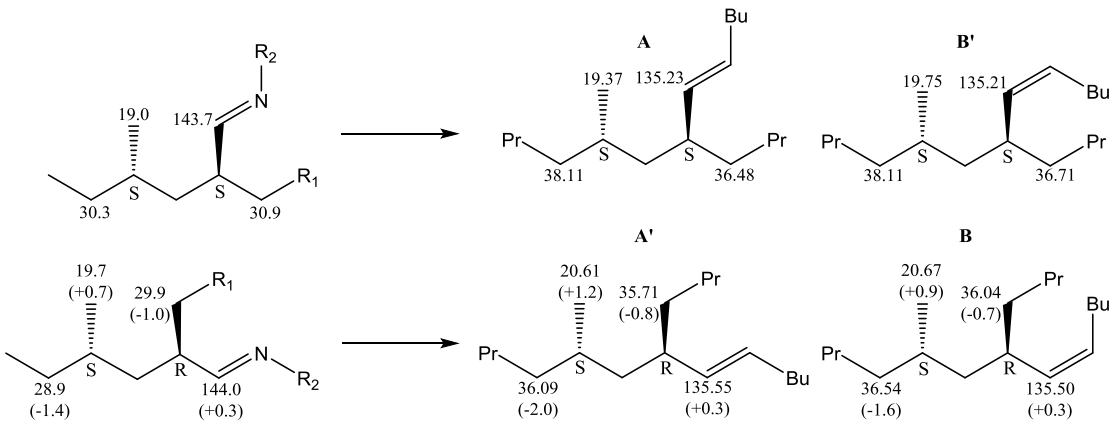

Scheme 3.6 - The variations in chemical shifts induced by the different diastereomers. The chemical shifts are shown in ppm, R_1 = -$CH_2CH_2OSiMe_2{}^tBu$, R_2 = *N*-(2-methoxymethyl)pyrrolidinyl.

As shown, the difference in chemical shifts for positions adjacent to the chiral centres are similar for both the trimer products and the chirally resolved reference compounds. Combination of this characterisation technique with ^{1}H NOESY NMR spectroscopy allowed for complete characterisation of diastereomers. When taken into consideration alongside the ^{13}C-^{13}C couplings and the ^{13}C chemical shifts of the structurally significant positions, all of the isomers could be characterised. The isomers identified have been labelled according to the proposed products and are presented below in alphabetical order with the information that allowed their characterisation. The key observations are made in reference to established chemical shift ranges for given environments.[227]

Isomers A and A'

Based on the data shown in Table 3.3 the formation of both diastereomers of *trans*-7-butyl-5-methyltridec-8-ene were confirmed, as shown in Figure 3.10.

Table 3.3 - The ^{13}C NMR data for the structurally significant positions.

	Chemical Shift (ppm)	
Position	Isomer A	Isomer A'
C_1	130.25	130.01
C_2	135.24	135.56
C_3	40.93	40.78
C_4	43.63	43.97
C_5	30.33	30.27
C_6	19.38	20.63
	Coupling Constant (Hz)	
Interaction	Isomer A	Isomer A'
$^2J_{2,4}$	1.5	1.5
$^2J_{4,6}$	0.5	< 0.1
$^4J_{2,6}$	< 0.1	< 0.1

The key observations on identification of the six structurally significant positions were as follows:

1. The olefinic carbon atoms (C_1 and C_2) match the expected shifts for an α-branched internal olefin.
2. The α-carbon (C_3) matched the shift expected for a tertiary carbon atom in the *trans* position.
3. C_4 was observed at a shift typical for a secondary carbon atom adjacent to two branching points.
4. C_5 was observed at a shift typical for a tertiary carbon atom.
5. C_6 was observed at a shift typical for a secondary methyl group.

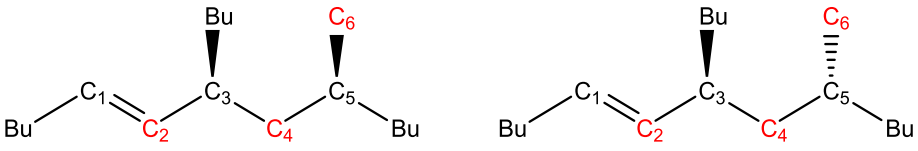

A (SS/RR) A' (SR/RS)

Figure 3.10 - The structure of isomers A and A'. Enriched positions are displayed in red.

Isomers B and B'

Based on the data shown in Table 3.4 the formation of both diastereomers of *cis*-7-butyl-5-methyltridec-8-ene were confirmed, as shown in Figure 3.11.

Table 3.4 - The ^{13}C NMR data for the structurally significant positions.

	Chemical Shift (ppm)	
Position	Isomer B	Isomer B'
C_1	129.32	129.67
C_2	135.48	135.19
C_3	35.01	35.15
C_4	44.49	44.06
C_5	30.30	30.54
C_6	20.70	19.76
	Coupling Constant (Hz)	
Interaction	Isomer B	Isomer B'
$^2J_{2,4}$	1.3	1.3
$^2J_{4,6}$	0.1	0.4
$^4J_{2,6}$	< 0.1	< 0.1

The key observations on identification of the six structurally significant positions were as follows:

1. The olefinic carbon atoms (C_1 and C_2) match the expected shifts for an α-branched internal olefin.
2. The α-carbon (C_3) matched the shift expected for a tertiary carbon atom in the *cis* position.
3. C_4 was observed at a shift typical for a secondary carbon atom adjacent to two branching points.
4. C_5 was observed at a shift typical for a tertiary carbon atom.
5. C_6 was observed at a shift typical for a secondary methyl group.

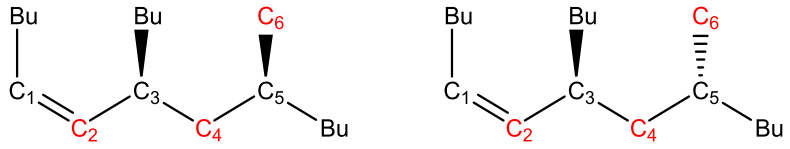

B (SS/RR) B' (SR/RS)

Figure 3.11 - The structure of isomers B and B'. Enriched positions are shown in red.

Isomer C

Based on the data shown in Table 3.5 the formation of 7-butyl-5-methylenetridecane was confirmed, as shown in Figure 3.12. This isomer matches that characterised by Harvey *et al.*, allowing the assignment to be confirmed by comparison.[225]

Table 3.5 - The ^{13}C NMR data for the structurally significant positions.

	Chemical Shift (ppm)
Position	Isomer C
C_1	110.68
C_2	148.14
C_3	41.59
C_4	35.68
C_5	33.80
C_6	26.86
	Coupling Constant (Hz)
Interaction	Isomer C
$^2J_{1,3}$	2.2
$^2J_{3,5}$	< 0.1
$^4J_{1,5}$	< 0.1

The key observations on identification of the six structurally significant positions were as follows:

1. The olefinic carbon atoms (C_1 and C_2) match the expected shifts for a vinylidene.
2. The α-position (C_3) matched the shift expected for a secondary carbon atom.
3. C_4 was observed at a shift typical for a tertiary carbon atom.
4. C_5 was observed at a shift typical for a secondary carbon atom adjacent to branching.
5. C_6 was observed at a shift typical for a secondary carbon atom.

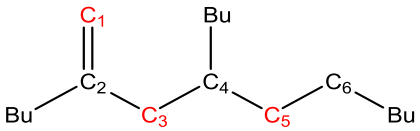

Figure 3.12 - The structure of isomer C. Enriched positions are shown in red.

The identity of this isomer was confirmed by comparison to the ^{13}C NMR spectra reported for this species by Harvey *et al*. On this occasion the spectroscopy was carried out in $CDCl_3$, therefore a solution of the trimer mix was made up in this solvent to allow direct comparison, Table 3.6. The slight variations result from comparison of a pure sample to a mixture of isomers.

Table 3.6 - The chemical shifts of the key structural positions recorded for Isomer C in $CDCl_3$ compared to those reported by Harvey *et al*.[225]

	Chemical Shift (ppm)	
Position	Isomer C	Isomer C (Lit.)
C_1	109.98	110.0
C_2	149.16	148.8
C_3	41.31	41.3
C_4	35.41	35.4
C_5	33.46	33.5
C_6	26.52	26.5

It can be seen that there is a very good correlation between the two samples, which were each produced according to completely different methods. Such accuracy indicates that this method of identification is highly reliable for the characterisation of the trimer products. The majority of isomers cannot be confirmed in this manner but the successful correlation demonstrated here strongly supports the assignments given herein.

Isomers D and D'

Based on the data shown in Table 3.7 the formation of both diastereomers of 6-butyl-8-methyl-5-methylenedodecane were confirmed, as shown in Figure 3.13. The key positions of Isomer D' match the 1-pentene trimer characterised by Bercaw *et al.*, allowing confirmation of the assignment by comparison.[193]

Table 3.7 - The ^{13}C NMR data for the structurally significant positions.

	Chemical Shift (ppm)	
Position	Isomer D	Isomer D'
C_1	109.17	109.57
C_2	152.17	151.53
C_3	44.49	44.94
C_4	42.63	41.88
C_5	30.51	30.34
C_6	20.52	19.67
	Coupling Constant (Hz)	
Interaction	Isomer D	Isomer D'
$^2J_{4,6}$	2.6	2.5
$^3J_{1,4}$	< 0.1	0.4
$^5J_{1,6}$	< 0.1	< 0.1

The key observations on identification of the six structurally significant positions were as follows:

1. The olefinic carbon atoms (C_1 and C_2) match the expected shifts for a vinylidene.
2. The α-carbon (C_3) matched the shift expected for a tertiary carbon atom.
3. C_4 was observed at a shift typical for a secondary carbon atom adjacent to two branching points.
4. C_5 was observed at a shift typical for a tertiary carbon atom.
5. C_6 was observed at a shift typical for a secondary methyl group.

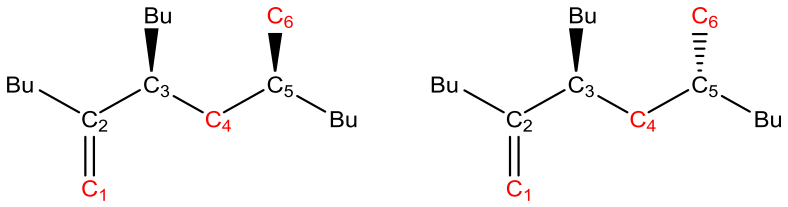

D (SS/RR) D' (SR/RS)

Figure 3.13 - The structure of isomers D and D'. Enriched positions are shown in red.

The identity of Isomer D' was confirmed by comparison to the ^{13}C NMR spectra reported for the C_{15} analogue by Bercaw *et al.* (in the Supporting Information).[193] On this occasion the spectroscopy was carried out in C_6D_6, therefore a solution of the trimer mix was made up in this solvent to allow direct comparison, Table 3.8. The slight variations result from the presence of propyl rather than butyl branching.

Table 3.8 - The chemical shifts of the key structural positions recorded for Isomer D' in C_6D_6 compared to those reported by Bercaw *et al*.[193]

	Chemical Shift (ppm)	
Position	Isomer D'	Isomer D' (Lit.)
C_1	109.62	109.68
C_2	152.23	151.97
C_3	45.08	44.81
C_4	41.90	41.85
C_5	30.42	30.31
C_6	19.80	19.76

The shifts observed again match nicely to literature precedent, in this case it allows identification of the majority diastereomer produced by the (FI)$TiMe_3$ system as being SR/RS. The successful correlation further supports the validity of the characterisation method.

Isomers E and E'

Based on the data shown in Table 3.9 the formation of both diastereomers of 6-butyl-5-methyl-8-methylenedodecane were confirmed, as shown in Figure 3.14.

Table 3.9 - The ^{13}C NMR data for the structurally significant positions.

	Chemical Shift (ppm)	
Position	Isomer E	Isomer E'
C_1	110.79	110.81
C_2	148.43	148.32
C_3	37.19	38.57
C_4	39.91	39.90
C_5	35.58	35.42
C_6	15.69	15.32
	Coupling Constant (Hz)	
Interaction	Isomer E	Isomer E'
$^2J_{1,3}$	2.3	2.1
$^3J_{3,6}$	2.8	1.1
$^5J_{1,6}$	< 0.1	< 0.1

The key observations on identification of the six structurally significant positions were as follows:

1. The olefinic carbon atoms (C_1 and C_2) match the expected shifts for a vinylidene.
2. The α-carbon (C_3) matched the shift expected for a secondary carbon atom.
3. C_4 and C_5 were observed at shifts typical for tertiary carbon atoms adjacent to branching.
4. C_6 was observed at a shift typical for a secondary methyl group.

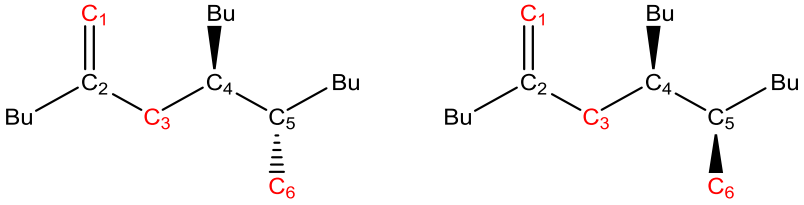

E (RR/SS) E' (RS/SR)

Figure 3.14 - The structure of isomers E and E'. Enriched positions are shown in red.

Isomers F and F'

Based on the data shown in Table 3.10 the formation of both diastereomers of *cis*-6-butyl-5-methyltridec-8-ene were confirmed, as shown in Figure 3.15.

Table 3.10 - The ^{13}C NMR data for the structurally significant positions.

	Chemical Shift (ppm)	
Position	Isomer F	Isomer F'
C_1	130.18	130.25
C_2	129.59	129.42
C_3	32.35	32.21
C_4	43.37	43.33
C_5	34.58	34.50
C_6	15.87	15.73
	Coupling Constant (Hz)	
Interaction	Isomer F	Isomer F'
$^1J_{2,3}$	43.1	43.1
$^3J_{3,6}$	2.8	1.4
$^4J_{2,6}$	< 0.1	< 0.1

The key observations on identification of the six structurally significant positions were as follows:

1. The olefinic carbon atoms (C_1 and C_2) match the expected shifts for an internal olefin without α-branching.
2. The α-carbon (C_3) matched the shift expected for a secondary carbon atom in the *cis* position.
3. C_4 and C_5 were observed at shifts typical for tertiary carbon atoms adjacent to branching.
4. C_6 was observed at a shift typical for a secondary methyl group.

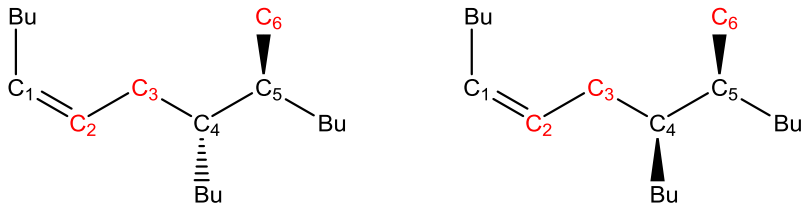

F (RS/SR) F' (SS/RR)

Figure 3.15 - The structure of isomers F and F'. Enriched positions are shown in red.

Isomers G and G'

Based on the data shown in Table 3.11 the formation of both diastereomers of *trans*-6-butyl-5-methyltridec-8-ene were confirmed, as shown in Figure 3.16.

Table 3.11 - The ^{13}C NMR data for the structurally significant positions.

	Chemical Shift (ppm)	
Position	Isomer G	Isomer G'
C_1	131.24	131.27
C_2	130.12	129.95
C_3	33.95	34.22
C_4	42.94	43.02
C_5	34.52	34.43
C_6	15.84	15.63
	Coupling Constant (Hz)	
Interaction	Isomer G	Isomer G'
$^1J_{2,3}$	43.5	43.6
$^3J_{3,6}$	2.8	1.3
$^4J_{2,6}$	< 0.1	< 0.1

The key observations on identification of the six structurally significant positions were as follows:

1. The olefinic carbon atoms (C_1 and C_2) match the expected shifts for an internal olefin without α-branching.
2. The α-carbon (C_3) matched the shift expected for a secondary carbon atom in the *trans* position.
3. C_4 and C_5 were observed at shifts typical for tertiary carbon atoms adjacent to branching.
4. C_6 was observed at a shift typical for a secondary methyl group.

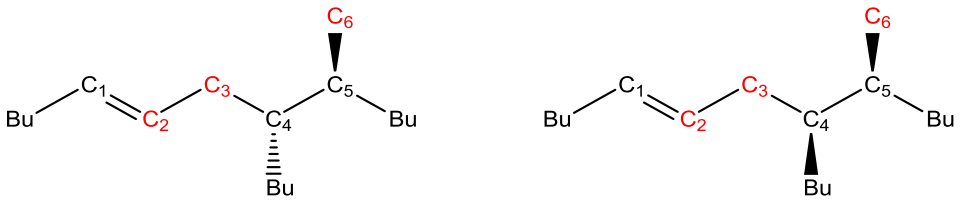

G (RS/SR) G' (SS/RR)

Figure 3.16 - The structure of isomers G and G'. Enriched positions are shown in red.

Isomer H

Based on the data shown in Table 3.12 the formation of 6-butyl-5-methylenetridecane was confirmed, as shown in Figure 3.17.

Table 3.12 - The ^{13}C NMR data for the structurally significant positions of isomer H.

Position	Chemical Shift (ppm)
C_1	109.22
C_2	151.77
C_3	47.14
C_4	34.56
C_5	27.85
C_6	~
Interaction	**Coupling Constant (Hz)**
$^1J_{2,3}$	2.5
$^3J_{1,4}$	35.1
$^4J_{1,5}$	< 0.1

The key observations on identification of the six structurally significant positions were as follows:

1. The olefinic carbon atoms (C_1 and C_2) match the expected shifts for a vinylidene.
2. The α-carbon (C_3) matched the shift expected for a tertiary carbon.
3. C_4 was observed at a shift typical for a secondary carbon atom adjacent to branching.
4. C_5 was observed at a shift typical for a secondary carbon atom.
5. C_6 was obscured by overlapping peaks.

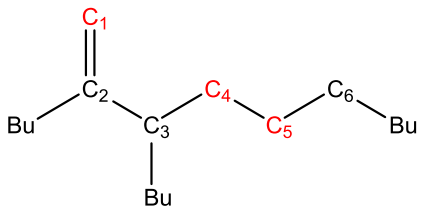

Figure 3.17 - The structure of isomer H. Enriched positions are shown in red.

Isomers I and K

Based on the data shown in Table 3.13 the formation of *trans*-8-butyltetradec-5-ene (I) and *cis*-8-butyltetradec-5-ene (K) were confirmed, as shown in Figure 3.18.

Table 3.13 - The ^{13}C NMR data for the structurally significant positions.

	Chemical Shift (ppm)	
Position	Isomer I	Isomer K
C_1	131.69	130.58
C_2	128.75	128.30
C_3	37.08	32.34
C_4	38.10	38.44
C_5	27.72	27.41
C_6	~	27.18
	Coupling Constant (Hz)	
Interaction	Isomer I	Isomer K
$^1J_{2,3}$	43.6	43.1
$^2J_{3,5}$	< 0.1	< 0.1
$^3J_{2,5}$	2.4	2.5

The key observations on identification of the six structurally significant positions were as follows:

1. The olefinic carbon atoms (C_1 and C_2) match the expected shifts for an internal olefin without α-branching.
2. The α-carbon (C_3) matched the shift expected for a secondary carbon atom in the *trans* position for I and the *cis* position for K.
3. C_4 was observed at a shift typical for a tertiary carbon atom.
4. C_5 and C_6 were observed at shifts typical for secondary carbon atoms. C_6 was obscured for Isomer I.

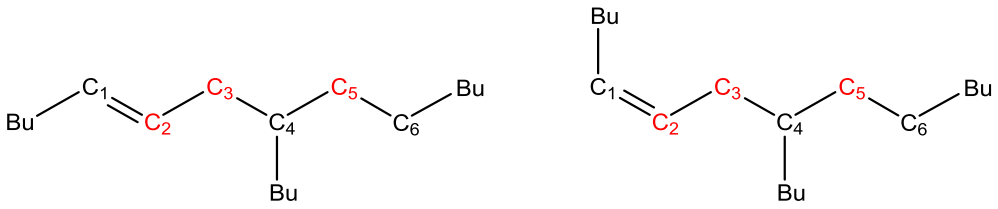

I K

Figure 3.18 - The structure of isomers I and K. Enriched positions are shown in red.

Isomers L and M

Based on the data shown in Table 3.14 the formation of *cis*-7-butyltetradec-5-ene (L) and *trans*-7-butyltetradec-5-ene (M) and were confirmed, as shown in Figure 3.19.

Table 3.14 - The ^{13}C NMR data for the structurally significant positions.

	Chemical Shift (ppm)	
Position	Isomer L	Isomer M
C_1	129.71	130.28
C_2	135.19	135.27
C_3	37.48	43.28
C_4	36.20	36.07
C_5	27.77	27.69
C_6	32.57	32.40
	Coupling Constant (Hz)	
Interaction	Isomer L	Isomer M
$^1J_{4,5}$	< 0.1	1.0
$^2J_{2,4}$	35.1	35.5
$^3J_{2,5}$	1.6	1.7

The key observations on identification of the six structurally significant positions were as follows:

1. The olefinic carbon atoms (C_1 and C_2) match the expected shifts for an internal olefin with α-branching.
2. The α-carbon (C_3) matched the shift expected for a tertiary carbon atom in the *cis* position for L and the *trans* position for M.
3. C_4 was observed at a shift typical for a secondary carbon atom adjacent to branching.
4. C_5 and C_6 were observed at shifts typical for secondary carbon atoms.

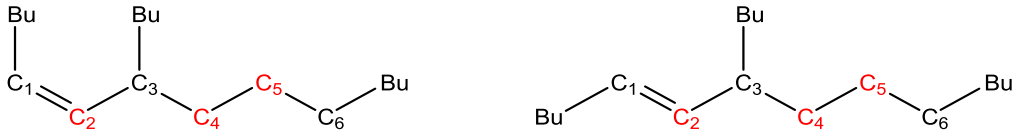

L M

Figure 3.19 - The structure of isomers L and M. Enriched positions are shown in red.

Characterisation of every predicted regioisomer, with the exception of N-U, provided strong evidence for the existence of the proposed metallacyclic mechanism. It also confirms the existence of all of the proposed pathways within the proposed mechanism, with the exception of *exo*-cyclic β-hydride elimination. These conclusions were later supported by R. D. Köhn in unpublished work in which the 2-position of 1-hexene was enriched. The same isomers were again identified and the chemical shifts determined using the original method were confirmed. Further information on the favourability of the different processes occurring during the catalyst cycle could be obtained by investigation of the relative abundance of the isomers.

3.2 Investigation of the Catalytic Intermediates

In order to investigate the various intermediates of the catalyst cycle it was necessary to calculate the relative abundance of each isomer. This was achieved by integration of long-delay inverse-gated ^{13}C NMR spectroscopy. This allowed accurate calculation of the relative abundance of the regioisomers by taking the average of all 18 signals found to correspond to each isomer. In cases where peaks were overlapping this signal was not used for either of the corresponding isomers. The relative abundance of the isomers produced by γ-Pe_2Cl are shown in Table 3.15, the sum of diastereomers has been shown for clarity. It is also worth noting that, while not shown, the diastereomers of each regioisomer vary considerably in abundance. Analysis of the causes of this selectivity are beyond the scope of this investigation, however, and require computational investigation.

Table 3.15 - The relative abundance of the C_{18} regioisomers produced by γ-Pe_2Cl.

Regioisomer Abundance (%)											
A	B	C	D	E	F	G	H	I	K	L	M
39.4	21.5	12.3	14.9	3.5	2.1	1.1	0.5	0.3	1.4	0.5	1.2

It is immediately apparent from the results that a large number of the isomers constitute only a minor proportion of the product mix while isomers A-D represent the vast majority. In order to assess the abundance of the different chromacyclic intermediates, the products must be grouped into those produced by the same chromacycloheptane, Table 3.16. An abbreviated mechanism is shown in Scheme 3.7, which demonstrates the pathways that could account for the different regioisomers according to the proposed mechanism. The abbreviations used for the chromacyclic intermediates will be used throughout the remainder of this chapter.

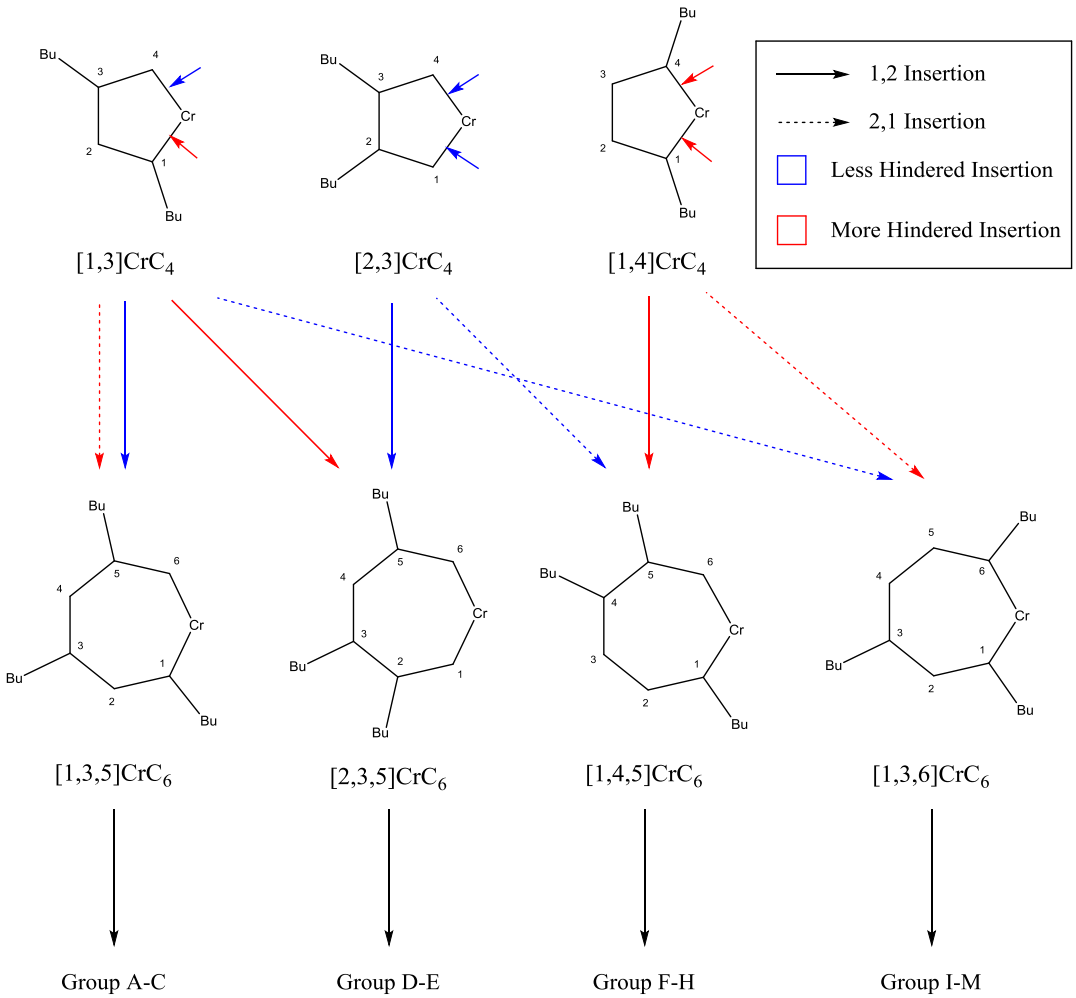

Scheme 3.7 - The groups of isomers produced according to the metallacyclic mechanism.

Table 3.16 - The relative abundance of the regioisomer groups produced from the same chromacycloheptane intermediate.

Group Abundance (%)			
A-C	D-E	F-H	I-M
73.2	18.4	3.7	3.4

As shown in Scheme 3.7, the relative abundance of the isomer groups is equivalent to the chromacycloheptane intermediates from which they are formed. It can also been seen that these intermediates can result from a total of eight pathways that, based on the variation in isomer abundance, must vary considerably in favourability. By analysing the abundance of the isomer groups it was possible to gain insights into the chromacyclopentane intermediates predicted by kinetic analysis to form the resting state of catalysis.

Group A-C, and therefore [1,3,5]CrC_6, is observed to be by far the most abundant isomer group and can only be produced *via* [1,3]CrC_4. As such, the minimum abundance of [1,3]CrC_4 is 73.2%, meaning this species accounts for the vast majority of the resting state of the active catalyst. Such favourability indicates that steric repulsion between the two butyl groups is of far greater significance than interaction between a butyl group in the 1-position and the ligand environment. However, electronic considerations could also account for such selectivity by promoting head-to-tail oxidative cyclisation.

The formation of [2,3,5]CrC_6 is more complex due to two possible formation pathways. The high abundance of [1,3]CrC_4 suggests that a considerable proportion of this group of isomers is formed as a result of hindered insertion into a substituted Cr-C bond. Equally, the effect of substitution at the 1-position could be significant and the majority could instead be formed from [2,3]CrC_4. Based on the abundance of [1,3]CrC_4 it appears clear that situation of the butyl branching in adjacent positions is strongly disfavoured. Therefore, the [1,3]CrC_4 route appears more likely and would suggest insertion into a less hindered Cr-C bond is at least four times more favourable. The maximum possible abundance of [2,3]CrC_4, based on isomers D-H, is observed to be 22.1%, though there is no conclusive evidence it is formed at all.

The formation of [1,4,5]CrC_6 is also possible *via* two intermediates, though only [1,4]CrC_4 provides a route that does not rely on [2,1] migratory insertion. Overall, the maximum proportion of [1,4]CrC_4 is observed to be 7.1% and it therefore constitutes a minor component of the active catalyst. This suggests that there is considerable steric interaction between the ligand environment and butyl chains at the 1-position, greatly reducing the likelihood of [1,4]CrC_4 formation despite avoidance of steric clash between butyl groups. The implication is, therefore, that chromacyclopentane formation is under steric control, with the [1,3]CrC_4 arrangement resulting in the least strain.

The low abundance of [1,4]CrC_4 suggests that the vast majority of [1,3,6]CrC_6 is accounted for by [2,1] migratory insertion into the non-substituted Cr-C bond of [1,3]CrC_4. In addition, [2,1] migratory insertion into the hindered bond of [1,3]CrC_4 is likely to represent a minute proportion of the A-C products formed. As such, the ratio of [1,3,5]CrC_6 to [1,3,6]CrC_6 is expected to give a good approximation of the favourability of [1,2] over [2,1] migratory insertion. The ratio was calculated to be 22:1 in favour of [1,2] insertion, considerably less than expected, and demonstrates that the assumption that the vast majority of insertions would occur with a [1,2] orientation cannot be made for these systems.

The observed ratio indicates that the maximum proportion of [1,4,5]CrC_6 that could result from [2,3]CrC_4 is 21%, based on the assumption that 100% of D-E results from this chromacyclopentane. Due to this being considered a very high estimate and the unlikelihood of F-H resulting from [1,4]CrC_4, the abundance of [1,3,6]CrC_6 provides a good estimate for that of [1,4]CrC_4. On this basis, the relative abundance of the three possible chromacyclopentanes can be approximated as 77-95% for [1,3]CrC_4, 0-18% for [2,3]CrC_4 and 4% for [1,4]CrC_4.

Overall, the trends expected for the formation of the intermediates were observed as expected. Firstly, insertion into a Cr-C bond in which a butyl branch was situated on the carbon was found to be disfavoured over unhindered insertion by at least a factor of four. Secondly, [2,1] migratory insertion was strongly disfavoured in comparison to [1,2] insertion but not to the degree expected. Thirdly, [1,3]CrC_4 was observed to be the most abundant chromacyclopentane due to steric repulsion between adjacent butyl groups and between butyl groups and the ligand. Fourthly, interaction between adjacent butyl groups appears to be more detrimental towards chromacyclopentane formation than steric interaction with the ligand environment.

3.2.1 The Effect of Ligand Bulk

The steric influence of the ligand was investigated by observation of the relative regioisomer abundance produced by catalysts with varying N-substituent branching point. The results of this investigation are shown in Table 3.17, with the sum of diastereomers shown where applicable. β-Bu_2 and α-Pe_2 were used for the first time in this study in order to minimise variation of the branching moieties and increase solubility. The catalysts were synthesised by R. D. Köhn according to the procedures described herein for β-Pr_2 and α-$^{i}Bu_2$.

Table 3.17 - The relative abundance of regioisomers produced by catalysts containing N-substituents with different branching points.

	Regioisomer Abundance (%)											
Catalyst	A	B	C	D	E	F	G	H	I	K	L	M
γ-Pe_2H	39.4	21.5	12.3	14.9	3.5	2.1	1.1	0.5	0.3	1.4	0.5	1.2
β-Bu_2	45.3	14.5	3.1	19.1	8.7	2.9	1.8	0.8	0.7	0.8	0.4	0.7
α-Pe_2	36.9	28.8	1.6	19.8	9.1	2.2	0.7	0.1	~	0.4	~	0.3

It is immediately apparent from the results that the bulk of the N-substituent has a considerable effect on the isomer mix. However, isomers A to E are again observed as the majority isomers in most cases. Among these, A, B and D are consistently the most abundant, suggesting their formation pathways are not prohibitively influenced by increased steric strain. In order to assess the effect of steric bulk on the different chromacyclic intermediates, the products were grouped into those produced by the same chromacycloheptane, Table 3.18.

Table 3.18 - The relative abundance of the groups of regioisomers produced from the same chromacycloheptane intermediate.

	Group Abundance (%)			
Catalyst	A-C	D-E	F-H	I-M
γ-Pe_2H	73.2	18.4	3.7	3.4
β-Bu_2	63.9	27.8	5.5	2.6
α-Pe_2	67.3	28.9	3.0	0.7

The results demonstrate that the steric bulk of the N-substituents has a considerable influence on the intermediates of the catalytic cycle. Despite this, [1,3,5]CrC_6 remains by far the most abundant chromacycloheptane. This further indicates the extent of the steric hindrance induced by adjacent butyl groups during chromacyclopentane formation. However, the ratio of Group A-C to Group D-E does fall considerably on moving from γ-Pe_2H to bulkier ligands (γ-Pe_2H = 4.0:1, β-Bu_2 = 2.3:1, α-Pe_2 = 2.3:1). Such a shift in selectivity is indicative of a shift towards [2,3]CrC_4 formation and away from [1,3]CrC_4. This observation therefore provides the first evidence for the existence of [2,3]CrC_4, while the magnitude of the shift indicates a considerable proportion of D-E is formed *via* this intermediate. It appears, therefore, that all three chromacyclopentanes are formed as intermediates during the catalyst cycle and that insertion into a substituted Cr-C bond is less likely than first thought.

Using the same approximation for the favourability of [1,2] over [2,1] migratory insertion as previously, the ratio was seen to vary markedly between catalysts (γ-Pe_2H = 22:1, β-Bu_2 = 25:1, α-Pe_2 = 96:1) and increase with increasing bulk. This implies that interaction between the third olefin and the ligand environment is considerable and determines the orientation of the molecule prior to insertion. As a result, the quantity of isomers I-M is severely reduced for α-Pe_2, with some not observed at all (I and L), indicating more selective catalysts can be produced by increasing the bulk of the N-substituents.

Broadly, the effects of increasing the ligand bulk agreed with the trends expected for the proposed mechanism, such as the observed shift from [1,3]CrC_4 to [2,3]CrC_4. A clear trend is not observed for the production of F-H, which is attributable to a weakening in the correlation between the relative abundance of the isomer group and [1,4]CrC_4. For example, the rise seen for β-Bu_2 relative to γ-Pe_2H can be linked to a considerable increase in the abundance of [2,3]CrC_4 and similar levels of [1,2] migratory insertion. In contrast, the considerable drop observed for α-Pe_2 can be linked to a lower abundance of [1,4]CrC_4 and a significant reduction in [1,2] migratory insertion.

Variation of the ligand has shown that the steric bulk of the ligand has considerable influence over the substitution pattern of chromacyclopentane intermediates. The steric control exerted by the ligand environment likely explains the considerable difference in selectivity between these systems and the (FI)$TiMe_3$ catalyst. This far bulkier catalyst was shown to be 85% selective towards formation of D, which would be expected based on the highly favourable formation of [2,3]CrC_4. The selectivity of the system described by Bercaw *et al*. therefore fully agrees with the steric control proposed here.

3.2.2 The Effect of α-Olefin Chain Length

Having established a strong link between the steric bulk of the catalyst and the abundance of the catalytic intermediates, the next logical step was to vary the bulk of the substrate. Firstly, the system was screened with a variety of α-olefins to identify the scope of the catalyst system. It was found that only LAOs (technically defined as mono-substituted α-olefins without branching at the carbon adjacent to the double bond) underwent trimerisation. Tests with vinylcyclohexane and 4,4-dimethylbut-1-ene both demonstrated no activity towards trimerisation.

This observation limited the number of commercial α-olefins available for investigation. However, it was recorded by Bercaw *et al*. that the turnover number of their catalyst was reduced on increasing the chain length of the LAO.[193] It appears, therefore, that simply extending the linear chain of the olefin can influence the catalysis. An investigation was carried out to determine whether increased chain length reduced the effectiveness of the catalyst and whether any effect on the catalyst selectivity was observed.

3.2.2.1 Effects on Catalyst Activity

In order to investigate whether the loss in activity observed by Bercaw *et al.* was replicated for $(R_3TAC)CrCl_3$ catalyst systems a series of trimerisations were carried out with liquid LAOs of varying chain length. Purification of the olefins was carried out in the same manner as described for the optimised 1-hexene work and the standard trimerisation procedure followed. The trimerisation was carried out with γ-Pe_2Cl in each case. The results are shown in Table 3.19.

Table 3.19 - The effect of substrate variation on catalyst performance.

Run	Substrate	Substrate (Eq.)	Activity (TOF)	Selectivity (%)	TON
1	1-Pentene	4992	4857	94	4228
2	1-Hexene	5008	4371	94	4077
3	1-Octene	5237	4212	93	3792
4	1-Octadecene	4912	1959	93	4107

It can be seen that increasing the length of the LAO's alkyl chain does indeed result in a reduction in activity. This could be attributable to the insertion rate of the third olefin, based on the kinetic investigations carried out previously. Alternatively, the greater proportion, as measured by mass, of LAO could result in a significant drop in solution polarity. This has shown previously to detrimentally affect the activity without reducing the turnover number. Whichever the cause, the activity remains at a satisfactory level even in the case of Run 4, suggesting considerable scope for the trimerisation of LAOs.

In contrast to the results reported for the (FI)$TiMe_3$ catalyst, the turnover number appears unaffected by increasing chain length.[193] The disparity in results is likely due to differing decomposition rates between the catalysts. The catalysts described here demonstrate very slow decomposition and therefore the lower activity has limited effect on the turnover number.

Observation that these catalysts can be applied to LAOs containing long chain lengths and achieve good turnovers indicates that (R_3TAC)$CrCl_3$ catalysts are far more suitable for application to lubricant synthesis (C_{30+}) than the only other known system. [193] The robust nature of these catalysts maximises the scope for trimerisation of other olefins, which may induce even lower activities. The ability to produce large quantities of a range of trimers led to investigation of their effects on isomer selectivity.

3.2.2.2 Effects on Catalyst Selectivity

In order to fully assess the effect of olefin bulk variation a larger range of olefins was required. Specifically, to reduce the bulk further it was necessary to carry out trimerisation of 1-butene and propylene. This required adaptation of the procedure in order to accommodate the use of gaseous substrates. A full description of the gaseous trimerisation reaction conditions and procedures that allowed synthesis of C_9 and C_{12} trimers is provided in Chapter 5. Unfortunately, the procedure did not allow for accurate calculation of catalyst activities but good yields of trimer were collected. In addition, 4-methylpent-1-ene was investigated as a branched substrate known to exhibit increased bulk.

The relative abundance of the major product isomers was again calculated using ^{13}C NMR integration and the observed isomers were grouped by the chromacycloheptane from which they formed. The effect of increased steric bulk on the olefin is shown in Figure 3.20.

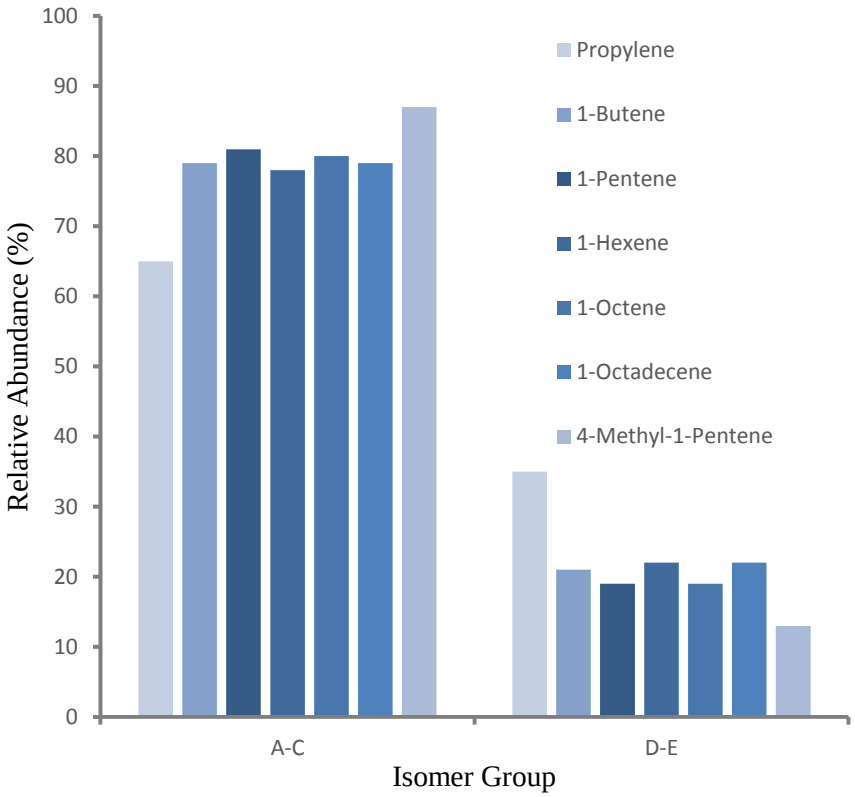

Figure 3.20 - The effect of increased steric bulk within the alkyl group of the LAO on the chromacycloheptane formed.

The results give another strong indication that the metallacyclic intermediates are formed under steric control. It can be seen that the ratio of Group A-C to D-E remains almost constant for the linear species larger than propylene. This would be expected due to no effective increase in steric bulk around the metallacycle. In contrast, a considerable shift in selectivity is observed for propylene and 4-methyl-1-pentene, which induce considerable variation in steric bulk. Both of these results indicate that reduction of the steric bulk on the alkyl group of the olefin leads to increased formation of D-E, while increasing the bulk results in a greater proportion of A-C.

These results clearly demonstrate that competition exists between olefin-olefin and olefin-ligand steric clash during the oxidative cyclisation step in the catalysis cycle. Larger olefins result in increased repulsion between themselves, which increasingly favours the formation of [1,3]CrC_4 in order to minimise this. On the other hand, reducing the bulk of the olefin minimises steric interaction and in turn enables avoidance of steric clash with the ligand environment, favouring the formation of [2,3]CrC_4. The fact that [1,3]CrC_4 is still favoured when propylene is used as the substrate indicates that the steric influence of the ligand is considerably weaker than that of the alkyl branches in the metallacycle.

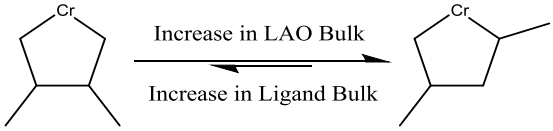

Figure 3.21 - The competition that exists between [1,3] and [2,3] substituted chromacyclopentanes and the influence of steric bulk.

3.2.3 The Effect of Counter-Ion Variation

Another factor that could influence the selectivity of the catalyst towards formation of different chromacyclopentanes is the counter-ion. The work of McGuinness *et al*. demonstrated clearly that catalytic intermediates can be influenced by counter-ion binding strength.[213] It follows therefore that the different counter-ions formed when using chromium triflate rather than chromium chloride catalysts could have a considerable impact on selectivity. It was shown by McGuiness *et al*. that MAO was the most weakly binding counter-ion of the considerable array investigated. It would be expected therefore that the $Al_xMe_y(OTf)_z$ counter-ion formed when activating a chromium triflate catalyst with $AlMe_3$ would bind more strongly.

1-Hexene was trimerised using the α-$^{i}Bu_2$ and α-$^{i}Bu_2$(OTf) catalysts. The triflate was activated with 20 equivalents of trimethylaluminium in *o*-$C_6H_4F_2$ before addition of 1500 equivalents of 1-hexene. Trimerisation of 1-hexene with the chloride catalyst was carried out according to the standard procedure. The effects on the relative abundance of the major isomer groups are shown in Figure 3.22.

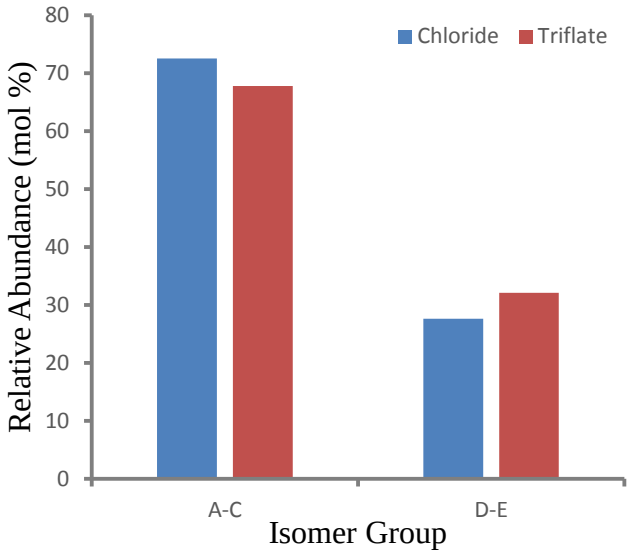

Figure 3.22 - The effect of the counter-ion on the relative abundance of the two isomer groups.

The results indicate a limited shift towards Group D-E was observed when using the chromium triflate catalyst. This mirrors the effects observed on increasing the bulk of the catalyst, as would be expected for a more strongly binding counter-ion. If the equilibrium predicted to exist between inner and outer sphere coordination of the counter-ion is shifted towards the inner sphere, then the effective bulk of the catalyst would be expected to increase. This would translate into a shift towards [2,3]CrC_4 and isomers D and E, as observed here. However, the different experimental procedures required for each catalyst may also lead to some variation in selectivity, such that no firm conclusions can be drawn.

Overall, it appears clear that the selectivity of intermediate formation is under steric control. This is demonstrated most clearly by comparison of isomer groups A-C and D-E, the relative abundance of which is indicative of the ratio of [1,3]CrC_4 to [2,3]CrC_4. It has been shown that increasing steric bulk around the metal centre, either through ligand modification or through more strongly binding counter-ions, leads to increased [2,3]CrC_4 formation. In contrast, increasing the bulk of the LAO substrate by incorporation of branching leads to a higher abundance of [1,3]CrC_4. Considerable steric control is also observed over the favourability of [2,1] migratory insertion, with increased bulk around the metal leading to a significant reduction in isomers I-M.

3.3 Investigation of the Elimination Pathways

Comparison of the relative abundance of isomer groups has allowed considerable insight into the different chromacyclic intermediates and the insertion pathways. However, the second process that determines the selectivity of the catalytic system is β-hydride elimination, which can be investigated by comparison of the abundance of isomers within a given group. While limited insights could be gained with the use of ^{13}C labelling studies, it was also necessary to investigate the elimination more directly with the use of deuterated systems.

3.3.1 The Effect of Ligand Bulk

A noticeable effect on increasing the ligand bulk was a shift in the relative abundance of isomers within the same group. This variation suggests that interaction between the ligand environment and the chromacycloheptane strongly influences the conformation of the ring and the ability of certain positions to form the dihedral angles required for elimination. While detailed analysis of the interaction is not possible based on calculation of the relative abundance of the regioisomers, several conclusions can be drawn. The data shown in Table 3.20 demonstrates the proportion of each regioisomer within the A-C isomer group.

Table 3.20 - The relative abundance of regioisomers within Group A-C for each catalyst.

	Relative Abundance (%)		
Catalyst	A	B	C
γ-Pe_2H	53.8	29.4	16.8
β-Bu_2	72.0	23.1	4.9
α-Pe_2	54.8	42.8	2.4

Increasing the ligand bulk appears to be detrimental towards the formation of vinylidene C in favour of internal olefins A and B. This suggests that repositioning the bulky butyl group also at the β-position presents a barrier to elimination. These results indicate that such alterations to the conformation of the ring are disfavoured and that formation of an acceptable dihedral angle with the β-hydride is sterically hindered. As such, the hindrance is increased with increasing steric bulk on the ligand, resulting in increased formation of the competing internal olefins.

Between the *cis* (B) and *trans* (A) isomers there is also considerable variation between catalysts that does not follow a simple trend. This must result from steric hindrance of the conformations that lead to their formation. Subtle differences in the ligand environment appear to determine whether the *syn* or *anti* hydride relative to the butyl branch in the 1-position is more accessible. However, further insights into this selectivity are difficult based on calculation of the regioisomer abundance.

It was not expected that any influence on elimination pathways would be observed within Group D-E, as no competition exists between internal olefins and vinylidenes. However, as shown in Table 3.21, there is in fact a considerable shift in the proportion of each vinylidene on increasing the bulk from γ-Pe_2H.

Table 3.21 - The relative abundance of regioisomers within Group D-E for each catalyst.

	Relative Abundance (%)	
Catalyst	D	E
γ-Pe_2H	81.0	19.0
β-Bu_2	68.7	31.3
α-Pe_2	68.5	31.5

Interestingly, the increased formation of E corresponds nicely with the observed increase in the abundance of [2,3]CrC_4. While the chromacyclopentane intermediate can have no impact on the elimination pathway according to the proposed mechanism, it suggests that the steric impact is similar in both cases. D appears to be favoured over E due to the beneficial influence of an alkyl branch in the 3-position, in an analogous manner to the selectivity observed for co-trimerisation of ethylene and 1-hexene, Chapter 4. Increasing the steric bulk of the ligand appears to nullify the promotion of elimination in this way, though with the information available no further conclusions could be drawn.

3.3.2 The Effect of Substrate Bulk

Considerable variation within the two major groups was also observed on variation of the LAO bulk. The relative abundance of the five major isomers is shown in Figure 3.23 for each of the substrates investigated.

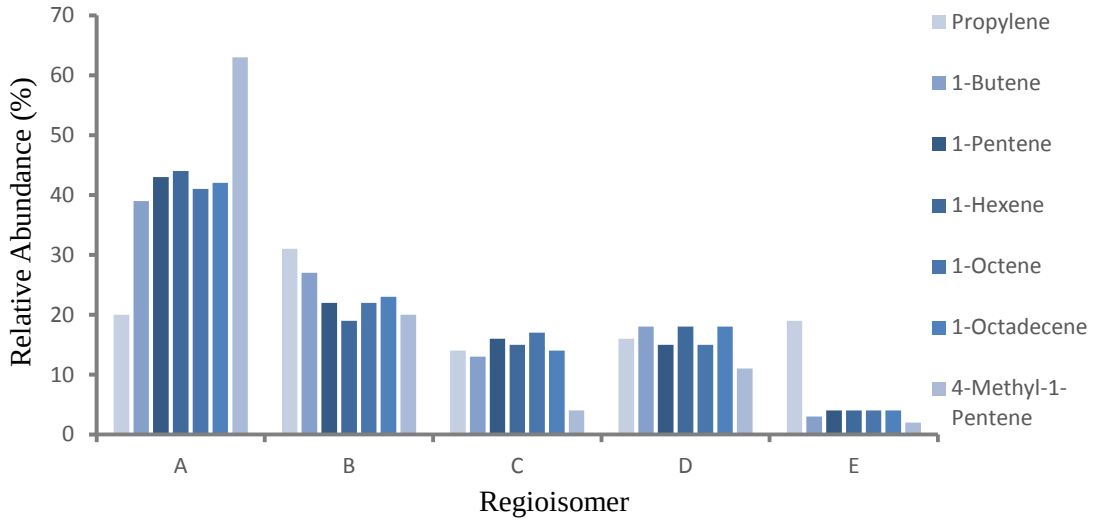

Figure 3.23 - The relative abundance of the five major regioisomers for each of the substrates tested.

Considerable shifts in selectivity based solely on the elimination pathways are again observed on increasing the strain on the system. Regarding group A-C, the vinylidene C is again disfavoured when the strain of the ring is increased by incorporation of additional branching. Both the propylene and 1-butene experiments demonstrate a shift away from A towards B relative to the average for longer linear chains. In contrast, a considerable increase in A is observed for 4-methylpent-1-ene at the expense of C. A clear trend appears to emerge, with increased bulk on the LAO favouring formation of A over B and C, though no explanation can be put forward based on these results.

Excluding the propylene experiment, almost no effect on the relative abundance of D and E is observed. For propylene there is a spike in the abundance of E such that it becomes the dominant isomer within the group. This was not observed on increasing the catalyst bulk and as such must result from reduced steric clash between the alkyl branches. It is also interesting that the overall increase in Group D-E is entirely accounted for by this increase in E, suggesting a tipping point has been reached in facilitating this pathway.

3.3.3 Deuterium Labelling Studies

In order to look at the elimination pathways more closely a series of deuteration experiments were carried out according to the procedures described by Eisch *et al*. and Muller *et al*.[229, 230] It was found that reaction of 1-hexyne with diisobutylaluminium hydride gave an aluminium alkenyl species which could be hydrolysed to give terminal alkenes. By incorporation of deuterium into different reagents it was then possible to selectively deuterate all three of the olefinic positions, as shown in Scheme 3.8.

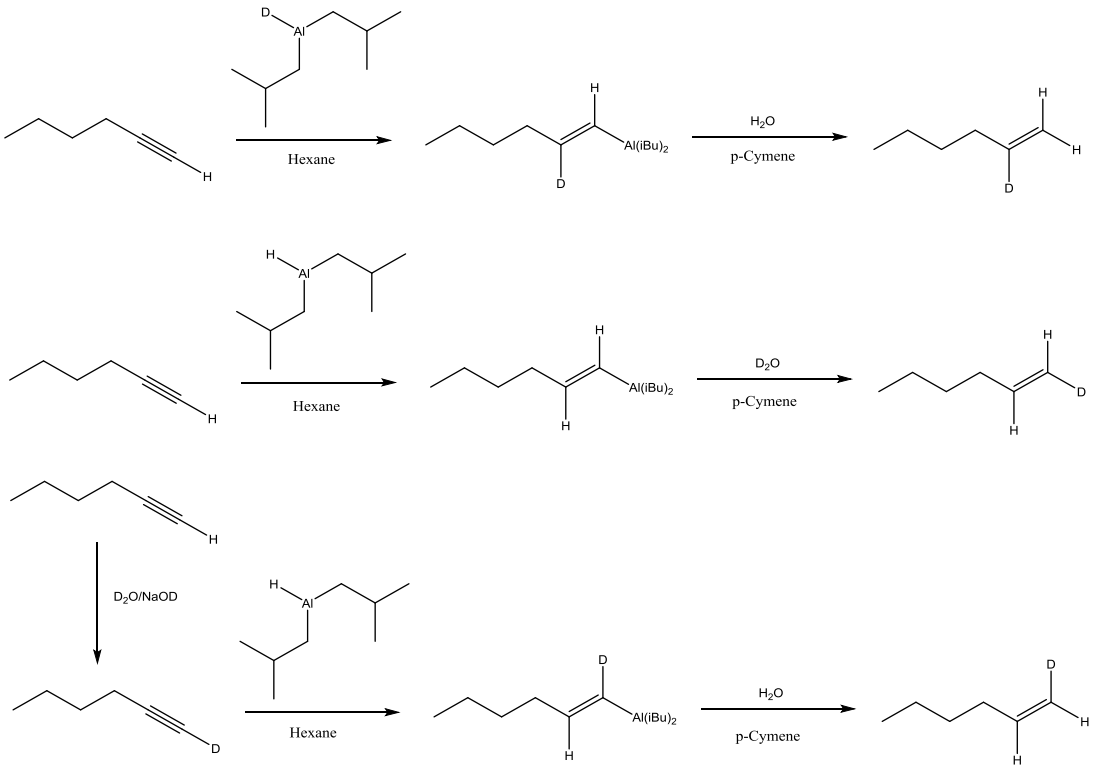

Scheme 3.8 - The procedure used to selectively deuterate each of the olefinic positions.

Complete deuteration could not be achieved for the samples, with some non-deuterated 1-hexene remaining. This equated to 95% deuteration for *cis*-1-D-1-hexene, 99% for *trans*-1-D-1-Hexene and 91% for 2-D-1-hexene due to limitations introduced by the procedure and/or reagents. The synthesis of 1,1-D_2-1-hexene by combination of the methods described for *cis* and *trans* led to unsatisfactory levels of deuteration at less than 85%. A different procedure was therefore used based on that used for the synthesis of ^{13}C labelled 1-hexene. Reaction of 1-bromopentane with triphenylphosphine, followed by deprotonation with sodium hydride gave the required ylide. Further reaction with 99% D_2-paraformaldehyde then resulted in the selective synthesis of 99% 1,1-D_2-1-hexene at an overall yield of 62%.

Each of the labelled 1-hexene species was then trimerised with γ-Pe_2Cl using the standard procedure. Each catalytic run was successful and produced considerable variation in the isomer distribution observed, as expected based on the kinetic isotope effect. This was demonstrated by Schrock and co-workers during analysis of metallacyclic dimerisation systems, who found that β-deuteride shift is considerably disfavoured relative to β-hydride shift.[54] As such, the position responsible for the elimination pathway should be immediately apparent where competition exists. In this manner it was hoped that the isomer grouping could be confirmed, which in turn would provide further evidence of a metallacyclic mechanism.

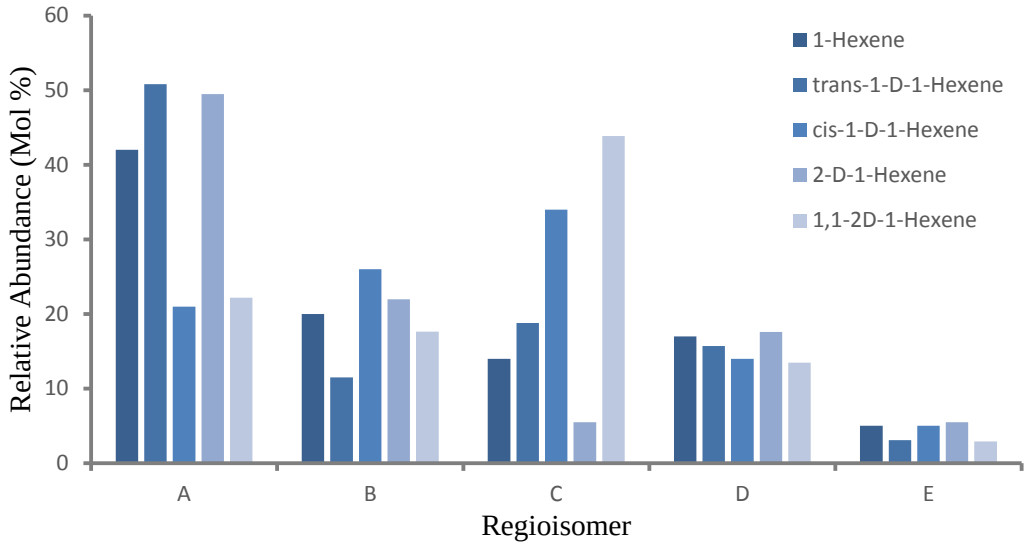

Figure 3.24 - The isomer distribution for the differently deuterated C_{18} trimers.

The relative abundance of the five major regioisomers, shown in Figure 3.24, demonstrate considerable variation between A-C but almost none between D-E on deuteration of the 1-hexene. This difference in behaviour agrees with the proposed mechanism, in which these two groups are formed solely from independent intermediates. No changes are observed in the ratio of D to E because no competition exists between elimination from different positions. Both products are vinylidenes and as such β-hydride/deuteride elimination occurs from the same position, that which is deuterated when using 2-D-1-hexene. Interestingly, the relative abundance of A-C compared to D-E remains constant throughout, indicating that there is no isotope effect on the formation of the chromacycloheptanes, as would be expected.

Group A-C shows considerable variation on deuteration of different positions. As expected, the use of 2-D-1-hexene leads to a considerable drop in the abundance of vinylidene C due to the unfavourability of β-deuteride shift and the fact its formation is in competition with internal olefins. The opposite observation is made on the use of 1,1-2D-1-hexene, which leads to a considerable increase in the abundance of C. Direct competition between elimination pathways that lead to a vinylidene or internal olefin product is therefore clearly evident. This could not occur if the catalyst cycle proceeded *via* a Cossee-Arlman mechanism. As such, this observation effectively rules out the chain growth mechanism and lends further support to the metallacyclic mechanism.

Within this expected trend is more subtle variation, however, because A and C appear to be in more direct competition than with B. This is demonstrated primarily by the runs carried out with 2-D-1-hexene and 1,1-2D-1-hexene, in which the shift in selectivity occurs almost entirely between A and C, with the proportion of B formed remaining fairly constant. This indicates that A and C must result from the same ring conformation, while B is formed from a different conformer with a significant energy barrier to transition. Some transition must occur, however, as a small shift in selectivity is observed between the use of *cis* and *trans* deuterated 1-hexene. This demonstrates that the *cis* product is formed by β-hydride elimination from the *anti* position relative to the butyl chain, while the *trans* product is formed by elimination from the *syn* position.

The selectivity resulting from the *cis* and *trans* deuteration indicates that β-hydride elimination can only occur from one position for each product. Based on the assumption that the metallacycloheptane adopts the chair conformation, it appears most likely that elimination would occur from an axial position. This position is in far closer proximity to both the chromium centre and the '6-position' to which the hydride will shift. Based on these assumptions the observed effects of deuteration can be explained according to Figure 3.25.

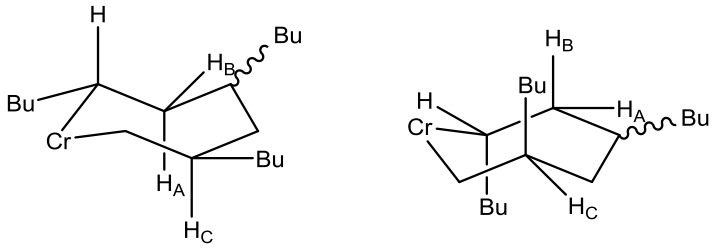

A/C B

Figure 3.25 - The proposed conformations of the chromacycloheptane intermediates leading to isomers A-C. Where H_A = a β-hydrogen atom *syn* to the butyl group in the 1-position, H_B = a β-hydrogen atom *anti* to the butyl group in the 1-position, H_C = a β-hydrogen atom on a tertiary carbon and H = an α-hydrogen atom.

The subscript letter assigned to each of the β-hydrogens indicates the isomer formed on β-hydride elimination from this position. These conformers have been proposed based on the reliance of *cis* or *trans* internal olefin formation on the deuteration of *syn* or *anti* positions. The conformations are also proposed based on the direct competition observed between A and C, as these isomers must both result from the same conformation in which the necessary hydrides are in axial positions.

The greater proportion of A compared to B can also be explained based on this proposal in relation to steric hindrance, shown previously to determine the relative abundance. The conformer leading to B must be more sterically hindered due to the orientation of at least two butyl groups in the more encumbered axial positions. Meanwhile, the two butyl groups closest to the ligand environment in the conformer leading to A and C are in equatorial positions. These two conformations are directly linked *via* ring-flip, which would account for the energy barrier to interconversion observed in competition between A and B.

Overall, significant steric influence has been demonstrated on the elimination pathways. Increases in the steric bulk of both the ligand and the LAO led to considerable shifts in selectivity within isomer group A-C. A thorough investigation with the use of deuterium labelling resulted in a detailed picture of the different elimination pathways and confirmed which isomers are formed from competing pathways. It was found that the two groups of major isomers are indeed formed from independent intermediates, with no competition between groups. This strongly supports the proposed metallacyclic mechanism.

Analysis of Group A-C clearly demonstrated competition between the product formation pathways. Observation of competition between vinylidene and internal olefin formation cannot be explained by the Cossee-Arlman mechanism, effectively ruling out its existence for this catalyst system. The changes in relative abundance induced by deuteration can be explained based on two different chromacycloheptane conformers accounting for A/C and B. The proposed conformations of [1,3,5]CrC_6 allow explanation of the general selectivity as well as the effects of deuteration and steric bulk on isomers A-C. While further computational research is required to test the assumptions made and to allow calculation of the orientation of the third butyl group, these partial conformations represent a good starting point.

3.4 GCMS Analysis and the Discovery of Dimerisation

Once the relative abundance of the different stereoisomers was accurately calculated by ^{13}C NMR integration, the samples were analysed using GCMS-FID (Gas Chromatography Mass Spectrometry - Flame Ionisation Detection). It was hoped that this highly sensitive analytical method would present a more facile route to isomer abundance calculation. However, separation and identification of the peaks proved difficult and only the major isomers could be identified by correlation with the results of ^{13}C NMR analysis. This was achieved with the use of the deuterated trimers described in the previous section in addition to two different column specifications. These trimers were used due to the considerable variations in the relative abundance of different isomers, which facilitated correlation.

The relative integration of each signal was determined relative to the entire C_{18} region in an analogous method to the results of the NMR analysis. Comparison of the results allowed the peaks to be correlated to their corresponding isomer/s to within a high degree of accuracy. The assignments are shown in Figure 3.26.

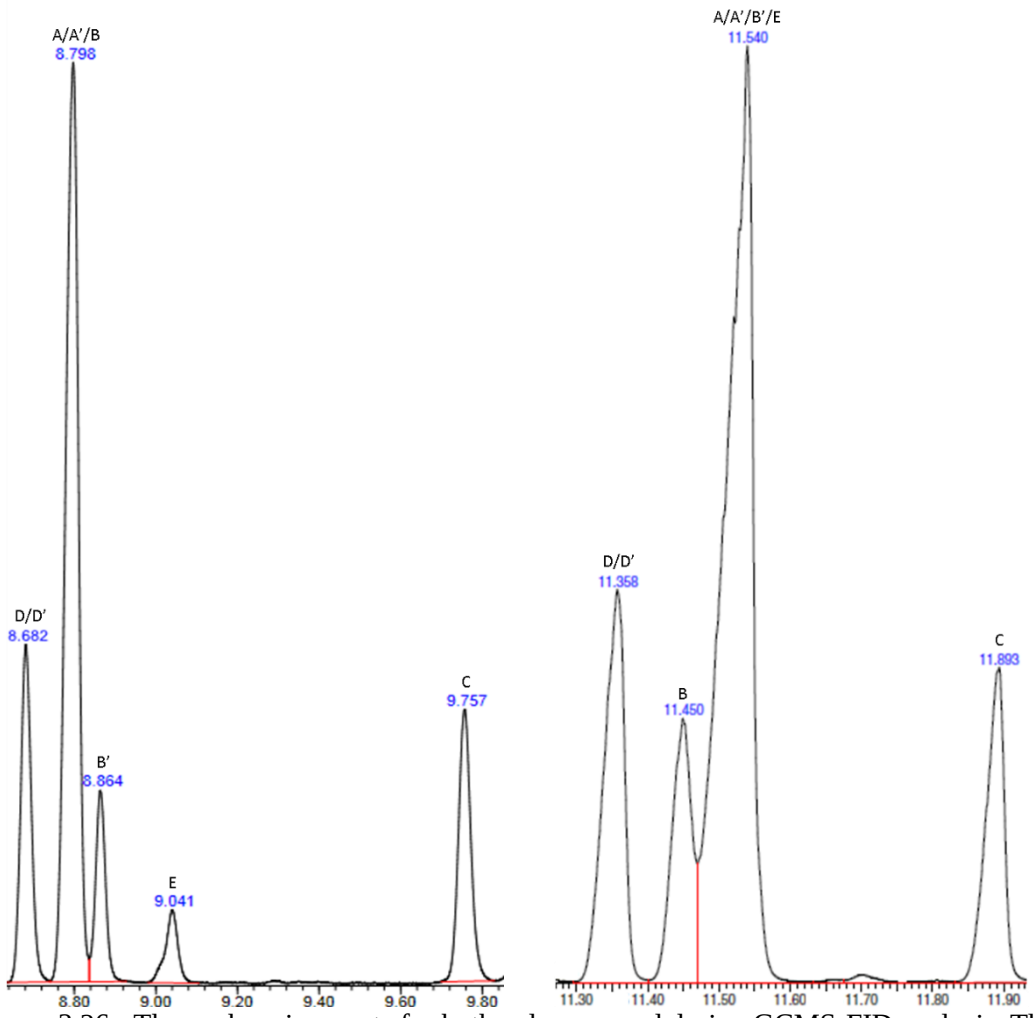

Figure 3.26 - The peak assignments for both columns used during GCMS-FID analysis. The sample shown corresponds to non-deuterated C_{18} trimer produced with γ-Pe_2Cl.

The results obtained using the DB-FFAP column (left) provided the best separation while comparison with the HP-5 column (right) allowed differentiation of the two diastereomers of B. Column specifications are available in Chapter 5. Isomer B was the only regioisomer for which the two diastereomers could be distinguished. The assignment was made based on correlation with the ^{13}C NMR integration data presented in Figure 3.24. The accuracy of the assignments for the DB-FFAP column is shown in Figure 3.27, while the correlation of the HP-5 column is shown in Figure 3.28. The substrates used for correlation were 1) 1-Hexene 2) 1,1-D_2-1-Hexene 3) *trans*-1-D-1-Hexene 4) *cis*-1-D-1-Hexene and 5) 2-D-1-Hexene.

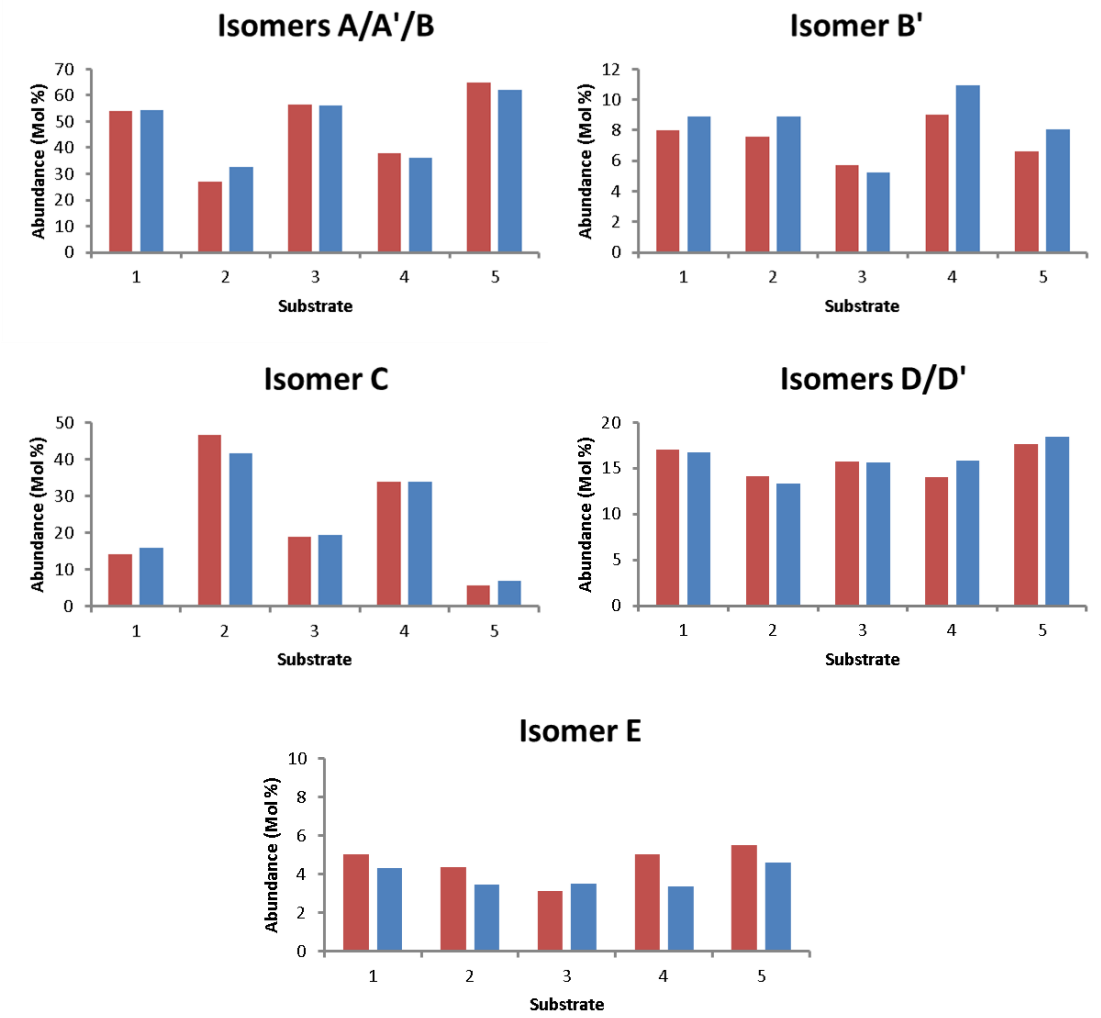

Figure 3.27 - The peak correlation for the DB-FFAP column. Red represents data calculated from NMR integration while blue represents GCMS derived data.

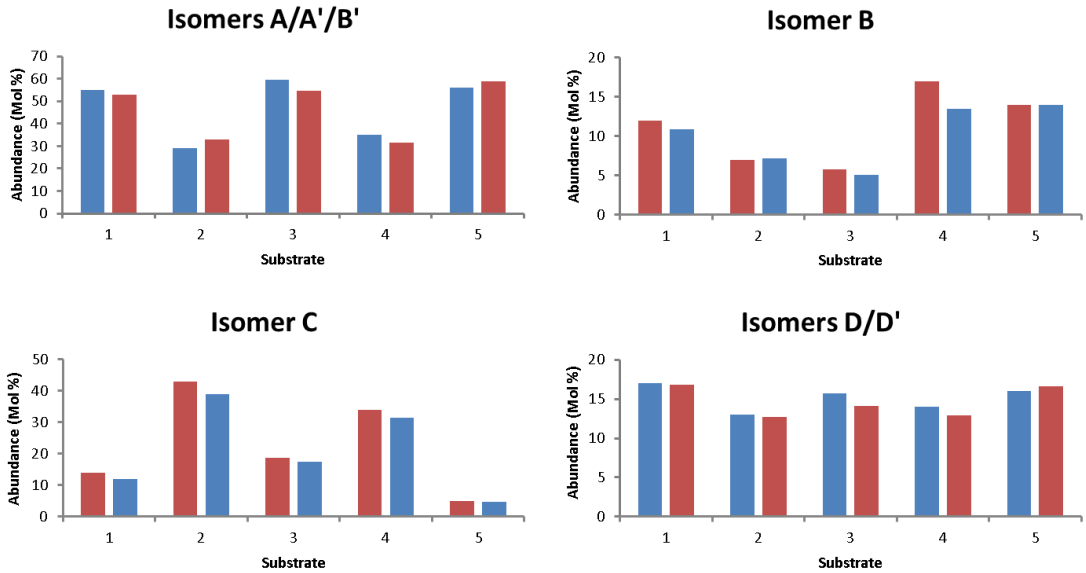

Figure 3.28 - Peak correlation for the HP-5 column. Red represents data calculated from NMR integration while blue represents GCMS derived data.

The correlation, even for the major isomers, demonstrated noticeable errors and had to be identified based on the observed trends for the differently deuterated 1-hexenes. This is likely induced by the presence of minor isomers at similar retention times. Ultimately, GCMS proved to be a less effective tool for calculation of the relative abundance when compared to NMR spectroscopy. This was principally as a result of the difficulty encountered on trying to differentiate between isomers A and B, which displayed unsurprisingly similar retention times. In addition, the similarity in the retention times of all products meant that minor isomers were not observed.

The use of GCMS did have a considerable advantage, however, when searching for additional side products. The high sensitivity of this analytical technique meant that impurities in highly concentrated samples of C_{18} trimer could be detected at concentrations as low as 0.01%. In this manner dimerisation was observed for the first time at quantities ranging from 0.01% to 0.1% abundance relative to the trimer, depending on the catalyst and conditions.

By comparison to the NIST database of MS spectra it was possible to gain insights into the identities of the dimers, though confirmation would require synthesis of reference compounds and this has not been carried out. The low intensity of the peaks prevented full characterisation due to uncertainty surrounding the stereoisomerism and position of internal olefins. However, the branching of the compounds could still be reliably predicted. The proposed identities are shown in Figure 3.29.

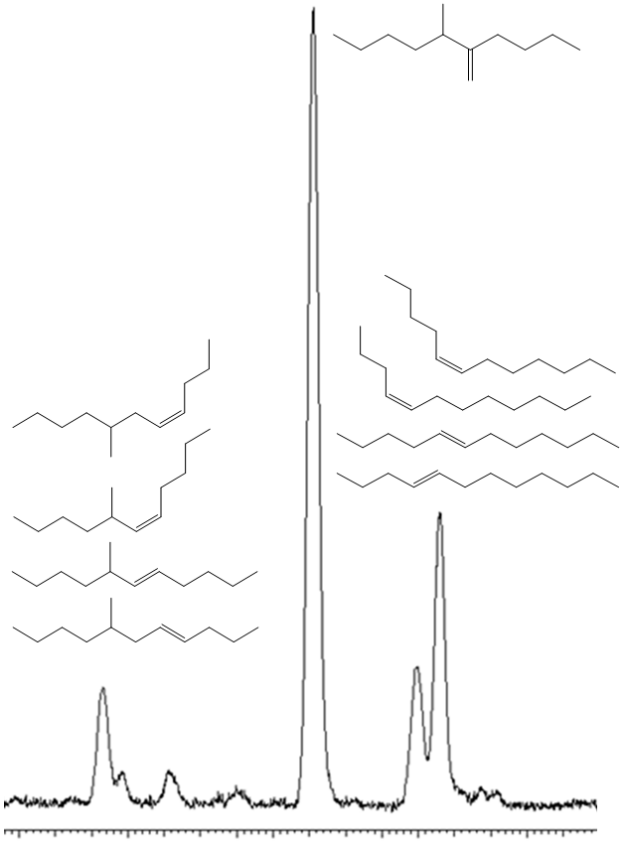

Figure 3.29 - The C_{12} region of the GCMS spectrum for a trimer sample produced using γ-Pe_2Cl and the peak allocation.

The major peak could be readily identified as 5-methyl-6-methylenedecane, which correlates well with one of the proposed chromacyclopentane intermediates. The other peaks could not be fully characterised, with the peaks at lower retention time shown to contain a secondary methyl group and the peaks at higher retention time shown to be linear. The observation of singularly branched and linear products also fits with the proposed chromacyclopentane intermediates. Interestingly, no fragmentation patterns correlated with 5-methyleneundecane, suggesting its formation is disfavoured. This would agree with the observation that vinylidene products are disfavoured relative to internal olefinic products when in direct competition.

The relative intensities of the dimers do not bear any resemblance to the predicted abundance of the intermediates based on analysis of the trimer. This suggests that the proportion of a given dimer is determined instead by the favourability of elimination from the chromacyclopentane. Based on the results observed, this would suggest that the stability of the intermediate towards β-hydride elimination increases from [2,3]CrC_4 to [1,4]CrC_4 to [1,3]CrC_4. The factors relating to the substitution pattern that determine the favourability of elimination remain unclear. It is also not possible to comment on the existence of *exo*-cyclic elimination due to the uncertainties around the internal olefin position.

Overall, GCMS proved to be ineffective as a means of calculating the relative abundance of the C_{18} regioisomers. The technique proved far more useful in searching for side products ad impurities, with its use leading to the discovery of dimerisation for these systems for the first time. Partial characterisation of these extremely low abundance products was achieved and gave an indication of the stability of the three chromacyclopentane intermediates towards β-hydride elimination. The observed branching patterns and the identification of 5-methyl-6-methylenedecane lend further support to the proposed metallacyclic mechanism.

3.5 Identification of the Side Products of Activation

Another aspect of the catalyst cycle, which has been investigated for numerous ethylene systems, is the activation mechanism and the resulting side-products.[19] Methane has been observed during kinetic investigations of $(R_3TAC)CrCl_3$ catalysts, Chapter 2, but does not represent conclusive evidence for the proposed mechanism. This is due to methane production also resulting from reaction of MAO and water. In order to prove the activation procedure, it was necessary to isolate side products that could only result from interaction between the LAO and the chromium centre.

The side products of activation are only produced in equimolar amounts to the catalyst and, as such, a large scale reaction was required in order to detect them. This could not be achieved with $(R_3TAC)CrCl_3$ catalysts due to the high equivalents of highly expensive MAO required to produce an active catalyst. This led to these experiments being conducted with the use of $(R_3TAC)Cr(OTf)_3$ catalysts, which require far fewer equivalents of the cheaper trimethylaluminium. The mechanism proposed to occur on activation of chromium triflate catalysts is shown in Scheme 3.9.

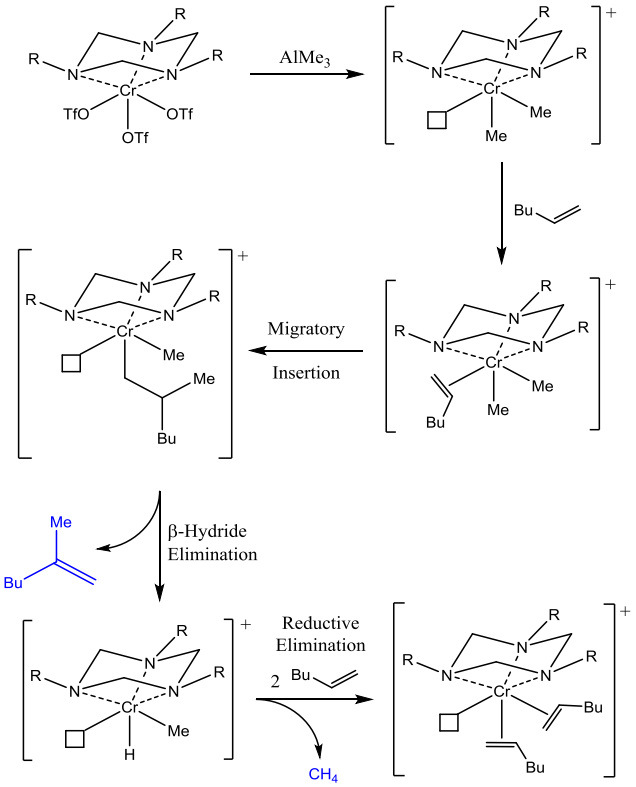

Scheme 3.9 - The proposed activation pathway for chromium triflate catalysts with the side products shown in blue.

According to the proposed mechanism, adapted directly from that originally proposed for $(R_3TAC)CrCl_3$ systems by Köhn *et al*, there should only be one product of activation besides methane.[2] 2-Methyl-1-hexene should be far easier to identify than the propene formed during ethylene reactions as it should not be incorporated into trimerisation. An investigation into whether the formation of 2-methyl-1-hexene could be confirmed was undertaken with the use of $(Cy_3TAC)Cr(OTf)_3$, synthesised by R. Köhn in an analogous procedure to that described for α-$^{i}Bu_2$.

The trimerisation was carried out with just 6 equivalents of 1-hexene, which were added to 0.5 g of the catalyst after activation with 20 equivalents of trimethylaluminium. After one hour the reaction was halted and the solution hydrolysed while cooling to ensure that no volatile species were lost. Extraction with pentane allowed isolation of the organic phase, which was analysed by GCMS. The FID spectrum observed is shown in Figure 3.30 with the peaks labelled according to correlation with the NIST database.

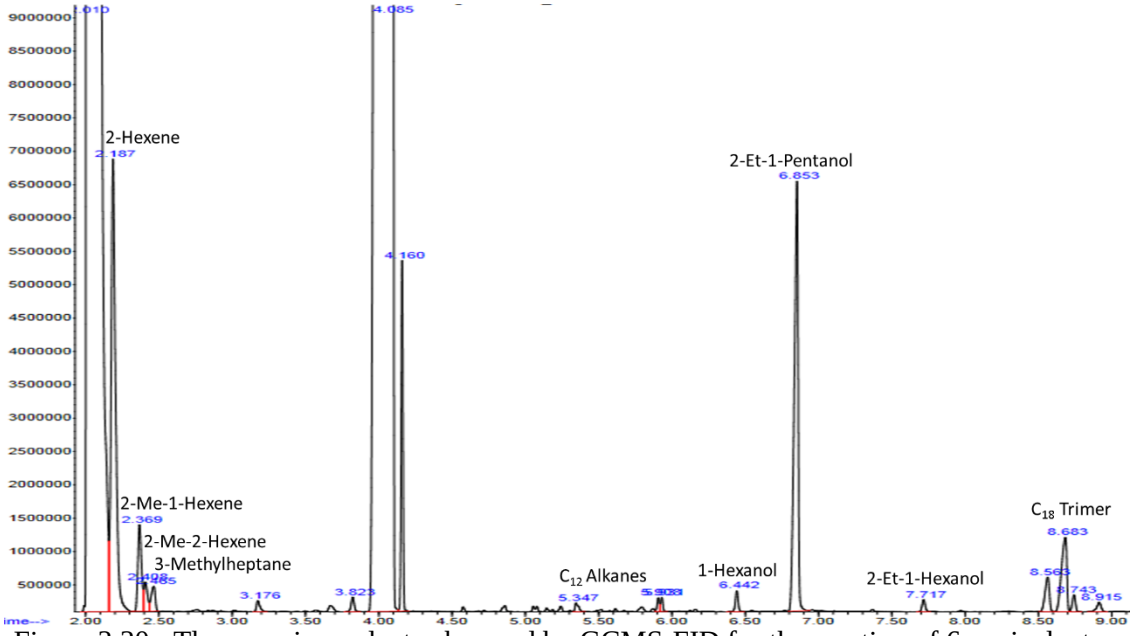

Figure 3.30 - The organic products observed by GCMS-FID for the reaction of 6 equivalents of 1-hexene with activated $(Cy_3TAC)Cr(OTf)_3$. Retention time is shown on the x-axis in minutes while the intensity is shown on the y-axis in arbitrary units. The solvent peaks at 2.010 and 4.085 have been cut off to better present the products.

On analysis of the organic products it is immediately apparent that more species are formed than predicted, suggesting more processes are occurring than described in the original proposal. In order to confirm the existence of the key products a set of reference compounds were run and the retention time recorded. The C_{18} trimer and 2-hexene could be identified by comparison to the products of standard chromium triflate trimerisation experiments. Otherwise, the peaks corresponding to 2-methyl-1-hexene, 1-hexanol, 2-ethyl-1-pentanol and 2-ethyl-1-hexanol were characterised using reference samples.

2-Ethyl-1-pentanol appeared inconsistent with the products that would be expected under these conditions. Therefore, a reference sample of 2-methyl-1-hexanol was also run in case of misassignment on correlation with the NIST database. It was thought this compound may represent a more likely product due to the expected formation of 2-methylhexyl moieties. Misassignment between these two species could result from its structural similarity and identical molecular mass. Neither of these species were commercially available and were synthesised according to the procedures described in Chapter 5. Comparison of the reference samples with the original spectrum is shown in Figure 3.31.

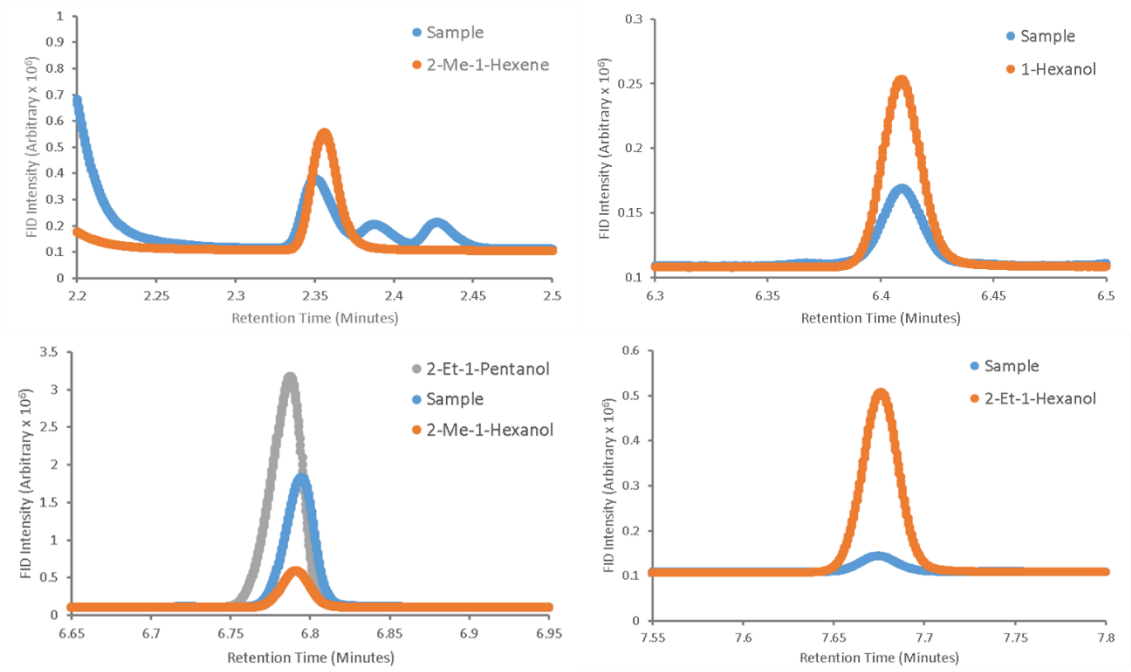

Figure 3.31 - Correlation of retention times between reference samples and the products of activation.

The formation of 2-methyl-1-hexene was confirmed as an activation product for the first time, giving a strong indication that the proposed activation route is correct. Based on correlation with the NIST database 2-methyl-2-hexene was also observed, indicating that 2-methyl-1-hexene still interacts with the catalyst and can be isomerised. A similar reactivity has been observed for the vinylidene products of chromium triflate catalysed trimerisation.[231] Both 1-hexanol and 2-ethyl-1-hexanol were also confirmed, indicating oxidation of organometallic species within the catalyst solution leads to their formation.

The species represented by the signal at 6.8 minutes remains unclear based on these results, with both reference compounds demonstrating very similar retention times. It was noted that the 2-methyl-1-hexanol reference was predicted to be 2-ethyl-1-pentanol by the NIST database, indicating an error exists within the software. In order to confirm the identity of this species the sample taken from the original experiment was gradually concentrated at 50 °C to remove all volatile components. The remaining liquids were then heated to 100 °C and the volatiles collected. This second fraction was analysed by NMR spectroscopy and found to contain predominantly 2-methyl-1-hexene based on comparison to the neat reference sample, as shown in Table 3.22. A full assignment is provided in Chapter 5.

Table 3.22 - Comparison of the ^{1}H and ^{13}C NMR spectra recorded for neat samples of the isolated activation product and 2-methyl-1-hexanol relative to an internal sample of TMS. The alcoholic proton is not shown.

^{1}H NMR Chemical Shifts (δ, ppm)		^{13}C NMR Chemical Shifts (δ, ppm)	
Activation Product	2-Me-1-Hexanol	Activation Product	2-Me-1-Hexanol
3.42	3.43	68.89	68.92
1.54	1.55	36.94	36.92
1.37	1.39	33.92	33.96
1.05	1.06	30.27	30.30
1.23	1.24	23.93	23.96
0.89	0.91	16.99	17.05
0.85	0.86	14.40	14.44

On identification of the major activation products it was also possible to accurately determine how many equivalents of 1-hexene had been converted into each. Integration of the GCMS-FID spectrum allowed calculation of the relative abundance after corrections based on the molecular mass of the product. The integration of FID spectra is measured relative to the molecular mass of a molecule, such that this must be taken into account when comparing species of different empirical formula. The product distribution is detailed in Table 3.23.

Table 3.23 - The equivalents of 1-hexene consumed during formation of the various activation products.

Activation Product	1-Hexene Equivalents Converted
2-Hexene	2.8
2-Methyl-1-Hexene	0.3
2-Methyl-2-Hexene	0.2
3-Methylheptane	0.1
C_{12} Alkanes	0.1
1-Hexanol	0.1
2-Methyl-1-Hexanol	1.7
2-Ethyl-1-Hexanol	< 0.1
C_{18} Trimer	0.9

According to the original proposal, one equivalent of 1-hexene should be consumed in the production of 2-methyl-1-hexene to give the active catalyst. The remaining 1-hexene would be expected to either trimerise or isomerise to 2-hexene. In fact, while 2-hexene and C_{18} trimers do indeed make up the bulk of the products, it appears that more than one equivalent of 1-hexene has been consumed in the formation of activation products. Only 0.5 equivalents of 2-methyl-1-hexene and 2-methyl-2-hexene are observed, suggesting some of these volatile compounds is lost during isolation of the sample. The sum of the 2-methyl branched species is 2.2 equivalents, indicating that additional processes must account for the excess produced and the conversion to an alcohol.

The most likely mechanism by which greater quantities than expected are formed is chain transfer between the alkylated chromium catalyst and the aluminium activator. Transfer of the 2-methylhexyl group from the chromium to the aluminium would result in substitution with a methyl. Therefore, an additional 1-hexene molecule would be required to activate the catalyst each time this occurred, increasing the amount of 1-hexene required for activation. By taking chain transfer into account a mechanism can be proposed which accounts for each of the products observed, with the exception of the minor quantity of 2-ethyl-1-hexanol which remains unexplained.

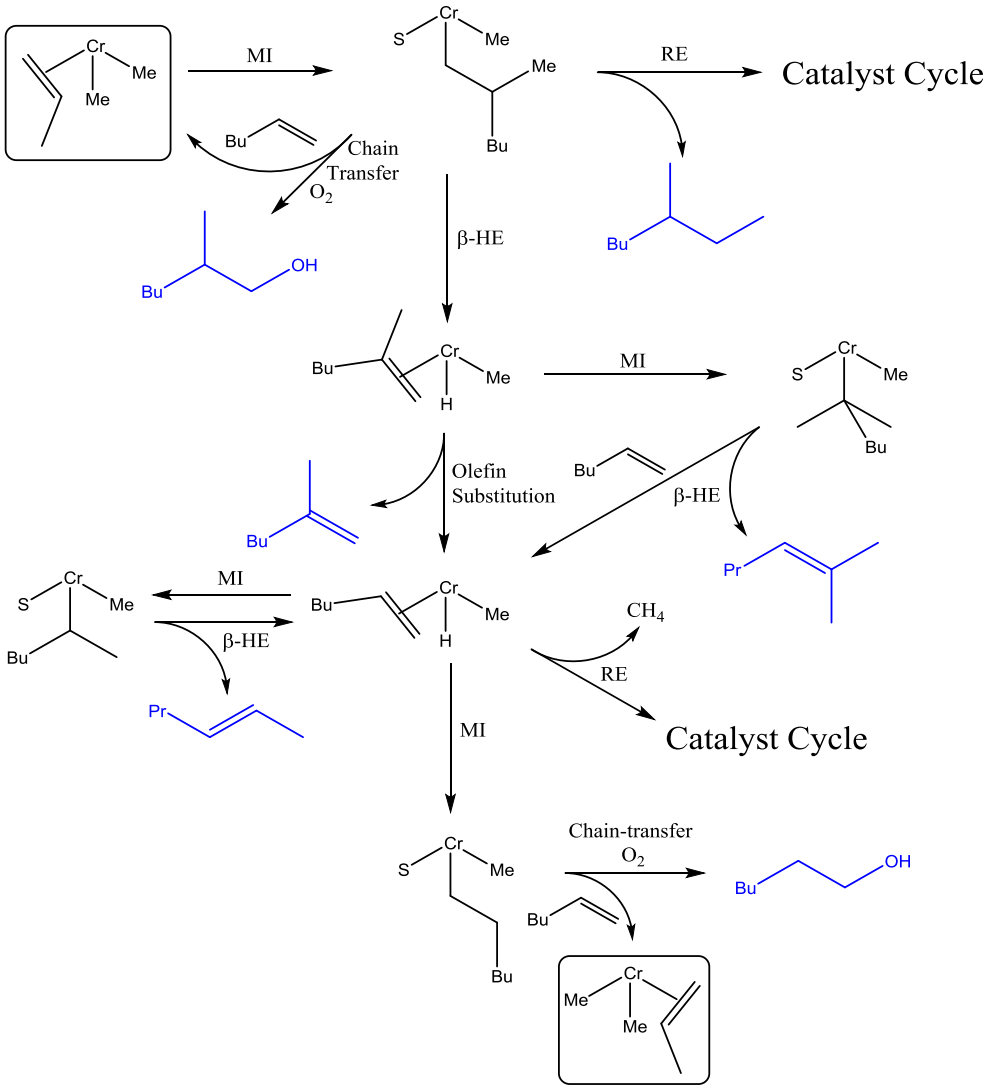

Scheme 3.10 - The processes proposed to occur during catalyst activation. MI = migratory insertion, RE = reductive elimination, β-HE = β-hydride elimination.

The mechanism shown is adapted directly from the original proposal with addition of the previously unexpected chain-transfer reactions. It is hypothesised that the alcohols result from oxidation of aluminium species. The isomerisation steps have been included as possibilities due to the presence of a chromium hydride intermediate but are more likely produced after catalyst activation according to the allyl mechanism described in Chapter 2. Cr^{III} hydrides are not stable and therefore this would either be a very short lived intermediate or a concerted β-hydride shift could occur.

Based on the side products observed it appears that two routes into the catalyst cycle are available. The predicted route, *via* methane evolution, appears to represent the major pathway based on the products observed. However, the unexpected observation of small quantities of 3-methylheptane suggests that reductive elimination can occur immediately after the initial olefin insertion. This would involve C-C bond formation between sp^3 carbon atoms, usually considered highly unlikely. However, there is limited precedent for this chemistry as similar coupling between sp^2 carbon atoms has been observed experimentally by Carney *et al.* for analogous Cr^{III} systems.[120]

Overall, the original mechanism proposed for activation of $(R_3TAC)CrCl_3$ LAO trimerisation catalysts has been modified to account for the side products observed. This investigation has produced the first experimental evidence for the formation of 2-methyl-1-hexene as an activation product, supporting the original proposal, and identified a variety of others. The greater than one equivalent of 2-methylhexyl derived species observed strongly suggests that chain transfer occurs between the catalyst and activator. This process would increase the time required for complete activation of the catalyst and may explain the induction period seen for these catalysts. All of the products observed, excluding 2-ethyl-1-hexanol, can be accounted for by adaptation of the original proposal, again supporting the existence of the metallacyclic mechanism.

3.6 Direct Observation of Catalytic Intermediates *via* Mass Spectrometry

A key feature of α-olefin trimerisation catalysts is the ionic nature of the active species. This was firmly established by Bercaw *et al*., who demonstrated that activity was entirely dependent on the presence of a cationic metal centre.[98] Mass spectrometry is therefore an ideal analytical technique for investigation of the intermediates and counter-ions of catalysis. To the best of my knowledge, however, this technique has not been applied to trimerisation systems until now. This is likely due to the considerable difficulties that result from the extremely air and moisture sensitive nature of the active catalyst, as well as the use of large and poorly soluble activating agents such as MAO.

With the use of α-$^{i}Bu_2(OTf)$ and trimethylaluminium as the activating agent it was possible to produce a system that featured a small, well-defined and highly soluble counter-ion suitable for this analysis. The air and moisture sensitivity was overcome by linking the mass spectrometer directly to a glove box, such that samples could be prepared and injected under a dry argon atmosphere. The tubing connections to the mass spectrometer were prepared in order to ensure the best seal possible, though it was impossible to eliminate all risks of exposure to air and moisture.

The mass spectrometry undertaken during this investigation was performed using the relatively benign ESI (Electrospray Ionisation) technique. Mass spectrometry is not normally quantitive due to unpredictable variations in the ionisability of the species investigated. However, in this case the ionisation step was not required as the species to be investigated are already ionic. In the absence of ionisation the peak intensity of the different species is dependent on the abundance and the dissociation constant of the different ion pairs. Throughout catalysis it is expected that the counter-ion will remain unchanged, while the chromium species will alternate between Cr^{I} and Cr^{III}. It is thought that dissociation constants between the counter-ion and chromium species of the same oxidation state would be of comparable magnitude. Therefore the relative peak intensity gives a good insight into the relative abundance of comparable species.

Two experiments were carried out, one in which cations were detected and one which the anionic counter-ions were investigated. Both were carried out separately using the same equipment and with the same reaction conditions applied to catalysis. In each case numerous minor peaks were detected which could not be satisfactorily identified. Therefore, the results published here provide evidence of the existence of the intermediates described but do not indicate that they are formed exclusively.

3.6.1 Investigation of the Cationic Intermediates

Direct analysis of the intermediates of metallacyclic catalyst cycles has, to date, been limited and inconclusive.[101] The key aim of this investigation was therefore to observe signals corresponding to the exact mass and isotope pattern of the proposed intermediates of both the activation and the catalyst cycle. In so doing, conclusive evidence for the intermediates could be collected. The potential intermediates proposed as part of the metallacyclic mechanism are shown in Figure 3.32.

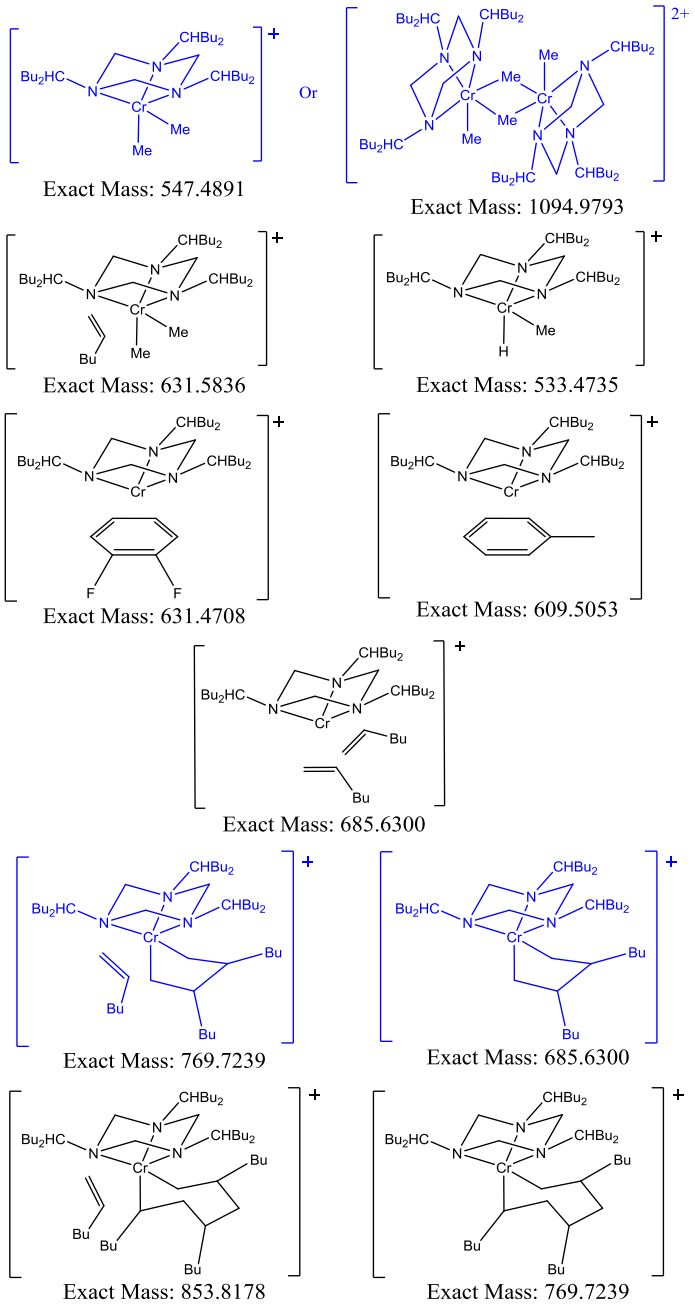

Figure 3.32 - The cationic intermediates possible within the proposed metallacyclic mechanism. Proposed resting states are shown in blue.

A minor complication associated with the use of mass spectrometry to identify these cationic species is that several have an identical isotopic mass. The inability to differentiate between coordinated 1-hexene and 1-hexene incorporated into a metallacycle leads to the introduction of some ambiguity. The predicted resting states are highlighted in blue and are based on the kinetic studies described in Chapter 2 and the proposed activation mechanism.

The reaction was carried out according to the standard procedure for chromium triflate trimerisation but with 5000 equivalents of 1-hexene in an attempt to extend the duration of the reaction. The analysis was carried out in two stages, firstly, after addition of the activator and secondly, after 1-hexene addition. This first analysis was undertaken with the aim of identifying a $[LCrMe_2]^+$ species, for which evidence has been found previously.[101] The spectrum collected featured only one significant peak, which corresponded to the proposed product of alkylation and abstraction, $[((\alpha\text{-}^{i}Bu_2)_3TAC)CrMe_2]^+$, as shown in Figure 3.33.

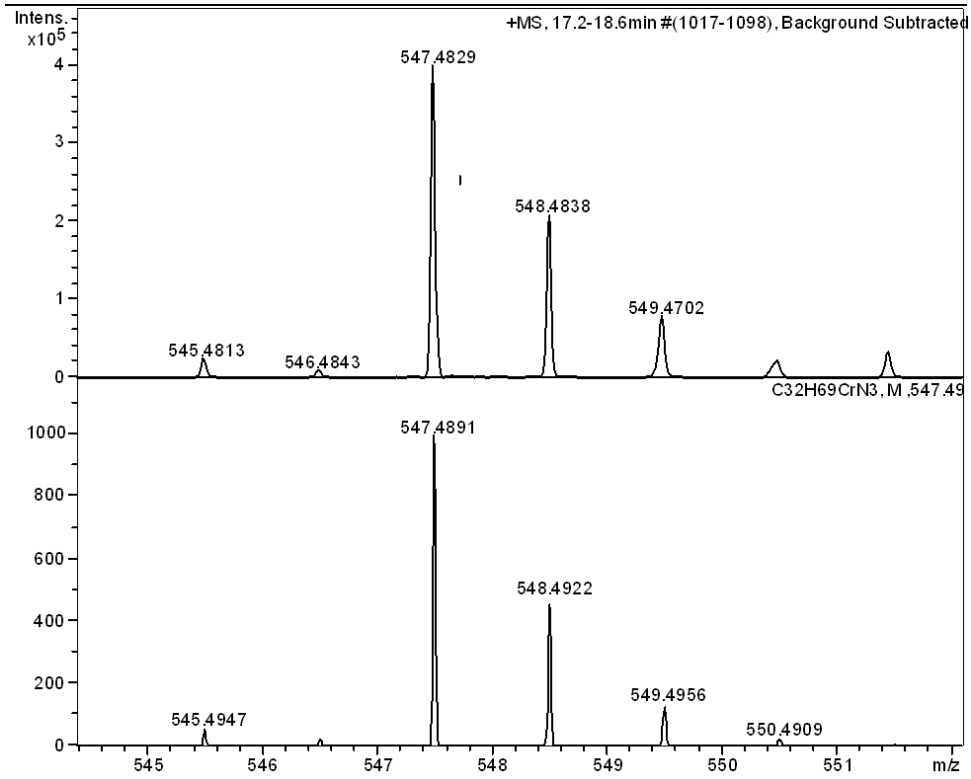

Figure 3.33 - The observed (top) and calculated (bottom) m/z peaks corresponding to $[((\alpha\text{-}^{i}Bu_2)_3TAC)CrMe_2]^+$.

The single chromium atom of the species gives a distinctive peak at M-2, alongside a more minor peak at M-1, which facilitates confirmation of the presence of chromium. The other elements present within the solution (C, H, N, O, S, F) have very high abundance in their most stable isotope and result in minimal influence on the isotope pattern. The large number of carbon atoms present in the ligand leads to the typical pattern seen for organics, with decreasing intensities from M to M+1 to M+2 etc.

Identification of the dimethyl chromium species lends considerable support to the proposed activation mechanism, especially in conjunction with characterisation of the side products. This analysis confirms that prior to addition of the α-olefin the chromium species exists as $[(R_3TAC)CrMe_2]^+$, as originally proposed. While no dimer was observed, it is unclear whether this is due to separation under the conditions of the mass spectrometer. Regardless of its form, the observation of this signal indicates that a dimethyl chromium species is formed. The predicted abstraction and alkylation reactions appear to proceed rapidly with the analysis run within one minute of addition. The very clean spectrum indicates that this is by far the majority species, indicating a clean and efficient partial activation.

This analysis was then followed by addition of 5000 equivalents of 1-hexene. The sample was again analysed within one minute, with the spectrum observed to contain numerous significant sets of peaks where previously there was just one. The most abundant peak was observed at 517.4338 and identified as $[((\alpha\text{-}^iBu_2)_3TAC)Cr]^+$, as shown in Figure 3.34.

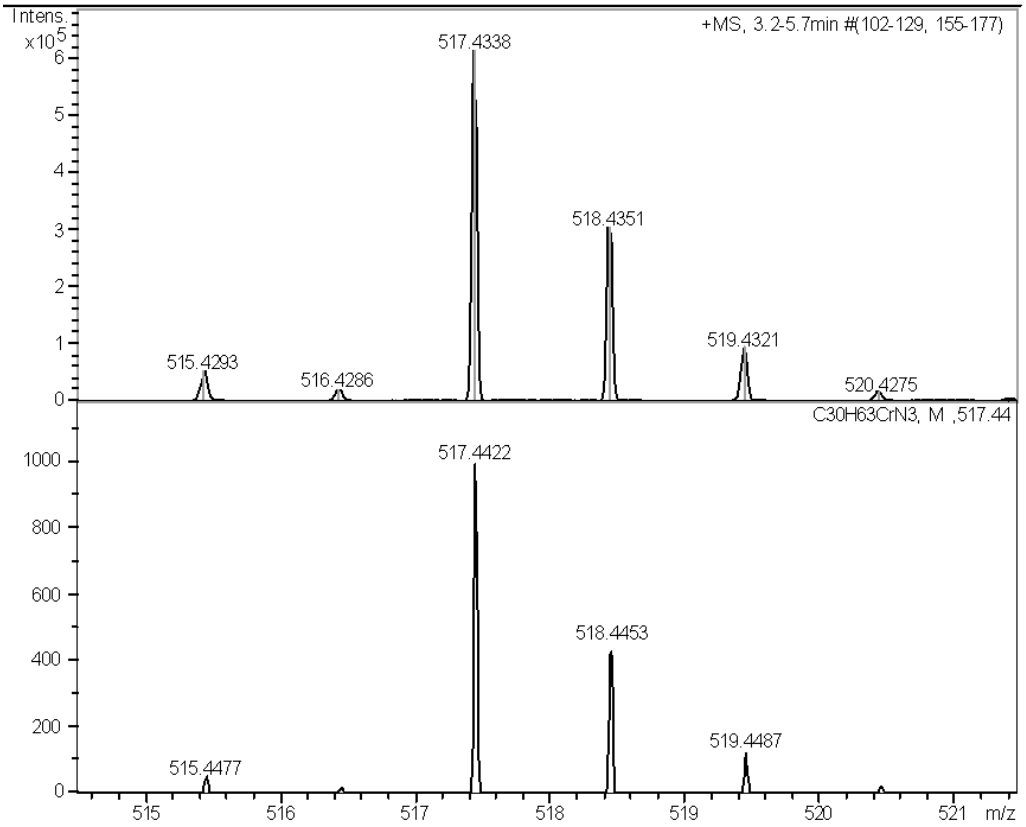

Figure 3.34 - The observed (top) and calculated (bottom) m/z peaks corresponding to $[((\alpha\text{-}^iBu_2)_3TAC)Cr]^+$.

Identification of this species gives definitive evidence for the existence of the Cr^I oxidation state within the catalytic solution. The high intensity of a Cr^I species indicates that loss in ionic attraction within the ion pair may lead to better detection as expected. This could then explain why this apparent high abundance is not replicated by the kinetic analysis, which demonstrates that a Cr^{III} species is the resting state.

Observation of this 'naked' cation was unexpected and indicates that the conditions within the mass spectrometer are not as benign as thought. It was hoped that in the absence of ionisation complexes would remain entirely intact. However, it is highly unlikely that this species exists as observed and, as such, must represent a weakly bound Cr^{I} adduct such as the two intermediates predicted. Further analysis of minor peaks within the spectrum indicated a peak at 609.4752 that can be assigned as $[(\alpha\text{-}^{i}Bu_2)_3Cr(toluene)]^{+}$, as shown in Figure 3.35.

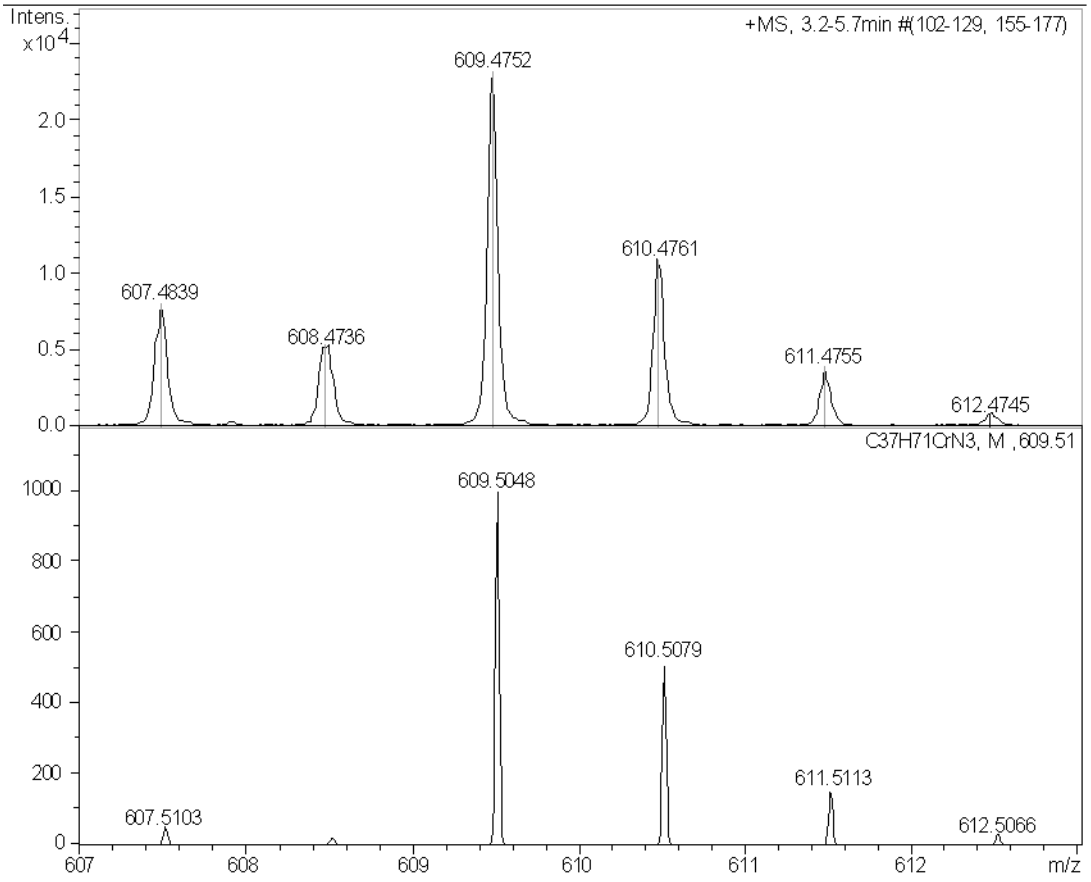

Figure 3.35 - The observed (top) and calculated (bottom) m/z peaks corresponding to $[((\alpha\text{-}^{i}Bu_2)_3TAC)Cr(toluene)]^{+}$.

The low intensity of this set of peaks leads to less accurate correlation with the calculated m/z values. In addition, the shoulders on the M-1 and M-2 indicate underlying signals which have increased their intensity to beyond that expected. As such, this signal can be less confidently assigned but still appears to indicate that the proposed Cr^{I} toluene adduct exists. No corresponding peak was observed for the 1,2-difluorobenzene analogue, indicating its lower π-basicity leads to weaker or no adduct formation. This would agree with a recent study into arene binding using similar techniques.[232] No further peaks could be conclusively identified as $(R_3TAC)Cr^{I}$ complexes but one ambiguous set of signals was also identified. The peak at 685.6142 corresponds to $[((\alpha\text{-}^{i}Bu_2)_3TAC)Cr(1\text{-hexene})_2]^{+}$, Figure 3.36.

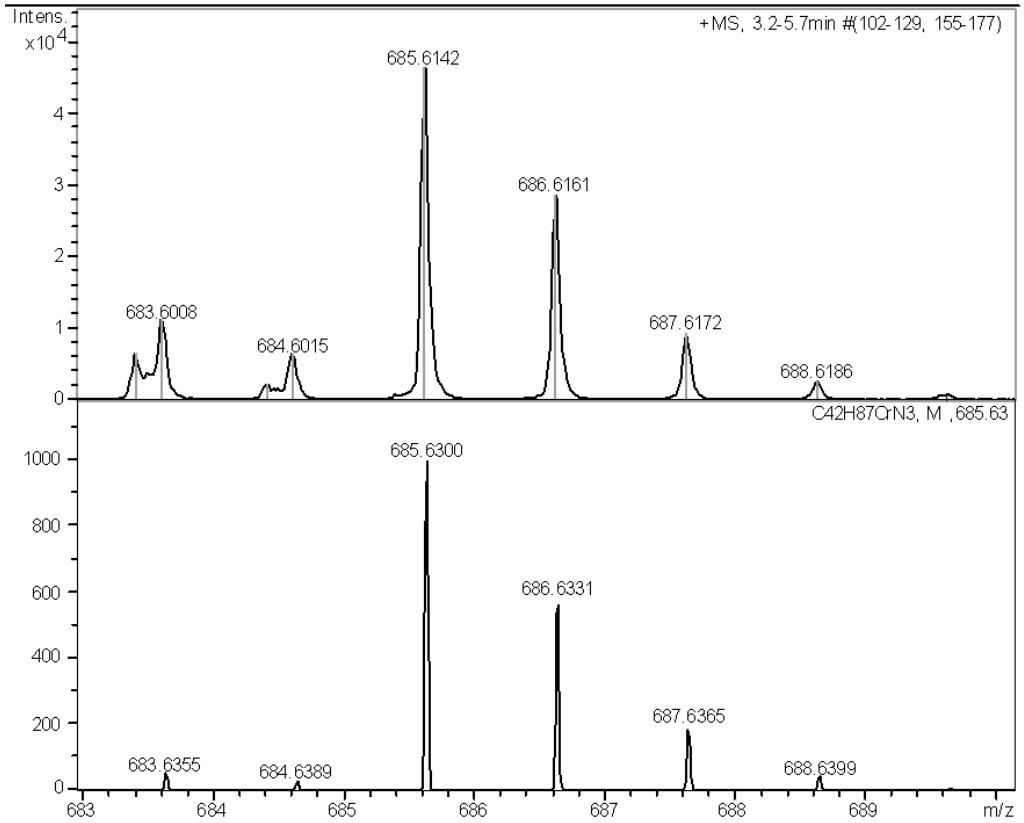

Figure 3.36 - The observed (top) and calculated (bottom) m/z peaks corresponding to $[((\alpha\text{-}^{i}Bu_2)_3TAC)Cr(1\text{-hexene})_2]^+$.

This set of peaks could either represent the Cr^{I} adduct or the Cr^{III} chromacyclopentane without a neutral compound occupying the vacant site. From the data collected it is impossible to differentiate between these two possibilities. However, two other peaks were also observed that when taken together give a clearer picture of the cations present. The second most abundant set of peaks in the spectrum was observed at 769.7140 and matched that expected for $[((\alpha\text{-}^{i}Bu_2)_3TAC)Cr(1\text{-hexene})_3]^+$, Figure 3.37.

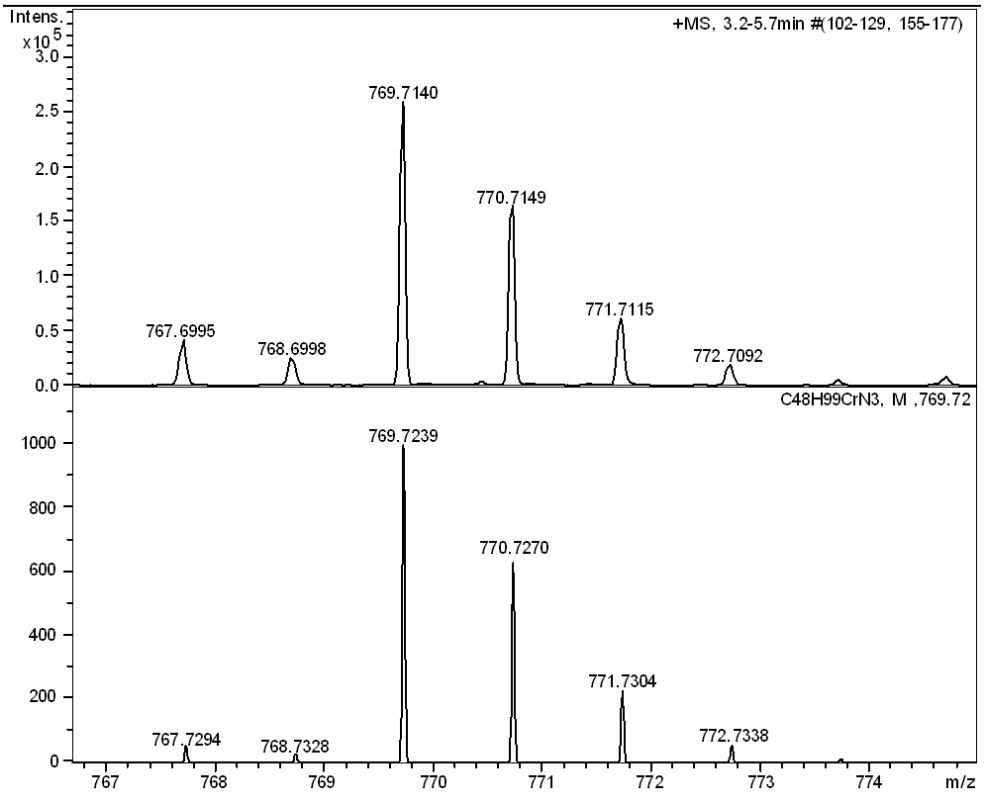

Figure 3.37 - The observed (top) and calculated (bottom) m/z peaks corresponding to $[((\alpha\text{-}^{i}Bu_2)_3TAC)Cr(1\text{-hexene})_3]^+$.

This signal is the first to be highly likely to correlate to a Cr^{III} species. With the significant signal observed for the 'naked' Cr^{I} species, it appears unlikely that three olefins could remain bound as adducts under the conditions of the spectrometer. However, unambiguous identification of the signal remains impossible as the peaks could correspond to either the chromacyclopentane with a 1-hexene adduct or the chromacycloheptane without. One final set of low intensity peaks was also observed at 853.7976 and corresponded to $[((\alpha\text{-}^{i}Bu_2)_3TAC)Cr(1\text{-hexene})_4]^+$, Figure 3.38.

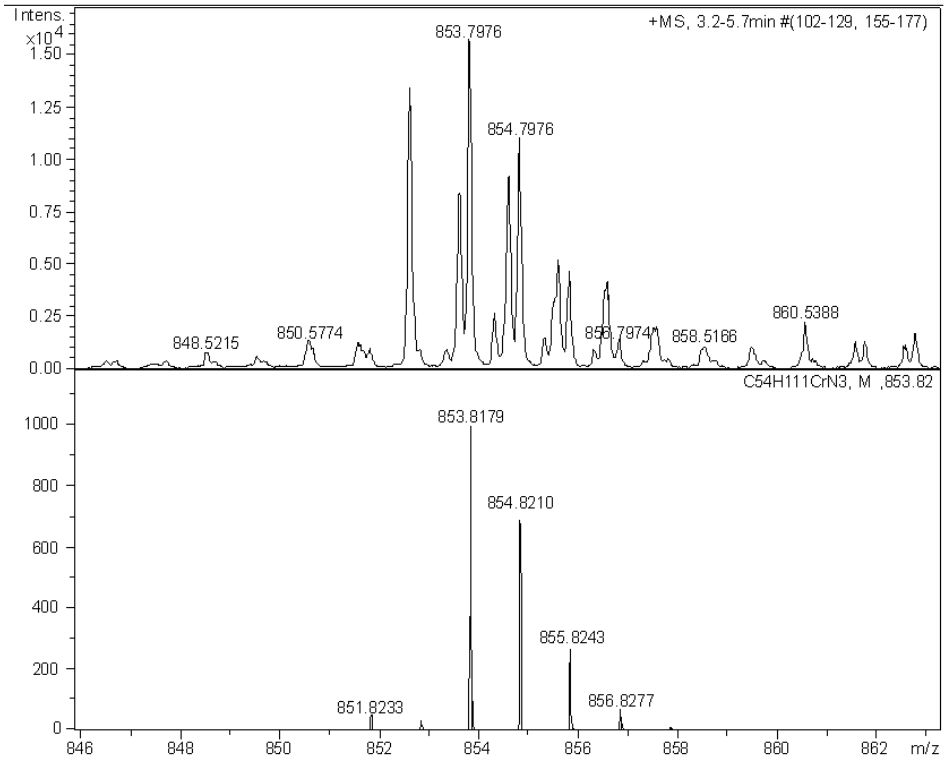

Figure 3.38 - The observed (top) and calculated (bottom) m/z peaks corresponding to $[((\alpha\text{-}^{i}Bu_2)_3TAC)Cr(1\text{-hexene})_4]^+$.

While these signals are a very low intensity relative to the others it is important in identifying the Cr^{III} species observed because it is unambiguous. In the absence of tetramerisation, which has been proven to be the case for these catalysts, this signal can only correspond to the chromacycloheptane with a 1-hexene adduct. Metallacycloheptanes are known to be highly unstable towards β-hydride elimination and, as such, would be expected to be short-lived.[38] Therefore, formation of 1-hexene adducts must be highly favourable for the Cr^{III} species in order for this species to be observed. This strongly indicates that the set of signals at 769.714, Figure 3.37, represent the chromacyclopentane with a 1-hexene adduct. In turn, this then suggests that the peak at 685.6142 predominantly represents the Cr^{I} bis 1-hexene adduct.

By comparison of the relative intensity of the signals observed, Table 3.24, these assignments would appear to agree with the kinetic results discussed earlier. The relative intensities were calculated based on comparison of the most abundant peak per set. Comparisons cannot be reliably made between Cr^{I} and Cr^{III} species, as discussed earlier.

Table 3.24 - The relative peak intensities of the cations observed. The dashed line separates species considered to contain chromium in different oxidation states.

Chromium Species	Relative Intensity
$[((\alpha\text{-}^{i}Bu_2)_3TAC)Cr]^+$	64.0
$[((\alpha\text{-}^{i}Bu_2)_3TAC)Cr(toluene)]^+$	2.4
$[((\alpha\text{-}^{i}Bu_2)_3TAC)Cr(1\text{-hexene})_2]^+$	4.9
$[((\alpha\text{-}^{i}Bu_2)_3TAC)Cr(1\text{-hexene})_3]^+$	27.1
$[((\alpha\text{-}^{i}Bu_2)_3TAC)Cr(1\text{-hexene})_4]^+$	1.7

Comparison of the species thought or known to feature chromium in the Cr^{I} oxidation state does not yield any meaningful information as the vast majority is detected as the 'naked' cation. The ratio of cations is therefore likely to represent the stability of the complex in the spectrometer environment rather than their abundance in solution.

In contrast, the Cr^{III} species appear to bind adducts far more strongly, allowing reliable comparison. Based on the known chemistry of metallacycles, it is highly unlikely that a chromacycloheptane represents the resting state of the catalysis. It is far more likely that a chromacyclopentane species accounts for the resting state and this would agree with the observed kinetics. On this basis $[((\alpha\text{-}^{i}Bu_2)_3TAC)Cr(1\text{-hexene})_3]^+$ must be considered to be a chromacyclopentane with a 1-hexene adduct.

This observation strongly suggests that the first order rate dependence on LAO seen for these catalysts is due to the trigger mechanism rather than complexation of the olefin.[233] This mechanism, first proposed in 1991, neatly explains the first and higher order kinetics observed for Ziegler-Natta LAO polymerisation catalysts. It is proposed that the approach of an α-olefin towards a site already occupied by a bound LAO induces insertion of the bound species into a pre-existing M-C bond. Weak interaction between the approaching olefin and the metal centre leads to stabilisation of the transition state of insertion and avoids the formation of a highly unfavourable vacant site. The dependence on the complexation of the approaching olefin provides a satisfactory explanation of first order kinetics relative to LAO concentration and agrees with the observations of the MS analysis described here.

Based on the information gained during this investigation a modification of the original metallacyclic mechanism can be proposed which takes account of the observed intermediates, Scheme 3.11.

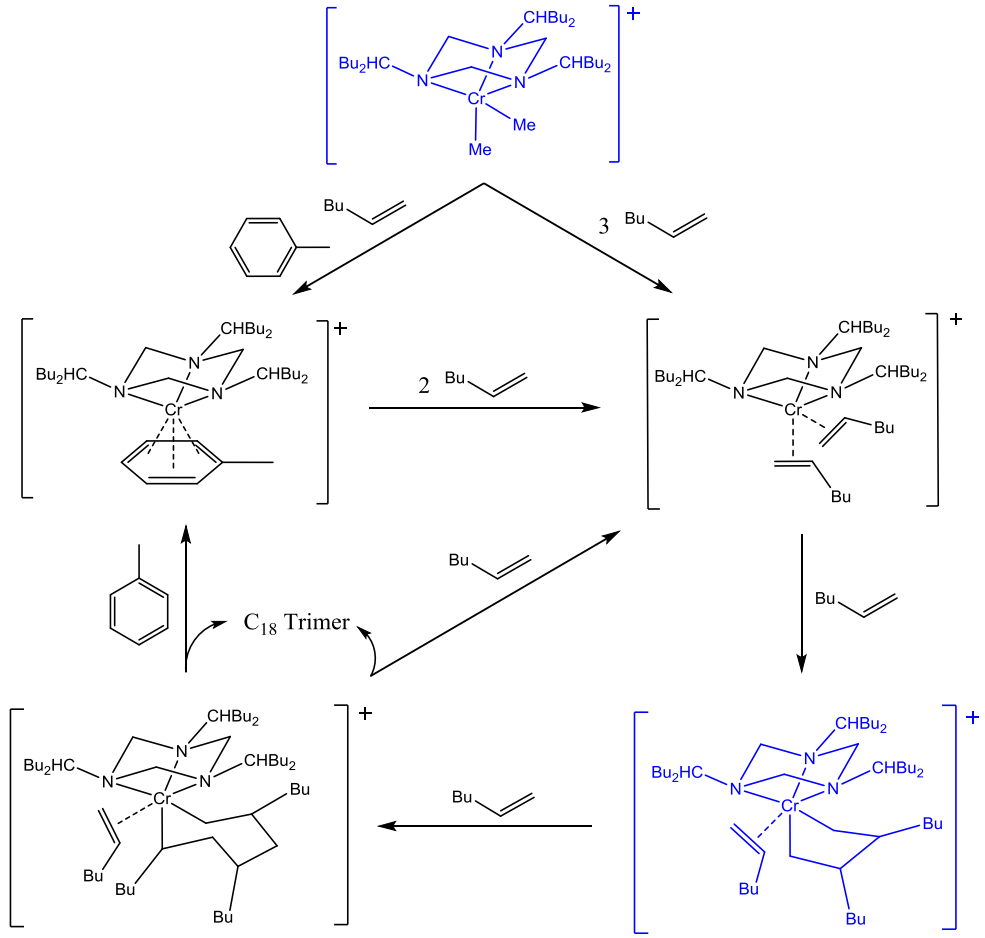

Scheme 3.11 - The modified metallacyclic mechanism. Resting states are shown in blue.

Despite most studies indicating that β-hydride elimination within the chromacycloheptane occurs *via* a concerted 5,1-hydride shift, it is likely that a vacant site is still required. Therefore the 1-hexene bound to the metallacycloheptane must be displaced prior to elimination. This would enable either toluene or two olefin units to replace the C_{18} product, suggesting that two routes are available for the progression of the catalytic cycle. The proposed modifications are minor and all evidence supports the metallacyclic mechanism originally proposed.

The results presented here also provide further evidence that the Cossee-Arlman mechanism does not account for the observed trimerisation. The reliance of the chain growth mechanism on an additional hydride results in all intermediates having a slightly higher mass relative to the metallacyclic alternatives. As such, it can be readily observed that the intermediates are metallacyclic in nature, as demonstrated in Figure 3.39.

Observed Exact Mass: 769.7140

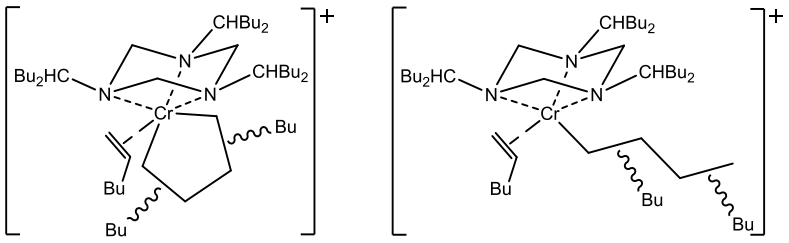

Chemical Formula: $C_{48}H_{99}CrN_3^+$
Exact Mass: 769.7239

Chemical Formula: $C_{48}H_{100}CrN_3^+$
Exact Mass: 770.7317

Figure 3.39 - Comparison of the exact mass of metallacyclic and chain growth intermediates.

A sample was taken from the reaction after three hours in order to investigate whether any variation had occurred in the relative abundance. Unfortunately, it was discovered that the signals representing the intermediates were no longer visible. Instead, the spectrum was dominated by a single set of peaks at 549.4282 that corresponded to $[((\alpha\text{-}^{i}Bu_2)_3TAC)CrO_2]^+$, Figure 3.40.

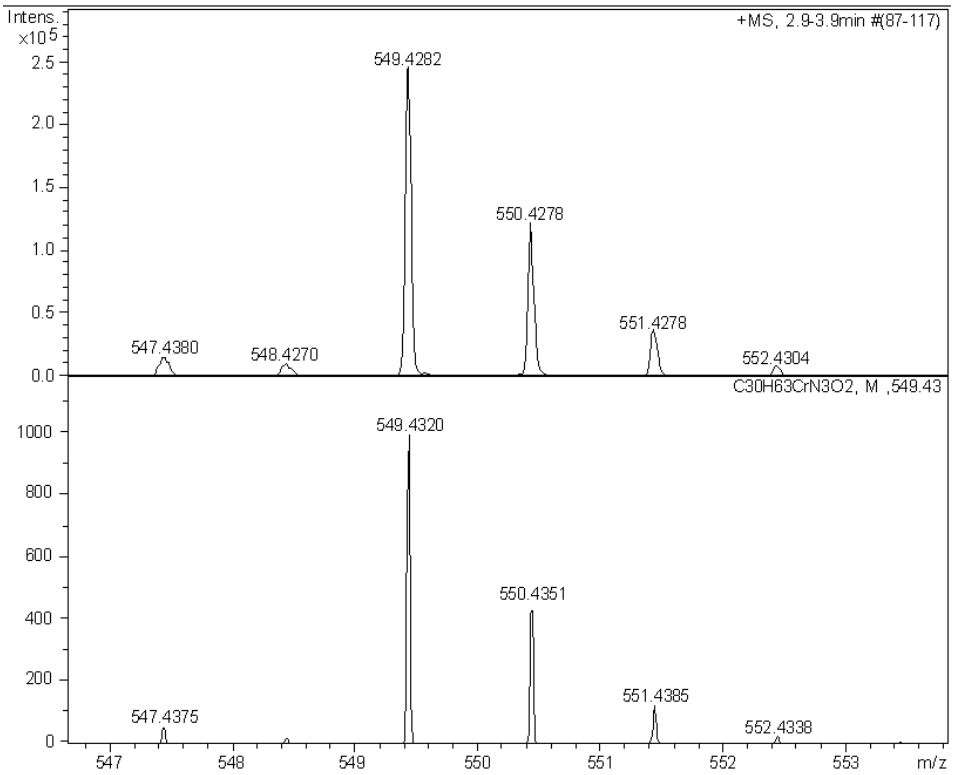

Figure 3.40 - The observed (top) and calculated (bottom) m/z peaks corresponding to $[((\alpha\text{-}^{i}Bu_2)_3TAC)CrO_2]^+$.

The emergence of this peak clearly indicates decomposition on contact with oxygen, suggesting the argon atmosphere was not as oxygen free as thought. The species could take the form of Cr^{V} with two oxo ligands or Cr^{III} with a single peroxo ligand.[234, 235] However, based on MS analysis it is not possible to distinguish between these two possibilities. It is remarkable that the TAC ligand has remained bound after the oxidation reaction. The reduced ionic radius of Cr^{V} would reduce the already constrained orbital overlap with the nitrogen donors, suggesting a Cr^{III} decomposition is more likely. While not a decomposition pathway that should be observed under ideal conditions, the facile oxidation does suggest an inherent instability towards low concentration oxidants. This supports the proposed explanation for the loss in activity on exposure to halogenoalkanes.

Overall, analysis of the cationic intermediates using mass spectrometry has provided direct evidence for the existence of metallacyclic intermediates for the first time. In combination with the previously discussed results, the Cossee-Arlman mechanism now appears unfeasible for selective trimerisation with this catalyst. Instead, the Cr^{I}/Cr^{III} redox cycle has been strongly supported, with observation of Cr^{I} in the active catalyst solution alongside the other intermediates predicted. Identification of the resting state gives a strong indication that the rate determining step is the insertion of an olefin into the metallacycle, as predicted by kinetic analysis. However, it appears that the trigger mechanism accounts for the first order dependence on 1-hexene, as coordination of the olefin appears rapid.[233]

3.6.2 Investigation of the Anionic Counter-Ions

With the exception of the investigation into co-catalysts carried out by McGuinness *et al*., very little attention has been paid to the counter-ion during catalysis.[213] While in some defined cases the structure of the counter-ion is evident due to the addition of an abstraction agent alongside the alkylating agent, in the case of $AlMe_3$ activation it is less clear.[19] The use of MS during the catalysis allowed insights into the species formed as the counter-ion after completion of the alkylation and abstraction steps.

It has been shown previously that $(R_3TAC)Cr(OTf)_3$ catalysts can be activated with four equivalents of $AlMe_3$ but no less.[231] This indicates that a 4:3 ratio of aluminium to triflate is essential for formation of the $[(R_3TAC)CrMe_2]^{+}$ activated catalyst. Based on this ratio, the complete activated catalyst can be hypothesised as that shown in Figure 3.41.

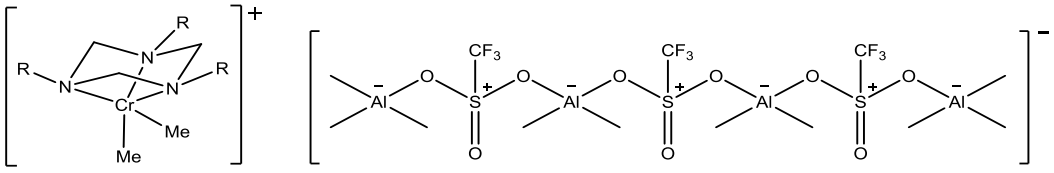

Figure 3.41 - The proposed ionic complex formed on reaction of 4 equivalents $AlMe_3$ with a $(R_3TAC)Cr(OTf)_3$ pre-catalyst.

The proposed counter-ion makes several assumptions that are unproven. Firstly, while the triflate group is known to act as a bidentate ligand in several complexes, this does not usually result in a formal positive charge on the sulphur atom.[236] Such an arrangement is therefore poorly understood, as is the formation of an extended alternately charged chain in this manner. Secondly, it is unclear how effective the bridging triflate would be at stabilising the terminal aluminium groups. $[AlMe_3OTf]^-$ is a known and readily synthesised species, while $Al(OTf)_3$ is commercially available and synthesised from the reaction of $AlMe_3$ with TfOH. Therefore, similar species in which the formal cationic charge is not present on the triflate group are well known.

The catalysis was run according to the same procedure as that used for the cationic investigation, with a minimum of $AlMe_3$ used in order to form a clear green solution. This was measured at approximately 10 equivalents, such that an excess of $AlMe_3$ was present to act as a scavenger and to increase the activation rate. The solution was then analysed within a minute of addition of the activator. Once complete, the 5000 equivalents of 1-hexene were added to give the active catalyst system and analysis was again carried out within a minute. The spectrum observed was nearly identical in both cases, with the same major peaks observed.

The counter-ions do not feature isotope patterns as distinctive as those of the cations, with sulphur the only element that influenced the set of peaks to any great degree. Increased intensity of the M+2 peak over that expected based on the influence of carbon indicated the presence of one or more sulphur atoms and provided evidence of the presence of triflate groups.

At relatively low m/z values there were two significant peaks that corresponded to the expected anions containing only one aluminium atom. These were characterised as $[AlMe_3OTf]^-$ and $[AlMe_2(OTf)_2]^-$, Figure 3.42, of which the dimethyl species was by far the most abundant on comparison of peak intensities. This indicates that $AlMe_3$ units which abstract a triflate group are typically also involved in alkylation of the chromium. The considerable number of higher molecular weight products observed were therefore predicted to result from this initial product. The proposed counter-ion would also result from this same initial product, lending some support to its existence.

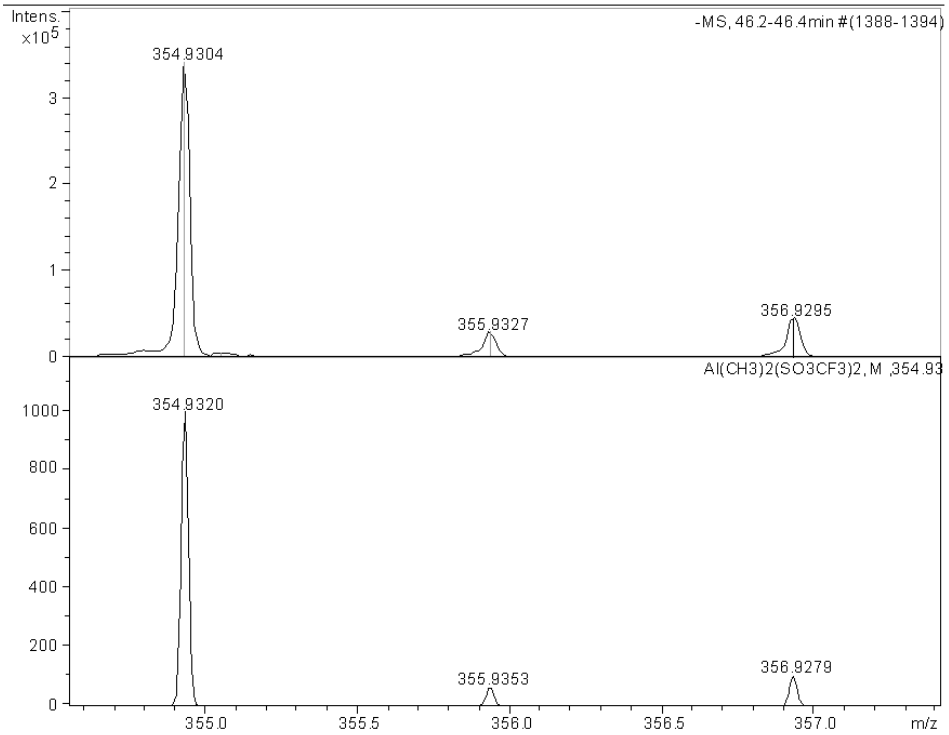

Figure 3.42 - The observed (top) and calculated (bottom) m/z peaks corresponding to $[AlMe_2(OTf)_2]^-$.

Analysis of the higher molecular weight products showed that most contained two triflate groups, as would be expected from the higher abundance of $[AlMe_2(OTf)_2]^-$. Unfortunately, the products also corresponded to products containing increased levels of oxygen than would have been expected. This indicated that either oxygen or moisture had contaminated the highly reactive aluminium species to give far more products than expected. These could be identified as those shown in Figure 3.43, in each case the isotope pattern was observed as expected.

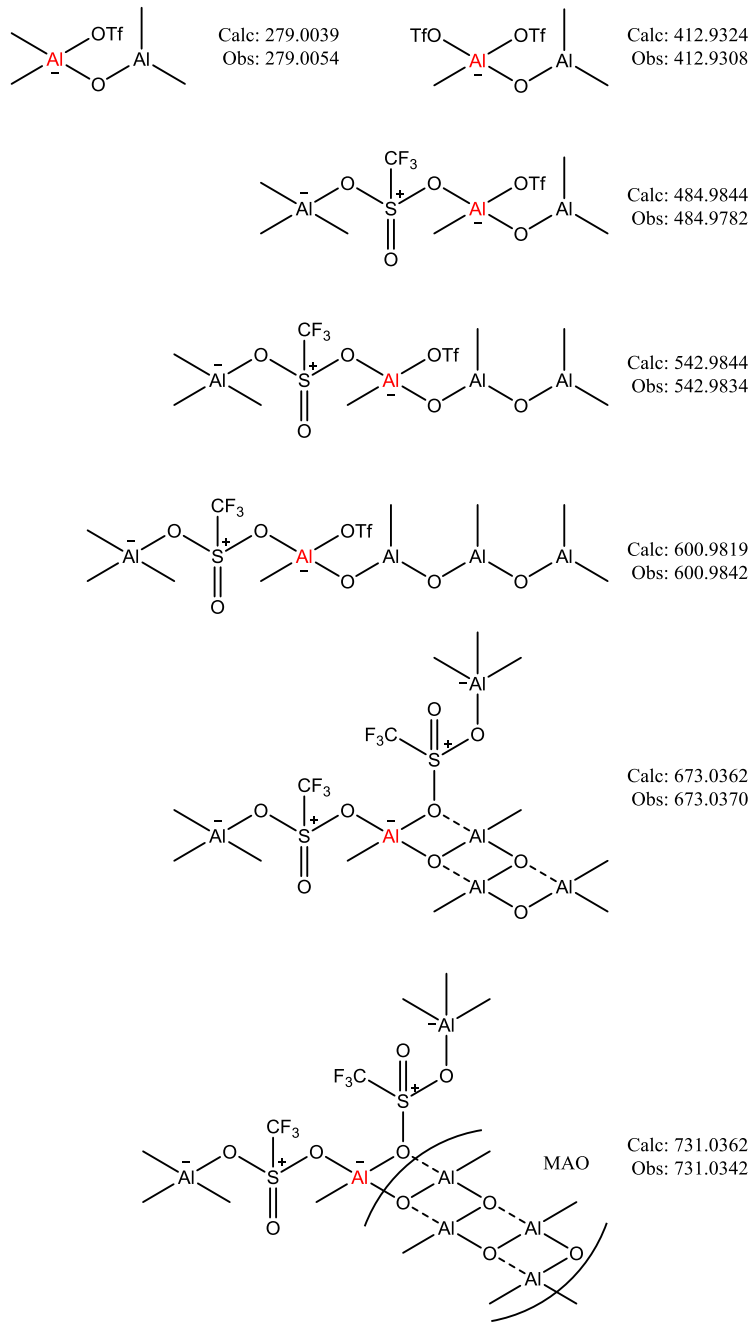

Figure 3.43 - The anionic aluminium species detected. The aluminium that is carried forwards from the original product is shown in red.

It can be seen that the number of major products is determined by the growth of methylaluminoxane chains. This strongly indicates that moisture is the source of contamination, with no methoxy groups detected. Larger molecules are probably formed but remain unobserved due to increasingly poor solubility in *o*-$C_6H_4F_2$. With the aluminium species thought to act as a scavenger in all cases it appears that this may in fact be beneficial, with the counter-ion becoming more like the highly effective MAO in the presence of low concentrations of moisture. Therefore, this activation route appears highly effective as the potency of the catalyst is unlikely to be lost due to low level contamination, assuming the scavenger prevents the chromium from being affected.

Despite these complications it was still possible to observe that the triflate groups can indeed act as bridging ligands that incorporate a formally positive charge. Peak 484.98, for example, cannot be accounted for by any other logical arrangement of the atoms shown to be present by MS analysis. This lends considerable support to the proposed counter-ion under ideal conditions. With the presence of moisture confirmed, the spectra were checked for peaks corresponding to species in which hydroxy groups had been incorporated. This led to the discovery of two peaks that gave even stronger evidence in favour of the proposed anionic species, Figure 3.44, in both cases the expected isotope pattern was observed.

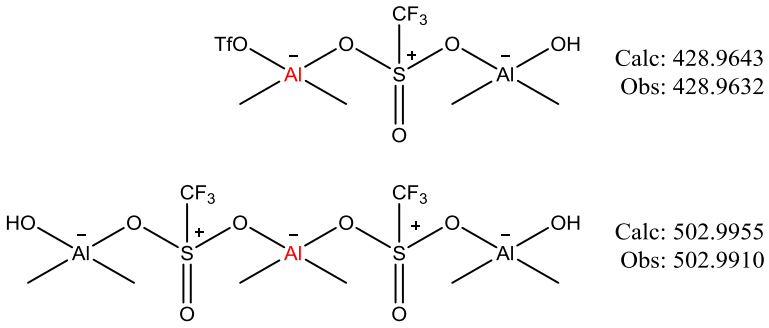

Figure 3.44 - The two large anions detected that were shown to contain hydroxyl groups.

These two species, and especially the anion observed at 502.99, bear a striking resemblance to the proposed counter-ion. These products demonstrate that formally cationic triflate groups are able to bridge between anionic aluminium centres, producing large anions of diffuse charge suitable for catalysis. Observation of these species strongly supports the proposed structure of the counter-ion and allows speculation on the mechanism by which it is formed.

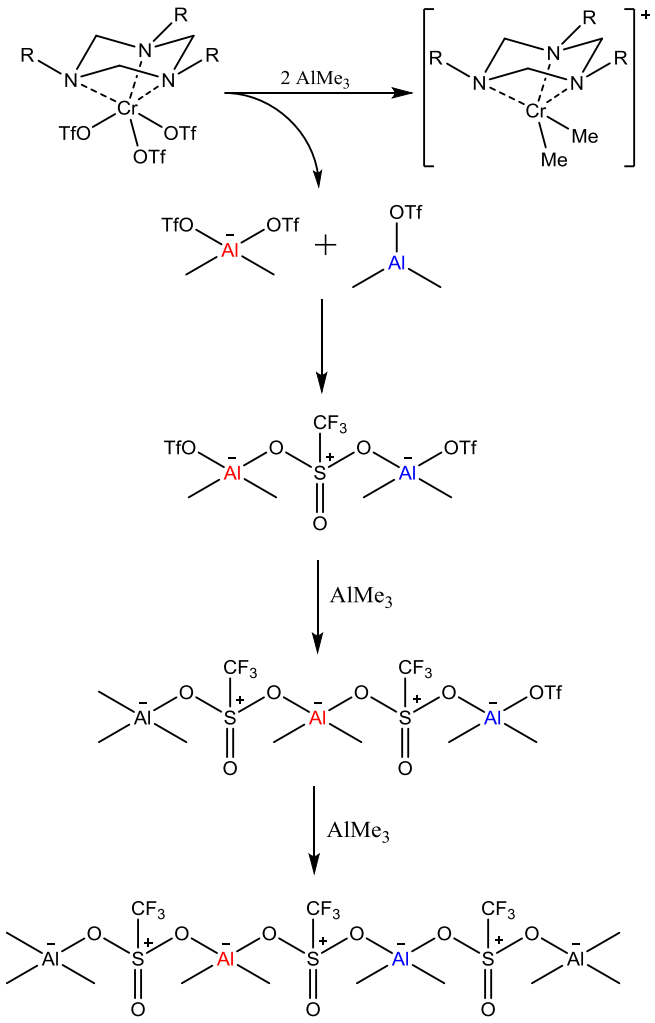

Scheme 3.12 - The proposed mechanism for formation of a weakly coordinating anion.

The MS results showed clearly that $[AlMe_2(OTf)_2]^-$ is the principal anionic product of alkylation and abstraction. On this basis a second neutral aluminium triflate must result from catalyst activation, as shown in Scheme 3.12. The MS results also showed that the monodentate triflate ligands can bind neutral aluminium species to form a larger anion. This would occur three times, as shown, with steps one and two being interchangeable. The observed requirement for four equivalents can therefore be explained by the need to convert all triflate groups to bidentate bridges between aluminium units, preventing direct coordination to the chromium.

Unfortunately, under the conditions of this reaction a species containing a 4:3 ratio of aluminium to triflate could not be detected. This is likely as a result of the disruption caused by the presence of moisture. Further optimisation of the reaction conditions is required before a concerted attempt at detection of the counter-ion under ideal catalytic conditions can be made.

Following on from investigation of the side-products of activation and the proposed chain transfer chemistry, the spectra were also studied for evidence of the related aluminium species. As predicted, two significant signals were observed in the sample taken after addition of 1-hexene that corresponded with 2-methylhexyl aluminium species, Figure 3.45.

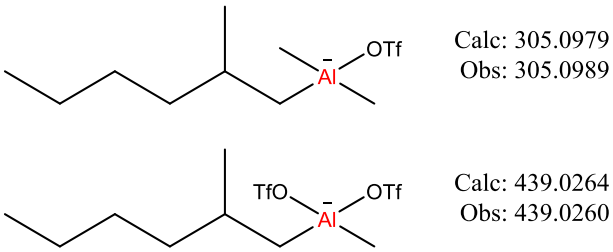

Figure 3.45 - The two principal aluminium species containing 2-methylhexyl groups.

Observation of these two species confirms chain transfer reactions as the source of the greater than expected equivalents of 2-methylhexyl based side products. In addition to these major species, numerous additional anions containing the 2-methylhexyl group were observed as a result of partial oxidation. The two corresponding species in which a second methyl group had been substituted were also observed, indicating that chain transfer is a fairly favourable process even when sterically hindered. These results strongly support the proposed activation mechanism and provide firm evidence that the alcohol containing species result from aluminium complexes. Aluminium species corresponding to the two minor alcohols formed, hexanol and 2-ethylhexanol, were not observed but it follows that they are formed in the same manner.

Overall, analysis of the anion with mass spectrometry provided considerable support for the proposed counter-ion. Principally, the analysis allowed observation of species containing cationic triflates as bridging ligands between anionic aluminium units. As such, the connectivity and chemistry proposed to account for the formation of the counter-ion has been demonstrated experimentally, though unfortunately the species itself has not been observed. Observation of this chemistry allowed the proposal of a counter-ion formation mechanism that accounts for the observed requirement for four equivalents of $AlMe_3$. Further analysis also confirmed the existence of chain transfer reactions, strongly supporting the proposed activation mechanism.

3.7 Summary

A series of mechanistic investigations have been carried out with the aim of determining whether the previously proposed metallacyclic mechanism is responsible for LAO trimerisation.[2] Firstly, extensive NMR analysis of the trimer product was carried out in order to determine the C_{18} regioisomers formed. The identification of 18 isomers was achieved by ^{13}C labelling of 1-hexene and subsequent one and two dimensional ^{13}C NMR spectroscopy on the enriched C_{18} product.

All of the products identified match those predicted by the metallacyclic mechanism. However, the distribution of the products was found to differ considerably from the original proposal. Firstly, it was found that [2,1]-migratory insertion cannot be discounted and accounts for up to 5% of the products in some cases. Secondly, *exo*-cyclic β-hydride elimination appears to be negligible in all cases, in contrast to the high favourability predicted. This results in considerably fewer isomers than originally proposed and suggests considerable steric constraints on the α-substituents of metallacycloheptanes.

In accordance with the proposed mechanism, quantification of the products *via* ^{13}C NMR integration allowed insights into the relative abundance of the differently substituted metallacyclic intermediates. It was found that greater than 75% of chromacyclopentanes adopted the [1,3]CrC_4 arrangement, with only minor quantities of the [2,3]CrC_4 and [1,4]CrC_4 intermediates. The formation of these intermediates *via* oxidative cyclisation was found to be strongly influenced by steric control, induced by either the LAO or the ligand. Chiefly, competition exists between LAO-LAO interaction and LAO-ligand interaction, of which LAO-LAO repulsion is the more significant. Increasing the bulk of the ligand or reducing the bulk of the LAO led to increased formation of [2,3]CrC_4, while the opposite promoted increased [1,3]CrC_4 formation.

The binding strength of the counter-ion was also found to have an effect. Use of a more strongly binding anion produced the same effect as increasing the ligand bulk, as would be expected. This demonstrated that the counter-ion is likely to be present within the inner sphere during catalysis, such that it has a steric influence over selectivity. The greatest effect of steric variation was on the orientation of migratory insertion. Increased bulk on the ligand or LAO led to a considerable reduction in the proportion of [2,1]-migratory insertion derived products. The ratio of [1,2] to [2,1] was shifted from around 20:1 up to 100:1 as a result of increased steric bulk, enabling considerable increases in selectivity to be achieved.

An unexpected and significant steric influence on elimination pathways was also discovered. This suggests considerable interaction between the metallacycloheptane and the ligand environment, which in turn influences the energy barriers towards conformational change. The elimination pathways were investigated more thoroughly with the use of selective deuterium labelling. The proportion of the different isomer groups which result from the same metallacycloheptane remained constant. This demonstrated clearly that deuteration had no effect on the cyclic oxidation or insertion steps and that no competition exists between metallacycloheptanes once they are formed.

More importantly, within group A-C, which accounts for the most abundant products, considerable competition was observed. Competition between formation of a vinylidene and an internal olefin was the most marked and would not be possible for Cossee-Arlman systems. As such, this provided strong evidence that a chain growth mechanism of any kind does not account for the selective trimerisation observed. Interestingly, isomers A and C appeared to be in direct competition while B displayed only limited effects. As a result, two different conformations can be proposed which account for this observation, as well as the far lower quantity of *cis* product relative to *trans*. Based on the effects of deuterating specific positions, it appears that B results from a more sterically hindered conformer, which on undergoing ring-flip gives the more favourable conformer that produces both A and C.

The side products of activation were also investigated by the large scale reaction of just 6 equivalents of 1-hexene with a chromium triflate catalyst. This allowed the identification and even isolation of a far greater number of products than originally expected. The formation of 2-methyl-1-hexene, the only product predicted by the proposed metallacyclic mechanism, was confirmed for the first time. In addition, a variety of other products derived from interaction of 1-hexene with the alkylated catalyst were discovered. Several alcohols were observed, including 2-methyl-1-hexanol, such that more than one equivalent of 1-hexene is required for catalyst activation. This demonstrated that chain transfer reactions must occur between the catalyst and the aluminium activator. A modified activation mechanism has been proposed that incorporates the newly discovered processes. While the activation procedure proved to be more complex than originally proposed, the results broadly agreed with the original proposal and further support the metallacyclic mechanism.

Finally, a different approach towards investigation of the mechanism was taken by attempting to look at the intermediates directly using mass spectrometry. This proved successful and signals were observed that corresponded with the predicted chromacyclopentanes and heptanes. To the best of my knowledge, this is the first time that direct evidence of these species has been obtained. This analysis confirmed the existence of Cr^{I} under catalytic conditions and provided strong evidence for Cr^{III} metallacycles. The relative abundance could also be gauged, with the chromacyclopentane resting state appearing to take the form of a 1-hexene adduct. This led to the proposal that the trigger mechanism is responsible for the first order rate dependence on 1-hexene.[233]

The same analytical approach was applied to the counter-ion and allowed the proposal of a pathway to a weakly coordinating anion from chromium triflate activation with $AlMe_3$. The MS analysis demonstrated that triflate groups are capable of acting as formally cationic bridging ligands between anionic aluminium units. The resulting anions are likely to feature a highly diffuse charge and, as such, be weakly coordinating towards the chromium cation. As a result, the prior observation that activation can be achieved with exactly 4 equivalents of $AlMe_3$ can be explained. The aluminium species formed *via* chain transfer reactions during activation were also discovered, confirming the existence of this process.

4. Ethylene Trimerisation: Optimisation and Product Identification

The area of selective oligomerisation that has attracted the most attention since it was first discovered is without a doubt that of ethylene trimerisation. As discussed in Chapter 1, there are numerous catalyst systems currently being investigated due to the value of 1-hexene as a monomer for LLDPE. One of the lesser known catalyst systems is that based on R_3TAC chromium complexes, as they have previously only been published in the form of patents for BASF or as models for the Phillips polymerisation catalyst.[147, 192]

Truly selective trimerisation of ethylene with this system was discovered in 2000, with the use of a range of TAC ligands derived from commercially available amines. Both branched and unbranched alkyl N-substituents, as well as phenyl and cyclohexyl containing species, were investigated, with 2-ethylhexyl and 2-propylheptyl moieties proving to be the most effective, Figure 4.1. Good activities of around 20,000 $g(C_2H_4)\ g(Cr)^{-1}\ h^{-1}$ were achieved although the system suffered from low selectivity compared to other systems.

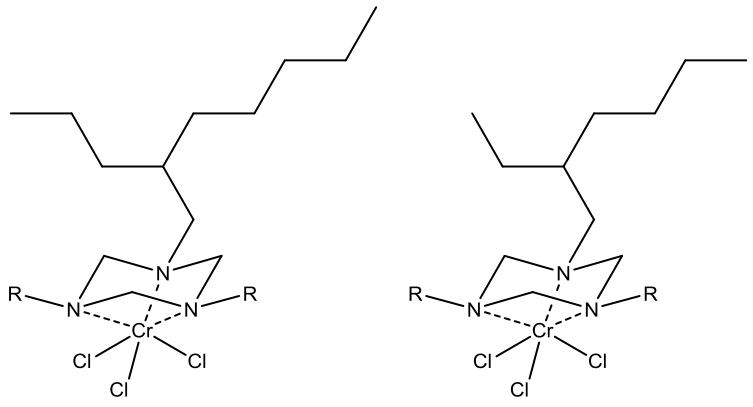

β-PrPe β-EtBu

Figure 4.1 - The two most effective pre-catalysts in the original patent and their abbreviations.

The poor selectivity was due to the high abundance of decenes and tetradecenes observed in the product mix, along with ~10 w% polymer. While decenes are often observed as a side product of ethylene trimerisation due to the co-trimerisation of ethylene and 1-hexene, the observation of tetradecenes is rare. The relative rate of re-incorporation of 1-hexene into the trimer is therefore much higher for this system than for most others, as would be expected for catalysts that readily trimerise LAOs. These published systems typically produced 1-hexene at poor selectivities of less than 50 w% of total products.

This chapter describes investigation of the reaction conditions, catalyst design and aluminium activator for ethylene trimerisation under both ambient and pressurised conditions. Optimisation of each of these components was carried out with the aim of increasing both the selectivity and activity of the system to levels competitive with the numerous well-defined homogeneous systems reported to date.

4.1 Ambient Pressure Testing

Two investigations were carried out under just 1 bar of ethylene, produced by the constant flow of ethylene through a catalyst solution. Firstly, polymerisation studies were carried out in this manner due to the significant problems associated with reactor fouling. The strong rate dependence of polymerisation reactions on ethylene concentration would lead to large quantities of polymer under pressurised conditions. The complexities related to accurately recording the yield and cleaning of the autoclave meant that all polymerisation reactions were carried out at ambient pressure using basic glassware.

A second study, in which a range of activators were investigated, was also conducted under these conditions due to safety considerations relating to the use of concentrated or pure aluminium alkyls. This far simpler technique removed the risk of damage to expensive equipment and, because of greater adaptability, allowed for the introduction of further safety precautions.

These studies were each carried out according to the same procedure. The reaction vessel was dried by heating whilst flushing with argon. Meanwhile, 20 μmol of the catalyst was activated under argon with 500 equivalents of the aluminium activator. Dry toluene was then added to the reaction vessel before being degassed and heated to 40 ˚C. The activated catalyst was then added by syringe under a flow of argon before a 40 L min^{-1} flow of ethylene through the system was initiated. The reaction was allowed to proceed for 10 minutes while stirring, at which point the system was flushed with argon to remove any residual ethylene.

The products were determined first by taking a 1 mL sample of the solution to be analysed by GCMS. Secondly, methanol was added to precipitate any polymer produced, which was then separated by filtration, dried and weighed to calculate the yield. As such, in combination with external calibration of the GCMS-FID (Gas Chromatography Mass Spectrometry – Flame Ionisation Detector) system a complete and quantitive calculation of the abundance of the different products could be carried out for each reaction.

Calibration of the GCMS was carried out externally with known concentrations of 1-hexene, 1-octene and 1-decene within the range expected for the standard catalyst procedure. External calibration was favoured over internal in order to ensure that all results were comparable without the risk of incorporating additional errors. The expected linear progression of FID peak integration with increasing concentration was observed and the line of best fit used for all of the data later described.

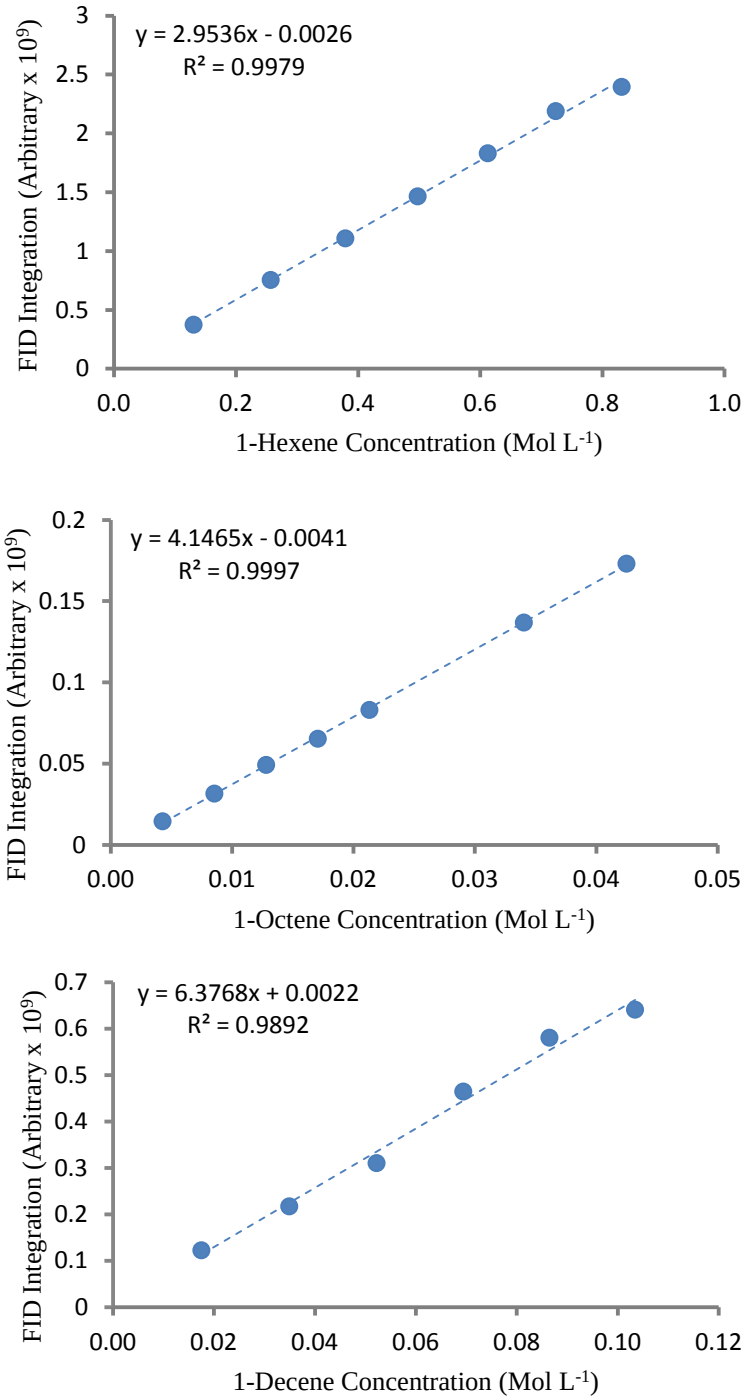

Figure 4.2 - The calibration curves used to determine the concentration of 1-hexene, 1-octene and decene isomers in the product solutions.

While 1-decene is not an exact reference for the range of decene isomers produced, the empirical formula is the same and therefore the FID integrations should be unaffected. The retention time, which if considerably different can effect peak width and alter the integration value, would be expected to be very similar. The good linear fits for concentration against the arbitrary integration values allowed the calculated relationships shown in Figure 4.2 to be used in calculating the overall yield in the experiments here described.

4.1.1 Polymerisation and the 'Halogen Effect'

Continuing on from the investigations into the 'halogen effect' described in Chapter 2, a study was conducted to see if the same relationship was observed for ethylene polymerisation systems. The same catalysts (Pe_2H, Pe_2Cl and Pe_2Br) were again applied alongside another available catalyst, synthesised by C. Hawkins, which contained six chlorines in the ligand.[151] While this catalyst is branched at the β-position, the structural analysis described in Chapter 2 indicates this should not increase the steric bulk of the system. The most significant effects are expected, therefore, to result from any potential 'halogen effect'. The abbreviation used for this catalyst is shown in Figure 4.3.

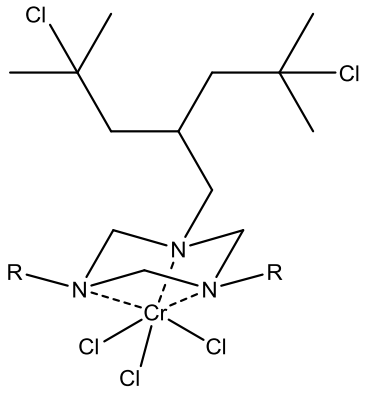

β-$^{i}Bu_2(Cl_2)$

Figure 4.3 - The additional catalyst containing six chlorine atoms and its abbreviation.

Prior investigation of catalysts with γ-branched N-substituents has shown that these systems were only poorly selective towards trimerisation and produced considerable polymer. Thus, they were expected to be well suited as probes for any internal 'halogen effect' on polymerisation activity and selectivity.

Table 4.1 – The catalytic activity of differently halogenated polymerisation catalysts.

	Selectivity (w%)			Activity (mol(C_2H_4) mol(Cr)$^{-1}$ h^{-1})	
Catalyst	1-C_6	C_{10}	PE	1-C_6	PE
γ-Pe_2H	6	0	94	1283	20,000
γ-Pe_2Cl	7	0	93	1889	26,000
γ-Pe_2Br	6	0	94	1604	26,000
β-$^{i}Bu_2(Cl_2)$	78	1	21	5382	1000

The data provided represents all products readily observable by GCMS-FID at an abundance of over 0.01 w% of liquid products. Trace quantities of C_{10} olefins were observed for each of the γ-branched catalysts at approximately 0.1 w% in total. The region associated with the decene products was observed to contain four peaks in each case, indicating the existence of at least four C_{10} isomers rather than pure 1-decene as would be expected for a chain growth or ring expansion pathway. It is immediately apparent, therefore, that the C_{10} products result from the co-trimerisation of 1-hexene with ethylene as previously proposed.[4]

It is clear from the data shown in Table 4.1 that catalyst selectivity is not determined by halogen incorporation but is instead highly dependent on the N-substituent branching point. The marked swing in the product distribution when β-$^{i}Bu_2(Cl_2)$ was used demonstrates that trimerisation becomes far more favourable. This is despite the crystallographic evidence that suggests that there is very limited or even less steric crowding on moving from γ- to β-branched ligand systems. The most reasonable explanation is therefore that the intermediates of the poly- and trimerisation mechanisms interact with the ligand in a distinctly different manner than the pre-catalyst.

In contrast, the halogenation of the ligand does appear to have a marked influence on the activity of the catalyst towards polymerisation. A considerably higher activity was recorded for both γ-Pe_2Cl and γ-Pe_2Br compared to the non-halogenated analogue. This positive 'halogen effect' contrasts markedly with the detrimental effects observed for the LAO trimerisation systems and suggests an alternative mechanism. As such, a ring-expansion polymerisation mechanism appears to be less likely with the observation of different reactivity.

Polymerisation induced by systems also known to demonstrate trimerisation has been proposed to occur *via* two different mechanisms, in much the same way as the debate over the selectivity of ethylene trimerisation.[19, 126] A simple Cossee-Arlman chain growth mechanism is the most common explanation and would likely result from decomposition of the catalyst to form an active Cr^{II} species. In contrast, a ring expansion mechanism has also been proposed in which ethylene insertion into the metallacycle continues way beyond the established tri- or tetramerisation selectivity.[19] The two proposals are shown in Scheme 4.1.

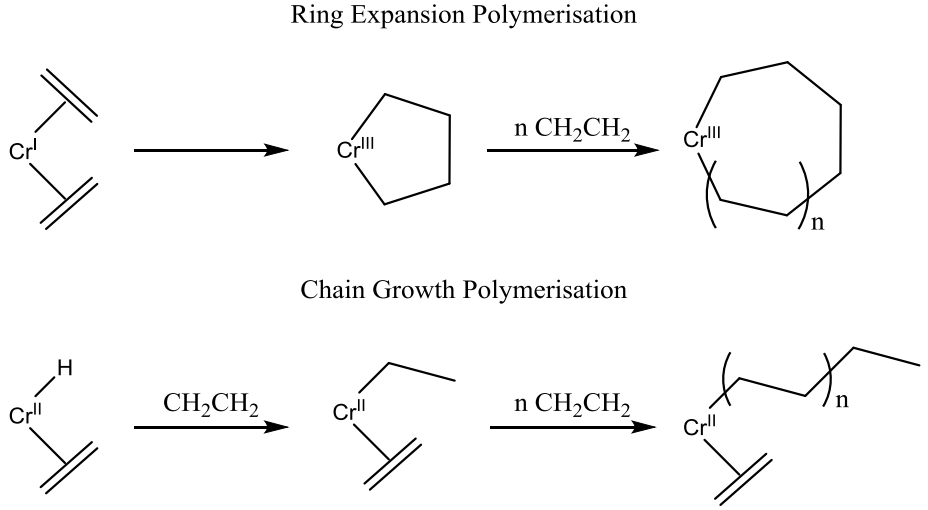

Scheme 4.1 – The two polymerisation pathways proposed to exist for systems of this type.

The ring expansion mechanism has been attributed to the observation of polyethylene at lower molecular weights (M_w < 30,000) than usually attributed to Cr^{II} systems.[237, 238] To give an insight into which mechanism may account for the polymerisation observed with these catalysts, the physical properties of the polymer were analysed. The average molecular weight (M_w) and polydispersity index (PDI) were calculated by gel permeation chromatography (GPC), while the melting point was determined by differential scanning calorimetry (DSC).

Table 4.2 – The physical properties of the polymer produced by each catalyst.

Catalyst	M_w (g mol^{-1})	PDI	m.p. (°C)
γ-Pe_2H	5000	3.2	125.3
γ-Pe_2Cl	8000	3.1	127.6
γ-Pe_2Br	6000	3.3	127.2
β-$^{i}Bu_2(Cl_2)$	51,000	32.4	124.7

A distinct difference can again be observed between the branching points. The average molecular weight and PDI are significantly higher for the β-branched system due to the formation of a bimodal polymer. This strongly suggests that for this species at least two mechanisms are available for ethylene polymerisation. By comparison to the established results for Cossee-Arlman and metallacyclic polymerisation systems it can be concluded that both pathways may play a role in the formation of the polymeric product.[239] The lower molecular weight product, in the 5000 to 8000 g mol^{-1} region, matching that of the other catalysts, can be tentatively attributed to ring expansion polymerisation.

γ-Pe_2Cl and γ-Pe_2Br both produced polymer with a greater average molecular weight than that of γ-Pe_2H, which is again indicative of greater activity towards polymerisation and reduced chain transfer. γ-Pe_2Cl produced the longest chain polyethylene, suggesting it is the most effective catalyst in this regard despite slightly lower activities than the brominated catalyst. The PDI was almost identical for each of the γ-branched catalysts but was very high compared to established ethylene polymerisation catalysts. The melting point appears to correlate nicely with the molecular weight as would be expected. The exception is β-$^{i}Bu_2(Cl_2)$, for which a lower melting point is observed despite the higher M_w. This suggests that the polymers are quite different in structure and mix poorly, leading to the lower melting points associated with impure samples.

Overall, the poor selectivity of γ-branched catalysts towards trimerisation has been confirmed relative to β-branched alternatives. Moderately active polymerisation catalysts have been described which produce a very low average molecular weight polymer. This is potentially indicative of a ring expansion mechanism, especially when the observation of a bimodal system for β-$^{i}Bu_2(Cl_2)$ is taken into account. This work demonstrates that a considerable increase in ligand bulk appears necessary in order to produce a truly selective ethylene trimerisation catalyst.

4.1.2 Activator Screening

The second ambient pressure study was conducted into activator variation. The greater reactivity of ethylene compared to LAOs should allow observation of any trimerisation or polymerisation activity that results. The same procedure was followed as for the polymerisation tests with the use of γ-Pe_2Cl as the catalyst due to its good polymerisation activity. A range of aluminium based activating agents were tested without inclusion of an additional abstracting agent to explore whether any cheaper alternatives to MAO could be utilised in the future. 500 equivalents of aluminium relative to the catalyst were used in each case.

Table 4.3 – The tri- and polymerisation activity of γ-Pe_2Cl after activation by a range of aluminium alkyls. '~' indicates the yield could not be accurately determined due to obscured peaks.

	Activity ($mol(C_2H_4)\ mol(Cr)^{-1}\ h^{-1}$)	
Activator	1-C_6	PE
MAO	2673	23,000
MMAO	~	28,000
PMAO	3493	26,000
Me_3Al	0	0
Et_3Al	0	0
$^{i}Bu_3Al$	0	0
Et_2AlCl	0	0
$EtAlCl_2$	0	0
Et_2AlOMe	0	0

The results of activator screening, shown in Table 4.3, were disappointing but not unexpected. Each of the activators that do not form a weakly coordinating counter-ion on halide/methyl abstraction did not produce an active catalyst. This is likely as a result of the formation of a strongly binding ionic pair. In each case a green solution was formed but the colour was quickly lost in favour of a yellow or vivid red/brown solution. The one exception was $EtAlCl_2$, which formed a blue solution which remained stable for some time. While other activators also produced a blue solution, it was short-lived in each case and the expected green solution was subsequently formed.

It has been shown previously within the group that the pre-catalysts react with $AlCl_3$ to form $[(R_3TAC)CrCl(\mu\text{-}Cl)_2CrCl(R_3TAC)]^{2+}$ dimers, which form navy blue solutions. It is highly likely therefore that similar dimeric species are formed on addition of $EtAlCl_2$. A variety of techniques were employed in an attempt to crystallise this species as an example of a partially activated catalyst in the presence of an aluminium alkyl. Unfortunately, all proved futile and this species could not be analysed further, with MS techniques also giving unsatisfactory results.

Each of the activators derived from aluminoxanes proved to successfully produce the active catalyst. Amongst these there was considerably greater variation than expected, with MMAO ('modified' methylaluminoxane, which incorporates a certain proportion of *iso*-butyl groups in order to induce solubility in non-aromatic hydrocarbons) proving to be most effective regarding polymerisation activity. It was not possible to calculate the trimerisation activity with this activator due to the commercial sample consisting of a heptane solution. This contained a considerable number of impurities which obscured the 1-hexene region in the GCMS spectrum and prevented accurate yield calculation. The general indication was of a greater activity than the other activators, suggesting the trend observed for polymerisation activity was replicated for trimerisation.

It is unclear what effect the solvent has on the overall activity and as such it is difficult to compare the aluminoxane activators directly. MAO and PMAO ('polymeric' methylaluminoxane, in which the oligomerisation of AlOMe units has been allowed to proceed further to give larger structures) are both supplied in toluene, while MMAO is supplied in heptane. The effect of the presence of aromatic species will be analysed in more detail later due to their implication in the ligand migration catalyst decomposition pathway.[201]

Overall, these catalysts appear to be severely restricted to methylaluminoxane-type activators in a similar manner to the majority of competing trimerisation catalysts.[19] However, considerable differences in the catalyst activity can be induced by variation of the MAO based activator, with modifications to the basic MAO species appearing to be beneficial. Further investigation is required to determine whether these observations result from other influences, such as solvent and activator concentration during catalyst activation.

4.2 Pressurised Autoclave Testing

In agreement with the vast majority of trimerisation catalyst testing, investigations into optimisation of the catalytic procedure were carried out under pressurised conditions. All of the reactions described herein were carried out under 5 bar of ethylene and 1 bar of argon to give 6 bar total reactor pressure. The bulk solvent used in each reaction was heptane and mechanical stirring was maintained at 300 rpm throughout. These conditions were found previously to provide the optimal selectivity towards 1-hexene formation.[151] Higher ethylene pressures and the use of aromatic solvents resulted in increased quantities of polymer, leading to loss of selectivity and considerable reactor fouling. Thus, the parameters stated were carried forward to the current investigation.

All pressurised experiments were carried out according to an optimised procedure, with any deviations detailed alongside the data presented. The standard ethylene trimerisation method was performed as described here.

A 1 litre Büchi autoclave was dried prior to each reaction by heating to 90 °C and flushing with argon for a total of two hours. Once complete, the reactor was cooled to 30 °C and charged with 250 mL of molecular sieve dried heptane, which was then heated to 70 °C. 10 µmol of the catalyst being investigated was then weighed into a Schlenk tube under argon and activated with 500 equivalents of MAO in toluene. No additional solvent was added, with a green solution forming in the solvent within which the activator was supplied.

After 1 hour the activated catalyst was injected into the autoclave while flushing with argon. The reactor was sealed and mechanical stirring at 300 rpm commenced. The autoclave was then opened to ethylene and the reactor pressure increased to 6 bar by addition of 5 bar ethylene over the course of two minutes. On attaining the desired reactor pressure, this was maintained using an automated ethylene flow regulator. The reaction was allowed to proceed for one hour during which the ethylene flow rate, total ethylene consumption, reactor temperature and reactor pressure were monitored in real time and recorded using the Pegasus software package.

Once the reaction was complete the ethylene flow was halted and the reactor cooled over the course of 10 minutes. Once the reactor had reached 30 °C the pressure was released and the solution removed and collected while flushing with argon. A 1 mL sample was taken for GCMS analysis of the liquid products and run according to procedure described in Chapter 5. The remaining suspension was filtered through sintered glass to remove the polymeric products, which were then dried and weighed in order to calculate the yield. Finally, the autoclave was washed with 200 mL of hexane before further use.

Beyond this procedure, further optimisation of ethylene trimerisation using this system focused primarily on the temperature and activation procedure alongside modification of the catalyst itself. The effects of these parameters will be analysed extensively in this section according to the same techniques applied to the ambient pressure testing. Kinetic analysis was also carried out by monitoring the ethylene consumption. Before comparison of different catalysts, the optimised procedure was determined with the use of β-PrPe, the catalyst previously used for the solvent and pressure investigations.[151] The catalyst was re-purified by column chromatography before use. All catalyst runs were carried out twice, with the average values of two successful experiments presented here. Experiments were considered successful when the key data demonstrated a variation of less than 10%, which was the standard applied by LyondellBasell GmbH.

4.2.1 The Effect of Aromatics on Catalyst Activation

The surprise observation of considerable differences in catalyst performance between different MAO based activator solutions led to an in-depth study into the effect of aromatic solvents on activation. Catalyst activation was achieved with the use of 750 equivalents of MMAO in heptane to avoid aromatic species. A control reaction was run followed by further reactions in which either 1 or 2 mL of toluene, previously dried according to the same procedure as heptane, was added to the catalyst immediately after the activator solution.

This mixture was then left for 1 hour before addition to the bulk solvent and exposure to ethylene according to the standard procedure. The catalyst performance was then assessed to determine the effect of toluene. The 1-hexene produced could be analysed despite the use of MMAO in heptane due to the far greater quantity of 1-hexene produced in pressurised runs. The integration value is therefore likely to be slightly overstated but this will be consistent between runs using this activator. The activity of C_{10} formation is not given as this is formed *via* a secondary reaction and is therefore not linked directly to catalyst performance.

Table 4.4 - The effect of toluene on catalyst activation.

	Selectivity (w%)				Activity ($mol(C_2H_4)\ mol(Cr)^{-1}\ h^{-1}$)		
Toluene Added (mL)	1-C_6	1-C_8	C_{10}	PE	1-C_6	1-C_8	PE
0	86	3	9	2	46,339	1640	2000
1	83	3	12	2	33,578	1212	2000
2	79	5	14	2	23,740	1426	1000

The most significant observation made as a result of this experiment, Table 4.4, was the observation of 1-octene formation for the first time, as confirmed by GCMS with a reference sample. This brings $(R_3TAC)CrCl_3$ catalysts into line with the large number of selective oligomerisation catalysts that display at least some activity towards both tri-and tetramerisation.[19] The formation of 1-hexene is strongly favoured in this case, such that these catalysts remain highly selective despite observation of this additional product.

The effect of toluene concentration on the trimerisation activity is marked, with a significant drop in reaction rate observed as the concentration was increased. This led to a corresponding drop in the 1-hexene selectivity which was compensated for by an increase in decene formation. The catalyst activity towards 1-octene and polymer formation also fell, in general, when the toluene was introduced into the activation procedure. This indicates a general increase in the decomposition rate of the active catalyst leading to the loss in activity. In turn, this also suggests that the species formed on decomposition does not induce polymerisation or alternative side reactions. This further indicates that the low molecular weight polymer formed results from a ring expansion mechanism rather than a chain growth mechanism involving a Cr^{II} decomposition product.

In order to resolve the true effectiveness of MAO, which is used as a toluene solution, a set of reactions were run to compare it with the toluene doped MMAO activations. Activation with 500 equivalents of MAO requires the use of almost exactly 1 mL of toluene solution. The equivalents of activator required was also analysed to a limited degree to test whether 750 equivalents was necessary for complete catalyst activation.

Table 4.5 – Comparison of MMAO and MAO as catalyst activation agents.

				Selectivity (w%)				Activity (TOF)*		
Run	Activator	Eq. (Al)	Tol. (mL)	1-C_6	1-C_8	C_{10}	PE	1-C_6	1-C_8	PE
1	MMAO	750	0	86	3	9	2	46,339	1640	2000
2	MMAO	750	1	83	3	12	2	33,578	1212	2000
3	MMAO	500	0	88	4	8	1	45,127	1782	2000
4	MAO	750	1.5	91	2	7	0	59,207	1319	100
5	MAO	500	1	89	3	7	1	37,321	1176	600

*TOF = mol(C_2H_4) mol(Cr)$^{-1}$ h^{-1}.

Of the experiments run, Table 4.5, activation with 750 equivalents of MAO appears the most effective. However, this technique consistently resulted in a highly exothermic reaction that led to a temperature increase of over 15 °C. Therefore, this result cannot be considered a true comparison to the other reactions, especially when the results of temperature variation (discussed in the next section) are taken into account. Run 4 should therefore be considered anomalous with respect to comparison between MAO and MMAO activators.

It can be seen that between Runs 1 and 3 very little change in catalyst behaviour is observed. Both selectivity and activity for all of the products remains very similar, suggesting complete activation of the catalyst is still achieved with 500 equivalents of activator. Further reductions in the quantity of activator were not attempted on the recommendation of LyondellBasell, due to reproducibility being considered more important than increasing the efficiency of the catalyst. The presence of such high concentrations of aluminium alkyl should prevent moderate fluctuations in moisture levels from affecting the results.

The equivalents of activator used has limited, if any, effect on catalyst performance within the range investigated. Therefore, it can be assumed that the results for Run 2 also accurately represent the effect of doping with 1 mL of toluene on 500 equivalents of MMAO. Comparison to Run 5 indicates the catalyst performance in the presence of the same quantity of toluene and indicates that MAO is a more effective activating agent. The cheaper MAO also appears to improve the selectivity of the system towards trimerisation. However, as MAO must always be used with toluene, this activator is strongly disadvantaged and comparison of Runs 3 and 5 indicates MMAO produces the more effective catalyst when used as supplied.

Overall, toluene has been shown to have a significant detrimental effect on catalysis. Based on these results, the only known decomposition mechanism, in which ligand migration results in the formation of a Cr^{I} bistoluene sandwich complex, appears to be promoted by increasing the concentration of toluene.[201] Alternatively, the proposed toluene adduct could reduce the catalyst activity by disrupting the oxidative cyclisation step. The avoidance of aromatic solvents appears essential in order to optimise the trimerisation activity of the system. On this basis, MMAO is the preferred activator going forwards, despite the slightly lower selectivities displayed in comparison to MAO.

4.2.2 Temperature Variation

Using 750 equivalents of MMAO, the ethylene trimerisation system was run at temperatures increasing from 50 to 90 °C to give a broad indication of any temperature effects. Higher reaction temperatures were not investigated due to the need to avoid complications resulting from reaching the boiling point of heptane. The reaction temperature was maintained to within a maximum error of 4 °C throughout the experiment. The solvent was heated in the autoclave prior to injection of the catalyst, such that there was no lag in attaining the desired temperature.

Table 4.6 – The effect of temperature on catalyst activity and selectivity.

		Selectivity (w%)				Activity ($mol(C_2H_4)\ mol(Cr)^{-1}\ h^{-1}$)		
Run	Temp. (°C)	1-C_6	1-C_8	C_{10}	PE	1-C_6	1-C_8	PE
1	50	66	5	7	22	40,957	3066	14,000
2	60	80	4	7	9	44,593	2067	5000
3	70	86	3	7	4	46,339	1640	2000
4	80	89	2	7	2	47,729	1141	900
5	90	88	2	8	2	34,683	642	1000

The results shown in Table 4.6 indicate that the reaction temperature has a considerable effect on the selectivity of the system, as well as a less pronounced but positive influence on the trimerisation activity. At 47,729 $mol(C_2H_4)\ mol(Cr)^{-1}\ h^{-1}$, Run 4 represents one of the most active systems yet produced for this catalyst.[151] Increasing the temperature further to 90 °C appears to result in thermal decomposition, as the trimerisation activity drops off sharply. As can be seen in Figure 4.4, the catalyst activity for the formation of the key side-products is considerably reduced with increasing temperature.

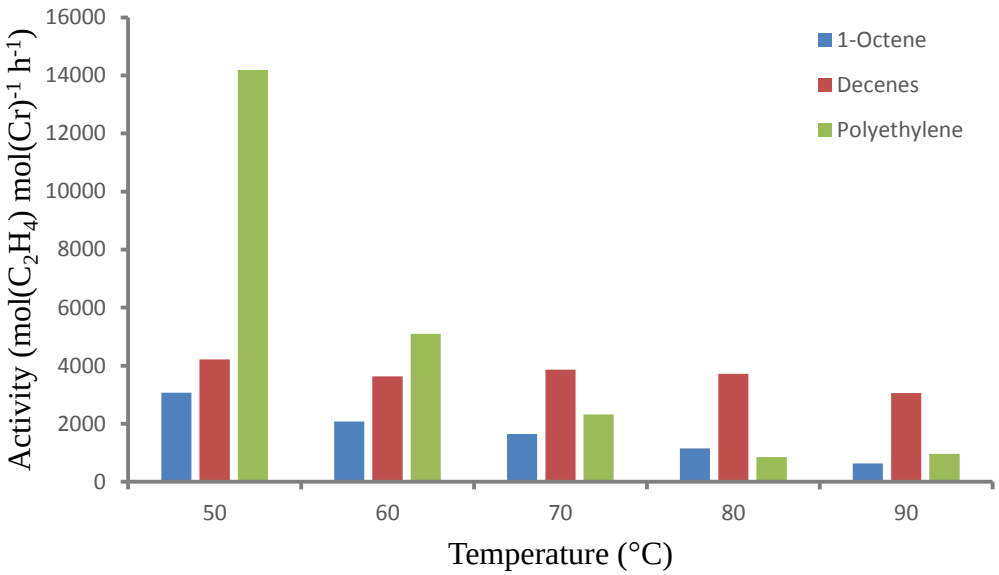

Figure 4.4 - The catalyst activities for 1-octene, decene and polyethylene formation.

Polymer formation is affected to the greatest degree, accounting for less than 2 w% of products at 80 °C. This brings considerable benefits, both in regards to the overall catalyst selectivity but also, and more importantly, in relation to reactor fouling. The maximum tolerance for most systems would be 1 w%, though the lower the proportion the lower the reactor down-time and the greater the likelihood of commercial application.[204] Application of MAO, which appears to produce more selective catalysts, at 80 °C would likely lead to catalysts which produce polymer at a significantly lower relative abundance than the 1 w% maximum.

The formation of 1-octene is also seen to be disfavoured at increasing temperatures. While the dependence of the ratio of trimerisation to tetramerisation has been investigated heavily in relation to the concentration of ethylene, far less attention has been paid to temperature dependence. For this system it appears that 1-octene is formed *via* a more thermodynamically favourable pathway. It is implied, therefore, that the formation of 1-hexene over 1-octene is under kinetic control and 1-octene is formed by a similar mechanism to that of trimerisation. This would appear to be in agreement with the ring expansion mechanism proposed by McGuinness *et al.*, with higher temperatures favouring insertion of the third ethylene before a fourth can coordinate to the metal.[217]

The activity of 1-decene formation is broadly unaffected by changes in reaction temperature and broadly reflects the concentration of 1-hexene in solution. This is as would be expected for the proposed co-trimerisation route to the formation of C_{10} isomers. On this basis it appears difficult to reduce the proportion of decenes formed by modification of the trimerisation procedure, instead it seems that alterations to the catalyst itself may be necessary.

The ethylene consumption of the different runs was recorded to give an insight into the reaction kinetics. This demonstrated a marked difference in the catalyst behaviour on increasing the temperature, as shown in Figure 4.5. The rapid consumption observed during the first couple of minutes is a result of ethylene dissolution into the heptane solvent and does not indicate a faster rate of reaction.

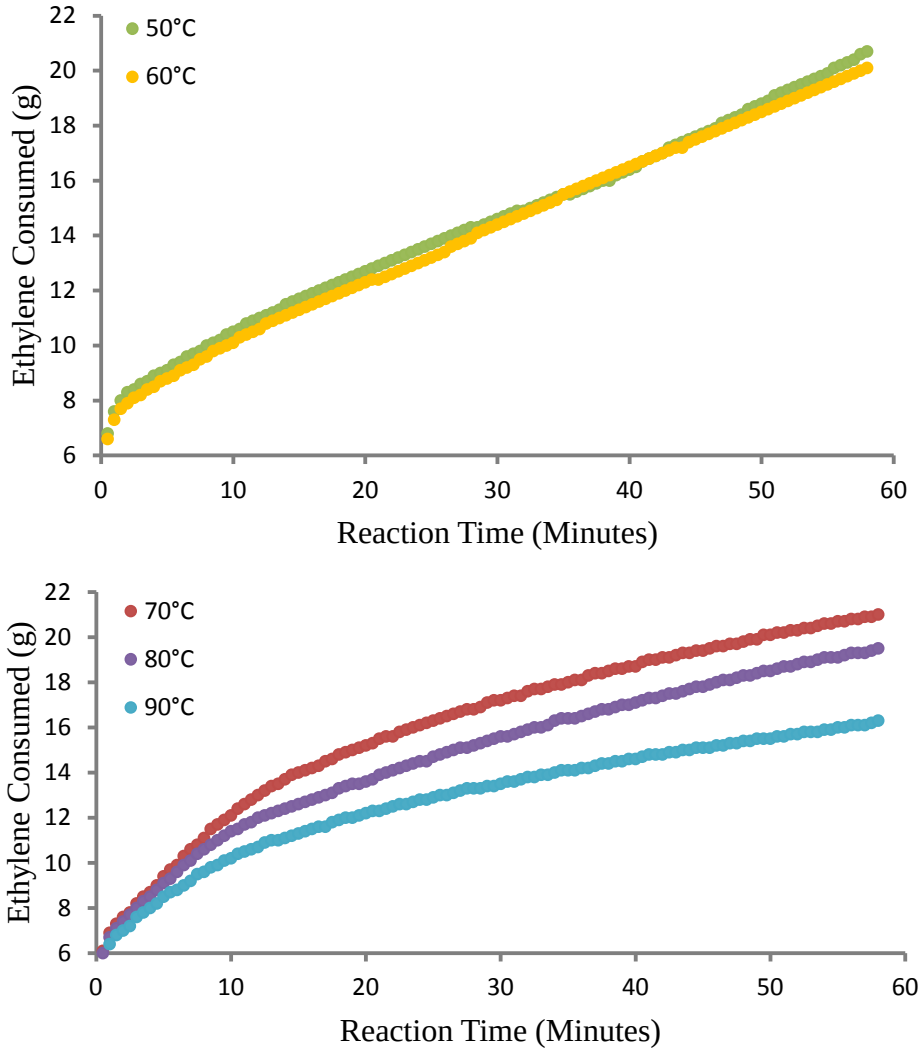

Figure 4.5 - The effect of temperature on ethylene consumption over the course of the reaction.

The lower temperature runs demonstrate linear kinetics during the course of the reaction, which contrasts starkly with the kink kinetics of the higher temperature runs. This must result from the different selectivities observed, such that high levels of polymer formation result in linear consumption. On the other hand, when very limited levels of polymerisation are observed consumption follows kink kinetics due to the transition from rapid 1-hexene formation to slower decene production. As the concentration of 1-hexene increases the favourability of co-trimerisation is increased until a tipping point occurs. This has been observed previously in other kinetic studies.[111]

It is noticeable that the 'kink' is most pronounced for Run 4, which produced the greatest proportion of 1-hexene. This results from the absence of underlying consumption due to 1-octene or polymer formation that would obscure the transition. It can be seen that the initial rate is very similar for Runs 3 and 4, which is reflected in their trimerisation activities shown in Table 4.6. The consumption of these two runs diverges at the transition point due to the higher proportion of side reactions in Run 3. Importantly, at 80 °C only a minor decay in the consumption rate can be observed over time suggesting that minimal catalyst decomposition is occurring within the first hour of reaction.

On the assumption that no 1-decene is formed in the initial stages of the reaction, due to the extremely low concentration of 1-hexene, the true rate of ethylene trimerisation can be estimated. Run 4 demonstrated very high selectivities and thus provided the most accurate estimation. The activity was calculated using the consumption data collected over a five minute period between 3 and 8 minutes after the start of the reaction. During this time period a linear consumption was observed, as the solvent had become saturated with ethylene and the 'kink' had not yet been reached, Figure 4.6.

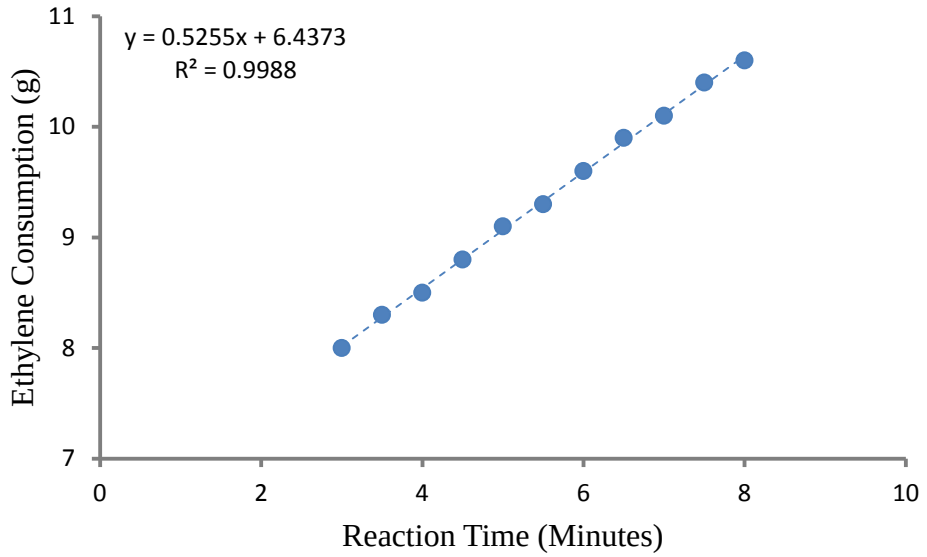

Figure 4.6 - Ethylene consumption during the linear region associated with ethylene trimerisation for Run 4.

Using these data the peak activity was calculated as 111,214 mol(C_2H_4) mol(Cr)$^{-1}$ h^{-1}. As such, in the initial stages this system is highly competitive with other homogeneous trimerisation systems, especially considering the lower pressures used for this system compared to most.[19]

Overall, the reaction temperature was found to play a key role in determining the selectivity and kinetics of the catalyst. While beyond 80 °C thermal decomposition appears to occur, up to this point the increases in temperature gave far more selective systems. Importantly, polymerisation seems to be highly dependent on temperature and can be reduced to less than 2 w% under optimal conditions. It is also noted that thermal decomposition does not appear to induce polymer formation, providing further evidence that it is formed as a side reaction of the active catalyst. This investigation demonstrates that simple modification of the methodology can produce a 90% selective $(R_3TAC)CrCl_3$ trimerisation system. The kink kinetics observed also suggest that reducing the reaction time could improve the selectivity further.

4.2.3 Reaction Time Variation

The effects of increasing the reaction time were explored with the aim of observing additional 'kinks' in longer runs, indicative of predominant C_{14} formation, or of decay caused by catalyst decomposition. In reducing the reaction time it was also hoped that a far more selective system could be produced. In so doing, the phase of the reaction in which the side products are formed should become apparent.

In experiments with shorter reaction times the inherent deviations from perfect practice within the procedure introduce considerably greater error, especially those relating to ethylene exposure time and autoclave pressure. Firstly, the reaction time is calculated from the point at which the system is first exposed to ethylene. It takes almost exactly 2 minutes to achieve 6 bar of pressure after initial exposure, which leads to under-reporting of activities. In addition, saturation of the heptane with ethylene at 6 bar is incomplete up until 6 minutes have elapsed, again introducing an underestimate of true activity.

In addition, over-reporting is introduced at the end of the experiment. Once the reaction time is complete the ethylene flow and stirring is halted and the reactor cooled to 30 °C. A brief investigation of the effect of stirring showed that ethylene dissolution into heptane at 6 bar was slow, at <0.02 g min^{-1}, in the absence of stirring. However, the ethylene in solution will continue reacting during the 10 minutes required to cool the reactor, after which the system is flushed with argon to remove any remaining ethylene. For the experiments with shorter reaction times it is expected that this will contribute only minor increases to the reaction time due to the high rate of ethylene consumption at the end of the reaction. Even when the over-reporting caused by the cooling period is taken into account, it is thought that activities quoted based on the reaction time relative to the quantity produced are likely to be considerably understated.

These reactions were undertaken with the use of a new pre-catalyst, $((Pe_2CH)_3TAC)CrCl_3$, abbreviated to α-Pe_2. This complex was synthesised by R. Kohn according to the original procedure described for α-$^{i}Bu_2$. An α-branched catalyst was considered a good candidate for application to ethylene trimerisation due to the potential to reduce the quantity of C_{10} co-trimers produced *via* steric hindrance. The effects of catalyst variation will be discussed in greater detail in the next section.

Table 4.7 – The effect of reaction time on the quantity of products and the selectivity of the catalysts.

Run	Reaction Time (min)	Selectivity (w%)				Mass (g)			
		1-C_6	1-C_8	C_{10}	PE	1-C_6	1-C_8	C_{10}	PE
1	15	93.5	0.8	0.5	3.6	9.2	0.1	0.2	0.4
2	30	93.4	0.6	0.7	3.3	12.1	0.1	0.4	0.4
3	60	93.3	0.5	0.8	3.0	14.6	0.1	0.5	0.5
4	120	92.6	0.4	1.0	2.5	18.3	0.1	0.9	0.5
5	180	93.2	0.3	1.0	2.4	18.8	0.1	1.0	0.5

The new catalyst performed far better than expected at reducing the quantity of C_{10} isomers produced and resulted in consistent selectivities in excess of 93 w%. Variation of the reaction time had less of an effect on the 1-hexene selectivity than expected, with only minor losses attributed to the increased formation of C_{10} isomers. More surprising was the very minor increase in the quantity of polymer produced, increasing from 356 to 533 mg, such that a 1200% increase in the reaction time only caused a 50% increase in polymer yield. The implication is that polymerisation activity is directly related to the trimerisation activity and, as such, the mechanisms appear linked. This observation lends further support to the proposal that the active catalyst accounts for this reactivity and favours the existence of a ring expansion mechanism.

The proportion of C_{10} isomers doubled from Run 1 to 5 in line with expectations. While a greater increase was predicted based on the behaviour of β-PrPe, the apparent steric hindrance towards their formation when using this catalyst seems to reduce the increase. In contrast, the proportion of 1-octene is seen to fall with increasing reaction time, suggesting that its formation occurs in the initial stages of the reaction. Based on the ring expansion mechanism, the tetramerisation activity would be expected to demonstrate a higher dependence on ethylene concentration. It appears that this also translates into the relative concentration of ethylene and 1-hexene. However, it is difficult to draw any firm conclusions due to the small yields recorded.

Activity data has not been presented in Table 4.7 due to the reaction time having by far the greatest influence on the calculation, resulting in the activity falling in all cases. This shows that none of the products are produced at a significantly increasing rate over time. The activity data is therefore only valid for 1-hexene production. This is shown in Table 4.8 for each run and demonstrates the commercial benefits of reducing the reaction time. However, these values are only a guide as the true reaction time contains considerable error due to the filling and cooling periods.

Table 4.8 – The influence of reaction time on 1-hexene activity.

Run	Reaction Time (min)	Activity ($mol(C_2H_4)\ mol(Cr)^{-1}\ h^{-1}$)
1	15	130,463
2	30	85,870
3	60	52,149
4	120	32,580
5	180	19,962

A considerable improvement in the efficiency of the reaction can be observed on reducing the reaction time, such that for any commercial application reactions would only be run for short periods. The results for Run 1 are likely to represent the optimal conditions as the transition period to a slower rate of reaction is observed at approximately 15 minutes. The improvement relative to β-PrPe can be attributed to the apparent unfavourability of 1-hexene binding, which would lead to co-trimerisation. The exclusion of 1-hexene, whether it is incorporated into a trimer or only transitory, would be expected to improve the ethylene activity. As such, it appears that optimising the steric bulk of the N-substituents of the ligand could lead to extremely active catalysts.

The kinetics of Run 5 were investigated further in order to calculate the peak activity of the system and investigate whether further transition points could be observed in the ethylene consumption, Figure 4.7.

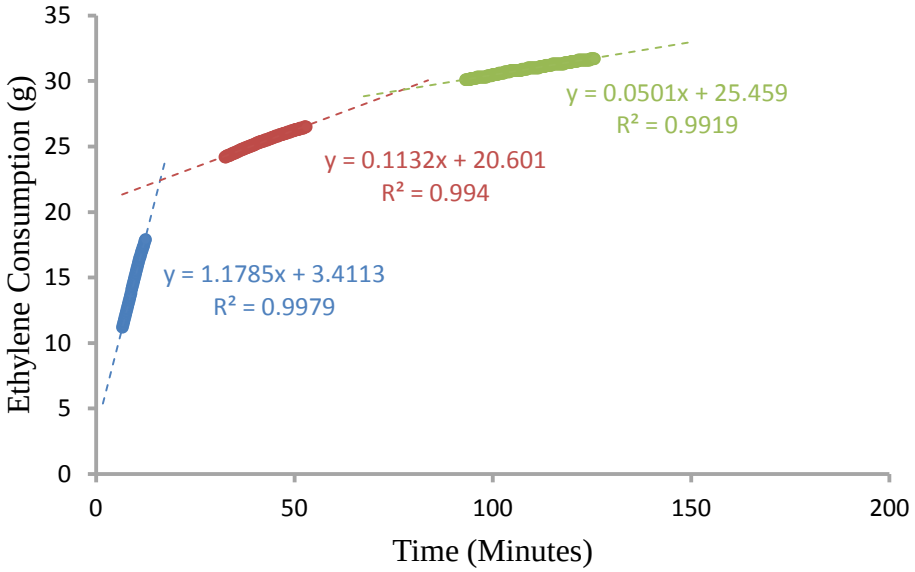

Figure 4.7 - Kinetic analysis of the different phases of the trimerisation.

Three distinct phases in the trimerisation reaction were observed in the ethylene consumption. The initial phase was found to be short lived, with the linear kinetics giving way to a relatively sharp transition period after 17 minutes. Associated with ethylene trimerisation, this phase accounts for the majority of consumption despite its short duration. The second period, associated with decene formation, proceeds at just a tenth of the rate of the first phase. It is longer lived, however, and represents the final phase for reactions under the standard conditions. It can be seen that a third phase appears to exist beyond this, however, at half again the rate of consumption. This phase is theoretically associated with tetradecane formation, though only a trace is observed.

It can be seen from the R^2 values that the linear fits become less accurate as the reaction proceeds. This is indicative of increasingly non-linear kinetics, which is associated with increasing catalyst decay over time. The deviations, even after 3 hours, remain small and suggest that the activated catalyst demonstrates impressive stability under catalytic conditions.

The low abundance of decenes and negligible yield of tetradecenes seems to contradict the observation of such distinct phases. A potential explanation is that the majority resting state of the reaction changes between these periods. These systems are known to be first order relative to ethylene, which is indicative of the metallacyclopentane acting as the resting state.[19] On this basis, it is proposed that variation of the metallacyclopentane results in the distinct difference in rates between phases. In keeping with the observation of three phases, there are three possible metallacyclopentanes that could act as the resting state, as shown in Figure 4.8. These species would then undergo ethylene insertion at different rates. It is assumed that ethylene insertion is fast compared to insertion of 1-hexene.

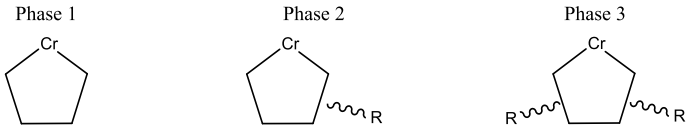

Figure 4.8 - The proposed majority resting states of the catalyst during the different phases of reaction.

During the first phase there is minimal 1-hexene present within the solution, thus the resting state must be a non-substituted chromacyclopentane formed from two ethylene units. Once the concentration of 1-hexene has reached a critical point, the majority of the chromacyclopentanes formed become mono-substituted due to cyclic oxidation of one 1-hexene unit and one ethylene unit. These species would be expected to demonstrate a slower rate of ethylene insertion, resulting in a reduction in overall consumption. During the third phase the trend is proposed to continue with disubstituted chromacycle formation, with an even slower rate of ethylene insertion predicted.

The results presented here clearly indicate that 1-hexene is produced throughout the reaction period, though at a decreasing rate. The substituted metallacyclic intermediates are therefore proposed to hinder the reaction until successful insertion leads to C_{10}, or in more seldom cases C_{14}, formation. At this point rapid ethylene trimerisation would proceed until another substituted intermediate was formed, leading to another delay. Therefore, as an increasing proportion of chromacyclopentanes incorporate 1-hexene, the overall rate of consumption is observed to fall markedly.

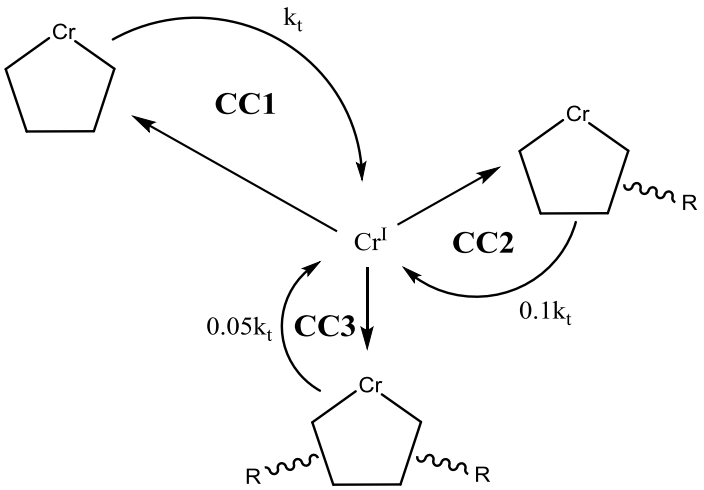

Scheme 4.2 - A simplified schematic of the three catalytic cycles proposed to occur during ethylene trimerisation. R = butyl.

The proposed explanation of the kinetic effects resulting from the varying concentrations of chromacyclopentane intermediates is shown in Scheme 4.2. The scheme excludes tetra- and polymerisation as minor side reactions of apparently constant relative rate. In Phase 1, the rate of consumption results entirely from catalyst cycle 1 (CC1) and proceeds at k_t. As the 1-hexene concentration increases, CC2 becomes more prevalent until the mono-substituted intermediate makes up the majority. At this point the reaction enters Phase 2 and ethylene is consumed at a rate of $0.1k_t$ due to CC2 acting as the rate determining step. The rapid rate of ethylene trimerisation would continue when the non-substituted intermediate was formed but the overall rate of reaction is determined by the relative abundance of the metallacyclopentanes. At even higher 1-hexene concentrations the disubstituted intermediate becomes the majority and leads to Phase 3. At this point the catalysis is proceeding through all three catalyst cycles but CC3 is the rate determining step, leading to a further drop in the overall rate of consumption to $0.05k_t$.

As expected, calculation of the peak activity during Phase 1 gave a considerably higher value than initial results would suggest at 265,203 mol(C_2H_4) mol(Cr)$^{-1}$ h^{-1}. At 93.5% selectivity this equates to a trimerisation activity of 246,631 mol(C_2H_4) mol(Cr)$^{-1}$ h^{-1}. Such efficiencies make this catalyst amongst the most active yet discovered, especially when the relatively low ethylene pressure is taken into account. Steric optimisation therefore presents the possibility of producing a catalyst capable of out-performing the best performing systems described to date.

4.2.4 Catalyst Bulk Variation

Comparison of the performance of β-PrPe and α-Pe_2 demonstrated clearly that modification of the N-substituent enabled considerable improvements in selectivity to be achieved. A selection of catalysts were tested in an attempt to identify the optimal steric bulk of the ligand for application to ethylene trimerisation. Only relatively limited scope exists, however, for modification of these ligands. Firstly, catalysts without alkyl branching or with branching at the γ-position demonstrate poor selectivity and produce large quantities of polymer. Secondly, the reactions are run in heptane and therefore the catalysts need to feature relatively long chain alkyl groups as the branching moieties to ensure solubility.

Within these limits, the performance of five catalysts was compared. Each of the catalysts was run under the same standard conditions and using the same procedure. The activity data has been quoted based on the isolated yield and therefore does not represent the peak activity.

Table 4.9 – Comparison of the ethylene trimerisation efficiency of a range of catalysts.

		Selectivity (w%)				Activity (TOF)*		
Run	Catalyst	1-C_6	1-C_8	C_{10}	PE	1-C_6	1-C_8	PE
1	β-EtBu	84.1	4.0	8.3	3.6	50,973	2424	2000
2	β-PrPe	84.5	3.4	7.5	4.2	45,127	1782	2000
3	β-$^{i}Bu_2(Cl_2)$	84.1	3.5	7.6	4.4	39,281	1640	2000
4	α-Pe_2	93.0	0.5	3.2	3.3	52,149	285	2000
5	α-$^{i}Bu_2$	93.3	0.6	2.4	3.7	43,951	281	2000

*TOF = mol(C_2H_4) mol(Cr)$^{-1}$ h^{-1}.

As was observed for the ambient pressure testing, the branching point appears to have a significant effect on the selectivity of these catalysts, as shown in Table 4.9. Runs 4 and 5 demonstrate considerable improvements over the β-branched catalysts to give far better selectivities. This comes as a result of a reduction in the quantity of 1-octene and decenes produced and indicates that steric bulk plays a key role in the regulation of these side products.

The significant reduction in 1-octene formation appears to support the ring growth tetramerisation mechanism, in which two ethylene units are thought to bind to the metallacyclopentane intermediate.[217] It follows that increased steric bulk around the metal centre would disfavour the second unit from coordinating and hence trimerisation selectivity would increase. However, should a dinuclear mechanism account for the tetramerisation of ethylene this would also likely be disfavoured by bulkier ligands.[80]

Disappointingly, the level of polymerisation does not undergo a reduction of the same magnitude, though a slight improvement can be seen for the α-branched catalysts. This observation appears to contradict the proposed ring expansion polymerisation as, based on this mechanism, the activity would be expected to mirror that of 1-octene formation. Therefore, the origins of the minor quantities of polyethylene seen here remain unclear.

The kinetics of β-EtBu, α-Pe_2 and α-$^{i}Bu_2$ were analysed more closely by looking at the ethylene consumption over time. The rapid initial consumption reflects the filling time prior to 6 bar of pressure being established, Figure 4.9.

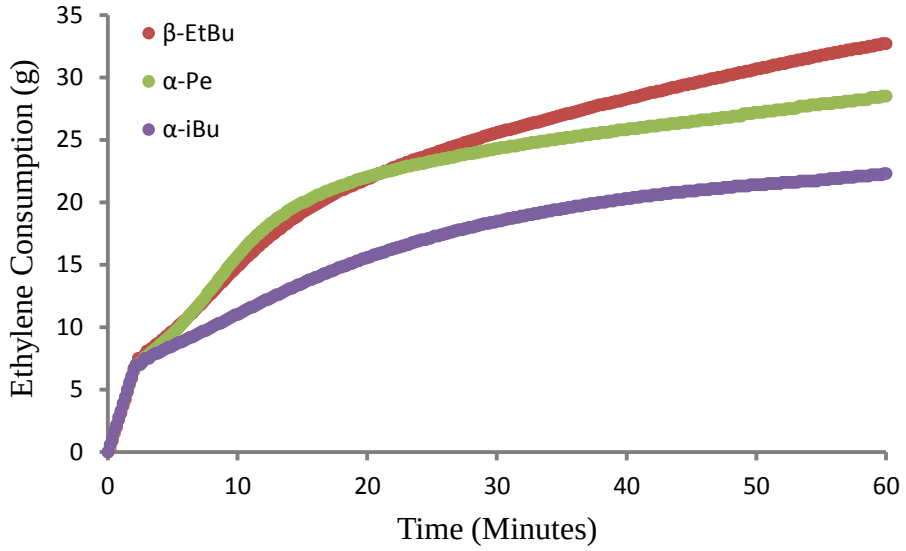

Figure 4.9 - Ethylene consumption over time for three catalysts of varying bulk.

Comparison of these three catalysts presents distinctly different behaviour for each. β-EtBu and α-Pe_2 demonstrate very similar consumption in Phase 1, which is reflected in the similarity in their overall trimerisation activity. In contrast, α-$^{i}Bu_2$ displays a slower rate of reaction in Phase 1 that is maintained for longer, such that the selectivity appears unaffected or even enhanced by this behaviour. Comparison of the peak activities, observed at between 5 and 10 minutes for the more active catalysts and between 10 and 15 minutes for α-$^{i}Bu_2$, in Table 4.10 reflects this observation.

Table 4.10 – The peak activities of the three differently substituted catalysts.

	Peak Activity (mol(C_2H_4) mol(Cr)$^{-1}$ h^{-1})	
Catalyst	Overall	1-Hexene
β-EtBu	222,428	187,068
α-Pe_2	265,203	246,631
α-$^{i}Bu_2$	183,931	171,598

Despite the similar consumption displayed by β-EtBu and α-Pe_2, the considerable difference in selectivity results in the α-branched species demonstrating a far greater trimerisation activity. By this measure, the more efficient use of ethylene by α-$^{i}Bu_2$ results in a similar trimerisation activity to β-EtBu despite considerably less total consumption. There is a stark difference between the two α-branched catalysts however, suggesting that increasing the bulk too far results in a loss in activity. In Phase 2 the difference in selectivity between catalysts can be plainly seen, with consumption continuing for β-EtBu at a far higher rate than for the other two catalysts. This is indicative of the formation of C_{10} isomers and higher oligomers, which are disfavoured for the bulkier catalysts.

Overall, the use of novel α-branched catalysts has resulted in > 93 w% selective ethylene trimerisation systems. Increasing the bulk of the ligand system successfully reduced the formation of 1-octene and higher oligomers, though it proved ineffective at preventing the formation of polyethylene as the majority side product. The peak activities of these systems, as measured over a 5 minute period in Phase 1, are impressive and compare favourably to more established systems reported previously. The optimal ethylene trimerisation activity reported herein has been compared to those described in Chapter 1 in Table 4.11, with the effect of using a lower pressure removed by quoting the activity per bar of ethylene pressure.

Table 4.11 - Comparison of the catalyst activities per bar of ethylene for a selection of the best performing systems.

Ligand Abbreviation	Transition Metal	Activity ($TOF.bar^{-1}$)	Selectivity (w%)
FI	Ti	225,000	92
Phillips	Cr	126,000	95
PNP	Cr	85,000	90
α-Pe_2	**Cr**	**49,326**	**94**
PP	Cr	47,000	25
PNN	Cr	30,000	94
CpAr	Ti	23,000	86
PNPO	Cr	16,000	85
SNS	Cr	10,000	98
NNC	Cr	5,000	83
NNN	Cr	3,000	97
PNPNH	Cr	2,000	87
Cl_5	Ta	100	96

It can be seen that the α-Pe_2 catalyst is highly competitive with the best systems published to date. The results recorded for this catalyst place (R_3TAC)$CrCl_3$ catalysts in the top five most active ethylene trimerisation reported to date. In addition, there are very few catalysts capable of producing 1-hexene at such high selectivities. This catalyst, which has undergone considerably less optimisation than the other best performing systems, therefore represents an ideal starting point for further improvements in relative performance. It is also notable that α-Pe_2 displays a far better activity than the NNN catalyst, which has a very similar structure around the metal centre, suggesting the coordination behaviour of the TAC ligand is essential for high activities.

4.2.5 Chromium Triflates as Ethylene Trimerisation Catalysts

The chromium triflate catalyst, α-$^{i}Bu_2$(OTf), was investigated as an ethylene trimerisation catalyst. The different conditions required for the use of these catalysts, principally the use of only 15 equivalents of trialkylaluminium activator, made their application more difficult due to the absence of an excess oxygen and moisture scavenger. In addition, the reaction was carried out at 40 °C rather than 70 °C due to their high sensitivity to thermal decomposition observed previously.[231] While it has been shown that increasing the equivalents of activator beyond a certain level led to a detrimental effect, the ethylene reaction did not proceed under the conditions typical to LAO trimerisation. A difference in activity would be expected to result from the different abstractable anion and counter-ion, though some reactivity should occur based on the activity toward LAOs. The lack of reactivity was therefore put down to decomposition as a result of exposure to moisture and/or oxygen in the absence of a scavenger.

A study was therefore undertaken in which various techniques were applied in order to either reduce any potential exposure to oxygen/moisture or to increase the quantity of scavenger present in the catalyst solution. Increases in the quantity of scavenger were achieved by addition of Et_3Al to the heptane solution during the heating of the autoclave. The solution was then stirred for an hour at 40 °C to ensure the heptane was completely moisture and oxygen free. The quantity of scavenger added was increased up to 200 equivalents, as shown in Table 4.12.

Table 4.12 – The effect of increasing the Et_3Al concentration in solution prior to catalyst addition.

		Selectivity (w%)			Activity (mol(C_2H_4) mol(Cr)$^{-1}$ h^{-1})	
Run	Et_3Al (Eq.)	1-C_6	C_{10}	PE	1-C_6	PE
1	30	9	0	91	71	700
2	100	85	1	15	1711	300
3	200	79	2	19	2852	700

Overall, the results were extremely poor relative to the performance of chloride catalysts. However, the results do show that increasing the amount of activator in solution does result in the formation of an active trimerisation catalyst. The marked increase in activity from Run 1 to Run 3 gave the impression that the heptane solution was not fully dried by the molecular sieves normally used. In order to determine whether the presence of moisture or oxygen was indeed the cause of the poor performance an alternative procedure for the reaction was devised.

300 mL of molecular sieve dried heptane was degassed and distilled under vacuum into a liquid nitrogen cooled Youngs flask. Under argon several droplets of Na/K alloy were added, with no effervescence observed. The heptane was stirred over the liquid alloy for 3 days to ensure that the solvent was completely dry and oxygen free. The catalyst was activated with 30 equivalents of $AlMe_3$ and added to a 250 mL sample of the dry heptane outside of the autoclave to ensure complete dissolution, another aspect that could result in the poor activity. The activated catalyst appeared to dissolve readily and was then transferred by cannula, rather than syringe, into the autoclave, which had been flushed with argon at 100 °C for five hours. The reaction was then initiated according to the standard procedure.

Using this modified procedure it is thought that any potential route by which the activated catalyst could be exposed to air or moisture was removed. The new technique was far from ideal, however, as addition of the 250 mL catalyst solution took ~5 minutes and the active catalyst was dissolved in heptane for ~15 minutes before exposure to ethylene. This method is therefore not directly comparable to the previous method, though the effects would not be expected to be severe.

Unfortunately, the stringent drying procedure did not improve the performance and this method resulted in similar results to Run 1, with polymer the major product. This indicates that the heptane solvent is not likely to be contaminated with moisture and that the higher Et_3Al equivalents are required for a different role in the catalysis. The marked difference in the chemistry of these species relative to LAO trimerisation remains poorly understood. As a result, serious questions remain over whether chromium triflate catalysts can be applied to the current ethylene trimerisation system. Further investigation is required into solvent variation and other parameters as it appears the more strongly binding counter-ion may be completely nullifying any activity.

To ensure that the limited reactivity was not a result of the Aufbau reaction, the non-selective oligomerisation of ethylene by Et_3Al, a control reaction was run. A quantity of Et_3Al equivalent to 200 equivalents in a catalyst run was added to heptane and exposed to ethylene at 40 °C for one hour. No activity was observed during this time, indicating that the 1-hexene production can be accurately attributed to the chromium catalyst. The inactivity of the $AlEt_3$ is likely a result of the far lower temperatures used in this case relative to those typically employed.[12]

4.3 Mechanistic Investigation of Co-trimerisation

The mechanism proposed herein for the observation of kink kinetics is dependent on direct competition between ethylene and 1-hexene on formation of the chromacyclopentane. However, this may not be the case if the 1-hexene formed remains bound and is immediately incorporated into a subsequent co-trimerisation, such that competition does not occur. The two possible pathways are shown in Scheme 4.3, whereby Pathway 1 lacks and Pathway 2 features free competition between the reagents. In order to test which pathway occurs, an experiment was run in which the solution was doped with 1-pentene. Should the C_{10} isomers only result from a process in which no competition occurs, then the 1-pentene should not be co-trimerised with ethylene.

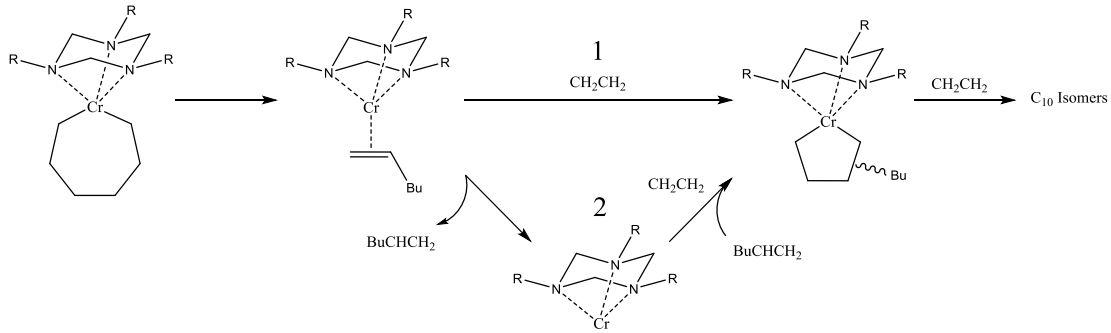

Scheme 4.3 – The two pathways that could lead to the formation of C_{10} isomers.

5 mL of 1-pentene was added to the heptane solution before addition of the activated β-PrPe catalyst and the experiment run according to the standard procedure without further modification. Ethylene consumption was considerably less than for typical experiments in which the additional LAO is not present. GCMS analysis showed that just 2.98 g of 1-hexene was formed, compared to at least 12 g for a standard run with the β-PrPe catalyst. Two additional products were observed in the liquid fraction and identified by GCMS with comparison to the NIST database. Firstly, the decene isomers were formed as before, though at low concentration due to the reduction in 1-hexene available. Secondly, a set of peaks with approximately the same distribution as those of the decenes were observed and identified as C_9 compounds.

Observation of a range of nonenes at greater concentration than the decenes, especially with a matching isomer distribution, indicates clearly that direct competition exists between 1-hexene and ethylene in the standard system. This confirms one of the key assumptions in the proposed explanation for the kink kinetics observed. In combination with the kinetic analysis, this suggests that the proposal accurately describes the distinct rate changes observed during the course of the reaction. The production of 0.74 g of nonene isomers, at an overall selectivity of 18 w%, also indicates that introduction of LAOs from the start of the reaction produces a moderately active co-trimerisation system.

4.4 Analysis of the Higher Oligomers

One of the most significant side products for these catalysts, as well as for the majority of other catalyst systems, are decene isomers. These species are formed even when using the catalysts with the greatest steric bulk, and are thought to result from the co-trimerisation of ethylene and 1-hexene.[4] To investigate the mechanism of their formation and to properly characterise these products a sample of the C_{10} isomers was isolated by the repeated distillation of a solution of the trimerisation products. A sample was procured which was >95% pure C_{10} isomers, originally produced by the β-PrPe catalyst under standard conditions. This was then analysed with both GCMS and NMR spectroscopic techniques.

The C_{10} side products were first characterised by Bercaw *et al.* with the use of GCMS analysis.[4] All of the potential products predicted by the metallacyclic co-trimerisation mechanism were synthesised or procured before they were run as reference compounds. By correlation of the retention times, the four major isomers observed could be identified and quantified alongside some minority linear species, Scheme 4.4. Characterisation of the isomers allowed several conclusions to be drawn about the selectivity of the intermediates, which apply to higher oligomerisation in general.

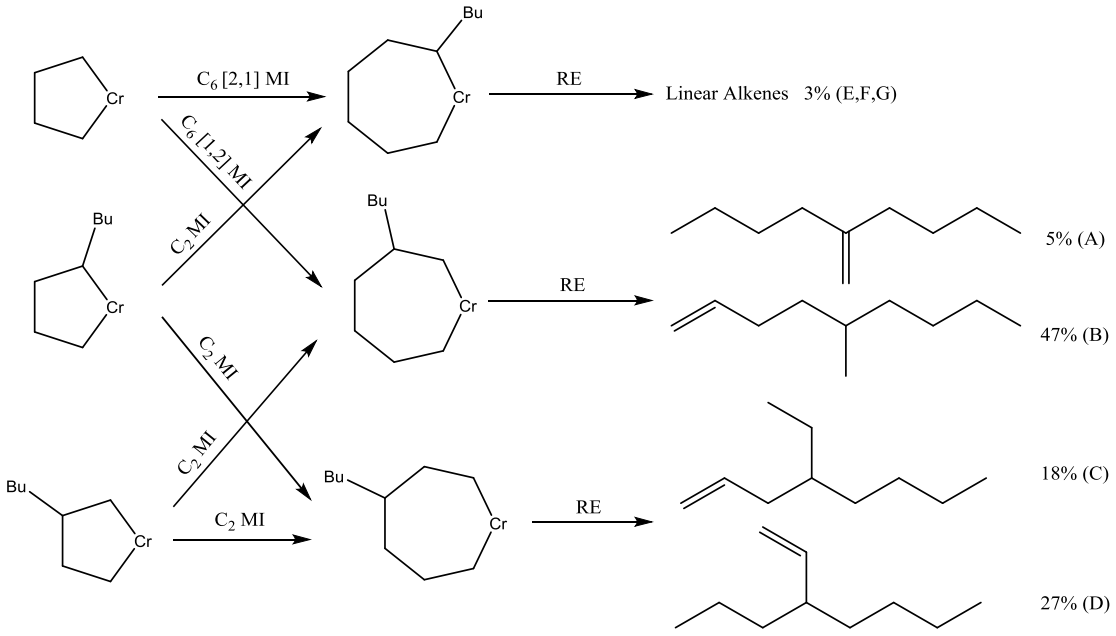

Scheme 4.4 - The characterised products of co-trimerisation between 1-hexene and ethylene. The labels refer to the nomenclature used herein rather than those proposed by Bercaw *et al*. MI = Migratory Insertion, RE = Reductive Elimination.

The principal mechanistic conclusion was that all the isomers produced corresponded to those predicted by the metallacyclic mechanism. The relative abundance of the different isomers could also be explained by several simple rules. The product distribution indicates that the 2-substituted chromacyclopentane is the most strongly favoured. This would be expected based on the unfavourable steric interaction with the ligand environment that would result from substitution at the α-position. Once formed, however, either of the two major chromacycloheptanes can still be produced based on the C-Cr bond that the second ethylene unit inserts into. Insertion into the bond furthest from the alkyl branching appears to be slightly more favourable, though there is no significant effect, again in-keeping with the idea of steric control.

There are marked differences in the β-hydride elimination pathways, which account for the majority of the variation in isomer abundance. The significant difference between the vinylidene and the corresponding α-olefin would be expected. Kinetic limitations must result from the availability of one rather than two hydrides, reducing the chance of an acceptable dihedral angle being achieved. In addition, the flexibility of this position would be significantly hindered by the need to reposition the large butyl group. More surprising is the difference in the isomers that result from the 3-substituted chromacycloheptane. Though not mentioned in the original publication, it appears that elimination from a position adjacent to the alkyl branching is beneficial. This is again presumably due to a steric effect resulting from the ability of conformers to reposition the butyl group.

The results also demonstrate clearly that LAO insertion into the non-substituted chromacyclopentane is severely disfavoured. This lends considerable support to the proposed explanation for the observation of kink kinetics. One of the key assumptions of which was that ethylene insertion into a metallacyclopentane proceeds at a much faster rate than LAO insertion. An additional observation made during this research was that minor quantities of LAO dimers were observed, complicating the assignment of higher oligomers slightly.

A later kinetic study into the formation of the C_{10} products was carried out by Zilbershtein *et al.*[240] This research investigated the commercialised Phillips catalyst, which produces decenes as the most significant side product. This work found that two distinct pathways to decene formation exist, with one dependent on 1-hexene concentration and one independent. The pathways described by Bercaw *et al.* were proposed to account for the 1-hexene dependent route, while Pathway 1 in Scheme 4.3 was put forward for the second mechanism. All kinetic observations supported the existence of a metallacyclic mechanism.

As part of this work the C_{10} products were identified using a mix of GCMS and ^{13}C NMR spectroscopy. It was demonstrated that the proportion of linear isomers produced was far greater than observed by Bercaw *et al.*, with the majority consisting of the products of *exo*-cyclic elimination. The marked difference in the product distribution was attributed to the variation in catalysts and conditions used. However, the partial characterisation of the products and the use of database comparison for GCMS correlation leads to some uncertainty in the assignment. The limited number of ^{13}C chemical shifts provided for the products are novel and have been used as a reference here.

The investigation described herein aims to fully characterise the C_{10} isomers using ^{13}C NMR spectroscopy as a more facile route to identification of all isomers, which avoids the need for GCMS reference synthesis. In addition, comparisons can then be made between the abundance of the characterised products produced by R_3TAC and PNP systems by correlation with GCMS analysis.

4.4.1 NMR Analysis of the C_{10} Fraction

A concentrated solution of the decene isomers in $CDCl_3$ was analysed with a trace of TMS added as a standard. This solution was analysed by ^{13}C NMR over the course of 15 hours with 30 second scan delays and a 5 second acquisition time to give a spectrum that could be quantitatively integrated. This indicated the existence of seven isomers which were assigned the letters A to G in order of their ^{13}C peak of highest shift, Table 4.13. Symmetry in isomers A, F and G resulted in less than ten signals being observed.

Table 4.13 – The ^{13}C NMR signals recorded for each of the C_{10} isomers. Where known, the previously reported chemical shifts are given in italics underneath the observed values and the reference provided.

Chemical shift relative to TMS (δ, ppm)						
A[241]	B[240]	C[240]	D[240]	E[242]	F[243]	G[244]
149.32	139.01	137.30	143.43	138.83	130.46	129.89
150.37	*139.5*	*137.8*	*143.8*	*139.2*	*130.77*	*129.85*
109.07	114.21	115.68	114.16	114.41	32.78	32.46
108.32	*114.1*	*115.6*	*114.0*	*114.1*	*32.92*	*31.98*
36.18	37.16	39.44	44.47	33.22	32.37	27.30
35.80		*39.0*	*44.2*	*33.8*	*32.61*	*26.91*
30.50	36.80	38.12	37.93	30.62	22.61	22.73
30.08				*31.8*	*22.78*	*22.35*
22.90	32.71	33.08	35.35	30.35	14.12	14.32
22.53	*32.5*			*29.5*	*14.16*	*14.00*
14.24	31.85	29.46	29.89	30.03		
13.98				*29.3*		
	29.76	26.15	23.24	29.68		
				29.3		
	23.45	23.48	20.67	29.32		
				29.2		
	19.71	14.32	14.29	23.03		
				22.7		
	14.29	11.08	14.16	14.42		
				14.1		

Based on these shifts the identity of the different isomers could be determined by comparison with the known ^{13}C spectra of the compounds. The minor variations observed are attributed to differences in concentration and the fact that a mixture of the isomers is being compared to the pure isomer in most cases. Distinctive features in the isomers, such as symmetry and the distance of the branching point from the double bond allowed facile identification.

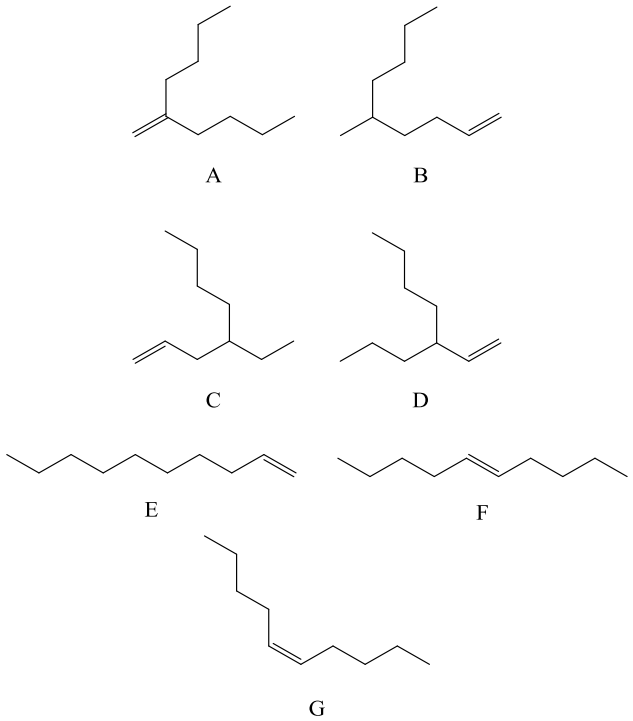

Figure 4.10 - The structures of the C_{10} isomers identified.

All of the isomers characterised, Figure 4.10, agree with the predicted co-trimerisation of 1-hexene and ethylene. To my knowledge, this is the first time the C_{10} side products of ethylene trimerisation have been fully characterised by NMR. The structures are all also consistent with the expectation that the isomers would be formed by insertion of ethylene rather than 1-hexene into the chromacyclopentane. Isomers C and D can only be accounted for based on this sequence of ring formation. By taking the average integration of a Laurentz-Gauss fitting for each of the peaks, the relative abundance could also be calculated from this data, Table 4.14. The results have been compared to those of Bercaw *et al.*, who obtained the relative abundance with the use of GCMS.[4]

Table 4.14 – The relative abundance of the seven C_{10} isomers produced by β-PrPe compared to those produced by the PNP catalyst.

	Relative Abundance (%)	
C_{10} Isomer	β-PrPe	PNP
A	11.9	5
B	39.8	47
C	21.0	18
D	25.5	27
E	0.2	} 3
F	0.6	
G	1.0	

It can be seen that the general trends observed are broadly the same for both catalysts. Meanwhile, it was found that NMR analysis is a superior tool for the analysis of the C_{10} isomers compared to GCMS, allowing the linear isomers to be identified and differentiated. This analysis, in much the same way as for the LAO trimers, also indicates that *exo*-cyclic β-hydride elimination is highly disfavoured for this system. While additional more minor peaks were observed in the internal olefinic region, corresponding aliphatic signals were not apparent. Therefore, the existence of *exo*-cyclic elimination cannot be conclusively ruled out. However, should this process occur, it is clear that regioisomers of only negligible quantity are produced. This contradicts markedly with the conclusions of Zilbershtein *et al*. who reported a significant quantity of dec-4-ene.[240]

The PNP catalyst demonstrates greater selectivity between competing elimination pathways within the co-trimerisation. The favourability of different β-hydrides towards elimination is increased, eg. the abundance of A compared to B and C compared to D. On the other hand, the selectivity towards chromacyclopentane formation is unchanged, eg. the sum of A and B compared to the sum of C and D. This would suggest that the ligand has very limited influence of the regioisomerism of the chromacyclopentane. Once formed, however, the metallacycle appears to be heavily influenced by the ligand, such that the elimination pathways vary considerably in energy between systems.

Overall, the conclusions are the same as those put forward by Bercaw *et al.*[4] However, elucidation of the linear isomers allows three further insights into the co-trimerisation process. Firstly, and in agreement with the results of LAO trimerisation, *exo*-cyclic hydride elimination is observed to be highly unfavourable if it occurs at all. Secondly, elimination from a secondary position adjacent to alkyl branching is the most favourable. This can be observed in the significantly greater abundance of F and G compared to E. Thirdly, the conformations that lead to formation of the *cis* or *trans* linear olefins are unequal either in terms of the favourability of their adoption or their ability to undergo β-hydride elimination. This clearly demonstrates the steric influence of the alkyl chain on the favourability of ring conformations.

4.4.2 GCMS Analysis of the C_{10} Fraction

The concentrated sample of C_{10} isomers was also analysed using GCMS. The observed spectrum, Figure 4.11, displayed seven peaks as hoped, indicating that each of the isomers could be distinguished using this technique. Unfortunately toluene, used as part of the calibration solution, is retained on the column for a similar period of time and slightly obscures one of the peaks. However, each of the seven peaks could be correlated to the NMR integration results to allow assignment, in combination with comparison of the MS fragmentation spectrum to the NIST database.

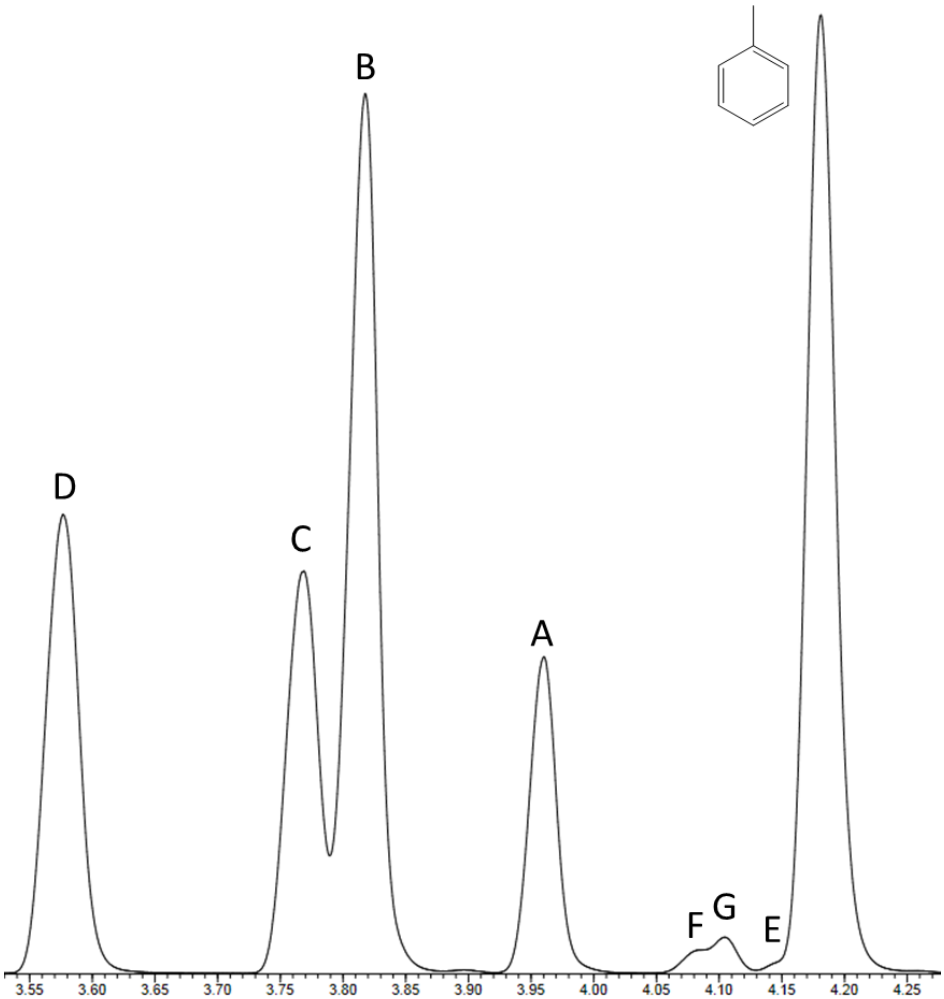

Figure 4.11 - The GCMS-FID spectrum of the C_{10} isomer mix. The x-axis indicates the retention time.

Correlation of the GCMS spectrum was achieved by integration of each FID peak and calculating the relative abundance without any corrections applied. This method should be highly accurate due to the identical empirical formula for each of the products. Where peaks overlapped the integrations of each peak were split linearly from the minima existing between them, according to the standard method of the installed Agilent software. As such, a slight underestimate would be expected for the larger peak and a slight overestimate for the smaller peak. The correlation accuracy is shown in Figure 4.12.

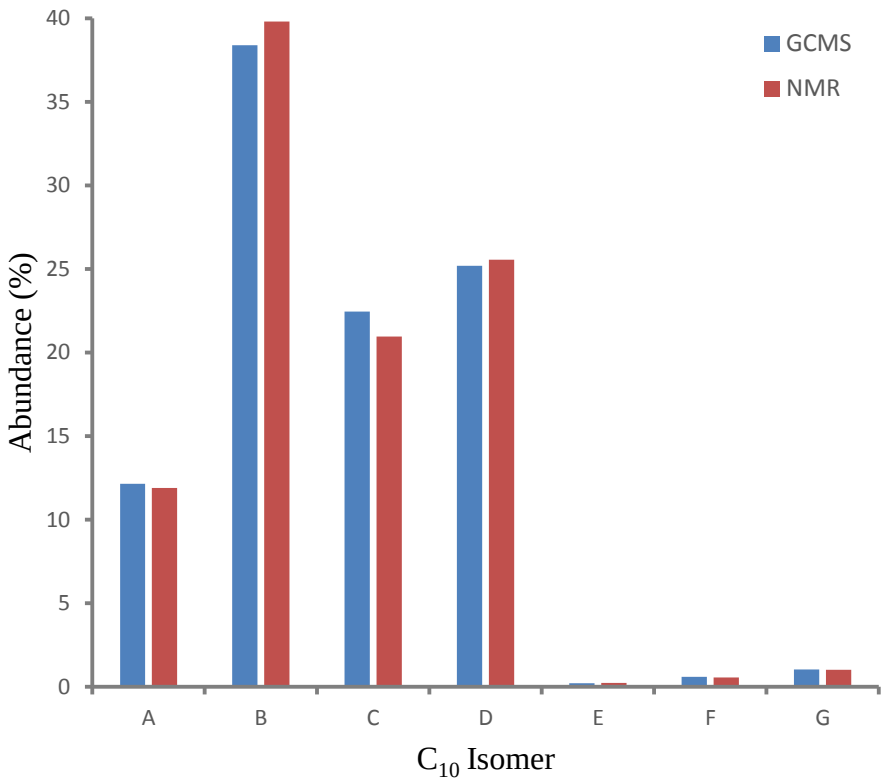

Figure 4.12 - Correlation of the peak integrations of NMR and GCMS analytical techniques.

The integrations correlate well between the two techniques with only minor deviations induced by integration techniques. The successful observation of the isomers by GCMS-FID allowed for direct comparison to the results of Bercaw *et al.* The strong correlation between the two analytical techniques confirms that the results presented herein are suitable for comparison to those of the PNP catalyst. GCMS analysis also allowed for the relative abundance of the C_{10} isomers to be observed directly from the product solution, avoiding the need for purification. This in turn allowed comparison between ligands of varying bulk.

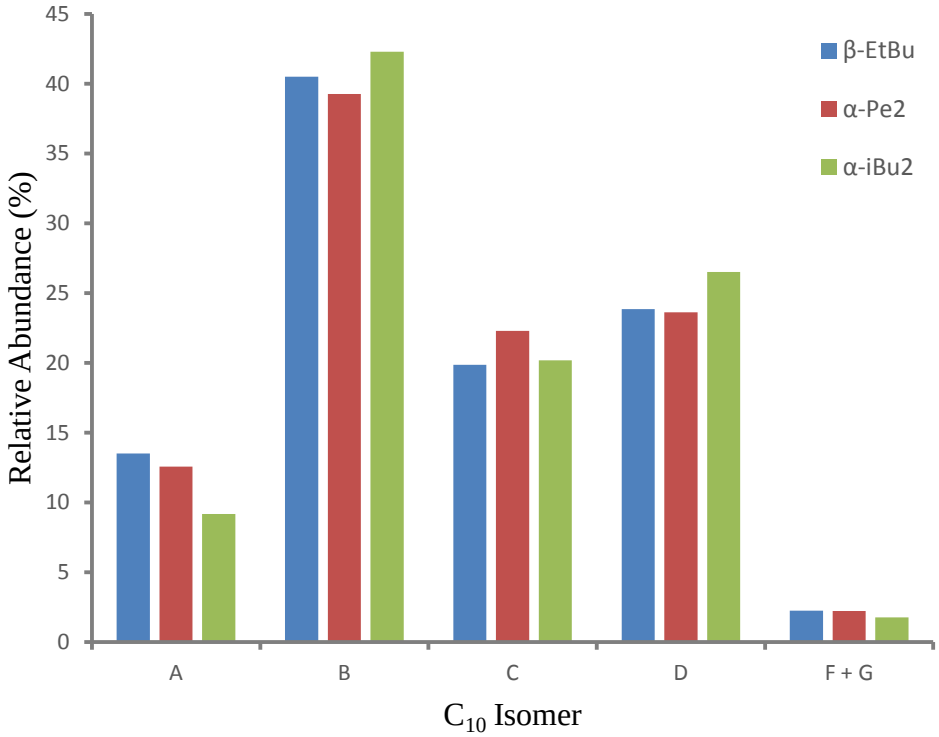

Figure 4.13 - The effect of ligand bulk on the relative abundance of the C_{10} isomers.

The relative abundance of C_{10} isomers was compared for the three catalysts that demonstrated the greatest steric influence in previous studies, β-EtBu, α-Pe_2 and α-$^{i}Bu_2$. The results displayed in Figure 4.13 demonstrate no definitive trends and suggest that the N-substituent bulk has no substantial impact on the isomer formed. This supports the proposal made by Bercaw *et al.* that the principal products each derive from the same chromacyclopentane. The research into LAO trimerisation described previously discovered significant steric influence from the ligand during chromacyclopentane formation, which would be expected to skew the selectivity of C_{10} formation if multiple intermediates were involved. It seems most likely, therefore, that the considerable differences in ligand coordination between R_3TAC and PNP ligands results in the different elimination behaviour, as opposed to steric interaction.

4.4.3 GCMS Analysis of the C_{12+} Oligomers

A closer look at the C_{12} region of the GCMS-FID spectrum, identified by comparison of the fragmentation spectra to the NIST database, demonstrates a remarkable similarity to that of the C_{10} region, Figure 4.14. It seems apparent, therefore, that the vast majority of the C_{12} products are produced in the same manner as the decenes *via* the co-trimerisation of 1-octene and ethylene. On this basis, the isomers can be labelled in the same way but in this case hexyl branching is present where previously there was a butyl group.

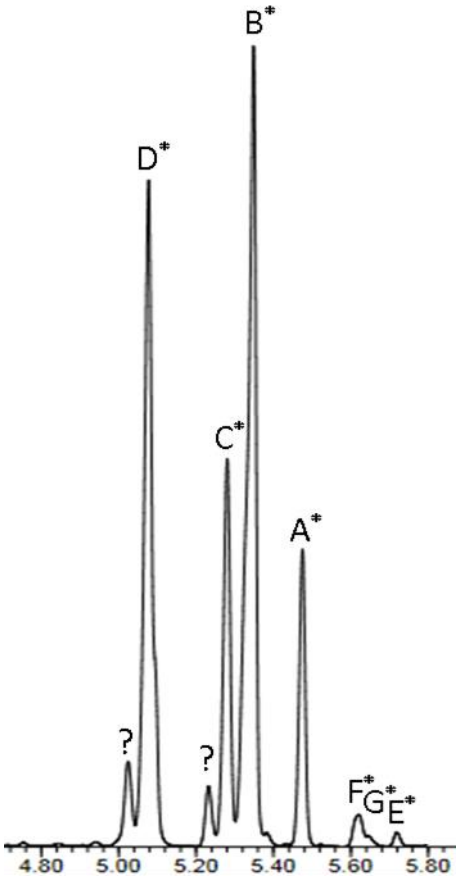

Figure 4.14 - The C_{12} region of the GCMS spectrum.

The matching peak distribution and relative intensity strongly suggests that the C_{12} isomers are formed *via* co-trimerisation in the same manner as C_{10} isomers. In accordance with this observation, these peaks were not observed for the α-branched catalysts that produced negligible quantities of 1-octene. The two peaks marked with a '?' do not correspond to co-trimers based on correlation with the C_{10} region. However, they were still shown to contain twelve carbon atoms, suggesting that these peaks represent 1-hexene dimerisation. This would agree with the observations of Bercaw *et al.*, who also observed low levels of homo-dimerisation.[4]

The second most abundant group of isomers after the decenes is the C_{14} fraction. This region of the GCMS spectra is crowded, containing many peaks of similar retention time. The pathway to formation of C_{14} isomers is more complex than for the lower molecular weight products due to several possible routes to their formation. The first route, presumed to be the most likely, is the co-trimerisation of two 1-hexene units with one molecule of ethylene, Scheme 4.5. A second route also exists, however, in which the C_{10} α-olefins could co-trimerise with ethylene.

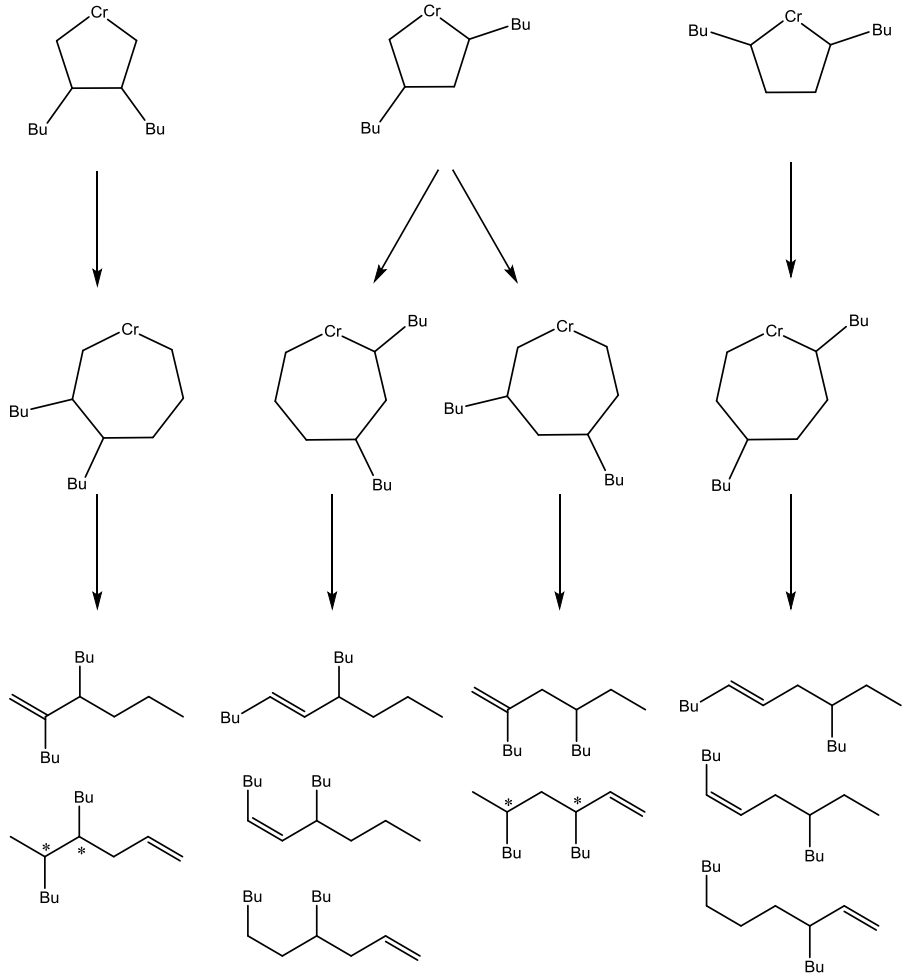

Scheme 4.5 – The full range of C_{14} products that can be formed by co-trimerisation of 1-hexene and ethylene. The chiral centres have been marked where diastereomers exist.

As shown, a maximum of twelve C_{14} products (including diastereomers) can be formed *via* this pathway, on the assumption that they are formed from a di-substituted chromacyclopentane. Based on the results of the investigations into LAO trimerisation, it is known that some of these species will be considerably less likely, such as the products that result from the 1,4-substituted chromacyclopentane. Based on these prior observations it would be expected that the six products which result from the 1,3-substituted intermediate would be the most abundant. While the C_{14} products could not be satisfactorily characterised, a closer look at the region allowed several conclusions to be drawn, Figure 4.15.

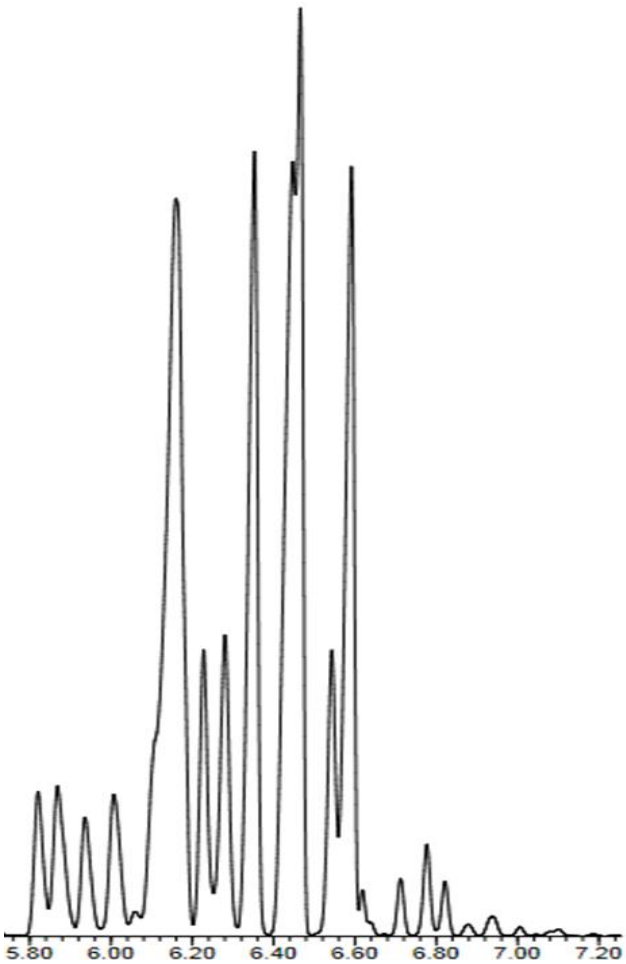

Figure 4.15 - The C_{14} region of the GCMS spectrum.

The principal observation is that there are more than twelve peaks visible, such that co-trimerisation of 1-hexene with ethylene is unlikely to account for all of the products. The co-trimerisation of terminal decenes with ethylene is therefore thought to account for the additional peaks, as dimerisation of any of the species present would not give C_{14} products. In addition, it would appear that there are six majority products, with observation of two unusually broad and two sharp peaks. This would agree with that expected according to the favourability of chromacyclopentane regioisomers, Scheme 4.5. However, in the absence of full characterisation this cannot be confirmed.

Based on the results of R group variation, discussed in Chapter 3, the number of C_{10} products that could potentially be incorporated into co-trimers is limited. Isomers A, F and G are known to be inert towards trimerisation as the active catalyst is selective towards terminal olefins. In addition, the unsuccessful attempts at vinylcyclohexane and vinyl-*tert*-butane trimerisation indicate that species with branching at the α-position are also inert. Thus, isomer D would also be expected to be inert, while the low abundance of E would cause any co-trimerisation products to be of negligible concentration. It can be assumed therefore that the additional peaks are accounted for by the 14 possible products of the co-trimerisation of isomers B and C with two units of ethylene. However, many of these products would be expected to overlap with other peaks and be of low concentration, such that it is not possible to observe all of them.

A less well defined GCMS spectrum that shows all of the higher oligomers is shown in Figure 4.16 to give a better indication of the relative concentrations. The most intense peaks of the C_{10} region have been cut off in order to display the less abundant higher molecular weight oligomers more clearly.

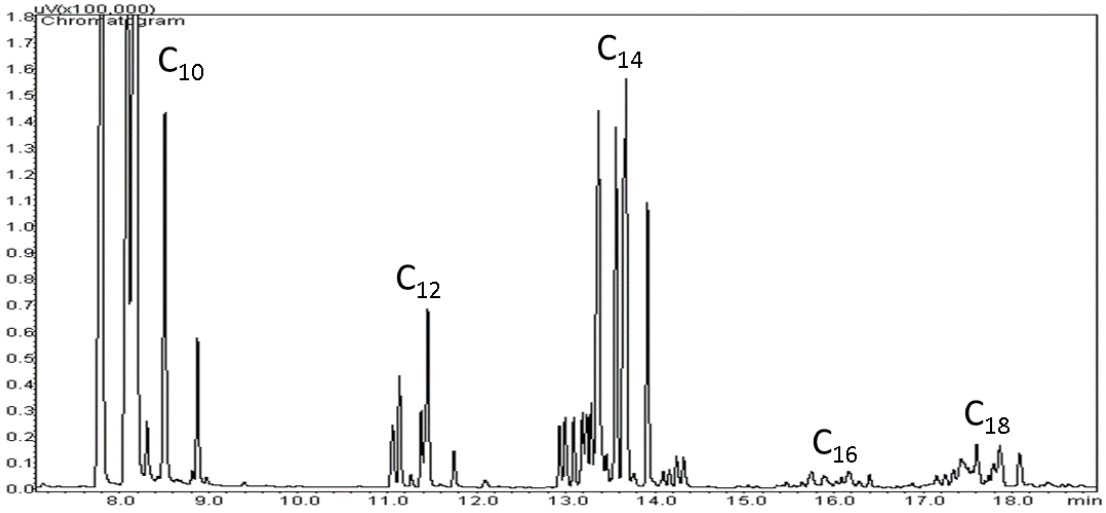

Figure 4.16 – The full GCMS spectrum of the higher oligomers.

The highest concentrations are observed for the oligomers which are formed by the co-trimerisation of 1-hexene and ethylene, ie. C_{10} and C_{14}. This is exactly what would be expected based on the observation that 1-hexene and ethylene are the reagents present in the highest concentrations. The oligomers reliant on the concentration of 1-octene, ie. C_{12} and C_{16} (C_8 + C_6 + C_2 or 2 x C_8), are far less abundant due to the lower concentration of 1-octene relative to 1-hexene. The C_{18} oligomers are of very low concentration due to the slow insertion of 1-hexene into a chromacyclopentane relative to ethylene. Such that after formation of a di-substituted chromacyclopentane, the production of C_{14} by insertion of an ethylene unit is far more favourable. No further oligomerisation products could be detected.

Overall, the use of ^{13}C NMR spectroscopy allowed the complete characterisation of the C_{10} side products and calculation of their relative abundance. The distribution of these products was found to be similar to those observed for the PNP catalyst, supporting the original conclusions of Bercaw *et al.* The characterisation of the linear products demonstrated that *exo*-cyclic β-hydride elimination is strongly disfavoured. The discovery that tetramerisation occurs for these systems explains the observation of C_{12} and C_{16} co-trimers and increases the complexity of the side-products formed. There is also compelling evidence for the incorporation of C_{10} isomers B and C into the C_{14} products.

4.5 Summary

The $(R_3TAC)CrCl_3$ based ethylene trimerisation system has been improved significantly over those originally patented, with selectivities increased from approximately 50 w% to beyond 90 w%. This has in turn resulted in considerable improvements in activity towards 1-hexene formation. The enhanced performance was principally achieved by optimisation of the reaction temperature, which resulted in the activity towards polymerisation dropping sharply. While increasing the overall 1-hexene selectivity, this also led to a considerable reduction in reactor fouling. The ratio of trimerisation to tetramerisation was also found to be temperature dependent, with the formation of 1-octene falling steadily with increasing temperature. The optimum reaction temperature was found to be 80 °C and gave selectivities of 89 w% with the β-PrPe catalyst, the best ever observed.[151]

Investigation of the effect of toluene on the reaction showed that it acts as a moderately potent catalyst poison. The presence of aromatics could be avoided with the use of a heptane soluble MMAO activator, resulting in better catalyst activities when compared to the use of MAO in toluene. Doping of the MMAO activated catalysts with toluene resulted in drops in activity related to the volume added, clearly indicating the inducement of decomposition by these species. It appears that MAO is a more effective activating agent but is strongly disadvantaged by the toluene solvent inherent in its use.

Modification of the catalyst in order to increase the steric bulk of the N-substituent resulted in further improvements. The introduction of α-branching led to the effective repression of 1-octene and decene formation, such that 1-hexene selectivities were further increased to 94 w%, the highest ever recorded for $(R_3TAC)CrCl_3$ catalysts. The detrimental effect on decene formation is readily explained by steric interaction between the ligand and the LAO. The effect of ligand bulk on tetramerisation would also be expected based on other studies but does not give any further information into which mechanism may account for it.[19]

The kinetics of the system were explored in detail by analysis of the rate of ethylene consumption over time. This revealed the existence of kink kinetics, with three distinct phases observed in which the consumption rate differed considerably. It is proposed that this can be explained by changes in the chromacyclopentane resting state, which are induced by the increasing 1-hexene concentration over time. By reducing the reaction time the activity of the first phase, associated with the majority of 1-hexene formation, was exploited to give a far more efficient process for application to commercial systems.

It was found that the selectivity of the systems towards 1-hexene remains almost constant regardless of reaction time, allowing calculation of the peak activity. This was measured over the course of five minutes during the linear period of the first phase and provided a true indication of the trimerisation activity of the catalyst. These data showed that these systems demonstrate similar activities per bar ethylene to the leading chromium catalysts published to date.

As the principal side product of many ethylene trimerisation reactions, the formation of decenes and higher oligomers was investigated in detail. All of the C_{10} products were fully characterised using ^{13}C NMR spectroscopy and correlated to GCMS analysis. The results fully supported the mechanism and pathway selectivity proposed by Bercaw *et al*. but proved more effective at identifying the minor linear products.[4] This demonstrated that *exo*-cyclic β-hydride elimination is negligible and that elimination from a secondary carbon adjacent to alkyl branching is the most favourable.

Further investigation showed that C_{14} oligomers were the next most abundant, in agreement with the proposed explanation of the kinetics. It was found that they are formed not just from co-trimerisation of 1-hexene with ethylene but also incorporate C_{10} isomers B and C. The vast majority of C_{12} oligomers were found to result from co-trimerisation of 1-octene with ethylene and gave the same isomer distribution as the C_{10} isomers, allowing for their identification. This work resulted in a greatly improved understanding of the key side products formed and the processes that account for them.

5. Experimental Details

All manipulations of air/moisture sensitive compounds were carried out under an atmosphere of argon or nitrogen using standard Schlenk techniques or under an argon atmosphere in a Saffron glove box. All reagents for which the synthetic technique is not given were obtained from major suppliers and used as received unless otherwise specified. 1,2-difluorobenzene was dried over molecular sieves before being vacuum transferred and stored over fresh molecular sieves under argon. Other dry solvents were obtained from the Innovative Technology Solvent Purification System.

NMR spectra were obtained on either a Bruker DRX500 MHz FT-NMR spectrometer [500MHz (^{1}H), 125MHz (^{13}C)], or a Bruker DRX400 MHz FT-NMR spectrometer [400MHz (^{1}H), 100MHz (^{13}C)] at 298 K. All ^{13}C spectra are H decoupled unless otherwise stated. Shift values are quoted in ppm relative to TMS or set internal solvent signals. Coupling constants (J) and line widths (W) are quoted in Hz. J-coupling is J_{H-H} for ^{1}H NMR spectra and J_{C-H} for coupled ^{13}C NMR spectra unless otherwise stated. Such spectra were assigned based on the line width of observed signals, which increases on increasing distance from the paramagnetic centre.[245, 246] NMR spectra are often taken without the use of deuterated solvent and referenced to the solvent signal externally referenced to TMS. The shift of 1,2-difluorobenzene (*o*-$C_6H_4F_2$) was set to 6.976 (^{1}H) and 117.98 (^{13}C) ppm, determined for the neat solvent relative to an added trace of TMS. When $CDCl_3$ was used, the residual proton peak was set to 7.27 and the carbon peak was set to 77.16. Effective magnetic moments were measured using the Evans method and corrected for the diamagnetic contribution.[247, 248]

Mass spectra were obtained using a micrOTOF electrospray time-of-flight (ESI-TOF) mass spectrometer (Bruker Daltonik) using acetonitrile as the solvent and collecting data in positive charge mode. The peaks quoted correspond to the calculated exact mass, the correct isotope patterns are present where the peak is quoted. For metal complexes a small amount of $Me_3N.HCl$ was added to obtain a predictable ion formation ($M+C_3H_{10}N^+$) unless otherwise stated.

Elemental analysis was performed externally by London Metropolitan University Elemental Analysis Service, UK.

GCMS analysis was performed on two different spectrometers fitted with different columns. The first was an Agilent 7890B with Agilent 5977A MSD and FID detectors. This spectrometer was equipped with a DB-FFAP column 30 m in length, with a diameter of 0.250 mm and a 0.25 µm film thickness. The second was an Agilent 7890A with Agilent 5975C MSD and FID detectors. This spectrometer was equipped with a HP-5 column 30 m in length, with a diameter of 0.320 mm and a 0.25 µm film thickness. A ramp rate of 3 °C per minute was used from 40 to 350 °C in both cases.

Intensity data for all crystal structures were collected at 150(2) K on a Nonius KappaCCD diffractometer or an Agilent Xcalibur equipped with an Oxford Cryostream, using graphite monochromated MoKα radiation (λ= 0.71073 Å). Data were processed using the affiliated Nonius[249249] and Agilent Software. For all structures a symmetry-related (multi-scan) absorption correction had been applied. Structure solution, followed by full-matrix least squares refinement was performed using the WINGX-1.80 suite of programs throughout.

5.1 Catalyst Synthesis

5.1.1 γ-Branched Chromium Chloride Triazacyclohexane Catalysts

5.1.1.1 Synthesis of $(Pentyl_2C(X)CH_2CH_2)_3TACCrCl_3$, X = Cl, Br

Synthesis of 3-pentyloct-2-enenitrile ($Pentyl_2C=CHCN$).

Sodium methoxide (10.74 g, 199 mmol) was dissolved in dry methanol (100 mL) and stirred for 5 minutes under N_2. Diethylcyanomethylphosphonate (28.22 g, 26.3 mL, 159 mmol) was pipetted into the solution and stirred for a further 5 minutes. 6-undecanone (22.9 g, 28.0 mL, 134 mmol) in 50 mL of dry methanol was added slowly by dropping funnel. The mixture was then heated at 70 ˚C for 4 days. The solvent was removed under reduced pressure and the product extracted from the remaining salts by washing with petroleum ether (3 x 50 mL) and then diethyl ether (50 mL). The combined fractions were reduced under vacuum. The resulting yellow oil was vacuum transferred at 10^{-2} mbar and ~300 ˚C to yield 12.6 g (45%) of a colourless oil.

^{1}H NMR (MeOH, Me set to 3.31): δ = 5.18 (1H, s, J = 1.3, =C**H**CN), 2.36 (2H, t, J = 7.8, -*trans*-C**H**$_2$Bu), 2.17 (2H, t of d, J = 7.7 / 1.3, -*cis*-C**H**$_2$Bu), 1.45 (4H, m, -C**H**$_2$Me), 1.30 (8H, m, -C**H**$_2$C**H**$_2$Et), 0.88 (6H, m, -C**H**$_3$).

^{13}C NMR (MeOH, set to 49.0): δ = 169.9 (-**C**=CHCN), 116.9 (-**C**N), 94.6 (=**C**HCN), 35.8 (-*trans*-**C**H$_2$Bu), 34.6 (-*cis*-**C**H$_2$Bu), 31.5/31.4 (-**C**H$_2$Et), 27.6/27.0 (-**C**H$_2$Pr), 22.42/22.37 (-**C**H$_2$Me), 13.53/13.52 (-**C**H$_3$).

This process was later shown to be significantly improved by substitution of the NaOMe with KO^{t}Bu and MeOH with THF. This gave 97% conversion and followed the same procedure except no heating was required; it was instead left to stir at room temperature for 20 hours. This was a test reaction as a significant quantity of product had already been synthesised, no isolated yield was collected.

Synthesis of 3-pentyloct-2-en-1-amine ($Pentyl_2C{=}CHCH_2NH_2$).

$AlCl_3$ (8.35 g, 62.5 mmol) was carefully dissolved into 400 mL of ice-cooled dry Et_2O under a nitrogen atmosphere. $LiAlH_4$ (7.51 g, 197.9 mmol) was then slowly added to avoid excessive boiling of the solvent during the highly exothermic reaction. The grey suspension was stirred for an hour at room temperature. A solution of $Pentyl_2C{=}CHCN$ (11.61 g, 59.6 mmol) in dry Et_2O (50 mL) was added drop-wise over the course of 30 minutes and left to stir for half an hour. Significant effervescence was observed on addition of each drop due to the highly exothermic nature of the reaction.

After complete addition the mixture was cooled in an ice bath and hydrolysed by the careful addition of 7.5 mL of water, 7.5 mL of 20% NaOH in water, 30 mL water and another 15 mL of 20% NaOH solution, in that order. The mixture was stirred vigourously for an hour to ensure complete hydrolysis. The suspension became white over this period. The suspension was left to settle before decanting off the clear Et_2O solution, followed by extractions with Et_2O (3 x 150 mL). The solvent was removed from the combined extracts under reduced pressure. Vacuum transfer at 10^{-2} mbar and ~300 ˚C yielded 9.68 g (44 mmol, 82%) of a colourless viscous oil.

^{1}H NMR, $CDCl_3$: δ = 5.13 (1H, t, J = 6.9, =C**H**CH_2NH_2), 3.17 (2H, d, J = 6.8, -C**H**$_2NH_2$), 1.89 (4H, m, J = 6.6, -C**H**$_2$Bu), 1.15-1.33 (12H, m, -C**H**$_2$C**H**$_2$C**H**$_2$Me), 0.99 (2H, broad s, -N**H**$_2$), 0.81 (6H, t, J = 6.5, -C**H**$_3$).

^{13}C NMR, $CDCl_3$: δ = 141.0 (-**C**=$CHCH_2NH_2$), 125.9 (=**C**HCH_2NH_2), 39.4 (-**C**H_2NH_2), 36.7 (-*trans*-**C**H_2Bu), 31.9/31.6 (-**C**H_2Et), 30.1 (-*cis*-**C**H_2Bu), 28.4/27.7 (-**C**H_2Pr), 22.5 (-**C**H_2Me), 14.0 (-**C**H_3).

Synthesis of 1,3,5-tris(3-pentyloct-2-en-1-yl)-1,3,5-triazinane ($(Pentyl_2C{=}CHCH_2)_3$TAC).

Paraformaldehyde (1.20 g, 40.0 mmol) was added to $Pentyl_2C{=}CHCH_2NH_2$ (7.93 g, 40.2 mmol) in 45 mL of toluene. The suspension was stirred for 3 days. During this time the particles were consumed and several droplets of water formed, indicating a complete reaction. The water was removed *via* azeotropic distillation of toluene (3 x 50 mL) and the remaining solvent removed under reduced pressure. The mixture was further dried at 10^{-2} mbar and 80 ˚C for 12 hours. The yield after drying was 7.86 g (93%) of a colourless viscous oil.

^{1}H NMR, $CDCl_3$: δ = 5.12 (3H, t, J = 6.6, =C**H**CH_2TAC), 3.22 (6H, broad s, NC**H**$_2$N), 2.99 (6H, d, J = 6.5, -C**H**$_2$TAC), 1.93 (12H, m,-C**H**$_2$Bu), 1.17-1.34 (36H, m, -C**H**$_2$C**H**$_2$C**H**$_2$Me), 0.81 (18H, m, -C**H**$_3$).

^{13}C NMR, $CDCl_3$: δ = 143.0 (-**C**=$CHCH_2$TAC), 121.5 (=**C**HCH_2TAC), 77.2 (N**C**H_2N), 50.2 (-**C**H_2TAC), 36.8 (-*trans*-**C**H_2Bu), 32.0/31.7 (-**C**H_2Et), 30.3 (-*cis*-**C**H_2Bu), 28.2/27.8 (-**C**H_2Pr), 22.6 (-**C**H_2Me), 14.0 (-**C**H_3).

Synthesis of (Pentyl$_2$C=CHCH$_2$)$_3$TACCrCl$_3$.

$CrCl_3(THF)_3$ (2.55 g, 6.8 mmol) was added to (Pentyl$_2$C=CHCH$_2$)$_3$TAC (4.04 g, 6.4 mmol) under an argon atmosphere. The reagents were then dissolved into 20 mL dry DCM and the solution stirred for 4 days. The resulting purple solution was separated by column chromatography, eluting with DCM. The solvent of the purple fractions was removed under reduced pressure and the resulting solid dried for 24 hours under high vacuum, yielding 4.32 g (90%) of a purple solid.

^{13}C NMR (DCM set to 54.0 (W = 10)): δ = 165.1 (W = 131, -**C**=CHCH$_2$TAC), 30.2 (W = 19, -**C**H$_2$Pr), 29.9 (W = 15, -**C**H$_2$Et), 28.3 (W = 36, -**C**H$_2$Bu), 27.8 (W = 19, -**C**H$_2$Pr), 25.6 (W = 42, -**C**H$_2$Bu), 21.02 (W = 13, -**C**H$_2$Me), 20.78 (W = 8, -**C**H$_2$Me), 12.16 (W = 11, -**C**H$_3$), -4 (W = 720, =**C**HCH$_2$TAC).

The line width measurements for this complex were complicated by the similar environments of nuclei in the two pentyl chains, preventing accurate Gaussian predictions. The values are therefore likely to include considerable error.

ESI-MS (m/z) [$C_{42}H_{81}Cl_3CrN_3.C_3H_{10}N$]$^+$: Calculated exact mass: 844.5714, found 844.5719.

Anal. Calc. for $C_{42}H_{81}Cl_3CrN_3$ (%): C, 64.14; H, 10.38; N, 5.34. Found: C, 64.10; H, 10.40; N, 5.29.

Magnetic moment (DCM) = 3.68 BM.

Synthesis of (Pentyl$_2$C(Cl)CH$_2$CH$_2$)$_3$TACCrCl$_3$.

(Pentyl$_2$C=CHCH$_2$)$_3$TACCrCl$_3$ (1.79 g, 2.27 mmol) was dissolved in a mixture of acetyl chloride (12 mL, 169 mmol) and DCM (10 mL) and cooled in an ice bath. Methanol (6.60 mL, 163 mmol) dissolved in 10 mL of dry DCM was added drop wise to the reaction mixture over the course of 2 hours before further stirring for 12 hours while warming to room temperature. Excess HCl was removed by bubbling nitrogen through the solution. The resulting purple solution was passed through a short silica column, eluting with DCM. The solvent of the purple fractions was removed under reduced pressure to yield a purple solid**,** which was further dried by heating to 40 ˚C at 10^{-2} mbar for 12 hours (0.330 g, 77%).

^{13}C NMR (DCM, set to 54.0 (W= 10)): δ = 102.3 (W = 188, -**C**ClCH$_2$CH$_2$TAC), 39.1 (W = 60, -**C**H$_2$Bu), 30.8 (W = 30, -**C**H$_2$Et), 24.7 (W = 52, -**C**H$_2$Pr), 21.8 (W = 26, -**C**H$_2$Me), 13.8 (W = 23, -**C**H$_3$), -26 (W = 930, -**C**H$_2$Bu).

ESI-MS [$C_{42}H_{84}Cl_6CrN_3.C_3H_{10}N$]$^+$: Calculated exact mass: 952.5015, found 952.4977.

Anal. Calc. for $C_{42}H_{84}Cl_6CrN_3$ (%): C, 56.31; H, 9.45; N, 4.69. Found: C, 56.16; H, 9.65; N, 4.81.

Magnetic moment (DCM) = 3.79 BM.

Synthesis of ($Pentyl_2C(Br)CH_2CH_2)_3TACCrCl_3$.

($Pentyl_2C{=}CHCH_2)_3TACCrCl_3$ (0.64 g, 0.82 mmol) was dissolved in a mixture of acetyl bromide (5 mL, 68 mmol) and DCM (6 mL) and cooled in an ice bath. Methanol (2.60 mL, 64 mmol) dissolved in 3 mL of dry DCM was carefully added drop wise to the reaction mixture over the course of an hour followed by stirring for 12 hours while warming to room temperature. The resulting purple solution was passed through a short silica column, eluting with DCM. The solvent of the purple fractions was removed under reduced pressure yielding a purple solid, which was further dried by heating the solid to 40 ˚C at 10^{-2} mbar overnight (603 mg, 69%).

^{13}C NMR (DCM, set to 54.0 (W= 10)) δ = 102.9 (W = 168, -**C**$BrCH_2CH_2TAC$), 40.4 (W = 59, -**C**H_2Bu), 30.7 (W = 28, -**C**H_2Et), 25.5 (W = 52, -**C**H_2Pr), 21.8 (W = 22, -**C**H_2Me), 13.2 (W = 20, -**C**H_3), -25 (W=810, -**C**H_2CH_2TAC).

ESI-MS (m/z) $[C_{42}H_{87}Br_3Cl_3CrN_3.C_3H_{10}N]^+$: Calculated exact mass: 1084.3499, found 1084.3526.

Anal. Calc. for $C_{42}H_{87}Br_3Cl_3CrN_3$ (%): C, 49.01; H, 8.23; N, 4.08. Found: C, 49.15; H, 8.32; N, 4.27.

Magnetic moment (DCM) = 3.85 BM.

5.1.1.2 Synthesis of ($Pentyl_2CHCH_2CH_2)_3TACCrCl_3$

Synthesis of 3-pentyloctan-1-amine ($Pentyl_2CHCH_2CH_2NH_2$).

10.87 g of saturated/unsaturated amine mix produced from unselective nitrile reduction attempts was dissolved into MeOH (120 mL). 10% Pd/C (430 mg) was added to form a black suspension. A large excess of hydrogen was generated by the drop-wise addition of water (2 mL, 2 g) to a suspension of CaH_2 (1.64 g, 39 mmol) in THF (20 mL). This was performed in a separate flask, connected to the reaction flask via a glass bridge, after evacuation of the whole system to the solvent vapour pressure. An oil bubbler was used to gauge the rate of H_2 produced. After the water addition the system was left stirring under a hydrogen atmosphere overnight. The solvent was removed under reduced pressure and the remaining liquid vacuum transferred off the Pd/C catalyst to yield 8.78 g of a clear oil (80%).

^1H NMR, $CDCl_3$: δ = 2.48 (2H, t, J = 6.8, -C**H**$_2NH_2$), 1.19 (2H, m, J = 6.5, -C**H**$_2CH_2NH_2$), 1.10 (1H, m, J = 6.8, -C**H**$CH_2CH_2NH_2$), 1.06 (16H, m, -C**H**$_2$C**H**$_2$C**H**$_2$C**H**$_2$Me), 0.89 (2H, s, -N**H**$_2$), 0.69 (6H, t, J = 7.1, -C**H**$_3$).

^{13}C NMR, $CDCl_3$: δ = 39.81 (-**C**H_2NH_2), 37.98 (-**C**$HCH_2CH_2NH_2$), 35.02 (-**C**$H_2CH_2NH_2$), 33.47 (-**C**H_2Bu), 32.08 (-**C**H_2Et), 26.03 (-**C**H_2Pr), 22.43 (-**C**H_2Me), 13.78 (-**C**H_3).

Synthesis of 1,3,5-tris(3-pentyloctyl)-1,3,5-triazinane ((Pentyl$_2$CHCH$_2$CH$_2$)$_3$TAC).

Paraformaldehyde (0.63 g, 21.1 mmol) was added to Pentyl$_2$CHCH$_2$CH$_2$NH$_2$ (4.67 g, 23.4 mmol) in 50 mL toluene. The suspension was stirred for 3 days. During this time the particles were consumed and several droplets of water formed, indicating a complete reaction. The water was removed *via* azeotropic distillation of toluene (3 x 50 mL) and the remaining solvent removed under reduced pressure. The mixture was further dried at 10^{-2} mbar and 80 ˚C for 12 hours. The yield after drying was 3.88 g (79%) of a colourless viscous oil.

^{1}H NMR, CDCl$_3$: δ = 3.30 (6H, broad s, NC**H**$_2$N), 2.39 (6H, t, J = 7.6, -C**H**$_2$TAC), 1.41 (6H, t, J = 6.6, -C**H**$_2$CH$_2$TAC), 1.29 (3H, m, J = 6.8, -C**H**CH$_2$CH$_2$TAC), 1.25 (48H, m, -C**H**$_2$C**H**$_2$C**H**$_2$C**H**$_2$Me), 0.88 (18H, t, J = 7.1, -C**H**$_3$).

^{13}C NMR – ^{1}H-coupled, CDCl$_3$: δ = 74.65 (t, J = 140.3, N**C**H2N), 50.44 (t, J = 130.9, -**C**H$_2$TAC), 35.62 (d, J = 126.5, -**C**HCH$_2$CH$_2$TAC), 33.48 (t, J = 124.8, -**C**H$_2$Bu), 32.11 (t, J = 127.2, -**C**H$_2$Et), 31.33 (t, J = 123.4, -**C**H$_2$CH$_2$TAC), 26.06 (t, J = 125.8, -**C**H$_2$Pr), 22.46 (t, J = 124.9, -**C**H$_2$Me), 13.83 (q, J = 124.4, -**C**H$_3$).

Synthesis of (Pentyl$_2$CHCH$_2$CH$_2$)$_3$TACCrCl$_3$.

CrCl$_3$(THF)$_3$ (2.19 g, 5.9 mmol) was added to (Pentyl$_2$CHCH$_2$CH$_2$)$_3$TAC (3.88 g, 6.1 mmol) under an argon atmosphere. The reagents were then dissolved into 20 mL dry DCM and the solution stirred for 2 days. The resulting purple solution was separated by column chromatography, eluting with DCM. The solvent of the purple fractions was removed under reduced pressure and the resulting solid dried for 24 hours under high vacuum, yielding 2.04 g (93%) of a purple solid.

^{13}C NMR, CDCl$_3$: δ = 62.1 (W = 142, -**C**HCH$_2$CH$_2$TAC), 34.8 (W = 67, -**C**H$_2$Bu), 29.2 (W = 43, -**C**H$_2$Pr), 33.7 (W = 29, -**C**H$_2$Et), 24.3 (W = 19, -**C**H$_2$Me), 15.9 (W = 15, -**C**H$_3$), -30.9 (W = 470, -**C**H$_2$CH$_2$TAC).

ESI-MS (m/z) [C$_{42}$H$_{87}$Cl$_3$CrN$_3$.C$_3$H$_{10}$N]$^+$: Calculated exact mass: 850.6184, found 850.6193.

Anal. Calc. for C$_{42}$H$_{87}$Cl$_3$CrN$_3$ (%): C, 63.65; H, 11.07; N, 5.30. Found: C, 63.83; H, 11.14; N, 5.47.

Magnetic moment (CDCl$_3$) = 3.80 BM.

5.1.1.3 Synthesis of ($^{i}Bu_2C=CHCH_2)_3TACCrCl_3$

Synthesis of 5-methyl-3-(2-methylpropyl)hex-2-enenitrile ($^{i}Bu_2C=CHCN$).

Sodium methoxide (3.62 g, 67 mmol) was dissolved in dry methanol (50 mL) and stirred for 5 minutes under a nitrogen atmosphere. Diethylcyanomethylphosphonate (9.12 g, 8.5 mL, 52 mmol) was pipetted into the solution and stirred for a further 5 minutes. 2,6-dimethylheptan-4-one (6.69 g, 8.0 mL, 47 mmol) in 25 mL of dry methanol was added drop-wise over the course of an hour. The mixture was then heated at 70 ˚C for 12 hours. The solvent was removed under reduced pressure and the product extracted from the remaining salts by washing with petroleum ether (3 x 50 mL) and then diethyl ether (50 mL). The combined fractions were reduced under vacuum. The resulting yellow oil was vacuum transferred at 10^{-2} mbar and ~300 ˚C to yield 1.96 g (26%) of a colourless oil.

^{1}H NMR, $CDCl_3$: δ = 5.03 (1H, s, =C**H**CN), 2.17 (2H, d, J = 7.6, *cis*-C**H**$_2$CHMe$_2$), 1.93 (2H, d, J = 7.3, *trans*-C**H**$_2$CHMe$_2$), 1.75 (2H, m, J = 6.9, -C**H**Me$_2$), 0.84/0.79 (6H/6H, d/d, J = 6.7/6.5, -C**H**$_3$).

^{13}C NMR, $CDCl_3$: δ = 167.2 (-**C**=CHCN), 117.1 (-**C**N), 96.6 (=**C**HCN), 45.3/43.3 (-**C**H$_2$CHMe$_2$), 27.0/26.3 (-**C**HMe$_2$), 22.3/22.2 (-**C**H$_3$).

Synthesis of 5-methyl-3-(2-methylpropyl)hex-2-en-1-amine ($^{i}Bu_2C=CHCH_2NH_2$).

$AlCl_3$ (2.00 g, 15.0 mmol) was carefully dissolved into 120 mL of ice-cooled dry Et_2O under a nitrogen atmosphere. $LiAlH_4$ (1.51 g, 40.1 mmol) was then slowly added to avoid excessive boiling of the solvent during the highly exothermic reaction. The grey suspension was stirred for an hour at ambient temperature. A solution of $^{i}Bu_2C=CHCN$ (1.96 g, 12 mmol) in dry Et_2O (20 mL) was added drop-wise over 30 minutes and left to stir for half an hour. Significant effervescence was observed on addition of each drop due to the highly exothermic nature of the reaction.

After complete addition the mixture was cooled in an ice bath and hydrolysed by the careful addition of 1.25 mL of water, 1.25 mL of 20% NaOH in water, 5 mL water and another 2.5mL of 20% NaOH solution, in that order. The mixture was stirred vigourously for an hour to ensure complete hydrolysis. The suspension became white over this period. The suspension was left to settle before decanting off the clear Et_2O solution, followed by extractions with Et_2O (5 x 30 mL). The solvent was removed from the combined extracts under reduced pressure. Vacuum transfer at 10^{-2} mbar and ~300 ˚C yielded 1.64 g (9.8 mmol, 82%) of a colourless viscous oil.

^{1}H NMR, neat (TMS): δ = 5.79 (1H, t, J = 6.5,=C**H**CH$_2$NH$_2$), 3.71 (2H, d, J = 6.5, -C**H**$_2$NH$_2$), 2.37/2.32 (2H/2H, d/d, J = 7.5, -C**H**$_2$CHMe$_2$), 2.21 (2H, m, J = 6.5, -C**H**Me$_2$), 1.91 (2H, broad s, -N**H**$_2$), 1.36/1.37 (6H/6H, d/d, J = 5, -C**H**$_3$).

^{13}C NMR, neat (TMS): δ = 137.4 (-**C**=CHCH$_2$NH$_2$), 130.5 (=**C**HCH$_2$NH$_2$), 47.1 (-C**H**$_2$NH$_2$), 40.0/39.3 (-**C**H$_2$CHMe$_2$), 27.2/26.6 (-**C**HMe$_2$), 22.94/22.91 (-**C**H$_3$).

Synthesis of 1,3,5-tris[5-methyl-3-(2-methylpropyl)hex-2-en-1-yl]-1,3,5-triazinane ((^{i}*Bu*$_2$*C=CHCH*$_2$*)*$_3$*TAC).*

Paraformaldehyde (0.29 g, 9.77 mmol) was added to $^{i}Bu_2C{=}CHCH_2NH_2$ (1.64 g, 9.8 mmol) in 15 mL toluene. The suspension was stirred for 3 days. During this time the particles were consumed and several droplets of water formed, indicating a complete reaction. The water was removed *via* azeotropic distillation of toluene (3 x 50 mL) and the remaining solvent removed under reduced pressure. The mixture was further dried at 10^{-2} mbar and 80 ˚C for 12 hours. The yield after drying was 1.78 g (92%) of a colourless viscous oil.

^{1}H NMR, $CDCl_3$: δ = 5.27 (3H, t, J = 5.8, =C**H**CH_2TAC), 3.28 (6H, broad s, -NC**H**$_2$N-), 3.10 (6H, d, J = 5.4, -C**H**$_2$TAC), 1.91/1.86 (6H/6H, d/d, J = 6.8/6.3, -C**H**$_2$CHMe$_2$), 1.74 (6H, m, -C**H**Me$_2$), 0.86 (36H, 2 overlapping d, -C**H**$_3$).

^{13}C NMR, $CDCl_3$: δ = 140.7 (-**C**=$CHCH_2$TAC), 124.5 (=**C**HCH_2TAC), 74.2 (-N**C**H_2N-), 50.5 (-**C**H_2TAC), 46.7/39.2 (-**C**H_2CHMe$_2$), 26.9/26.2 (-**C**HMe$_2$), 22.70/22.65 (-**C**H_3).

Synthesis of (^{i}*Bu*$_2$*C=CHCH*$_2$*)*$_3$*TACCrCl*$_3$*.*

$CrCl_3(THF)_3$ (1.194 g, 3.2 mmol) was added to ($^{i}Bu_2C{=}CHCH_2)_3$TAC (1.633 g, 3.0 mmol) under an argon atmosphere. The reagents were then dissolved into 20 mL dry DCM and the solution stirred for 2 days. The resulting purple solution was separated by column chromatography, eluting with DCM. The solvent of the purple fractions was removed under reduced pressure and the resulting solid dried for 24 hours under high vacuum, yielding 1.626 g (77%) of a purple solid.

ESI-MS (m/z) $[C_{36}H_{69}Cl_3CrN_3.C_3H_{10}N]^+$: Calculated exact mass: 762.4746, found 762.5051.

Anal. Calc. for $C_{36}H_{69}Cl_3CrN_3$ (%): C, 61.75; H, 9.90; N, 5.98. Found: C, 61.47; H, 9.75; N, 6.08.

5.1.1.4 Synthesis of (^{i}Bu$_2$CHCH$_2$CH$_2$)$_3$TACCrCl$_3$

Synthesis of 5-methyl-3-(2-methylpropyl)hexan-1-amine (^{i}*Bu*$_2$*CHCH*$_2$*CH*$_2$*NH*$_2$*).*

$^{i}Bu_2C{=}CHCH_2NH_2$ (0.44 g, 2.6 mmol) was dissolved into MeOH (50 mL). 10% Pd/C (132 mg) was added to form a black suspension. A large excess of hydrogen was generated by the drop-wise addition of water (4 mL, 4 g, 220 mmol) to a suspension of CaH_2 (451 mg, 10.7 mmol) in THF (20 mL). This was performed in a separate flask, connected to the reaction flask *via* a glass bridge, after evacuation of the whole system to the solvent vapour pressure. An oil bubbler was used to gauge the rate of H_2 produced. After the water addition the system was left stirring under a hydrogen atmosphere overnight. The solvent was removed under reduced pressure and the remaining liquid vacuum transferred off the Pd/C catalyst to yield 402 mg (91%) of a colourless oil.

^{1}H NMR, $CDCl_3$: δ = 2.77 (2H, broad s, -N**H**$_2$), 2.44 (2H, t, J = 7.6 Hz, -C**H**$_2$NH$_2$), 1.41 (2H, m, J = 6.7, -C**H**Me$_2$), 1.23 (1H, m, J = 6.3, -C**H**CH$_2$CH$_2$NH$_2$), 1.16 (2H, m, J = 6.0, -C**H**$_2$CH$_2$NH$_2$), 0.83 (4H, t, J = 6.8, -C**H**$_2$CHMe$_2$), 0.63 (12H, d, J = 6.8, -C**H**$_3$).

^{13}C NMR, $CDCl_3$: δ = 44.0 (-**C**H$_2$CHMe$_2$), 39.1 (-**C**H$_2$NH$_2$), 37.8 (-**C**H$_2$CH$_2$NH$_2$), 30.6 (-**C**HCH$_2$CH$_2$NH$_2$), 24.9 (-**C**HMe$_2$), 22.7/22.5 (-**C**H$_3$).

Synthesis of 1,3,5-tris[5-methyl-3-(2-methylpropyl)hexyl]-1,3,5-triazinane ((^{i}*Bu$_2$CHCH$_2$CH$_2$)$_3$TAC).*

Paraformaldehyde (66 mg, 2.2 mmol) was added to ^{i}Bu$_2$CHCH$_2$CH$_2$NH$_2$ (402 mg, 2.3 mmol) in 20 mL toluene. The suspension was stirred for 3 days. During this time the particles were consumed and several droplets of water formed, indicating a complete reaction. The water was removed *via* azeotropic distillation of toluene (5 x 20 mL) and the remaining solvent removed under reduced pressure. The mixture was further dried at 10^{-2} mbar and 80 ˚C for 16 hours. The yield after drying was 380 mg (90%) of a colourless viscous oil.

^{1}H NMR, $CDCl_3$: δ = 3.38 (6H, broad s, -NC**H**$_2$N-), 2.35 (2H, t, J = 7.8, -C**H**$_2$TAC), 1.49 (2H, m, J = 6.6, -C**H**Me$_2$), 1.36 (2H, m, J = 6.0, -C**H**$_2$CH$_2$TAC), 1.21 (1H, m, J = 6.4, -C**H**CH$_2$CH$_2$TAC), 0.81 (4H, t, J = 6.7, -C**H**$_2$CHMe$_2$), 0.65 (12H, d, J = 6.6, -C**H**$_3$).

^{13}C NMR, $CDCl_3$: δ = 73.69 (-N**C**H$_2$N-), 49.1 (-**C**H$_2$NH$_2$), 44.4 (-**C**H$_2$CHMe$_2$), 33.1 (-**C**H$_2$CH$_2$NH$_2$), 30.2 (-**C**HCH$_2$CH$_2$NH$_2$), 25.2 (-**C**HMe$_2$), 22.5/22.3 (-**C**H$_3$).

Synthesis of (^{i}*Bu$_2$CHCH$_2$CH$_2$)$_3$TACCrCl$_3$.*

$CrCl_3(THF)_3$ (275 mg, 0.74 mmol) was added to (^{i}Bu$_2$CHCH$_2$CH$_2$)$_3$TAC (380 mg, 0.69 mmol) under an argon atmosphere. The reagents were then dissolved into 20 mL dry DCM and the solution stirred for 2 days. The resulting purple solution was separated by column chromatography, eluting with DCM. The solvent of the purple fractions was removed under reduced pressure and the resulting solid dried for 24 hours under high vacuum, yielding 248 mg (50%) of a purple solid.

ESI-MS (m/z) $[C_{36}H_{75}Cl_3CrN_3.C_3H_{10}N]^+$: Calculated exact mass: 766.5245, found 766.5224.

Anal. Calc. for $C_{36}H_{75}Cl_3CrN_3$ (%): C, 61.04; H,10.67; N, 5.93. Found: C, 61.18; H, 10.56; N, 6.08.

5.1.2 β-Branched Chromium Chloride Triazacyclohexane Catalysts

5.1.2.1 Synthesis of $(Pr_2CHCH_2)_3TACCrCl_3$

Synthesis of methyl 2-cyano-2-propylpentanoate ($MeOC(=O)C(Pr)_2CN$).

Sodium methoxide (12.00 g, 222 mmol) was dissolved into 100 mL of dry methanol under nitrogen, with the evolution of a considerable amount of heat. Half (50 mL) of the base solution was added drop-wise to ethyl cyanoacetate (11.7 mL,110 mmol, 12.44 g) and the solution left to stir for 15 minutes, leading to a yellowing of the mixture. 1-Bromopropane (10 mL, 110 mmol, 13.54 g) was then added. The system was kept under nitrogen for three hours with vigourous stirring, leading to a cloudy orange solution. The second half of base solution was then added followed by another 10 mL of 1-bromopropane and the mixture left stirring overnight.

Overnight a vivid red suspension had formed. The solution was allowed to cool to room temperature before being decanted from the white precipitate. The salts were extracted with petroleum ether (3 x 100 mL) and the solvent of the combined extractions removed under reduced pressure. The resulting liquid was vacuum transferred at 10^{-2} mbar and 300 ˚C using a water bath to cool the collection vessel. 16.8 g (92 mmol, 84%) of a clear liquid was collected.

^{1}H NMR, $CDCl_3$: δ = 3.79 (3H, s, -OC**H**$_3$), 1.87 (2H, t of d, J = 13.1/4.8, -C**H**$_2$Et), 1.77 (2H, t of d, J = 12.8/4.0, -C**H**$_2$Et), 1.58 (2H, m, -C**H**$_2$Me), 1.33 (2H, m, -C**H**$_2$Me), 0.96 (6H, t, J = 7.3, -C**H**$_3$).

^{13}C NMR, $CDCl_3$: δ = 169.09 (-**C**=O), 118.56 (-**C**N), 52.49 (-O**C**H$_3$), 49.35 (-**C**(Pr)$_2$CN), 38.99 (-**C**H$_2$Et), 18.32 (-**C**H$_2$Me), 13.06 (-**C**H$_3$).

Synthesis of 2-propylpentanenitrile (Pr_2CHCN).

De-ionised water (2.5 mL, 2.48 g, 138 mmol) was dissolved into 100 mL of DMSO. Lithium chloride (11.73 g, 277 mmol) was then dissolved into the mixture (very exothermic) and the system was put under nitrogen. Once dissolved, $MeOC(=O)C(Pr)_2CN$ (16.81 g, 92 mmol) was added and the mixture heated to 150 ˚C whilst stirring overnight.

The resulting brown solution was decanted off yellow solids and 100 mL de-ionised water was added. The aqueous solution was then extracted with pentane (100 mL), which was washed with further de-ionised water (3 x 100 mL). The water washings were extracted with pentane (25 mL) which was then combined with the original pentane solution. The solvent was removed under reduced pressure to give a yellow oil. This was vacuum transferred (~150 ˚C, 10^{-2} mbar, liquid nitrogen bath) to give 8.90 g (71 mmol, 77%) of a colourless oil.

^{1}H NMR, $CDCl_3$: δ = 2.54 (1H, m, -C**H**CN), 1.42-1.62 (8H, m, -C**H**$_2$C**H**$_2$Me), 0.96 (6H, t, J = 7.5, -C**H**$_3$).

^{13}C NMR, $CDCl_3$: δ = 121.70 (-**C**N), 34.04 (-**C**H$_2$Et), 30.80 (-**C**HCN), 20.05 (-**C**H$_2$Me), 13.11 (-**C**H$_3$).

Synthesis of 2-propylpentan-1-amine ($Pr_2CHCH_2NH_2$).

$AlCl_3$ (10.69 g, 80.1 mmol) was carefully dissolved into 400 mL of ice-cooled dry Et_2O under a nitrogen atmosphere. $LiAlH_4$ (9.07 g, 240.0 mmol) was then slowly added to avoid excessive boiling of the solvent during the highly exothermic reaction. The grey suspension was stirred for an hour at ambient temperature. A solution of Pr_2CHCN (8.90 g, 71.0 mmol) in dry Et_2O (50 mL) was added drop-wise over 30 minutes and left to stir for half an hour. Significant bubbling was observed on addition of each drop due to the highly exothermic nature of the reaction.

After complete addition the mixture was cooled in an ice bath and hydrolysed by the careful addition of 50 mL of water, 50 mL of 20% NaOH in water, 100 mL water and another 100 mL of 20% NaOH solution, in that order. The mixture was stirred vigourously for an hour to ensure complete hydrolysis. The suspension became white over this period. The suspension was left to settle before decanting off the clear Et_2O solution, followed by extractions with Et_2O (3 x 150 mL). The solvent was removed from the combined extracts under reduced pressure. The product was vacuum transferred (2 x 10^{-2} mbar, ~150 ˚C, ice bath) to give 7.05 g (54.6 mmol, 77%) of a colourless oil.

^{1}H NMR, $CDCl_3$: δ = 2.60 (2H, d, J = 5.3, -C**H**$_2$NH$_2$), 1.18-1.38 (9H, m, -C**H**C**H**$_2$C**H**$_2$Me), 1.01 (2H, broad s, -N**H**$_2$), 0.90 (6H, t, J = 7.6, -C**H**$_3$).

^{13}C NMR, $CDCl_3$: δ = 44.70 (-**C**H$_2$NH$_2$), 39.99 (-**C**HCH$_2$NH$_2$), 33.43 (-**C**H$_2$Et), 19.40 (-**C**H$_2$Me), 13.89 (-**C**H$_3$).

Synthesis of 1,3,5-tris(2-propylpentyl)-1,3,5-triazinane ($(Pr_2CHCH_2)_3TAC$).

Paraformaldehyde (1.65 g, 55.0 mmol) was added to $^{i}Bu_2CHCH_2CH_2NH_2$ (7.05 g, 54.6 mmol) in 100 mL toluene. The suspension was stirred for 3 days. During this time the particles were consumed and several droplets of water formed, indicating a complete reaction. The water was removed *via* azeotropic distillation of toluene (3 x 50 mL) and the remaining solvent removed under reduced pressure. The mixture was further dried at 10^{-2} mbar and 150 ˚C for 16 hours. The yield after drying was 6.44 g (15.2 mmol, 90%) of a colourless viscous oil.

^{1}H NMR, $CDCl_3$: δ = 3.26 (6H, broad s, -NC**H**$_2$N-), 2.26 (6H, d, J = 7.2, -C**H**$_2$TAC), 1.43 (3H, m, -C**H**CH$_2$TAC), 1.18-1.38 (24H, m, -C**H**$_2$C**H**$_2$Me), 0.88 (18H, t, J = 7.2, -C**H**$_3$).

^{13}C NMR, $CDCl_3$: δ = 75.48 (-N**C**H$_2$N-), 57.38 (-**C**H$_2$TAC), 35.77 (-**C**HCH$_2$TAC), 34.97 (-**C**H$_2$Et), 19.98 (-**C**H$_2$Me), 14.66 (-**C**H$_3$).

Synthesis of ($Pr_2CHCH_2)_3TACCrCl_3$.

$CrCl_3(THF)_3$ (3.71 g, 10.0 mmol) was added to $(Pr_2CHCH_2)_3TAC$ (4.28 mg, 10.1 mmol) under an argon atmosphere. The reagents were then dissolved into 20 mL dry DCM and the solution stirred for 2 days. The resulting purple solution was separated by column chromatography, eluting with DCM. The solvent of the purple fractions was removed under reduced pressure and the resulting solid dried for 24 hours under high vacuum, yielding 4.97 mg (8.5 mmol, 85%) of a purple solid.

^{13}C NMR, *o*-$C_6H_4F_2$/DCM (DCM set to 54 ppm): δ = 49.50 (W = 153, -**C**H_2Et), 21.64 (W = 62, -**C**H_2Me), 15.16 (W = 41, -**C**H_3), -39.68 (W = 814, -**C**HPr_2).

ESI-MS (m/z) $[C_{27}H_{57}Cl_3CrN_3.C_3H_{10}N]^+$: Calculated exact mass: 640.3836; found: 640.3875.

Anal. Calc. for $C_{27}H_{57}Cl_3CrN_3$ (%): C, 55.71; H, 9.87; N, 7.22. Found: C, 55.59; H, 9.99; N, 7.33.

5.1.3 α-Branched Chromium Chloride Triazacyclohexane Catalysts

Synthesis of 2,6-dimethylheptan-4-amine ($^iBu_2CHNH_2$).

Ammonium acetate (35.02 g, 454 mmol) was dissolved into MeOH (100 mL) under nitrogen before addition of 10 mL (8.08 g, 56.8 mmol) of 2,6-dimethylheptan-4-one. This was stirred for 90 minutes at room temperature. Sodium cyanoborohydride (2.58 g, 41.0 mmol) was dissolved into MeOH (20 mL) and added to the reaction mixture which was left stirring overnight at 30 °C.

The reaction vessel was placed in a cold water bath and a liquid nitrogen cooled trap was added. 10 mL of 32% aqueous HCl was added dropwise over the course of 30 minutes, leading to a highly exothermic reaction and considerable white precipitate. CARE: Hydrolysis of the cyanoborohydride leads to the evolution of hydrogen cyanide which should be caught in the trap and disposed of properly. The MeOH was removed under reduced pressure to give a white slurry. This was extracted with pentane (3 x 50 mL) and Et_2O (3 x 50 mL) and the solvents again removed to give a clear oil. This was dissolved in Et_2O (50 mL) before addition of 5.32 g (133 mmol) of NaOH. The mixture was stirred for 2 hours before addition of 5 mL of water to form two phases and dissolve the solids. The organic phase was removed and collected and the aqueous phase extracted with Et_2O (3 x 50 mL) and pentane (2 x 50 mL). The solvent was then removed at reduced pressure. The resulting oil was distilled at 160 °C and 300 mbar to give 5.44 g (38 mmol, 67%) of a colourless non-viscous oil.

^1H NMR, $CDCl_3$: δ = 2.83 (1H, quintet, J = 6.6, -C**H**NH_2), 1.73 (2H, nonet, J = 6.7, -C**H**Me_2), 1.17 (4H, m, -C**H**$_2$CHMe_2), 0.90 (12H, t, J = 6.4, -C**H**$_3$).

^{13}C NMR, $CDCl_3$: δ = 47.99 (-**C**H_2CHMe_2), 46.24 (-**C**HCH_2NH_2), 24.44 (-**C**HMe_2), 23.24 (-**C**H_3), 21.79 (-**C**H_3).

Synthesis of 1,3,5-tris(2,6-dimethylheptan-4-yl)-1,3,5-triazinane ($(^{i}Bu_2CH)_3TAC$).

Paraformaldehyde (1.03 g, 34.4 mmol) was added to $^{i}Bu_2CHNH_2$ (4.93 g, 34.4 mmol) in 100 mL toluene. The suspension was stirred for 2 days. During this time the particles were consumed and several droplets of water formed, indicating a complete reaction. The water was removed *via* azeotropic distillation of toluene (3 x 50 mL) and the remaining solvent removed under reduced pressure. The mixture was further dried at 50 mbar and 50 ˚C for 6 hours. The yield after drying was 4.00 g (25.7 mmol, 75%) of a colourless viscous oil. NMR spectroscopy indicated a mixture of imine and triazacyclohexane was formed at a ratio of 3:2.

Imine:

^{1}H NMR, $CDCl_3$: δ = 7.35 (1H, d, J = 17.4, =C**H**-*cis*), 7.14 (1H, d, J = 17.4, =C**H**-*trans*), 3.06 (1H, m, -C**H**N=CH_2), 1.24 (2H, m, -C**H**Me_2), 1.05 (4H, d of t, J = 13.7/7.0, -C**H**$_2$CMe_2), 0.86/0.83 (6H/6H, d/d, J = 6.5/6.5 -C**H**$_3$).

^{13}C NMR, $CDCl_3$: δ = 250.91 (-N=**C**H_2), 68.63 (-**C**HN=CH_2), 40.51 (-**C**H_2CMe_2).

Triazacyclohexane:

^{1}H NMR, $CDCl_3$: δ = 3.48 (6H, s, -NC**H**$_2$N-), 2.62 (3H, quintet, J = 6.9, -C**H**N), 1.69 (2H, m, -C**H**Me_2), 1.46 (4H, m, -C**H**$_2$CMe_2), 0.88/0.87 (6H/6H, d/d, J = 6.8/6.8, -C**H**$_3$).

^{13}C NMR, $CDCl_3$: δ = 67.39 (-N**C**H_2N-), 56.46 (-**C**HN), 45.36 (-**C**H_2CMe_2).

Six further ^{13}C peaks were observed which represent (-**C**HMe_2) and the pairs of (-**C**H_3) for each molecule. These were not assigned but were recorded at 24.98, 24.24, 23.59, 23.13, 22.88 and 21.54.

Synthesis of ($^{i}Bu_2CH)_3TACCrCl_3$.

$CrCl_3(THF)_3$ (3.23 g, 8.7 mmol) was added to the ($^{i}Bu_2CH)_3TAC$ / $^{i}Bu_2CHNCH_2$ mix (4.00 g) under an argon atmosphere. The reagents were then dissolved into 20 mL dry DCM and the solution stirred for 2 days. The resulting purple solution was separated by column chromatography, eluting with DCM. The solvent of the purple fractions was removed under reduced pressure and the resulting solid dried for 24 hours at 50 °C under high vacuum, yielding 3.81 g (6.1 mmol, 71%) of a purple solid.

^{13}C NMR, $CDCl_3$: δ = 37.64 (W = 111, -**C**HMe_2), 28.55 (W = 91, -**C**H_3), 20.16 (W = 32, -**C**H_3), -37.31 (W = 1940, -**C**$H_2{}^{i}$Pr).

ESI-MS (m/z) of $[C_{30}H_{63}Cl_3CrN_3.C_3H_{10}N]^+$: Calculated exact mass: 684.4276; found: 684.4388.

Anal. Calc. for $C_{30}H_{63}Cl_3CrN_3$ (%): C, 57.73; H, 10.17; N, 6.73. Found: C, 57.64; H, 10.25; N, 6.82.

5.1.4 Chromium Triflate Triazacyclohexane Catalysts

5.1.4.1 Chromium Triflates Synthesised from Chromium Chlorides

Synthesis of $(Pr_2CHCH_2)_3TACCr(OTf)_3$

$(Pr_2CHCH_2)_3TACCrCl_3$ (1.97 g, 3.4 mmol) was cooled with liquid nitrogen and approximately 10 mL of triflic acid was condensed onto the purple solids across all-glass linkages. The acid was then allowed to melt and the system opened up to a trap cooled with liquid nitrogen to catch any hydrogen chloride given off. Once the acid melts a violent reaction proceeds with considerable effervescence. Once the reaction was complete the acid was distilled off at 40 °C and 10^{-2} mbar over the course of a day. The dark blue solids were then washed twice with 25 mL of dry Et_2O under a nitrogen atmosphere to remove any further acid. Subsequent drying at reduced pressure led to 2.73 g (3.0 mmol, 88%) of a pale blue solid.

^{13}C NMR, *o*-$C_6H_4F_2$, **C**F doublet set to 149.9 ppm: δ = 49.52 (W = 138, -**C**H_2Et), 21.64 (W = 62, -**C**H_2Me), 15.16 (W = 41, -**C**H_3), -39.35 (W = 527, -**C**HPr_2).

^{19}F NMR, *o*-$C_6H_4F_2$, C**F** set to -139.4 ppm: δ = -45.56 (W = 3300).

Anal. Calc. for $C_{30}H_{57}CrF_9N_3O_9S_3$ (%): C, 39.04; H, 6.23; N, 4.55. Found: C, 38.81; H, 6.38; N, 4.32.

Synthesis of $(^iBu_2CH)_3TACCr(OTf)_3$

$(^iBu_2CH)_3TACCrCl_3$ (1.06 g, 1.7 mmol) was cooled with liquid nitrogen and approximately 10 mL of triflic acid was condensed onto the purple solids across all-glass linkages. The acid was then allowed to melt and the system opened up to a trap cooled with liquid nitrogen to catch any hydrogen chloride given off. Once the acid melts a violent reaction proceeds with considerable effervescence. Once the reaction was complete the acid was distilled off at 40 °C and 10^{-2} mbar over the course of a day. The dark blue solids were then washed four times with 25 mL of dry Et_2O under a nitrogen atmosphere to remove any further acid. Subsequent drying at reduced pressure led to 1.43 g (1.5 mmol, 87%) of a pale blue solid.

^{13}C NMR, *o*-$C_6H_4F_2$, **C**F doublet set to 149.9 ppm: δ = 36.85 (W = 111, -**C**HMe_2), 29.41 (W = 91, -**C**H_3), 23.51 (W = 32, -**C**H_3), -41.47 (W = 1240, -**C**$H_2{}^iPr$).

^{19}F NMR, *o*-$C_6H_4F_2$, C**F** set to -139.4 ppm: δ = -44.36 (W = 3400).

Anal. Calc. for $C_{33}H_{63}CrF_9N_3O_9S_3$ (%): C, 41.07; H, 6.58; N, 4.35. Found: C, 40.90; H, 6.75; N, 4.34.

5.1.4.2 Synthesis of Chromium(III) Triflate.

Trifluoromethanesulphonic acid (32.64 g, 19.2 mL, 218 mmol) was dissolved into de-ionised water (75 mL) by drop-wise addition due to the highly exothermic reaction. Considerable fuming was observed on addition of each drop. Granulated chromium (4.16 g, 80 mmol) was then added and stirred vigourously with no initial reaction observed. The solution was heated to 90 °C in the presence of oxygen and over the course of 48 hours became blue/violet in colour, indicative of $[Cr(H_2O)_6]^{3+}$ formation.[223]

The solution was filtered through sintered glass to remove the excess chromium before the solvent was removed under reduced pressure to give a viscous blue oil. The oil was heated to 100 °C under reduced pressure for one hour, leading to a pale green solid. Further heating to 300 °C under high vacuum (10^{-2} mbar), led to a dark green solid and a considerable quantity of water being collected over the course of an hour. The product demonstrated strong hydrophilicity, reverting back to a blue/green oil within seconds of exposure to air. The solid was ground by pestle and mortar under an argon atmosphere to give an extremely fine powder which was further dried under high vacuum. After drying, 32.2 g (64.4 mmol, 89%) of dark green powder was collected.

^{19}F NMR, *o*-$C_6H_4F_2$, C**F** set to -139.4 ppm: δ = -52.92 (W = 2900).

Anal. Calc. for $C_3CrF_9N_3O_9S_3$ (%): C, 7.22; H, 0.00; N, 0.00. Found: C, 7.12; H, 1.17; N, 0.00.

5.2 Chromium Triflate Substitution Reactions

Synthesis of $(Pr_2CHCH_2)_3TACCrCl_3$.

$(Pr_2CHCH_2)_3TACCr(OTf)_3$ (51.8 mg, 56 µmol) was added to tetramethylammonium chloride (35.4 mg, 320 µmol) before addition of *o*-$C_6H_4F_2$ (10 mL) to form a blue solution. The expected blue to purple colour change occurred within 10 minutes. The reaction was left overnight to ensure complete reaction. The purple solution was then eluted through a silica column with DCM, which was subsequently removed from the purple eluent under reduced pressure. The resulting solids were dried under high vacuum to give 24 mg (41 µmol, 74%) of a purple powder. Mass spectrometry and elemental analysis results correlated with those already stated.

Synthesis of ($Pr_2CHCH_2)_3TACCrBr_3$.

$(Pr_2CHCH_2)_3TACCr(OTf)_3$ (60.1 mg, 65 µmol) was added to tetramethylammonium bromide (53.0 mg, 344 µmol) under an argon atmosphere. *o*-$C_6H_4F_2$ (10 mL) was then added to give a blue solution over undissolved ammonium salts, which was stirred vigourously for 12 hours. A purple solution formed after two hours. The suspension was separated by column chromatography, eluting with DCM. The purple eluent was collected and the DCM removed under reduced pressure to give 35 mg (49 µmol, 75%) of a purple solid after drying under high vacuum for two hours. Crystals were obtained by evaporation of DCM from a saturated solution.

ESI-MS (m/z) $[C_{27}H_{57}Br_3CrN_3.C_3H_{10}N]^+$: Calculated exact mass: 772.2321; found: 772.2349.

Anal. Calc. for $C_{27}H_{57}Br_3CrN_3$ (%): C, 45.33; H, 8.03; N, 5.87. Found: C, 45.15; H, 7.90; N, 5.66.

Synthesis of ($Pr_2CHCH_2)_3TACCrI_3$.

$(Pr_2CHCH_2)_3TACCr(OTf)_3$ (51.4 mg, 56 µmol) was added to tetramethylammonium iodide (58.3 mg, 290 µmol) before addition of *o*-$C_6H_4F_2$ (10 mL) to form a saturated blue solution over solids. This was stirred vigourously over the course of 48 hours. The solution had changed from blue to a dark orange/brown colour during this time. The suspension was run through a silica column while eluting with *o*-$C_6H_4F_2$, which led to retention of a considerable quantity of green solid throughout, suggesting slow decomposition on contact with silica and leading to a severe reduction in yield. The orange/brown eluent was collected and the solvent removed to give 20 mg (23 µmol, 42%) of a dark orange solid after drying under high vacuum for two hours.

ESI-MS (m/z) $[C_{27}H_{57}I_3CrN_3.C_3H_{10}N]^+$: Calculated exact mass: 916.1905; found: 916.1934.

Anal. Calc. for $C_{27}H_{57}CrI_3N_3$ (%): C, 37.86; H, 6.71; N, 4.91. Found: C, 37.80; H, 6.64; N, 4.86.

Synthesis of ($Pr_2CHCH_2)_3TACCr(SCN)_3$.

$(Pr_2CHCH_2)_3TACCr(OTf)_3$ (52.4 mg, 57 µmol) was added to potassium thiocyanate (33.8 mg, 348 µmol) before addition of *o*-$C_6H_4F_2$ (10 mL) to form a saturated blue solution over solids. This was stirred vigourously over the course of 3 days. After one day the colour had changed from blue to dark blue/green. The solution was separated by column chromatography with *o*-$C_6H_4F_2$ eluent to give a blue solution which was collected and combined. The solvent was removed at reduced pressure to give 5.3 mg (8.2 µmol, 14%) of an oily turquoise solid

ESI-MS (m/z) $[C_{30}H_{57}CrN_6S_3.C_3H_{10}N]^+$: Calculated exact mass: 709.4025; found: 709.4060.

ESI-MS (m/z) $[C_{31}H_{57}CrN_7S_4]^-$: Calculated exact mass: 707.2963; found: 707.3060.

5.3 Optimised Liquid LAO Trimerisation Method

2 mg of catalyst, 250 equivalents of DMAO and 7500 equivalents of dry *o*-$C_6H_4F_2$ are added to the reaction vessel under argon to form a green solution which is agitated until completely homogenous (~2 minutes). 5000 equivalents of Na/K dried 1-hexene is then added, resulting in a yellow solution, and the vessel left under an argon atmosphere for the entirety of the reaction. An NMR sample is taken after one hour to test the initial activity of the catalyst before being returned to the bulk solution. The reaction is complete after 6 hours.

The trimer is extracted from the reaction mixture by exposing the solution to air before the drop-wise addition of methanol. This results in significant effervescence and the formation of white precipitate. Once no further reaction is observed, several drops of hydrochloric acid are added to solubilise the alumina solids, resulting in further effervescence. Addition of pentane results in the formation of a green 'aqueous' phase containing the aluminium and chromium species and a clear organic phase, which is collected.

The majority of the *o*-$C_6H_4F_2$ and hexenes are removed from the organic phase at 50 mbar and 40 ˚C. The remaining colourless liquid is transferred under high vacuum (10^{-3} mbar) at ~300 ˚C across a short bridge to a receiving flask in a cold water bath. A liquid nitrogen cooled trap is used to collect any remaining volatile components. The pure trimer collected is then analysed by NMR after addition of an internal TMS reference.

5.4 LAO Trimerisation Conditions

5.4.1 Activator Isomerisation Testing

The experimental data for testing of the isomerisation activity of the aluminium activators. The MAO was used as a toluene solution while TMA (trimethylaluminium) was used as a heptane solution.

Table 5.1 - The experimental data for the isomerisation testing of activators.

Activator	DMAO	MAO	TMA
Mass of Solution (mg)		541.2	115.1
Effective Mass (mg)	48.3	54.1	2.9
Mol (mmol Al)	0.80	0.90	0.04
***o*-$C_6H_4F_2$**			
Mass (mg)	3090	3240	1010
Mol (mmol)	27.1	28.4	8.9
Equivalents	34	32	222
1-Hexene			
Mass (mg)	1332	1439	85.1
Mol (mmol)	15.8	17.1	1.0
Equivalents	20	19	25
Isomerisation after 1 hour (mol%)	0.01	0.00	0.01
Isomerisation after 5 days (mol%)	0.51	0.07	0.02

5.4.2 Dilution Testing

The experimental data for increasing the dilution of the catalyst solution.

Table 5.2 - The experimental data for the testing of γ-Pe_2Cl at different dilutions.

Run	1	2	3
γ-Pe_2Cl			
Mass (mg)	4.4	4.2	5.6
Mol (μmol)	4.9	4.7	6.3
DMAO			
Mass (mg)	47.8	42.4	48.62
Mol (mmol Al)	0.79	0.70	0.81
Equivalents (Al)	162	150	129
***o*-$C_6H_4F_2$**			
Mass (mg)	477.9	849.6	1817.6
Mol (mmol)	4.2	7.4	15.9
Equivalents	853	1588	2549
1-Hexene			
Mass (mg)	880.7	792.8	1078.2
Mol (mmol)	10.5	9.4	12.8
Equivalents	2131	2009	2049
Conversion after 1.5 hours (%)	52	64	56
Conversion after 3 days (%)	90	87	81
Trimerisation (mol%)	79	83	91
Isomerisation (mol%)	21	17	10
Activity (TOF)	423	717	685
TON	1500	1451	1499

5.4.3 Analysis of Activity

The experimental data for increasing the equivalents of CaH_2 dried 1-hexene.

Table 5.3 - The experimental data for the activity testing of γ-Pe_2Cl.

Run	1	2	3	4
γ-Pe_2Cl				
Mass (mg)	5.6	5.6	5.1	4.8
Mol (μmol)	6.3	6.3	5.7	5.4
DMAO				
Mass (mg)	48.2	48.6	44.4	41.4
Mol (mmol Al)	0.80	0.81	0.74	0.69
Equivalents (Al)	128	129	130	128
***o*-$C_6H_4F_2$**				
Mass (mg)	1800.1	1817.6	1661.1	1549.3
Mol (mmol)	15.8	15.9	14.6	13.6
Equivalents	2524	2549	2557	2534
1-Hexene				
Mass (mg)	533.1	1078.2	1432.2	1852.2
Mol (mmol)	6.3	12.8	17.0	22.0
Equivalents	1013	2049	2989	4107
Conversion after 1.5 hours (%)	84	56	28	10
Conversion after 3 days (%)	93	81	63	20
Trimerisation (mol%)	87	91	87	38
Isomerisation (mol%)	13	10	13	62
Activity (TOF)	499	685	496	170
TON	827	1499	1627	311

5.4.4 Purification

The experimental data for increasing the equivalents of Na/K dried 1-hexene.

Table 5.4 - The experimental data for the activity testing of γ-Pe_2Cl.

Run	1	2	3	4
γ-Pe_2Cl				
Mass (mg)	1.1	1.0	1.0	1.0
Mol (μmol)	1.2	1.1	1.1	1.1
DMAO				
Mass (mg)	10.8	10.5	9.8	10.5
Mol (mmol Al)	0.18	0.18	0.16	0.17
Equivalents (Al)	153	154	153	153
***o*-$C_6H_4F_2$**				
Mass (mg)	1270.2	1243.5	1156.3	1233.5
Mol (mmol)	11.1	10.9	10.1	10.8
Equivalents	9499	9573	9557	9496
1-Hexene				
Mass (mg)	102.3	204.1	275.0	419.2
Mol (mmol)	1.2	2.4	3.3	5.0
Equivalents	1037	2130	3081	4375
Conversion after 1.5 hours (%)	74	81	81	82
Conversion after 3 days (%)	90	95	93	93
Trimerisation (mol%)	82	82	92	93
Isomerisation (mol%)	18	18	8	7
Activity (TOF)	512	1154	1664	2380
TON	767	1661	2644	3778

5.4.5 DMAO Equivalents Optimisation

The experimental data for increasing the equivalents of DMAO.

Table 5.5 - The experimental data for DMAO equivalents optimisation.

Run	1	2	3	4
γ-Pe_2Cl				
Mass (mg)	2.0	2.0	2.0	2.0
Mol (μmol)	2.2	2.2	2.2	2.2
DMAO				
Mass (mg)	5.9	11.8	28.9	58.2
Mol (mmol Al)	0.10	0.20	0.48	0.97
Equivalents (Al)	44	88	215	433
***o*-$C_6H_4F_2$**				
Mass (mg)	3160	3520	3430	3390
Mol (mmol)	27.7	30.9	30.1	29.7
Equivalents	12406	13820	13466	13309
1-Hexene				
Mass (mg)	1430	1360	1400	1380
Mol (mmol)	17.0	16.2	16.6	16.4
Equivalents	7611	7238	7451	7345
Conversion after 1.5 hours (%)	5	14	22	24
Conversion after 3 days (%)	9	39	73	72
Trimerisation (mol%)	76	90	93	92
Isomerisation (mol%)	24	10	7	8
Activity (TOF)	247	654	1105	1172
TON	687	2820	5441	5302

5.4.6 Halogen Effect - Activity Testing

The experimental data for increasing the equivalents of Na/K dried 1-hexene for the differently halogenated catalysts. The data for γ-Pe_2Cl was taken from Section 5.4.3.

Table 5.6 - The experimental data for the activity testing of γ-Pe_2Br.

Run	1	2	3	4
γ-Pe_2Br				
Mass (mg)	1.1	1.1	1.2	1.2
Mol (μmol)	1.0	1.0	1.1	1.1
DMAO				
Mass (mg)	9.3	9.2	9.4	10.0
Mol (mmol Al)	0.16	0.15	0.16	0.17
Equivalents (Al)	148	148	148	147
***o*-$C_6H_4F_2$**				
Mass (mg)	1268.5	1245.7	1279.4	1358.8
Mol (mmol)	11.1	10.9	11.2	11.9
Equivalents	10595	10601	10588	10567
1-Hexene				
Mass (mg)	90.0	166.9	259.8	390.1
Mol (mmol)	1.1	2.0	3.1	4.6
Equivalents	1019	1926	2915	4113
Conversion after 1.5 hours (%)	59	65	73	69
Conversion after 3 days (%)	67	77	80	78
Trimerisation (mol%)	98	94	86	66
Isomerisation (mol%)	2	6	14	34
Activity (TOF)	399	832	1420	1892
TON	675	1401	2009	2119

Table 5.7 - The experimental data for the activity testing of γ-Pe_2H.

Run	1	2	3	4
γ-Pe_2H				
Mass (mg)	1.1	1.1	1.1	0.8
Mol (μmol)	1.4	1.4	1.4	1.0
DMAO				
Mass (mg)	9.0	9.2	9.0	6.8
Mol (mmol Al)	0.15	0.15	0.15	0.11
Equivalents (Al)	108	110	108	112
***o*-$C_6H_4F_2$**				
Mass (mg)	1354.5	1379.6	1352.5	1019.8
Mol (mmol)	11.9	12.1	11.9	8.9
Equivalents	8554	8712	8541	8855
1-Hexene				
Mass (mg)	117.1	263.9	373.1	384.0
Mol (mmol)	1.4	3.1	4.4	4.6
Equivalents	1002	2260	3194	4520
Conversion after 1.5 hours (%)	26	78	62	78
Conversion after 3 days (%)	30	98	89	97
Trimerisation (mol%)	91	87	90	92
Isomerisation (mol%)	9	13	10	8
Activity (TOF)	176	1171	1318	2347
TON	274	1918	2558	4042

5.4.7 Halogen Effect - Stability Testing

The experimental data for stability testing of the differently halogenated catalysts.

Table 5.8 - The experimental data for the stability testing of γ-Pe_2Cl.

Addition Delay (hrs)	0	1	2	3	23
γ-Pe_2Cl					
Mass (mg)	4.9	4.7	4.4	4.8	4.8
Mol (μmol)	5.5	5.2	4.9	5.4	5.4
DMAO					
Mass (mg)	45.6	45.5	44.3	45.1	42.0
Mol (mmol Al)	0.76	0.76	0.74	0.75	0.70
Equivalents (Al)	136	146	151	139	129
***o*-$C_6H_4F_2$**					
Mass (mg)	446	480	422	449	500
Mol (mmol)	3.9	4.2	3.7	3.9	4.4
Equivalents	709	808	755	722	815
1-Hexene					
Mass (mg)	458	464	460	478	465
Mol (mmol)	5.4	5.5	5.5	5.7	5.5
Equivalents	995	1051	1113	1060	1031
Conversion after 1.5 hours (%)	68	71	67	66	65
Conversion after 3 days (%)	78	87	76	90	88
Trimerisation (mol%)	82	91	79	98	93
Isomerisation (mol%)	18	9	11	2	7
Activity (TOF)	451	497	497	466	447
TON	776	914	846	954	907

Table 5.9 - The experimental data for the stability testing of γ-Pe_2Br.

Addition Delay (hrs)	0	1	2	3	23
γ-Pe_2Br					
Mass (mg)	4.9	5.2	5.3	4.9	5.1
Mol (μmol)	4.8	5.1	5.1	4.8	5.0
DMAO					
Mass (mg)	44.9	43.3	44.0	45.3	45.2
Mol (mmol Al)	0.75	0.72	0.73	0.75	0.75
Equivalents (Al)	157	142	142	158	151
***o*-$C_6H_4F_2$**					
Mass (mg)	460	421	432	428	500
Mol (mmol)	4.0	3.7	3.8	3.8	4.4
Equivalents	847	730	735	788	884
1-Hexene					
Mass (mg)	465	458	449	484	467
Mol (mmol)	5.5	5.4	5.3	5.8	5.5
Equivalents	1161	1077	1036	1208	1120
Conversion after 1.5 hours (%)	27	24	37	17	3
Conversion after 3 days (%)	74	70	79	57	61
Trimerisation (mol%)	97	95	99	86	85
Isomerisation (mol%)	3	5	1	14	15
Activity (TOF)	209	172	256	137	22
TON	859	754	818	689	683

Table 5.10 - The experimental data for the stability testing of γ-Pe_2H.

Addition Delay (hrs)	0	1	2	3	23
γ-Pe_2H					
Mass (mg)	4.4	4.4	4.2	4.1	4.2
Mol (μmol)	5.6	5.6	5.3	5.2	5.3
DMAO					
Mass (mg)	42.4	49.6	45.4	44.9	45.0
Mol (mmol Al)	0.70	0.82	0.75	0.75	0.75
Equivalents (Al)	127	148	142	144	141
***o*-$C_6H_4F_2$**					
Mass (mg)	435.2	394.7	508.1	432.4	439.0
Mol (mmol)	3.8	3.5	4.5	3.8	3.8
Equivalents	687	623	840	733	726
1-Hexene					
Mass (mg)	440.8	530.9	453.2	440.2	452.5
Mol (mmol)	5.2	6.3	5.4	5.2	5.4
Equivalents	943	1136	1016	1011	1015
Conversion after 1.5 hours (%)	67	60	66	68	60
Conversion after 3 days (%)	69	65	64	63	65
Trimerisation (mol%)	72	69	69	67	71
Isomerisation (mol%)	28	31	31	33	29
Activity (TOF)	421	454	447	458	406
TON	651	739	650	637	659

5.4.8 External Halogen Effect

The experimental data for testing the effect of halogenoalkane additives.

Table 5.11 - The proportion of reagents within the stock solution used.

Reagent	Mass (mg)	Mol (mmol)	Equivalents
γ-Pe_2H	12	0.0151	
DMAO	228	3.78	250
o-$C_6H_4F_2$	12780	112	7398
1-Hexene	6358	75.5	4989
Total	19378		

Table 5.12 - The experimental data for addition of 1-chlorohexadecane.

Run	Control	1	2	3	4
Mass of Stock Solution (g)	5.2500	3.5302	3.5582	3.5012	3.6018
Mass Percentage (w%)	27	18	18	18	18
γ-Pe_2H					
Mass (mg)	3.3	2.2	2.2	2.2	2.2
Mol (mmol)	4.1	2.8	2.8	2.7	2.8
DMAO					
Mass (mg)	61.8	41.5	41.7	41.3	42.2
Mol (mmol Al)	1.0	0.7	0.7	0.7	0.7
***o*-$C_6H_4F_2$**					
Mass (mg)	3463.4	2326.0	2333.0	2313.2	2361.6
Mol (mmol)	30.4	20.4	20.4	20.3	20.7
1-Hexene					
Mass (mg)	1723.0	1157.1	1160.6	1150.8	1174.8
Mol (mmol)	20.5	13.7	13.8	13.7	14.0
1-Chlorohexadecane					
Mass (mg)	0	23.9	39.6	239.2	390.4
Mol (mmol)	0	0.09	0.15	0.92	1.50
Equivalents	0	33	55	335	535
Conversion after 1 hour (%)	10	7	2	1	~
Conversion after 3 days (%)	85	29	10	4	~
Trimerisation (mol%)	93	94	81	76	~
Isomerisation (mol%)	7	6	19	24	~
Activity (TOF)	479	335	94	38	~
TON	4214	1429	475	210	~

Table 5.13 - The experimental data for addition of 1-bromododecane.

Run	5	6	7	8
Mass of Stock Solution (g)	3.5344	3.5152	3.5356	3.5519
Mass Percentage (w%)	18	18	18	18
γ-Pe_2H				
Mass (mg)	2.2	2.2	2.2	2.2
Mol (μmol)	2.7	2.7	2.7	2.8
DMAO				
Mass (mg)	41.4	41.3	41.4	41.8
Mol (mmol Al)	0.69	0.69	0.69	0.69
***o*-$C_6H_4F_2$**				
Mass (mg)	2317.4	2313.2	2318.2	2338.7
Mol (mmol)	20.3	20.3	20.3	20.5
1-Hexene				
Mass (mg)	1152.9	1150.8	1153.2	1163.5
Mol (mmol)	13.7	13.7	13.7	13.8
1-Bromododecane				
Mass (mg)	22.7	37.2	228.4	374.0
Mol (mmol)	0.09	0.15	0.92	1.50
Equivalents	33	54	334	542
Conversion after 1 hour (%)	0.8	0.7	0.9	0.0
Conversion after 3 days (%)	1.6	1.3	2.1	0.6
Trimerisation (mol%)	34	32	38	18
Isomerisation (mol%)	66	68	62	82
Activity (TOF)	39	34	44	0
TON	78	63	105	31

5.4.9 Effect of *o*-$C_6H_4Cl_2$

The experimental data for testing the effect of *ortho*-dichlorobenzene.

Table 5.14 - The experimental data for *o*-$C_6H_4Cl_2$ doping.

Run	1	2	3
γ-Pe_2Cl			
Mass (mg)	2.0	2.0	2.0
Mol (μmol)	2.2	2.2	2.2
DMAO			
Mass (mg)	39.0	35.1	35.5
Mol (mmol Al)	0.65	0.58	0.59
Equivalents (Al)	290	261	264
***o*-$C_6H_4F_2$**			
Mass (mg)	2010	2143	0
Mol (mmol)	17.6	18.8	0
Equivalents	7891	8414	0
***o*-$C_6H_4Cl_2$**			
Mass (mg)	0	154.3	2120.1
Mol (mmol)	0	1.0	14.4
Equivalents	0	470	6460
1-Hexene			
Mass (mg)	925	833	926
Mol (mmol)	11.0	9.9	11.0
Equivalents	4923	4433	4928
Conversion after 1.5 hours (%)	28	20	2
Conversion after 3 days (%)	45	33	7
Trimerisation (mol%)	95	86	82
Isomerisation (mol%)	5	14	18
Activity (TOF)	1361	879	104
TON	2199	1476	349

5.4.10 Catalytic Potential of Alternative Chromium Halides

The experimental data for testing the performance of differently halogenated chromium catalysts.

Table 5.15 - The experimental data for each of the differently halogenated catalysts tested.

Catalyst	β-Pr_2	β-Pr_2(Br)	β-Pr_2(I)
Mass (mg)	2.0	2.4	2.9
Mol (μmol)	3.4	3.4	3.4
DMAO			
Mass (mg)	52.3	51.2	51.5
Mol (mmol Al)	0.87	0.85	0.86
Equivalents (Al)	255	250	252
***o*-$C_6H_4F_2$**			
Mass (mg)	2010	2110	1990
Mol (mmol)	17.6	18.5	17.4
Equivalents	5182	5439	5130
1-Hexene			
Mass (mg)	1530	1583	1551
Mol (mmol)	18.2	18.8	18.4
Equivalents	5347	5532	5420
Conversion after 1.5 hours (%)	7.4	1.4	1.2
Conversion after 3 days (%)	14.1	3.5	1.8
Trimerisation (mol%)	84	90	68
Isomerisation (mol%)	16	10	32
Activity (TOF)	397	79	64
TON	**756**	**196**	**97**

5.5 Defined Aluminate Synthesis and Doping

Synthesis of Potassium 1,1,1,3,3,3-hexafluoro-2-(trifluoromethyl)propan-2-olate (C_4F_9OK).

Potassium hydroxide (1.89 g, 33.7 mmol) was dissolved into water (50 mL) while cooling with an ice bath. Once the solution had reached 0 °C 1,1,1,3,3,3-hexafluoro-2-(trifluoromethyl)propan-2-ol (5 mL, 8.05 g, 34 mmol) was added and stirred for one hour. MS-TOF analysis indicated formation of the desired product. The solvent was removed at 100 °C under 10^{-3} mbar to give a white solid. Purification was achieved by sublimation of these solids at 190 °C under 10^{-3} mbar to give a white solid (6.00 g, 23.5 mmol, 69%). This process was slow but necessary as sublimation at higher temperatures led to decomposition and the formation of brown solids.

ESI-MS (m/z) $[C_4F_9O]^-$: Calculated exact mass: 234.9805; found: 234.9804.

Synthesis of $KAl(OC_4F_9)_4$.

Potassium 1,1,1,3,3,3-hexafluoro-2-(trifluoromethyl)propan-2-olate (0.31 g, 2.73 mmol) and 1,1,1,3,3,3-hexafluoro-2-(trifluoromethyl)propan-2-ol (2 mL, 3.22 g, 13.6 mmol) were dissolved into 50 mL of dry toluene under an argon atmosphere. Once fully dissolved the solution was frozen at -278 °C before drop-wise addition of 16.75 g of 1.1% $AlMe_3$ in toluene solution (0.18 g, 2.56 mmol). The $AlMe_3$ solution froze on contact. Once addition was complete the solution was allowed to warm to the melting point of toluene, -95 °C, at which the reaction was maintained. After 2 hours a white precipitate had formed as a suspension. The toluene was removed at 50 mbar to give a white solid, which was shown by NMR to be a mixture of $KAl(OC_4F_9)_4$, $KAl(OC_4F_9)_3F$ and $KAl(OC_4F_9)_2F_2$.

The solids were heated to 90 °C under 10^{-3} mbar, which led to partial sublimation. The sublimed solids were found to be the aluminium fluoride containing species. The remaining solids were left overnight under the same conditions, resulting in further sublimation and leaving the product as a pure white solid (1.83 g, 1.89 mmol, 74%).

ESI-MS (m/z) $[C_{16}AlF_{36}O_4]^-$: Calculated exact mass: 966.9037; found: 966.9115.

Catalyst Doping

The catalysis was carried out according to the optimised procedure for two parallel reactions. For the doped reaction the aluminate was added after the DMAO, prior to dissolution into a *o*-$C_6H_4F_2$ solution. No problems with solubility were observed. The quantities and catalyst performance are shown in Table 5.16.

Table 5.16 - The experimental data for aluminate doping.

Run	1	2
γ-Pe_2Cl		
Mass (mg)	2.0	2.0
mMol	2.2	2.2
DMAO		
Mass (mg)	26.9	26.5
Mol (mmol Al)	0.45	0.44
Equivalents (Al)	200	197
$KAl(OC_4F_9)_4$		
Mass (mg)	140.6	0
Mol (mmol)	0.14	0
Equivalents	63	0
***o*-$C_6H_4F_2$**		
Mass (mg)	2160	2040
Mol (mmol)	18.9	17.9
Equivalents	8480	8009
1-Hexene		
Mass (mg)	910	967
Mol (mmol)	10.8	11.5
Equivalents	4843	5147
Trimer Conversion at 1 hour (%)	7	7
Trimer Conversion at 3 days (%)	89	88
Trimerisation (mol%)	93	92
Isomerisation (mol%)	7	8
Activity (TOF)	334	355
TON	4315	4514

5.6 ^{13}C 1-Hexene Labelling

Due to the high costs associated with the use of ^{13}C labelled compounds it was imperative that yields were as high as possible. For this reason only limited analysis was performed at the intermediate stages of the synthesis.

Synthesis of [$Ph_3P^{13}CH_3$]I.

^{13}C-Enriched methyl iodide (1 g, entire contents of commercial vial, 7 mmol) was dissolved into toluene (20 mL) and cooled to -14 ˚C. Triphenylphosphine (1.90 g, 7.2 mmol) was then dissolved into the solution, which was stirred for 6 days. A white precipitate was gradually produced over this period. The toluene was removed under reduced pressure to give a white solid. The toluene was collected in a liquid nitrogen cooled trap and analysed by NMR spectroscopy, which indicated no methyl iodide was present. Based on this observation a 100% yield was assumed, 2.83 g (7 mmol) of phosphonium salt.

Synthesis of $Ph_3P^{13}CH_2$.

Sodium hydride (0.17 g, 7.2 mmol) was added to [$Ph_3PC^*H_3$]I (2.83 g, 7 mmol) followed by tetraglyme (8.44 g, 47.4 mmol) as solvent. A viscous white suspension was formed. This was stirred for 5 days under argon and gradually became a clear dark yellow solution.

Synthesis of $BuCH^{13}CH_2$.

Pentanal (0.60 g, 7.0 mmol) was added to the ylide solution under nitrogen along with *p*-cymene (1.5 g) to aid solubility. The solution was left to stir for 4 hours, during which time the triphenylphosphonate precipitated out. The solvent and 1-hexene were distilled off the white solid. Triisobutylaluminium (9.42 g, 47.4 mmol) was added to the solution in order to dry the 1-hexene and remove the tetraglyme *via* adduct formation. The remaining volatile components were removed under reduced pressure to give a 24.8 w% solution of enriched 1-hexene in *p*-cymene. NMR spectroscopy indicated 443 mg (74% over all three steps) was present in the solution.

^{1}H NMR, [*p*-cymene: 6.98 (4H, m), 2.75 (1H, m), 2.19 (3H, s), 1.18 (6H, d)]: δ = 5.72 (1H, m, J = 10.2 Hz, -C**H**C*H_2), 4.95 (2H, Two sets of d of d of d, $J_{C,H}$ = 152.2 Hz, =C***H**$_2$), 1.99 (2H, m, J = 6.5 Hz, -C**H**$_2$Pr), 1.30 (4H, m, -C**H**$_2$C**H**$_2$Me), 0.88 (3H, t, J = 6.8 Hz, -C**H**$_3$).

^{13}C NMR, [*p*-cymene: 145.1, 135.1, 129.4, 126.6, 34.3, 24.5, 21.2]: δ = 138.3 (d, $J_{C,C}$ = 69.4 Hz, -**C**HC*H_2), 114.6 (=**C***H_2), 34.1 (-**C**H_2Pr), 32.6 (-**C**H_2Et), 22.8 (-**C**H_2Me), 14.3 (-**C**H_3).

5.7 ^{2}H 1-Hexene Labelling

Synthesis of trans-1-D-1-Hexene.

Under an argon atmosphere, diisobutylaluminium hydride in hexane (34.8 g, 21 w%, 51.4 mmol) was added drop-wise to 1-hexyne (4.81 g, 58.6 mmol), previously dried over molecular sieves, at 0 °C over the course of five hours. The mixture was stirred for 2 days.

The solvent was removed under reduced pressure and the remaining oil diluted into *p*-cymene (10 mL) and again cooled to 0 °C before careful hydrolysis with D_2O (5 g, 250 mmol). The volatiles were vacuum transferred (10^{-2} mbar and 100 °C), then distilled at ambient pressure and 100 °C to give *trans*-1-D-1-hexene (3.02 g, 35.2 mmol, 60%) in *p*-cymene.

^{1}H NMR, [*p*-cymene: 7.23 (4H, m), 3.01 (1H, m), 2.45 (3H, s), 1.43 (6H, d)]: δ = 5.97 (1H, m, -C**H**CHD), 5.15 (1H, d, J = 9.9, =C**H**D), 2.24 (2H, q, J = 6.8, -C**H**$_2$Pr), 1.56 (4H, m, -C**H**$_2$C**H**$_2$Me), 1.14 (3H, m, -C**H**$_3$).

^{13}C NMR, [*p*-cymene: 145.6, 134.7, 129.0, 126.2, 34.0, 24.1, 20.8]: δ = 138.6 (-**C**HCHD), 113.9 (1:1:1 t, $J_{C,D}$ = 24.1, =**C**HD), 33.7 (-**C**H$_2$Pr), 31.4 (-**C**H$_2$Et), 22.4 (-**C**H$_2$Me), 13.9 (-**C**H$_3$).

^{2}H NMR, *p*-cymene [set to internal reference]: δ = 5.56 (d, $J_{C,D}$ = 16.6, =C**D**H).

Synthesis of cis-1-D-1-Hexene.

1-Hexyne (10 mL, 7.15 g, 87 mmol) was dissolved into *p*-cymene (50 mL) before addition of sodium hydride (2.21 g, 92 mmol). After being stirred for 2 hours, D_2O (1.8 mL, 1.8 g, 100 mmol) was added. The solution was then stirred for 3 hours. NMR spectroscopy indicated 60% deuteration after vacuum transfer of the product. Two repetitions of this technique gave an eventual deuteration of >99% and yielded 5.27 g (63.4 mmol, 73%) 1-D-1-hexyne in *p*-cymene.

Under an argon atmosphere, diisobutylaluminium hydride in hexane (49.9 g, 21 w%, 74 mmol) was added drop-wise to 1-D-1-hexyne (5.27 g, 61.9 mmol) at 0 °C over the course of five hours. The mixture was stirred for 2 days. The solvent was removed under reduced pressure to give a colourless viscous oil. The oil was diluted into *p*-cymene (10 mL) and cooled to 0 °C before careful hydrolysis with de-ionised water (1.65 g, 250 mmol) and left to stir for 12 hours. The volatile componants were vacuum transferred (10^{-2} mbar and 100 °C), then twice distilled at ambient pressure and 100 °C to give 1.01 g (12 mmol, 19%) of a colourless non-viscous oil.

^{1}H NMR, neat (TMS): δ = 5.88 (1H, m, -C**H**CHD), 5.01 (2H, d, J = 9.8, =C**H**D), 2.18 (2H, q, J = 7, -C**H**$_2$Pr), 1.49 (4H, m, -C**H**$_2$C**H**$_2$Me), 1.04 (3H, t, J = 6.7, -C**H**$_3$).

^{13}C NMR, neat (TMS): δ = 138.5 (-**C**HCHD), 113.8 (1:1:1 t, $J_{C,D}$ = 23.6, =**C**HD), 33.8 (-**C**H$_2$Pr), 31.5 (-**C**H$_2$Et), 22.7 (-**C**H$_2$Me), 13.8 (-**C**H$_3$).

^{2}H NMR, neat [set to internal reference]: δ = 5.30 (d, $J_{D,H}$ = 2.5, =CH**D**).

Synthesis of 2-D-1-Hexene.

Diisobutylaluminium deuteride was synthesized by addition of lithium aluminium deuteride (1.91 g, 45.5 mmol, 3.1 Eq.) to aluminium chloride (1.98 g, 14.8 mmol, 1 Eq.) and triisobutylaluminium (24.13 g, 121.7 mmol, 8.2 Eq.) and heating to 60 °C for 24 hours. The resulting grey slurry was extracted with hexane (3 x 100 mL) before all extractions were combined and the solvent removed under reduced pressure.

Under an argon atmosphere, diisobutylaluminium deuteride in hexane (12.22 g, 38 w%, 38.5 mmol) was added drop-wise to 1-hexyne (3.78 g, 46 mmol) at 0 °C over the course of five hours. The mixture was stirred for 2 days. The solvent was removed under reduced pressure to give a colourless viscous oil.

The oil was diluted into *p*-cymene (10 mL) and cooled to 0 °C before careful hydrolysis with de-ionised water (5 mL, 5.0 g, 250 mmol) and left to stir for 12 hours. The volatile componants were vacuum transferred (10^{-2} mbar and 100 °C), then twice distilled at ambient pressure and 100 °C to give 1.43 g (16.8 mmol, 31%) of a colourless non-viscous oil.

^{1}H NMR, [*o*-$C_6H_4F_2$: 6.99 (2H, m), 7.08 (2H, m)]: δ = 4.95 (1H, broad s, =C**H**H) 4.90 (1H, broad s, =CH**H**), 1.96 (2H, t, J = 7.2, -C**H**$_2$Pr), 1.26 (4H, m, -C**H**$_2$C**H**$_2$Me), 0.94 (3H, m, -C**H**$_3$).

^{13}C NMR, [*o*-$C_6H_4F_2$: 151.4, 149.4, 124.3, 116.8]: δ = 138.4 (1:1:1 t, $J_{C,D}$ = 22.3, -**C**DCH$_2$), 113.3 (=**C**H$_2$), 33.2 (-**C**H$_2$Pr), 30.9 (-**C**H$_2$Et), 21.9 (-**C**H$_2$Me), 13.0 (-**C**H$_3$).

^{2}H NMR, *o*-$C_6H_4F_2$ [set to internal reference]: δ = 5.89 (m, -C**D**=CH$_2$).

Synthesis of 1,1-D$_2$-1-Hexene.

Synthesis of Pentyltriphenylphosphonium Bromide:

Triphenylphosphine (8.90 g, 34.0 mmol) was placed under nitrogen and suspended in 1-bromopentane (10 mL, 12.18 g, 80.6 mmol). The mixture was heated to 110 °C and stirred for 15 hours, by which time a white paste had precipitated. The mixture was then cooled to room temperature and diluted with dry Et_2O (50 mL) before the solids were filtered off. The remaining solids were washed with further dry Et_2O (2 x 50 mL) and the solvent removed in vacuo to give a white solid (12.5 g, 30.3 mmol, 89%).

^{1}H NMR, $CDCl_3$: δ = 7.53-7.63 (15H, m, -P(C$_6$**H**$_5$)$_3$), 3.45 (2H, m, -C**H**$_2$Bu), 1.41 (4H, m, -C**H**$_2$C**H**$_2$Et), 1.09 (2H, m, -C**H**$_2$Me), 0.60 (3H, t, J = 7.3, -C**H**$_3$)

^{13}C NMR, $CDCl_3$: δ = 135.4 (d, J = 3, *p*-Ph), 133.0 (d, J = 10, *o*-Ph), 130.0 (d, J = 13, *m*-Ph), 117.6 (d, J = 86, *i*-Ph), 31.8 (d, J = 16, -**C**H$_2$Et), 22.2 (d, J = 50, -**C**H$_2$Bu), 21.6 (d, J = 5, -**C**H$_2$Pr), 21.5 (d, J = 1, -**C**H$_2$Me), 13.1 (-**C**H$_3$).

^{31}P NMR, $CDCl_3$ [set to internal reference]: δ = 24.1.

Synthesis of $Ph_3P{=}CHBu$:

Sodium hydride (280 mg, 11.67 mmol) and [Ph_3PCH_2Bu]Br (4.78 g, 11.56 mmol) were suspended in tetraglyme (13.3 g) under argon and stirred for three days. An orange solution formed during this time with some white/yellow solids precipitating. The solution was filtered to give 15.2 g of a clear solution. ^{1}H NMR integration indicated 21.9 w% product (3.33 g, 10.0 mmol, 87%).

^{1}H NMR, [Tetraglyme: -OC**H**$_3$ set to 3.27 (6H, s)]: δ = 7.39-7.59 (15H, m, =P(C$_6$**H**$_5$)$_3$), 2.04 (2H, m, -C**H**$_2$Pr), 1.35 (4H, m, -C**H**$_2$C**H**$_2$Me), 0.81 (3H, t, J = 6.91, -C**H**$_3$), 0.60 (1H, d of t, J = 17.3 and 7.5, -P=C**H**Bu).

^{13}C NMR, [Tetraglyme: -OC**H**$_3$ set to 58.58]: δ = 133.8 (d, J = 82.9, *i*-Ph,), 132.7 (d, J = 9.2, *o*-Ph), 130.9 (d, J = 2.6, *p*-Ph), 128.6 (d, J = 11.1, *m*-Ph), 38.8 (d, J = 11.7, -**C**H$_2$Pr), 29.4 (d, J = 5.8, -**C**H$_2$Et), 22.3 (-**C**H$_2$Me), 14.3 (-**C**H$_3$), 10.9 (d, J = 117.6, -P=**C**HBu).

^{31}P NMR, Tetraglyme [set to internal reference]: δ = 12.6.

Synthesis of 1,1-D_2-1-Hexene:

D_2-paraformaldehyde (280 mg, 8.8 mmol) was added to the entire ylide solution and left stirring overnight. The still orange solution was transferred under vacuum to yield a colourless liquid (558 mg, 6.5 mmol, 74%), with an orange solution remaining behind.

^{1}H NMR, neat [benzene reference set to 7.15]: δ = 5.66 (1H, m, -C**H**CD$_2$), 1.96 (2H, q, J = 7, -C**H**$_2$Pr), 1.28 (4H, m, -C**H**$_2$C**H**$_2$Me), 0.82 (3H, t, J = 6.7, -C**H**$_3$).

^{13}C NMR, neat [benzene reference set to 128.6]: δ = 138.8 (-**C**HCD$_2$), 113.9 (m, $J_{C,D}$ = 23.2, =**C**D$_2$), 34.1 (-**C**H$_2$Pr), 31.9 (-**C**H$_2$Et), 22.8 (-**C**H$_2$Me), 14.1 (-**C**H$_3$).

^{2}H NMR, neat [set to an internal reference]: δ = 4.86 (d, $J_{D,H}$ = 16.7, *trans*-CHC**D**D), 4.79 (d, $J_{D,H}$ = 6.4, *cis*-CHC**D**D).

5.8 Gaseous α-Olefin Trimerisation

Trimerisation of Propene.

26.9 mg (30 µmol) $(Pe_2(Cl)CHCH_2CH_2)_3TACCrCl_3$, 447.4 mg (7.5 mmol, 250 Eq.) DMAO and 22.49 g *o*-$C_6H_4F_2$ were weighed out under argon to give an activated catalyst solution. This was frozen with liquid nitrogen and degassed under high vacuum before being returned to room temperature and put under an atmosphere of propylene while stirring. No immediate colour change was observed but a water bath was required to cool the highly exothermic reaction. The progress of the reaction was monitored with the use of an oil bubbler by setting the propene cylinder regulator to equal the initial rate of propylene uptake. After 3 hours propene flowed through the bubbler unless the cylinder was completely sealed off, indicating the reaction was complete. The reaction was left to stir overnight under propylene, during which time a gradual change in colour from green to yellow was observed.

On complete reaction the system was opened to the air and the catalyst solution carefully hydrolysed with methanol and, subsequently, 32% hydrochloric acid in water. After extraction with pentane (3 x 50 mL) the extractions were combined and the pentane removed under reduced pressure. The remaining *o*-$C_6H_4F_2$ solution was then distilled at 140 °C and ambient pressure to concentrate the trimer. NMR spectroscopy indicated the remaining solution constituted 46 w% trimer (332 mg) and this was used for further analysis.

Trimerisation of 1-Butene.

Attempts at trimerising 1-butene according to the procedure described for propene proved unsuccessful due to the presence of a poison in the 1-butene. In order to ensure a successful reaction a system incorporating a sacrificial reaction was set up.

The sacrificial solution was made up of 30 µmol catalyst (26.9 mg), 185.6 mg (3 mmol, 100 Eq.) DMAO and 23.98 g *o*-$C_6H_4F_2$. The solution was frozen using liquid nitrogen and degassed under high vacuum before being warmed to -78 °C. Approximately 2 mL of 1-butene was then condensed into the solution which went cloudy after 30 minutes. A secondary flask was then attached containing 10 µmol catalyst (9.0 mg), 152.9 mg (2.5 mmol, 250 Eq.) DMAO and 8.62 g *o*-$C_6H_4F_2$. The fresh catalyst solution was frozen and degassed before the 1-butene of the original solution was condensed across at -78 °C in the same manner. After transfer of the 1-butene the secondary solution became yellow over the course of 12 hours. A third flask was attached, containing 10 µmol catalyst (9.0 mg), 150.8 mg (2.5 mmol, 250 Eq.) DMAO and 8.91 g *o*-$C_6H_4F_2$, and the process repeated. NMR analysis showed that 33.3 mg of trimer was present in the secondary flask and 19.7 mg was present in the third.

In order to get reasonable NMR analysis of the product these were combined, the aluminium species hydrolysed with water and extracted with pentane (3 x 50 mL). The pentane was removed at reduced pressure before the remaining solution was distilled at 100 mbar and 300°C without cooling of the receiving flask. This was repeated four times until there was >50 w% trimer by NMR spectroscopy integration.

The overall quantity of trimer had been reduced to 16 mg and this was analysed by ^{13}C NMR.

5.9 Branched Alcohol Synthesis

5.9.1 Synthesis of 2-Methyl-1-Hexanol

Synthesis of Diethyl Butylmethylmalonate.

Diethyl methylmalonate (2 mL, 2.04 g, 11.7 mmol) was diluted into dry THF (25 mL) under nitrogen. Sodium hydride (60 w% in mineral oil, 480.6 mg, 12 mmol) was suspended in a further 30 mL of dry THF and added drop-wise, resulting in considerable effervescence and a clear solution. After 30 minutes, 1-bromobutane (1.4 mL, 1.78 g, 13 mmol) was added. No immediate reaction was observed and the solution was heated to 50 °C. After two hours a precipitate became visible and the reaction was left to stir under nitrogen for three days.

The THF was removed under reduced pressure to give a viscous slurry, which was extracted with pentane (3 x 50 mL). The pentane was then removed at reduced pressure to give a pale yellow oil. This was transferred under vacuum (10^{-2} mbar and 150 °C) to give 1.67 g (7.2 mmol, 62%) of a colourless oil.

^1H NMR, $CDCl_3$: δ = 4.18 (4H, q, J = 7.2, -OC**H$_2$**Me), 1.85 (2H, t, J = 8.4, -C**H$_2$**Pr), 1.39 (3H, s, -CC**H$_3$**), 1.32 (4H, m, -C**H$_2$**C**H$_2$**Me), 1.25 (6H, t, J = 7.5, -OCH$_2$C**H$_3$**), 0.90 (3H, t, J = 7.2, -CH$_2$CH$_2$C**H$_3$**).

^{13}C NMR, $CDCl_3$: δ = 172.41 (**C**=O), 60.96 (-O**C**H$_2$Me), 53.59 (-**C**(Bu)Me), 35.19 (-**C**H$_2$Pr), 26.39 (-**C**H$_2$Et), 22.93 (-CH$_2$**C**H$_2$Me), 19.75 (-C**C**H$_3$), 13.99 (-OCH$_2$**C**H$_3$), 13.81 (-CH$_2$CH$_2$**C**H$_3$).

Synthesis of Ethyl 2-Methylhexanoate.

DMSO (10 mL) was mixed with de-ionised water (0.25 mL, 0.25 g, 13.8 mmol). Lithium chloride (1.24 g, 29.2 mmol) was then dissolved into the mixture which took some time and required vigourous stirring (very exothermic) and the system was put under nitrogen. Once dissolved, diethyl butylmethylmalonate (1.668 g, 7.2 mmol) was added and the mixture heated to 150 °C whilst stirring overnight.

The brown solution was decanted off yellow solids before 100 mL of pentane was added followed by 100 mL of de-ionised water to give two distinct phases, a brown aqueous layer and a yellow organic layer. The organic layer was extracted with further water (3 x 50 mL) and the combined water washings were extracted with 25 mL of pentane which was then combined with the original solution. The solvent was removed under reduced pressure to give a yellow oil. The oil was vacuum transferred (~150˚C, 10^{-2} mbar, liquid nitrogen bath) to give 0.61 g (3.9 mmol, 54%) of a colourless non-viscous oil.

^1H NMR, $CDCl_3$: δ = 4.11 (2H, q, J = 7.3, -OC**H$_2$**Me), 2.39 (1H, sextet, J = 7.0, -C**H**(Bu)Me), 1.64 and 1.39 (2H, m and m, -C**H$_2$**Pr), 1.29 (4H, m, -C**H$_2$**C**H$_2$**Me), 1.24

(3H, t, J = 7.0, -$OCH_2C\mathbf{H}_3$), 1.13 (3H, d, J = 7.3, -$CHC\mathbf{H}_3$), 0.89 (3H, t, J = 7.3, -$CH_2CH_2C\mathbf{H}_3$).

^{13}C NMR, $CDCl_3$: δ = 176.03 (**C**=O), 59.46 (-O**C**H_2Me), 39.14 (-**C**H**(**Bu)Me), 33.24 (-**C**H_2Pr), 29.13 (-**C**H_2Et), 22.28 (-$CH_2\mathbf{C}H_2$Me), 16.64 (-CH**C**H_3), 13.82 (-$OCH_2\mathbf{C}H_3$), 13.46 (-$CH_2CH_2\mathbf{C}H_3$).

Synthesis of 2-Methylhexanol.

Lithium aluminium hydride (0.45 g, 12.0 mmol) was added to 20 mL of dry Et_2O under nitrogen. The grey suspension was stirred vigourously and cooled to -0 °C as ethyl 2-methylhexanoate (0.610 g, 3.9 mmol) was added drop-wise. Considerable effervescence was observed with addition of each drop. After 30 minutes the suspension was hydrolysed with sequential addition of 5 mL water, 5 mL aqueous NaOH (20 w%) solution, 10 mL water and 10 mL aqueous NaOH (20 w%) solution. This gave a clear colourless organic phase above an aqueous phase containing a white slurry. The Et_2O was decanted off and the remaining aqueous phase washed with a further 3 x 100 mL of Et_2O, with all the Et_2O extractions then being combined. The Et_2O was removed at reduced pressure to give 0.28 g (2.4 mmol, 62%) of a colourless non-viscous oil.

^{1}H NMR, $CDCl_3$: δ = 3.74 (1H, broad s, -O**H**), 3.39 (2H, broad d of d, J = 30.7 and 6.8, -C**H**$_2$OH), 1.57 (1H, m, -C**H**(Bu)Me), 1.0 - 1.50 (6H, m, -$C\mathbf{H}_2C\mathbf{H}_2C\mathbf{H}_2$Me), 0.91 (3H, d, J = 6.9, -$CHC\mathbf{H}_3$), 0.89 (3H, t, J = 6.9, -$CH_2CH_2C\mathbf{H}_3$).

^{13}C NMR, $CDCl_3$: δ = 67.80 (**C**H_2OH), 35.62 (-**C**H**(**Bu)Me), 32.90 (-**C**H_2Pr), 29.19 (-**C**H_2Et), 22.93 (-$CH_2\mathbf{C}H_2$Me), 16.50 (-CH**C**H_3), 13.91 (-$CH_2CH_2\mathbf{C}H_3$).

5.9.2 Synthesis of 2-Ethyl-1-Pentanol

Synthesis of Diethyl Ethylpropylmalonate.

Diethyl ethylmalonate (2 mL, 2.00 g, 10.6 mmol) was diluted into dry THF (25 mL) under nitrogen. Sodium hydride (60 w% in mineral oil, 442.8 mg, 11 mmol) was suspended in a further 30 mL of dry THF and added drop-wise, resulting in considerable effervescence and a clear solution. After 30 minutes, 1-bromopropane (1.2 mL, 1.48 g, 12 mmol) was added. No immediate reaction was observed and the solution was heated to 50 °C. After two hours a precipitate became visible and the reaction was left to stir under nitrogen for three days.

The THF was removed under reduced pressure to give a viscous slurry, which was extracted with pentane (3 x 50 mL). The pentane was then removed at reduced pressure to give a pale yellow oil. This was transferred under vacuum (10^{-2} mbar and 150 °C) to give 1.45 g (6.3 mmol, 59%) of a colourless oil.

^{1}H NMR, $CDCl_3$: δ = 4.17 (4H, q, J = 7.3, -OC**H**$_2$Me), 1.92 (2H, q, J = 7.6, -CC**H**$_2$Me), 1.84 (2H, m, -CC**H**$_2$Et), 1.24 (6H, t, J = 7.1, -OCH$_2$C**H**$_3$), 1.23 (2H, m, -CH$_2$C**H**$_2$Me), 0.92 (3H, t, J = 7.3, -CCH$_2$C**H**$_3$), 0.82 (3H, t, J = 7.3, - CH$_2$CH$_2$C**H**$_3$).

^{13}C NMR, $CDCl_3$: δ = 171.32 (**C**=O), 60.43 (-O**C**H$_2$Me), 57.59 (-**C(**Pr)Et), 33.65 (-**C**H$_2$Et), 24.94 (-C**C**H$_2$Me), 17.00 (-CH$_2$**C**H$_2$Me), 14.03 (-CH$_2$CH$_2$**C**H$_3$), 13.72 (-OCH$_2$**C**H$_3$), 8.02 (-CCH$_2$**C**H$_3$).

Synthesis of Ethyl 2-Ethylpentanoate.

DMSO (10 mL) was mixed with de-ionised water (0.25 mL, 0.25 g, 13.8 mmol). Lithium chloride (1.21 g, 29.1 mmol) was then dissolved into the mixture which took some time and required vigourous stirring (very exothermic) and the system was put under nitrogen. Once dissolved, diethyl ethylpropylmalonate (1.447 g, 6.3 mmol) was added and the mixture heated to 150 °C whilst stirring overnight.

The brown solution was decanted off yellow solids before 100 mL of pentane was added followed by 100 mL of de-ionised water to give two distinct phases, a brown aqueous layer and a yellow organic layer. The organic layer was extracted with further water (3 x 50 mL) and the combined water washings were extracted with 25 mL of pentane which was then combined with the original solution. The solvent was removed under reduced pressure to give a yellow oil. The oil was vacuum transferred (~150 ˚C, 10^{-2} mbar, liquid nitrogen bath) to give 0.50 g (3.2 mmol, 51%) of a colourless non-viscous oil.

^{1}H NMR, $CDCl_3$: δ = 4.12 (2H, q, J = 7.0, -OC**H**$_2$Me), 2.39 (1H, m, -C**H**(Pr)Et), 1.62 (2H, m, -CHC**H**$_2$Me), 1.51 and 1.40 (2H, m, -CHC**H**$_2$Et), 1.31 (2H, m, -CHCH$_2$C**H**$_2$Me), 1.24 (3H, t, J = 7.1, -OCH$_2$C**H**$_3$), 0.91 (3H, t, J = 7.2, -CHCH$_2$C**H**$_3$), 0.89 (3H, t, J = 7.2, -CH$_2$CH$_2$C**H**$_3$).

^{13}C NMR, $CDCl_3$: δ = 175.46 (**C**=O), 59.30 (-O**C**H$_2$Me), 46.70 (-**C**H**(**Pr)Et), 34.00 (-**C**H$_2$Et), 25.16 (-CH**C**H$_2$Me), 20.24 (-CH$_2$**C**H$_2$Me), 13.83 (-OCH$_2$**C**H$_3$), 13.46 (-CHCH$_2$CH$_2$**C**H$_3$), 11.25 (-CHCH$_2$**C**H$_3$).

Synthesis of 2-Ethylpentanol.

Lithium aluminium hydride (0.39 g, 10.4 mmol) was added to 20 mL of dry Et_2O under nitrogen. The grey suspension was stirred vigourously and cooled to -0 °C as ethyl 2-ethylpentanoate (0.50 g, 3.2 mmol) was added drop-wise. Considerable effervescence was observed with addition of each drop. After 30 minutes the suspension was hydrolysed with sequential addition of 5 mL water, 5 mL aqueous NaOH (20 w%) solution, 10 mL water and 10 mL aqueous NaOH (20 w%) solution. This gave a clear colourless organic phase above an aqueous phase containing a white slurry. The Et_2O was decanted off and the remaining aqueous phase washed with a further 3 x 100 mL of Et_2O, with all the Et_2O extractions then being combined. The Et_2O was removed at reduced pressure to give 0.22 g (1.9 mmol, 59%) of a colourless non-viscous oil.

^{1}H NMR, $CDCl_3$: δ = 3.51 (2H, d of d, J = 30.2 and 7.1 -C**H$_2$**OH), 1.20 – 1.50 (7H, m, -C**H**(C**H**$_2$Me)C**H**$_2$C**H**$_2$Me), 0.91 (3H, t, J = 7.3, -CHCH$_2$C**H**$_3$), 0.89 (3H, t, J = 7.7, -CH$_2$CH$_2$C**H**$_3$).

^{13}C NMR, $CDCl_3$: δ = 64.61 (-**C**H$_2$OH), 41.63 (-**C**H(Pr)Et), 32.68 (-**C**H$_2$Et), 23.20 (-CH**C**H$_2$Me), 19.89 (-CH$_2$**C**H$_2$Me), 14.23 (-CHCH$_2$CH$_2$**C**H$_3$), 10.80 (-CHCH$_2$**C**H$_3$).

5.10 Air Sensitive Mass Spectrometry Procedure

A Bruker Daltonik micrOTOFQ electrospray quadrupole time-of-flight mass spectrometer was used. This was coupled to an MBraun glove box containing an argon atmosphere. An air-tight connector in the side of the glove box allowed for PEEK tubing to pass from the glove box to the mass spectrometer without exposure to air or moisture. The sample was injected directly into the tubing *via* syringe and the use of an adaptor. The instrument was calibrated post-acquisition using a range of sodium formate clusters. The observed mass and isotope pattern were considered to match the corresponding theoretical values calculated from the empirical formula when an error of less than 20 ppm was observed. The background spectrum was established before each run with the use of samples of each reagent.

The trimerisation catalysis analysed using the positive ion detection mode was carried out with the use of α-^{i}Bu$_2$(OTf) (2.5 mg, 2.6 µmol), AlMe$_3$ (2.5 w% in toluene, 4.9 mg, 68 µmol, 26 equivalents), 1-hexene (1.226 g, 14.6 mmol, 5600 equivalents) and *o*-$C_6H_4F_2$ (2.07 g, 18.2 mmol, 7000 equivalents). The reaction analysed using the negative ion detection mode was carried out using very similar conditions, though fewer equivalents of activator were used. The reagent and quantities were α-^{i}Bu$_2$(OTf) (2.5 mg, 2.6 µmol), AlMe$_3$ (2.5 w% in toluene, 1.9 mg, 26 µmol, 10 equivalents), 1-hexene (1.106 g, 13.1 mmol, 5000 equivalents) and *o*-$C_6H_4F_2$ (2.01 g, 18.1 mmol, 6900 equivalents).

Analysis of the sample was carried out in two stages, firstly within one minute of activator addition and secondly within one minute of 1-hexene addition. At least three aliquots of *o*-$C_6H_4F_2$ were run through the system before each sample was analysed to reduce the risk of contamination.

Conclusions

The work described herein demonstrates a significant contribution to the field of selective α-olefin trimerisation. Firstly, ethylene trimerisation is an intensively researched area of organometallic chemistry that is attracting ever more attention.[19] The results presented take this research further *via* the development of chromium chloride triazacyclohexane catalysts that demonstrate efficiencies similar to the best systems known. A significant improvement on previously published results for $(R_3TAC)CrCl_3$ systems has been demonstrated.[192] Activities have been drastically increased from 20,000 to 250,000 $mol(C_2H_4)\ mol(Cr)^{-1}\ h^{-1}$ while 1-hexene selectivities have also improved markedly from around 50 w% to 93 w%. As such, these systems are the fourth most active yet described, when measured per bar of ethylene pressure.[19] These extremely cheap catalysts therefore represent the first phosphine-free systems capable of competing with the expensive PNP catalyst.[97]

The vast improvements in performance were achieved principally by modification of the ancillary ligand and optimisation of the reaction conditions. The catalyst selectivity was found to be highly dependent on reaction temperature, with optimisation from 50 °C to 80 °C leading to a considerable improvement. Importantly, the formation of polyethylene was markedly reduced by the rise in temperature, which resulted in less reactor fouling. The presence of toluene was also found to be detrimental, while MAO was shown to be a more effective activator than MMAO. Catalyst modification focused on increasing the ligand bulk and resulted in further improvements in selectivity. Tetramerisation was almost completely repressed in this manner, while the formation of C_{10} co-trimers was significantly reduced. The activity of the system was unaffected, unless very bulky systems were used, resulting in greatly improved efficiencies.

Secondly, the bulk of this research focused on expanding the scope of trimerisation to include LAOs. This area of selective oligomerisation has only recently been established, with $(FI)TiMe_3$ and $(R_3TAC)CrCl_3$ catalysts the only active systems known.[2, 3, 193] The synthesis of a novel range of catalysts and the development of optimal reaction conditions led to highly active and >95 w% selective trimerisation systems. The species described outperformed previously published $(R_3TAC)CrCl_3$ species by a factor of five whilst also improving on selectivities. This also represents a twenty fold increase in activity over the $(FI)TiMe_3$ systems, making the catalysts described the most efficient LAO trimerisation catalysts yet discovered.

The principal side product was found to be 2-hexene, which was shown to result from a side reaction of the active catalyst. The mechanism for its production is proposed to be the π-allyl complex mechanism, based on the known chemistry of analogous chromium species. In addition, kinetic analysis indicated that the rate of trimerisation is first order relative to LAO concentration, suggesting a metallacyclopentane resting state.[19] The catalysts were found to behave differently to similar ethylene trimerisation systems, especially regarding the 'halogen effect'. The presence of halogenoalkanes induced decomposition rather than improved performance, which is proposed to result from the ready oxidation of Cr^I intermediates.

These systems presented an opportunity to investigate the metallacyclic mechanism in greater detail than is possible for ethylene systems. The slower rate of reaction, combined with branching in the intermediates, allowed for considerable insight into the chromacyclic species. Characterisation of the product regioisomers down to 0.1% abundance was in agreement with those proposed for the metallacyclic mechanism, with some alterations. [1,2] Migratory insertion was found to be considerably more favourable than initially envisaged while *exo*-cyclic β-hydride elimination could not be observed at all.[2] Product quantification also allowed the relative abundance of intermediates and catalytic pathways to be accurately estimated for the first time.

Analysis of elimination pathways using deuterium labelling provided further evidence of the metallacyclic mechanism. Direct competition was observed between β-hydride elimination from different positions within intermediates that gave the same product structure. This can only be explained by the simultaneous binding of the alkyl species to the metal at two positions, indicative of a metallacyclic species. Ligand and LAO bulk variation was also investigated intensively with considerable steric influence observed. Marked effects on the proportions of the chromacyclopentane intermediates strongly indicated that the oxidative cyclisation step is under steric control. In addition, considerable influence on elimination pathways was observed, indicating the significance of conformational change during β-hydride elimination.

Further mechanistic investigations led to characterisation of the side products of activation. The 2-methyl-1-hexene predicted by the original proposal was confirmed alongside several unexpected additional products.[2] These were found to result from chain transfer reactions between the alkylated catalyst and the aluminium activator. As a result, greater than one equivalent of LAO is required to activate the catalyst, which would reduce the rate of activation and could explain the initiation period observed during kinetic analysis. The intermediates of the catalysis were also investigated directly using air sensitive mass spectrometry. Using this method, signals were observed that matched those expected for the proposed chromacyclic intermediates, while those predicted for chain growth intermediates were absent. The existence of Cr^{I} and Cr^{III} under catalytic conditions was also confirmed, giving conclusive evidence for the proposed redox cycle for the first time.

This work has established $(R_3TAC)CrCl_3$ catalysts as highly efficient and adaptable selective trimerisation systems that can be used with a range of α-olefins. These cheap and readily synthesised species present considerable potential for future application in the production of co-monomers, fuels and lubricants.[71] Their stable and defined nature has also allowed considerable new insights into the mechanism. Both analysis of the products and direct observation of intermediates has provided firm evidence for the proposed metallacyclic mechanism and discredited the possibility of chain growth pathways to selective trimerisation.

Going forward, considerable scope remains for improving the performance of chromium triflate pre-catalysts and further exploiting their favourable properties for mechanistic investigations. In addition, the performance of the various trimers requires testing in order to determine their suitability for application as lubricants, fuels or chemical precursors. Overall, this work has established a strong foundation for the continued improvement of chromium triazacyclohexane pre-catalysts.

Acknowledgements

First and foremost, my thanks go to Dr Randolf Köhn for his guidance, advice and support throughout my time in his group. Your interest and enthusiasm, regardless of the outcome of experiments, was indispensable during difficult periods and greatly appreciated when progress was being made. The time and effort you have devoted towards supporting this research cannot be understated and has played a significant role in the discoveries made.

I would also like to thank my colleagues at LyondellBasell who were so welcoming during my three month placement in Frankfurt. The kindness extended by those I worked with, especially Daniella Jahn, Michael Schiendorfer, Volker Fraaije, Shahram Mihan and Heike Gregorius, allowed me to settle into the unfamiliar surroundings quickly and enjoy the city to its fullest. The training and experience you provided is greatly appreciated and will be incredibly useful going forward.

During this research I have relied on technical support from several people in order to use a variety of analytical techniques. I would like to thank Dr Rhodri Owen and Heather Parker for the considerable amount of time they put aside to help with GCMS analysis. I also need to thank Dr Anneke Lubben, without whom the air sensitive mass spectrometry research would not have been possible. My appreciation goes to Dr John Lowe for the work he performed in setting up the ^{13}C-^{13}C COSY NMR program that was essential for this research. Dr Gabriele Kociok-Köhn also receives my sincere thanks for performing all of the single crystal X-ray diffraction analysis and never tiring of my hedgehogs. Your patience and perseverance led to some important results that contributed significantly to this work.

I would also like to thank those colleagues with whom I have shared an office and the last three years. The friendly and supportive environment ensured that spirits were always high and ideas could always be discussed. My thanks go to Ben Hodges, James Tyson, David Gonzalez Calatayud and Sophia Sarpaki. In particular, I need to thank Fernando Cortezon Tamarit for being so hard working that I felt guilty leaving before 7 pm, a great deal of work can be attributed to the extra hours you provoked.

Finally, I need to thank those who have supported me during my postgraduate degree and the writing of this thesis. My family and that of my girlfriend have provided me with constant support for the many aspects of a thesis that don't get written down. Most importantly, I need to thank Katie for responding to my frequent protestations about formatting errors with a smile and a patronising pat on the head. Producing this thesis has been infinitely easier with you by my side and for that you have my deepest gratitude.

My thanks also go jointly to the EPSRC and LyondellBasell GmbH for financial support.

References

1. J. Skupinska, *Chem. Rev.*, 1991, **91**, 613-648.
2. R. D. Köhn, M. Haufe, G. Kociok-Köhn, S. Grimm, P. Wasserscheid and W. Keim, *Angew. Chem., Int. Ed.*, 2000, **39**, 4337.
3. P. Wasserscheid, S. Grimm, R. D. Köhn and M. Haufe, *Adv. Synth. Catal.*, 2001, **343**, 814-818.
4. L. H. Do, J. A. Labinger and J. E. Bercaw, *Organometallics*, 2012, **31**, 5143-5149.
5. D. F. Wass, *Dalton Trans.*, 2007, **8**, 816-819.
6. *US Pat.*, US7081557-B2, 2005.
7. G. Wilke, *Angew. Chem., Int. Ed.*, 2003, **42**, 5000-5008.
8. *US Pat.*, US2943125, 1960.
9. A. F. Hill, *Organotransition Metal Chemistry*, The Royal Society of Chemistry, Cambridge, 2002.
10. P. Cossee, *J. Catal.*, 1964, **3**, 80-88.
11. S. Wang, J. Li, G. Wang, B. Zhang and J. Qu, *Gaofenzi Tongbao*, 2012, **106**, 122-126.
12. *Eur. Pat.*, DE2053758A, 1971.
13. *Eur. Pat.*, DE2062293A, 1971.
14. P. Kuhn, D. Semeril, D. Matt, M. J. Chetcuti and P. Lutz, *Dalton Trans.*, 2007, **5**, 515-528.
15. *U. S. Pat.*, US3686351, 1972.
16. W. Keim, *Chem. Ind.*, 1984, **36**, 397-399.
17. A. Forestiere, H. Olivier-Bourbigou and L. Saussine, *Oil Gas Sci. Technol.*, 2009, **64**, 649-667.
18. M. J. Hanton, L. Daubney, T. Lebl, S. Polas, D. M. Smith and A. Willemse, *Dalton Trans.*, 2010, **39**, 7025-7037.
19. D. S. McGuinness, *Chem. Rev.*, 2011, **111**, 2321-2341.
20. P. Boulens, E. Pellier, E. Jeanneau, J. N. H. Reek, H. Olivier-Bourbigou and P.-A. R. Breuil, *Organometallics*, 2015, **34**, 1139-1142.
21. M. L. H. Green, *Adv. Organomet. Cat.*, 1970, **8**, 29.
22. A. R. Fraser, P. H. Bird, S. A. Bezman, J. R. Shapley, R. White and J. A. Osborn, *J. Amer. Chem. Soc.*, 1973, **95**, 597-598.
23. M. J. Doyle, J. McMeeking and P. Binger, *J. Chem. Soc., Chem. Commun.*, 1976, **11**, 376-379.
24. J. R. Blackborow, U. Feldhoff, F. W. Grevels, R. H. Grubbs and A. Miyashita, *J. Organomet. Chem.*, 1979, **173**, 253-261.
25. P. Binger, *Angew. Chem., Int. Ed.*, 1972, **11**, 433-434.
26. P. Binger, *Angew. Chem., Int. Ed.*, 1972, **11**, 309-310.
27. C. G. Biefeld, H. A. Eick and R. H. Grubbs, *Inorg. Chem.*, 1973, **12**, 2166-2170.
28. J. X. McDermott, J. F. White and G. M. Whitesides, *J. Amer. Chem. Soc.*, 1973, **95**, 4451-4452.
29. G. B. Young and G. M. Whitesides, *J. Am. Chem. Soc.*, 1978, **100**, 5808-5815.
30. P. Diversi, G. Ingrosso, A. Lucherini, W. Porzio and M. Zocchi, *J. Chem. Soc., Chem. Commun.*, 1977, **22**, 811-812.
31. P. Diversi, G. Ingrosso and A. Lucherini, *J. Chem. Soc., Chem. Commun.*, 1977, **2**, 52-53.
32. J. X. McDermott, M. E. Wilson and G. M. Whitesides, *J. Am. Chem. Soc.*, 1976, **98**, 6529-6536.
33. T. Takahashi, M. Tamura, M. Saburi, Y. Uchida and E. Negishi, *J. Chem. Soc., Chem. Commun.*, 1989, **13**, 852-853.
34. P. Diversi, G. Ingrosso and A. Lucherini, *J. Chem. Soc., Chem. Commun.*, 1978, **17**, 735-736.
35. J. X. McDermott and G. M. Whitesides, *J. Amer. Chem. Soc.*, 1974, **96**, 947-948.

36. R. Emrich, O. Heinemann, P. W. Jolly, C. Krueger and G. P. J. Verhovnik, *Organometallics*, 1997, **16**, 1511-1513.
37. R. DiCosimo, S. S. Moore, A. F. Sowinski and G. M. Whitesides, *J. Am. Chem. Soc.*, 1982, **104**, 124-133.
38. J. X. McDermott, J. F. White and G. M. Whitesides, *J. Am. Chem. Soc.*, 1976, **98**, 6521-6528.
39. R. H. Grubbs, A. Miyashita, M. Liu and P. Burk, *J. Am. Chem. Soc.*, 1978, **100**, 2418-2425.
40. R. H. Grubbs and A. Miyashita, *J. Am. Chem. Soc.*, 1978, **100**, 1300-1302.
41. R. H. Grubbs and A. Miyashita, *J. Chem. Soc., Chem. Commun.*, 1977, **23**, 864-865.
42. R. H. Grubbs and A. Miyashita, *J. Am. Chem. Soc.*, 1978, **100**, 7416-7418.
43. R. H. Grubbs and A. Miyashita, *Fundam. Res. Homogeneous Catal.*, 1979, **3**, 151-163.
44. U. Dorf, K. Engel and G. Erker, *Angew. Chem.*, 1982, **94**, 916-917.
45. G. Erker, K. Engel, U. Dorf, J. L. Atwood and W. E. Hunter, *Angew. Chem.*, 1982, **94**, 915-916.
46. H. G. Alt and C. E. Denner, *J. Organomet. Chem.*, 1990, **390**, 53-60.
47. M. D. Spencer, P. M. Morse, S. R. Wilson and G. S. Girolami, *J. Am. Chem. Soc.*, 1993, **115**, 2057-2059.
48. Y. You and G. S. Girolami, *Organometallics*, 2008, **27**, 3172-3180.
49. G. P. Belov, T. S. Dzhabiev and I. M. Kolesnikov, *J. Mol. Catal.*, 1982, **14**, 105-112.
50. B. Bogdanovic and G. Wilke, *Brennstoff-Chemie*, 1968, **49**, 323.
51. B. Bogdanovic, B. Spliethoff and G. Wilke, *Angew. Chem., Int. Ed.*, 1980, **19**, 622-623.
52. G. Wilke, B. Bogdanovic, P. Hardt, P. Heimbach, W. Keim, M. Kroner, W. Oberkirch, K. Tanaka, E. Steinruc, D. Walter and H. Zimmerman, *Angew. Chem., Int. Ed.*, 1966, **5**, 151.
53. J. K. Hambling, *Chem. Brit.*, 1969, **5**, 354-359.
54. S. J. McLain, J. Sancho and R. R. Schrock, *J. Am. Chem. Soc.*, 1980, **102**, 5610-5618.
55. W. E. Piers, P. J. Shapiro, E. E. Bunel and J. E. Bercaw, *Syn. Lett.*, 1990, **2**, 74-84.
56. J. Christoffers and R. G. Bergman, *J. Am. Chem. Soc.*, 1996, **118**, 4715-4716.
57. *Universal Pat.*, WO2011003046A1, 2011.
58. *Universal Pat.*, WO2011003044A1, 2011.
59. *Universal Pat.*, WO2011003047A1, 2011.
60. J. R. V. Lang, C. E. Denner and H. G. Alt, *J. Mol. Catal. A: Chem.*, 2010, **322**, 45-49.
61. J. Christoffers and R. G. Bergman, *Inorg. Chim. Acta*, 1998, **270**, 20-27.
62. E. Hauptman, S. Sabo-Etienne, P. S. White, M. Brookhart, J. M. Garner, P. J. Fagan and J. C. Calabrese, *J. Am. Chem. Soc.*, 1994, **116**, 8038-8060.
63. C.-Y. Ho and L. He, *Angew. Chem., Int. Ed.*, 2010, **49**, 9182-9186.
64. A. Miyashita, S. Ikezu and H. Nohira, *Chem. Lett.*, 1985, 1235-1238.
65. T. V. RajanBabu, *Chem. Rev.*, 2003, **103**, 2845-2860.
66. *US Pat.*, US2846425, 1958.
67. V. N. Panchenko, V. A. Zakharov and E. A. Paukshtis, *Appl. Catal., A*, 2006, **313**, 130-136.
68. R. Messere, A. F. Noels, P. Dournel, N. Zandona, J. Breulet and S. A. Solvay, *Proceedings of International Congress on Metallocene Polymers*, Schotland Business Research, Duesseldorf, 1996, 309-322.
69. M. P. McDaniel, *Review of Phillips Chromium Catalyst for Ethylene Polymerization*, Wiley, New York, 2010, 291-446.
70. *Eur. Pat.*, EP 0417477, 1991.
71. J. T. Dixon, M. J. Green, F. M. Hess and D. H. Morgan, *J. Organomet. Chem.*, 2004, **689**, 3641-3668.
72. R. W. J. Van, C. Grove, J. P. Steynberg, K. B. Stark, J. J. Huyser and P. J. Steynberg, *Organometallics*, 2004, **23**, 1207-1222.

73. A. Jabri, C. B. Mason, Y. Sim, S. Gambarotta, T. J. Burchell and R. Duchateau, *Angew. Chem. Int. Ed.*, 2008, **47**, 9717-9721.
74. I. Y. Skobelev, V. N. Panchenko, O. Y. Lyakin, K. P. Bryliakov, V. A. Zakharov and E. P. Talsi, *Organometallics*, 2010, **29**, 2943-2950.
75. Y. Fang, Y. Liu, Y. Ke, C. Guo, N. Zhu, X. Mi, Z. Ma and Y. Hu, *Appl. Catal., A*, 2002, **235**, 33-38.
76. J. R. Briggs, *J. Chem. Soc., Chem. Commun.*, 1989, **11**, 674-675.
77. R. M. Manyik, W. E. Walker and T. P. Wilson, *J. Catal.*, 1977, **47**, 197-209.
78. A. Bollmann, K. Blann, J. T. Dixon, F. M. Hess, E. Killian, H. Maumela, D. S. McGuinness, D. H. Morgan, A. Neveling, S. Otto, M. Overett, A. M. Z. Slawin, P. Wasserscheid and S. Kuhlmann, *J. Am. Chem. Soc.*, 2004, **126**, 14712-14713.
79. J. F. Young, G. P. A. Yap and K. H. Theopold, *234th ACS National Meeting*, American Chemical Society, Boston, 2007, INOR-554.
80. S. Peitz, B. R. Aluri, N. Peulecke, B. H. Mueller, A. Woehl, W. Mueller, M. H. Al-Hazmi, F. M. Mosa and U. Rosenthal, *Chem. Eur. J.*, 2010, **16**, 7670-7676.
81. C. Pellecchia, M. Mazzeo and G.-J. Gruter, *Macromol. Rapid Commun.*, 1999, **20**, 337-340.
82. D. J. Gillis, R. Quyoum, M.-J. Tudoret, Q. Wang, D. Jeremic, A. W. Roszak and M. C. Baird, *Organometallics*, 1996, **15**, 3600-3605.
83. D. J. Gillis, M. J. Tudoret and M. C. Baird, *J. Am. Chem. Soc.*, 1993, **115**, 2543-2545.
84. J. Sassmannshausen, *Organometallics*, 2000, **19**, 482-489.
85. B. Hessen, *J. Mol. Catal. A: Chem.*, 2004, **213**, 129-135.
86. P. J. W. Deckers, B. Hessen and J. H. Teuben, *Angew. Chem., Int. Ed.*, 2001, **40**, 2516-2519.
87. P. J. W. Deckers, B. Hessen and J. H. Teuben, *Organometallics*, 2002, **21**, 5122-5135.
88. J. Huang, T. Wu and Y. Qian, *Chem. Commun.*, 2003, **22**, 2816-2817.
89. T. Wu, Y. Qian and J. Huang, *J. Mol. Catal. A: Chem.*, 2004, **214**, 227-229.
90. Y. Zhang, H. Ma and J. Huang, *J. Mol. Catal. A: Chem.*, 2013, **373**, 85-95.
91. Y. Suzuki, S. Kinoshita, A. Shibahara, S. Ishii, K. Kawamura, Y. Inoue and T. Fujita, *Organometallics*, 2010, **29**, 2394-2396.
92. I. E. Soshnikov, N. V. Semikolenova, J. Ma, K. Q. Zhao, V. A. Zakharov, K. P. Bryliakov, C. Redshaw and E. P. Talsi, *Organometallics*, 2014, **33**, 1431-1439.
93. C. Andes, S. B. Harkins, S. Murtuza, K. Oyler and A. Sen, *J. Am. Chem. Soc.*, 2001, **123**, 7423-7424.
94. R. Arteaga-Muller, H. Tsurugi, T. Saito, M. Yanagawa, S. Oda and K. Mashima, *J. Am. Chem. Soc.*, 2009, **131**, 5370-5371.
95. *Eur. Pat.*, WO2001068572A1, 2001.
96. M. Ohashi, T. Kawashima, T. Taniguchi, K. Kikushima and S. Ogoshi, *Organometallics*, 2015, **34**, 1604-1607.
97. A. Carter, S. A. Cohen, N. A. Cooley, A. Murphy, J. Scutt and D. F. Wass, *Chem. Commun.*, 2002, 858-859.
98. T. Agapie, S. J. Schofer, J. A. Labinger and J. E. Bercaw, *J. Am. Chem. Soc.*, 2004, **126**, 1304-1305.
99. T. Agapie, J. A. Labinger and J. E. Bercaw, *J. Am. Chem. Soc.*, 2007, **129**, 14281-14295.
100. T. Agapie, J. A. Labinger and J. E. Bercaw, *J. Am. Chem. Soc.*, 2007, **129**, 14281-14295.
101. L. H. Do, J. A. Labinger and J. E. Bercaw, *ACS Catal.*, 2013, **3**, 2582-2585.
102. K. Blann, A. Bollmann, H. De Bod, J. T. Dixon, E. Killian, P. Nongodlwana, M. C. Maumela, H. Maumela, A. E. McConnell, D. H. Morgan, M. J. Overett, M. Pretorius, S. Kuhlmann and P. Wasserscheid, *J. Catal.*, 2007, **249**, 244-249.
103. N. Cloete, H. G. Visser, I. Engelbrecht, M. J. Overett, W. F. Gabrielli and A. Roodt, *Inorg. Chem.*, 2013, **52**, 2268-2270.

104. M. J. Overett, K. Blann, A. Bollmann, J. T. Dixon, D. Haasbroek, E. Killian, H. Maumela, D. S. McGuinness and D. H. Morgan, *J. Am. Chem. Soc.*, 2005, **127**, 10723-10730.
105. S. Sa, S. M. Lee and S. Y. Kim, *J. Mol. Catal. A: Chem.*, 2013, **378**, 17-21.
106. J. A. Suttil, P. Wasserscheid, D. S. McGuinness, M. G. Gardiner and S. J. Evans, *Catal. Sci. Technol.*, 2014, **4**, 2574-2588.
107. T. E. Stennett, T. W. Hey, L. T. Ball, S. R. Flynn, J. E. Radcliffe, C. L. McMullin, R. L. Wingad and D. F. Wass, *Chem. Cat. Chem.*, 2013, **5**, 2946-2954.
108. *Eur. Pat.*, WO2009006979A2, 2009.
109. B. R. Aluri, N. Peulecke, S. Peitz, A. Spannenberg, B. H. Muller, S. Schulz, H.-J. Drexler, D. Heller, M. H. Al-Hazmi, F. M. Mosa, A. Wohl, W. Muller and U. Rosenthal, *Dalton Trans.*, 2010, **39**, 7911-7920.
110. A. Woehl, W. Mueller, S. Peitz, N. Peulecke, B. R. Aluri, B. H. Mueller, D. Heller, U. Rosenthal, M. H. Al-Hazmi and F. M. Mosa, *Chem. Eur. J.*, 2010, **16**, 7833-7842.
111. A. Woehl, W. Mueller, N. Peulecke, B. H. Mueller, S. Peitz, D. Heller and U. Rosenthal, *J. Mol. Catal. A: Chem.*, 2009, **297**, 1-8.
112. N. Peulecke, B. H. Mueller, S. Peitz, B. R. Aluri, U. Rosenthal, A. Woehl, W. Mueller, M. H. Al-Hazmi and F. M. Mosa, *Chem. Cat. Chem.*, 2010, **2**, 1079-1081.
113. S. Peitz, N. Peulecke, B. R. Aluri, S. Hansen, B. H. Mueller, A. Spannenberg, U. Rosenthal, M. H. Al-Hazmi, F. M. Mosa, A. Woehl and W. Mueller, *Eur. J. Inorg. Chem.*, 2010, 1167-1171.
114. Y. Zhou, H. Wu, S. Xu, X. Zhang, M. Shi and J. Zhang, *Dalton Trans.*, 2015, **44**, 9545-9550.
115. I. Thapa, S. Gambarotta, I. Korobkov, R. Duchateau, S. V. Kulangara and R. Chevalier, *Organometallics*, 2010, **29**, 4080-4089.
116. Y. Shaikh, K. Albahily, M. Sutcliffe, V. Fomitcheva, S. Gambarotta, I. Korobkov and R. Duchateau, *Angew. Chem., Int. Ed.*, 2012, **51**, 1366-1369.
117. Y. Shaikh, J. Gurnham, K. Albahily, S. Gambarotta and I. Korobkov, *Organometallics*, 2012, **31**, 7427-7433.
118. Y. Yang, J. Gurnham, B. Liu, R. Duchateau, S. Gambarotta and I. Korobkov, *Organometallics*, 2014, **20**, 5749-5757.
119. Y. Yang, Z. Liu, B. Liu and R. Duchateau, *ACS Catal.*, 2013, **3**, 2353-2361.
120. O. L. Sydora, T. C. Jones, B. L. Small, A. J. Nett, A. A. Fischer and M. J. Carney, *ACS Catal.*, 2012, **2**, 2452-2455.
121. K. Albahily, D. Al-Baldawi, S. Gambarotta, R. Duchateau, E. Koc and T. J. Burchell, *Organometallics*, 2008, **27**, 5708-5711.
122. K. Albahily, V. Fomitcheva, Y. Shaikh, E. Sebastiao, S. I. Gorelsky, S. Gambarotta, I. Korobkov and R. Duchateau, *Organometallics*, 2011, **30**, 4201-4210.
123. D. S. McGuinness, P. Wasserscheid, W. Keim, C. Hu, U. Englert, J. T. Dixon and C. Grove, *Chem. Commun.*, 2003, 334-335.
124. A. Alzamly, S. Gambarotta and I. Korobkov, *Organometallics*, 2013, **32**, 7204-7212.
125. D. S. McGuinness, P. Wasserscheid, W. Keim, D. Morgan, J. T. Dixon, A. Bollmann, H. Maumela, F. Hess and U. Englert, *J. Am. Chem. Soc.*, 2003, **125**, 5272-5273.
126. D. S. McGuinness, D. B. Brown, R. P. Tooze, F. M. Hess, J. T. Dixon and A. M. Z. Slawin, *Organometallics*, 2006, **25**, 3605-3610.
127. C. Temple, A. Jabri, P. Crewdson, S. Gambarotta, I. Korobkov and R. Duchateau, *Angew. Chem., Int. Ed.*, 2006, **45**, 7050-7053.
128. C. N. Temple, S. Gambarotta, I. Korobkov and R. Duchateau, *Organometallics*, 2007, **26**, 4598-4603.
129. M. E. Bluhm, O. Walter and M. Doering, *J. Organomet. Chem.*, 2005, **690**, 713-721.
130. M. J. Overett, K. Blann, A. Bollmann, V. R. de Villiers, J. T. Dixon, E. Killian, M. C. Maumela, H. Maumela, D. S. McGuinness, D. H. Morgan, A. Rucklidge and A. M. Z. Slawin, *J. Mol. Catal. A: Chem.*, 2008, **283**, 114-119.
131. J. Zhang, X. Wang, X. Zhang, W. Wu, G. Zhang, S. Xu and M. Shi, *ACS Catal.*, 2013, **3**, 2311-2317.

132. *US Pat.*, WO2006096881A1, 2006.
133. M. Ronellenfitsch, H. Wadepohl and M. Enders, *Organometallics*, 2014, **20**, 5758-5766.
134. *US Pat.*, US20020035029A1, 2002.
135. J. Zhang, A. Li and T. S. A. Hor, *Dalton Trans.*, 2009, 9327-9333.
136. J. Zhang, P. Braunstein and T. S. A. Hor, *Organometallics*, 2008, **27**, 4277-4279.
137. *US Pat.*, US5087788A, 1992.
138. *Jap. Pat.*, JP09268134A, 1997.
139. S. Licciulli, K. Albahily, V. Fomitcheva, I. Korobkov, S. Gambarotta and R. Duchateau, *Angew. Chem., Int. Ed.*, 2011, **50**, 2346-2349.
140. A. Jabri, C. B. Mason, S. Gambarotta, T. J. Burchell and R. Duchateau, *Angew. Chem., Int. Ed.*, 2008, **47**, 9717-9721.
141. H. Mahomed, A. Bollmann, J. T. Dixon, V. Gokul, L. Griesel, C. Grove, F. Hess, H. Maumela and L. Pepler, *Appl. Catal., A*, 2003, **255**, 355-359.
142. *Eur. Pat.*, EP699648A1, 1996.
143. D. H. Morgan, S. L. Schwikkard, J. T. Dixon, J. J. Nair and R. Hunter, *Adv. Synth. Catal.*, 2003, **345**, 939-942.
144. *Br. Pat.*, WO2002004119A1, 2002.
145. *Jap. Pat.*, JP11222445A, 1999.
146. T. Monoi and Y. Sasaki, *J. Mol. Catal. A: Chem.*, 2002, **187**, 135-141.
147. R. D. Köhn, M. Haufe, S. Mihan and D. Lilge, *Chem. Commun.*, 2000, 1927-1928.
148. S. R. C. A. Brocher, *Comp. Rend.*, 1895, 449.
149. A. Bouchemma, P. H. McCabe and G. A. Sim, *Acta Crystallogr., Sect. C: Cryst. Struct. Commun.*, 1990, **46**, 671-674.
150. A. Bouchemma, P. H. McCabe and G. A. Sim, *Acta Crystallogr., Sect. C: Cryst. Struct. Commun.*, 1988, **44**, 1469-1472.
151. C. R. Hawkins, PhD Thesis, University of Bath, 2012.
152. A. R. Martin and H. J. Yallop, *Trans. Faraday Soc.*, 1958, **54**, 257-263.
153. B. L. Ahuja, P. Jain, J. Sahariya, N. L. Heda and P. Soni, *J. Phys. Chem. A*, 2013, **117**, 5685-5692.
154. G. Zhao and M. Lu, *Comput. Theor. Chem.*, 2013, **1018**, 13-18.
155. A. Luttringhaus and W. Kullick, *Tetrahedron Lett.*, 1959, 13-15.
156. R. Fuchs and P. Kluefers, *J. Organomet. Chem.*, 1992, **424**, 353-370.
157. H. Schumann, *Z. Naturforsch., B: Chem. Sci.*, 1995, **50**, 1038-1044.
158. M. V. Baker, D. H. Brown, B. W. Skelton and A. H. White, *J. Chem. Soc., Dalton Trans.*, 1999, 1483-1490.
159. M. V. Baker and M. R. North, *J. Organomet. Chem.*, 1998, **565**, 225-230.
160. M. V. Baker, M. R. North, B. W. Skelton and A. H. White, *Inorg. Chem.*, 1999, **38**, 4515-4521.
161. N. L. Armanasco, M. V. Baker, A. G. Barnes, D. H. Brown, V. J. Hesler, M. R. North, D. Lee, M. J. Paroline and T. B. Rauchfuss, *Inorg. Synth.*, 2010, **35**, 109-114.
162. N. L. Armanasco, M. V. Baker, M. R. North, B. W. Skelton and A. H. White, *J. Chem. Soc., Dalton Trans.*, 1998, 1145-1150.
163. N. L. Armanasco, M. V. Baker, M. R. North, B. W. Skelton and A. H. White, *J. Chem. Soc., Dalton Trans.*, 1997, 1363-1368.
164. M. V. Baker, D. H. Brown, B. W. Skelton and A. H. White, *Dalton Trans.*, 2000, 763-768.
165. G. S. Gol'din, M. G. Gruntfest, A. I. L'Vov, L. S. Baturina, S. V. Sin'ko, Y. V. Kolodyazhnyi, N. L. Sin'ko and N. L. Chikina, *Koord. Khim.*, 1981, **7**, 82-86.
166. M. V. Baker, M. C. Palermo, B. W. Skelton and A. H. White, *Aust. J. Chem.*, 1999, **52**, 179-183.
167. A. Venugopal, I. Kamps, D. Bojer, R. J. F. Berger, A. Mix, A. Willner, B. Neumann, H. G. Stammler and N. W. Mitzel, *Dalton Trans.*, 2009, 5755-5765.
168. R. D. Köhn, Z. Pan and G. Kociok-Köhn, *223rd ACS National Meeting*, American Chemical Society, Orlando, 2002, INOR-462.

169. H. Braband, S. Imstepf, M. Felber, B. Spingler and R. Alberto, *Inorg. Chem.*, 2010, **49**, 1283-1285.
170. G. R. Willey, T. J. Woodman, U. Somasundaram, D. R. Aris and W. Errington, *J. Chem. Soc., Dalton Trans.*, 1998, 2573-2576.
171. C. S. Tredget, S. C. Lawrence, B. D. Ward, R. G. Howe, A. R. Cowley and P. Mountford, *Organometallics*, 2005, **24**, 3136-3148.
172. M. Huelsmann, B. Neumann, H. G. Stammler and N. W. Mitzel, *Eur. J. Inorg. Chem.*, 2012, **26**, 4200-4209.
173. C. Strohmann and V. H. Gessner, *Chem. Asian J.*, 2008, **3**, 1929-1934.
174. M. V. Baker, D. H. Brown, B. W. Skelton and A. H. White, *J. Chem. Soc., Dalton Trans.*, 2000, 763-768.
175. R. D. Koehn and G. Kociok-Koehn, *Angew. Chem.*, 1994, **106**, 1958-1960.
176. A. Bianchi and E. Garcia-Espana, *Supramolecular Chemistry: From Molecules to Nanomaterials*, 2012, **3**, 753-784.
177. G. C. Silver and W. C. Trogler, *J. Am. Chem. Soc.*, 1995, **117**, 3983-3993.
178. F.-J. Wu, G. P. Stahly, F. R. Fronczek and S. F. Watkins, *Acta Crystallogr., Sect. C: Cryst. Struct. Commun.*, 1995, **51**, 18-20.
179. R. D. Koehn, Z. Pan, M. F. Mahon and G. Kociok-Koehn, *Dalton Trans.*, 2003, 2269-2275.
180. G. Kickelbick, D. Rutzinger and T. Gallauner, *Monatsh. Chem.*, 2002, **133**, 1157-1164.
181. R. D. Köhn, L. L. Tomas, Z. Pan, F. Speiser and G. Kociok-Kohn, *Dalton Trans.*, 2009, 4556-4568.
182. R. D. Köhn, G. Seifert, Z. Pan, M. F. Mahon and G. Kociok-Kohn, *Angew. Chem., Int. Ed.*, 2003, **42**, 793-796.
183. N. L. Armanasco, M. V. Baker, M. R. North, B. W. Skelton and A. H. White, *J. Chem. Soc., Dalton Trans.*, 1997, 1363-1368.
184. R. D. Koehn, G. Kociok-Koehn and M. Haufe, *J. Organomet. Chem.*, 1995, **501**, 303-307.
185. C. N. Nenu and B. M. Weckhuysen, *Chem. Commun.*, 2005, 1865-1867.
186. C. N. Nenu, J. N. J. van Lingen, F. M. F. de Groot, D. C. Koningsberger and B. M. Weckhuysen, *Chem. Eur. J.*, 2006, **12**, 4756-4763.
187. C. N. Nenu, P. Bodart and B. M. Weckhuysen, *J. Mol. Catal. A: Chem.*, 2007, **269**, 5-11.
188. R. D. Koehn, Z. Pan, G. Kociok-Koehn and M. F. Mahon, *Dalton Trans.*, 2002, 2344-2347.
189. R. D. Köhn, Z. Pan, J. Sun and C. Liang, *Catal. Commun.*, 2003, **4**, 33-37.
190. *Eur. Pat.*, WO2000058369A1, 2000.
191. *US Pat.*, US6887958-B1, 2001.
192. *Eur. Pat.*, WO2000058319A1, 2000.
193. A. Sattler, J. A. Labinger and J. E. Bercaw, *Organometallics*, 2013, **32**, 6899-6902.
194. J. T. Dixon, M. J. Green, F. M. Hess and D. H. Morgan, *J. Organomet. Chem.*, 2004, **689**, 3641-3668.
195. L. Horner, H. Hoffmann, W. Klink, H. Ertel and V. G. Toscano, *Chem. Ber.*, 1962, **95**, 581-601.
196. X. Chen, G. Li and C. Qian, *Res. Chem. Intermed.*, 2012, **38**, 645-649.
197. B. Badet, M. Julia and C. Rolando, *Synthesis*, 1982, 291-294.
198. L. H. Slaugh, *Tetrahedron*, 1966, **22**, 1741-1746.
199. R. F. Nystrom, *J. Am. Chem. Soc.*, 1955, **77**, 2544-2545.
200. J.-H. Xie, S.-F. Zhu and Q.-L. Zhou, *Chem. Rev.*, 2011, **111**, 1713-1760.
201. R. D. Kohn, D. Smith, M. F. Mahon, M. Prinz, S. Mihan and G. Kociok-Kohn, *J. Organomet. Chem.*, 2003, **683**, 200-208.
202. D. B. G. Williams and M. Lawton, *J. Org. Chem.*, 2010, **75**, 8351-8354.

203. M. Schormann, K. S. Klimek, H. Hatop, S. P. Varkey, H. W. Roesky, C. Lehmann, C. Roepken, R. Herbst-Irmer and M. Noltemeyer, *J. Solid State Chem.*, 2001, **162**, 225-236.
204. *Based on private correspondance with Sasol and LyondellBasell*.
205. R. D. Köhn, D. Smith, M. F. Mahon, M. Prinz, S. Mihan and G. Kociok-Köhn, *J. Organomet. Chem.*, 2003, **683**, 200-208.
206. L. H. Do, J. A. Labinger and J. E. Bercaw, *ACS Catal.*, 2013, **3**, 2582-2585.
207. C. Ramsden, *Comprehensive Organic Functional Group Transformations II*, Elsevier Ltd., 2005.
208. P. Girard, J. L. Namy and H. B. Kagan, *J. Am. Chem. Soc.*, 1980, **102**, 2693-2698.
209. B. W. Knettle and R. A. Flowers, II, *Org. Lett.*, 2001, **3**, 2321-2324.
210. H. J. Lim, C. R. Smith and T. V. RajanBabu, *J. Org. Chem.*, 2009, **74**, 4565-4572.
211. P. W. Jolly, *Acc. Chem. Res.*, 1996, **29**, 544-551.
212. S. Liu, R. Pattacini and P. Braunstein, *Organometallics*, 2011, **30**, 3549-3558.
213. D. S. McGuinness, A. J. Rucklidge, R. P. Tooze and A. M. Z. Slawin, *Organometallics*, 2007, **26**, 2561-2569.
214. A. Kraft, J. Beck and I. Krossing, *Chem. Eur. J.*, 2011, **17**, 12975-12980.
215. A. Kraft, J. Beck, G. Steinfeld, H. Scherer, D. Himmel and I. Krossing, *Organometallics*, 2012, **31**, 7485-7491.
216. A. Kraft, N. Trapp, D. Himmel, H. Boehrer, P. Schlueter, H. Scherer and I. Krossing, *Chem. Eur. J.*, 2012, **18**, 9371-9380.
217. G. J. P. Britovsek, D. S. McGuinness, T. S. Wierenga and C. T. Young, *ACS Catal.*, 2015, Ahead of Print.
218. T. E. Stennett, M. F. Haddow and D. F. Wass, *Organometallics*, 2012, **31**, 6960-6965.
219. T. Agapie, M. W. Day, L. M. Henling, J. A. Labinger and J. E. Bercaw, *Organometallics*, 2006, **25**, 2733-2742.
220. C. K. Ryu, R. B. Lessard, D. Lynch and J. F. Endicott, *J. Phys. Chem.*, 1989, **93**, 1752-1759.
221. M. Brorson, C. J. H. Jacobsen, C. M. Jensen, I. Schmidt and J. Villadsen, *Inorg. Chim. Acta*, 1996, **247**, 189-194.
222. S. J. Manning, W. Bogen and L. A. Kelly, *J. Org. Chem.*, 2011, **76**, 6007-6013.
223. H. Taube and A. Scott, *Inorg. Chem.*, 1971, **10**, 62-66.
224. P. Andersen, A. Doessing, J. Glerup and M. Rude, *Acta Chem. Scand.*, 1990, **44**, 346-352.
225. B. G. Harvey and H. A. Meylemans, *Green Chem.*, 2014, **16**, 770-776.
226. Z. Liu, E. Somsook, C. B. White, K. A. Rosaaen and C. R. Landis, *J. Am. Chem. Soc.*, 2001, **123**, 11193-11207.
227. H. Kalinowski, *Carbon 13 NMR Spectroscopy*, Wiley, New York, 1987.
228. D. Enders, J. Tiebes, N. De Kimpe, M. Keppens, C. Stevens, G. Smagghe and O. Betz, *J. Org. Chem.*, 1993, **58**, 4881-4884.
229. J. J. Eisch and S.-G. Rhee, *J. Am. Chem. Soc.*, 1974, **96**, 7276-7284.
230. D. Muller and A. Alexakis, *Org. Lett.*, 2012, **14**, 1842-1845.
231. C. Heron, Masters Thesis, University of Bath, 2015.
232. S. D. Pike, I. Pernik, R. Theron, J. S. McIndoe and A. S. Weller, *J. Organomet. Chem.*, 2015, **784**, 75-83.
233. M. Ystenes, *J. Catal.*, 1991, **129**, 383-401.
234. K. Qin, C. D. Incarvito, A. L. Rheingold and K. H. Theopold, *Angew. Chem., Int. Ed.*, 2002, **41**, 2333-2335.
235. K. Qin, C. D. Incarvito, A. L. Rheingold and K. H. Theopold, *J. Am. Chem. Soc.*, 2002, **124**, 14008-14009.
236. M. Gjikaj and A. Adam, *Z. Anorg. Allg. Chem.*, 2006, **632**, 2475-2480.
237. A. K. Tomov, J. J. Chirinos, D. J. Jones, R. J. Long and V. C. Gibson, *J. Am. Chem. Soc.*, 2005, **127**, 10166-10167.

238. A. K. Tomov, J. J. Chirinos, R. J. Long, V. C. Gibson and M. R. J. Elsegood, *J. Am. Chem. Soc.*, 2006, **128**, 7704-7705.
239. A. K. Tomov, J. J. Chirinos, D. J. Jones, R. J. Long and V. C. Gibson, *J. Am. Chem. Soc.*, 2005, **127**, 10166-10167.
240. T. M. Zilbershtein, V. A. Kardash, V. V. Suvorova and A. K. Golovko, *Appl. Catal., A*, 2014, **475**, 371-378.
241. R. W. Alder, P. R. Allen, K. R. Anderson, C. P. Butts, E. Khosravi, A. Martin, C. M. Maunder, A. G. Orpen and C. B. St. Pourcain, *J. Chem. Soc., Perkin Trans. 2*, 1998, 2083-2108.
242. S. Datta, C.-L. Chang, K.-L. Yeh and R.-S. Liu, *J. Am. Chem. Soc.*, 2003, **125**, 9294-9295.
243. J. W. De Haan and L. J. M. Van de Ven, *Org. Magn. Resonance*, 1973, **5**, 147-153.
244. B. K. Keitz, K. Endo, M. B. Herbert and R. H. Grubbs, *J. Am. Chem. Soc.*, 2011, **133**, 9686-9688.
245. R. D. Köhn, M. Haufe, D. Smith, G. Kociok-Kohn and S. Mihan, *223rd ACS National Meeting*, American Chemical Society, Orlando, 2002.
246. R. D. Köhn, A. G. N. Coxon, C. R. Hawkins, D. Smith, S. Mihan, K. Schuhen, M. Schiendorfer and G. Kociok-Kohn, *Polyhedron*, 2014, **84**, 3-13.
247. D. F. Evans, *J. Chem. Soc.*, 1959, 2003-2005.
248. D. H. Grant, *J. Chem. Educ.*, 1995, **72**, 39-40.
249. Z. Otwinowski and W. Minor, *Methods Enzymol.*, 1997, **276**, 307-326.

Appendix 1 - ^{13}C NMR Data for the C_{18} Trimers

All chemical shifts were measured for a pure sample of the isomer mix relative to an internal TMS reference. The assignments are as quoted in the main text, the remaining signals corresponding to the butyl chains could not be distinguished from one another.

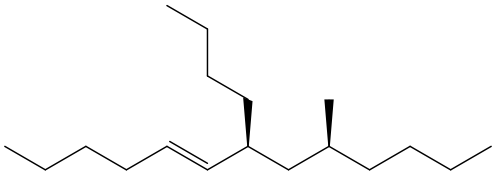

A (SS/RR)

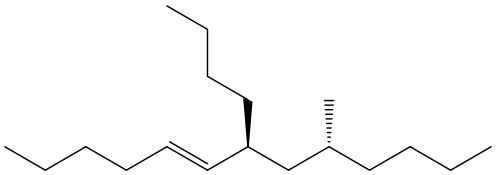

A' (SR/RS)

Isomer A

^{13}C NMR, neat (TMS): δ = 135.24, 130.25, 43.63, 40.93, 38.14, 36.52, 32.61, 32.29, 30.33, 29.9, 29.64, 23.32, 23.13, 22.41, 19.38, 14.28, 14.26, 14.04.

Isomer A'

^{13}C NMR, neat (TMS): δ = 135.56, 130.01, 43.97, 40.78, 36.10, 35.75, 32.65, 32.33, 30.27, 29.82, 29.44, 23.38, 23.14, 22.45, 20.63, 14.29, 14.25, 14.06.

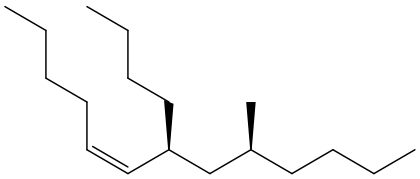

B (SS/RR)

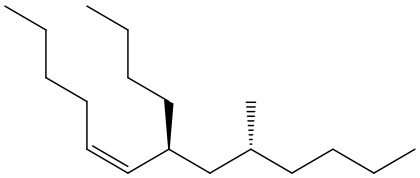

B' (SR/RS)

Isomer B

^{13}C NMR, neat (TMS): δ = 135.48, 129.32, 44.49, 36.56, 36.09, 35.01, 32.56, 30.63, 29.92, 29.67, 27.87, 23.47, 23.26, 22.81, 20.70, 14.31, 14.26, 14.15.

Isomer B'

^{13}C NMR, neat (TMS): δ = 135.19, 129.67, 44.06, 38.15, 36.75, 35.15, 32.60, 30.54, 29.95, 29.61, 27.88, 23.34, 23.25, 22.76, 19.76, 14.28, 14.26, 14.16.

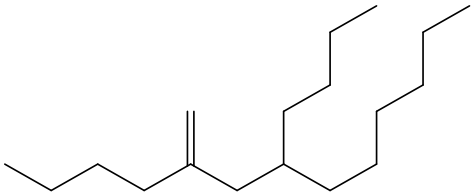

C

Isomer C

^{13}C NMR, neat (TMS): δ = 148.14, 110.68, 41.59, 35.68, 35.55, 33.80, 33.48, 32.33, 30.31, 30.14, 29.14, 26.86, 23.42, 23.04, 22.79, 14.27, 14.24, 14.14.

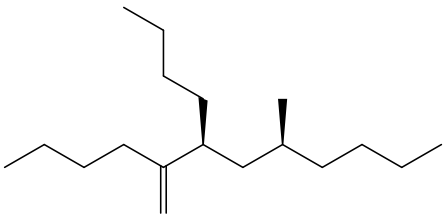

D (SS/RR)

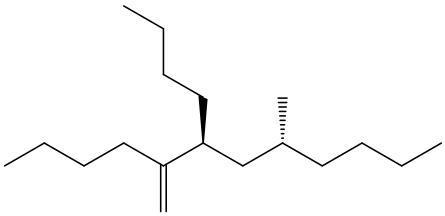

D' (SR/RS)

Isomer D

^{13}C NMR, neat (TMS): δ = 152.17, 109.17, 44.49, 42.63, 36.55, 34.06, 32.42, 30.51, 30.44, 30.01, 29.52, 23.34, 23.20, 23.05, 20.52, 14.29, 14.22, 14.21.

Isomer D'

^{13}C NMR, neat (TMS): δ = 151.53, 109.57, 44.94, 41.88, 38.11, 34.91, 31.57, 30.34, 30.49, 30.14, 29.62, 23.38, 23.17, 23.09, 19.67, 14.27, 14.26, 14.24.

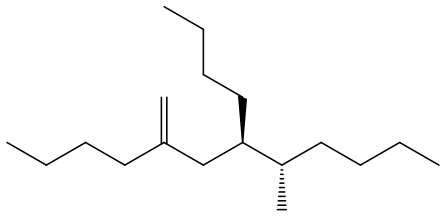

E (RR/SS)

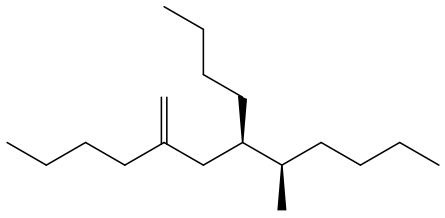

E' (RS/SR)

Isomer E

^{13}C NMR, neat (TMS): δ = 148.43, 110.79, 39.91, 37.19, 35.58, 33.89, 33.72, 30.54, 30.50, 30.37, 30.30, 23.36, 23.33, 22.79, 15.65, 14.30, 14.27, 14.14.

Isomer E'

^{13}C NMR, neat (TMS): δ = 148.32, 110.81, 39.90, 38.57, 35.42, 34.09, 33.82, 32.57, 30.47, 30.43, 29.31, 23.38, 23.39, 22.75, 15.32.

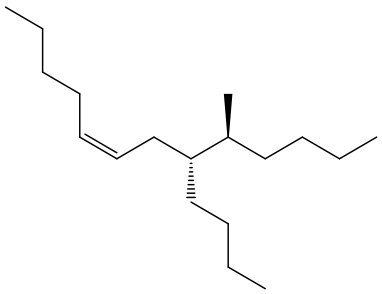

F (RS/SR)

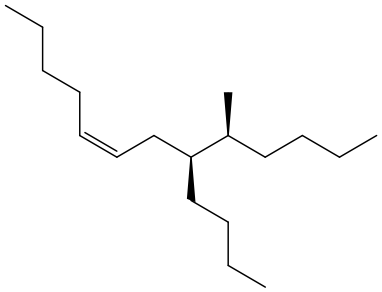

F' (SS/RR)

Isomer F

^{13}C NMR, neat (TMS): δ = 130.18, 129.59, 43.37, 34.58, 34.04, 32.35, 32.30, 31.00, 30.19, 28.01, 27.38, 15.87.

Isomer F'

^{13}C NMR, neat (TMS): δ = 130.25, 129.42, 43.33, 34.50, 34.15, 32.21, 29.30, 15.73.

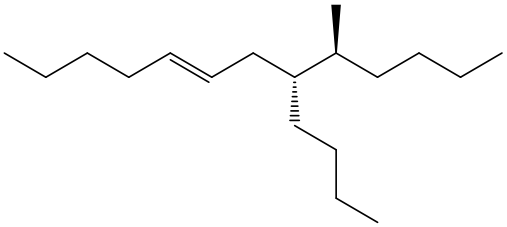

G (RS/SR)

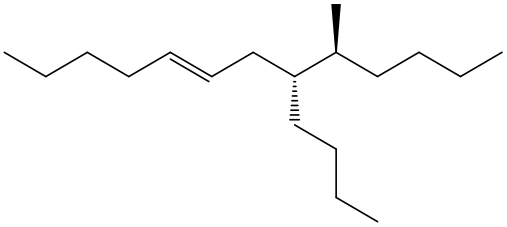

G' (SS/RR)

Isomer G

^{13}C NMR, neat (TMS): δ = 131.24, 130.12, 42.94, 34.52, 33.95, 33.72, 32.73, 32.24, 30.83, 30.66, 30.32, 15.84.

Isomer G'

^{13}C NMR, neat (TMS): δ = 131.27, 129.95, 43.02, 36.03, 34.98, 34.43, 34.22, 15.63.

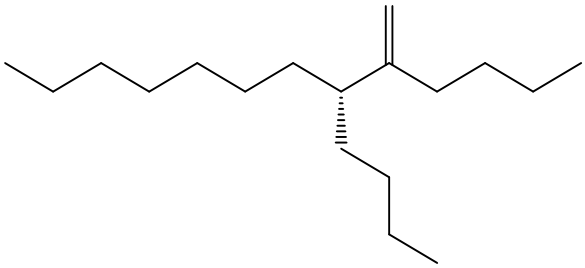

H

Isomer H

^{13}C NMR, neat (TMS): δ = 151.77, 109.22, 47.14, 34.56, 27.85.

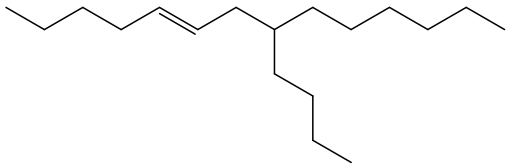

I

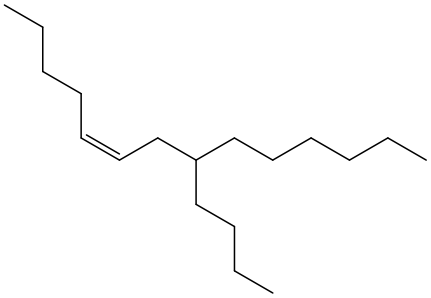

K

Isomer I

^{13}C NMR, neat (TMS): δ = 131.69, 128.75, 38.10, 37.08, 27.72.

Isomer K

^{13}C NMR, neat (TMS): δ = 130.58, 128.30, 38.44, 33.97, 33.65, 32.34, 31.50, 29.75, 29.46, 27.41, 27.18.

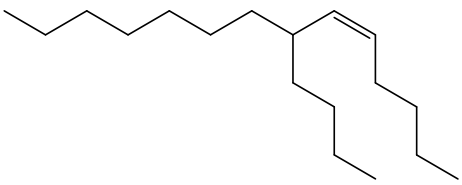

L

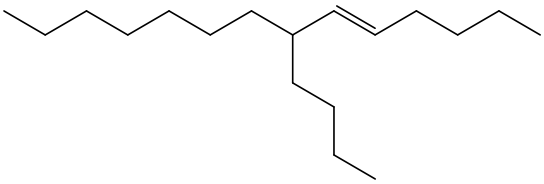

M

Isomer L

^{13}C NMR, neat (TMS): δ = 135.19, 129.71, 37.48, 36.48, 36.20, 32.57, 32.41, 30.34, 30.04, 29.81, 27.78, 27.77, 23.30, 23.09, 22.77, 14.27, 14.26, 14.17.

Isomer M

^{13}C NMR, neat (TMS): δ = 135.27, 130.28, 43.28, 36.07, 35.76, 32.76, 32.40, 32.38, 30.19, 29.90, 29.83, 27.69, 23.19, 23.09, 22.52, 14.27, 14.26, 14.08.

Appendix 2 - Single Crystal X-Ray Diffraction Data

Crystal data and structure refinement for $(Pe_2CHCH_2CH_2)_3TACCrCl_3$.

Empirical formula	C42 H87 Cl3 Cr N3	
Formula weight	792.50	
Temperature	150(2) K	
Wavelength	0.71073 Å	
Crystal system, space group	monoclinic, P 2_1/a	
Unit cell dimensions	a = 13.353(4) Å	α = 90°.
	b = 24.402(7) Å	β = 91.319(11)°.
	c = 14.056(4) Å	γ = 90°.
Volume	4579(2) $Å^3$	
Z	4	
Calculated density	1.150 Mg/m^3	
Absorption coefficient	0.455 mm^{-1}	
F(000)	1740	
Crystal size	0.50 x 0.10 x 0.08 mm	
Theta range for data collection	2.93 to 25.19°.	
Limiting indices	-15<=h<=15, -28<=k<=27, -15<=l<=16	
Reflections collected / unique	15641 / 5712 [R(int) = 0.2488]	
Completeness to theta = 25.19	69.4 %	
Max. and min. transmission	0.9645 and 0.8044	
Refinement method	Full-matrix least-squares on F^2	
Data / restraints / parameters	5712 / 66 / 233	
Goodness-of-fit on F^2	1.745	
Final R indices [I>2sigma(I)]	R1 = 0.3070, wR2 = 0.6010	
R indices (all data)	R1 = 0.4623, wR2 = 0.6616	
Extinction coefficient	0.31(5)	
Largest diff. peak and hole	2.165 and -1.225 $e.Å^{-3}$	

Crystal data and structure refinement for $(Pe_2CBrCH_2CH_2)_3TACCrCl_3$.

Empirical formula	C42 H84 Br3 Cl3 Cr N3	
Formula weight	1029.20	
Temperature	150(2) K	
Wavelength	0.71073 Å	
Crystal system, space group	Monoclinic, P 2_1/n	
Unit cell dimensions	a = 13.9501(8) Å	α = 90°.
	b = 14.1189(7) Å	β = 91.458(4)°.
	c = 25.0564(12) Å	γ = 90°.
Volume	4933.5(4) A^3	
Z	4	
Calculated density	1.386 Mg/m^3	
Absorption coefficient	2.855 mm^{-1}	
F(000)	2148	
Crystal size	0.40 x 0.25 x 0.20 mm	
Theta range for data collection	3.26 to 27.4°.	
Limiting indices	-17<=h<=18, -17<=k<=18, -27<=l<=32	
Reflections collected / unique	30961 / 10700 [R(int) = 0.0575]	
Completeness to theta = 25.00	99.4 %	
Absorption correction	Semi-empirical from equivalents	
Max. and min. transmission	0.5990 and 0.3947	
Refinement method	Full-matrix least-squares on F^2	
Data / restraints / parameters	10700 / 18 / 493	
Goodness-of-fit on F^2	0.847	
Final R indices [I>2sigma(I)]	R1 = 0.0459, wR2 = 0.1020	
R indices (all data)	R1 = 0.1059, wR2 = 0.1117	
Largest diff. peak and hole	1.272 and -1.042 e.$Å^{-3}$	

Crystal and Structural Refinement Data for ($^{i}Bu_2CH)_3TACCrCl_3$

Empirical formula	C30 H63 Cl3 Cr N3	
Formula weight	624.18	
Temperature	150(2) K	
Wavelength	0.71073 Å	
Crystal system	Monoclinic	
Space group	$P2_1/c$	
Unit cell dimensions	a = 13.05720(10) Å	α = 90°.
	b = 22.5768(3) Å	β = 117.2045(7)°.
	c = 14.04180(10) Å	γ = 90°.
Volume	3681.48(7) $Å^3$	
Z	4	
Density (calculated)	1.126 Mg/m^3	
Absorption coefficient	0.549 mm^{-1}	
F(000)	1356	
Crystal size	0.500 x 0.300 x 0.250 mm^3	
Theta range for data collection	2.913 to 27.459°.	
Index ranges	-16<=h<=15, -29<=k<=29, -18<=l<=18	
Reflections collected	63189	
Independent reflections	8390 [R(int) = 0.0615]	
Completeness to theta = 25.242°	99.8 %	
Absorption correction	Semi-empirical from equivalents	
Max. and min. transmission	0.874 and 0.782	
Refinement method	Full-matrix least-squares on F^2	
Data / restraints / parameters	8390 / 0 / 381	
Goodness-of-fit on F^2	1.020	
Final R indices [I>2sigma(I)]	R1 = 0.0418, wR2 = 0.0905	
R indices (all data)	R1 = 0.0623, wR2 = 0.0986	
Largest diff. peak and hole	0.487 and -0.387 $e.Å^{-3}$	

Crystal data and structure refinement for ($^{i}Bu_2CH)_3TACCrBr_3$.

Empirical formula	C30 H63 Br3 Cr N3	
Formula weight	757.56	
Temperature	150(2) K	
Wavelength	0.71073 Å	
Crystal system	Triclinic	
Space group	P1	
Unit cell dimensions	a = 12.5950(2) Å	α= 91.9340(10)°.
	b = 14.4290(2) Å	β= 90.9760(10)°.
	c = 21.2180(3) Å	γ = 105.4670(10)°.
Volume	3712.89(10) $Å^3$	
Z	4	
Density (calculated)	1.355 Mg/m^3	
Absorption coefficient	3.558 mm^{-1}	
F(000)	1572	
Crystal size	0.550 x 0.500 x 0.100 mm^3	
Theta range for data collection	3.049 to 27.488°.	
Index ranges	-16<=h<=16, -18<=k<=18, -26<=l<=27	
Reflections collected	52378	
Independent reflections	28808 [R(int) = 0.0650]	
Completeness to theta = 25.242°	98.2 %	
Absorption correction	Semi-empirical from equivalents	
Max. and min. transmission	0.714 and 0.375	
Refinement method	Full-matrix least-squares on F^2	
Data / restraints / parameters	28808 / 244 / 1604	
Goodness-of-fit on F^2	1.030	
Final R indices [I>2sigma(I)]	R1 = 0.0641, wR2 = 0.1484	
R indices (all data)	R1 = 0.0918, wR2 = 0.1659	
Absolute structure parameter	0.221(11)	
Largest diff. peak and hole	1.523 and -0.859 e.$Å^{-3}$	

Crystal data and structure refinement for [(^{i}Bu$_2$CH)$_3$TACCrBr$_2$(H$_2$O)][OTf]-DCM.

Empirical formula	C32 H67 Br2 Cl2 Cr F3 N3 O4 S	
Formula weight	929.66	
Temperature	150(2) K	
Wavelength	1.54184 Å	
Crystal system	Monoclinic	
Space group	$P2_1/n$	
Unit cell dimensions	a = 14.70360(10) Å	α= 90°.
	b = 15.72900(10) Å	β= 91.2990(10)°.
	c = 18.9512(2) Å	γ = 90°.
Volume	4381.77(6) Å^3	
Z	4	
Density (calculated)	1.409 Mg/m^3	
Absorption coefficient	6.253 mm^{-1}	
F(000)	1932	
Crystal size	0.300 x 0.150 x 0.050 mm^3	
Theta range for data collection	4.116 to 71.951°.	
Index ranges	-18<=h<=18, -17<=k<=19, -22<=l<=23	
Reflections collected	34190	
Independent reflections	8508 [R(int) = 0.0601]	
Completeness to theta = 67.684°	99.9 %	
Absorption correction	Semi-empirical from equivalents	
Max. and min. transmission	1.00000 and 0.39511	
Refinement method	Full-matrix least-squares on F^2	
Data / restraints / parameters	8508 / 2 / 469	
Goodness-of-fit on F^2	1.023	
Final R indices [I>2sigma(I)]	R1 = 0.0539, wR2 = 0.1446	
R indices (all data)	R1 = 0.0572, wR2 = 0.1488	
Largest diff. peak and hole	1.099 and -0.968 e.Å^{-3}	

Crystal data and structure refinement for $(Pr_2CHCH_2)_3TACCrCl_3$.

Empirical formula	C27 H57 Cl3 Cr N3	
Formula weight	582.10	
Temperature	150(2) K	
Wavelength	1.54184 Å	
Crystal system	Monoclinic	
Space group	$P2_1/n$	
Unit cell dimensions	a = 13.9121(8) Å	α= 90°.
	b = 21.190(2) Å	β= 94.558(7)°.
	c = 22.010(2) Å	γ = 90°.
Volume	6468.0(9) $Å^3$	
Z	8	
Density (calculated)	1.196 Mg/m^3	
Absorption coefficient	5.319 mm^{-1}	
F(000)	2520	
Crystal size	0.150 x 0.120 x 0.030 mm^3	
Theta range for data collection	4.190 to 67.028°.	
Index ranges	-16<=h<=16, -25<=k<=25, -26<=l<=25	
Reflections collected	15774	
Independent reflections	15774	
Completeness to theta = 67.028°	99.3 %	
Absorption correction	Semi-empirical from equivalents	
Max. and min. transmission	1.00000 and 0.60277	
Refinement method	Full-matrix least-squares on F^2	
Data / restraints / parameters	15774 / 81 / 673	
Goodness-of-fit on F^2	0.774	
Final R indices [I>2sigma(I)]	R1 = 0.0595, wR2 = 0.1013	
R indices (all data)	R1 = 0.1424, wR2 = 0.1157	
Largest diff. peak and hole	0.483 and -0.487 $e.Å^{-3}$	

Crystal data and structure refinement for $(Pr_2CHCH_2)_3TACCrBr_3$.

Empirical formula	C27 H57 Br3 Cr N3	
Formula weight	715.48	
Temperature	150(2) K	
Wavelength	1.54184 Å	
Crystal system	Orthorhombic	
Space group	Pbcn	
Unit cell dimensions	a = 21.5170(5) Å	α= 90°.
	b = 14.2483(2) Å	β= 90°.
	c = 21.7431(6) Å	γ = 90°.
Volume	6666.0(3) $Å^3$	
Z	8	
Density (calculated)	1.426 Mg/m^3	
Absorption coefficient	7.163 mm^{-1}	
F(000)	2952	
Crystal size	0.280 x 0.100 x 0.020 mm^3	
Theta range for data collection	5.516 to 71.933°.	
Index ranges	-26<=h<=26, -10<=k<=17, -26<=l<=25	
Reflections collected	38776	
Independent reflections	6505 [R(int) = 0.0709]	
Completeness to theta = 67.684°	99.8 %	
Absorption correction	Semi-empirical from equivalents	
Max. and min. transmission	1.00000 and 0.56392	
Refinement method	Full-matrix least-squares on F^2	
Data / restraints / parameters	6505 / 0 / 313	
Goodness-of-fit on F^2	1.034	
Final R indices [I>2sigma(I)]	R1 = 0.0611, wR2 = 0.1614	
R indices (all data)	R1 = 0.0711, wR2 = 0.1741	
Largest diff. peak and hole	1.097 and -0.824 e.$Å^{-3}$	

Crystal data and structure refinement for $(Pr_2CHCH_2)_3TACCrI_3$.

Empirical formula	C27 H57 Cl3 Cr N3	
Formula weight	582.10	
Temperature	150(2) K	
Wavelength	1.54184 Å	
Crystal system	Monoclinic	
Space group	$P2_1/n$	
Unit cell dimensions	a = 13.90570(10) Å	α= 90°.
	b = 21.1031(15) Å	β= 95.605(7)°.
	c = 22.1570(16) Å	γ = 90°.
Volume	6471.0(7) $Å^3$	
Z	8	
Density (calculated)	1.199 Mg/m^3	
Absorption coefficient	5.333 mm^{-1}	
F(000)	2520	
Crystal size	0.300 x 0.100 x 0.100 mm^3	
Theta range for data collection	5.272 to 72.527°.	
Index ranges	-11<=h<=17, -25<=k<=25, -26<=l<=27	
Reflections collected	15988	
Independent reflections	15988	
Completeness to theta = 67.684°	99.6 %	
Absorption correction	Semi-empirical from equivalents	
Max. and min. transmission	1.00000 and 0.58393	
Refinement method	Full-matrix least-squares on F^2	
Data / restraints / parameters	15988 / 21 / 655	
Goodness-of-fit on F^2	0.903	
Final R indices [I>2sigma(I)]	R1 = 0.0940, wR2 = 0.2070	
R indices (all data)	R1 = 0.1550, wR2 = 0.2271	
Largest diff. peak and hole	0.886 and -0.964 $e.Å^{-3}$	